

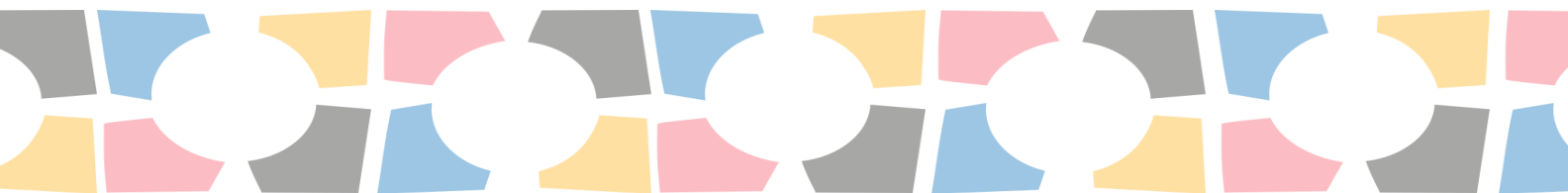
MoDeSt 2024

11th Conference of the
Modification, Degradation, Stabilization of
Polymers

BOOK OF ABSTRACTS

September 1-4, 2024

University of Palermo
PALERMO, ITALY



Under Auspices of:



AIM

Associazione Italiana di Scienza e
Tecnologia delle Macromolecole



AIMAT

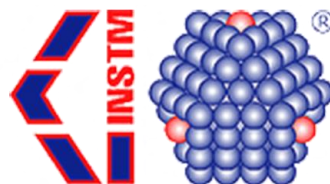
Associazione Italiana Materiali



**Università
degli Studi
di Palermo**

UNIPA

Università degli Studi di Palermo



INSTM

Interuniversity Consortium of
Science and Technology of
Materials

Our Sponsors:



MP Strumenti

Distributore di strumenti scientifici
per la ricerca e il controllo qualità



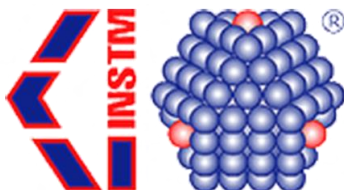
ZwickRoell

Leader mondiale nelle prove
dei materiali



AMAPLAST

Promozione nel mondo della tecnologia italiana per la
trasformazione delle materie plastiche e della gomma



INSTM

Interuniversity Consortium of
Science and Technology of
Materials



FKV

Soluzioni per il laboratorio

MoDeSt 2024
11th Conference of the
Modification, Degradation, Stabilization of Polymers

WELCOME

Dear MoDeSt friends,
thank you for being here.

The first MoDeSt Conference was held in Palermo in 2000 when MoDeSt Society did not even exist!! Actually, the Society was established just after this successful Conference (more than 350 participants!). After that Meeting, this Conference was held every couple of years.

Unfortunately, the pandemic has interrupted our biennial conference and, after five years, now we start again coming back in Palermo where everything started.

The decision in 2000 to combine these three topics - *Modification, Degradation and Stabilization* - was taken by Gianni Camino and myself as a recognition of the overlapping of these subjects in polymer science and technology. The Modification - voluntary or involuntary - by chemical or physical methods of a polymer matrix is the very essence of the scientific work of all of us.

The participation of about 200 researchers from 20 countries is a tangible proof of the success of this idea even after 24 years and of the great interest in these topics, but, it is also a tangible proof of affection towards MoDeSt and towards the colleagues of the University of Palermo who, with great effort and in a very short time, succeeded in organizing this meeting.

I wish to thank all of those who made this event possible, and especially the younger, who took on their shoulders the burden of this complex organization task. Without their help, we would not be here.

The remarkable number of communications has been divided into three parallel sessions but not according to the topics of the conference.

I think that all of these topics are very "*compatible*" and, at least in part, "*superimposable*" each other, and "*Blending*" is always a good and fruitful idea!

Furthermore, I wish to give my warmest thanks to University of Palermo, to the Department of Engineering and to the sponsors of this Conference who allowed the organization of this scientific meeting, including the social events. Finally, thanks to the journal "*Polymer Degradation and Stability*" and the editor prof. Mathew Celina for the publication of the communications of this Conference.

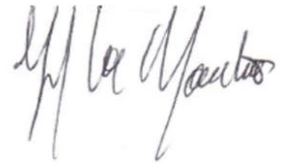
MoDeSt is about a quarter of century old and many colleagues and friends who founded and supported this society are no more with us, among them; Les Utracki, Jean-Pierre Pascault, Maria Omastova, Mario Malinconico, Toni Recca and others. We need to remember them because memory is the soul of a community.

I am seventy-five and I have been retired for 4 years, 10 months, 1 day and about 9 hours, but, ... refrain your enthusiasm, don't enjoy, this is not my good-bye! I will

continue to stimulate (and maybe to bore!) my younger successors for a number of more years, until GOD and the existing laws will allow me to do so. Later, I am sure they will not lose our habit and they will go further in the direction followed during these our previous fifty years: scientific rigour, intellectual honesty, opening toward others and work, work, work.

Thank you again for being here.

Franco La Mantia

A handwritten signature in black ink, appearing to read 'F. La Mantia', written in a cursive style.

Organisers and Committees

Organizing Committee

F.P. La Mantia, University of Palermo, (Chairman)
A. Valenza, University of Palermo
R. Scaffaro, University of Palermo
G. Cicala, University of Catania
N.Tz. Dintcheva, University of Palermo
M. Morreale, University of Enna
L. Botta, University of Palermo
V. Fiore, University of Palermo
L. Calabrese, University of Messina
M.C. Mistretta, University of Palermo

Scientific Committee

S. A-Malaika, England
F. P. La Mantia, Italy
J. Covas, Portugal
P. Gijsman, The Netherlands
S. Therias, France
N. Allen, England
M. Celina, USA
J.L. Gardette, France
J. F. Gerard, France
T. Iwata, Japan
A. J. Müller, Spain
C. Papaspyrides, Greece
P. Potschke, Germany
P. Saha, Czech Republic

Local Committee

F.P. La Mantia, University of Palermo, (Chairman)
M. Ceraulo, University of Palermo
E.F. Gulino, University of Palermo
A. Maio, University of Palermo
M.C. Citarrella, University of Palermo
V. Titone, University of Palermo
M. Gammino, University of Palermo

Scientific program

September 2nd			
	Session 1 - Hall F120	Session 2 -Hall F220	Session 3 - Hall F230
09.00	OPENING CEREMONY		
09.30	PL.1 Celina		
10.15	O1-1 Carfagna	O2-1 Dorigato	O3-1 Benzemma 1
10.30	O1-2 Gomez-Sanchez	O2-2 Stanzione	O3-2 Benzemma 2
10.45	O1-3 Mauro	O2-3 Pantani	O3-3 Cruz
11.00	O1-4 Jean	O2-4 Palmieri	O3-4 Torresi
11.15	O1-5 Skyronka	O2-5 Baron	O3-5 Stam
11.30	Coffee Break - Poster	Coffee Break - Poster	Coffee Break - Poster
12.00	PL.4 Muller		
12.45	O1-6 Hiejima	O2-6 Tamburri	O3-6 Delarue
13.00	O1-7 Muranaka	O2-7 Mincheva	O3-7 Paul
13.15	O1-8 Noè	O2-8 Balsamo	O3-8 Niccolai
13.30	O1-9 Mayer-Gall	O2-9 Rijavec	O3-9 Combeau
13.45	Lunch - Poster	Lunch - Poster	Lunch - Poster
15.15	O1-10 Torre	O2-10 Kruczala	O3-10 Nag
15.30	O1-11 Gkalliou	O2-11 Lo Re	O3-11 Chervanyov
15.45	O1-12 Tang	O2-12 Avella	O3-12 Metzsch-Zilligen 1
16.00	O1-13 Gratier	O2-13 Berner	O3-13 Metzsch-Zilligen 2
16.15	O1-14 Kozlowski	O2-14 Panagiotopoulos	O3-14 Leem
16.30	Coffee break - poster	Coffee Break - Poster	Coffee Break - Poster
17.00	Assembly		

Scientific program

September 3rd		
Session 1 - Hall F120	Session 2 -Hall F220	Session 3 - Hall F230
09.00	PL.2 Schartel	
09.45	O1-15 Papaspyrides	O2-15 Ambrosio
10.00	O1-16 Arrigo	O2-16 Garofalo
10.15	O1-17 Jankowski	O2-17 Szostak
10.30	O1-18 Rizzarelli	O2-18 Regnier
10.45	O1-19 Yarahmadi	O2-19 Vaytet
11.00	O1-20 Covas	O2-20 Paiva
11.15	Coffee Break - Poster	Coffee Break - Poster
11.45	PL.5 Pegoretti	
12.30	O1-21 Richaud	O2-21 Maffezzoli
12.45	O1-22 Bajer	O2-22 Grommer
13.00	O1-23 Colucci	O2-23 Pyrzyński
13.15	O1-24 Killinger	O2-24 Cicala
13.30	Lunch - Poster	Lunch - Poster
15.00	O1-25 Fukata	O2-25 Lazeregue
15.15	O1-26 Goncalves Marquez	O2-26 Schiera
15.30	O1-27 Doriat	O2-27 Gammino
15.45	O1-28 Buccella	O2-28 Abe
16.00	O1-29 Rizzo	O2-29 Carbone
16.15	O1-30 Di Liberto	O2-30 Watt
16.30	Coffee Break - Poster	Coffee Break - Poster
		Coffee break - Poster

Scientific program

September 4th			
	Session 1 - Hall F120	Session 2 -Hall F220	Session 3 - Hall F230
09.00	PL.3 Iwata		
09.45	O1-31 Fredi	O2-31 Duchamp	O3-31 Bruzaud
10.00	O1-32 Jost	O2-32 Ishida	O3-32 Kabe
10.15	O1-33 Milazzo	O2-33 Visco	O3-33 Puglia
10.30	O1-34 Coltelli	O2-34 Merijs Meri	O3-34 Rodi
10.45	O1-35 Koike	O2-35 Frache	O3-35 Latteri
11.00	O1-36 Fiorica	O2-36 Bernagozzi	O3-36 Calabrese
11.15	Coffee Break	Coffee Break	Coffee Break
11.45	O1-37 Valenza		
12.00	O1-38 Gerard		
12.15	O1-39 Therias		
12.30	CONCLUDING and AWARDS		
13.00	Lunch		

Scientific program - Poster presentations

September 2nd

P1 Adoumaz
P2 Aleeva
P3 Antonucci
P4 Arrigo
P5 Badia 1
P6 Baiamonte
P7 Bajer
P8 Becker
P9 Benito
P10 Botta
P11 Calabrese
P12 Cavodeau
P13 Celauro
P14 Ceraulo
P15 Citarrella 1
P16 Cruz
P17 Di Maio
P18 Diaz-Carrasco
P19 Filippone
P20 Frache
P21 Galbis
P22 Gamez 1
P23 Garcia-Martin
P24 Gnoffo
P25 Gorecki
P26 Gutierrez Silva
P27 Infurna
P28 Inguanta
P29 Kozłowska
P30 Kruczala
P31 Moretti
P32 Morreale 1
P33 Scaffaro 1
P34 Zasada 1
P35 Nakashima

September 3rd

P1 Badia 2
P2 Ciaramitaro
P3 Cicala
P4 Citarrella 2
P5 de Paz Banez
P6 Di Marco
P7 Gamez 2
P8 Gulino
P9 Höhne
P10 Ishida
P11 Ivanova
P12 Jakubowicz
P13 Kowalonek
P14 Leanza
P15 Luciano
P16 Maio
P17 Masek
P18 Fiore
P19 Mistretta
P20 Morreale 2
P21 Otto
P22 Paul
P23 Petrucci
P24 Puglia
P25 Rech
P26 Riccelli
P27 Rizzarelli
P28 Scaffaro 2
P29 Scarfato
P30 Testa
P31 Titone
P32 Tomasik
P33 Visco
P34 Zasada 2
P35 Tamburri
P36 Sanfilippo

Table of contents

Plenary lectures

SEPTEMBER, 2ND

MOVING FORWARD: TRACK RECORD AND OUTSTANDING CHALLENGES
IN THE FIELD OF POLYMER DEGRADATION

M. Celina 29

TOUGHENING BRITTLE BACTERIAL POLYHYDROXYBUTYRATE BY CONTROLLING
ITS STEREOMICROSTRUCTURE THROUGH SEVERAL APPROACHES

A.J. Müller 30

SEPTEMBER, 3RD

THERMAL DECOMPOSITION FEATURES FLAME RETARDANCY

B. Scharrel 32

MULTIFUNCTIONAL SANDWICH COMPOSITES WITH THERMAL ENERGY
STORAGE CAPABILITY

G. Fredi, E. Boso, A. Sorze, A. Pegoretti 34

SEPTEMBER, 4TH

DEVELOPMENT OF HIGH-PERFORMANCE BIODEGRADABLE BIOMASS
PLASTICS AND DEEP-SEA BIODEGRADATION

T. Iwata 36

SEPTEMBER, 2ND - SESSION 1

FROM LIQUID CRYSTALLINE TO BIOBASED EPOXY RESINS: INSIGHT INTO MORE SUSTAINABLE THERMOSETS <u>C. Carfagna</u> , V. Ambrogi, P. Cerruti, G. Gentile, M. Salzano De Luna, A. Marotta, L. Gioiella, A. Mija	38
NATURAL AGEING OF CLOSED-CELL POLYESTER URETHANE FOAM <u>E. Gómez-Sánchez</u> , S. Kunz, J. Köppen, S. Brunner, E. Rettler, E. Bresolin	40
ONE-POT SYNTHESIS OF POLY(D,L-LACTIDE)-CARBON NANODOTS NANOCOMPOSITES BY MELT-EXTRUSION TRANSESTERIFICATION: A VERSATILE WAY TO PRODUCE PHO-TOSTABLE FLUORESCENT BIOMATERIALS <u>N. Mauro</u> , M.A. Utzeri, F. Messina, A. Sciortino, G. Cavallaro, G. Giammona	43
MICRONIZATION AND REGENERATION OF VULCANIZED RUBBER SCRAP BY TWIN-SCREW EXTRUSION <u>Q. Jean</u> , Y. Chalamet, J.C. Majesté, C. Carrot, C. Janin, B. Cantaloube, P. Heuillet	45
EFFECT OF PROCESSING CONDITIONS ON THE COMPATIBILISATION OF A RECLAIMED EPDM IN A PP MATRIX <u>V. Skyronka</u> , J.C. Majesté, C. Carrot, Y. Chalamet, C. Janin, B. Cantaloube	47
FORMATION OF PARALLEL CRACKS DRIVEN BY CHEMICRYSTALLIZATION AND SUBSEQUENT FRAGMENTATION INTO MICROPLASTICS <u>Y. Hiejima</u> , D. Hara, R. Ippitsu, A. Ito, K.H. Nitta	49
DEGRADATION BEHAVIOR OF POLYBUTYLENE SUCCINATE WITH FILLERS <u>Y. Muranaka</u> , T. Koike, T. Osuga, T. Maki	51
NEW TYRE COMPOUNDS WITH REDUCED ENVIRONMENTAL IMPACT <u>C. Noè</u> , C. Di Bernanrdo, M. Dadkhah, F. Demichelis, M.Messori	53
N-P-SILANES AS MULTIPURPOSE FLAME RETARDANTS <u>T. Mayer-Gall</u> , W. Ali, R. Otto, V. Shabani, D. Danielski, J.S. Gutmanna	55
CHALLENGES ON THE CURRENT CAPABILITIES TO DETERMINE THE THERMAL DIFFUSIVITY OF CARBON/PHENOLIC COMPOSITES EXPOSED TO HARSH HYPERTHERMAL ENVIRONMENTS: A THEORETICAL ASSESSMENT AND AN EXPERIMENTAL PROTOCOL M. Natali, <u>L. Torre</u> , M. Buconi, M. Rallini	57

ACCELERATED HYDROLYTIC DEGRADATION OF GLASS FIBER-POLYAMIDE (PA66) COMPOSITES <u>K. Gkaliou</u> , M.V. Ørsnæs, A.H. Holm, A.E. Daugaard	59
LIFETIME PREDICTION MODEL OF CARBON FIBER REINFORCED EPOXY RESIN COMPOSITES UNDER HYGROTHERMAL AGING <u>G. Tang</u> , R. Yang	61
ENGINEERING FLAME-RETARDANT PROPERTIES IN THERMOPLASTIC POLYURETHANE THROUGH REACTIVE EXTRUSION <u>L. Gratier</u> , J.-M. Raquez, M. Cochez, F. Laoutid, H. Vahabi	63
PROGRESS IN FLEXIBLE AND RIGID FIRE BARRIERS <u>R. Kozlowski</u> , Z. Malkowski, M. Muzyczek	65
 SEPTEMBER, 2ND - SESSION 2	
INVESTIGATING THE POTENTIAL OF NOVEL FURANOATE POLYESTERS FOR PACKAGING APPLICATIONS <u>A. Dorigato</u> , G. Fredi, D. Rigotti, D. Perin, M. Soccio, N. Lotti, D.N. Bikiaris, A. Pegoretti	68
ZEIN-BASED NANOPARTICLES AS SUSTAINABLE AND ACTIVE PLATFORMS WITH POTENTIAL APPLICATIONS IN AGRICULTURE <u>M. Stanzione</u> , E. Oleandro, G. G. Buonocore, S. P. Nastasi, B. M. Orlando Marchesano, M. C. Bonza, M. Lavorgna	70
THE IMPORTANCE OF MELTING IN 3D PRINTING S. Liparoti, D. Cavallo, M. L. Di Lorenzo, T. Hashemi, A. Romano, <u>R. Pantani</u>	72
BLENDS OF VIRGIN AND RECYCLED PP FROM PERSONAL PROTECTIVE EQUIPMENT: CORRELATION BETWEEN RHEOLOGICAL, STRUCTURAL AND MECHANICAL PROPERTIES <u>F. Palmieri</u> , M. C. Riccelli, G. Infurna, N. Tz. Dintcheva, A. Romani, M. Levi, L. Incarnato	73
DURABILITY OF FLAME RETARDED POLYMER , 3D PRINTABLE FOR RAILWAY INDUSTRY <u>R. Baron</u> , L. Geoffroy, N. Gay, G. Fontaine, B. Fayolle, S. Bourbigot	75
MULTIFUNCTIONAL POLYMER COMPOSITES PRODUCED BY ADDITIVE MANUFACTURING <u>E. Tamburri</u> , L. Montaina, F. Pescosolido, R. Carcione, S. Battistoni	77
SOLID-STATE MODIFICATION FOR IMPROVED FLAME RETARDANCY <u>R. Mincheva</u> , C. Gerbehaye, Katrien V. Bernaerts, G. Fontaine, Serge Bourbigotc, J.M. Raquez	79

3D PRINTED HIGHLY POROUS HOLLOW DEVICES FOR LONG-TERM CONTROLLED RELEASE <u>M. Balsamo</u> , M.C. Mistretta, R. Scaffaro	81
NON-DESTRUCTIVE ANALYSIS OF DEHP SURFACE CONCENTRATIONS AND DIFFUSION-EVAPORATION IN HERITAGE PVC OBJECTS <u>T. Rijavec</u> , S. Bujok, S. Antropov, G. A. Newsome, J. Grau-Bové, I. Kralj Cigić, K. Kruczała, Ł. Bratasz, M. Strlič	83
TOWARDS THE UNDERSTANDING OF THE THERMAL DEGRADATION BEHAVIOR OF THE RIGID AND PLASTICIZED POLY(VINYL CHLORIDE) <u>K. Kruczała</u> , M. Saad, M. Bucki, S. Bujok, D. Pawcenis, T. Rijavec, K. Górecki, Ł. Bratasz, I. Kralj Cigic, M. Strlič	85
PLASTICIZATION OF DIALCOHOL CELLULOSE AND EFFECT ON THE THERMOMECHANICAL PROPERTIES E. Pellegrino, <u>G. Lo Re</u> , A. Fina	87
RING OPENING POLYMERIZATION OF ETHYLENE BRASSYLATE IN REACTIVE EXTRUSION AND ITS END OF LIFE OPTIONS <u>A. Avella</u> , R. Mincheva, D. Pappalardo, G. Lo Re	89
THERMAL AND FLAME RETARDANT PROPERTIES OF EPOXY VITRIMERS BASED ON DISULFIDE BONDS <u>V. Berner</u> , A. Huegun, L. Hammer, A. M. Cristadoro, C.C. Hoehne	91
ADDRESSING INHOMOGENEITY IN PLASTIC WASTE STREAMS: A COMPREHENSIVE EVALUATION OF SAMPLING AND SAMPLE PREPARATION STRATEGIES <u>C. Panagiotopoulos</u> , C. Podara, M. Karamitrou, T. Kosanovic-Milickovic, M. Silber, L. Meyer, B. von Vacano, A.N. Carvalho Neiva, J.H. Knoop, A. Martínez García, A. Ibáñez-García, E. Santamarina, C. Prieto, S. Pavlidou, L. Poudeh, C. Charitidis, S.N. Vouyiouka	93
 SEPTEMBER, 2ND - SESSION 3	
RECYCLING OF MULTI LAYER POLYMER FILMS BY MECHANOCHEMISTRY IN EXTRUSION_1 <u>A. Benzemma</u> , C. Chalamet	96
RECYCLING OF MULTI LAYER POLYMER FILMS BY MECHANOCHEMISTRY IN EXTRUSION_2 <u>A. Benzemma</u> , C. Chalamet	98

UV-C INDUCED PHOTODEGRADATION OF POLYPROPYLENE J.C.F. Gimenez, S.H.F. Bonatti, M.V. Basaglia, R.H.S. Garcia, A. dos Santos, L.H. Staffa, M. Samara, S.H.P. Bettini, E.R. de Azevedo, E. Helal, N.R. Demarquette, M.G.P. Homem, <u>S.A. Cruz</u>	100
THE USE OF CLICK CHEMISTRY FOR THE PRODUCTION OF CROSSLINKED BIOBASED POLYURETHANE CORE/SHEATH NANOFIBERS AND THEIR FUNCTIONALIZATION <u>S. Torresi</u> , I. Larraza, N. Gabilondo, A. Eceiza	102
THERMAL OXIDATIVE STABILITY AND CONSUMPTION OF ANTIOXIDANTS DURING CLOSED LOOP RECYCLING OF POLYPROPYLENE <u>R. Stam</u> , B. Leurs, P. Gijsman, K. Ragaert, R. Fiorio	104
CHARACTERISATION OF AGED ABS LAYERS FORMED DURING LONG-WAVELENGTH UV EXPOSURE <u>L. Delarue</u> , A. Dazzi, J. Mathurin, M.F. Pucci, P.-J. Liotier, P. Ienny, A.-S. Carobretelle, D. Perrin	106
CHROME TANNED LEATHER TRIMMINGS STABILIZED WITH GYPSUM THROUGH THERMAL INSULATION PANEL PRODUCTION <u>A.C. Paul</u> , M.T. Islam, P. Roy, N. Saha, T. Saha, P. Saha	108
SULFONATED POLYETHER ETHER KETONE-BASED PROTON EXCHANGE MEMBRANES FOR SEMI-ORGANIC REDOX FLOW BATTERIES <u>F. Niccolai</u> , L. Calzolari, Z. El Koura, I. Pucher, E. Martinelli	110
HOW POSS IN INTUMESCENT FLAME-RETARDANT SYSTEMS CAN CONTRIBUTE TO THE IMPROVEMENT OF THE FIRE BEHAVIOR OF VIRGIN AND RECYCLED HDPE? <u>M. Combeau</u> , M. Batistella, A. Breuillac, A. Impola, D. Perrin, J.M. Lopez-Cuesta	112
PERFORMANCE BIOPLASTIC SYNTHESIS UTILIZING PLATFORM MOLECULES DERIVED FROM RENEWABLE FEEDSTOCKS <u>A. Nag</u> , T. Kaneko	114
EFFECT OFFILLERS ON THE SPINODAL DECOMPOSITION AND ELECTRICAL CONDUCTIVITY OF POLYMER BLENDS AND DIBLOCK COPOLYMERS <u>A.I. Chervanyov</u>	116
RADICAL SCAVENGING AND PROCESSING STABILITY OF NOVEL BIOBASED STABILIZERS IN POLYPROPYLENE K. Markus, <u>E. Metzsch-Zilligen</u> , R. Pfaendner	118
ENHANCING THE HYDROLYTIC STABILITY OF POLY(LACTIC ACID) USING NOVEL STABILIZER COMBINATIONS J. Hallstein, <u>E. Metzsch-Zilligen</u> , R. Pfaendner	121

MICROSTRUCTURAL CHANGES OF XPS FOAMED PLASTIC ADDING GRAPHITE FILLERS <u>Y. Leem</u> , R.Kitagaki	123
--	-----

SEPTEMBER, 3RD - SESSION 1

RESTABILIZING PVB INTERLAYER AGAINST HEAT DEGRADATION FOR CLOSED-LOOP RECYCLING IN LAMINATED GLASS V. Nikitakos, A.D. Porfyris, K. Beltsios, R. Pfaendner, A. Perez, <u>C.D. Papaspyrides</u>	125
--	-----

MECHANICAL RECYCLING OF POLYPROPYLENE: EFFECT OF A REPAIR ADDITIVE ON FLOW CHARACTERISTICS AND PROCESSABILITY <u>R. Arrigo</u> , G. Bernagozzi, A. Frache	127
--	-----

RIGID POLYURETHANE FOAMS WITH LIMITED FLAMMABILITY AND BIOCIDAL PROPERTIES <u>P. Jankowski</u> , I. Grzywa-Niksińska	129
---	-----

SUSTAINABLE BIOCOMPOSITES BASED ON MATER-BI AND GRAPE POMACE FOR A CIRCULAR ECONOMY: PERFORMANCE EVALUATION AND DEGRADATION IN COMPOST V. Titone, M. Rapisarda, L. Pulvirenti, E. Napoli, G. Impallomeni, L. Botta, M.C. Mistretta, <u>P. Rizzarelli</u>	131
---	-----

DEGRADATION OF RIGID POLYURETHANE FOAM IN DISTRICT HEATING PIPES -ACCELERATED VS NATURAL AGEING I. Jakubowicz, <u>N. Yarahmadi</u>	133
---	-----

IN PROCESS CHARACTERIZATION OF POLYMER COMPOSITES USING SMALL SCALE EXTRUDERS P.F. Teixeira, L. Hilliou, <u>J.A. Covas</u>	135
---	-----

MACROMOLECULAR MOBILITY IN AGED AND VIRGIN EPOXIES <u>E. Richaud</u>	137
---	-----

BIOPOLYMERIC FLUORESCENT MATERIALS DEDICATED TO PACKAGING PERISHABLE PRODUCTS <u>D. Bajer</u>	139
--	-----

3D PRINTING OF ACRYLATE EPOXIDIZED SOYBEAN OIL (AESO)-BASED COMPOSITES CONTAINING LIGNIN <u>G. Colucci</u> , F. Sacchi, F. Bondioli, M. Messori	141
--	-----

LEWIS PAIR CATALYZED DEPOLYMERIZATION OF POST-CONSUMER PET WASTE <u>L. Killinger</u> , R. Hanich-Spahn, A.S.K. Hashmi	143
DEVELOPMENT OF LOW DIELECTRIC POLYSACCHARIDE ESTERS FOR ELECTRICAL INSULATING RESINS <u>Y. Fukata</u> , S. Kimura, T. Iwata	145
HOW TO ENHANCE IMPACT PROPERTIES OF POLYETHYLENE TEREPHTHALATE IN A MECHANICAL RECYCLING CONTEXT <u>G. Gonçalves Marques</u> , V. Bounor-Legaré, R. Fulchiron, R. Inoubli, P. Hajji, A. Couffin	148
EFFECT OF HIGH-SPEED AIRFLOW ON POLYMER THERMO-OXIDATION <u>A. Doriat</u> , M. Gigliotti, M. Beringhier, G. Lalizel, E. Dorignac, P. Berterretche, M. Minervino	150
ABOUT THE DEGRADATION MECHANISM OF EPOXY RESIN EXPOSED TO PARTIAL DISCHARGES <u>G. Buccella</u> , A.S. Basso Peressut, L. Brambilla, A. Villa, L. Barbieri, D. Palladini, G. D'Avanzo, S. Venturini	152
ENHANCING SELF-HEALING AND RECYCLING CAPABILITIES IN UNSATURATED POLYESTER RESIN: A WAY TO INTRODUCE TRANSESTERIFICATION CATALYSTS <u>G. Rizzo</u> , S. Dattilo, L. Saitta, C. Tosto, I. Blanco, G. Cicala	154
CONSUMPTION AND BIODEGRADATION OF POLYMERS BY INSECT LARVAE <u>E.A. Di Liberto</u> , G. Battaglia, R. Pellerito, G. Curcuruto, N. Tz. Dintcheva	156
SEPTEMBER, 3RD - SESSION 2	
TAILORING THE FUNCTIONALITY OF POLYMER BASED BIOMATERIALS FOR HEALTH <u>L. Ambrosio</u> , U. D'Amora, P. Manini, A. Pezzella, M.G. Raucchi, A. Ronca, S. Scialla, A. Soriente	158
A PRELIMINARY STUDY ON THE EXTRUSION FOAMING OF MIXED RECYCLED POLYOLEFIN WASTE WITH A CHEMICAL BLOWING AGENT <u>E. Garofalo</u> , L. Di Maio, C. Di Costanzo, L. Incarnato	160
THE USE OF PACKAGING INDUSTRY WASTE FOR THE MODIFICATION OF POLYPROPYLENE D. Dziadowiec, P. Szymczak, J. Andrzejewski, <u>M. Szostak</u>	162

FULLY BIOBASED FLAME RETARDANTS FOR POLYAMIDE 11 COMPATIBLE WITH THE MELT SPINNING PROCESS <u>J. Regnier</u> , S. Giraud, J.J. Flat, B. Mulot, S. Bourbigot, G. Fontaine, A. Cayla	164
AGING OF MEDIUM VOLTAGE JOINTS UNDER COMBINED AGEING CONDITIONS AT LOW TEMPERATURE <u>T. Vaytet</u> , O. Gain, F. Gouanvé, E. Espuche, C. Moreau, M. Broudin, H. Tanzeghti	166
SOFT ACTUATORS BASED ON THERMOPLASTIC POLYURETHANE COMPOSITES WITH YTTRIUM IRON GARNET <u>M. C. Paiva</u> , M.M. da Silva, J. A. Covas, M. P. Proença	168
PET NANOPLASTIC PRODUCTION AND THEIR EFFECT ON MODEL LIVING SYSTEMS <u>A. Maffezzoli</u> , G. Polo, M. G. Lionetto, C. Mele, C. Esposito Corcione, F. Lionetto	170
A CHARACTERIZATION METHOD FOR EVALUATING ADDITIVES SUITABLE FOR ODOR CONTROL IN PLASTICS <u>R. Grömmner</u> , E. Metzsch-Zilligen, M. Großhauser, R. Pfaendner, H. Haug, C.C. Höhne	172
THE LATEST RESEARCH FOR IMPROVING INTUMESCENT COATING FOR PROTECTION AGAINST FIRE <u>K. Pyrzynski</u>	174
RECYCLABLE AND REUSABLE BIO-EPOXY RESINS FOR COMPOSITES: THE APPROACH OF THE RE-COMP PROJECT <u>G.Cicala</u> , L.Saitta, A. Latteri, S.Dattilo, G.Rizzo, C.Tosto	176
CHARACTERIZATION OF WATER TRANSPORT PROPERTIES OF ACRYLIC URETHANE CLEAR COAT AND UV AGEING EFFECT <u>H. Lazeregue</u> , B. Fayolle, C. Sollogoub, S. Delalande, J.-C. Menetrier, R. Bougnot	178
3D COMPOSITE SCAFFOLD BASED ON PLLA AND NATURAL ANTIOXIDANT MOLECULES <u>V. Schiera</u> , F. La Monica, F. Carfi Pavia, P. Poma, G. Ghersi, V. La Carrubba, V. Brucato, N. Tz. Dintcheva	180
ENHANCING RHEOLOGICAL AND MECHANICAL PROPERTIES OF BIOSOURCED POLY(BUTYLENE SUCCINATE-CO-BUTYLENE ADIPATE) THROUGH GREEN REACTIVE EXTRUSION <u>M. Gammino</u> , C. Gioia, R. Scaffaro, G. Lo Re	182
DEVELOPMENT OF HIGH PERFORMANCE BIODEGRADABLE BACTERIAL POLYESTER MATERIALS BASED ON POLYMER ALLOY TECHNIQUES <u>H. Abe</u> , I. Farahin Jeepery, K. Sudesh	185

ON THE EFFECT OF THE THERMAL HISTORY ON PORE SIZE ARCHITECTURE IN POLYMERIC SCAFFOLDS PREPARED VIA TIPS <u>C. Carbone</u> , D. Davi, V. La Carrubba, V. Brucato, F. Carfi Pavia	187
DEVELOPMENT OF PHOSPHONATE-(CO-)POLYMER-FUNCTIONALIZED SILICA NANOPARTICLES AS ALTERNATIVE FLAME RETARDANTS FOR TRANSPARENT THERMOPLASTIC POLYMERS <u>F.A. Watt</u> , D. Frosien, W. Ali, R. Weberskirch, T. Mayer-Gall, S. Fuchs	189
 SEPTEMBER, 3RD - SESSION 3	
MECHANISTIC STUDIES ON PROCESSING AND FIRE BEHAVIOR OF A NEW CELLULOSE BASED FLAME RETARDANT IN POLYPROPYLENE A. Polster, M. Kaplan, M. Ciesielski, C. Getterle, S. Fuchs, <u>H.-O. Fabritius</u>	191
EXPLORING BIODEGRADATION PROCESS TO ADVANCE BIOPLASTIC SUSTAINABILITY A. Marín, P. Feijoo, A. Jáuregui, E. Ventura, E. Sánchez-Safont, J. Gámez-Pérez, <u>L.Cabedo</u>	193
CARBONATATION OF [ETHYLENE-GLYCIDYL METHACRYLATE]-BASED COPOLYMERS WITH CARBON DIOXIDE AS REAGENT BY REACTIVE EXTRUSION: IMPACT ON POLYMERS BLENDS COMPATIBILIZATION B. Guerdener, V. Ayzac, P. Besognet, S. Norsic, V. Monteil, V. Dufaud, J. Raynaud, Y. Chalamet, <u>V. Bounor-Legaré</u>	195
THERMAL DEGRADATION OF AN AROMATIC AMINE CURED EPOXIDIZED LINDSEED OIL VITRIMER <u>S. Serrano</u> , S. Berlioz, H. Hajjoul, E. Richaud, P. Carriere	197
LIFETIME PREDICTION OF POLY (BUTYLENE ADIPATE/ TEREPHTHALATE) UNDER VARIOUS CLIMATE CONDITIONS <u>Y. Ye</u> , G. Tang, X. Meng, R. Yang	199
WASP NEST INSPIRED BIOBASED FLAME RETARDANT <u>B. Schwind</u> , J. Stahlmecke, M.-J. Wesemann, T. Rust, S. Fuchs, H.-O. Fabritius	201
RADICAL RING OPENING COPOLYMERIZATION OF CYCLIC KETENE ACETALS: A NEW ROUTE FOR THE SYNTHESIS OF DEGRADABLE AND FUNCTIONAL POLYMERS FOR CANCER THERAPY <u>T. Pesenti</u> , C. Zhu, D. Domingo-Lopez, S. Ishii, M.I. Gibson, S. Messaoudi, J. Nicolas	203
POLY(ISOPROPYLACRYLAMIDE) HOMOPOLYMER, COPOLYMER AND AERO GEL THERMOSENSITIVE BEHAVIOR AND AGEING EFFECT <u>C. Mathieu</u> , S. Issa, E. Richaud	205

THE SIMULATION METHOD AND APPLICATION OF PHOTO-OXIDATIVE DEGRADATION/AGING OF POLYMERS <u>X. Meng</u> , Y. Ye, R. Yang	207
RECYCLASS, A VALUE CHAIN APPROACH TO BOOST A CIRCULAR USE OF PLASTICS <u>P. Glerean</u>	209
DURABILITY AND PERFORMANCE OF SUSTAINABLE COMPOSITE FILM BY ALIPHATIC AROMATIC POLYESTER AND CARBON BASED PARTICLES PRODUCED BY SLOW PYROLYSIS AND HYDROTHERMAL CARBONIZATION <u>N. Tz. Dintcheva</u> , G. Infurna, M. Volpe, A. Messineo	210
SURFACE MICRO-CRACKING ON NBR/PVC/CARBON BLACK BLENDS: INFLUENCE OF THE ENVIRONMENTAL STRESSES C. Thoral, G. Soulagnet, <u>P.-O. Bussiere</u> , S. Therias	212
GEPOLYMERS BEYOND CONSTRUCTION: ENHANCED ADSORPTION AND FLAME RETARDANCY IN NANOCOMPOSITE SYSTEMS <u>A. Lo Bianco</u> , M.M. Calvino, G. Cavallaro, P. Pasbakhsh, G. Lazzara, S. Milioto	214
UV-C/H ₂ O-DRIVEN ABIOTIC DEGRADATION OF PBAT/TPS-BASED COMMERCIAL FILMS <u>K. Gutiérrez-Silva</u> , O. Gil-Castell, J.D. Badia	216
RECYCLING OF PERSONAL PROTECTION EQUIPMENT: SANITISATION, DEGRADATION AND POLYMER BLEND FORMULATIONS <u>G. Infurna</u> , A. Romani, M.C. Riccelli, M. Levi, L. Incarnato, N. Tz. Dintcheva	218
CHARACTERIZATION AND FLAME RETARDANT PROPERTIES OF A SET OF STYRENIC COPOLYMERS CONTAINING (METH-)ACRYLATE PHOSPHATES AND ORGANIC SULFIDES <u>S. Fuchs</u> , M. Andruschko, P. Frank, U. Jonas	220
 SEPTEMBER, 4TH - SESSION 1	
BIOMEDICAL POTENTIAL OF ELECTROSPUN MATS BASED ON FURANOATE POLYESTERS S. Santi, <u>G. Fredi</u> , N. Lotti, M. Soccio, A. Dorigato	222
INVESTING THERMAL OXIDATIVE AGING MECHANISMS IN EPDM <u>C. Jost</u> , J. Sahyoun, M. Lacuve, X. Colin, E. Espuche	224

FABRICATION AND CHARACTERIZATION OF PIEZOELECTRIC POLYHYDROXYBUTYRATE/BARIUM TITANATE NANOCOMPOSITE MATERIALS AND SCAFFOLDS FOR BONE TISSUE APPLICATIONS <u>M. Milazzo</u> , M. Labardi, M. Seggiani, G. Gallone, S. Danti	226
CHITIN AND CHITOSAN MATERIALS FROM BLACK SOLDIER FLY (HERMETIA ILLUCENS): AN INSIGHT ONTO NEW PERSPECTIVES OF CIRCULARITY <u>M.B. Coltelli</u> , V. Gigante, L. Panariello, L. Aliotta, C. Scieuzo, P. Falabella, A. Lazzeri	228
KINETIC MODELS FOR A HYDROLYSIS REACTION WITH MARINE DEGRADABLE BIOPOLYMERS BASED ON THE WATER SORPTION BEHAVIOR <u>T. Koike</u> , Y. Muranaka, T. Maki	230
NANOCOMPOSITE GELLAN GUM BASED INJECTABLE AND PRINTABLE HYDROGEL WITH ANTIMICROBIAL PROPERTIES <u>C.Fiorica</u> , G. Barberi, G. Pitarresi, F.S. Palumbo, V. Catania, D. Schillaci, G. Giammona	232
HUMID/DRY CYCLES IN NATURAL FIBER REINFORCED COMPOSITES ARE A REAL AGING ISSUE? <u>A. Valenza</u> , V. Fiore, L. Calabrese, E. Proverbio	234
IONIC LIQUIDS AS MULTIFUCNTIONAL POLYMER ADDITIVES <u>J.F. Gérard</u> , J. Duchet-Rumeau, S. Livi	236
STUDY OF THE ABIOTIC DEGRADATION OF ELASTOMERS (VULCANISED OR NOT) FOR THEIR BIODEGRADATION M. Dieng, L. Calarnou, <u>S. Therias</u> , J.-L. Gardette, P.-O. Bussière, L. Malosse, S. Dronet, P. Besse-Hoggan, B. Eyheraguibel	239
 SEPTEMBER, 4TH - SESSION 2	
EFFECT OF THE INCORPORATION OF RECYCLED MATERIALS ON THE DURABILITY OF POLYETHYLENE FILMS <u>A. Duchamp</u> , J. Christmann, J.-L. Gardette, J. Charbonnier, B. Bouchut, S. Therias	241
ELUCIDATE INTRINSIC ORIGIN OF HETEROGENEOUS OXIDATIVE AGING USING COARSE-GRAINED MOLECULAR DYNAMICS SIMULATION <u>T. Ishida</u>	243
A STUDY ON BIOPLASTIC OBTAINED FROM RENEWABLE SOURCES: MATERIAL'S CHARACTERIZATION AND BIO-DEGRADATION IN SOIL <u>A. Visco</u> , C. Scolaro, S. Brahim, N. Bardella , V. Beghetto	245

SYNTHESIS OF BIOBASED COMPATIBILISER FOR MODIFICATION OF RECYCLED POLYPROPYLENE COMPOSITES WITH BUCKWHEAT STRAW S. Motrončiks, R. Bērziņš, <u>R. Merijs-Meri</u> , A. Ābele, J. Zicāns	247
CHAR FORMATION IN POLYETHYLENE: EFFECT OF THE MACROMOLECULAR ARCHITECTURE <u>A. Frache</u> , R. Arrigo, G. Malucelli, G. Camino	249
A NOVEL ROUTE FOR OBTAINING HIGH MELT STRENGTH RECYCLED HIGH-DENSITY POLYETHYLENE <u>G. Bernagozzi</u> , R. Arrigo, A. Frache	251
SEPTEMBER, 4TH - SESSION 3	
DESIGN OF TAILOR-MADE POLYHYDROXYALKANOATES: FROM BIOSYNTHESIS TO BIODEGRADATION G. Derippe, G. Brouchon, P. Lemechko, <u>S. Bruzaud</u>	253
PREPARATION AND FUNCTIONALITY OF MICROBIAL PRODUCED POLYESTER POROUS MATERIAL BY LIQUID PHASE DEPOSITION METHOD <u>T. Kabe</u> , R. Suzuki, T. Iwata	255
EFFECT OF GAMMA RADIATION ON THE THERMOMECHANICAL BEHAVIOUR OF POLYBUTYLENE FURANOATE <u>D. Puglia</u> , F. Dominici, A. Coatti, M. Giannetto, M. Soccio, N. Lotti, E. Macerata, M. Negrin, M. Mariani, A. Soldini, I. Solaberrieta, M.C. Garrigós, A. Jimenez	258
IRRIGATION DRIPLINES WITH REDUCED CARBON FOOTPRINT <u>E.G. Rodi</u> , A. Oliveri, S. Corviseri, C. Giuffré, M. Baiamonte, F.P. La Mantia	260
COMPARING ADDITIVE VS CONVENTIONAL MANUFACTURING VIA LCA <u>A. Latteri</u> , G. Cicala, C. Tosto	262
DURABILITY OF FLAX FIBER REINFORCED COMPOSITES UNDER ALTERNATE SALT FOG AND DRYING CYCLES <u>L. Calabrese</u> , V. Fiore, C. Sanfilippo, E. Proverbio, A. Valenza	264

Poster presentations

SEPTEMBER, 2ND

- PHOSPHORUS PENTOXIDE (P₂O₅) CATALYST FOR RING OPENING
POLYMERIZATION OF ε-CAPROLACTONE (ε-CL)
I. Adoumaz, M. Save, M. Lahcini 267
- PVA-PVP-LIGNIN-SODIUM OLEATE FILMS FOR CATIONIC DYE
DEGRADATION
Y. Aleeva, D.F. Chillura Martino 269
- THERMAL BEHAVIOR OF POLYSACCHARIDES MODIFIED CASEIN
M.R. Ricciardi, V. Antonucci, L. Affatato, A. Langella 271
- PROTECTIVE NANOSTRUCTURED FLAME RETARDANT COATINGS FOR
CABLE INDUSTRY APPLICATIONS
R. Arrigo, F. Cravero, E. Lorenzi, A. Frache 273
- ULTRAVIOLET IRRADIATION EFFECT AT DRY AND WATER IMMERSION
CONDITIONS ON PLA/PBAT COMMERCIAL FILMS
K. Gutiérrez-Silva, R. Muñoz-Espí, C.M. Gómez, M. Culebras, O. Gil-Castell, J.D.
Badia 275
- DEVELOPMENT OF BIOFORMULATIONS BASED ON NATURAL CARRIERS
AND ESSENTIAL OILS FOR AGRICULTURAL APPLICATIONS: PRELIMINARY
RESULTS
M. Baiamonte, H. Tsolakis, G. Lo Verde, E. Ragusa, R. Rizzo, E. Spinozzi, F.
Maggi, L. Botta 277
- NANO-STARCH FOR MULTIDIRECTIONAL APPLICATION IN MEDICINE,
FOOD, AND COSMETIC INDUSTRIES
D. Bajer 279
- CONCEPTUAL FRAMEWORK FOR THE HAZARD ASSESSMENT OF
RECYCLED PLASTICS
R. Becker, M. Lukas, C. Drago and U. Braun 281
- SUPER-POROUS AND SUPER-SWELLING CHITOSAN-BASED MATRICES FOR
WOUND AND BURN TREATMENT
F. Díaz-Carrasco, Á. Torrecillas-Cortés, E. Galbis, M.G. García-Martín, M.V. de-
Paz, E. Benito 283

CACTUS PEAR BY-PRODUCTS AS FILLERS FOR THE DEVELOPMENT OF BIOCOMPOSITES: REINFORCEMENT OR DEGRADATION EFFECT? M.C. Mistretta, G. Lamattina, F. Gargano, G. Liguori, P. Rizzarelli, P. Scarfato, <u>L. Botta</u>	285
EFFECT OF ALTERNATING HUMIDITY AND DRYNESS ON THE DURABILITY OF ADSORBENT SHEETS USED IN OPEN-CYCLE ADSORPTION PROCESSES <u>L. Calabrese</u> , E. Mastronardo, E. Piperopoulos, G. Scionti, S. De Antonellis, A. Freni, C. Milone	287
STUDY OF THE DEGRADATION OF WATER SOLUBLE THERMOSET POLYMERS BASED ON AZA-MICHAEL ADDITION - EFFECTS OF POLAR/NONPOLAR CHARACTERISTICS OF MONOMERS <u>F. Cavodeau</u> , J-F. Stumbe, M. Brogly	289
UV AGING RESISTANCE OF MODIFIED BITUMEN: COMPARISON OF SBS AND BIOCHAR <u>C. Celauro</u> , R. Teresia, N.Tz. Dintcheva	291
INFLUENCE OF A RUBBERY COMPATIBILIZER ON GNPS NANOCOMPOSITES: ANALYSIS ON ISOTROPIC AND ANISOTROPIC SAMPLE <u>M. Ceraulo</u> , V. Titone, M. Baiamonte, L. Botta, F. P. La Mantia	295
MULTIFUNCTIONAL 3D-PRINTED COMPOSITES BASED ON BIOPOLYMERIC MATRICES AND TOMATO PLANT (SOLANUM LYCOPERSICUM) WASTE FOR CONTEXTUAL FERTILIZER RELEASE AND CU(II) IONS REMOVAL <u>M.C. Citarrella</u> , E.F. Gulino, R. Scaffaro	297
BIO-BASED POLYMER RECYCLING FOR FOOD CONTACT: AN APPROACH OF FOOD SECURITY R. Paiva, M. Azna, M. Wrona, A.P. Lima Batista, C. Nerín, <u>S.A. Cruz</u>	299
ENHANCEMENT OF BIODEGRADABLE FOOD PACKAGING FILMS BY COEXTRUSION OF PBS, PBSA AND NANO-COMPOSITE PHB SYSTEMS F. Palmieri, J. Nii Ayi Tagoe, <u>L. Di Maio</u>	301
IMPROVING THE STABILITY OF GUAR GUM-BASED HYDROGELS <u>F. Díaz-Carrasco</u> , M.V. de-Paz, M.G. García-Martín, E. Benito	303
ASSESSING THE PERCOLATION THRESHOLD IN PLA/KENAF BIOCOMPOSITES FOR BIODEGRADATION PURPOSES <u>G. Filippone</u>	305
FLAME RETARDANT PP-BASED MATERIAL: THE EFFECT OF 3D PRINTING PROCESS <u>A. Frache</u> E. Lorenzi, R. Arrigo	307

BIODEGRADABLE POLYHYDROXYURETHANE (PHU) BIOMATERIALS DEVELOPED USING THE NIPU METHODOLOGY A.I. Carbajo-Gordillo, <u>E. Galbis</u> , E. Benito, F. Díaz-Carrasco, R. Grosso, N. Iglesias, M.G. García-Martín, R. Lucas, M.V. de-Paz	309
REACTIVE EXTRUSION FOR COMPATIBILIZING BIODEGRADABLE PHBV/PBSA BLENDS E. Sánchez-Safont, I. Pisa Ripoll, K. Samaniego-Aguilar, L. Cabedo, <u>J. Gámez-Pérez</u>	311
L-TARTARAMIDE AND GUAR GUM-BASED MATRICES FOR GASTRO-RETENTIVE DRUG DELIVERY SYSTEMS F. Díaz-Carrasco, E. García-Pulido, M. Katavić, <u>M.G. García-Martín</u> , M.V. de-Paz, E. Benito	313
SIMULATING THE MECHANICAL RECYCLING OF PET- AND HDPE-BASED PACKAGING: THE INTERACTION BETWEEN PRESENCE OF CONTAMINANTS, DEGRADATION AND REPROCESSING <u>C. Gnoffo</u> , R. Arrigo, A. Frache	315
THE EFFECT OF PLASTICISER TYPE ON THE THERMAL DEGRADATION OF POLY(VINYL CHLORIDE): MULTIMODAL SPECTROSCOPIC ANALYSIS <u>K. Górecki</u> , S. Bujok, Ł. Bratasz and K. Kruczała	317
HYDRO/CHEMO-THERMAL PERFORMANCE OF COMMERCIAL PBAT/TPS-BASED FILMS <u>K. Gutiérrez-Silva</u> , A. Jordán-Silvestre, M. Izquierdo, V. Martínez-Soria, O. Gil-Castell, J.D. Badia	319
COMPOSITES FROM WASTE POLYPROPYLENE AND RECOVERED CARBON FIBRE E. Zolfaghari, <u>G. Infurna</u> , S. Alessi, C. Dispenza, N.Tz. Dintcheva	321
A NEW CASE IN ABS POLYMER FOR NANOSTRUCTURED LEAD BATTERIES: STABILITY STUDY IN 5M SULFURIC ACID M. Insinga, L. Oliveri, N. Moukri, B. Patella, <u>R. Inguanta</u>	323
MODIFICATION OF POLYMER MATRICES COMPOSED OF SODIUM ALGINATE AND STARCH BY INCORPORATION OF MICROSPHERES <u>J. Kozłowska</u>	325
EFFECT OF ACCELERATED THERMAL DEGRADATION OF POLY(VINYL CHLORIDE): THE CASE OF UNPLASTICIZED PVC M. Saad, M. Bucki, S. Bujok, D. Pawcenis, T. Rijavec, K. Górecki, Ł. Bratasz, I. Kralj Cigic, M. Strlič, <u>K. Kruczała</u>	327

INJECTION MOLDING OF POLYMER-ALUMINIUM NANOCOMPOSITES TO TUNE OPTICAL PROPERTIES <u>F. Moretti</u> , M. Fischer, S. Fornasaro, A. Leuteritz, I. Kühnert, V. Lughi, P Posocco	329
MICROPLASTICS AND NANOPLASTICS: MAIN SOURCES AND ISSUES <u>M. Morreale</u> , F.P. La Mantia	331
3D PRINTED AND COMPRESSION MOLDED BIO-COMPOSITES BASED ON OFI WASTE AND BIODEGRADABLE POLYMERS FOR NPK FERTILIZER CONTROLLED RELEASE <u>R. Scaffaro</u> , M.C. Citarrella, E.F. Gulino	332
HYALURONIC ACID/TANNIC ACID FOR APPLICATIONS AS WOUND DRESSINGS <u>L. Zasada</u> , M. Wekwejt, M. Małek, A. Ronowska, A. Michno, A. Pałubicka, A. Klimek, B. Kaczmarek-Szczepańska	334
POLYMER PYROLYSIS PATHWAYS AFFECTING THE CHARACTERISTICS OF POLYMER COMBUSTION <u>E. Nakashima</u> , T. Fuji, T. Ueno	336
SEPTEMBER, 3RD	
ULTRAVIOLET IRRADIATION EFFECT AT DRY AND WATER IMMERSION CONDITIONS ON PLA/PBAT COMMERCIAL FILMS K. Gutiérrez-Silva, R. Muñoz-Espí, C.M. Gómez, M. Culebras, O. Gil-Castell, <u>J.D. Badia</u>	338
POLYSACCHARIDE-BASED BIODEGRADABLE POLYMERS FOR MEDICAL APPLICATIONS <u>V. Ciaramitaro</u> , F. Vitale, E. Piacenza, A. Presentato, D.F. Chillura Martino	340
IMPACT OF PRINTING PROFILES ON THERMAL CONDUCTIVITY AND TENSILE STRENGTH IN METAL FUSED FILAMENT FABRICATION C. Tosto, L. Saitta, R. Barbagallo, I. Blanco, <u>G. Cicala</u>	342
FROM WASTE TO SUSTAINABLE RESOURCE: 3D-PRINTED BIOCOMPOSITE FISH CRATES BASED ON BIODEGRADABLE POLYMERS AND ANCHOVY FISHBONE SCRAPS <u>M.C. Citarrella</u> , E.F. Gulino, R. Scaffaro	345
ENHANCING THE THERMAL STABILITY OF GELATIN-BASED HYDROGELS AT PHYSIOLOGICAL TEMPERATURES F. Díaz-Carrasco, E. Vidal-Nogales, Á. Santos-Medina, M.J. Díaz, <u>M.V. de-Paz</u> , M.G. García-Martín, E. Benito	347

ENHANCED MECHANICAL AND RHEOLOGICAL PROPERTIES OF CHITOSAN-BASED HYDROGELS WITH HYDROXYAPATITE FOR BONE TISSUE ENGINEERING <u>C. Di Marco</u> , M. Trapani, M. Testa , B. Di Stefano, V. La Carrubba, F. Lopresti	349
MARINE BIODEGRADATION OF BIODEGRADABLE VS. CONVENTIONAL PLASTICS A. Marín, P. Feijoo , A. Jáuregui, E. Sánchez-Safont, J. Tena-Medialde, J.R. García-March, L. Cabedo, <u>J. Gámez-Pérez</u>	351
ONE-STEP FABRICATION AND THERMAL STABILIZATION OF PVA NANOFIBER MEMBRANES VIA HEAT-ASSISTED SOLUTION BLOW SPINNING <u>E.F. Gulino</u> , R. Scaffaro	353
FLAME RETARDANT PROPERTIES OF S-TRIAZINE PHOSPHONATES IN PU RIGID FOAMS <u>C.C. Höhne</u> , J. Limburger, A. König, T. Wagener, E. Kroke	355
COARSE-GRAINED MOLECULAR DYNAMICS SIMULATIONS OF OXIDATIVE AGING IN AMORPHOUS REGIONS OF SEMI-CRYSTALLINE POLYMERS - DECAY OF STRESS TRANSMITTER CONTENT- <u>T. Ishida</u>	357
CHITOSAN AND NANOCCLAY MODIFIED POLYBUTADIENE SUCCINATE COMPOSITES RHEOLOGICAL AND MECHANICAL PROPERTIES FOR ANTIMICROBIAL PACKAGING <u>T. Ivanova</u> , R. Berzina, A. Lebedeva, I. Bochkovs, J. Biteniekis, R. Merijs-Meri, J. Zicans	359
PIPEOPSY: A NOVEL METHOD FOR STATUS ASSESSMENT OF DISTRICT HEATING PIPES IN OPERATION <u>I. Jakubowicz</u> , N. Yarahmadi	361
ZINC OXIDE NANOPARTICLES AND SAGE ESSENTIAL OIL AS ACTIVE COMPONENTS OF ALGINATE FILMS FOR FOOD PACKAGING <u>J. Kowalonek</u> , N. Stachowiak-Trojanowska, Z. Ciecierska, A. Richert	363
HDPE AND PP BASED SYSTEMS WITH PVP-I ADDITIVE: MECHANICAL AND BARRIER PROPERTIES <u>M. Leanza</u> , D.C. Carbone, M. Baiamonte, M. Rapisarda, E.T.A. Spina, F.P. La Mantia, P. Rizzarelli	365
MECHANICAL CHARACTERIZATION AND THERMAL DEGRADATION OF SUSTAINABLE ADHESIVES BASED ON BIO-EPOXY RESINS ADDITIVATED WITH THERMOPLASTIC POLYMERS FOR SEPARABLE JOINTS <u>M. Luciano</u> , R. Miranda, C. Sanfilippo, F. Mazzara, V. Fiore, A. Valenza	367

ONE-STEP FABRICATION AND MODIFICATION OF BIOPOLYMER FIBERS COATED WITH ACTIVE NANOPARTICLES FOR SUSTAINABLE TECHNOLOGIES <u>A. Maio</u> , M. Gammino, R. Scaffaro	369
BIODEGRADABLE POLYMER MATERIALS OF BACTERIAL ORIGIN <u>A. Masek</u> , S. Bielecki, K. Rulka, V. Brunnela, M. Arese	371
EFFECTS OF SALT SPRAY AGEING ON BIO-BASED EPOXY RESINS <u>V. Fiore</u> , B. Megna, F. Sarasini, D. Rossano, R. Miranda	373
PHOTO-OXIDATIVE DEGRADATION OF BIOCOMPOSITES BASED ON MATER-BI AND GRAPE POMACE: PROPERTIES AND SOIL BURIAL PERFORMANCE M. Rapisarda, V. Titone, L. Pulvirenti, E. Napoli, G. Impallomeni, L. Botta, P. Rizzarelli, <u>M.C. Mistretta</u>	375
RHEOLOGICAL AND SPINNING BEHAVIOUR OF A STARCH-BASED POLYMER <u>M. Morreale</u> , M. Baiamonte, F.P. La Mantia	377
EXPLORING THE IMPACT OF SILOXANE NETWORKS ON THE THERMAL BEHAVIOR OF P/N-ENRICHED FLAME RETARDANT FINISHES FOR COTTON FABRIC <u>R. Otto</u> , W. Ali, J. S. Gutmann, T. Mayer-Gall	378
BIODEGRADABILITY OF POLY URATHANE SHOE SOLE' ENSUING BY THE SOIL BURIAL DEGRADATION N. Saha, <u>A.C. Paul</u> , T. Saha, N. Saha, P. Saha	380
RECYCLING OF HDPE FROM BUSHES USED IN RAILWAYS CROSSBEAMS FASTENING AND ITS REINFORCEMENTS WITH THE SCRAPED FRACTION OF CARBON FIBERS WASTES UPCYCLING <u>R. Petrucci</u> , L. Torre, M. Rallini	382
ROLE OF NANOLIGNIN AND METAL OXIDE NANOPARTICLES ON PLLA UV PHOTODEGRADATION <u>D. Puglia</u> , E. Lizundia, I. Armentano, F. Luzi, A. Di Michele, R. Sardella, A. Carotti, A. Macchiarulo, L. Torre	384
UNDERSTANDING AND COUNTERATING THERMO-OXIDATIVE DEGRADATION DURING MECHANICAL RECYCLING OF PA 6,6 <u>A. Rech</u> , K. Almdal, A.E. Daugaard	386
INCORPORATING RECYCLED MASKS INTO BITUMEN: A SUSTAINABLE SOLUTION <u>M.C. Riccelli</u> , P. Scarfato, A. Romano, M. Levi, G. Infurna, N.Tz. Dintcheva, L. Incarnato	388

CHARACTERIZATION, PHOTO-OXIDATION AND DEGRADATION IN COMPOST OF WOOD FLOUR AND HAZELNUT SHELLS POLYLACTIDE-BASED BIOCOMPOSITES M. Baiamonte, M. Rapisarda, M.C. Mistretta, G. Impallomeni, F.P. La Mantia, <u>P. Rizzarelli</u>	390
CHEMICAL AND PHOTOCHEMICAL DEGRADATION OF PLA BASED GREEN COMPOSITES A. Maio, E.F. Gulino, M. Gammino, M.C. Citarrella, <u>R. Scaffaro</u>	392
DEVELOPMENT, PERFORMANCE, AND DEGRADATION BEHAVIOR OF BIOCOMPOSITES BASED ON PBS AND GLOCHIDS FROM OPUNTIA FICUS-INDICA F. Marchetta, L. D'Arienzo, L. Di Maio, L. Botta, M.C. Mistretta, P. Rizzarelli, M. Lanza, <u>P. Scarfato</u>	394
POLYLACTIC ACID ELECTROSPUN MEMBRANE AS A PROOF OF CONCEPT FOR INTESTINAL BARRIER RECONSTRUCTION <u>M. Testa</u> , C. Di Marco, G. Serio, C. Gentile, V. La Carrubba, F. Lopresti	396
PHYSICAL AND ANTIBACTERIAL PROPERTIES OF BIODEGRADABLE PLA/PBAT BLENDS CONTAINING CARVACROL <u>V. Titone</u> , L. Botta, M.C. Mistretta, S. Russello, G. Garofalo, R. Gaglio	398
FLAME RETARDANTS ON TEXTILES: A NOVEL STEADY-STATE EXPERIMENTAL APPROACH FOR MECHANISTIC INVESTIGATIONS <u>N. Tomasik</u> , R. Otto, T. Mayer-Gall, B. Atakan	400
PHOTO-DEGRADATION EFFECTS OF BIO-POLYBUTYLENE-SUCCINATE EXPOSED TO UVC RAYS C. Scolaro, <u>A. Visco</u> , S. Brahim	402
FILMS BASED ON HYALURONIC ACID/ELLAGIC ACID BIOLOGICAL STUDIES <u>L. Zasada</u> , B. Kaczmarek-Szczepańska, K. Kleszczyński, D. Chmielniak, M.B. Hollerung, K. Steinbrink, S. Grabska-Zielińska	404
ENHANCING STABILITY: THE PROTECTIVE ROLE OF NANODIAMONDS AGAINST DEGRADATION AND BIODEGRADATION IN CELLULOSE ETHER DISPERSIONS E. Palmieri, A. Alabiso, L. Migliore, <u>E. Tamburri</u> , S. Orlanducci	406
IMPACT OF CALCIUM HYDROXIDE TREATMENT ON SISAL FIBER PROPERTIES AND THEIR GEOPOLYMER COMPOSITES <u>C. Sanfilippo</u> , V. Fiore, L. Calabrese, B. Megna, A. Valenza	408

Plenary lectures
and
Oral communications

MOVING FORWARD: TRACK RECORD AND OUTSTANDING CHALLENGES IN THE FIELD OF POLYMER DEGRADATION

M. Celina

Visiting Scientist to Los Alamos National Laboratory, Editor-in-chief PDST
Albuquerque, NM, USA
MCelinaEditorPDST@netscape.com

INTRODUCTION

Polymer degradation is as old as the beginning of polymer science. According to Nat. Geographic in 2010 “Ancient mesoamerican cultures blended plant juices to make rubber bouncier or more durable, a new study says”. This means additives and stability determined polymer applications right at the beginning. Since then our field has come a long way. A good understanding of how to design polymers, advanced characterization methods and endless application opportunities. This means our efforts regarding polymer design, optimization and understanding of degradation behavior will continue to be very important, particularly if we wish to engage in sustainable economic activities, master our needs for energy changes, implement improved waste management, and continue our modern life style (food choices, health, transportation, electronics, communication etc.). Let’s focus on some trends.

DISCUSSION

This presentation gives us a chance to consider our significant collective achievements in polymer degradation obtained over decades. Polymer degradation depends on the combination of materials chemistry, physics and engineering. Reaction mechanisms and their kinetics, organic chemistry for polymer reactions, material property correlations, the differences in behavior between rubbery, amorphous and crystalline materials, material physics and diffusion, scission and crosslinking chemistry, UV versus thermal degradation, additive choices and modeling. What are some of our key achievements in these areas and where do we struggle?

We shall consider a number of outstanding challenges. Some areas are important but have traditionally been avoided at the interface of degradation science versus materials engineering and testing. To move forward we have to reflect occasionally and focus on the framework. Many questions come up that ought to be addressed as best as possible moving forward. We will consider examples of what has worked well and where current limits are found. Some questions remaining to be important come to mind:

- Accelerated ageing under combined environments; what is challenging?
- Accelerated ageing offering better predictions for applications, is this possible?
- Are there accelerated aging approaches that we have overlooked or avoided?
- How do we tackle the issue of accelerated ageing with the need for extrapolations?
- Are modern diagnostic tools and near automated rapid data acquisition a solution for everything or a curse? When do we need to be cautious?
- What are the current limits for standardized testing or aging of polymer?
- How are testing standards derived and where is our input? Do they matter?
- How do we balance degradation science with industry preferences for material testing?
- Where has degradation science really made a difference?
- What about modeling? Can we balance experiments, truth and perhaps speculation?
- How do we handle the increasing volume of publications by all means?
- Is a career involving polymer degradation still attractive? What might be the trend?

TOUGHENING BRITTLE BACTERIAL POLYHYDROXYBUTYRATE BY CONTROLLING ITS STEREO-MICROSTRUCTURE THROUGH SEVERAL APPROACHES

Alejandro J. Müller¹⁻²

¹POLYMAT and Department of Polymers and Advanced Materials: Physics, Chemistry and Technology, Faculty of Chemistry, University of the Basque Country UPV/EHU, Paseo Manuel de Lardizabal 3, 20018 Donostia-San Sebastián, Spain

²IKERBASQUE, Basque Foundation for Science, Plaza Euskadi 5, 48009 Bilbao, Spain
Email: alejandrojesus.muller@ehu.es

Poly(3-hydroxybutyrate) (P3HB) is a biologically produced, biodegradable natural polyester with excellent thermal and barrier properties but suffers from several weaknesses limiting its applications. It degrades when the temperature surpasses its melting point, making its processing challenging. On the other hand, it possesses a very low intrinsic nucleation density and a high tendency to crystallize due to its stereo-perfect (*sp*-P3HBb) nature with an absolute (*R*)-stereoconfiguration¹⁻². This leads to very large spherulites (see Figure 1a) concentrating stresses at their inter-spherulitic boundaries. At the same time, the crystallinity tends to increase with aging time at room temperature due to its sub-ambient T_g value and crystallization ability.

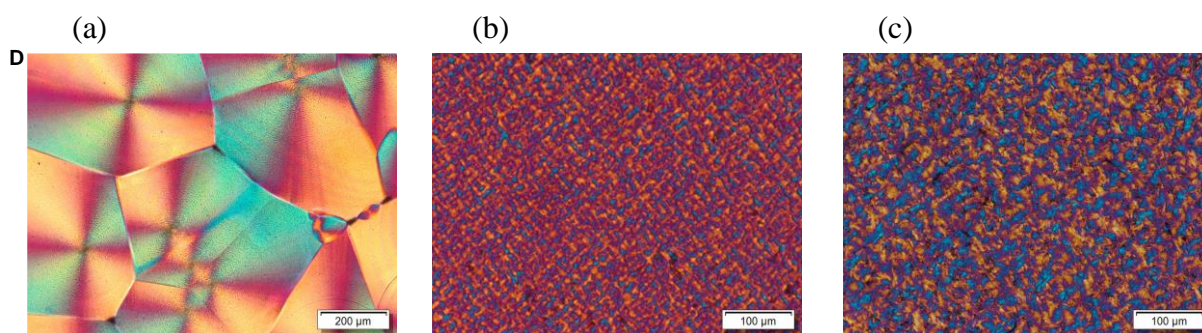


Figure 1. Polarized Light Optical Micrographs for: (a) Bio-PHB (*sp*-P3HBb), (b) Iso-rich PHB (*ir*-P3HB_{788k}), and (c) a 50/50 blend of *sp*-P3HBb and *ir*-P3HB_{788k} (modified from ref. 3)

Hence, bio-PHB is inherently brittle. Recently, we reported³ a mono-material product design strategy to toughen stereo-perfect, brittle bio, or synthetic P3HB by blending it with stereomicrostructurally engineered P3HB. The chemical synthesis of these specially designed P3HB with varying tacticities was developed by the group Prof. Eugene Chen (Department of Chemistry, Colorado State University, USA)¹⁻⁴. Through tacticity ([mm] from 0 to 100%) and molecular weight (Mn to 788 kDa) tuning, high-performance synthetic P3HB materials with tensile strength up to ~30 MPa, fracture strain to ~800%, and toughness to 135 MJ m⁻³ (>120 tougher than bio-P3HB) have been produced. As an example, the effect of stereomicrostructure on the spherulitic texture is shown in Figure 1b, where one material with an iso-rich composition, *ir*-P3HB_{788k}, displays a submicron spherulite texture, indicative of a much higher nucleation density. This high nucleation density is due to the stereo defects present in *ir*-P3HB_{788k}.

Stereodefects disrupt the crystallizable sequences (thus reducing T_m and crystallinity) but also provide many more nucleation sites. This is the perfect molecular key to enhanced ductility and improved transparency (large spherulites scatter light; if their size is similar or below the wavelength of visible light, 0.4 microns, the material becomes transparent as no light can be scattered by these smaller superstructures)¹⁻⁴. Figure 1c demonstrates how a miscible

50/50 blend of *sp*-P3HBb and *ir*-P3HB_{788k} can keep the submicron spherulitic texture, producing a highly transparent material (which also has high ductility³).

The physical blending of the brittle biological P3HB with such specially engineered stereodefected P3HB in 10 to 90 wt.%, which leads to miscible blends, dramatically increases its ductility from ~5% to 95 – 450% while still maintaining a desirably high elastic modulus (>1 GPa), tensile strength (>35 MPa), and melting temperature (160 – 170 °C). This mono-material P3HB-toughening-P3HB methodology departs from the traditional heterogeneous approach of incorporating different polymers to toughen P3HB, hindering chemical or mechanical recycling, highlighting the potential of the mono-material product design solely based on biodegradable P3HB to deliver P3HB materials with diverse performance properties³.

References

[1] Caputo, M. R.; Tang, X.; Westlie, A. H.; Sardon, H.; Chen, E. Y.-X.; Müller, A. J. *Biomacromolecules*, **2022**, *23*, 3847-3859 (September). “Effect of Chain Stereoconfiguration on Poly(3-hydroxybutyrate) Crystallization Kinetics”. DOI: 10.1021/acs.biomac.2c00682.

[2] Quinn, E. C.; Westlie, A. H.; Sangroniz, A.; Caputo, M. R.; Xu, S.; Zhang, Z.; Urgun-Demirtas, M.; Müller, A. J.; Chen, E. Y.-X. *Journal of the American Chemical Society*, **2023**, *145*, 5795-5802 (March). “Installing Controlled Stereo-Defects Yields Semicrystalline and Biodegradable Poly(3-Hydroxybutyrate) with High Toughness and Optical Clarity”. DOI: 10.1021/jacs.2c12897.

[3] Zhang, Z.; Quinn, E. C.; Olmedo-Martínez, J. L.; Caputo, M. R.; Franklin, K. A.; Müller, A. J.; Chen, E. Y.-X. *Angewandte Chemie International Edition*, **2023**, *62*, e202311264, 1-6 (December). “Toughening Brittle Bio-P3HB with Synthetic P3HB of Engineered Stereomicrostructures”. DOI: 10.1002/anie.202311264.

[4] Caputo, M. R.; Shi, C.; Tang, X.; Sardon, H.; Chen, E. Y.-X.; Müller, A. J. *Biomacromolecules*, **2023**, *24*, 5328-5341 (November). “Tailoring the Nucleation and Crystallization Rate of Polyhydroxybutyrate by Copolymerization”. DOI: 10.1021/acs.biomac.3c00808.

THERMAL DECOMPOSITION FEATURES FLAME RETARDANCY

B. Schartel

Bundesanstalt für Materialforschung und -prüfung (BAM), Berlin Germany
bernhard.schartel@bam.de

INTRODUCTION

Most polymeric materials in most fire scenarios burn based on an anaerobe pyrolysis feeding the flame with fuel. Understanding the thermal decomposition in the condensed phase is key to tailor flame retardancy. Adjusting the decomposition temperature of flame retardant and polymer as well as providing the desired chemical structure for specific reactions determine the molecular mechanisms and thus the flame-retardant modes of action. Hereby, it is not only charring in the condensed phase and radical scavenging in the gas phase, but also physicochemical and physical effects such as melt flow and protective layer formation. This paper delivers thought-provoking impulses on how the understanding of the pyrolysis can be used for evidenced-based development and optimization of flame-retardant polymeric materials. Some rather overseen details are picked up as well as rethinking of concepts memorized long ago is encouraged to discover something new. The talk tries to fill some gaps between flame-retardant mechanisms, flame-retardant modes of action, and fire performance.

EXPERIMENTAL

Materials

This paper deduces its conclusions from results of several research projects performed in the working group of the author. For a detailed description of the materials, their compounding, and the preparation of test specimens please go for the comprehensive description in the original papers.[1-10]

Methods

A multi-methodical approach based on thermogravimetry (TGA), TGA coupled with evolved gas analysis (TGA-FTIR), hot stage FTIR, pyrolysis GC/MS, and residue analysis was used for investigating the pyrolysis. The flammability in the fire scenario ignition was addressed using oxygen index (OI) and testing in the UL 94 burning chamber. The fire behaviour in developing fires was investigated using a cone calorimeter. Additional efforts complete the studies, such as other fire tests, advanced analysis of the fire residue, melt rheology, or particle finite element simulations (PFEM). Tailored and self-designed experiments and advanced data evaluation described fire phenomena or modes of action. For a detailed description of the experimental the reader is relegated to the original papers.[1-10]

RESULTS AND DISCUSSION

One important aspect in achieving, adjusting, and optimising flame retardancy is exploiting specific chemical reactions in the condensed phase between the pyrolyzing polymer and the flame retardant at the right place, time, and temperature.[1-3] At the same time, these reactions of partly decomposed or hydrolysed flame retardants in the condensed phase competes with releasing as volatile into the gas phase. Based on three comparisons this field is illuminated in detail: reactive phosphine oxide, phosphinate, phosphonate, and phosphate are compared in the same epoxy resins evaluating the influence of the oxidation state,[1] different phosphorous flame retardants in different epoxy resins underlining the specific reactions between the partly decomposed or hydrolysed flame retardant and the partly decomposed polymer,[3] and the comparison of three aryl phosphates with different volatility highlights the competition of chemical reaction in the condensed phase and gasification.[2]

Any fire residue reduces fire risks, when the release of hydrocarbon fuel into the gas phase is replaced by storing fuel in the condensed phase as carbonaceous char. Thus, charring describing crosslinking, dehydration, aromatization, and graphitization is the flame retardancy mechanisms, whereas charring describing the reduction in fire load the flame-retardant mode of action. The phenomenon charring belongs to a complete pyrolysis or complete pyrolysis step; the char yield indicates the amount of fuel stored in the residue. Further, any fire residue works as protective layer. The barrier properties depend on the physical properties of the residue but not necessarily on its amount.[4] Usually, a residue design such as a tailored morphology of the fire residue is demanded. The mass loss rate and heat release rate are reduced. The main mechanisms are heat shielding and thermal insulation.[5] Sometimes the protective layer is good enough to cause incomplete pyrolysis due to extinguishing before the pyrolysis front went through the whole sample.[6,7] Analogous to charring also incomplete pyrolysis can result in efficient reduction in fire load. Proper data evaluation and key experiments are used to sort out and understand these different phenomena. Flame retardant polyurethane foams passing the heat release and smoke toxicity requirements of EN 45545 are discussed as evidence-based development using charring and incomplete pyrolysis due to an efficient protective layer.[7,8]

The thermal decomposition into liquid intermediate products increases crucially the melt flow during burning,[9] whereas charring and the ablation of the polymer matrix increasing the content of fillers yield melt viscosities enlarged by orders of magnitude.[10] Violent burning of some polymers at the end of a cone calorimeter test can be understood as pyrolysis enabling a pool fire. The understanding of the thermal decomposition of the polymeric material harbours the explanation of non-flaming dripping extinguishing the flame via sufficient cooling, retreat effects preventing ignition, and efficient nondripping flame retardancy.

This paper leads the audience from chemistry over complex macroscopic fire phenomena of physicochemical nature to fire performance. Thought-provoking impulses are given how the scientific understanding of the pyrolysis in the condensed phase can be used for research and evidenced-based development of future flame-retardant polymeric materials.

Acknowledgement

The talk uses results from distinct projects; thus, thanks go to the German Research Foundation DFG SCHA 730/6-1, SCHA 730/8, SCHA 730/10-1, and Scha 730/19-1, Bayer MaterialScience AG, and the BMWi (BMWK) AiF: IGF No.: 19078 N/2 for financial support. Many thanks to former working group members U. Braun, Y. Y. Chan, B. Perret, S. Rabe, K. H. Richter, A. Weiß, and G. Wu, and to our co-operation partners A. Hartwig (IFAM), M. Döring and M. Ciesielski (at that time KIT), and J. M. Marti (CIMNE) as well.

References

- 1) U. Braun, A. I. Balabanovich, B. ScharTEL, et al. *Polymer* **47**, 8495, 2006.
- 2) B. Perret, K. H. Pawlowski, B. ScharTEL. *J Therm Anal Calorim* **97**, 949, 2009.
- 3) B. ScharTEL, B. Perret, B. Dittrich, et al. *Macromol Mater Engin* **301**, 9, 2016.
- 4) B. ScharTEL, A. Weiß, H. Sturm, et al. *Polym Adv Technol* **22**, 1581, 2011.
- 5) G. M. Wu, B. ScharTEL, H. Bahr, et al. *Combust Flame* **159**, 3616, 2012.
- 6) S. Rabe, Y. Chuenban, B. ScharTEL. *Materials* **10**, 455, 2017.
- 7) Y. Y. Chan, B. ScharTEL. *Polymers* **14**, 2562, 2022.
- 8) Y. Y. Chan, B. ScharTEL. *KGK* **75**, 39–46, 2022
- 9) J. Marti, B. ScharTEL, E. Oñate. *J Fire Sci* **40**, 3, 2022.
- 10) A. Turski Silva Diniz, B. ScharTEL. *e-Polymers* **24**, 20230194, 2024.

MULTIFUNCTIONAL SANDWICH COMPOSITES WITH THERMAL ENERGY STORAGE CAPABILITY

G. Fredi, E.Boso, A.Sorze and A. Pegoretti

Department of Industrial Engineering and INSTM Research Unit, University of Trento, Via Sommarive 9, Trento, Italy

INTRODUCTION

Sandwich composite structures, composed of two thin yet stiff face sheets separated by a lightweight core material, have garnered significant attention due to their outstanding specific stiffness and strength, particularly under flexural load. Beyond their mechanical performance, improving the thermal management capabilities of these structures has become increasingly important, driven by the rising demand for energy-efficient systems and effective temperature regulation in various applications. This can be achieved by reducing the thermal diffusivity of the foam core and by incorporating phase change materials (PCMs). Integrating PCMs into structural composites offers an attractive approach to creating multifunctional materials that can simultaneously meet load-bearing and thermal energy storage needs. To harness the known benefits of PCM-enhanced polyurethane (PU) foams and address the mechanical property limitations that hinder their widespread use in structural applications, this study introduces, for the first time, a novel sandwich composite system. This system combines the advantages of PU/PCM foams as the core material with high-performance epoxy/carbon fiber laminates as the structural skins.

EXPERIMENTAL

Materials. For the preparation of the sandwich cores, polyol HDR R 150 (viscosity at 23 °C = 1050 mPa·s; density at 23 °C = 1.1 g/cm³) and isocyanate ISN 1 (viscosity at 23 °C = 200 mPa·s; density at 23 °C = 1.23 g/cm³) were both provided by Kairos Srl (Verona, Italy). PU foams for the sandwich cores were produced by mixing polyol and isocyanate in a ratio of 100:130. MPCM 32D® microencapsulated phase change material was supplied by Microtek Laboratories Inc. (OH, USA) in the form of a dry powder with a mean particle size of 15-30 μm, a density of 0.9 g/cm³, a nominal melting point of 32 ± 2 °C, and a latent heat of fusion of 160 J/g. For the preparation of the epoxy/carbon sandwich skins, the epoxy base Elan-tech® EC 152 and the hardener Elan-tech® W 152 MR were kindly provided by Elantas Europe Srl (Parma, Italy) and mixed at a ratio 100:30. Balanced plain weave carbon fabric Angeloni GG 200 P (mass per unit area = 192 g/cm³) was supplied by G. Angeloni Srl (Venezia, Italy).

Preparation. First, the required amounts of polyol and isocyanate were weighed and poured into separate beakers. For the PCM-containing compositions, the necessary PCM mass was weighed and split equally into the two beakers. Primary mixing by hand was then performed in each beaker using a spatula. Then, the content of the two beakers was combined, mechanically mixed for approx. 25-30 s, and then poured into a mold with an inner cavity of 250 × 250 × 20 mm³, preheated at 40 °C. The mold was rapidly covered and cured in an oven at 40 °C for 20 min. After the characterization of the foams, the sample PU-PCM20 presented an optimal balance between thermal and mechanical properties. Hence, composite sandwich panels were prepared with either neat PU or PU-PCM20 core materials. Three carbon fiber (CF) laminae were impregnated with the epoxy/hardener mixture and placed on the top of a flat steel plate. Then, the foam panel was placed onto them, and finally, three more CF laminae were added on top, each one of them impregnated with the epoxy/hardener mixture. The vacuum bag was then sealed, and the composite was left curing under vacuum for 24 h at room temperature. Each sandwich panel was then demolded and post-cured at 60 °C for 15 h. Two specimens were

produced with the neat PU foam as a core and two additional specimens with the PU-PCM20 foam.

Thermal characterization. Differential scanning calorimetry (DSC) was performed via a Mettler DSC 30 (Mettler Toledo Inc., Columbus, Ohio, USA). Specimens of approx. 10 mg were subjected to a heating/cooling/heating cycle between $-50\text{ }^{\circ}\text{C}$ to $100\text{ }^{\circ}\text{C}$ at $\pm 10\text{ }^{\circ}\text{C}/\text{min}$, under a constant nitrogen flow of $100\text{ ml}/\text{min}$.

Mechanical characterization. Mechanical testing was performed with an Instron 5969 universal testing machine (Instron, Norwood, MA, USA), equipped with a 1 kN load cell and a thermal chamber allowing measurements at different temperatures.

RESULTS AND DISCUSSION

The combination of the increased thermal buffering effect provided by the PCM, as investigated in DSC, and the increase in thermal conductivity, as measured via HFM, was studied on a larger scale via infrared thermography (1a-d). The results of this test demonstrate that an increase in the PCM content prolongs the time required to reach the equilibrium temperature, both during heating and during cooling, due to the heat stored or released by the PCM during its phase transition. For instance, during heating to $50\text{ }^{\circ}\text{C}$, a nominal addition of 20 wt% PCM extends the time needed from 8 min of neat PU to 14 min of PU-PCM20.

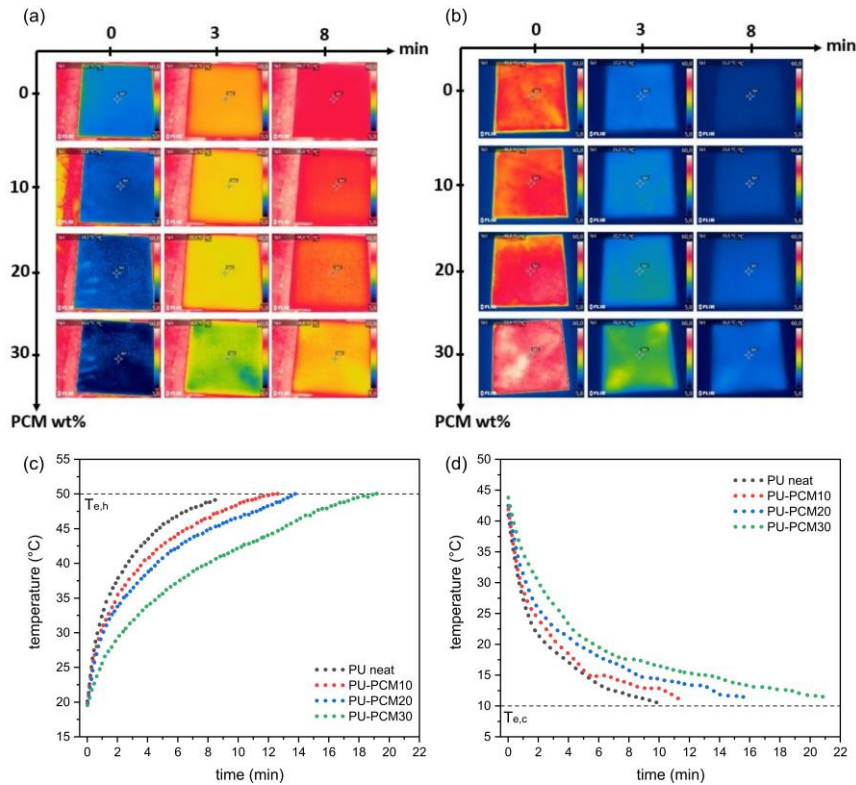


Fig. 1 Results of infrared thermography on foam samples. (a-b) Camera frames recorded at test start, after 3 min, and after 8 min as a function of the PCM nominal concentration in the heating (a) and cooling (b) experiments. (c-d) Temperature profiles of the foam surfaces (average temperature) as a function of time in the heating (c) and (d) cooling experiments. $T_{e,h}$ and $T_{e,c}$ indicate the environment temperature in the heating and cooling experiments, respectively.

Acknowledgment

This research activity has been supported by the Air Force Office of Scientific Research (AFOSR) within the project “Multifunctional polymer composites for thermal energy storage: current trends and future perspectives”, Grant Number: FA8655-23-1-7039.

DEVELOPMENT OF HIGH-PERFORMANCE BIODEGRADABLE BIOMASS PLASTICS AND DEEP-SEA BIODEGRADATION

T. Iwata

Department of Biomaterial Sciences, Graduate School of Agricultural and Life Sciences, The University of Tokyo, 1-1-1 Yayoi, Bunkyo-ku, Tokyo 113-8657, Japan
atiwata@g.ecc.u-tokyo.ac.jp

INTRODUCTION

To establish a sustainable material production system and preserve the beautiful global environment forever, it is desirable to develop “biomass plastics” that are made from renewable biomass instead of petroleum, and “biodegradable plastics” that are completely degraded into carbon dioxide and water by enzymes secreted by microorganisms in the environment [1]. This paper presents processing and marine-biodegradation of microbial polyester strong or elastic fibers [2,3], self-degradable aliphatic polyesters in sea-water environment by embedding lipases via melt extrusion [4,5]. More recently, we succeeded to confirm microbial decomposition of representative biodegradable plastics (polyhydroxyalkanoates, biodegradable polyesters, and polysaccharide esters) at diverse deep-sea floor locations ranging in depth from 757 to 5552 m [6].

RESULTS AND DISCUSSION

Processing and Marine-biodegradation of Microbial Polyesters [2,3]

Marine degradable fibers with both strength and elasticity were successfully fabricated by a new melt-spinning method from P(3HB-co-16mol%-4HB) that is one of microbial polyesters. Polymers was melted at the temperature lower than melting temperature to leave thick lamellar crystals and obtained fibers were stretched at room temperature. The obtained fibers have tensile strength of over 200 MPa and elongation at break of ca. 200% that are comparable to those of non-biodegradable elastic fibers processed from Polyethylene and Polypropylene. The elasticity is generated by changing the molecular structures of tie molecules between lamellar crystals and the free molecular chains in amorphous regions around stacked lamellae from helix structure to planar zigzag one. It was confirmed that these fibers were completely degraded by both seawater from Tokyo-Bay and freshwater from Sanshiro-Pond less than one month. It was revealed that P(3HB-co-16 mol%-4HB) becomes high-performance biodegradable fibers with excellent mechanical properties and marine biodegradability.

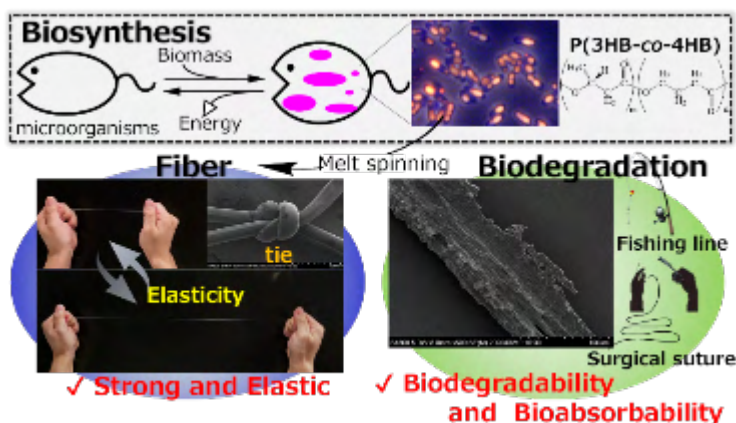


Fig.1 PHA fibers and

Self-degradable aliphatic polyesters by embedding enzymess via melt extrusion [4,5]

Non-biodegradable microplastics have become a global problem. we propose a new enzyme-embedded biodegradable plastic that can be self-biodegraded anytime and anywhere. PLLA extruded films embedding immobilized proteinase K encapsulated in polyacrylamide were produced at 200 °C and embedded-enzyme degradation was monitored. Immobilized proteinase K embedded in the extruded film maintained its degradation activity and degraded the PLLA film from inside to make small holes and cavities, suggesting that immobilization is

a powerful technique to prepare thermoforms with embedded enzymes. The rate of embedded-enzyme degradation was accelerated by dividing the film into smaller pieces, which can be regarded as a model experiment for biodegradation of microplastics.

Several lipases were embedded into the aliphatic biodegradable polyesters poly(butylene succinate), poly(butylene succinate-co-adipate) and polycaprolactone, all of which normally exhibit limited environmental degradation. Observed composite films were all enzymatic self-degraded in buffered solutions. Even low concentrations of these lipases embedded in the polyester films resulted in significant degradation after a short time period, suggesting that the lipases retained their activities after melt extrusion. These studies demonstrate the viability of using embedded enzymes to obtain self-degradable polymers as an approach that can provide the existing polymers a degradation initiation function to solving environmental issues related to plastic waste.

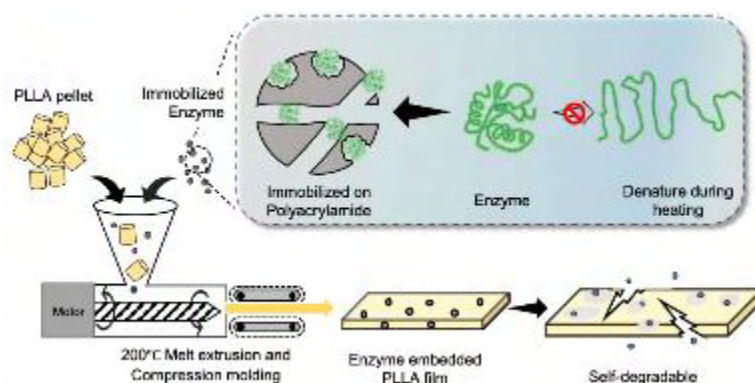


Fig.2 Enzyme embedded biodegradable plastics

Microbial decomposition of biodegradable plastics on the deep-sea floor [6]

We succeeded to confirm microbial decomposition of representative biodegradable plastics (polyhydroxyalkanoates, biodegradable polyesters, and polysaccharide esters) at diverse deep-sea floor locations ranging in depth from 757 to 5552 m. The rate of degradation slowed with water depth. We analyzed the plastic-associated microbial communities by 16S rRNA gene amplicon sequencing and metagenomics. Several dominant microorganisms carried genes potentially encoding plastic-degrading enzymes such as polyhydroxyalkanoate depolymerases and cutinases/polyesterases. Our results confirm that biodegradable plastics can be degraded by the action of microorganisms on the deep-sea floor, although with much less efficiency than in coastal settings.

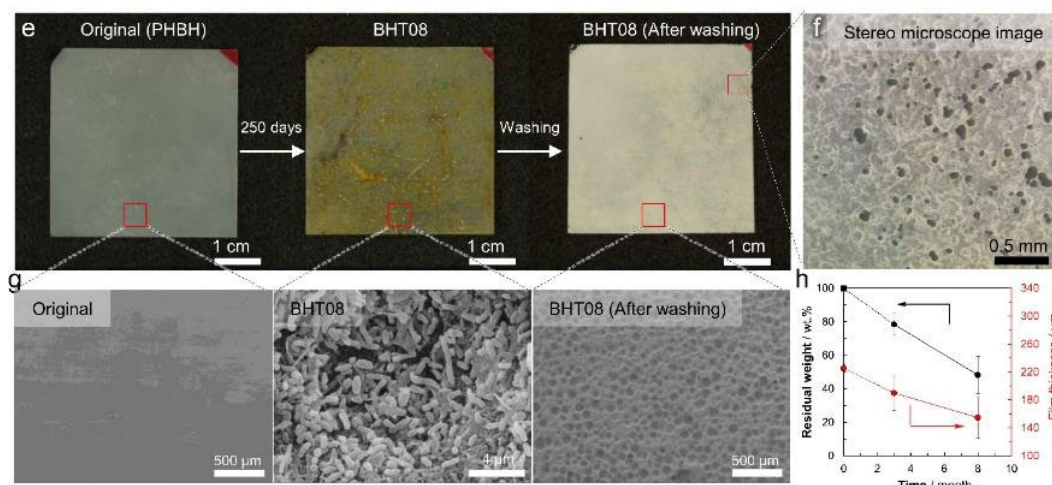


Fig.3 PHBH film degradation at deep-sea floor (BHT, 855m)

References

- [1] T. Iwata, *Angew. Chem. Int. Ed.* **54**, 3210 (2015). [2] T. Omura, *et al.*, *ACS Appl. Polym. Mater.* **3**, 6479 (2021). [3] T. Iwata, *et al.*, *Polym. J.* **53**, 221 (2021). [4] Q.Y. Huang, *et al.*, *Biomacromolecules* **21**, 3301 (2020). [5] Q.Y. Huang, *et al.*, *Polym. Degrad. Stab.* 109647 (2021). [6] T. Omura *et al.*, *Nat. Commun.*, **15**, 568 (2024).

FROM LIQUID CRYSTALLINE TO BIOBASED EPOXY RESINS: INSIGHT INTO MORE SUSTAINABLE THERMOSETS

Cosimo CARFAGNA^{2,4}, Veronica AMBROGI^{1,2}, Pierfrancesco CERRUTI², Gennaro GENTILE², Martina SALZANO DE LUNA¹, Angela MAROTTA¹, Lucia GIOIELLA¹, Alice MIJA³

¹ Department of Chemical, Materials and Production Engineering (DICMaPI), University of Naples Federico II, Naples, Italy

² Institute for Polymers, Composites and Biomaterials (IPCB), CNR, Pozzuoli (NA), Italy

³ Laboratoire de Physique de la Matière Condensée (LPMC) CNRS – UMR 7336, Université Nice Sophia Antipolis, Nice, France

⁴ Centro Regionale di Competenze CRdC scarl Nuove Tecnologie, via Nuova Agnano, Napoli, Italy.

Epoxy resins are covalently cross-linked networks with high dimensional stability, excellent mechanical resistance and chemical stability over a broad range of temperatures. Due to their properties epoxies find application as structural composites, adhesives and coatings.

The successful applications of high performance liquid crystalline (LC) polymers, such as Kevlar, stimulated the interest in designing crosslinked LC polymers. The prediction by de Gennes to develop liquid crystalline networks through the crosslinking reaction of reactive LC monomers resulted in the development of a class of materials known as liquid crystalline thermosets (LCTs). These polymers combine the useful properties of liquid crystals (self-assembly, reversible phase transition, macroscopic orientation) and thermosets (good thermal, mechanical, and barrier properties). A variety of LCTs were developed in the 1990s with monomers such as acrylate, methacrylate, epoxy, isocyanate, and maleimide. Liquid crystalline epoxy networks (LCENs) have been among the most investigated LCTs because of their unique range of properties and potential applications^[1,2,3].

Since epoxies in general have a pivotal role in many industrial fields, the improvement of their sustainability is becoming a crucial challenge, since traditional production protocols are in conflict with the recent principles of green chemistry, being the used monomers oil-based and frequently toxic. This is the case, for example, of the DGEBA, whose use is now limited due to its demonstrated disruptive endocrine activity and adverse impact on human health^[4]. Moreover, due to their crosslinked structure, epoxy resins pose serious problems at the end of their service life, being typically incinerated or landfilled, causing severe environmental problems.

To address these issues and to apply the principles of circular economy to this class of thermosets, several strategies have been adopted. On one hand, the design of new formulations of resins including Covalent Adaptable Networks (CANs) has made possible the reprocessing of these materials, prolonging their service life. On the other hand, the identification of new platform molecules of biological origin for the production of epoxy resins from renewable, non toxic resources has been proposed^[5]. Indeed, molecules derived from vegetable oils, lignin and cellulose have been used to produce new epoxy resins with a variety of features, achievable for different applications. Among the most promising alternatives to BPA, precursors derived from cellulose and sugars have received a huge interest, as they are prone to a variety of modification processes that allow the production of compounds of different chemical structure from linear, cyclic to aromatic^[6]. Herein, the eco-design, production and potential applications of furan-based epoxy resins is discussed. Furan molecule represents a suitable alternative building block, not only for its aromatic nature, but also for its environmental safety, and its easy availability. Furan derivatives can be easily obtained from vegetal biomass and efficiently modified to get many monomers and curing agents for the production of epoxy thermosets. In this communication, a comprehensive overview on the

recent synthetic approaches based on the use of furan biorenewable precursors for epoxy resins is provided ^[6]. Among the different alternatives, 2,5-dihydroxy methyl furandiol (BHMF) has been selected as starting compound for the synthesis of the corresponding diepoxy monomer the 2,5-bis[(2-oxiranylmethoxy)methyl] furan (BOMF). The synthesis of BOMF/anhydride resins is discussed, considering the influence of the nature of anhydride and catalyst, and the anhydride-to-epoxy content ratio on the curing behaviour, as well as on the physico-chemical and mechanical properties of the final products. The use of furan-based epoxy resins as coatings for metal substrates for food can packaging is also presented, demonstrating the potential of this class of bio-based resins for industrial applications ^[7].

References

- [1] Carfagna C, Amendola E, Giamberini M. Liquid crystalline epoxy based thermosetting polymers. *Prog Polym Sci.* 1997;22(8):1607–1647.
- [2] Carfagna C, Amendola E, Giamberini M. Liquid crystalline epoxy resins containing binaphthyl group as rigid block with enhanced thermal stability. *Macromol Chem Phys.* 1994;195(7):2307–2315.
- [3] Carfagna C, Amendola E, Giamberini M, et al. Liquid-crystalline epoxy resins: a glycidyl-terminated benzaldehyde azine cured in the nematic phase. *Macromol Chem Phys.* 1994;195(1):279–287.
- [4] Gonçalves, F. A., Santos, M., Cernadas, T., Ferreira, P., & Alves, P. (2022). Advances in the development of biobased epoxy resins: insight into more sustainable materials and future applications. *International Materials Reviews*, 67(2), 119-149.
- [5] Alabiso, W., and Schlögl, S. (2020). The impact of vitrimers on the industry of the future: Chemistry, properties and sustainable forward-looking applications. *Polymers*, 12(8), 1660.
- [6] Marotta, A., Faggio, N., Ambrogi, V., Cerruti, P., Gentile, G., & Mija, A. (2019). Curing behavior and properties of sustainable furan-based epoxy/anhydride resins. *Biomacromolecules*, 20(10), 3831-3841.
- [7] Marotta, A., Faggio, N., Ambrogi, V., Mija, A., Gentile, G., & Cerruti, P. (2021). Biobased furan-based epoxy/TiO₂ nanocomposites for the preparation of coatings with improved chemical resistance. *Chemical Engineering Journal*, 406, 127107.

NATURAL AGEING OF CLOSED-CELL POLYESTER URETHANE FOAM

Elena Gómez-Sánchez,¹ Simon Kunz,¹ Janine Köppen,² Susanne Brunner, Erik Rettler¹ and Eleonora Bresolin

¹Material Sciences Department, Deutsches Bergbau-Museum Bochum, Leibniz Research Museum for Geo-resources. Correspondence: elena.gomezsanchez@bergbaumuseum.de

² Objects Conservator M.A., Seattle, WA

³Technical University of Munich, TUM School of Engineering and Design

INTRODUCTION

PU-ES elastomer foams are prone to hydrolysis [1], [2] which mainly affects the ester groups of the soft segments [3]. The process is autocatalytic [2] and leads to chain scission and the release of the dicarboxylic acid used for the synthesis, e.g. adipic acid. The degradation of PU-ES has been studied with a range of spectroscopic, chromatographic and mechanical testing techniques, thanks to which insight has been gained on a wide range of issues, such as stabilising structural features [2], and the effects of chain scission in phase separation [5]. Often, studies base their results in artificially aged (AA), their focus lying in the changes in mechanical properties upon ageing of newly synthesised materials to compare its performance with other materials [6] and/or to predict its lifetime. This approach is convenient, as it would be unviable to wait for natural aging to introduce a given formulation in the market.

However, it is generally accepted that artificial ageing protocols are only an approximation of what happens in the normal course of time [7], [8], [9]; here, diffusion limited oxidation and hydrolysis need to be particularly considered [10]. Availability of NA polymeric materials of known composition would allow drawing comparisons between the degradation processes, both chemical and physical, developing under artificial and natural ageing regimes. Parallel to this research, the heritage science literature offers a complementary viewpoint by studying NA material aged indoor well after its intended lifespan. Here, research on PU-ES has mostly focused on consolidation methods to increase the mechanical stability of singular pieces of contemporary works of art like sculptures and design objects [11], [12], [13] by testing the methods first in AA mockups. Pellizzi [14] described a positive correlation between NA and AA open-cell materials based on FTIR (I_{3323}/I_{1727} , C=O/OH ratio) and their state of degradation as visually evaluated.

The present work presents a systematic approach for the study of the ageing of closed-cell polyester urethane foams in museum conditions. It describes a) the systematical characterization of the ageing phenomena observed upon natural ageing with microscopic and spectroscopic techniques, and b) the attempts at reproducing the observed phenomena under artificial ageing conditions and a comparison of NA and AA material as based on visual, chemical and, as far as possible, mechanical characterization techniques. The objects of study, 19 pairs of shoe soles from the 1980s/90s of a collection of miners' gear of the Deutsches Bergbau-Museum Bochum (German Mining Museum), make up a sample of relatively diverse material from a well-defined time, space and use. Newly synthesized material, similar to the naturally aged (NA) material, was aged according to typical industrial standards.

EXPERIMENTAL

Material for artificial ageing was kindly provided by BASF Lemförde according to a historical recipe for PU shoe soles chosen based on py-GCMS data of the miners' shoe soles. *Shore hardness* A and 00 were measured following international standards (ISO 7619-1:2012, ASTM D 2240-00, with testers by Sauter GmbH and Bareiss. *Compression set* was carried out according to DIN ISO 815-1:2016. *Tensile strength* tests were carried out according to DIN 53504:2017 with a tensile strength tester Zugprüfmaschine T1000 with a mechanical extensometer and a 10 kN load cell (MSC Sensortechnik GmbH) (25 mm starting length; preload 0.1 N, testing speed 200 mm/min). *Fourier Transform Infrared* spectrometer from Thermo Fischer Scientific, Nicolet iS50, gold optic, diamond ATR sampling unit, KBr beam splitter and DTGS detector, region 7,000 – 400 cm⁻¹, resolution of 4 cm⁻¹. *Evolved gas*

analysis – mass spectrometry and double shot – gas chromatography mass spectrometry were performed in a multi-shot pyrolyzer EGA/PY-3030D (Frontier Lab), coupled with a Thermo Fisher TRACE 1310 GC with an SSL injection port, and a single quadrupole mass spectrometer unit (Thermo Fisher, ISQ 7000). Artificial ageing was performed in a climatic chamber KS 600/45 (RS-Simulatoren Prüf- und Messtechnik GmbH) under constant, controlled temperature of 70°C and relative humidity of 98 %RH (ISO 188, DIN EN ISO 2440) for up to 56 days.

RESULTS AND DISCUSSION

The systematic study of the shoe sole collection allowed identifying four distinct ageing phenomena (Fig. 1), which could all be confirmed as related to the hydrolysis of the polyester polyol by FTIR and Raman. While pox, blooming and flaking all contain free adipic acid, the dried fluid involves organometallic complexes between iron ions and oligomers of the polyester polyol [15].

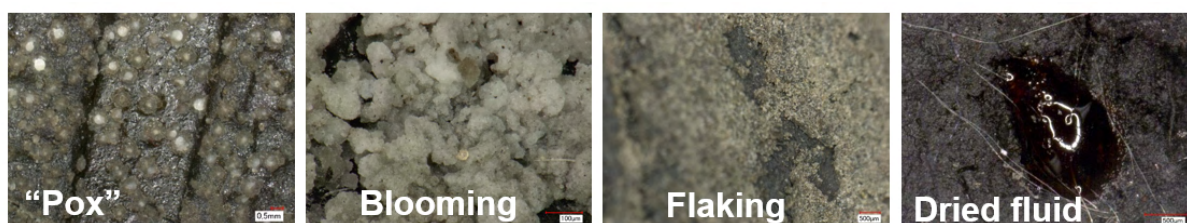


Figure 1. Ageing phenomena documented in most of the naturally aged shoe soles.

The present study also offers a comparison between NA and AA material. In FTIR (Fig. 3), the ratio I_{1727}/I_{1708} decreases with time, and is consistently lower in the surface than in the bulk, where less water is available for hydrolysis.

While the artificial ageing protocol used in the industry for this material reproduced well the loss of mechanical properties observed in the NA museum objects (Fig. 2), validating the use of this protocol for the intended purpose in the industry, and also the reached I_{1727}/I_{1708} value is similar for NA and AA material, the ageing phenomena observed in NA material were not replicated at the end of the artificial ageing period. Interestingly, these appeared in the AA material several months after the end of the artificial ageing. This indicates that the AA material, directly after artificial ageing, fundamentally differs from the NA samples from historical objects. The systematical study of representative NA material from museums offers very interesting possibilities in the study of polymer.

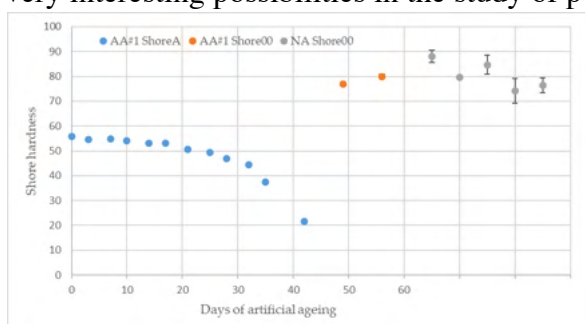


Figure 2. Shore hardness A (blue) and Shore 00 (orange and grey) for AA and NA samples.

NA samples not assigned to a value on the X-axis since exact day of production unknown (age: ca 30 years).

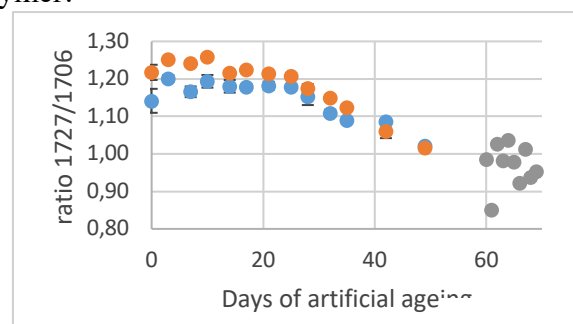


Figure 3. I_{1727}/I_{1708} of skin (blue) and bulk (orange) for AA and NA (grey) aged samples.

References

- [1] M. Szycher, *Szycher's Handbook of Polyurethanes*, 2nd ed. Boca Raton: CRC Press, 2013.
- [2] F. Xie, T. Zhang, P. Bryant, V. Kurusingal, J. M. Colwell, and B. Laycock, "Degradation and stabilization of polyurethane elastomers," *Progress in Polymer Science*, vol. 90, pp. 211–268, Mar. 2019, doi: 10.1016/j.progpolymsci.2018.12.003.
- [3] A. Bardin, P.-Y. Le Gac, S. Cérantola, G. Simon, H. Bindi, and B. Fayolle, "Hydrolytic kinetic model predicting embrittlement in thermoplastic elastomers," *Polymer*

- Degradation and Stability*, vol. 171, p. 109002, Jan. 2020, doi: 10.1016/j.polymdegradstab.2019.109002.
- [4] M. Hakkarainen, G. Adamus, A. Höglund, M. Kowalczyk, and A.-C. Albertsson, “ESI-MS Reveals the Influence of Hydrophilicity and Architecture on the Water-Soluble Degradation Product Patterns of Biodegradable Homo- and Copolyesters of 1,5-dioxepan-2-one and ϵ -Caprolactone,” *Macromolecules*, vol. 41, no. 10, pp. 3547–3554, May 2008, doi: 10.1021/ma800365m.
 - [5] D. G. Thompson, J. C. Osborn, E. M. Kober, and J. R. Schoonover, “Effects of hydrolysis-induced molecular weight changes on the phase separation of a polyester polyurethane,” *Polymer Degradation and Stability*, vol. 91, no. 12, pp. 3360–3370, Dezember 2006, doi: 10.1016/j.polymdegradstab.2006.05.019.
 - [6] G. Oertel, G. W. Becker, and D. Braun, *Polyurethane*, 3., neu Bearb. Aufl., Neuausg. in Kunststoff-Handbuch, no. 7. München: Hanser, 1993.
 - [7] M. Frigione and A. Rodríguez-Prieto, “Can Accelerated Aging Procedures Predict the Long Term Behavior of Polymers Exposed to Different Environments?,” *Polymers*, vol. 13, no. 16, p. 2688, Aug. 2021, doi: 10.3390/polym13162688.
 - [8] A. S. Maxwell, W. R. Broughton, G. Dean, and G. D. Sims, “Review of accelerated ageing methods and lifetime prediction for polymeric materials,” Teddington, Middlesex (UK), NPL National Physical Laboratory NPL Report DEPC MPR 016, Mar. 2005.
 - [9] M. Koehl *et al.*, “Round robin testing of various polymeric back-sheets for PV-modules with different ultra-violet radiation sources and sample temperatures,” in *Natural and Artificial Ageing of Polymers*, T. Reichert, Ed., Naples (Italy): Gesellschaft für Umweltsimulation e.V. GUS, 2015, pp. 289–293.
 - [10] E. Linde, N. H. Giron, and M. C. Celina, “Diffusion-limited hydrolysis in polymeric materials,” *Polymer Degradation and Stability*, vol. 204, p. 110095, Oct. 2022, doi: 10.1016/j.polymdegradstab.2022.110095.
 - [11] J. Langenbacher and B. Sommermeyer, “Material reversion: Investigation into degradation mechanisms of polyurethane elastomers,” in *Future talks 013: lectures and workshops on technology and conservation of modern materials in design*, T. Bechthold, Future talks, and Die Neue Sammlung, Eds., München: Die Neue Sammlung, 2013, pp. 228–236.
 - [12] S. De Groot, A. Laganà, T. van Oosten, H. van Keulen, and M. Palmeira, “The Wear and Tear of Polyurethane Elastomers. Investigation into properties, degradation and treatments,” in *Future talks 011: technology and conservation of modern materials in design ; October 26/28 2011, Die Neue Sammlung, The International Design Museum Munich*, T. Bechthold, Future talks, and Die Neue Sammlung, Eds., München: Die neue Sammlung, 2013, pp. 85–96.
 - [13] J. Köppen, S. Brunner, and E. Gómez-Sánchez, “Shoemaker’s nightmare - Deterioration of shoe soles and tests for the conservation of degraded closed-cell polyester urethane museum objects,” in *Future talks 019: Surfaces. Lectures and workshops on technology and conservation of the modern ; November 11/13 2019, Die Neue Sammlung, The Design Museum*, T. Bechthold and Die Neue Sammlung, Eds., München: Die Neue Sammlung, 2021, pp. 94–102.
 - [14] E. Pellizzi, A. Lattuari-Derieux, B. Lavédrine, and H. Cheradame, “Degradation of polyurethane ester foam artifacts: Chemical properties, mechanical properties and comparison between accelerated and natural degradation,” *Polymer Degradation and Stability*, vol. 107, pp. 255–261, Sep. 2014, doi: 10.1016/j.polymdegradstab.2013.12.018.
 - [15] H. Lotz and E. Gómez-Sánchez, “Organometallic complexation phenomenon observed during the natural aging of polyester urethane in the presence of iron corrosion,” *npj Materials Degradation*, vol. 74, p. 9, 2022, doi: <https://doi.org/10.1038/s41529-022-00286-6>.

ONE-POT SYNTHESIS OF POLY(D,L-LACTIDE)-CARBON NANODOTS NANOCOMPOSITES BY MELT-EXTRUSION TRANSESTERIFICATION: A VERSATILE WAY TO PRODUCE PHOTOSTABLE FLUORESCENT BIOMATERIALS

N. Mauro*¹, M.A. Utzeri¹, F. Messina², A. Sciortino², G. Cavallaro¹, G. Giammona¹

¹Department of Biological, Chemical and Pharmaceutical Sciences and Technologies (STEBICEF), University of Palermo, via Archirafi 32, 90123 Palermo, Italy

²Department of Physics and Chemistry (DiFC) “E. Segrè”, University of Palermo, via Archirafi 36, 90123 Palermo, Italy

*Department STEBICEF, University of Palermo, via Archirafi 32, 90123 Palermo, Italy.
nicolo.mauro@unipa.it

INTRODUCTION

The design of nanocomposite biomaterials is a promising approach for creating innovative biodegradable materials with superior properties. Incorporating nanofillers like carbon nanodots (CDs) into poly(D,L-lactide) (PLA) enhances structural and functional characteristics, addressing limitations in tissue engineering. These nanocomposites enable self-tracking using fluorescence imaging and allow tunable biodegradability and mechanical properties, useful for 3D-printed or porous implantable medical devices. They facilitate real-time, non-invasive monitoring of localization and degradation through fluorescence imaging. (1).

Building on this concept, we have recently developed an efficient protocol to produce decagram-scale quantities of CDs with a narrow size distribution (5.3 ± 0.4 nm), paving the way to real-world applications (2). These CDs are zero-dimensional carbon nanoparticles of graphitic structure, which contain structural defects (e.g., N-, S-doping), that can be obtained with high yields and exhibit single nanostructure multicolor emission, ranging from blue to near-infrared (NIR), along with different surface polar groups such as carboxyl and hydroxyl functions, amenable to further surface functionalization. In detail, hydroxyl groups can provoke heterophase transesterification of PLA chains by melt-extrusion (ME) (Figure 1), yielding single CDs-PLA conjugates dispersed in the PLA matrix and leading to thermoplastic nanocomposites endowed with bright multicolor photoluminescence and peculiar mechanical and physicochemical properties.

EXPERIMENTAL

Materials

Urea (99.5%), citric acid (99%), anhydrous N,N-dimethylformamide (DMF), indocyanine green (IGC) (99.5%), PLA (M_n 14 kDa, PD 1.8), Sephadex G15 and Sephadex G25 were purchased from Sigma-Aldrich and used as received.

Preparation

CDs were synthesized using a solvothermal process from urea (11.56 g), citric acid (36.95 g), and indocyanine green (100 mg) in anhydrous DMF (100 mL) at 170 °C for 6 hours in an autoclave ($P_{max}=18$ bar). The resulting brownish slurry was purified by size exclusion chromatography (SEC) with Sephadex® G15 and G25, yielding a 43% pure product. Then, CDs (100 mg, 2.98 mg/mL) were dispersed in acetone/water (95:5) by sonication and added dropwise to a PLA solution in chloroform (20% w/v, 100 mL), creating a clear PLA@CDs dispersion. Approximately 30 mL of the organic solvent was then removed using a rotary evaporator, resulting in a slurry, which was spread on a glass crystallizer to remove the remaining solvents overnight at room temperature. The resulting brown PLA@CDs film was cut into small pieces. These pieces (20 g) were then extruded at 185 °C using a Noztek Pro

Filament Extruder, producing ePLA@CDs filaments with a diameter of 1.75 ± 0.05 mm (Figure 1). These filaments were employed to print different fluorescent objects (orthopedic screws, grids, dishes) or were further dispersed in 1,4-dioxane/water 87:13 in order to produce porous scaffolds by means of the thermal-induced phase separation (TIPS) technique.

RESULTS AND DISCUSSION

The ePLA@CDs nanocomposite was designed to combine the thermoplastic features of PLA, which imply versatile printability to get 3D biocompatible and biodegradable biomaterials, and the multicolor fluorescence of water soluble and biocompatible CDs that can provide smart self-tracking capabilities. However, the high interfacial energy between polar CDs and non-polar polyesters such as PLA precludes the formation of homogeneous physical blends. In addition, CDs undergo photobleaching in solid state due to dot-to-dot interactions. To circumvent these limitations, CDs were functionalized on the surface with PLA chains by melt-transesterification during the extrusion process yielding a homogeneous blend in which CDs-PLA ultrasmall nanoparticles are dispersed throughout the PLA matrix.

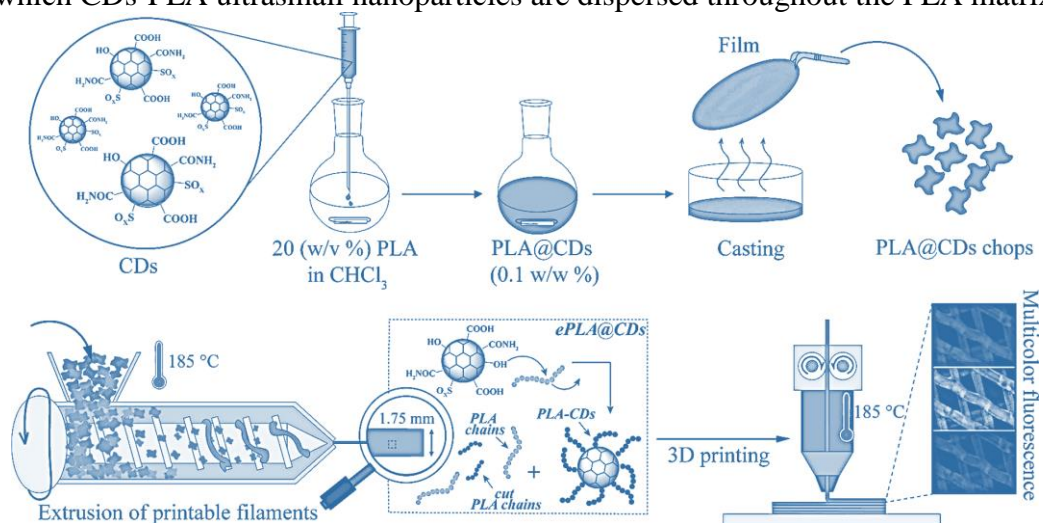


Fig. 1 Representation of the process adopted to obtain nanocomposite fibers for 3D printing applications (1)

SEC traces showed a bimodal molecular weight distribution (14 kDa and 8.3 kDa) due to the partial transesterification of PLA chains (not reported) and the presence of nanoparticles. Also, DSC analysis reveal two melting temperatures at 167 and 176 °C, confirming that the chosen extrusion conditions triggered a partial PLA degradation due to transesterification processes. DSC/TGA data show that conjugating CDs with PLA chains to form a nanocomposite enhances the thermal stability of ePLA/CDs without affecting the typical glass transition and melt temperature of plain PLA. We demonstrated that 1.7 mm ePLA/CDs filaments can be readily produced and utilized to print a range of complex objects, including orthopedic screws, with high morphological and structural homogeneity and characteristic fluorescence properties. We also demonstrated that the CDs filler enhances PLA degradation rate and *in vitro* cell adhesion and proliferation, desired features in tissue engineering applications. We proved that ePLA/CDs can be adopted to get microporous scaffold with tunable mechanical and biological properties through TIP.

Further studies can delve into optimizing processes to print micro-QR-codes endowed with an optical fingerprint for anticounterfeiting applications in several industrial fields.

References

- 1) N. Mauro, M.A. Utzeri, A. Sciortino, F. Messina, M. Cannas, G. Cavallaro, G. Giammona, *Chem. Eng. J.*, **443**, 136525 (2022)
- 2) N. Mauro, M.A. Utzeri, A. Sciortino, F. Messina, M. Cannas, R. Popescu, D. Gerthsen, G. Buscarino, G. Cavallaro, G. Giammona, *ACS Appl. Mater. Int.*, **14**, 2551-2563 (2022)

Micronization and regeneration of vulcanized rubber scrap by twin-screw extrusion

Quentin Jean¹, Yvan Chalamet¹, Jean-Charles Majesté¹, Christian Carrot¹, Claude Janin², Bernard Cantaloube², Patrick Heuillet²

¹ Univ Lyon, UJM-Saint-Etienne, CNRS, IMP UMR 5223, F-42023, Saint Etienne, France

² ELANOVA (ex: LRCCP) - 60 rue Auber, Vitry-sur-Seine, FRANCE

INTRODUCTION

Managing the end-of-life of vulcanized elastomers is a major environmental issue. Many studies have tried to develop or to improve recycling methods by means of devulcanization processes, most of the time in a continuous way[1]-[3]. But few of them tried to characterize the regenerated rubber in order to understand and control the mechanisms involved during the regeneration process. In a previous work, it was demonstrated, by means of the Horikx's analysis[4]-[5], that once corrected from fillers and bound rubber correction regeneration using a twin-screw extruder leads to a random chain scission (Fig.1)[6].

In the present work, the regeneration process operated in a twin-screw extruder, enabling both reduction of the size of the scrap particles and control of the thermal energy was studied. In the present work, the regeneration process operated in a twin-screw extruder, enabling both reduction of the size of the scrap particles and control of the thermal energy was studied.

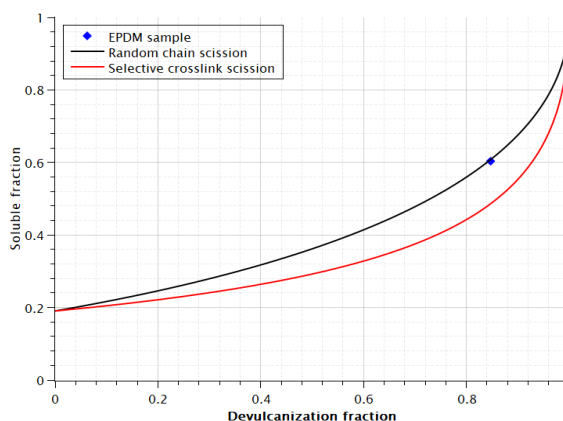


Fig. 1 Horikx's diagram plotted for the devulcanized rubber after correction by the amount of filler and of bound rubber[6]

EXPERIMENTAL

Materials

Ethylene-propylene-diene (EPDM) rubber composition containing EPDM polymer filled with carbon black and additives (plasticizers and sulfur vulcanizing agent) was used as a test material for the experiments and calculation. This industrial rubber was vulcanized in a salt bath at 230°C for 2 minutes, then cooled and cleaned with water.

Regeneration process

The first step consists in reducing the particle size in the first zones of the extruder.

The second step is to create a soluble fraction by increasing the temperature of the barrel. A study on different screw profiles enables to discriminate parameters that are efficient in creating the soluble fraction.

Physico-chemical characterization

The efficiency of the first step was assessed by analysis of the particle size using an optical microscope.

Deep analysis of the structure of the soluble fraction was carried out using various different methods such as size exclusion chromatography.

RESULTS AND DISCUSSION

Various offset angles of the kneading blocks were tested, such as (0° , 30° , 45° , 90° , -30° , -45°). The powder was analysed using optical microscopy. It is necessary to add a reverse screw element to fill the kneading block zone and reduce the particle size. Angular offset angle is an important parameter because for positive offset angle, the powder is confined between the kneading elements and forced to pass between the two kneaders' tops. The 0° angular offset works like a blade, forcing the particles to pass between the two kneaders' top. With this configuration, particle size can be reduced from 3-4 mm to 10-20 μm (**Fig.2**).

Various profiles were tested to design a regeneration zone. The first profile consists in using 90° angular offset kneading block to increase the residence time and control the temperature imposed on micronized particles. The second one is the same profile where a reverse screw element is added at the end of the profile. For the third, the reverse screw element is directly positioned after the kneading block zone in order to fill this zone and increase the residence time. Residence time distribution was measured for each screw profile, using a white filled EPDM, and they are respectively 94s, 114s and 232s.

Finally, the analysis of the structure of the soluble fraction by size exclusion chromatography (**Fig.3**) shows that it is essentially made of short linear chains ($M_n = 14\,500$ g/mol, $M_w = 117\,000$ g/mol) and microgels (30 wt.%).

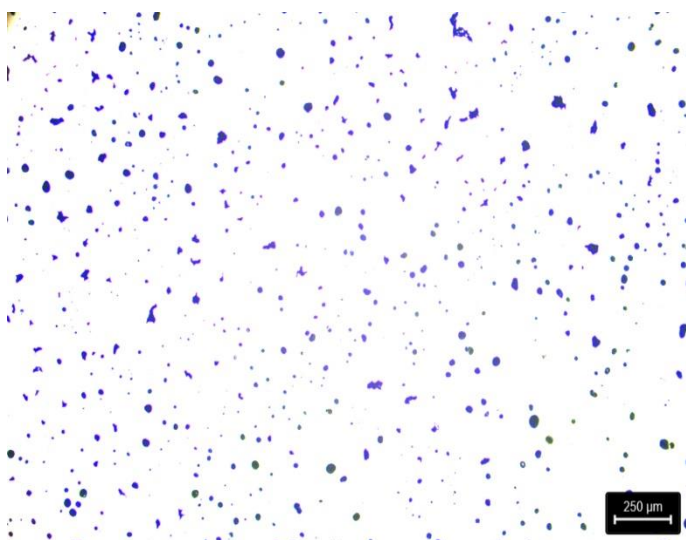


Fig. 2 Binary images of the particles obtained after the micronization step

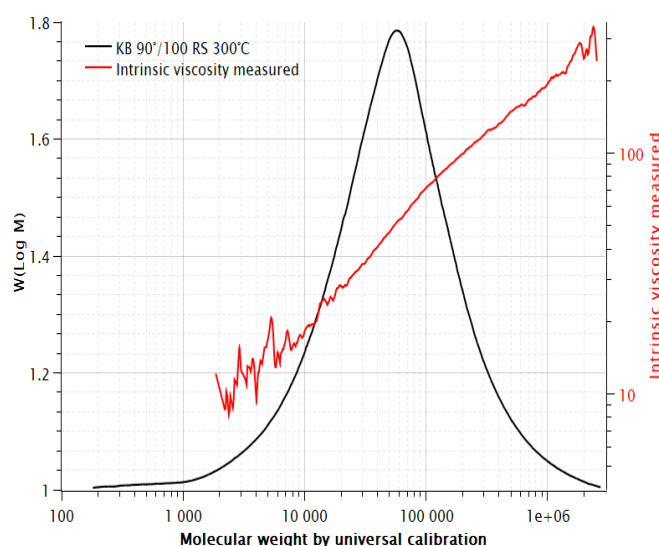


Fig. 3 GPC on soluble fraction after regeneration

References

- [1] M. Meysami, et al, "Devulcanization of Scrap Tire Rubber with Supercritical CO_2 : A Study of the Effects of Process Parameters on the Properties of Devulcanized Rubber." *International Polymer Processing* 32, pp. 183-193, doi:10.3139/217.3290
- [2] S. Seghar et al, "Thermo-mechanical devulcanization and recycling of rubber industry waste" *Resour Conserv Recycl*, vol. 144, pp. 180–186, May 2019, doi: 10.1016/j.resconrec.2019.01.047.
- [3] K. Formela et al, "The influence of screw configuration and screw speed of co-rotating twin screw extruder on the properties of products obtained by thermomechanical reclaiming of ground tire rubber," *Polimery/Polymers*, vol. 59, no. 2, pp. 170–177, 2014, doi: 10.14314/polimery.2014.170.
- [4] M. M. Horikx, "Chain scissions in a polymer network", *Rubber Chemistry and Technology* 29, pp. 1166–1173, 1956, doi.org/10.5254/1.3542617
- [5] M M. A. L. Verbruggen, L. Van Der Does, W. K. Dierkes, and J. W. M. Noordermeer, "Experimental validation of the Charlesby and Horikx models applied to de-vulcanization of sulfur and peroxide vulcanizates of NR and EPDM," *Rubber Chemistry and Technology*, 89, 4, pp. 671–688, 2016, doi: 10.5254/rct.16.83776.
- [6] Jean et al, "Application of Horikx's Theory for devulcanized Scrap Rubbers," *KGK-rubberpoint*, 2024.

Effect of processing conditions on the compatibilisation of a reclaimed EPDM in a PP matrix

V. Skyronka, J-C. Majesté*, C. Carrot*, Y. Chalamet*, C. Janin, B. Cantaloube****

*Université Jean Monnet, Université Claude Bernard Lyon 1, INSA Lyon, CNRS UMR 5223, Ingénierie des Matériaux Polymères F-42023 Saint Etienne Cedex, France

** Elanova Lab, 60 Rue Auber, 94408 Vitry-sur-Seine
victor.skyronka@univ-st-etienne.fr, majeste@univ-st-etienne.fr

INTRODUCTION

End-of-life and recycling is a major issue urging the research on elastomeric materials, regardless of their nature or source. Among the numerous recycling paths, reclaiming has many advantages, especially if it is carried out in a continuous thermomechanical process as twin-screw extrusion (1).

Polypropylene (PP) is a polyolefin used in many fields for its chemical and mechanical properties, except impact properties compared with other polyolefins. A way to enhance its impact properties is to blend it with an elastomer (2,3). Such a blend is called a thermoplastic elastomer blend (TPE). Ethylene propylene diene monomer rubber (EPDM) is widely used as the elastomeric phase due to its affinity and low interfacial tension with PP (4).

The use of reclaimed EPDM in TPE blend with a PP matrix appears to be a relevant path of reclaimed rubber valorization (5). In this work it was demonstrated that during reclaiming by twin-screw extrusion, polymer chains with low molecular mass (soluble fraction), are generated and plasticize the rubber to make it thermoplastic again. However, during the process, most of the reclaimed rubber remains crosslinked (insoluble fraction) and has poor adhesion with PP leading to bad mechanical properties.

Nevertheless, because both EPDM and PP are chemically similar, it was also shown that, in proper conditions, free radicals generated in both polymers are able to combine at the interface between phases, inducing compatibilization. The conditions of such a compatibilization have been studied in an internal mixer. A protocol has been developed and applied on several EPDM formula, or other elastomeric phases. Resulting blends show significantly increased elongation at break, indicating compatibilization between PP and reclaimed EPDM.

EXPERIMENTAL

Materials

Isotactic homopolymer of polypropylene, PPH 3060 from Total Energie, was used as the thermoplastic phase. In order to avoid chain scission during melt blending, a small amount of a mix of stabilizers (Irganox B225) was added to polypropylene. The density of PP is 0.900 g/cm³ at room temperature and 0.735 g/cm³ at 200°C.

Ethylene propylene diene monomer (EPDM) was selected as the reclaimed rubber, due to its expected affinity with polypropylene (interfacial tension between 0.06 and 0.6 mN/m) and because some PP-EPDM blends are used as industrial products. Before reclaiming, EPDM was formulated as an industrial material, by using paraffinic oil as plasticizer (35 wt%) and carbon black as a filler (40 wt%). Thermomechanical reclaiming with a twin-screw extruder was ensured by the Phénix Technologies company. The density of the non-crystalline reclaimed EPDM is 1.200 g/cm³ and assumed to remain constant with temperature.

Preparation

Blends of PP and reclaimed EPDM were prepared in an internal mixer (Haake PolyLab, Thermo Fisher Scientific) at 200°C with rotation speed of 120 rpm during 15 min. The

volume filling ratio of the mixing chamber was 70%. Several blend compositions with different volume fractions were prepared in order to cover a large range of morphologies and mechanical properties. Blends were prepared following two distinct protocols: simple protocol and compatibilization protocol.

Physico-chemical and mechanical characterization

Morphological investigations were carried out using SEM micrographs. Mechanical investigations were carried out using a tensile testing fixture.

RESULTS AND DISCUSSION

Compatibilization is investigated by means of two main characterization techniques. First, mechanical properties, especially elongation at break, are significantly improved with compatibilization protocol (Fig. 1). This can be related to the diminution of inclusion size between both protocols observed on SEM micrographs (Fig. 2).

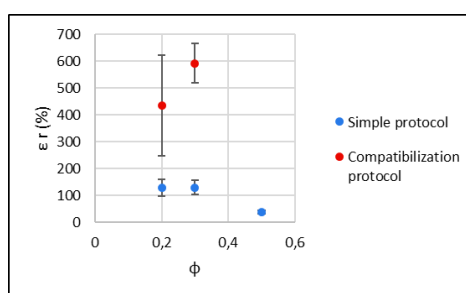


Fig. 1 Elongation at break of PP/reclaimed EPDM blends prepared by simple and compatibilization protocols

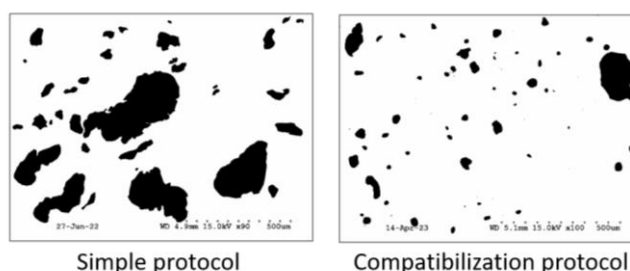


Fig. 2 Detoured SEM micrographs of a PP/reclaimed EPDM blends ($\Phi_{EPDM} = 0.2$) prepared by simple and compatibilization protocols

These results suggest that compatibilization occurs between reclaimed EPDM inclusions and PP matrix. Some PP chains have been grafted on the surface of EPDM inclusion which results in a stronger interphase and a significant reduction of the reagglomeration process in the blend.

References

- (1) S. Seghar, L. Asaro, M. Rolland-Monnet, N. Aït Hocine, Resources, Conservation and Recycling, 144 (2019)
- (2) Chiang, Tai-Chin, Liu, Huan-Li, Tsai, Lung-Chang, Jiang, Tao, Ma, Ning, Tsai, Fang-Chang, Scientific Reports, 10 (2020)
- (3) S. Tantayanon, S. Juikham, Journal of Applied Polymer Science, 91 (2004)
- (4) C. L. Hel, V. Bounor-Legaré, M. Catherin, A. Lucas, A. Thèvenon, P. Cassagnau, Polymers, 12 (2020)
- (5) L. Asaro, M. Gratton, S. Seghar, N. Aït Hocine, Resources, Conservation and Recycling, 133 (2018)

Formation of parallel cracks driven by chemicrystallization and subsequent fragmentation into microplastics

Y. Hiejima*, D. Hara, R. Ippitsu, A. Ito and K.-H. Nitta

Polymer Physics Laboratory, Graduate School of Natural Science and Technology, Kanazawa University, Kakuma Campus, Kanazawa 920-1192, Japan

hiejima@se.kanazawa-u.ac.jp

INTRODUCTION

Microplastics (MPs) are recognized as a potential threat for biological system. It has been widely accepted that degradation of plastic products in the environments leads to formation of secondary MPs, which is the major source of MPs. Despite intensive investigation, the formation mechanism of MPs in the environment is still unclear.

In this work, we conducted thermal degradation of isotactic polypropylene (iPP) sheets. We found that columnar structure with the width of ~0.2 mm was formed, and the collapse of the columnar structure gave MPs. The physical and chemical mechanisms for formation of MPs under accelerated conditions are discussed in detail.

EXPERIMENTAL

The iPP ($M_w=6.2 \times 10^5$) pellets were melted at 230 C and pressed at 40 MPa for 5 min, followed by quenching in boiled water at 100 C. The iPP sheets of 40 50 mm² with thicknesses from 0.1 to 2 mm were prepared. The volumetric crystallinity determined with the Archimedes method was about 63 %. The iPP sheet was exposed in hot air in a temperature chamber equipped with a rotating specimen rack. The exposure temperatures were from 130 to 140 C.

The morphology of the thermally-degraded iPP sheet was observed by the optical microscope. Local structural changes in the vicinity of the cracks were investigated by Raman and Fourier-transform infrared (FT-IR) microscopes. The crystallinity of iPP was determined from the intensity of the Raman bands in the 800 cm⁻¹ range¹. The carbonyl index (CI) was determined by the ratio of the intensity of the carbonyl band in the 1700 cm⁻¹ region to the C-H stretching band at 2700 cm⁻¹ as the reference.

RESULTS AND DISCUSSION

The photograph of the thermally-degraded iPP sheet exposed at 130 C for 93 days is shown in Fig. 1(a). Yellowing was observed in the edge region of the iPP sheet, whereas the central portion remained translucent. We confirmed that the decrease of the molecular weight and the increase of the CI were concentrated in this yellow region. This inhomogeneous degradation is caused by the temperature gradient within the sheet, where the temperature in the outer edge was higher than in the central portion by about 15 C owing to enhanced heat transfer. The microscopic image of the yellow region is shown in Fig. 1(b). We observed that

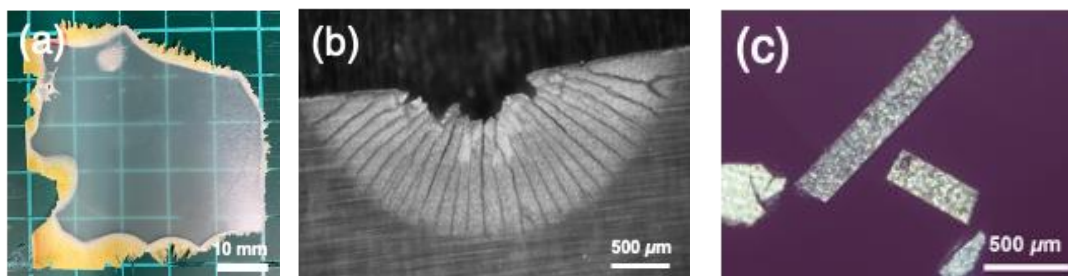


Fig. 1 (a) Photograph and (b) microscopic image of thermally-degraded iPP sheet. (c) A polarized optical microscopic image of MPs formed by collapse of the columnar structure.

columnar structure the width of about 0.2 mm was formed by propagation of parallel cracks. The crack propagation speed was almost constant throughout each exposure test, and the speed significantly increased with increasing the temperature from 0.3 mm/day at 130 C to 0.7 mm/day at 140 C. In addition, the columnar width significantly increased with increasing the thickness of the iPP sheet. Similar parallel cracks are observed for directional drying, where wet starch confined between two glass plates undergoes drying from a single side²⁾. Since drying of colloidal pastes lead to volume shrinkage, cracks are formed spontaneously. Physical mechanism of pattern formation in the parallel cracks owing to shrinkage (*e.g.* desiccation cracks in muds and columnar joints of rocks) is explained by one-dimensional stationary propagation of the crack fronts, where the stress gradient is concentrated³⁾.

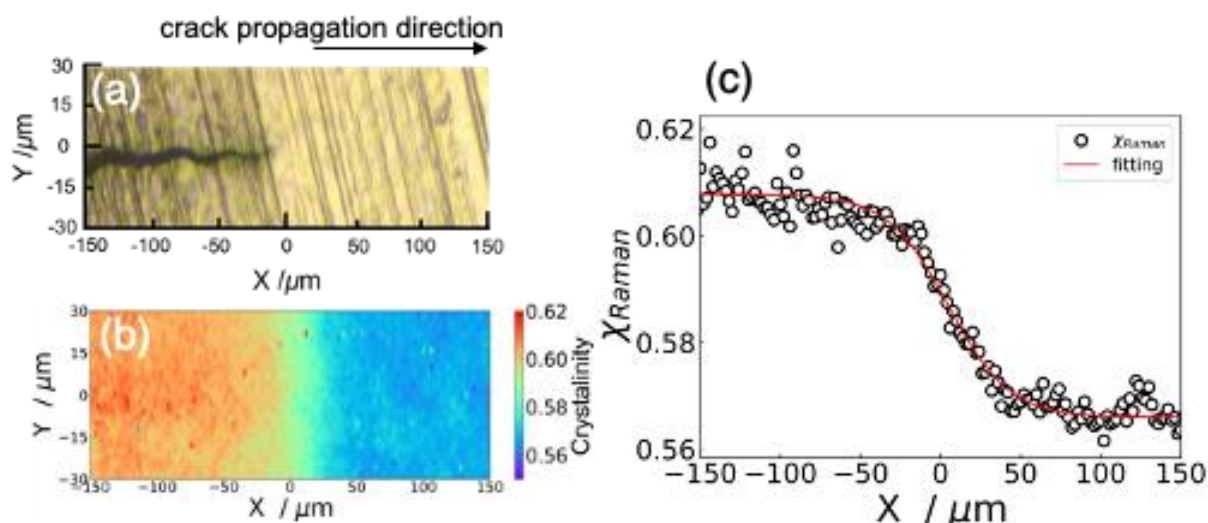


Fig. 2 (a) Microscopic image of a crack tip, (b) mapping and (c) profile of crystallinity. The crack tip is located at the origin.

The crack front in thermally-degraded iPP was visualized by Raman microscopy in Fig. 2. The crystallinity of iPP sharply increased in the vicinity of the crack tip. The front region where the crystallinity shows a step-wise increase forms a band perpendicular to the crack propagation direction next to the crack tip, suggesting one-dimensional propagation of the front region along the horizontal axis in Fig. 2(b). The width of the transitional region between the high- and low-crystallinity regions was determined to be about 40 μm by the fitting to a sigmoidal profile reflecting the interfacial region between two phases of before and after chemocrystallization. From the FT-IR microscopy, we also observed similar sigmoidal profile of the CI. Thus, it is concluded that the chemocrystallization induces the parallel-crack propagation, resulting in formation of MPs.

Acknowledgment

This work was financially supported by a grant of Long-range Research Initiative (LRI) by Japan Chemical Industry Association (JCIA).

References

- 1) A.S. Nielsen, D.N. Batchelder, R. Pyrz, *Polymer*, **43**, 2671 (2002)
- 2) C. Allain, L. Limat, *Phys. Rev. Lett.*, **74**, 2981 (1995)
- 3) L. Goehring, A. Nakahara, T. Dutta, S. Kitsunozaki, S. Tarafdar, *Desiccation Cracks and their Patterns*, Wiley (2015)

Degradation behavior of polybutylene succinate with fillers

Y. Muranaka*, T. Koike, T. Osuga and T. Maki

Department of Chemical Engineering, Kyoto University, Kyoto, Japan

*muranaka@cheme.kyoto-u.ac.jp

INTRODUCTION

Biodegradable plastics are used for agricultural materials and packaging materials, and it is important to clarify the physical properties of them for further applications. There have been many reports to improve the mechanical properties of biodegradable plastics by blending additives. However, few studies have quantitatively evaluated degradation rates, and it is difficult to predict degradation times. In addition, there are many examples of studies conducted with additive content of 0-10 wt%, and little is known about the impact of additives blended in large amounts. In this study, the degradation behavior under the influence of additives with large amounts was examined.

EXPERIMENTAL

Pelletized polybutylene succinate (BioPBS™) (PBS) and coconut shell derived activated carbon (6 μm) (AC) were purchased from Mitsubishi Chemical (Japan) and UES (Japan), respectively. Pellets of resin and AC were melt-blended at 140 °C, and molded by hot-pressing at 140 °C for 3 min at 30 MPa, and then cooled to 40 °C under the pressure by circulating water within the apparatus. Thus produced AC blended plastic was cut into a square (10 mm × 10 mm) with a thickness of 1 mm, and used in the experiment. In this study, a PBS sample with n wt% AC is denoted as PBS_AC n . Degradation in a compost was performed according to the ISO 14855-1 standard. A plastic sample was placed in a polypropylene cup with 30 g of compost which has 50 % moisture content, and then placed in an incubator preheated to 58 °C. For hydrothermal degradation, a plastic sample was sealed in a vial with 30 mL of deionized water, and then placed in an incubator preheated to 80 °C. After an elapse of reaction time, the remaining sample was collected via suction filtration washing with deionized water. The number average molecular weight (M_n), the crystallinity (χ_c), and the elemental composition of collected sample were analyzed using a gel permeation chromatography (Shimadzu, Japan), differential scanning calorimetry (DSC) analyzer (DSC-60A, Shimadzu, Japan), and elemental analyzer (JM-11, J-science, Japan), respectively. Dissolved fraction was analyzed by a total organic carbon (TOC) analyzer (TOC-VCSH, Shimadzu, Japan)

RESULTS AND DISCUSSION

PBS, PBS_AC5, and PBS_AC10 were degraded for 12 weeks in a compost. Fig. 1(a) shows the change in M_n . M_n decreased as biodegradation progressed, and approached a constant value. This was because the sample started leaching at certain range of M_n . Judging from Fig. 1(a), the AC content had little effect on the degradation rate. Fig. 1(b) shows the change in χ_c through degradation. χ_c increased during the degradation process. This was probably because the experiment was conducted at above the glass transition temperature. Judging from the results, the AC content had little effect on the crystallinity as well. It is known that during biodegradation plastics decreases M_n through hydrolysis in the first stage, and then decomposes by microorganisms activities. Eq. (1) shows the model equation for the hydrolysis reaction, where n is degree of polymerization [-], $[P_n]$ is molar density of polymer [mol/m^3], $[\text{COOH}]$ is molar density of carboxy group [mol/m^3], k is kinetic constant [$\text{m}^3/(\text{mol s})$], and t is reaction time [s]. Because the hydrolysis reaction of polyester is an autocatalytic reaction of carboxy groups, the hydrolysis depends on the concentrations of both ester bonds and carboxy groups. Eq. (2) expresses the change in M_n over time derived from Eq. (1). The

kinetic constant k was calculated from parameter fitting, and the calculation result was shown in Fig. 1(a). There was a good agreement with the experimental values, demonstrating the validity of the model. Because k was constant through the experiment, it was speculated that the degradation rate was independent of crystallinity. The polydispersity index (PDI) did not change during the degradation, which also indicated that the degradation progressed uniformly in the crystalline and amorphous regions.

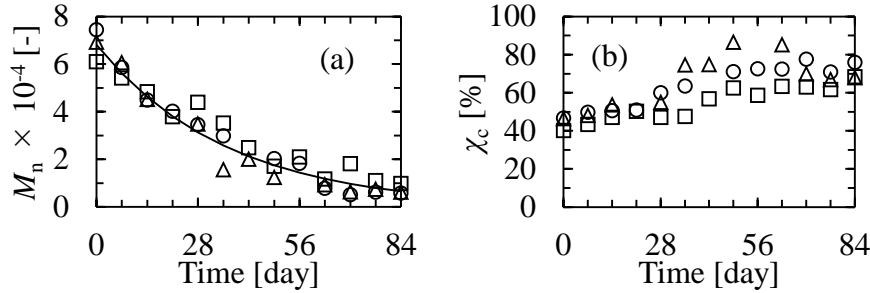


Fig. 1 Change in (a) M_n and (b) χ_c during the degradation in compost. Circles – PBS, triangles – PBS_AC5, squares – PBS_AC10, solid line – calculation according to Eq. (2)

$$d(\sum [P_n])/dt = k \{ \sum (n-1)[P_n] \} [\text{COOH}] \quad \text{Eq. (1)}$$

$$\ln(M_n) = \ln(M_{n0}) - k (\sum n[P_n])t \quad \text{Eq. (2)}$$

PBS, PBS_AC5, 10, 20, 30 and 50 were hydrothermally degraded for 1 week. Similar to compost degradation, there was no change in the M_n profiles even at high AC content. On the other hand, when the AC content was high, PDI increased with degradation. The crystallinity decreased when the AC content was high. If the crystallization of PBS was inhibited by AC, the crystal becomes thinner and the molecular chains folded in the crystal become shorter. When these are cleaved by hydrolysis, small M_n fractions dissolve into water. For these reasons, PDI increased during degradation for higher AC content samples. Besides, because no AC fraction was observed in solutions after hydrolysis, it was suggested that only PBS dissolved while AC remained in the sample. If degradation progresses while AC remains in the sample, the amount of TOC in the solution should match the value TOC' calculated according to Eq. (3) because PBS can be expressed as $(C_8H_{12}O_4)_n$, where Δm is weight decrease [g], and M_i is atomic weight of element (= C, H, or O) [-]. Fig. 2 shows a comparison between TOC and TOC'. TOC₀ is the original carbon content in the samples. The results showed that TOC corresponded to TOC' in a 1:1 ratio, which indicated that only PBS in the sample dissolved. Therefore, it can be concluded that the hydrolysis rate of PBS was relatively slow around the blended AC.

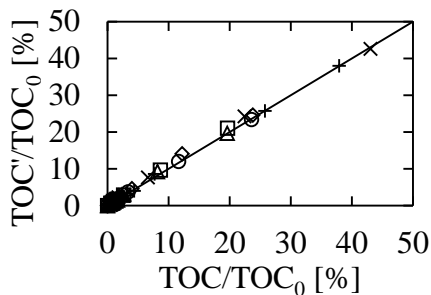


Fig. 2 Ratio of analyses and calculated dissolved carbon. Circles – PBS, triangles – PBS_AC5, squares – PBS_AC10, diamonds – PBS_AC20, crosses – PBS_AC30, pluses – PBS_AC50

$$\text{TOC}' = \Delta m \times M_C \times 8 / (M_C \times 8 + M_H \times 12 + M_O \times 4) \quad \text{Eq. (3)}$$

Acknowledgment

YM acknowledges support from AUN/SEED-Net (Grant No. BUU REd-UC 2301) for Research and Education Grant for the University Consortium (Consortium name: CES-CHEM).

New tyre compounds with reduced environmental impact

C. Noè¹, C. Di Bernanrdo¹, M. Dadkhah¹, F. Demichelis¹, M.Messori^{1,2}

¹Department of Applied Science and Technology (DISAT), Politecnico di Torino, Corso Duca degli Abruzzi 24, 10129 Torino

²National Interuniversity Consortium of Materials Science and Technology (INSTM), Via G. Giusti 9, 50121 Firenze, Italy

*camilla.noe@polito.it

INTRODUCTION

In 2018, the global pneumatics market reached a substantial volume of 29.2 million tons, driving significant demand for elastomeric products and carbon black (CB). The most used elastomers in tyre composites are natural rubber (NR), which is biobased and comes from the latex of *Hevea brasiliensis*, a plant native to the rainforest, and styrene butadiene rubber (SBR), which is, instead, synthetic. However, the highest environmental concern comes from CB, which is based on fossil fuel resources and has a high environmental impact, particularly regarding waste management and greenhouse gas emissions. Thanks to increasing public awareness and government funding, developing and designing new sustainable tyres have become a top priority in the automotive sector.

Using sustainable and renewable fillers in tire composites is one of the best strategies to reduce the CB environmental impact [1].

This study aims to characterize and assess various biomass wastes as potential reinforcement materials and explore substituting CB with materials produced through pyrolytic processes. This includes examining char derived from discarded tires and biomass sources. Furthermore, the sustainability effectiveness of the novel elastomeric compounds will be thoroughly investigated using a comprehensive life cycle assessment (LCA).

EXPERIMENTAL

Materials

Different rubber composites were prepared by adding different CB-biofiller amounts in the (NR:SB, 50wt%:50wt%) matrix, while keeping the remaining additive's quantity equal. SBR, NR, sulfur (S), stearic acid (SA), zinc oxide (ZnO), oil, and N-tert-butyl-2-benzothiazyl sulfonamide (TBBS), Commercial N326 carbon black (BET area of 77 m²/g, average pore dimensions 27nm) and pyrolyzed waste tires (Gen1.5) were provided by Michelin company. Agricultural waste derived from food by-products (ESF), maize by-products (GTF), sunflower by-products (SFF), and wine by-product (WPL) was provided by AgroMateriae srl and utilized as a biofiller.

Preparation

The rubber composites were prepared by mixing different CB-biofillers content in a Brabender (MT 1902140.1289) mixer at T=130 °C and rotor speed of 90 rpm for 30 min. After obtaining a homogeneous formulation, the composites were cured at T=140°C for 15 min in compression molding (Gibitre).

Characterization

The morphological analysis of the fillers and the composites was performed using the scanning electron microscopy SEM (Zeiss EVO 15) instruments. The filler's specific surface area was investigated by Brunauer–Emmett–Teller (BET) adsorption analysis. The bound rubber content (BRC) was analyzed using the swelling method in toluene. The Payne effect was evaluated measuring the storage modulus as a function of strain amplitude using an oscillatory disc rheometer (Anton Paar (MCR702E)). The thermal resistance of both the

fillers and the composites was investigated with thermogravimetric analysis. Hardness measurement was carried out using a Shore A durometer (Wallace, UK) in accordance with ISO 7619-1. Mechanical properties of the filled rubber composites, such as tensile strength, elongation at break, and modulus, were determined using an INSTRON universal testing machine (Ulm, Germany) in accordance with ISO 527 (die type 5A). The life cycle assessment was performed with the software SimaPro 3.5 using Ecoinvent 3.5.0 database.

RESULTS AND DISCUSSION

From the scanning electron microscope (SEM) images, it was evident that all the fillers had irregular shapes and some degree of porosity, differing significantly from carbon black (CB), which has a spherical shape without pores. Moreover, with SEM images, it was possible to calculate the average filler dimension, which was found to be in the micrometres scale, contrasting with CB's nanometer range.

Subsequently, using BET analysis, the specific surface area and average pore dimensions of the fillers were calculated. Compared to CB, the BET area was considerably lower for biofiller and biochar (max 1.8 m²/g) but surprisingly comparable for Gen1.5 (73 m²/g - char from waste tyres). A BRC test was conducted to assess the interaction between rubber and filler; results indicated that the best affinity was achieved in composites containing Gen1.5, followed by those with WSP550 biochar. In other formulations, the filler exhibited poor interaction with the matrix.

To characterize the magnitude of the filler-filler interaction, the Payne effect was investigated. In all cases, the partial substitution of CB with the new fillers leads to a decrease in the $\Delta G'$ value, indicating reduced filler-filler interaction and potential formation of a percolation filler network within the matrix [2]. All composites exhibit high thermal stability (up to 250°C) and excellent hardness (Shore A), mostly exceeding the minimum acceptable value of 65 for tire compounds.

The addition of biofiller and biochar slightly reduced the Young's Modulus of the composites while the elongation at break remained almost unchanged. However, when Gen1.5 was used, the strength of the composites improved, with Young's Modulus increasing from 24.9 MPa (pure CB) to 26.1 MPa (30 phr CB + 70 phr Gen1.5).

Finally, the LCA analysis conducted on all the formulations revealed that partially substituting CB with recycled or bio-based fillers successfully reduced greenhouse gas emissions. Therefore, this strategy can effectively provide a more sustainable alternative for tyre production.

Acknowledgement

This work has been financially supported by the project Pneumatici NEXT GENERATION di Michelin Italia ad Alte Performance, Innovativi, Circolari e Sostenibili

References

- 1) B. P. Chang, A. Gupta, R. Muthuraj, T. H. Mekonnen, *Green Chem.*, (2021), 23, 5337–5378 | 5337.
- 2) P. Pangamol, W. Malee, R. Yujaroen, P. Sae-Oui, C. Siritwong, *Arab J Sci Eng* (2018) 43:221–227.

N-P-Silanes as multipurpose flame retardants

T. Mayer-Gall,^{a,b} **W. Ali**,^{a,b} **R. Otto**,^a **V. Shabani**,^{a,b} **D. Danielski**,^a **J.S. Gutmann**^{a,b}

^a *Deutsches Textilforschungszentrum Nord-West gGmbH, Adlerstr. 1, D-47798 Krefeld, Germany, mayer-gall@dtmw.de*

^b *University Duisburg-Essen, Institute of Physical Chemistry and CENIDE, Universitätsstr. 5, D-45117 Essen, Germany*

mayer-gall@dtmw.de

INTRODUCTION

N-P silanes can be synthesised on the basis of industrial available educts, whereby, one-to-two reaction-steps are needed and a yield between 80-95 % are obtained. On this basis, a wide library of versatile N-P-silane-based FRs are developed. Based on these FR library, cotton, polyamide, polyester and their blends were applied and their thermal behavior and durability were assessed. A combination of nitrogen and phosphorous-based flame retardants with boron-based silanes exhibit smoke suppressant properties also offer a green alternative to halogenated flame retardants for composite materials.

RESULTS AND DISCUSSION

In this presentation an overview will be given about the currently flame retardants developed in our group and the main trends seen with respect to fire protection of materials, including fabrics, composites, wood and polymers. In **Figure 1** an overview of the different FR is given. Finished textiles passes different standardized test, e.g. for personal protective clothing (DIN EN 15025) or building materials with a rating (DIN 4102-B2) and show a high washing resistance. In **Figure 1** (below) a comparison of a FR-finished and native nylon-cotton (NYCO) fabric is given. In cooperation with abcr GmbH we could commercialize different N-P-silanes for textile finishing, for WPC applications or for the modification of glass fibers for polyamide in E&E applications.

The FRs in **Figure 1** (top) can have different functionalities for intumescence applications. A typical intumescence mixture consists of three components, an acid source, a gas source and a carbon donor. All these functionalities can be included into the silane. But these can be designed easily as acid and gas source. Different FR have been tested for wood coatings in intumescent mixtures, all of the FR acted with the desired function in the mixture.

This presentation should not only give an overview on the different new flame retardants and there application possibilities, furthermore an insight into the decomposition mechanism of the different FR is given.

CHALLENGES ON THE CURRENT CAPABILITIES TO DETERMINE THE THERMAL DIFFUSIVITY OF CARBON/PHENOLIC COMPOSITES EXPOSED TO HARSH HYPERTHERMAL ENVIRONMENTS: A THEORETICAL ASSESSMENT AND AN EXPERIMENTAL PROTOCOL

M. Natali, L. Torre, M. Buconi, and M. Rallini

Civil and Environmental Engineering Department, University of Perugia, Strada di Pentima 4, 05100 Terni, Italy

maurizio.natali@unipg.it, luigi.torre@unipg.it, michele.buconi@unipg.it, marco.rallini@unipg.it

INTRODUCTION

Carbon/Phenolic Composite (CPC) materials are essential to manufacture many portions of the nozzle assembly of Solid Rocket Motors (SRMs) which are essential both to preserve the independent access to space as well as for the homeland security [1, 2]. The thermal conductivity of these materials presents a strong dependence on the temperature. In terms of heat transfer analysis and exploitation of the experimental in-depth temperature profiles, the knowledge of the surface thermal boundary conditions is a critical task to properly design the related TPS. This is a concern both in the real operational environment of the TPS material as well as in the laboratory test which exploits torches such as Oxy-Acetylene Torch (OAT). In fact, harsh ambient conditions related to the given hyperthermal environment or other practical limitations may preclude the use of surface-mounted sensors for measuring the surface temperature and heat flux.

To overcome this problem, the temperature profiles obtained from thermocouples (TCs) located below the exposed surface can be used to retrieve the surface thermal boundary conditions. The exploitation of the in-depth temperature data to estimate the surface boundary conditions of the tested article (or of the real item) is known as the Inverse Heat Conduction Problem (IHCP). One of the challenges of the IHCP is to exploit the temperature profile at the TC site to estimate the temperature change that occurred at the surface. In addition to the IHCP approach, which is closely related to the determination of the boundary conditions applied at the tested article (or of the real TPS item), analytical models have also been developed to predict the response of polymeric ablatives such as CPCs exposed to different hyperthermal environments once the thermo-physical properties of the given material are known in the proper range of temperature. Finite Difference Method (FDM) is the most tunable and effective approach for obtaining numerical solutions which satisfy the real boundary conditions of these problems. However, for many problems of interest in rocketry and re-entry flight, some analytical solutions based on certain idealized boundary conditions can predict the in-depth temperature profiles with sufficient accuracy [3, 4].

The simplest model that it is possible to introduce only considers the effect of the transient heat conduction whilst, the more sophisticated approaches consider many thermal, chemical, and physical processes involved in ablation. This starting model is generally based on a one-dimensional (1D) analysis that considers the heat conduction in the through-thickness direction of a material heated from one side (referred as hot or exposed surface). This model assumes that a polymeric based TPS material is shaped like a flat semi-infinite slab (numerically speaking with a thickness higher than 100 mm) with constant thermo-physical properties. The cold (or unexposed) surface of the slab is assumed to be adiabatic (or at a constant temperature). In this basic approach the thermal diffusivity (α) i.e., the heat capacity (C_p), the thermal conductivity (k), and the density (ρ) are all assumed to be constant (independent from the temperature). Consequently, for a CPC, this model can be properly

applied only at very small heat fluxes i.e., the maximum temperature imposed at the CPC slab has to remain below the starting of the irreversible processes the phenolic matrix (~ 200 °C).

In the following research, the exact solutions of certain selected hyperthermal heating scenarios will be identified and presented, and criteria will be given for their use in solving heat conduction problems. It is worth to remind that in these cases, the solutions of the in-depth temperature profiles can be analytically obtained through the assumption of constant thermo-physical properties (i.e., constant α). A 1D finite element analysis model in presence of temperature dependent thermo-physical properties (with no degradation i.e. constant density) was adopted to better determine the in-depth temperature profiles. At a more advanced level, in addition to the temperature dependent thermal conductivity and heat capacity of the solid material, the effect of the non-constant density of the solid phase has to be considered. Then the effect of the gaseous phase can also be considered.

The aim of this presentation is to introduce the basic yet most relevant mechanisms behind the degradation of CPCs starting from the roots of the ideal heat transfer models, then filling the gap between the knowledge provided in traditional heat transfer books and more advanced review or research papers summarizing the state-of-the-art findings in the field of the modeling of ablative materials. These theoretical findings will be at the base of a protocol aimed at retrieving the in-plane and out-plane thermal diffusivity of CPCs through OAT test.

EXPERIMENTAL

Starting from the assumption of one-dimensional (1D) semi-infinite solid (thickness higher than 100 mm) and then moving to a finite element heat transfer model applied on a CPC sample having the size of the real testing coupons (10 mm large cubes), the in-depth temperature profiles were reported and discussed. The effect of the gaseous phase was not considered. On the other hand, the effect of the thermal losses in the tested sample will be considered.

At the same time, the temperature profiles of Carbon/Phenolic Composites (CPCs) exposed to Oxy-Acetylene Torch (OAT) were used to evaluate the thermal diffusivity of these materials. A comprehensive work of comparison of the obtained data with state-of-the-art CPCs such as MX-4926 and FM-5014 was carried out.

RESULTS AND DISCUSSION

The theoretical and experimental efforts were combined. The effect of the density, heat capacity, thermal conductivity was evaluated providing an evaluation of the experimental protocol. The thermal losses in the real tested samples were also taken into account and compared with the experimental results of the OAT tests.

Acknowledgment

This work has been financially supported by PRIN project DAPHNE - Development of Advanced testing Protocols and of High temperature materials for NExt generation solid and hybrid rocket motors

References

- [1] M. Natali, J.M. Kenny, L. Torre. *Prog. Mater. Sci.*, **84**, 192 (2016)
- [2] M. Natali, L. Torre, M. Rallini. *Compos. Part. A Appl. Sci. Manuf.*, **175**, 107801 (2023)
- [3] D. Baer, A. Ambrosio. *Planetary and Space Science*, **4**, 436 (1961)
- [4] D. Bianchi, A. Turchi, F. Nasuti, M. Onofri, 48th AIAA/ASME/SAE/ASEE Joint Propulsion Conference & Exhibit 30 July - 01 August 2012, Atlanta, Georgia

Accelerated hydrolytic degradation of glass fiber-polyamide (PA66) composites

K. Gkaliou, M. V. Ørsnaes, A. H. Holm, A. E. Daugaard*

Department of Material Technology, Grundfos Holding A/S, Bjerringbro, Denmark

*Department of Chemical and Biochemical Engineering, The Danish Polymer Center, Technical University of Denmark, Kongens Lyngby, Denmark
kgkaliou@grundfos.com, mvoersnaes@grundfos.com, aholm@grundfos.com, adt@kt.dtu.dk

INTRODUCTION

Polyamides (PAs) are thermoplastic engineering materials that find applications across a broad range of applications due to their high elasticity, mechanical strength, high melting point, and barrier properties against liquids and gases [1]. Polyamide 6.6 (PA6.6) is the primary polymer used by Grundfos to make housings for their circulator pumps. Although PA6.6 is known for its excellent mechanical behavior, pumps are exposed to various environmental conditions during use that decrease their performance over time [2] and ultimately limit a pump's lifetime. The design lifetime of a pump is 10-15 years, and the evaluation of new compounds meets very stringent requirements to ensure satisfactory performance.

In this work, we investigated the degradation behavior of unfilled PA66 and glass fiber (GF)-reinforced PA66 composites under hydrolytic acceleration. The main objective of this study is to develop a degradation model that can rapidly evaluate GF-PA66 grades for use in heating applications to enable faster qualification of new or recycled materials.

EXPERIMENTAL

Materials

PA66 (Zytel 101L) and GF-reinforced PA66 (Zytel FG70G30 HSR2) pellets have been supplied by Celanese.

Preparation of sample specimens and accelerated testing

Rectangular bars with dimensions of 0.6 (T) x 7 (W) x 85 (L) mm were injection molded and then immersed in vials with DI (deionized) water. The water was bubbled with nitrogen prior to aging to ensure that any changes in molar mass exclusively result from hydrolytic processes. The vials were placed into the ovens at 40°C and 95°C. Moreover, hydrolytic degradation was performed at 120°C using pressure vessel autoclaves. A range of conditioning times was used: 0 h; 100 h; 500 h; 1.000 h; 2.500 h and 5.000 h. In the case of 120°C, the samples were exposed up to 2500 h. All samples were dried prior to aging in a vacuum oven at 80°C for 2 days. Before further analysis, the samples were placed in a desiccator to avoid moisture absorption.

Characterization methods

Three samples of each material exposed to the water conditions were weighed on a standard balance with an accuracy of 0.1 mg. After aging, the samples were wiped with paper tissue, and the measurement was taken after the balance had stabilized. Mass variations were calculated using the following equation:

$$\Delta_m = (m_t - m_0) / m_0 * 100$$

Where Δ_m is the mass variation in %, $m(t)$ is the sample mass at a specific time t in g, and m_0 is the initial mass of the sample in g.

Gel Permeation Chromatography (GPC) was employed to evaluate the acceleration conditions' effect on the molar mass. Approximately 20 mg sample was dissolved in 2 mL HFIP (Hexafluoro-2-propanol) in a 4 mL vial, resulting in a 10 mg/ml concentration. After dissolution, the solution was filtered through a PTFE syringe filter with a pore size of 0.2 μm

and transferred to a 1.5 mL vial for auto-injection. Calibration standards of narrowly distributed poly (methyl methacrylate) (PMMA) were used to calculate the molar mass. The obtained molar mass is presented as the weight average molar mass, M_w .

RESULTS AND DISCUSSION

In Fig 1 a, it can be observed that there is a rapid initial water uptake for all the samples in the first exposure period of 100 h ($10 \text{ h}^{1/2}$). This has been associated with water absorption within the amorphous regions of the polymer. Zytel 101L, the base PA material without glass fibers, absorbed more water than Zytel FG70G30 HSR2, which contains 30 wt% glass fibers. After the equilibrium point, the water uptake profile of the materials depended on the temperature. Specifically, the water uptake (%) remains constant at 40°C , whereas at 95°C , the materials show a weight loss, which is attributed to degradation and wash-out of low molecular weight species. In contrast, the saturation level is lower at 120°C , which is believed to be due to increased degradation and wash-out competing with water uptake in the early phase of the test. From 1.000 h ($32 \text{ h}^{1/2}$), specimens become porous and incorporate more water, resulting in a competition between hydrolysis, wash-out and weight increase due to porosity.

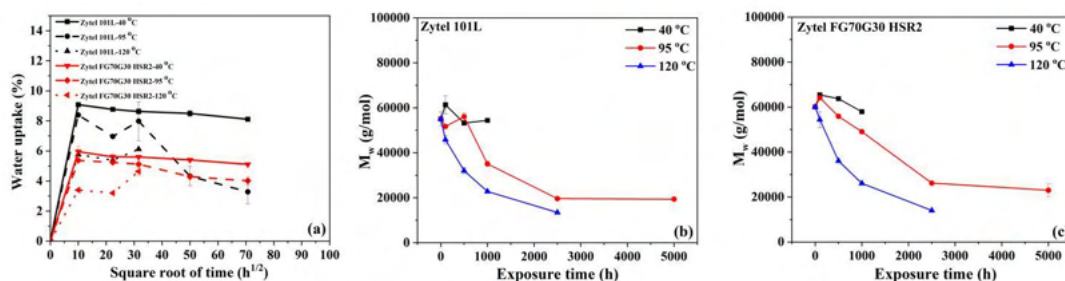


Fig. 1 Water uptake of Zytel 101L and Zytel FG70G30 HSR2 (a), changes in the weight average molar mass (M_w) for Zytel 101L (b) and Zytel FG70G30 HSR2 (c) when fully immersed in distilled water at 40°C , 95°C & 120°C under different exposure time periods.

The changes in molar mass of Zytel 101L (Fig. 1 b) and Zytel FG70G30 HSR2 (Fig. 1 c) were monitored by GPC. According to these data, temperature, not surprisingly, plays a significant role in the acceleration of PA66 hydrolysis. The reduction in molar mass resulting from hydrolysis exhibits a linear correlation with time. Initially, this is attributed to chain scission at the amide linkages, leading to a reduction in molar mass and, consequently, in the concentration of amide groups. Once the concentration of amide groups diminishes sufficiently, the hydrolysis rate becomes slower, indicating an equilibrium point. A molar mass of 20 kg/mol is considered the end-life point [3], which this material reaches after more than 2500 hours of exposure at 95°C , while 1000 hours at 120°C is sufficient. Following these acceleration conditions, a fast screening of different GF-PA66 grades can be performed by evaluating the degradation level (hydrolysis rate) via the reduction in molecular mass.

Acknowledgment

This work has been financially supported by Innovation Fund Denmark.

References

- [1] M.M. Brette, A.H. Holm, A.D. Drozdov, J. de C. Christiansen, *Chemistry (Easton)* 6 (2023) 13–50.
- [2] A. Plota, A. Masek, *Materials* 13 (2020) 4507.
- [3] C. El-Mazry, O. Correc, X. Colin, *Polym Degrad Stab* 97 (2012) 1049–1059.

LIFETIME PREDICTION MODEL OF CARBON FIBER REINFORCED EPOXY RESIN COMPOSITES UNDER HYGROTHERMAL AGING

Guoshuo Tang and Rui Yang*

Department of Chemical Engineering, Tsinghua University, Haidian District, Beijing, China.

tgs22@mails.tsinghua.edu.cn, yangr@mail.tsinghua.edu.cn

INTRODUCTION

Carbon fiber reinforced epoxy resin (CFRP) is widely used in various industries because of their low density, high strength, easy forming, corrosion resistance, fatigue resistance and other excellent properties. The actual use conditions of CFRP are very complex and harsh. So people are concerned about how long it can be used without problems. Therefore, the aging rate and life prediction of CFRP are particularly important.

In this paper, a new life prediction model of CFRP is presented. Through mathematical derivation, environmental condition equation and aging state equation are obtained. Under the condition of hygrothermal aging, the model was verified with the experimental results of accelerated aging, and a better fitting result was obtained.

EXPERIMENTAL

Lifetime prediction model

A service property P is a function of service environmental conditions (including temperature T, humidity H, solar irradiance I, O₂ concentration) and service time t, as shown in equation (1)

$$P(T, H, I, [O_2], t) = f_1(T) \cdot f_2(H) \cdot f_3(I) \cdot f_4([O_2]) \cdot f_5(t) \quad \#1$$

After the derivation of the formula, we can get equation(2).

$$\Delta P = \frac{\Delta P}{\Delta v} \cdot \Delta v(T, H, I, [O_2]) + \frac{\Delta P}{\Delta t} \Delta t \quad \#2$$

Equation (2) consists of three very important parts: $\frac{\Delta P}{\Delta v}$, $\Delta v(T, H, I, [O_2])$, $\frac{\Delta P}{\Delta t} \Delta t$. $\frac{\Delta P}{\Delta v}$

is the relationship between the service property P and the aging rate v. $\Delta v(T, H, I, [O_2])$ is the Environmental Condition Equation, which gives the aging rate in a certain environment.

Materials

Carbon fiber reinforced epoxy resin(CFRP) were from Fuhegu Science and Technology Limited company, Chengdu.

Accelerated aging

The accelerated aging of CFRP samples was performed in a ventilated oven (DGG-9070A, QIXIN SCIENTIFIC INSTRUMENT). The hygrothermal accelerated aging conditions (T/H) are: 120°C/(1g/m³), 85°C/(17.3g/m³), 85°C/(19.6g/m³) for up to 60 days.

The tensile strength and interlaminar shear strength of the samples were measured after accelerated aging.

Environment condition equation

The CO₂ generation rate of CFRP, as the aging rate under various combinations of temperature and humidity, was determined using the Comprehensive Aging Evaluation System (CAES) developed in our lab. The environmental condition equation is obtained through multiple regression.

Aging state characterization

The aging state of hygrothermal aged samples was characterized by CAES by measuring the CO₂ generation rates under the condition (T/H/I) of 70°C/(6.9g/m³)/(60mW/cm²@340nm).

RESULTS AND DISCUSSION

We used CAES to measure the environmental equation of CFRP under hygrothermal aging condition. The environmental condition equation can directly compare the aging rates of CFRP under different conditions. The aging state equation and lifetime prediction model were verified by the accelerated aging data with the error of <15%.

This model can be extended to CFRP for outdoor applications.

References

- [1]An Z, Xu Z, Ye Y, et al. A rapid and highly sensitive evaluation of polymer composite aging with linear correlation to real-time aging. *Anal Chim Acta* 2021; 1169: 338632.
- [2]Zhen-hua An, Rui Yang. A Novel Aging Evaluation System and the Application to Polyethylene Composites[J]. *Acta Polymerica Sinica*, 2021,52(2):196-203. DOI: 10.11777/j.issn1000-3304.2020.20150.
- [3]An Zhen-hua, Ye Yan, Xu Zhi-ping, et al. Study on Multi-factor Coupling Aging Kinetics of Polyolefins: Yearly and Monthly Aging Speed Maps[J]. *ACTA POLYMERICA SINICA*, 2021,52(11):1514-1522. DOI: 10.11777/j.issn1000-3304.2021.20122.

Engineering flame-retardant properties in thermoplastic polyurethane through reactive extrusion

Léa Gratier^{1,2,3}, Jean-Marie Raquez², Marianne Cochez¹, Fouad Laoutid³, Henri Vahabi¹

¹University of Lorraine, CentraleSupélec, LMOPS, F-57000 Metz, France

²University of Mons UMONS, Place du Parc 20, 7000 Mons, Belgium

³Materia Nova Research Center, 7000 Mons, Belgium

lea.gratier@univ-lorraine.fr

INTRODUCTION

This study is a part of a PhD thesis which aims to prepare flame-retardant thermoplastic polyurethane (TPU) by a solvent-free reactive extrusion process. The adopted strategy involves using bifunctional phosphorus-containing diols to replace diols segments commonly used in TPU production. These phosphorus-containing polyols will be thus incorporated directly into the macromolecular chain, through reactions with isocyanate groups leading to the formation of urethane bonds [1]. Reactive extrusion was chosen due to its advantages [2].

EXPERIMENTAL

Materials

For this work, 1,4-butanediol (BDO), Methylene diphenyl 4,4'-diisocyanate (4,4'-MDI) and Polyethylene glycol 1500 (PEG 1500) were purchased from Sigma-Aldrich. A phosphorated flame retardant and polyol was kindly provided by Clariant.

Preparation

TPU precursors and the reactive flame-retardant diols were directly incorporated into the extruder hopper (Fig. 1) at different contents to prepare flame-retardant TPU with different phosphorus contents. Extrusion conditions and blends compositions were studied to determine optimal conditions and compositions. The obtained materials were obtained in shape of rods and used for structural, thermal, mechanical, and flame-retardant analyses.

Physico-chemical and fire characterization

FTIR was performed using a Bruker Tensor 27 device in ATR-IR mode. TGA test was performed using TAQ500 device, in a temperature range of 20°C to 600°C, with a temperature ramp of 10°C/min. Preliminary flame-retardant tests were conducted with a lighter to assess an influence of the fire-retardant.

RESULTS AND DISCUSSION

FTIR was performed, and the results showed three areas of interests on the spectra (Fig 2) which show the conversion of isocyanate groups into urethane groups. No major difference was observed between raw materials and flame-retardant TPUs. To assess the thermal performance of the materials, TGA was performed, and the results exhibited a two-step thermal degradation pathway (Fig 3). Preliminary flame-retardant tests showed a clear enhancement of the flame-retardant behavior of phosphorylated TPU, owing to the formation a char during the combustion.



Fig. 1 Reactive extrusion of thermoplastic polyurethane using a microcompounder, adapted from [3]

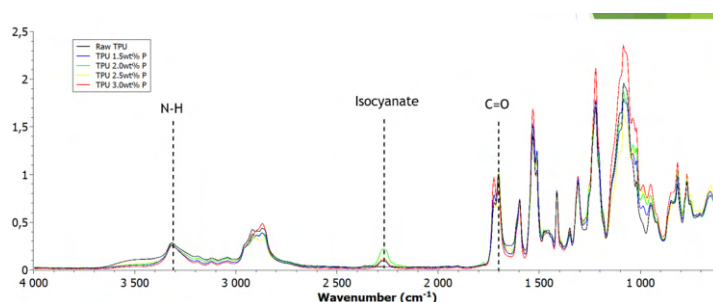


Fig. 2 : FTIR spectra of raw TPU and flame-retardant materials

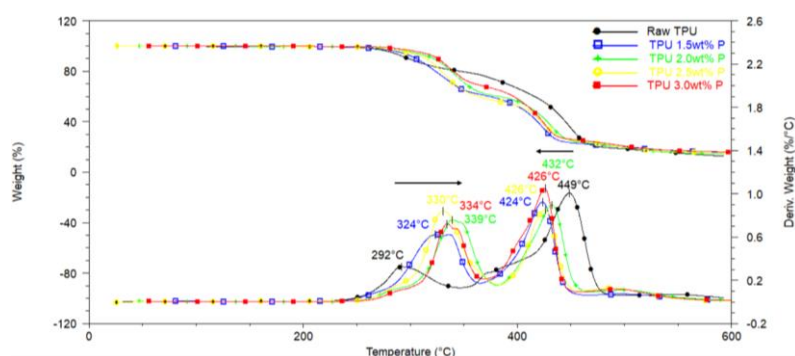


Fig. 3: TGA curves of raw TPU and flame-retardant materials

Acknowledgment

This work has been financially supported by UMONS and University of Lorraine

References

- [1] I. Zagożdżon, P. Parcheta, et J. Datta, « Novel Cast Polyurethanes Obtained by Using Reactive Phosphorus-Containing Polyol : Synthesis, Thermal Analysis and Combustion Behaviors », *Materials*, vol. 14, n° 11, p. 2699, mai 2021, doi: 10.3390/ma14112699.
- [2] H. Vahabi, F. Laoutid, K. Formela, M. Reza Saeb, et P. Dubois, « Flame-Retardant Polymer Materials Developed by Reactive Extrusion : Present Status and Future Perspectives », *Polymer Reviews*, vol. 62, 2022, doi: <https://doi.org/10.1080/15583724.2022.2052897>.
- [3] H. Orelma, A. Tanaka, M. Vuoriluoto, A. Khakalo, et A. Korpela, « Manufacture of all-wood sawdust-based particle board using ionic liquid-facilitated fusion process », *Wood Sci Technol*, vol. 55, n° 2, p. 331-349, mars 2021, doi: 10.1007/s00226-021-01265-x.

PROGRESS IN FLEXIBLE AND RIGID FIRE BARRIERS

R. Kozłowski¹, Z. Malkowski², M. Muzyczek³

1. Journal of Natural Fibers, Editor-in-chief, Professor consultant, Makow Polnych 4, Poznań, Poland

2. ASSA ABLOY. Małkowski-Martech S.A., Kórnik, Poland

3. Journal of Natural Fibers Editorial Board member, Poznań, Poland

INTRODUCTION

Developing innovative and progressive, with high efficiency two types: rigid and flexible barriers, on the base of 3D fibrous structure - protective against fire, acoustic waves, radiation and against biodeterioration for application in transportation, building and defense area – are of great importance. These barriers are the composites characterized by: low density, high strength, high thermal insulation, stability against biodeterioration, shielding radiation and high fire resistance. These barriers are characterized by significant progressive properties in comparison to currently produced and used composites. These improved composites and barriers could be applied in transport as fire blockers in aircraft, in busses, railway wagons, and ships and in building industry mainly as the blockers of fire propagation, more effective fire doors, gates and curtains, as more effective blocker of radiation, bioweapons for construction of specialty military-defense vehicles also resistant to napalm and penetration of toxic gases, shielding the UV, and X-radiation. These barriers can be explored with high thermal insulation properties relevant in whole range of mentioned applications, also in other areas of economy. It is planned the application of newly developed textile 3D fibrous relief and distance knitting materials. The reinforcing this multilayer composites will characterize sufficient strength, light, cool and fire resistance, shielding radiation and acoustic waves. The fibres used for construction of these 3D knittings - are alumina on base of $Al_2O_3 \cdot xSiO_2$ fibres, flexible basalt, melamine, in combination with some chemical fibres (like Aramid Kevlar) and natural fibres (carbon). (1)

EXPERIMENTAL

I. Flexible fire barriers:

1. The experiments on flexible fire barriers based on natural non-woven textiles made of blended wool/hemp fibres, wool/man-made fibres, Lin/Lin FR (flax), were conducted using LOI and cone calorimetry methods. Fire performances were determined. (2)

2. Experiments dealing with assessment of flame retardancy were conducted on upholstery composite with fluffy non-woven as a barrier (Interlinear) and on upholstery composite with needle-punched non-woven PINKWOOL as a barrier with limited flammability (Interlinear). Tests were conducted by cone calorimetry (3)

II. Rigid fire barriers:

1. Rigid fire blockers were tested, containing fire barriers based on exfoliated vermiculite joined by liquid mineral binding agents (products of polycondensation of ammonium polyphosphate with urea and boric acid). The following tests were conducted: thermogravimetric analyses (DTA), studies of non-combustibility of composites 2L[FL+V], evaluation of thermoinsulating properties of composites boards 2L[FL+V] (4)

2. Alumina fibres and basalt fibres, together with carbon and some other ceramic fibres, are the most advanced as reinforcing material in the area of new hybrid composites and modern technologies. (5) Flexible hollow basalt fibres are the future promising fibres reinforcing composites which can be used in difficult extremal working conditions. (6) Flexible hollow fibrous basalt fibres like: straps, roving, threads and fabrics (including 3D) are relatively new perspective in reinforcing materials for obtaining composites of organic and inorganic matrices (7). In comparison to various glass fibres like alkali free alumino – boro – silicate (E-glass), magnesium alumino – silicate (S-glass), their thermo-mechanical and chemical properties are comparable and some uses even better. For example: the modulus of elasticity of basalt roving is better than E-glass. Modern continuous basalt fibres (roving), has a strength close to E-glass and its high modulus of elasticity is typical to high strength magnesium alumino - silicate S-Glass. (8). The adhesive properties of basalt fibres to various polymeric matrices like: phenolic, epoxy, polyurethane, poly-urea, imide and mineral (lime and Portland cement) is stronger than glass-fibres. Also chemical resistance of basalt fibres to acid is high and alkali resistance of basalt fibres is higher in comparison to glass fibres. Below sequence: zirconium > basalt > quartz > alkali free materials shows that expensive zirconium glass fibre could be replaced by cheaper basalt fibres. Addition of some rare earths improve the resistancy of basalt fibres to nuclear radiation including UV and gamma radiation (9). In construction of fire barriers with high fire resistance application of composite, flexible, special barrier materials is latest and the new solution, when we take into consideration so important role of air layer between layers.

RESULTS AND DISCUSSION

I. Flexible fire barriers:

Ad 1. The flammability tests results confirmed, that the tested non-woven fabrics possess the properties of difficult-to-ignite materials and may be used as effective barriers in upholstery systems for furniture, car seats and in bedding in which the ecological aspects are of high significance. (2) (10) (11).

Ad. 2. Needle-punched non-woven made of flax and wool as well as of polyacrylate blend plays excellent role in decreasing flammability and improved significantly the comfort and safety of using home upholstery and mattress. (3)

II. Rigid fire barriers.

The flammability test results performed by LOI and cone calorimetry methods showed significant effect on fire retardancy, viz. prolonged time of ignition, which increased significantly several times, and improved: total heat release rate (total HRR), and maximum heat release rate (max. HRR) (4).

REFERENCES:

- 1) R.M. Kozłowski, M. Muzyczek, J. Walentowska, Flame Retardancy and Protection against Biodeterioration of Natural Fibers: State-of-Art and Future Prospects, In *Polymer Green Flame Retardants*, 801 (2014)
- 2) R. Kozłowski, B. Mieleniak, M. Muzyczek, A. Kubacki. *FIRE MATER Journal*, **26**, 243 (2002)
- 3) R. Kozłowski, M. Muzyczek, B. Mieleniak, *Polym. Degrad. Stab.*, **96**, 396 (2011)
- 4) R. Kozłowski, B. Mieleniak, R. Fiedorow, K. Bujnowicz. *Composites. Part A* **36**, 1047 (2005)
- 5) D. Price D., A.R. Horrocks, Flame resistant ceramic fibres, In: *Handbook of fire resistant textiles*, 272 (2013)

- 6) M. Barczewski et al. Mechanical and thermo-mechanical properties of polyurea composites filled with micro-basalt fibres for spray coatings applications, Book of abstracts of the First ICBFC-2019, Nanjing & Hengshii, China, 39 (2019)
- 7) J.P. West J. P. (ed), Basalt. Types, petrology and uses (Earth Sciences in the 21st century), 1-189 (2012)
- 8) D.D. Johnson, T.E. Sheehan, *J. Coat. Fabr.*, **13**, 97 (1983)
- 9) B.I. Lazoryak, S.I. Gutnikov, Basalt fibers chemical composition variations, Book of abstracts of the ICBFC-2019, Nanjing & Hengshii, China, 7 (2019)
- (10) R.M. Kozłowski, F. Kajzar, Nyszko G., Wertejuk, Majewski K., Mackiewicz-Talarczyk M. & Małkowski Z., *MOL CRYST LIQ CRYST Journal*, **655** (1), 195 (2017)
- (11) R. Kozłowski, Z. Małkowski, Flexible layered fire barriers possibilities of applying basalt fibres, Book of abstracts of the First ICBFC-2019, Nanjing & Hengshii, China, 37 (2019)

INVESTIGATING THE POTENTIAL OF NOVEL FURANOATE POLYESTERS FOR PACKAGING APPLICATIONS

A. Dorigato¹, G. Fredi¹, D. Rigotti¹, D. Perin¹, M. Soccio², N. Lotti², D.N. Bikiaris³ and A. Pegoretti¹

¹ Department of Industrial Engineering and INSTM Unit, University of Trento, via Sommarive 9, Trento, Italy

² Department of Civil, Chemical, Environmental, and Materials Engineering, University of Bologna, via Terracini 28, Bologna, Italy

³ Chemistry Department, Aristotle University of Thessaloniki, Thessaloniki, Greece
andrea.dorigato@unitn.it

INTRODUCTION

One of the most attractive bioderived monomers for novel bioplastics is furandicarboxylic acid (FDCA), obtainable from the fermentation and dehydration of biomass and listed among the twelve strategic building blocks derived from renewable raw materials [1]. Among the wide variety of polymers derivable from FDCA, furan-based polyesters or poly(alkylene furanoate)s (PAFs) are among the most important ones. Obtained through the polycondensation of FDCA with alkylene glycols, PAFs have already demonstrated comparable or superior thermo-mechanical and gas barrier properties than those of the corresponding poly(alkylene terephthalate)s (PATs), which make them suitable for packaging applications [2,3]. On the other hand, Polylactide (PLA) is a promising biopolymer from renewable resources, but its brittleness and poor gas barrier properties limit flexible packaging applications. Therefore, in this work PLA was blended with a biobased rubbery poly(pentamethylene furanoate) (PPeF), acting as a toughening agent, and a commercial epoxy functionalized compatibilizer was added to improve the interfacial interaction. The effect of PPeF loading on phase morphology, mechanical properties, oxygen permeability, and degradability in compost was characterized.

EXPERIMENTAL

Materials

An extrusion-grade PLA Ingeo™ Biopolymer 2500HP was provided by NatureWorks LLC (Minnetonka, MN, USA), having a density of 1.24 g/cm³ and a melt flow index of 8 g/10 min (210 °C, 5 kg). PPeF was synthesized via a two-stage polycondensation synthesis, and had a number-average molecular weight (M_n) of 29600 g/mol. The employed compatibilizer was a poly(styrene-acrylic-co-glycidyl methacrylate), commercially known as Joncryl® ADR 4468 (J), supplied by BASF GmbH (Ludwigshafen am Rhein, Germany), having a density of 1.08 g/cm³, a glass transition temperature of 59 °C, an M_n of 7250 g/mol and an epoxy equivalent weight of 310 g/mol.

Preparation

PLA/PPeF blends compatibilized by J were produced through melt compounding in a Haake™ Rheomix PolyLab™ System (Thermo Scientific, Waltham, MA, USA). The rotational speed of the rotors was set to 60 rpm, and PLA and PPeF were slowly poured into the working chamber, operating at 190 °C for 10 min. The obtained blends were further processed by hot pressing to produce square plates 120 mm wide and 2 mm thick using a Carver hot press, operating at 190 °C for 5 minutes with an applied pressure of 3.4 MPa. Additionally, small pieces cut out from these plates have been further hot pressed for 5 min at 190 °C, to prepare thin films with nominal dimensions of 30×30×0.2 cm³. Samples were prepared with a PPeF concentration variable from 1 wt% to 30 wt% and with a fixed J content of 1 phr.

Characterization techniques

The processability of the prepared blends was investigated through dynamic rheological measurements at 190 °C, while the structural and morphological properties were studied via field-emission scanning electron microscopy (FESEM) and Fourier-transform infrared (FT-IR) spectroscopy. The thermal properties were studied through thermogravimetric analysis (TGA), differential scanning calorimetry (DSC) and dynamic-mechanical thermal analysis (DMTA) in single cantilever bending mode. The mechanical behaviour of the prepared samples was investigated through quasi-static tensile tests. Because some of the examined materials exhibited ductile fracture behavior, the fracture resistance of the prepared films was investigated through an elastoplastic fracture mechanics approach, based on the Essential Work of Fracture (EWF) under plane-strain conditions. The functional properties of the prepared films were investigated in terms of UV-Vis-Near IR transmittance and oxygen permeability. The degradability in compost was studied through compost burial tests at 58 °C under moisture-controlled conditions.

RESULTS AND DISCUSSION

The addition of Joncryl clearly acted as a chain extender, that increased the complex viscosity, storage and loss moduli, and melt elasticity of PLA. The increased frequency dependence and shear thinning behavior confirmed the chain branching and extension induced by the compatibilizer. The incorporation of 10 wt% PPeF into PLA lead to a slight decrease in viscosity compared to neat PLA, and this could depend on the lower viscosity of PPeF compared to PLA. All blends displayed a sea-island morphology, with refined PPeF domains upon compatibilization. The phase separated morphology was also confirmed by FTIR and DSC investigations. Moreover, the crystallinity of PLA was strongly decreased upon the addition of the compatibilizer. Incorporating PPeF induced major tensile ductility enhancements from 5% strain at break for neat PLA up to 200% for the blend with 30 wt% PPeF, accompanied by progressive stiffness and strength declines. Through the application of the Essential Work of Fracture (EWF) approach on the prepared films, the specific essential work of fracture (w_e) was seen climbing from 6.2 to 40.0 kJ/m² with rising PPeF content, confirming its effectiveness as a toughness enhancer. PPeF contributed to increase the UV- and gas barrier properties of PLA. For example, the oxygen permeability dropped by 37% for the blend with 30 wt% PPeF. Moreover, compost burial tests also revealed 26% weight loss of PPeF after 60 days, proving its biodegradability. Hence, finely dispersed PPeF domains induced synergistic property improvements, making PLA/PPeF blends a promising sustainable option for flexible and biodegradable packaging.

Acknowledgments

This research activity has been funded by Fondazione Cassa di Risparmio di Trento e Rovereto (CARITRO, grant number 2020.0265), and has been based upon work from COST (European Cooperation in Science and Technology) Action FUR4Sustain (CA 18220).

References

- 1) G. Fredi, A. Dorigato, M. Bortolotti, A. Pegoretti, D.N. Bikiaris, *Polymers*, **12**, 2459 (2020)
- 2) D. Perin, D. Rigotti, G. Fredi, G.Z. Papageorgiou, D.N. Bikiaris, A. Dorigato, *J. Polym. Environ.*, **29**, 3948 (2021)
- 3) S. Santi, M. Soccio, G. Fredi, N. Lotti, A. Dorigato, *Polymer*, **279**, 126021 (2023)

Zein-Based Nanoparticles as Sustainable and Active Platforms with potential applications in agriculture

Mariamelia Stanzone^{1*}, Emilia Oleandro¹, Giovanna Giuliana Buonocore¹, Sara Paola Nastasi², Bianca Maria Orlando Marchesano², Maria Cristina Bonza² and Marino Lavorgna^{1,3}

¹ Institute of Polymers, Composites and Biomaterials-CNR, Piazzale E. Fermi 1, 80055 Portici, Italy

² Department of Biosciences, University of Milano, Via Celoria 26, 20133 Milano-Italy

³ Institute of Polymers, Composites and Biomaterials-CNR, Via Previati 1/E, 23900 Lecco, Italy

*mariamelia.stanzione@cnr.it; Tel.: +39-34-9386-0676

INTRODUCTION

Due to their unique structural and functional properties, nanomaterials are widely investigated for potential applications in different industrial sectors, from cultural heritage to agriculture. In this context, protein-based nanoparticles represent a promising and sustainable platform for encapsulating and protecting bioactive compounds due to their abundance, non-toxicity and stability and, as engineered nanocarriers, tailoring the active release of compounds on demand [1,2].

The aim of this work is to develop nanoparticles based on plant protein, such as zein extracted from maize as nanocarriers with twofold functionalities, respectively, to preserve the integrity and efficiency of selected molecules with bioinsecticide activity against phytopathogens and to act as carrier to deliver biomolecules into plant leaves, under appropriate pH and temperature conditions. As model system the nanoparticles embed fluorescein, to track the nanoparticles fate inside plant tissues. Their compatibility with plant physiology has been also analyzed.

EXPERIMENTAL

Materials

Zein protein (CAS number 9010-66-6), Fluorescein-5-maleimide (Ultra-Pure; CAS number ENZ-52502, MW: 427,37 g/mol) and Ethanol Absolute (CAS: 64-17-5, density: 0.79 kg/l) were purchased by Merc (Sigma Aldrich), by Enzo Biochem Inc and by VWR Chemicals, respectively. All reagents were used as received.

Preparation

Zein-based nanoparticles were obtained by an antisolvent precipitation method. Zein powder was dissolved in a hydroalcoholic solvent phase under magnetic stirring for three hours, subsequently a suitable amount of fluorescein was added. The resulting zein/fluorescein-based solution was dripped into the antisolvent phase, consisting of deionized water using a burette. A solvent/antisolvent ratio of 1:4 was considered and the antisolvent phase was maintained under magnetic stirring at 750 rpm. The NPs suspension was stored at 4°C, while 5 mL of the suspension was frozen and lyophilized, for physico-chemical and morphological characterization.

Dynamic Light Scattering, morphological characterization and analysis in plant tissues

DLS measurements were performed with a Malvern Zetasizer Nano ZS instrument. Morphological investigations were carried out by using scanning electron microscope (Quanta 200 FEG, FEI, The Netherlands).

Localization of fluorescein-labelled zein-based NPs was performed by a confocal laser scanning Nikon AX Eclipse Ti2 microscope.

Potential phytotoxicity of zein-based NPs was monitored by estimating the photosynthetic performance of tomato leaves [effective quantum yield —Y(II)— of photosystem II] by Imaging PAM MAXI-mode (WALZ).

RESULTS AND DISCUSSION

Figure 1A reports SEM captures of both zein and zein/fluorescein NPs used to compute the average particle size (MD) and polydispersity index (PDI). It is worth noting that when the NPs are marked with fluorescein, the average NPs dimension is lower than the corresponding zein NPs. Moreover, the smaller PDI value for the Zein/fluorescein supports the conclusion that the resulting size curve distribution becomes narrow.

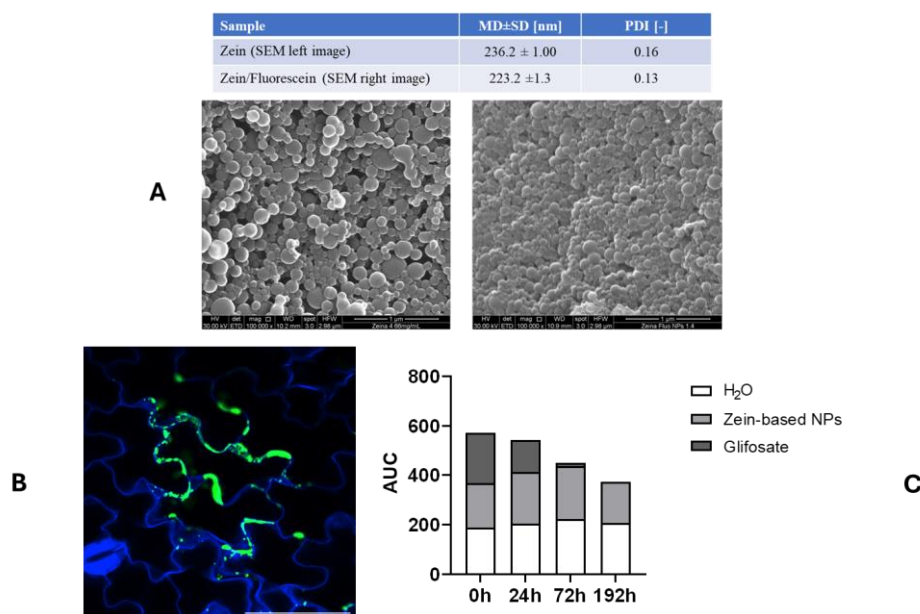


Figure 1. **A**: Average particle size, polydispersity index (PDI) SEM captures of both zein and zein/fluorescein NPs; **B**: Localization of fluorescein-labelled zein-based NPs by confocal laser scanning microscopy 24h after foliar spraying; **C**: Photosynthetic efficiency of treated plants measured by PAM imaging. AUC (area under the curve) of light curves.

Tomato leaves were sprayed with fluorescein-labelled zein based NPs, washed with water, stained with Renaissance® dye and imaged by confocal microscopy. Zein-based NPs (in green in Fig. 1B) rapidly penetrate within the tomato leaves and accumulate in the apoplast of the epidermal layer as indicated by the co-localization which marks the cell walls (in blue in Fig. 1B).

Tomato plants were sprayed respectively with water (negative control), with zein/fluorescein-based NPs or with glyphosate (an herbicide used as positive control) and later analyzed at different time points. The glyphosate rapidly impairs photosynthesis, whereas zein-based NPs do not affect photosynthetic efficiency, therefore the synthesized Zein based NPs results fully compatible with plant physiology.

Acknowledgment

This work has been financially supported by the “Bio-Inspired Plant Protection-BIPP” PRIN2020.0000454.23-01-2021 research project.

References

- 1) Mittal D., Kaur G., Singh P., Yadav K., Ali S.A. Nanoparticle-based sustainable agriculture and food science: Recent advances and future outlook. *Front. Nanotechnol.* 2020, 2, 579954.
- 2) Oleandro E., Stanzione M., Buonocore G.G., Lavorgna M. Zein-Based Nanoparticles as Active Platforms for Sustainable Applications: Recent Advances and Perspectives. *Nanomaterials* 2024, 14, 41.

The importance of melting in 3D printing

Sara Liparoti¹, Dario Cavallo², Maria Laura Di Lorenzo³, Targol Hashemi¹, Aldo Romano¹, Roberto Pantani^{1*}

¹ Dipartimento di Ingegneria Industriale, University of Salerno, Italy

² Dipartimento di Chimica e Chimica Industriale, University of Genova, Italy

³ CNR - Istituto di Chimica e Tecnologia dei Polimeri, Caserta, Italy

*rpantani@unisa.it

INTRODUCTION

Additive manufacturing, namely 3D printing, is attracting increasing interest in the industrial field since it allows obtaining parts with complex shape that are challenging to obtain with conventional processes. In particular, 3D printing of polymers is able to construct the object through the deposition of extruded bead on a deposition plate. Although interesting, 3D printing of polymers is challenging due to several phenomena that are not completely understood. For instance, the presence of seeds of crystallization due to an incomplete melting induces a faster crystallization with consequent effects on the adhesion between adjacent beads. If the crystallization is faster than the reorganization of molecules at the interface between adjacent beads, the molecules will not interact and the adhesion will be poor. Otherwise, if crystallization occurs later in the process, it will increase the interaction at the interface, and the adhesion will be strong. This work aims at assessing the effect of previous crystallization on the mechanical performances of 3D printed parts. A PLA filament has been obtained by extrusion and annealed at different temperatures to achieve desired crystallization degree. The filament has been used during the process conducted with different extrusion ratios to obtain the parts. The higher the extrusion ratio, which means flow rate, the higher the crystallinity and the orientation of the part are. The crystallinity degree and the orientation achieved during the process are correlated with the residence time of polymer inside the extruder.

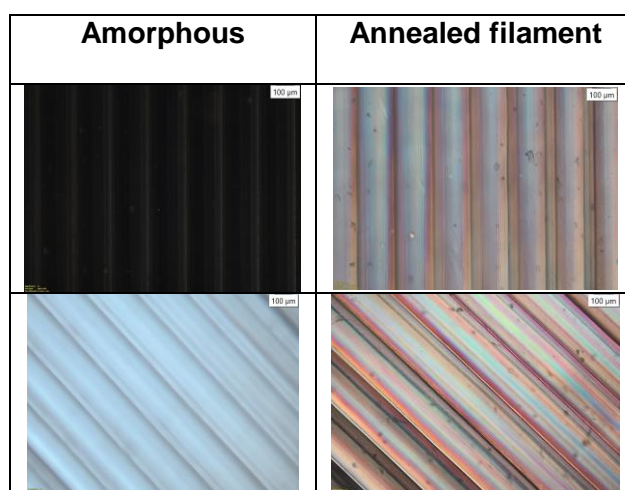


Figure 1 Optical micrographs of the parts obtained from an amorphous filament and from an annealed crystalline filament with 170°C nozzle temperature. The topmost micrograph is related to the part oriented at 45° with respect to the analyzer, the bottommost micrograph is related to the part oriented parallel to the analyzer.

Blends of Virgin and Recycled PP from Personal Protective Equipment: Correlation Between Rheological, Structural and Mechanical properties

Francesco Palmieri¹, Maria Chiara Riccelli¹, Giulia Infurna², Nadka Tz. Dintcheva², Alessia Romani³, Marinella Levi³, Loredana Incarnato¹

¹Department of Industrial Engineering, University of Salerno, Fisciano, SA, Italy

²Department of Engineering, University of Palermo, Palermo, Italy

³Department of Chemistry, Materials, and Chemical Engineering "Giulio Natta", Politecnico di Milano, Milano, Italy

INTRODUCTION

Despite being the mostly used polymer in EU, polypropylene (PP) is one of the least recycled plastics at a rate of ca. 5% of post-consumer recovery (1), in fact the heterogeneity of the waste stream and the rapid thermo- and photo-degradation, occurring during its service life and reprocessing, strongly hinder its recycling. PP is also used for the production of Personal Protective Equipment (PPE), such as face masks, single use gowns, etc., that are responsible for the 28% of total urban waste, creating an emerging threat to the environment (2).

This study involved a thorough face masks characterization followed by their mechanical recycling. Virgin/recycled PP blends at different weight proportions were then prepared by melt compounding and analyzed through an extensive rheological characterization, with the aim to assess their processability with the conventional technologies of film extrusion. Additionally, the structural characteristics (morphology and crystallinity) of the obtained samples were correlated with their final mechanical performances.

EXPERIMENTAL

Materials

In this study Moplen HP515M, grade for extrusion film with a density of 0.90 g/cm³, was supplied by LyondellBasell and used as virgin PP. Recycled PP (rPP) was produced by mechanical recycling of 3-ply face masks (net weight 4.41 0.05 g).

Preparation

The recycled PP was produced by mechanical recycling of the face masks, that were thermopressed with a Carver laboratory press (T = 200°C, P = 6000 Pa, for 5 min), grinded and fed to a Brabender Do-Corder 330 single-screw extruder (D=20 mm; L/D=20). A screw speed of 30 rpm was imposed, and a temperature profile of 165 - 170 - 170 °C was set along the barrel.

The PP and rPP pellets at different PP/rPP ratios (50/50, 70/30, 90/10 by weight) were melt and mixed in a Collin ZK 25-48D co-rotating twin extruder (D = 25 mm, L/D = 42), at a screw speed of 100 rpm and with a temperature profile of 185 - 185 - 185- 190 - 190 - 190 - 190 - 185 °C. The extruded strand was air-cooled and then pelletized.

Mechanical and rheological characterization

Mechanical tests were carried out using the CMT 4000 Series tensile tester (SANS, China) in accordance with ASTM D882-18.

Dynamic shear rheological experiments were performed out with an ARES rotational rheometer. Tests were performed with parallel-plate geometry (d=25 mm), at 190°C.

RESULTS AND DISCUSSION

Figure1 illustrates the rheological behavior of virgin and rPP and their blends at 190°C. The recycled material exhibits the lowest viscosity values across the investigated frequency

range, while the blends show intermediate η^* values compared to those of the two pure components. These findings align with the melt flow index data.

The Van Gurp–Palmen plots were determined for all the materials investigated which showing one phase and a plateau in the low G^* region tending towards 90°C , which is the typical behavior of linear polymer melts.

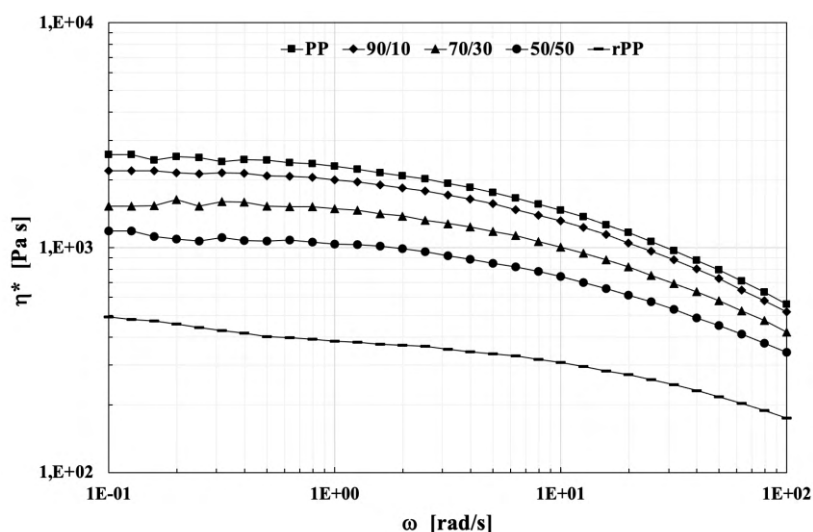


Fig. 1 (a) Viscosity curves of all the materials investigated at 190°C

Increasing the amounts of recycled PP in the blends a progressive stiffening of the materials is observed. Specifically, the elastic modulus increased from 648 ± 7 MPa, for the virgin PP to 738 ± 32 MPa for the blend at 50wt% of rPP. This was associated with a decrease of ca. 30% in the strain at break for all the blends compared with the virgin PP. These outcomes can be reasonably attributed to the increased crystallinity of the blends respect to the virgin PP.

Further analyses are ongoing to assess the processability of the recycled PP and its potential use in film extrusion and 3D printing.

Acknowledgment

This work has been financially supported by the MIUR Project "FUTUREVAL-PPE" (FUnctional Technology Unlocking and VALorization of Personal Protective Equipment production scrap and waste).

References

- 1) Selvaranjan, K. et al., 2023. Environmental challenges induced by extensive use of face masks during COVID-19: A review and potential solutions, *Environmental Challenges*, Volume 3, p. 19683–19704
- 2) Battegazzore, D., Cravero, F., Frache, A., 2020. Is it possible to mechanical recycle the materials of the disposable filtering masks? *Polymers*, Volume 12, p. 2726.

DURABILITY OF FLAME-RETARDED POLYMER, 3D PRINTABLE FOR RAILWAY INDUSTRY

R. Baron^{a, b, c}, L. Geoffroy^a, N. Gay^a, G. Fontaine^b, B. Fayolle^c and S. Bourbigot^{b, d*}

^a 4D Pioneers, 59650 Villeneuve d'Ascq, France

^b Univ. Lille, CNRS, INRAE, Centrale Lille, UMR 8207 – UMET – Unité Matériaux et Transformations, F-59000 Lille, France

^c Laboratoire PIMM, Arts et Métiers Sciences et Technologies, CNRS, Cnam, HESAM Université, 151 Boulevard de l'Hôpital, 75013, Paris, France

^d Institut Universitaire de France (IUF), Paris, France

roxane.baron@4dpioneers.com, *serge.bourbigot@centralelille.fr

INTRODUCTION

The railway industry employs a range of plastic materials that are subject to rigorous fire and smoke requirements to comply with the specifications of the EN 45545 standard. However, only a limited number of plastic materials have been able to meet the HL2-R1 criteria. In this project, a novel 3D printable polymer, composed of HDPE and meeting HL2-R1 criteria, was developed in collaboration between 4D Pioneers and UMET for the railway industry. This matrix can be 3D printed, is known for its excellent oxidation stability and was selected for use within the trains. The new formulation is printable and certified HL2-R1 on unaged material. The initial objective of this project is to investigate the influence of ageing on the fire and smoke properties of the material. To this end, accelerated thermal ageing tests were conducted under air on samples prepared by thermocompression. The fabrication of 3D printed parts will be the subject of a subsequent investigation.

In this work, the preparation and characterization of the material used are described and some results about the evolution of fire properties after thermal ageing are shown.

EXPERIMENTAL

Materials

The material used in this work is composed of fibers reinforced high-density polyethylene (HDPE) with flame-retardant (FR) fillers (patent pending). This formulation contains a combination of flame-retardants: (1) intumescent fillers, (2) smoke suppressors and (3) synergistic agents.

Preparation

The formulation was extruded with a co-rotative twin screw extruder from Thermo Scientific (HAAKE Rheomix OS PTW 16) with a screw diameter of 16 mm and a barrel length of 40 mm. The filament at the end of the extruder was cooled down with air and then granulated. The pellets obtained were thermocompressed with a hydraulic hotpress (Fontune, Fontijne Grotnes B. V., Niles, Michigan, United States) at 150 °C and 250 kN for 28 min to obtain 100 × 100 × 3 mm³ samples. Finally, these plates were placed in ventilated ovens at 3 different temperatures (120 °C, 110 °C and 100 °C).

Fire/smoke characterizations

The fire/smoke properties were measured with 3 different machines: (1) critical flux at extinguishment was determined with a lateral flame spread at small scale bench, (2) smoke opacity and toxicity were analyzed thanks to an adapted smoke box and (3) the maximum average rate of heat emission was measured with a mass loss calorimeter (MLC). These tests were derived from ISO 5658, ISO 5659 and ISO 5660 standards respectively as required for HL2-R1 of EN 45545.

RESULTS AND DISCUSSION

Samples were fire tested after several days of thermal ageing under air. The 3 fire tests were realized on aged plates at 120 °C, 110 °C and 100 °C and several exposure times for these temperatures. Results of MLC test on aged samples at 120 °C up to 96 days are shown in Fig. 1. Char formed after 1200 s of MLC test (**Fig. 1.a**) and heat release rate (HRR) curves (**Fig. 1.b**) are shown for each ageing time. It appears that thermal exposure has an impact on the charring and the heat released: the structure of the char (creation of a hollow structure vs. well distributed foamy structure) and the peak of heat release rate (increase of the peak of HRR) are modified because of the ageing.

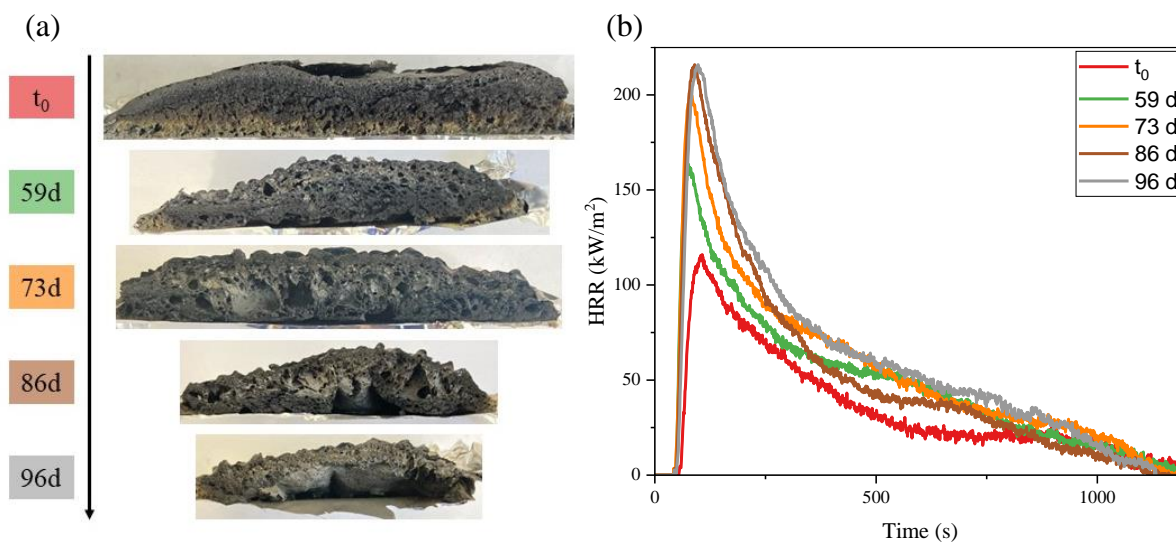


Fig. 1 (a) Pictures of char after MLC test and (b) Heat release rate (HRR) curves at several exposure times.

The char acts as a barrier that protects the material from the heat or the flame and allows it to decrease its decomposition¹. For instance, the aged samples, tested after 59 days, exhibited a distinct char development during the fire test. In particular, the size of the internal pores increased as a function of time, ultimately forming a hollow structure beneath the material after 96 days at 120 °C. This porosity growth can be linked to the HRR rise for a given exposure time. This HRR increase indicates a significant drop in fire properties with ageing.

Other fire tests were performed as lateral flame spread and will be also discussed in the talk. Physico-chemical analyses (IR, rheological properties, microscopy, solid state NMR of ³¹P, ¹³C and ²⁷Al, ...) of the matrix, FR fillers or on the char have been carried out to gain a better understanding of the mechanisms involved and will be presented.

Acknowledgment

This work has been financially supported by the National Research and Technology Association (ANRT) and 4D Pioneers for this thesis

References

1. Bourbigot, S., Le Bras, M., Duquesne, S. & Rochery, M. Recent Advances for Intumescent Polymers. *Macromol. Mater. Eng.* **289**, 499–511 (2004).

MULTIFUNCTIONAL POLYMER COMPOSITES PRODUCED BY ADDITIVE MANUFACTURING

Emanuela Tamburri¹, Luca Montaina¹, Francesca Pescosolido¹, Rocco Carcione², Silvia Battistoni²

¹Dip.to di Scienze e Tecnologie Chimiche, Università degli Studi di Roma “Tor Vergata”, Via della Ricerca Scientifica, Rome, Italy

²Consiglio Nazionale delle Ricerche - Institute of Materials for Electronics and Magnetism (CNR-IMEM) Parco Area delle Scienze 37A, Parma, Italy

emanuela.tamburri@uniroma2.it

INTRODUCTION

Additive manufacturing (AM), or 3D printing, has greatly facilitated the production of polymer composites by allowing precise fabrication of complex geometries and internal structures. This flexibility enables the creation of materials with tailored mechanical, electrical, and thermal properties for specific applications. Common 3D printing methods include Fused Deposition Modelling (FDM) and Stereolithography (SLA). Polyvinyl alcohol (PVA), polycaprolactone (PLC), and polyethylene glycol diacrylate (PEGDA) were chosen as polymeric matrices to develop printable inks using these two techniques, while detonation nanodiamonds (ND) [1], graphene platelets (GP), poly(3,4-ethylene-dioxythiophene) (PEDOT) [2], and polyaniline (PANI) [3-6] were used as fillers to enhance mechanical, thermal, and electrical properties of the printed polymer samples.

In this work we report the best results we obtained in printing by FDM and SLA 3D polymer composite items having the suitable characteristics as active materials for implementing volatile organic compounds' (VOCs) sensing devices [2], scaffold substrates for cell growth and proliferation [3], as well as for electrocardiogram (ECG) [4] and pH [5] monitoring systems.

EXPERIMENTAL

Extrusion Printing

PVA-ND inks were prepared starting from PVA and ND dispersions that were mixed to obtain aqueous dispersions with a final concentration of 10%_{w/w} of PVA and of 0.1, 0.5, 1 and 5%_{w/w} of ND with respect to PVA.

PVA-GP inks were prepared by dispersing GP, which were extracted from the shungite mineral by means of a proper optimized protocol, into 5%_{w/v} PVA aqueous solution (1%_{w/w}).

The PVA-ND and PVA-GP inks were printed by a Mendel 3-RepRapPro[®] 3D printer specifically designed and custom-assembled for layering slurries with different physical properties [1].

Stereolithography Printing

PEGDA-PEDOT inks were obtained by dispersing from 5 to 45 %_{w/w} polystyrene sulfonate – doped PEDOT (PEDOT:PSS) in a PEGDA/photoinitiator photosensitive resin [2].

Three different processing methodologies were adopted for using PANI as filler of 3D SLA printed items: i) PANI addition into the photosensitive resin [3]; ii) in situ polymerization of aniline monomer during the printing process [4]; iii) in-situ polymerization of aniline monomer within PEGDA printed items [5][6].

A commercial ELEGOO Mars SLA 3D printer was appropriately customized to enable prints with a reduced amount of material. The printer was equipped with a 405 nm LED with a power of 40 W and characterized by a printing resolution of 47 μm on the XY plane and of 1.25 μm on the Z axis.

RESULTS AND DISCUSSION

In Fig. 1 typical 3D items produced by modified polymer inks are reported. In particular, in Fig. 1-a a PVA-GP sample printed by extrusion is shown while a PEGDA-PEDOT:PSS double helical and a PEGDA-PANI woodpile printed by stereolithography are illustrated in Fig. 1-b and c, respectively.

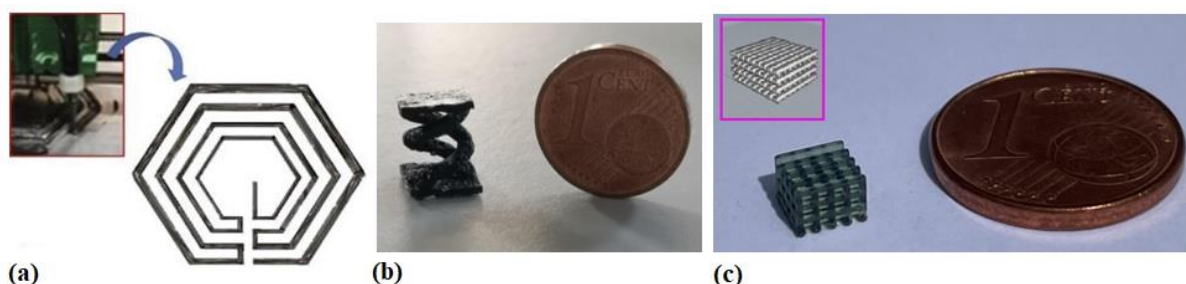


Fig. 1 (a) PVA-GP sample produced by extrusion printing [1]; (b) PEGDA-PEDOT:PSS helical item [2] and (c) PEGDA-PANI woodpile structure both produced by stereolithography.

The appropriate experimental conditions, both relating to the relative concentrations of the various inks and to the printing parameters, have allowed the production of objects with a controlled electrical conductivity and specific functional properties suitable for the creation of: i) scaffolds that imitate the hierarchical structure of cardiac myofibers (Fig. 2-a); ii) systems that can interact with chemical vapors in the long term for VOCs monitoring systems based on cumulative adsorption effects (Fig.2-b); iii) soft and flexible electrodes implementable in ECG devices (Fig. 3-c).

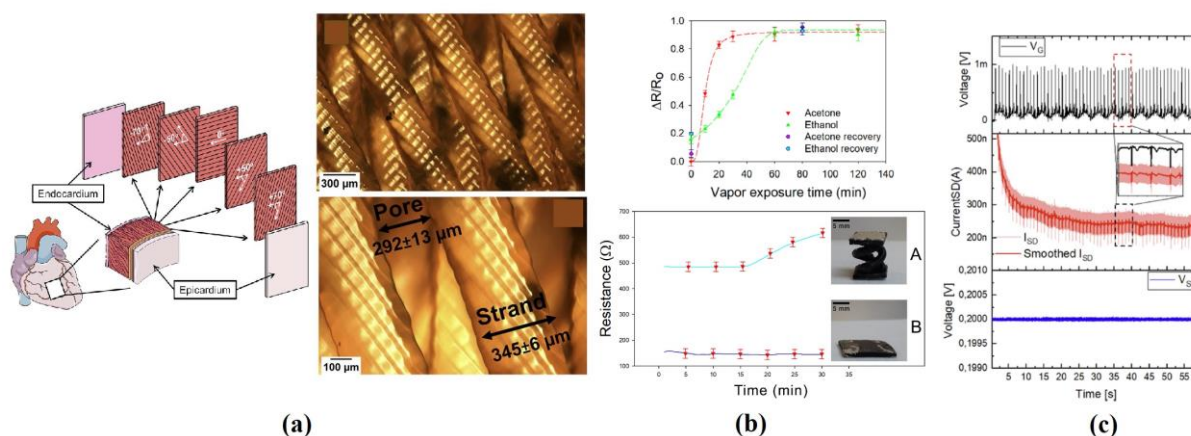


Fig. 2 (a) PEGDA-PANI sample mimicking the structure of cardiac myofibers [3]; (b) Normalized resistance variation of PEGDA:PEDOT double helical sample vs acetone and ethanol exposure times, and comparison between the resistivity of the double helical and parallelepiped shape under acetone exposure [2]; (c) Amplitudes of the FFT analysis for the ECG monitoring from PEGDA-PANI electrodes [4].

References

- 1) M. Angjellari, E. Tamburri, L. Montaina, et al., *Materials Design*, **119**, 12–21 (2017)
- 2) G. Scordo, E. Tamburri, L. Scaltrito, et al., *Nanomaterials*, **11**, 94 (2021)
- 3) A. Ul Haq, E. Tamburri, P. Di Nardo, et al., *Scientific Reports*, **13**, 1–14 (2023)
- 4) L. Montaina, S. Battistoni, E. Tamburri, et al., *ACS Applied Electronic Materials*, **5**, 164–172 (2023)
- 5) R. Carcione, E. Tamburri, S. Battistoni, et al., *Gels*, **9**, 784 (2023)
- 6) R. Carcione, E. Tamburri, S. Battistoni, et al., *ACS Applied Polymer Materials*, **6**, 1159–1168 (2024).

Solid-State Modification for Improved Flame Retardancy

R. Mincheva^{a*}, Carolane Gerbehaye^a, Katrien V. Bernaerts^b, Gaëlle Fontaine^c, Serge Bourbigot^{c,d} and J.M. Raquez^a

^a Laboratory of Polymeric and Composite Materials, University of Mons, Mons, Belgium

^b Sustainable Polymer Synthesis Group, Aachen-Maastricht Institute for Biobased Materials (AMIBM), Maastricht University, Brightlands Chemelot campus, Urmonderbaan 22, 6167 RD, Geleen, the Netherlands.

^c University of Lille, CNRS, INRAE, Centrale Lille, UMR 8207 - UMET - Unité Matériaux et Transformations, F-59000 Lille, France.

^d Institut Universitaire de France, Paris, Île-de-France, FR 75005.

*Laboratory of Polymeric and Composite Materials, University of Mons, Mons, Belgium

Rosica.Mincheva@umons.ac.be

INTRODUCTION

The flammability of polymers raises concerns with an average of 5,000 building fires daily in Europe¹ and requires intumescent polymer-based flame-retardant materials (FR). Intumescence via polymer additivation evokes concerns and guides FR chemistry to (1) the use of renewable and sustainable resources², and (2) the use of inherently intumescent materials and the pathways to obtain them are very limited.³

This study is the proof-of-concept towards an inherently flame-retardant semi-crystalline aromatic polyester using biobased (co)monomers via solid-state modification (SSM) technique. The SSM process was optimized on PBT and a diol sugar derivative as model couple and the thermal resistance and flammability of the resulting copolyesters were assessed. These polymers in combination with ammonium polyphosphate could be used to form an intumescent material.

EXPERIMENTAL

Materials

The PBT (Ultradur® B 6550, BASF AG, \overline{M}_n given by the supplier is 13,000 g/mol) was used as received. The diol sugar derivative (GalX) was synthesized through three steps from mucic acid (Sigma Aldrich) following the procedure reported by Prömpers et al. (yield: 75 %).⁴ The catalyst, dibutyl tin oxide (DBTO, 98%), was purchased from Sigma-Aldrich and used as received. The ammonium polyphosphate (APP) is an Exolit® AP 422 purchased from Clariant.

Preparation

PBT pellets were milled beforehand in an IKATM analytical mill to obtain a raw granulometry powder (250 μm) and five different compositions (PBT, P(BT-co-GalXT), PBT₅₀P(BT-co-GalXT)₅₀, PBT₃₂P(BT-co-GalXT)₃₂APP₃₆, PBT₆₀APP₄₀) were prepared using a Retsch CryoMill© with an auto pre-cooling cycle. SSM was performed in a specially designed Inox Autoclave-France reactor with an anchor shaped overhead stirrer in the presence of DBTO (300 ppm relative to the polymer mass) as catalyst. Bar specimens (127 x 12.7 x 3.2 mm) were prepared by compression molding (Carver 4122CE manual thermopress).

Rheological and physico-chemical characterization

¹H and ³¹P dipolar decoupling (DD) solid-state magic angle spinning (MAS) NMR experiments and Fourier-Transform Infrared Spectroscopy (FTIR) were performed to determine chemistry and composition of samples after SSM and UL 94 tests. The molecular weight of the polyesters was determined by size exclusion chromatography (SEC). Thermal properties were investigated with differential scanning calorimetry (DSC) and

thermogravimetric analysis (TGA). UL 94 (ASTMD 3801) vertical burning tests were used to test the flammability.

RESULTS AND DISCUSSION

The synthesis of P(BT-*co*-GalXT) via SSM of PBT with GalX as comonomer (Figure 1A) can be described as consisting of two major steps: (1) chain scission and transesterification reactions between GalX, and butanediol residues in PBT at temperatures between the polyester T_g and T_m ; (2) chain recombination reactions rebuilding P(BT-*co*-GalXT) molar mass. The occurrence of transesterification reactions was followed by ^1H NMR and quantitative analyses estimated GalX conversion and content in the P(BT-*co*-GalXT) to be around 80% and above 30%, respectively.

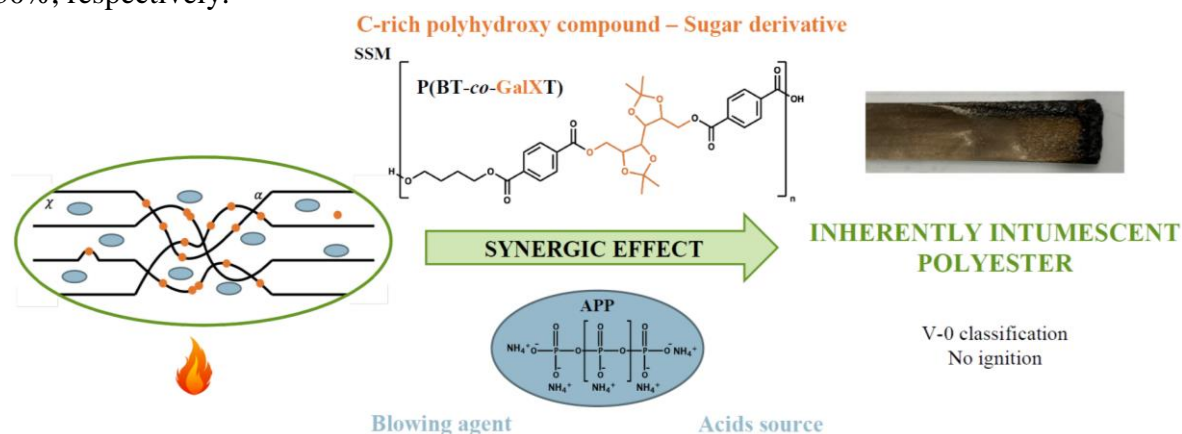


Fig. 1 Schematic representation of the SSM between PBT and GalX for the obtaining of intumescent materials

The thermal decomposition behavior of PBT and P(BT-*co*-GalXT) analyzed by TGA in pyrolysis conditions changed from single-step degradation to double-stage thermal decomposition, respectively while the residue at 800 °C increased by a factor of 2.5.

A standard UL 94 test - one of the most widely used fire tests for studying the relative flammability of plastic materials - was then performed to evaluate the flammability of the newly obtained copolyester and showed P(BT-*co*-GalXT) samples V-2 behavior at a thickness of 1.6 mm and a V-0 rating at 3.2 mm. To reduce material cost, a blend of PBT and P(BT-*co*-GalXT) at a 1:1 wt ratio was prepared and proved V-0 but with not inflammable plastic dripping. Despite these overall good results, no real carbonaceous layer was formed on the surface, attesting for the lack of intumescence. To this, APP was added to PBT/P(BT-*co*-GalXT) 1:1 at 4.5 % phosphorous content to result in a PBT/P(BT-*co*-GalXT)/APP composition satisfying all requirements for V-0 intumescent materials.

Acknowledgment

Authors acknowledge support from the European Community (FEDER) in the frame of LCFM-BIOMAT, and OPTI2MAT program of excellence. The Bioprofiling platform (NMR tests) was also supported by the European Regional Development Fund and the Walloon Region, Belgium. Jean-Marie Raquez is a FRS-FNRS senior scientific researcher.

References

- 1) S.V. Sokolov, P. Wagner, J.R. Hall, Report No 10 of Centre of Fire Statistics of CTIF (2021)
- 2) V.M. Kolb, Green Organic Chemistry and Its Interdisciplinary Applications (2017)
- 3) H.B. Zhao, Y.Z. Wang, Macromol. Rapid Commun., **38**, 1 (2017)
- 4) G. Prömpers, H. Keul, H. Höcker, Green Chem., **8**, 467 (2006)

3D PRINTED HIGHLY POROUS HOLLOW DEVICES FOR LONG-TERM CONTROLLED RELEASE

Balsamo M.^{1,2}, Mistretta M.C.^{1,2}, Scaffaro R.^{1,2}

¹Department of Engineering, University of Palermo, Palermo, Italy

²National Interuniversity Consortium of Materials Science and Technology (INSTM),
Florence, Italy

marta.balsamo01@unipa.it, mariachiara.mistretta@unipa.it, roberto.scaffaro@unipa.it

INTRODUCTION

The possibility to obtain resistant and reusable hollow devices with differentiated high porosity for storage and tunable long-term controlled release of substances is difficult to achieve efficiently. To solve this problem, we propose a combined melt-wet processing, which allows predictable and tunable morphologies. The process consists in combining Material Extrusion (MEX) with an eco-friendly salt leaching in distilled water, by using a biostable polymer and high percentages of saline porogen. The mixtures were extruded and the filaments were printed in devices that appear porous after leaching. Morphological, chemical and mechanical characterizations were conducted before and after printing and before and after leaching in order to analyze the properties of the blends and devices. Finally, the release kinetics of methylene blue, selected as a model molecule, was evaluated, to demonstrate the possibility of using them as reusable and tunable controlled release reservoir-type devices.

EXPERIMENTAL

Materials

The raw materials used in this work were nylon 6 (Ny6) (Radilon S35 100 NAT, $\rho_{\text{Ny6}} = 1.14 \text{ g/cm}^3$), as matrix, and sodium chloride (NaCl) (Fluka, Honeywell, $\rho_{\text{NaCl}} = 2.16 \text{ g/cm}^3$), as porogen.

NaCl was processed in three different ways in order to produce three samples with different particles dimensions. The prepared three samples were coded on the base of NaCl size fraction: NaCl_A, with particles diameter ranging between 1 and 250 μm ; NaCl_B with particles diameter ranging between 0.5 and 50 μm ; NaCl_C with particles diameter ranging between 0.5 and 15 μm .

Preparation

Ny6/NaCl filaments in the three blends were produced by extrusion (260°C, 6 bar, 50 rpm, 1 min of recirculating) using HAAKE Minilab II (Thermo Scientific, USA), with composition 30/70%wt, producing three different filaments, namely Fil_A, Fil_B and Fil_C. All filaments produced have diameters of 1.75 mm, suitable for the 3D printer. The porous hollow devices (HD), coded HD_A, HD_B and HD_C, were produced by Material Extrusion (MEX) additive manufacturing process (Sharebot Next Generation, Nibionno) of previously extruded blends filaments Fil_A, Fil_B and Fil_C respectively. The aim was to produce cylindrical hollow devices with inner diameter of 7 mm, height of 5 mm, base thickness of 1 mm and lateral wall thickness of 1 mm. The devices produced were subjected to salt leaching in distilled water and vacuum drying.

Rheological and physico-chemical characterization

Filaments and printed devices were characterized from a morphological, physico-chemical and functional point of view. In particular, the morphology of particles and pores was evaluated by SEM Phenom ProX (Thermo Scientific, USA). The rheological tests were conducted using a rotational rheometer (ARES-G2, TA Instruments, USA), in frequency sweep mode, in order to assess the processability of blends. Mechanical tensile (on the filaments) and compression (on the printed devices) tests were conducted in order to assess

the printability of the former and to simulate the application conditions of the latter, by using an Instron 3365 machine (UK). Moreover, the thermal behaviour of Ny6 and of Ny6/NaCl leached filaments subjected to the various extrusion/leaching processes was investigated by differential scanning calorimetry (DSC), in order to assess any changes in crystallinity to be attributed to processing. The real porosity of the printed devices was evaluated by gravimetric analysis and pycnometry to verify the leaching efficiency. Finally, methylene blue was used as a model molecule to verify the device capability to control release and data were fitted according to Korsmeyer-Peppas kinetic model.

RESULTS AND DISCUSSION

All blends exhibited rheological and mechanical behaviour sufficiently suitable for 3D printing: in fact, the final devices were successfully manufactured, using all prepared formulations. The porogen showed good dispersion in both the filaments and the printed devices, and the pores appeared well distributed in the cross-sections after leaching. Pore distribution range was consistent with the distribution range of the three salt samples, so the morphology of the systems is predictable and adjustable. An interesting decrease in particles and pores size was found in all lateral surfaces, which can be attributed to the fluid dynamics of the porogen inside the extruder and printer nozzle, as shown in Figure 1.

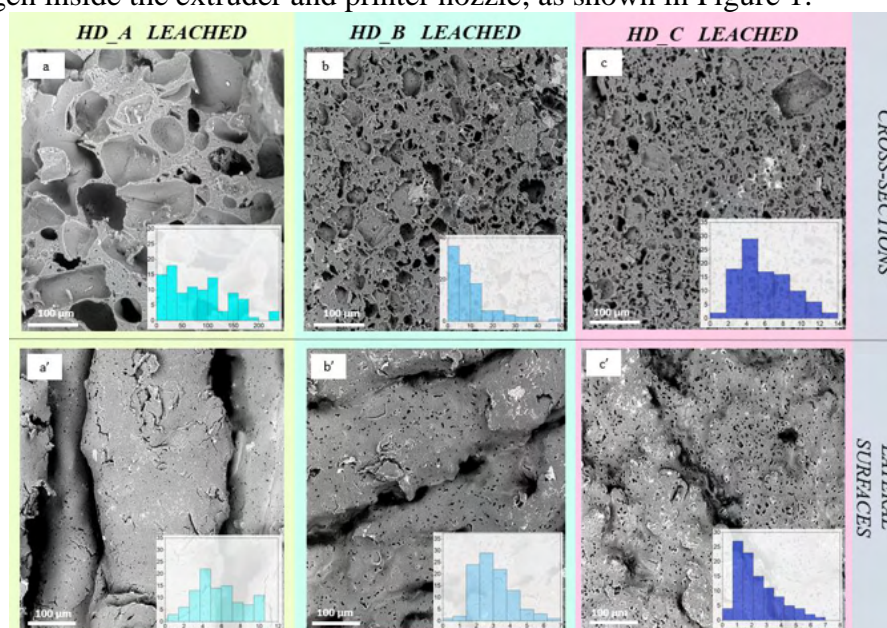


Figure 1 SEM images of leached printed devices sections (a - c), lateral surfaces (a' - c') and histograms of pores diameters distribution: HD_A leached (a, a'), HD_B leached (b, b'), HD_C leached (c, c'). Scale bar is 100 μm .

Printed devices after leaching showed high percentages of real porosity, similar to theoretical porosity, a quantitative symptom of total leaching. Despite the high degree of voids, they have maintained sufficient compressive mechanical properties, even in wet conditions, so the devices were confirmed as possible to handle and suitable for the application. Hollow devices were filled with methylene blue (MB) as model molecule, to test the functionality of the devices in releasing in a controlled manner. MB's release tests demonstrated the interconnection of the pores in the wall of the devices and the different kinetics confirm the possibility of tailoring the release through the morphology of the device pores, i.e. through the granulometry of the porogen. The Peppas-Korsmeyer model showed that the release mechanism for all devices is anomalous, thus influenced by swelling and porosity, and confirmed faster kinetics for the devices with the largest pores. These properties would allow the controlled release of other molecules, such as drugs, fertilizers and pesticides, confirming the versatility of the process.

Acknowledgment

This study was carried out within the SAMOTHRACE (Sicilian micro and nano technology research and innovation center) Extended Partnership and received funding from the European Union Next-GenerationEU (PIANO NAZIONALE DI RIPRESA E RESILIENZA (PNRR) – MISSIONE 4 COMPONENTE 2, INVESTIMENTO 1.5). This manuscript reflects only the authors' views and opinions, neither the European Union nor the European Commission can be considered responsible for them.

NON-DESTRUCTIVE ANALYSIS OF DEHP SURFACE CONCENTRATIONS AND DIFFUSION-EVAPORATION IN HERITAGE PVC OBJECTS

T. Rijavec^{1,2*}, S. Bujok³, S. Antropov³, G. A. Newsome², J. Grau-Bové⁴, I. Kralj Cigić¹, K. Kruczala⁵, L. Bratasz³, M. Strlič¹

¹Heritage Science Laboratory Ljubljana, Faculty of Chemistry and Chemical Technology, University of Ljubljana, Večna pot 113, Ljubljana, Slovenia

²Museum Conservation Institute, Smithsonian Institution, Suitland, Maryland, United States of America

³Jerzy Haber Institute of Catalysis and Surface Chemistry, Polish Academy of Sciences, Kraków, Poland

⁴Institute for Sustainable Heritage, University College London, London, United Kingdom

⁵Faculty of Chemistry, Jagiellonian University in Krakow, Kraków, Poland

Tjasa.rijavec@fkkt.uni-lj.si

INTRODUCTION

Poly(vinyl chloride) (PVC) objects are common in contemporary art and design collections, often exceeding their originally intended lifespans as consumer products (1). PVC's versatility, particularly its flexibility achieved by using plasticizers, makes it a popular material. Traditional phthalate plasticizers, which can make up to 50% of the material, are only physically mixed with PVC and other additives (2). These plasticizers migrate to the surface through bulk diffusion, where they can evaporate, leading to reduced flexibility and causing shrinkage. Visible signs of degradation include sticky surfaces and exudates that trap dust, which are quickly recognized as ongoing plastic deterioration. There is a lack of systematical chemical characterization of the exudates and their surface concentrations. The presence of surface exudates and changes to the material properties due to plasticizer loss present a significant conservation challenge to museums housing plastic objects.

In this study, we summarize the process of developing a non-destructive quantitative method for characterizing surface exudates to survey the current state of heritage PVC objects. Further, accurate data on bulk loss of bis(2-ethyl hexyl) phthalate (DEHP), traditionally the most common plasticizer (2), was acquired to create a general model and predict plasticizer loss for typical heritage PVC on a time-scale relevant to collection management.

EXPERIMENTAL

Determination of surface DEHP concentration

Knitted lint-free polyester swabs with a low total organic content residue and no adhesives were used to swab a 5-cm x 5-cm area of a PVC object without the use of a solvent. Each object was swabbed in triplicate. DEHP was extracted from the swab with hexane and the solution was analysed with an Agilent 7890B-5977B GC-MS. The quantitation was based on surface calibration off glass panels in the range of 0.2 mg/m² to 40 mg/m² DEHP.

Accelerated degradation

Reference historical PVC samples P178 (25% DEHP, 220 µm) and P417 (19% DEHP, 100 µm) were exposed to accelerated degradation in climate chambers at 60 °C and 80 °C at 55% RH (Weissttechnik ClimeEvent C/180/0) at different air velocities (0, 0.05, 0.2, 0.8 m/s). Five 2x2 cm² pieces of a sample were exposed to each degradation experiment and removed from the degradation chamber after 2, 7, 17, 35, and 56 days. The original and the degraded

pieces were characterized using gravimetry (Sartorius Entris Analytical Balance) and chromatography (Thermo Fisher Scientific).

Modelling plasticizer loss from accelerated degradation experiments

In the proposed diffusion-evaporation model, the overall plasticizer migration results from the diffusion of plasticizer molecules from the bulk to the surface (Fick's second law) and their subsequent evaporation (boundary condition) (3). The COMSOL Multiphysics® software was used to compute a solution for a one-dimensional diffusion problem with symmetric boundary conditions and compared with experimental values based on a reduced χ^2 function.

RESULTS AND DISCUSSION

The investigation into realistic surface concentrations of DEHP on heritage PVC objects enabled us to determine visually recognizable levels and estimate the number of heritage objects experiencing plasticizer loss through diffusion-evaporation or phase-separation. By monitoring bulk plasticizer content via gas chromatography and conducting gravimetric analysis of mass loss, we obtained comprehensive data to better understand the complex diffusion-evaporation process. A clear trend was observed between air velocity and plasticizer loss at 80 °C, which became less pronounced at 60 °C and was considered less significant at lower temperatures (10–30 °C). The experimentally obtained data was used to create a general model for DEHP diffusion-evaporation, considering the starting plasticizer content, object thickness and storage temperature.

Heritage PVC objects near room temperature can be categorized into three main groups: I - highly plasticized objects (rubbery state), II - slightly plasticized objects (glassy state, transparent), III - slightly plasticized objects (glassy state, opaque, i.e. high filler content); which significantly effects the diffusivity of DEHP. These classifications significantly affect the diffusivity of DEHP. In real heritage collections, PVC objects are expected to mostly belong to Groups I and II, where plasticizer loss is generally evaporation controlled. However, the dimensions of real objects (affecting the diffusion rate) must be considered for more precise determination. Diffusion-controlled loss results in non-homogeneous plasticizer distribution, increasing the risk of mechanical damage due to uneven stress distribution. Considering typical object thickness and the calculated critical thickness at room temperature, thin objects (0.2 mm) were identified as most at risk for damage from plasticizer loss.

Acknowledgment

Part of the research was carried out within the PVCARE project (Slovenian Research and Innovation Agency project no. N1-0241 and National Science Centre Poland NCN project OPUS-LAP 20, No. 2020/39/I/HS2/00911). Further acknowledged are the projects founded by Slovenian Research and Innovation Agency: E-RIHS.si (I0-E012), MRIC UL (I0-0022), NextGenHS (J7-50226) and Research Core Funding (P1-0447). TR acknowledges support through the Smithsonian Institution Predoctoral Fellowship and the “Women in Science 2024” Award granted by L’Oréal Adria d.o.o. and the Slovenian National Commission.

References

- 1) T. Rijavec, M. Strlič, I. Kralj Cigić, *Acta Chim. Slov.* **2020**, *67*, 993.
- 2) T. Rijavec, D. Ribar, J. Markelj, M. Strlič, I. Kralj Cigić, *Sci. Rep.* **2022**, *12*, 1.
- 3) E. Linde, U. W. Gedde, *Polym. Degrad. Stab.* **2014**, *101*, 24.

TOWARDS THE UNDERSTANDING OF THE THERMAL DEGRADATION BEHAVIOR OF THE RIGID AND PLASTICIZED POLY(VINYL CHLORIDE)

Krzysztof Kruczala^{1*}, Marwa Saad¹, Marek Bucki², Sonia Bujok³, Dominika Pawcenis¹, Tjaša Rijavec⁴, Karol Górecki¹, Łukasz Bratasz³, Irena Kralj Cigic⁴, Matija Strlič⁴

¹Faculty of Chemistry, Jagiellonian University in Krakow, Krakow, Poland

² Doctoral School of Exact and Natural Sciences, Jagiellonian University, Krakow, Poland

³ Jerzy Haber Institute of Catalysis and Surface Chemistry, PAS, Kraków, Poland

⁴ Faculty of Chemistry and Chemical Technology, University of Ljubljana, Ljubljana, Slovenia

kruczala@chemia.uj.edu.pl

INTRODUCTION

Works of art made of plasticized poly(vinyl chloride) (PVC) present unique and pressing conservation challenges. Until the 1990s, the poor qualities of plastics were not widely known and considered within the art conservation community (1). Due to inherently unstable formulations, PVC can deteriorate rapidly, producing dramatic alterations unanticipated by artists and collectors. The aging leads to changes in chemical and mechanical properties (2). The latter is mostly related to plasticizer migration by diffusion and evaporation, while chemical changes primarily involve dehydrochlorination, leading to polyene sequence formation and thus yellowing of PVC objects over time (3,4). The major objective of the current research is to gain valuable scientific information not only about plasticizer migration but also about polymer degradation of the PVC polymer chain. In particular, this study aims to link structural changes related to the discoloration of pristine and plasticized PVC with mechanical changes to assess the potential risk of damage originating from dehydrochlorination frequently observed in heritage PVC collections.

EXPERIMENTAL

Materials

The commercial materials used in this work were: (1) stabilized rigid PVC samples (2) plasticized PVC samples containing 19, 21, and 27% of DOTP (3) plasticized PVC samples with two plasticizers of DOTP and DEHA

Preparation

Accelerated aging was performed for rigid and plasticized PVC in a climate chamber for up to 22 weeks at 60°C and 80°C with 60% relative humidity (RH) and at 80°C without humidity control (estimated <7% RH).

Mechanical and physio-chemical characterization

SEM and wettability were used to characterize the rigid and plasticized PVC morphologically, and XPS was used to examine the surface compositions. The molecular fingerprint and the change in the plasticizer content were studied using ATR-FTIR and Raman spectroscopy, whereas paramagnetic resonance spectroscopy (EPR) was used to detect the formation of the radicals. Color changes and yellowing index were determined with the color analyzer ColorQuest, while UV-Vis spectrophotometry was employed to quantify the number of polyene sequences. The distribution of molar mass and change in molecular weight was determined using size exclusion chromatography (SEC). The mechanical properties of PVC samples were investigated using dynamic mechanical analysis (DMA).

RESULTS AND DISCUSSION

As presented in **Fig. 1**, the bands in Raman spectra assigned to polyene, 1100 cm⁻¹ and 1514 cm⁻¹ peaks originated from polyenes ν_1 (C-C=C) and ν_2 (C-C=C) stretching vibrations, started to appear after six weeks of degradation at 80°C without humidity control. The bands from polyenes were even more distinguished at 60% relative humidity (RH), leading to the conclusion that the higher humidity caused faster degradation of PVC. The Raman spectra

correlated with the samples' color change; all of them becoming more yellow with increasing aging time. According to the UV-Vis results, not only did the number of carbon-carbon double bonds increase, but the length of polyenes also increased. For the sample aged at 80°C without humidity control for 22 weeks the formation of 14 conjugated double bonds was detected (absorption at 521 nm). Since there were no statistically significant changes in the molecular weight of PVC after artificial aging for up to 22 weeks, we conclude that neither chain scission nor cross-linking occurs during artificial aging at 60°C and 80°C.

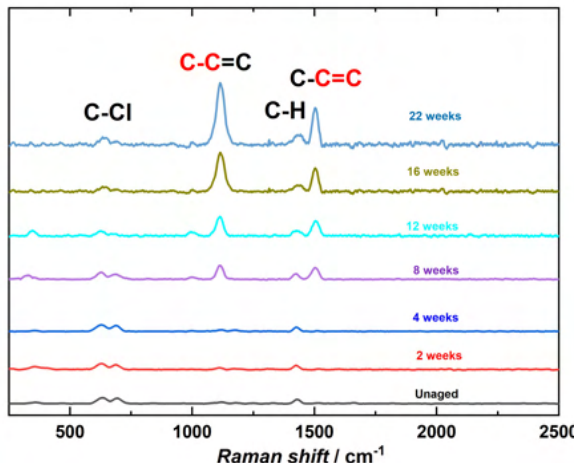


Fig. 1. Raman spectra of unaged and aged rigid PVC at 80°C

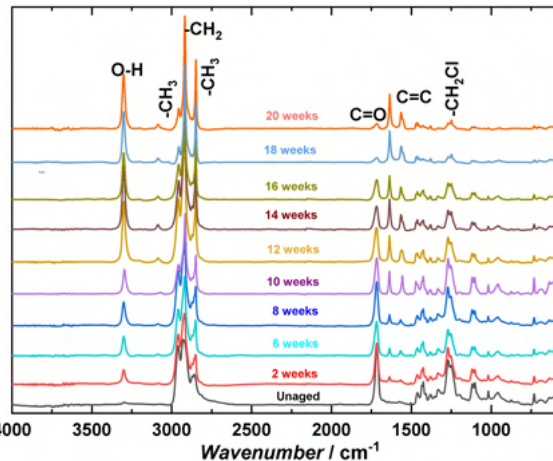


Fig. 2. ATR-FTIR spectra of PVC plasticized with 19% DOTP at 80°C

ATR-FTIR measurements (**Fig. 2**) for plasticized samples aged at 80°C revealed a decrease in the intensity of the band assigned to C=O, which can be explained by the plasticizer's loss [5]. In addition, a new band that appeared during the aging process was assigned to the vibrations of the -OH groups, and it may be related to the decomposition of the DOTP. The infrared spectra of PVC aged at 60°C did not exhibit any changes.

The water contact angle showed an increase in the hydrophobicity of the plasticized PVC samples because of the loss of the plasticizer, whereas the rigid PVC aged at the same conditions exhibited an increase of surface hydrophilicity due to partial oxidation.

Up to 22 weeks of artificial aging, the structural changes caused by the dehydrochlorination reaction did not affect the stiffness of rigid PVC, however, rigid PVC degraded at 80°C and 60% RH became stiffer after a prolonged time of treatment.

Surprisingly, EPR measurements reveal the formation of stable radicals, a small peak with $g=2.003$, even in the samples degraded at 60°C and 60%. This peak becomes even more intense for samples treated at 80°C. This observation may suggest that even at low temperatures the radical mechanism of PVC degradation needs to be taken into account.

Acknowledgment

The research is carried out within the OPUS LAP 20, National Science Centre, Poland 2020/39/I/HS2/00911 and Slovenian Research Agency, N1-0241 project, CEUS scheme. The infrastructure funded by the European Union in the framework of the Smart Growth Operational Programme, Measure 4.2; Grant No. POIR.04.02.00-00-D001/20, was used.

References

- 1) T. Rijavec, M. Strlič, I. Kralj-Cigić, *Acta Chim. Slov.*, 67, 993-1013 (2020)
- 2) T. Rijavec, M. Strlič, I. Kralj-Cigić, *Polym. Degrad. Stab.*, 211, 110329 (2023)
- 3) T. Rijavec, D. Pawcenis, K. Kruczała, M. Strlič, I. Kralj-Cigić, *Herit. Sci.* 11, 155 (2023)
- 4) K. Kopacz B. Kopczyńska, M. Czarnecka, T. Koźlecki, *J. Raman Spectrosc.*, 50, 2 (2019)
- 5) T. Rijavec, S. Bujok, S. Antropov, G. A. Newsome, J. Grau-Bové, I. Kralj Cigić, K. Kruczała, Ł. Bratasz, M. Strlič, *Sci. Adv.*, under review

PLASTICIZATION OF DIALCOHOL CELLULOSE AND EFFECT ON THE THERMOMECHANICAL PROPERTIES

E. Pellegrino, G. Lo Re* and A. Fina

Politecnico di Torino, Dipartimento di Scienza Applicata e Tecnologia, viale Teresa Michel 5, 15121 Alessandria, Italy

*Chalmers University of Technology, Department of Industrial and Materials Science, Rännvägen 2A, 412 58 Göteborg, Sweden

giadal@chalmers.se

INTRODUCTION

The interest in renewable and biodegradable polymers is increasing due to the awareness of the negative environmental impact of non-biodegradable and fossil-based plastics, in particular, considering disposable packaging applications. Cellulose and its derivatives seem good alternatives because of their biobased origin, biodegradability and physical-chemical properties. One problem of cellulosic materials is the abundance of hydroxyl groups in cellulose structure, which creates strong hydrogen bonds between the cellulose fibres. These bonds remain largely intact as the temperature rises, resulting in cellulose having a melting point higher than its degradation temperature. This prevents cellulose from being processed using standard melt processing equipment typically used in plastic packaging production, which are advantageous in terms of energy and solvent consumption. Chemical modification of cellulose fibres to dialcohol cellulose (DAC) was demonstrated to significantly decrease the crystallinity and lower the glass transition temperature of cellulose [1]. The chemical modification is obtained by first oxidation using sodium periodate followed by a reduction with sodium borohydride, which converts the so-formed aldehydes into hydroxyl groups [2] (Figure 1).

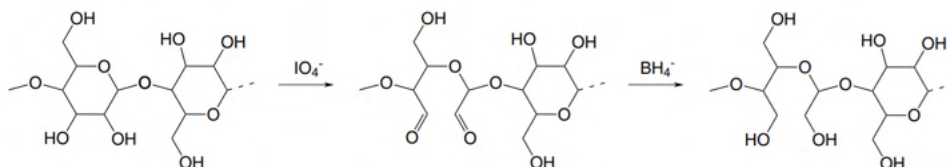


Fig 1: chemical modification from cellulose to dialcohol cellulose [1].

It has been demonstrated that DAC fibres are melt processable in the temperature window between the glass transition and degradation temperatures for cellulose. However, water is needed as a processing aid during melt processing, acting as a temporary plasticizer [3]. Although water is the most sustainable option, its exchange with the environment causes the material properties to be highly dependent on ambient conditions. This study aims to investigate the partial replacement of water with less volatile, green plasticizers, to control processability and physical properties of DAC-based materials.

EXPERIMENTAL

Materials

Dialcohol cellulose (in form of sheets), deionized water, urea, glycerol, sorbitol and isosorbide were used as received for the preparation of the mixtures.

Melt compounding, injection moulding and compression moulding

DAC melt compounding was performed in a micro-extruder at 100°C.

The injection moulding was performed in a micro-injection moulding machine; DAC specimens suitable for tensile tests were produced. Compression moulding was exploited for the preparation of specimens suitable for dynamic mechanical thermal analysis (DMTA) analyses.

Thermal, mechanical properties and morphology investigation

The thermal stability was evaluated exploiting thermal gravimetric analysis (TGA). The tensile properties were investigated using a tensile tester, while the thermal-mechanical properties using a dynamic mechanical thermal analysis (DMTA). The morphology was investigated using a scanning electron microscope (SEM).

RESULTS AND DISCUSSION

Systems containing both a plasticizer and water have been successfully melt-processed in a mini-extruder at a relatively low temperature (100°C).

From TGA is observed how the materials containing urea showed a slight decrease in thermal degradation temperature ($T_{10\%}$ from 285 to 261°C), while the materials containing sorbitol a slight increase ($T_{10\%}$ from 285 to 293°C). Mechanical and thermomechanical properties for DAC and plasticized materials were studied by tensile test and DMTA. DAC is a rigid material at room temperature, owing an elastic modulus of 316 MPa, a stress at break of 17 MPa, and elongation at break of 72%. The addition of plasticizers leads to a reduction in the elastic moduli in the range between 119 and 7 MPa, as well as in the stress at break in the range between 9 and 2 MPa. An increase in the elongation at break is observed in the range between 87 and 125%, depending on the type and concentration of the plasticizer. The systems containing sorbitol and isosorbide appear to be promising, as they provide a good increase in deformability while maintaining high mechanical properties. From the DMTA tests, the glass transition is assigned as the maximum in $\tan\delta$ at 30°C. The glass transitions for plasticized materials decrease in the range between 20 and 1°C, confirming the plasticization effect. The highest decrease in T_g is observed for the materials containing glycerol. A plateau in the Storage Modulus was observed above T_g for both pristine DAC and plasticized materials. In particular, the presence of a plasticizer reduces the value of such E' plateau (range between 52 and 19 MPa @140°C). The highest decrease in the plateau is observed for materials containing urea. From morphological analyses observed on cryo-fractured surfaces, compact materials have been observed, demonstrating that the DAC fibres can easily intercalate leading to homogeneous materials.

References

- 1) P.A. Larsson, L. Wågberg, Green Chemistry, **18**(11), 3324-3333 (2016).
- 2) S.H. Zeronian, F.L. Hudson, R.H.Peters, Tappi 47:557–564, (1964).
- 3) G. Lo Re, E.R Engel, L. Björn, M.G. Sicairos, M. Liebi, J. Wahlberg, ... & P.A. Larsson, Chemical Engineering Journal, **458**, 141372 (2023)..

Ring-opening polymerization of ethylene brassylate in reactive extrusion and its end-of-life options

A. Avella,¹ R. Mincheva,² D. Pappalardo³ and G. Lo Re^{1*}

¹*Chalmers University of Technology, Department of Industrial and Materials Science, Rännvägen 2A, 412 58 Göteborg, Sweden giadal@chalmers.se

²Laboratory of Polymeric and Composite Materials, University of Mons (UMONS), 7000 Mons, Belgium

³Dipartimento di Scienze e Tecnologie, Università del Sannio, via dei Mulini 59/A, 82100 Benevento, Italy

INTRODUCTION

In the search for solutions to contrast the environmental impact of plastics, the development of novel circular materials through scalable methods is of interest. Ethylene brassylate (EB) is a macrolactone sourced from rapeseed and castor oils that can be polymerized via ring-opening polymerization (ROP) to obtain a fully bio-sourced polyester, poly(ethylene brassylate) (PEB). In the literature, EB has been polymerized at laboratory scale with the aid of enzymatic [1], organometallic [2]–[5] or organic [3], [6], [7] catalysts. To our knowledge, in all previous studies, the ROP of EB has been carried out in batch conditions, in solution or bulk. In this work, the synthesis of PEB was tested via reactive extrusion (REx), a technique that uses conventional melt processing equipment for chemical reactions, eliminating the need for organic solvents. Thanks to the relatively powerful mixing, REx increases the monomer diffusion during polymerizations, often hindered in bulk due to higher polymer viscosity [8], thus leading to higher conversion and faster kinetics [9]. Therefore, REx could provide a scalable continuous method for EB polymerization and manufacturing in a single processing step. Given the novelty of this polyester, three end-of-life options of PEB were assessed in this work: mechanical recycling, enzymatic depolymerization and disintegration in compost.

EXPERIMENTAL

Materials

The following chemicals were purchased from Sigma Aldrich (Sweden): ethylene brassylate (1,4-dioxacycloheptadecane-5,17-dione) (> 95%), 1,5,7-triazabicyclo[4.4.0]dec-5-ene (TBD), Lipase B *Candida antarctica* (CALB) recombinant from *Aspergillus oryzae* in powder form (9 U/mg).

Preparation

The reagents were first dried in a ventilated oven overnight at 75 °C. The polymerization of EB was tested with different catalysts. In the case of TBD, the monomer:catalyst ratio was 42:1. The reactions were carried out in an Xplore microcompounder (MC15HT) with a recirculating system under a constant nitrogen flow. The processing was performed at 130 °C, 100 rpm for up to 60 min.

The extruded PEB samples were injection molded with an Xplore IM12 into dumbbell-shaped specimens, with a barrel and mold temperature of 80 °C and 25 °C, respectively. The injection followed a program of 2 s at 280 bar and holding for 10 s at 420 bar.

End-of-life: mechanical recycling, disintegration in compost and enzymatic depolymerization

For the simulation of post-industrial recycling, the dumbbell-shaped specimens of PEB were manually shredded and extruded in an Xplore microcompounder (total volume 5 cm³) at 130 °C and 100 rpm for 10 min. The process was repeated four times.

Disintegration tests under aerobic composting conditions were performed on a laboratory scale for 90 days according to the standard ISO 20200:2015. Materials from compression-molded sheets were cut into squares (15 mm x 15 mm x 1 mm), which were

weighed and placed in a mesh to ease their withdrawal during composting. Samples of each formulation were withdrawn from the disintegration container at different times and the mass loss was calculated with respect to the initial weight.

PEB was enzymatically depolymerized according to the procedure reported by Martínez-Cutillas et al. [10]. The sample was dissolved in toluene 0.5% w/v in a round-bottomed flask with a magnetic stirrer, and 300% w/w CALB was added. The reaction was carried out for 72 h at 55 °C and the products were analysed.

RESULTS AND DISCUSSION

Several catalysts and reaction conditions were studied in this work, and PEB synthesized with the organic base TBD achieved the largest molar mass (9 kg/mol) and monomer conversion (98%). From structural analyses, it was proven that TBD was both catalyzing and initiating the polymerization of EB.

After 90 days in simulated industrial composting, PEB disintegrated and lost 93% of its initial mass (Fig.1), therefore it could be classified as industrially compostable if additional tests are carried out.

Four extrusion cycles were performed to simulate the post-industrial mechanical recycling of PEB. The tensile tests at room temperature and a strain rate of 10% carried out on the recycled PEB indicated no significant change in the mechanical properties, whereas thermogravimetric analysis in nitrogen showed a 15 °C decrease in the onset-of-degradation temperature.

The enzymatic depolymerization with CALB yielded EB oligomers and monomer, confirming this route for potential chemical recycling.

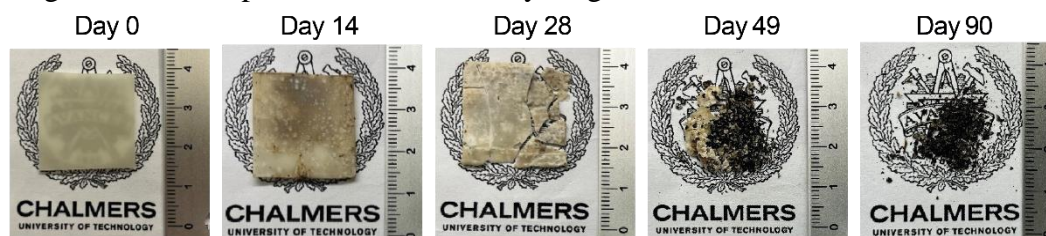


Fig. 1 Photographs of PEB samples extracted on different days during industrial composting.

References

- [1] S. Müller, H. Uyama, and S. Kobayashi, "Lipase-catalyzed ring-opening polymerization of cyclic diesters," *Chem. Lett.*, vol. 28, no. 12, pp. 1317–1318, 1999.
- [2] A. Butron, O. Llorente, J. Fernandez, E. Meaurio, and J. R. Sarasua, "Morphology and mechanical properties of poly(ethylene brassylate)/cellulose nanocrystal composites," *Carbohydr. Polym.*, vol. 221, no. June, pp. 137–145, 2019.
- [3] J. Fernández, H. Amestoy, H. Sardon, M. Aguirre, A. L. Varga, and J. R. Sarasua, "Effect of molecular weight on the physical properties of poly(ethylene brassylate) homopolymers," *J. Mech. Behav. Biomed. Mater.*, vol. 64, pp. 209–219, 2016.
- [4] J. Li et al., "Helical Crystals in Aliphatic Copolyesters: From Chiral Amplification to Mechanical Property Enhancement," *ACS Macro Lett.*, vol. 12, no. 3, pp. 369–375, 2023.
- [5] X. Wang et al., "Sodium complexes bearing cavity-like conformations: a highly active and well-controlled catalytic system for macrolactone homo- and copolymerization," *Polym. Chem.*, vol. 12, no. 13, pp. 1957–1966, Apr. 2021.
- [6] A. Pascual et al., "Experimental and computational studies of ring-opening polymerization of ethylene brassylate macrolactone and copolymerization with ϵ -caprolactone and TBD-guanidine organic catalyst," *J. Polym. Sci. Part A Polym. Chem.*, vol. 53, no. 4, pp. 552–561, Feb. 2015.
- [7] S. Kim and H. Chung, "Synthesis and Characterization of Lignin-graft-poly(ethylene brassylate): a Biomass-Based Polyester with High Mechanical Properties," *ACS Sustain. Chem. Eng.*, vol. 9, no. 44, pp. 14766–14776, Oct. 2021.
- [8] A. Pascual, H. Sardon, A. Veloso, F. Ruipérez, and D. Mecerreyes, "Organocatalyzed Synthesis of Aliphatic Polyesters from Ethylene Brassylate: A Cheap and Renewable Macrolactone," *ACS Macro Lett.*, vol. 3, no. 9, pp. 849–853, Sep. 2014.
- [9] S. Spinella et al., "Enzymatic reactive extrusion: moving towards continuous enzyme-catalysed polyester polymerisation and processing," *Green Chem.*, vol. 17, no. 8, pp. 4146–4150, 2015.
- [10] A. Martínez-Cutillas, S. León, S. Oh, and A. Martínez de Ilarduya, "Enzymatic recycling of polymacrolactones," *Polym. Chem.*, vol. 13, no. 11, pp. 1586–1595, Mar. 2022.

THERMAL AND FLAME RETARDANT PROPERTIES OF EPOXY VITRIMERS BASED ON DISULFIDE BONDS

V. Berner^a, A. Huegun^b, L. Hammer^c, A. M. Cristadoro^d, C.-C. Hoehne^a

^a Fraunhofer Institute for Chemical Technology ICT, Joseph-von-Fraunhofer Str. 7, 76327 Pfinztal, Germany

^b CIDETEC, Basque Research and Technology Alliance (BRTA), Po. Miramón 196, 20014 Donostia-San Sebastian, Spain

^c BASF SE, 67056 Ludwigshafen, Germany

^d BASF Polyurethanes GmbH, Elastogranstr. 60, 49448 Lemfoerde, Germany

valeria.berner@ict.fraunhofer.de

INTRODUCTION

Linear plastic economy leads to an unmanageable accumulation of plastic waste in the ecosystem. A change towards a sustainable circular plastics economy must be achieved.

Especially the recyclability of thermosets and thermoset composites is limited and challenging. The development of reprocessable, reusable and recyclable thermosets is therefore of great importance.

Vitrimers offer great potential in terms of recyclability as the incorporation of dynamic covalent bonds into a thermoset network provides a powerful method to recycle and reshape these plastics by topology rearrangements.

For many applications especially in the transportation sector the thermal and mechanical properties of plastics are essential. Currently, thermoset based composites are mainly and extensively used for several interior applications. Vitrimers show very similar mechanical properties to thermosets. However, vitrimers consist of a dynamic covalent network, which changes its topology by thermal activation – offering a great potential to be more safe-, sustainable- and recyclable-by design.

For application in the transportation sector, the thermal behavior and flame-retardant properties are of great importance.

EXPERIMENTAL

Materials

In this work an epoxy vitrimer based on bisphenol A diglycidyl ether (DGEBA) and 4-aminophenyl disulfide was studied. In total, the influence of 16 different phosphorous-based flame-retardant additives and reactive flame retardants with different oxidation numbers of the phosphorus were investigated. From the most promising formulations carbon fiber reinforced composites were manufactured and analyzed.

Preparation

The phosphorous based flame retardant and the epoxy resin were premixed. The phosphorous content of this mixture was 2 wt%. The formulation was cured with 4-aminophenyl disulfide. The carbon fiber reinforced composites were produced via Resin-Transfer-Moulding (RTM) process.

Thermal and flame retardant properties

The thermal behavior and flame-retardant properties were investigated using differential scanning calorimetry (DSC), thermal gravimetric analyses (TGA) as well as limiting oxygen index (LOI) tests, UL94 tests, and cone calorimeter as well as smoke chamber tests.

Mechanical recycling process

The most promising formulations were grinded and hot pressed again. The flame retardant properties of the obtained second generation plate were analyzed again.

RESULTS AND DISCUSSION

The vitrimer properties were achieved due to the disulfide containing hardener. A model of the mechanism of the dynamic covalent disulfide bond exchange is shown in Fig. 1.

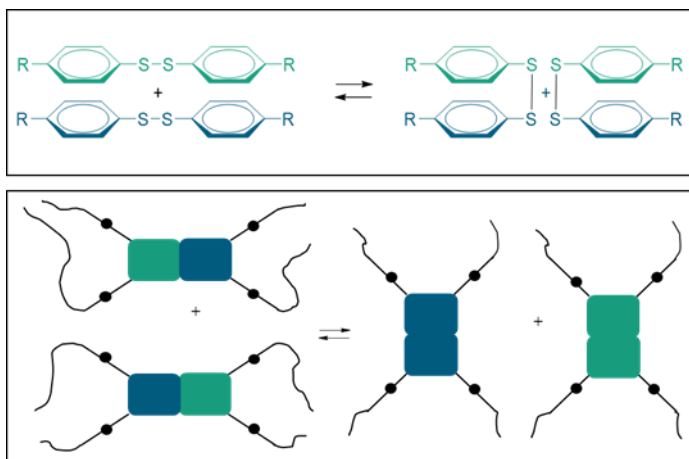


Fig. 1 Schematic exchange mechanism of disulfide bonds. (1)

During flame treatment, epoxy vitrimer-based composites showed charring and the release of large quantities of soot. Without any flame retardant, epoxy vitrimers and epoxy vitrimer-based composites do not pass the UL94 test. The LOI values of the studied cured fiber-free epoxy vitrimer is 20.9 O₂%. With the addition of phosphorus based flame retardants LOIs up to 38 % O₂ and UL94 V-0 classification were achieved. Gas phase active phosphorous based flame retardants tend to be more suitable for this epoxy vitrimer.

In cone calorimeter tests the peak heat release rate (pHRR) was reduced by 43 %. Carbon fiber reinforced composites with reactive phosphorous based flame retardants showed a pHRR of 179 kW*m⁻² and a maximum average rate of heat emission (MARHE) of 101 kW*m⁻².

In UL94 tests the same classification were achieved after a mechanical recycling process. LOI values decreased slightly for some formulations.

Acknowledgment

The authors would like to thank their colleagues from Fraunhofer ICT, Pfinztal: Beatrice Tübke, Yvonne Kasimir, Kristin Bergmann and Eyleen Napoli for analytical support and the Fraunhofer ICT research group for Flame, Fire and Explosion Protection for fruitful discussions and support. This project has received the funding from the European Union's Horizon Europe research and innovation program under grant no. 101057901. Views and opinions expressed are however those of the authors only and do not necessarily reflect those of the European Union. Neither the European Union nor the granting authority can be held responsible for them.

References

- 1) Li X, Zhang J, Zhang L, Ruiz de Luzuriaga A, Rekondo A, Wang D-Y. *Compos. Commun.*, **25**, 100754 (2021).

Addressing Inhomogeneity in Plastic Waste Streams: A Comprehensive Evaluation of Sampling and Sample Preparation Strategies

C. Panagiotopoulos¹, C. Podara², M. Karamitrou², T. Kosanovic-Milickovic², M. Silber³, L. Meyer³, B. von Vacano³, A.N. Carvalho Neiva⁴, J.H. Knoop⁵, A. Martínez García⁶, A. Ibáñez-García⁶, E. Santamarina⁷, C. Prieto⁷, S. Pavlidou⁸, L. Poudeh⁹, C. Charitidis² and S.N. Vouyiouka^{1,*}

¹Laboratory of Polymer Technology, School of Chemical Engineering, Zographou Campus, National Technical University of Athens, 157 72 Athens, Greece

²Research Lab of Advanced, Composites, Nanomaterials and Nanotechnology, School of Chemical Engineering, Zographou Campus, National Technical University of Athens, 157 72 Athens, Greece

³Group Research, BASF SE, 67056 Ludwigshafen am Rhein, Germany

⁴Coolrec Plastics BV, Van Hilststraat 7, 5145 RK, Waalwijk, The Netherlands

⁵Fraunhofer Institute for process engineering and packaging IVV, 85354 Freising, Germany

⁶Innovative Materials and Manufacturing Area, AIJU, Technological Institute for Children's Products and Leisure, 03440 Ibi, Alicante Spain

⁷AIMEN Technology Centre, O Porriño (Pontevedra), Spain

⁸MIRTEC S.A. 76th km Athens – Lamia Nat. Road, Schimatari Viotias, 32009, Greece

⁹Arçelik Global, Central R&D, Polymer & Chemistry Department, Tuzla 34950, Istanbul, Turkey

(*mvuyiuka@central.ntua.gr)

INTRODUCTION

In the perspectives of circular economy and minimization of environmental pollution, high-quality recycling strategies have been increasingly getting attention for utilizing and valorizing polymeric waste materials towards reusable and (if possible) upgraded, value-added products. However, these plastic waste streams (PWS) even when they are sorted, they often exhibit a low degree of homogeneity for a number of reasons which complicate their sampling, analytical characterization, processability, selection of upcycling strategy, *etc.* Therefore, developing sampling and sample analysis methodologies—that yield results accurate and representative enough to describe the contents and the safety of the bulk while being cost-effective—is crucial. In this context¹, a “model waste” was conceptualized, *i.e.*, a mixture of polymers (ABS, HIPS, PP and HDPE) of known composition which reflects a typical sorted ABS-rich electrical and electronic equipment waste stream (WEEE). The main objectives of this work lie in establishing a correlation of the sampling steps with low deviation values between replicates as well as determining the proximity of the targeted additives/substances contents to the actual values.

EXPERIMENTAL

Materials

Blends were prepared using the following commercially available virgin polymers with the respective composition given by wt. %: Acrylonitrile butadiene styrene (90.50 or 90.95 %, ABS Kumho 750SW, Kumho Petrochemical Co. Ltd., South Korea), high-impact polystyrene (6.00 %, HIPS Styron X-Tech 2175, Trinseo, Wayne, PA, USA), polypropylene (2.00 %, PP Borealis HE 125MO, Borealis AG, Austria), and high-density polyethylene (1.00 %, HDPE, Petkim Petilen YY S0464, Petkim Petrokimya Holding A.Ş., Turkey). Also, a masterbatch of ABS with 10 % wt. of the chosen brominated flame retardant (BFR-ABS), TBBPA (3,3',5,5'-Tetrabromobisphenol A, ICL Group Ltd., Israel), was prepared by twin-screw extrusion and then diluted to achieve a final concentration of 50 or 500 ppm TBBPA.

Preparation

Polymeric mixtures containing 50 or 500 ppm TBBPA were prepared *via* three different blending procedures: cryogenic grinding (ZM 200 centrifugal mill with 750 µm pore size sieve), extrusion (Collin ZK25 twin-screw extruder), injection molding (Arburg Allrounder 370C machine), and their combination.

Analytical methods

The main analytical methods were HPLC-MS/UV (ThermoFisher QExactive Plus), $^1\text{H-NMR}$ (700 MHz Bruker Avance III HD spectrometer with TCI CryoProbe), XRF (Spectro Xepos), ATR-FTIR (Alpha II instrument with a diamond crystal), thermal properties (TA Instruments Q200 and Q500), MFR (ZwickRoell MFlow at 220 °C, 10 kg), GPC analysis (Agilent 1100 G1312A) and LIBS (Surelite Nd:YAG nanosecond-pulsed laser at 1064 nm coupled with a Czerny-Turner spectrometer). For all analyses five replicates were performed and the results are presented as boxplots.

RESULTS AND DISCUSSION

The first objective was the quantification of TBBPA and identification of the homogenization approach that yielded the lowest deviation of between replicates as well as proximity to the actual concentration values. In view of that, the samples after homogenization were analyzed by $^1\text{H-NMR}$ spectroscopy and XRF. For NMR, the TBBPA concentration was calculated from its evident peak areas (**Fig. 1**) and the pertinent results are represented as boxplots in **Fig.2a** for the 500 ppm blends.

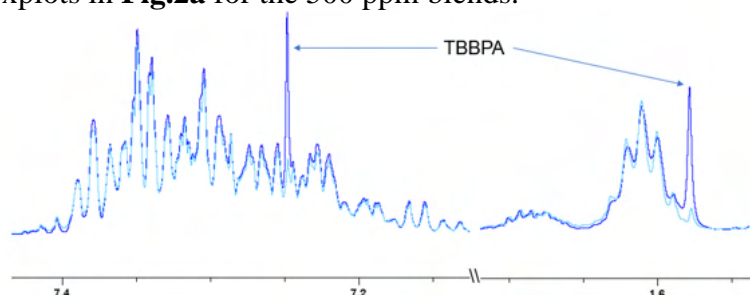


Fig. 1. $^1\text{H-NMR}$ spectra of samples containing 500 (dark blue) and 50 ppm TBBPA (light blue).

Samples that were prepared by cryogenic grinding, even though they showed closest values to the nominal ones (500 ppm), they also exhibited the largest boxes and therefore the largest variation between the individual measurements, both in NMR and XRF analyses. On the other hand, extrusion, injection molding and their combination obviously led to significantly more homogenous samples, but the measured concentration was significantly lower compared to the expected one. This was attributed to possible degradation of TBBPA during melt processing towards other chemical products. Interestingly, this was not followed by an analogous decrease of the Br content monitored by XRF, because Br as an element was not lost through homogenization.

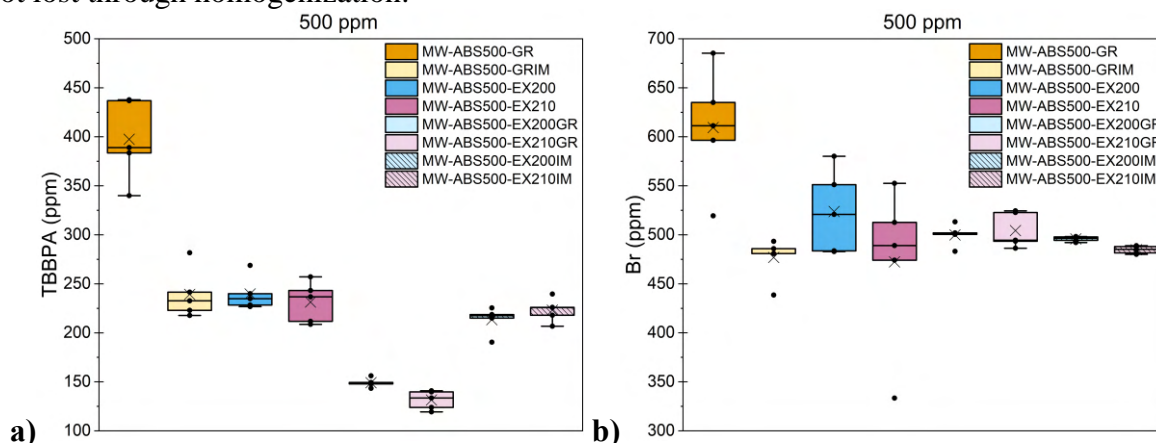


Fig. 2. a) NMR and **b)** XRF analysis of blends containing 500 ppm TBBPA.

As far as ATR-FTIR analysis is concerned, the BFR was not identified in any of the different sample homogenization approaches, meaning that such concentrations (even 500 ppm) were below the detection limits of this analytical technique. In terms of polymeric contamination, HIPS could not be easily discriminated from ABS (pre-dominant polymer)

due to their chemical similarity. PP peaks, on the other hand, were easily distinguished in the spectra, while HDPE was undetectable due to its low quantity (1 % wt.) and overlapping of peaks. Thermal analyses (DSC, TGA) were very reproducible and the samples presented the typical T_g of ABS, T_m of PP and PE, as well as single degradation steps around 400 °C, with no remarkable differences. Interestingly, the grinded samples exhibited ~ 10 °C lower T_g values, possibly due to some plasticization effect from the contained additives (*e.g.*, lubricant, TBBPA), which were evaporated/degraded in the other (melt-based) homogenization strategies. This was also corroborated by an analogous increase of MFR in the same samples. GPC analysis in overall showed no significant molecular weight decrease, regardless of the homogenization approach, while LIBS results did not provide strong evidence for assessing the homogenization degree.

Acknowledgment



**Funded by
the European Union**

This project has received funding from the European Union's Horizon Europe research and innovation program under grant agreement No 101058670.

Views and opinions expressed are however those of the author(s) only and do not necessarily reflect those of the European Union or European Health and Digital Executive Agency (HADEA). Neither the European Union nor the HADEA can be held responsible for them.

References

[1] Precycling Project website <https://www.precycling-project.eu/>

RECYCLING OF MULTI-LAYER POLYMER FILMS BY MECHANOCHEMISTRY IN EXTRUSION

A. Benzemma* and C. Chalamet *

* Jean Monnet University, Ingénierie des Matériaux Polymères (IMP), CNRS, UMR 5223, St Etienne, France

anais.benzemma@univ-st-etienne.fr

INTRODUCTION

Multilayer films, made of different layers of materials, are hard to recycle because they are heterogeneous. Traditional methods of separating and then recycling these materials are often ineffective, limiting material recovery rates [1], [2]. As a result, their recycling rates remain very low [3].

Shear pulverization in the solid state is emerging as an alternative technique to produce polymer blends with improved properties. This method creates submicron-sized dispersed domains without the need for heat, monomers, or solvents [4], [5], [6]. This solid-state polymer processing offers a simple and effective approach for making incompatible polymer blends more compatible. By mechanically treating two polymers together, block copolymers can form, stabilizing the interface between the two polymers [7], [8].

In this context, our study aims to use mechanochemistry as a method to make low-density polyethylene (LDPE) and isotactic polypropylene (iPP) more compatible. These are two commonly used polymers in flexible films. We aim to generate copolymers directly within the PE/PP blend without using external compatibilizers.

We will study the mechanical, rheological, and morphological properties of PE/PP blends produced by three continuous mechanochemical processes suitable for recycling complex materials: twin-screw extrusion (TSE), solid-state melt extrusion (SSME), and solid-state shear pulverization (SSSP).

EXPERIMENTAL

Materials

For this study, two polymers were selected: a low-density polyethylene (LDPE, reference 2102 NOW, SABIC) and an isotactic polypropylene (PP, reference 500P, SABIC). The LDPE has a density of 0.92 g/cm³, a melting temperature of 110°C, and a melt flow rate (MFR, 190°C, 2.16 kg) of 2.5 g/10 min. The PP has a density of 0.90 g/cm³, a melting temperature of 170°C, and a melt flow rate (MFR, 230°C, 2.16 kg) of 3 g/10 min.

Preparation of blends

Several PE/PP blends were prepared with different formulations including antioxidants (1% by weight), varying the percentage of PP from 0 to 100%. The antioxidants used (Irganox 1010 and Irgafos 168) were mixed in equal weight percentages. The blends were made in a co-rotating twin-screw extruder (BC21-Clextral, L/D=36 with D 25 mm). The feed rate and screw speed were set to 2 kg/h and 600 rpm.

Three extrusion processes were tested: Solid State Shear Pulverization (SSSP), with a barrel temperature set to 25°C, cooled by a water system, producing powder; Solid State Melt Extrusion (SSME), where the barrel temperature is maintained at 25°C up to the third mixing zone (600 mm), then raised to 200°C in the last zones; and Twin Screw Extrusion (TSE), with all extruder zones regulated at 200°C.

Mechanical and Morphological Characterization

The mechanical properties were evaluated using pre-injected specimens. Tensile tests, performed at 23°C with a displacement speed of 20 mm/min, were used to assess the linear and ultimate properties of the materials. Impact tests were conducted at -10°C using a 5 Joule hammer.

Morphological investigations were carried out using a scanning electron microscope (SEM, Quanta 250, FEI) equipped with a backscattered electron diffraction detector. Ruthenium tetroxide (RuO₄) was used as a staining agent to enhance phase contrast by increasing electron density.

RESULTS AND DISCUSSION

The study of PE/PP blends obtained by TSE reveals significant variations in their mechanical properties depending on their composition. An increase in the proportion of PP leads to an increase in elongation at break and elastic modulus, these results differ from those reported in the literature [9]. They also show the significant impact of composition on the mechanical properties of PE/PP blends. In particular, for blends containing 50% and 75% PP, the elastic modulus and elongation at break do not follow the classical blending law. For the 50/50 PE/PP blend, the properties are equivalent to those of PP extruded under similar conditions. This deviation from the blending law highlights complex interactions between polymers, offering the possibility of obtaining improved mechanical properties within certain composition ranges. The impact resilience measurement of the 50% PP blend stands out from other blends, as no rupture is observed.

It is now well established that the properties of polymer blends are closely related to the morphology of these blends. Thus, a microstructural analysis by SEM was performed to define the structure and morphology of the 50% PP blends with and without antioxidant. For the 50% PP blends, a co-continuous morphology is observed. The results show fine dispersions obtained by all three extrusion processes without AO, especially with the SSME process (Fig 1). The presence of a cold zone reduces the size of the morphology, enhancing interactions between phases and mechanical properties.

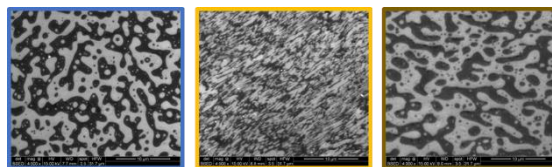


Fig. 1 Scanning electron micrographs of 50/50 LDPE/iPP blends prepared by S3P (blue), SSME (orange), TSE (brown) (x4000)

PE/PP blends containing an antioxidant were also studied to limit the effects of radicals on potential phase compatibilization at their interfaces. Mechanical properties, especially elongation at break, drop sharply in the presence of antioxidant, suggesting a lack of cohesion between the materials. SEM images confirm coalescence or even demixing between the phases, indicating a lack of compatibilization.

References

- [1] Chomon, "Flexible and rigid complexes used in packaging", *Techniques de l'Ingénieur*, (2017).
- [2] Coulon, "Characteristics of a multilayer packaging", *Techniques de l'Ingénieur*, 2008.
- [3] Schächtele, *Plastic Atlas - Facts and Figures about the World of Synthetic Polymers*. Heinrich Böll Stiftung, 2020.
- [4] Lebovitz and al. "Sub-micron Dispersed-Phase Particle Size in Polymer Blends: Overcoming the Taylor Limit via Solid-State Shear Pulverization", *Polymer*, vol. 44, no 1, p. 199-206, 2003.
- [5] Lebovitz and al. "In Situ Block Copolymer Formation during Solid-State Shear Pulverization: An Explanation for Blend Compatibilization via Interpolymer Radical Reactions", *Macromolecules*, vol. 35, no 26, p. 9716-9722, 2002.
- [6] Furgiuele and al., "Efficient Mixing of Polymer Blends of Extreme Viscosity Ratio: Elimination of Phase Inversion via Solid-State Shear Pulverization", *Polymer Engineering & Science*, 2000.
- [7] Gleixner and al., "Combination and Disproportionation of Model Radicals for the Growing Polystyrene Chain", *Die Makromolekulare Chemie*, vol. 180, no 11, p. 2581-2590, 1979.
- [8] Schreck and al., "Self-Reactions of 1,3-Diphenylpropyl and 1,3,5-Triphenylpentyl Radicals: Models for Termination in Styrene Polymerization", *Aust. J. Chem.*, vol. 42, no 3, p. 375-393, 1989.
- [9] Kostosz and al., "Mechanical and Thermal Properties of Gamma Irradiated iPP-LDPE Blends," *Boris Kidrič Institute of Nuclear Sciences*, 1986.

RECYCLING OF MULTI-LAYER POLYMER FILMS BY MECHANOCHEMISTRY IN EXTRUSION

A. Benzemma* and C. Chalamet *

* Jean Monnet University, Ingénierie des Matériaux Polymères (IMP), CNRS, UMR 5223, Saint-Etienne, France

anais.benzemma@univ-st-etienne.fr

INTRODUCTION

Polyethylene (PE)/polyamide (PA) multilayer films are particularly challenging to recycle due to the nonpolar structure of PE and the polar nature of PA. This results in poor miscibility and adhesion between the layers, leading to a heterogeneous morphology and suboptimal mechanical and thermal properties in the absence of compatibilizers.

Solid-state shear pulverization (SSSP) emerges as an alternative technique for producing polymer blends with enhanced properties. This method allows the creation of submicron-sized dispersed domains without the need for heat input, monomer addition, or solvents [1],[2],[3]. This solid-state polymer processing technique offers a simple and efficient approach for compatibilizing immiscible polymer blends. By mechanically processing two polymers together, block copolymers can form, thereby stabilizing the interface between the two polymers [4],[5].

In this context, our study aims to apply mechanochemistry as a recycling method for PE/PA multilayer films. We seek to directly compatibilize the two phases of the blend without resorting to external compatibilizers.

We will investigate the mechanical, rheological, and morphological properties of PE/PA blends obtained through three continuous mechanochemical processes adapted for recycling complex materials: twin-screw extrusion (TSE), solid-state then melt extrusion (SSME), and solid-state shear pulverization (SSSP).

EXPERIMENTAL

Materials

The post-industrial complex films used in this study were provided by Leygatch (Loire, France) in the form of production scraps from the extrusion of PE/PA multilayer films. These wastes contain PA and primarily polyolefins, with an unknown mass fraction of the components, as well as a binder whose name and quantity are also unknown.

Processes Involved

The experiments were conducted using a co-rotating twin-screw extruder (BC21-Clextral, L/D=36 with D=25 mm). The feed rate and screw speed were set to 2 kg/h and 300 rpm, respectively. Three extrusion processes were tested :

- Solid-State Shear Pulverization (SSSP) : The barrel temperature was set to 25°C, cooled by a water system, producing powder.
- Solid-State Melt Extrusion (SSME) : Up to the third mixing zone (600 mm), the barrel temperature was maintained at 25°C, then increased to 220°C in the subsequent zones.
- Twin-Screw Extrusion (TSE): All zones of the extruder were regulated at 220°C.

Morphological and Mechanical Characterization

The mechanical properties were evaluated using specimens that were previously injection-molded and conditioned under controlled humidity. Tensile tests, conducted at 23°C with a crosshead speed of 20 mm/min, were used to assess the linear and ultimate properties of the materials.

Morphological studies were carried out using a scanning electron microscope (SEM, Quanta 250, FEI) equipped with a backscattered electron diffraction detector. A 2% aqueous solution of a mixture of phosphotungstic acid and benzyl alcohol was used as a staining agent to enhance phase contrast by increasing electron density.

RESULTS AND DISCUSSION

SEM images of cryo-fractured tensile specimens show the morphology of the samples, both unextruded and processed by various methods. The morphology reveals a continuous PE phase with

dispersed PA droplets of varying sizes, consistent with observations by other authors [6]. The multilayer films that were not subjected to an extrusion process but merely injection-molded exhibited the largest average particle diameters, with a number-average diameter ($\overline{d_n}$) of 0.42 μm and a volume-average diameter ($\overline{d_v}$) of 4.15 μm , indicating a relatively coarse morphology.

Processing the films using the SSSP method resulted in a significant reduction in both the number-average and volume-average particle diameters ($\overline{d_n} = 0.28 \mu\text{m}$ and $\overline{d_v} = 1.495 \mu\text{m}$). The morphology of the blends became finer and more homogeneous. Tensile tests on samples obtained by SSSP showed a slight improvement in mechanical properties, notably an increase in elongation at break from 90% to 110%. The reduction in particle size promotes better internal cohesion and a more uniform distribution of stresses during deformation, thereby enhancing the overall mechanical performance of the material.

The morphologies of systems obtained after the SSME process showed an even more pronounced reduction in the number-average and volume-average particle diameters ($\overline{d_n} = 0.24 \mu\text{m}$ and $\overline{d_v} = 0.555 \mu\text{m}$). Materials produced by SSME exhibited tensile properties that were twice as strong as the unextruded reference and superior to those obtained by the SSSP process. The SSME process, combining intensive cold mixing that facilitates shear, followed by hot mixing that aids homogenization, promotes the formation of fine and well-distributed structures, enhancing the material's ability to withstand mechanical stresses.

Twin-screw extrusion (TSE) also reduced particle diameters ($\overline{d_n}=0.23 \mu\text{m}$ and $\overline{d_v}=0.665 \mu\text{m}$). The materials obtained by TSE showed a significant improvement over the unextruded samples, with good mechanical strength and elongation at break comparable to those achieved by SSME. The TSE process enables a homogeneous dispersion of the polymers, contributing to satisfactory mechanical properties.

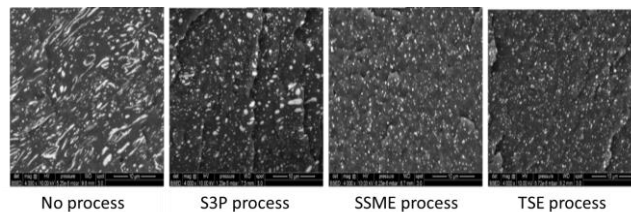


Figure 1: Influences of Extrusion Processes on the Recycling of PE/PA Films (X4000)

Conversely, in the absence of a binder between the polymer layers, the microscopic images reveal a complete lack of cohesion within the material. The two polymers do not form an identifiable morphology, resulting in very weak mechanical properties that are inferior to those obtained with a binder. The absence of a binder prevents interaction and adhesion between the polymer phases, leading to a heterogeneous and incoherent structure. This confirms that the improved properties of the material are due not only to the processing method used but also to the presence of a binder.

References

- [1] Lebovitz and al. "Sub-micron Dispersed-Phase Particle Size in Polymer Blends: Overcoming the Taylor Limit via Solid-State Shear Pulverization", *Polymer*, vol. 44, no 1, p. 199-206, 2003.
- [2] Lebovitz and al. "In Situ Block Copolymer Formation during Solid-State Shear Pulverization: An Explanation for Blend Compatibilization via Interpolymer Radical Reactions", *Macromolecules*, vol. 35, no 26, p. 9716-9722, 2002.
- [3] Furguele and al., "Efficient Mixing of Polymer Blends of Extreme Viscosity Ratio: Elimination of Phase Inversion via Solid-State Shear Pulverization", *Polymer Engineering & Science*, 2000.
- [4] Gleixner and al., "Combination and Disproportionation of Model Radicals for the Growing Polystyrene Chain", *Die Makromolekulare Chemie*, vol. 180, no 11, p. 2581-2590, 1979.
- [5] Schreck and al., "Self-Reactions of 1,3-Diphenylpropyl and 1,3,5-Triphenylpentyl Radicals: Models for Termination in Styrene Polymerization", *Aust. J. Chem.*, vol. 42, no 3, p. 375-393, 1989.
- [6] Ararat and al., « Compatibilization of LDPE/PA6 by Using a LDPE Functionalized with a Maleinized Hyperbranched Polyester Polyol », *Macromol. Res.*, 2020

UV-C INDUCED PHOTODEGRADATION OF POLYPROPYLENE

J. C. F. Gimenez^{a,d}, S. H. F. Bonatti^a, M. V. Basaglia^b, R. H. S. Garcia^c, A. dos Santos^a,
L. H. Staffa^b, M. Samara^d, S. H. P. Bettini^b, E. R. de Azevedo^c, E. Helal^{d,e}, N. R.
Demarquette^d, M. G. P. Homem^a, S. A. Cruz^{a*}

^aDepartment of Chemistry, Exact Sciences and Technology Centre (CCET), Federal University of São Carlos (UFSCar), São Carlos, São Paulo, Brazil

^bDepartment of Materials Engineer, CCET, UFSCar

^cPhysics Institute of São Carlos, IFSC, University of São Paulo, São Carlos, São Paulo, Brazil

^dMechanical Engineering, École de Technologie Supérieure, Montréal, Quebec, Canada

^eNanoXplore Inc., Saint-Laurent, Quebec, Canada

jessica.gimenez@estudante.ufscar.br, sandra.cruz@ufscar.br

INTRODUCTION

With the increasing use of germicidal lamps emitting UV-C radiation in hospitals to clean surfaces and reduce cross-contamination from pathogens (1), the study of UV-C's impact on polymer materials became crucial. However, only a few studies in the literature examined the effect of UV-C on PP photodegradation (4–6), and an in-depth investigation of the extended UV-C exposure on PP has not yet been undertaken.

In this work, we studied the impact of UV-C photodegradation of PP using rheology, FTIR-ATR, scanning electron microscopy (SEM), the contact angle formed by drops of water and diiodomethane, 1H Time-Domain Nuclear Magnetic Resonance (¹H TD-NMR), and differential scanning calorimetry (DSC).

EXPERIMENTAL

Materials

The polypropylene pellets were HP 523J grade supplied by BRASKEM. PP pellets were extruded in a Thermo Fisher Process 11 Parallel Twin-Screw Extruder at 200°C in the eight zones and a screw speed of 100 rpm. The films with 0.1 to 0.2 mm thickness were produced in a hot-pressed TIL MARCON MPH-10 hydraulic press, at 200°C and 0.5 bar.

Photodegradation

PP samples were exposed to UV-C for 0, 1, 2, 4, 6, 12, 24, 48, 96, 192, and 384 hours. The UV-C chamber source was two commercial Hg lamps (Philips TUV 4 W), positioned 26 cm apart, with 254 nm. The sample surface irradiation intensity was approximately 1.3 mW/cm². The sample holder was placed between them for dual-side exposure.

Physico-chemical analysis

Rheological characterization was performed in an Anton Paar MCR 302 rheometer using a 25 mm parallel plate geometry and 1 mm gap, at 200°C. The experiments were performed in the linear viscoelastic region with 3% strain in a nitrogen (N₂) atmosphere. ¹H TD-NMR experiments were performed in a 0.5-T Bruker Minispec mq20 NMR, VT probe head with a dead time of 11.5 μs. $\pi/2$ and π pulse lengths of 2.5 and 4.8 μs. Mixed-Magic Sandwich Echo Experiments (mixed-MSE) and Dipolar Filtered MSE (DF-MSE) experiments were also performed. FTIR-ATR were obtained in a Thermo Scientific Nicolet 6700-FTIR spectrometer, ranging from 400 to 4000 cm⁻¹, 64 scans, and 4 cm⁻¹ resolution. SEM micrographs were obtained using an FEI Inspect S50 microscope at 10 kV. All samples were coated with Au. Contact angles formed by drops of water and diiodomethane were measured using a Ramé-hart 260-F4 Series, running DROPimage Advanced v2.7 goniometer. A Netzsch DSC 200 F3 was used for DSC. Samples weighing ~10.0 mg were heated from 20°C to 210°C with a heating rate of 10 °C/min under N₂ flow.

RESULTS AND DISCUSSION

Fig. 1 (a) shows the normalized double quantum and reference intensities, associated with all ^1H spins in the sample (I_{REF}) and the intensity related to double quantum coherences between ^1H nuclear spins (I_{DQ}), as a function of the evolution period (τ_{DQ}), at 190 °C for PP 0h and PP 384h of UV-C. Fig. 1 (b) illustrates the $I_{REF} - I_{DQ}$ and the fitting of the long $2\tau_{DQ}$ region of the curves for both samples.

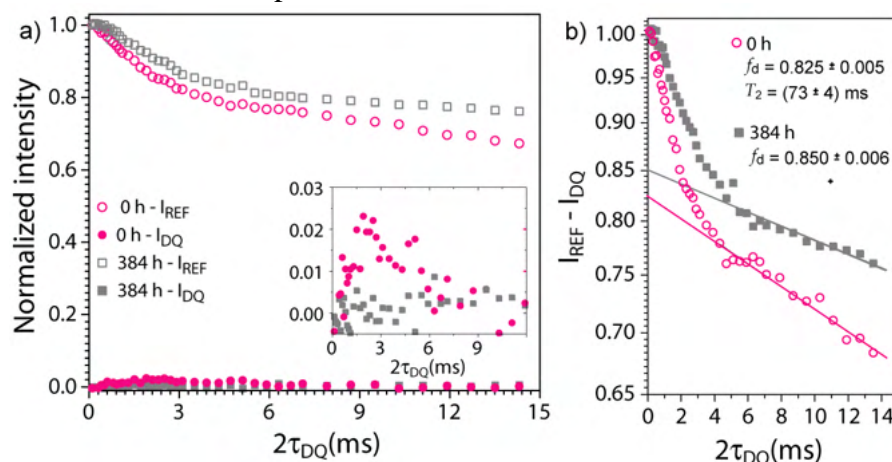


Fig 1. (a) I_{REF} and I_{DQ} as a function of τ_{DQ} for PP 0h and 384h, (b) $I_{REF} - I_{DQ}$ vs. τ_{DQ} , the fraction of free mobile chains f_d and the T_2 relaxation time for PP 0h and PP 384h.

A rather small I_{DQ} intensity is observed for PP 0h, which drops for the PP 384h. This drop indicates an increase in the fraction of unconstrained molecular segments, shown in the inset in Fig. 1 (a). An increase in the fraction of unconstrained molecular segments (f_d) and the corresponding relaxation time (T_2) is seen in Fig. 1 (b), indicating that the chains' mobility increased with the free mobile chain. Thus, the absence of I_{DQ} intensity (inset Fig. 1 (a)) and the increase in the fraction of free mobile chains (Fig.1 (b)), in UV-C samples suggests that UV-C photodegradation does not produce a detectable fraction of crosslinks. Instead, it decreases the fraction of the entangled chains.

Data from rheological measurements, DF-MSE, and DSC also report that PP tends to form branching during UV-C photodegradation. SEM images showed no cracks. The contact angle formed by drops of water decreased while the surface energy increased with the increase of the exposure time, indicating that photooxidation changed the surface hydrophilicity and wettability. FTIR-ATR showed that the methyl index is better in verifying the early stages of photodegradation under UV-C than the carbonyl index.

Acknowledgment

The authors would like to thank the financial funding given by the Coordination of Higher Education Personnel – CAPES (001), CAPES Institutional Internationalization Program – CAPES-PrInt (88887.889025/2023-00), and the São Paulo Research Foundation – FAPESP (2016/25703-2). ERdA thanks for the CNPq research grant 308760/2022-0.

References

- (1) E. Alisson, Agência FAPESP, J. Da USP, 2–5, (2021)
- (2) J. F. Rabek, Dordrecht, 1995
- (3) N.S. Allen, A. Chirinos-Padron, T.J. Henman, Prog. Org. Coatings, **13**, 97–122, (1985)
- (4) S. Aslanzadeh, M. Haghightat Kish, Fibers Polym., **11**, 710–718 (2010)
- (5) A. de S.M. de Freitas, J.S. Rodrigues, V.R. Botaro, A.P. Lemes, S.A. Cruz, W.R. Waldman, J. Polym. Res. **29**, 506, (2022)
- (6) C. Boronat, V. Correcher, J. García-Guinea, J.C. Bravo-Yagüe, Polym. Degrad. Stab. 225 (2024)

THE USE OF CLICK CHEMISTRY FOR THE PRODUCTION OF CROSSLINKED BIOBASED POLYURETHANE CORE/SHEATH NANOFIBERS AND THEIR FUNCTIONALIZATION

Stefano Torresi , Izaskun Larraza , Nagore Gabilondo , Arantxa Eceiza

'Materials + Technologies' Research Group, Department of Chemical and Environmental Engineering, Faculty of Engineering of Gipuzkoa, University of the Basque Country UPV/EHU, Donostia, 20018, Spain.

INTRODUCTION

Two biobased polyurethane formulations, one containing maleimide pendant group (PU-MAL) and the other one containing thiol pendant group (PU-SH) in the polymer backbone, were synthesized using both solvent and catalyst-free production process. Once characterized, the new compositions were used for the fabrication of nanofibers membranes through electrospinning. The two compositions were co-electrospun in a PU-MAL core/PU-SH sheath nanofiber configuration using stoichiometric maleimide to thiol ratio. The pendant counterpart moieties of each composition was used for a post-electrospinning click crosslinking upon UV irradiation. Clicked and not-clicked electrospun membranes were characterized and compared. Finally, changing the ratio of the two compositions, a membrane with excess of thiol was produced and functionalized using thiol-ene reaction to improve the hydrophobicity of the membrane.

EXPERIMENTAL

Materials

Biobased castor-oil derived poly(butylene sebacate)diol (PBSD) with an hydroxyl index of 32.01 mg KOH g⁻¹ and a Mn of 3505 g mol⁻¹ was used as polyol. 1,6-Hexamethylene diisocyanate (HDI, 168 g mol⁻¹) was used as diisocyanate, while 3-mercapto-1,2-propanediol (3MP, 108 g mol⁻¹) and N-(2,3-dihydroxypropyl) maleimide (DHPM, 174 g mol⁻¹) were used chain extenders. As functionalizing agent was used 1H,1H,2H-Perfluoro-1-decene.

Polyurethanes and electrospinning solutions synthesis

The polyurethanes were synthesized using a two-step or prepolymer bulk polymerization method, following previously reported protocol (1). Briefly, semicrystalline PBSD was melted in a two-necked round flask purged with N₂, HDI was added, mechanically stirred, and left it to react at 90 °C for 2 h. Then, the chain extender (DHPM for PU-MAL and 3MP for PU-SH) was added to the prepolymer, mixed vigorously for 10 min, and after that, the viscous liquid was transferred to a mould and pressed at 50 bar and 100 °C for 13 h. The polyurethanes were synthesized using a polyol:diisocyanate:chain extender ratio of 1:6:5. Once produced as films, PU-MAL and PU-SH films were cut in small pieces and dissolved separately in DMF:CHCl₃ (2:1 v/v) at different polymer concentrations, 15 wt% for PU-SH and 20 wt% for PU-MAL. The electrospinning parameters were set on: 18 cm tip-to-collector distance, 10 kV voltage and 1.4 ml h⁻¹ and 1.1 ml h⁻¹ flow rates for PU-SH (sheath) and PU-MAL (core), respectively.

Physico-chemical characterization

The polyurethane films were characterized using FTIR, NMR, DSC and TGA. For the electrospun membranes FTIR, NMR, TGA, SEM, DMA, WCA, tensile and solvent resistance tests were performed.

RESULTS AND DISCUSSION

The two electrospinning solutions were coaxially electrospun to obtain a crosslinkable nanofibrous membrane. Indeed, thanks to the UV-promoted thiol-Maleimide reaction, the nanofibers can be crosslinked after the electrospinning process, using UV light at 365 nm for 90 minutes. The clicked (crosslinked) membrane showed improved mechanical properties, higher hydrophobicity and better solvent resistance with respect the not-clicked one.

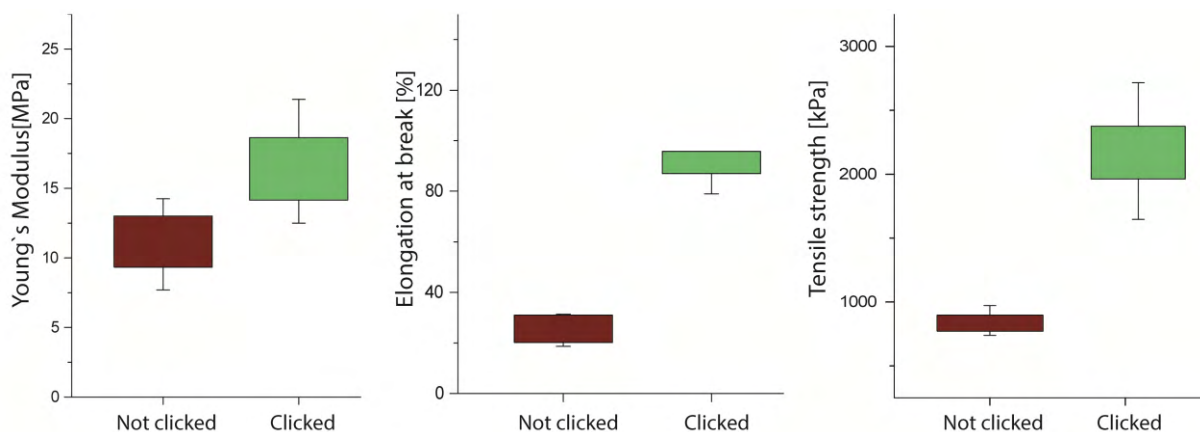


Fig. 1 Mechanical properties comparison between clicked and not-clicked membranes.

Finally, a composition containing an excess of thiols was electrospun, changing the flow rates of PU-MAL and PU-SH. The thiols not involved in the crosslinking were further functionalized with 1H,1H,2H-Perfluoro-1-decene, through thiol-ene reaction, resulting in a more hydrophobic membrane.

Acknowledgment

Financial support from Spanish Ministry of Science and Innovation and State Research Agency (MCIN/ AEI/ 10.13039/501100011033) in the frame of PID2019-105090RB-I00 project and from the Basque Country Government in the frame of Grupos Consolidados (IT-1690-22) are gratefully acknowledged. Stefano Torresi wishes to acknowledge the Ministry of Science and Innovation for his PhD grant (PRE2020-092538).

References

- 1) S. Torresi, T. Calvo-Correas, S. Basasoro, O. Guaresti, A. Alonso-Varona, N. Gabilondo, A. Eceiza, Furan-containing biobased polyurethane nanofibers: A new versatile and green support clickable via Diels-Alder reaction, *Reactive and Functional Polymers* 178 (2022) 105353. <https://doi.org/10.1016/j.reactfunctpolym.2022.105353>

THERMAL-OXIDATIVE STABILITY AND CONSUMPTION OF ANTIOXIDANTS DURING CLOSED-LOOP RECYCLING OF POLYPROPYLENE

R. Stam¹, B. Leurs¹, P. Gijsman^{1,2}, K. Ragaert¹ and R. Fiorio¹

1. Circular Plastics, Department of Circular Chemical Engineering, Faculty of Science and Engineering, Maastricht University, the Netherlands

2. Gijsman Durability Advisory, the Netherlands

rachel.stam@maastrichtuniversity.nl, r.fiorio@maastrichtuniversity.nl

INTRODUCTION

Antioxidants (AOs) are essential additives for plastics aiming to hinder the degradation of polymer chains. During processing, use, and recycling of plastics, AOs are gradually consumed and their complete depletion may lead to severe degradation, compromising the quality of the material and impeding the closed-loop recycling concept (1)-(3). Therefore, the evaluation of the thermal-oxidative stability as well as the determination of the active AO content in discarded plastics is fundamental to assess their recyclability and also to define a proper restabilization level.

In this work, we assessed the effects of closed-loop recycling on the thermal-oxidative stability and consumption of AOs in polypropylene (PP).

EXPERIMENTAL

Materials

Irganox 1010 (IR 1010, 98% pure), a phenolic primary antioxidant, was obtained from Merck (Germany). Irgafos 168 (IF 168, 98% pure), a phosphite secondary antioxidant, was obtained from TCI (Japan). Acetonitrile (ACN, HPLC grade), chloroform (AR quality) and toluene (HPLC grade) were obtained from Biosolve (France). A commercial PP grade was studied, containing both Irganox 1010 and Irgafos 168 with similar concentrations.

Preparation

The PP was submitted to consecutive extrusion and granulation cycles mimicking closed-loop recycling. The extrusions were carried out in an Xplore MC5 mini extruder at 230°C and 100 rpm. PP was fed into the extruder in batches of *ca.* 5-6 g. A fraction of the processed PP was collected for characterization after each processing cycle, and the remaining part of the material was used in the next processing cycle.

Antioxidant concentrations were determined by Soxhlet extraction and by dissolution-precipitation. Soxhlet extraction was carried out using chloroform for 48 h. The solvent was removed via rotary evaporation. Dissolution-precipitation was carried out in boiling toluene for 30 min. After dissolution, the polymer was precipitated by adding ACN, followed by vacuum filtration of the suspension. The solvent was evaporated using a nitrogen flow and the extracts were redissolved in acetonitrile before analysis.

High-performance liquid chromatography with UV detection (HPLC-UV) was employed for the analysis of the AOs. Chemiluminescence analysis (CL) was used to evaluate the oxidation induction time (OIT) of the PP samples at 180°C using dry air.

RESULTS AND DISCUSSION

The dissolution-based extraction method was substantially faster than the Soxhlet extraction (*ca.* 6 and 48h, respectively), and a higher yield of AOs was obtained via dissolution (*ca.* 20% for IF 168 and 30% for IR 1010) than the Soxhlet one. Therefore, the dissolution-precipitation method was used in the further steps of this study.

The consumption of AOs as a function of extrusion cycles is shown in Figure 1 and it is shown that *ca.* 90% of IF 168 is depleted after the first processing cycle, while IR 1010 reaches 90% depletion after the third processing cycle.

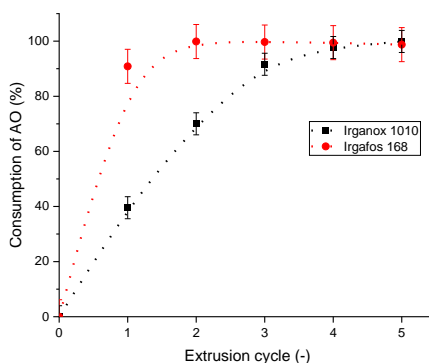


Fig. 1 Consumption of AOs as a function of consecutive extrusion cycles.

The CL results are shown in Figure 2a and indicate that the thermal-oxidative stability of PP decreases with the increase in the number of extrusion cycles. The consumption of IR 1010 leads to a proportional decrease in OIT, as shown in Figure 2b.

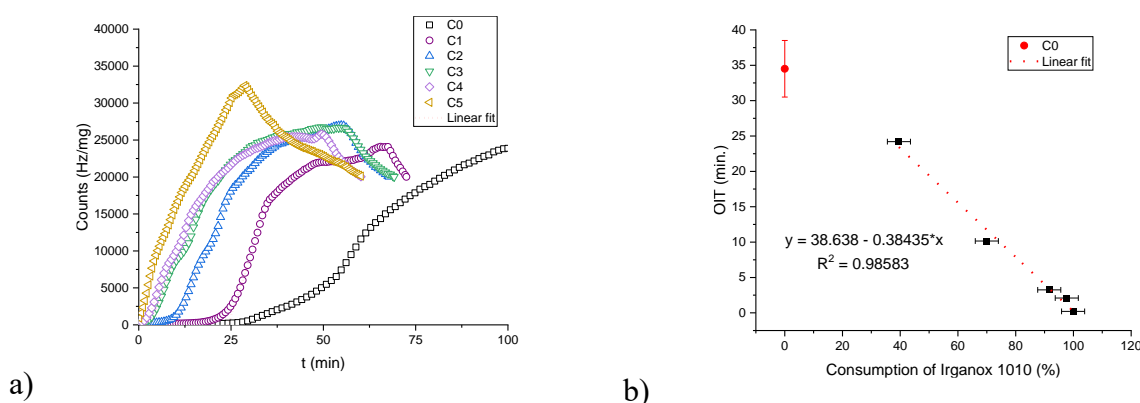


Fig. 2 a) Chemiluminescence as a function of time for the samples submitted to consecutive extrusion cycles. b) OIT as a function of the consumption of Irganox 1010.

The results show that melt processing of PP leads to a gradual consumption of the stabilization package. IF 168 was depleted faster than IR 1010, indicating that restabilization of the PP here evaluated is necessary before its first mechanical recycling cycle. Chemiluminescence analysis provides a good indication of the state of thermal-oxidative stability of PP. Furthermore, OIT values correlate well with the active content of Irganox 1010 and indicate the required level of restabilization for the polymer.

Acknowledgment

This work has been financially supported by the European Union's Horizon Europe research and innovation programme under grant agreement No 101058487.

References

1. Jansson, Anna, Kenneth Möller, and Thomas Gevert. *Polymer Degradation and Stability* 82.1 (2003): 37-46.
2. Gijsman, Pieter. *e-Polymers* 8.1 (2008): 065.
3. Gijsman, Pieter, and Rudinei Fiorio. *Polymer Degradation and Stability* 208 (2023): 110260.

CHARACTERISATION OF AGED ABS LAYERS FORMED DURING LONG-WAVELENGTH UV EXPOSURE

L. Delarue^{1,2}, A. Dazzi³, J. Mathurin³, M.F. Pucci², P.-J. Liotier¹, P. Ienny², A.-S. Caro-Bretelle², D. Perrin^{1*}.

¹ Polymers, Composites, Hybrids (PCH) – IMT Mines Alès, Alès, France

² Sustainability of eco-materials and structures (DMS) – IMT Mines Alès, Alès, France

³ Laboratoire de Chimie Physique, CNRS, Université Paris-Saclay, France.

*didier.perrin@mines-ales.fr

INTRODUCTION

Acrylonitrile Butadiene Styrene (ABS) is a polymer extensively used in the field of electronic, in household equipment, or in vehicles. More than a third of the overall quantity of this polymer can be found in this type of waste (1).

ABS is a rubber-toughened polymer. It is composed of a majority styrene-acrylonitrile copolymer phase (SAN) with spherical nodule-shaped elastomer inclusions of polybutadiene (PB). These nodules enhance the fracture toughness of the polymer allowing it to be more resilient. Yet, ABS is very sensitive to photo-oxidation risking rendering the product unusable through typical mechanical recycling (2,3). Literature relates the loss of mechanical properties with the aging of polybutadiene nodules (2,4,5).

In the present work, aged ABS layers formed during UV-exposure and their impact on the overall mechanical behavior are characterized.

EXPERIMENTAL

Materials

The ABS used in this study is the ABS Teluran GP22®. The materials were used as received.

Films elaboration

Two kinds of films were produced. A 450µm thick film was obtained through extrusion CAST. 30 µm thick films were obtained by solvent casting using acetone.

Aging conditions

The accelerated aging was done using the SEPAP 12-24 device. This chamber features 4 mercury vapor lamps on each corner and a central carousel allowing a homogeneous exposure of all the sides. Long UV wavelengths λ were used, with $300 < \lambda < 600$ nm.

Macro and micro scale

Infrared spectra were performed using a Vertex 70 FT MIR spectrometer from Bruker with a wavelength between 400 and 4000 cm^{-1} . Transmission mode through the 30 µm films was chosen to analyze the samples.

Aged layers were observed, morphology was characterized, and length was measured using the optical microscope VHX-7000 produced by Keyence. The mechanical behavior was analyzed using a low-velocity tensile test on the 450 µm thick films with an impact velocity of 4.5 m/s. This test allows the application of homogeneous stress across the sample, unlike the Izod and Charpy tests which lead to a heterogeneous state of stress.

Nano-scale characterization

The mechanical behavior of each phase was analyzed at the nanoscale using bimodal tapping mode (AM-FM) by means of an Atomic Force Microscope (MFP-3D Infinity by Asylum Research). This nano-scale characterization was completed by mapping the oxidized

compounds thanks to AFM-IR analysis using Icon-IR system (Bruker Nano) at the Institut de Chimie Physique, CNRS, Paris-Saclay University, France. Those nano-scale characterizations were conducted on both the sample surface and the core of the sample. For AM-FM analysis, a smooth surface was prepared using Leica Ultramicrotome device with a temperature of $-120\text{ }^{\circ}\text{C}$. Thin shaving $\sim 100\text{ nm}$ thick of ABS was collected, placed on silicon wafer, and used in the AFM-IR.

RESULTS AND DISCUSSION

Optical observations revealed distinct thin layers of oxidized ABS on the sample surface, with their lengths increasing with exposure time. At the nanoscale, rigid PB nodules were found in the aged layers of ABS, while soft nodules were present in the sample core (Figure 1). These rigid PB nodules contained carbonyl compounds formed due to oxidation, whereas no oxidized compounds were detected in the sample core. Consequently, because of these aged layers, a significant change in mechanical behavior was observed during mechanical testing. Initially ductile, the exposed ABS exhibited brittle behavior after 12 hours of aging (Figure 2).

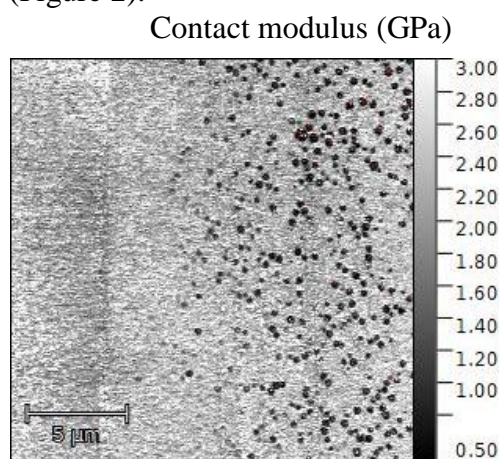


Figure 1 – AM-FM mapping (scan size $10 \times 10\ \mu\text{m}^2$) of the calculated contact modulus of 10-days aged ABS. The values presented are indicative and not intended to represent effective mechanical modulus values.

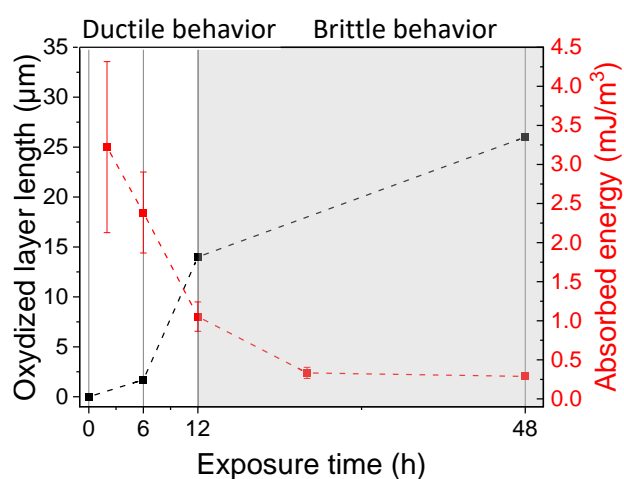


Figure 2 - Evolution of ABS oxidized layer length and mechanical properties tested through dynamic tensile test during UV exposure.

Acknowledgment

This work has been financially supported by Skytech SLP and IMT Mines Alès.

References

1. Maris E, Botané P, Wavrer P, Froelich D. Characterizing plastics originating from WEEE: A case study in France. *Miner Eng.* 2015;76:28–37.
2. Signoret C, Edo M, Lafon D, Caro-Bretelle AS, Lopez-Cuesta JM, Ienny P, et al. Degradation of Styrenic Plastics During Recycling: Impact of Reprocessing Photodegraded Material on Aspect and Mechanical Properties. *J Polym Environ* [Internet]. 2020;28(8):2055–77. Available from: <https://doi.org/10.1007/s10924-020-01741-8>
3. Bucknall CB, Street DG. Fracture behavior of rubber-modified thermoplastics after aging. *J Appl Polym Sci.* 1968;12(6):1311–20.
4. Jouan X, Gardette JL. Photooxidation of ABS of long-wavelengths. *J Polym Sci A Polym Chem.* 1991;29(5):685–96.
5. Adeniyi JB, Kolawole EG. Thermal and photo-degradation of unstabilized ABS. *Eur Polym J.* 1984 Jan;20(1):43–7.

CHROME TANNED LEATHER TRIMMINGS STABILIZED WITH GYPSUM THROUGH THERMAL INSULATION PANEL PRODUCTION

A.C. Paul^{1,3,*}, M.T. Islam³, P. Roy³, N. Saha^{1,2}, T. Saha² and P. Saha^{1,2}

¹Centre of Polymer Systems, University Institute, Tomas Bata University in Zlin, Trida Tomase Bati 5678, 76001 Zlin, Czech Republic

²Footwear Research Centre, University Institute, Tomas Bata University in Zlin, Nad Ovcirnou IV, 3685 Zlin, Czech Republic

³Department of Leather Engineering, Khulna University of Engineering & Technology, Khulna-9203, Bangladesh

*apaul@utb.cz

INTRODUCTION

Raw hides and skin industries are the major polluting industries in the world. In tanneries, only 20% of raw hides and skin are converted to finished leather, and the rest of the amount is discharged as solid, liquid, and gaseous waste. Statistically, leather solid waste comprises 50-60% lime flesh, 30-40% shaving dust, buffing dust and wet-blue splits, 5-7% chrome-tanned leather trimming (CTLT), and 2-5% hair (1). In Bangladesh, it was estimated that 105 tons of CTLT were generated each year, including the lean and pic season (2). At present, improper disposal of leather solid waste, often ending up in landfills without treatment, can contaminate soil and groundwater due to the leaching of chromium and other metals. However, Researchers and stakeholders in the leather industry have been exploring innovative solutions to convert waste materials like CTLT into value-added products. Due to the low thermal conductive value, CTLT can be used for thermal insulation panel-type composite materials. So far, insulation panels utilized as rooftop ceilings in the building can reduce heat transfer and minimize energy consumption (3). Presently, many researchers have already developed innovative approaches to stabilize leather solid waste through brick production (4, 5). However, the above-mentioned approaches consume very little waste. Furthermore, when this chrome-containing waste was combusting at a higher temperature, there was a possibility to convert Cr (III) to Cr (VI), which is carcinogenic.

In this approach, hazardous CTLTs stabilize through solidification with gypsum (G) as construction materials such as '*thermal insulation panels*', which have not been attempted yet, could get preference. The salient objective of this research endeavor is to minimize hazardous chrome-containing solid waste through the production of value-added products. A feasible insulating panel could open a new window for stabilizing CTLTs with gypsum as well as promote its safe waste management.

EXPERIMENTAL

Materials

Chrome-tanned leather trimmings (CTLTs) were collected from SAF Tannery Ltd, Jashore, Bangladesh. Gypsum (BK-90) was purchased from B. K. Plaster & Gypsum Corporation (Bangkok, Thailand). Wooden mold was prepared with the dimensions (6 inch × 5 inch × 0.5 inch) from the carpenter outlet of the KUET campus, Khulna, Bangladesh.

Preparation of 'Thermal Insulation Panel'

At first, collected CTLTs were converted to fine tiny particles using a laboratory pulverizer (Pulverisette, Germany). Each insulation panel was prepared by varying the amount (5% to 25% (w/w) of grounded CTLT and G; were mixed with water and then poured into the wooden mold. A control sample was also developed with 100% gypsum and 0% CTLT. Finally, samples were kept at room temperature for drying until reached into constant

weight. The ‘CTLT-G’ biocomposites are designated as (S₁-0, S₂-5, S₃-10, S₄-15, S₅-20 and S₆-25).

Characterization

Bulk density was investigated according to ASTM C373-88, and thermal conductivity was measured via Lee’s Disc apparatus at room temperature. Furthermore, FTIR, TGA, and surface morphology (SEM) were examined to evaluate its structural and physico-chemical properties.

RESULTS AND DISCUSSION

The density and thermal conductivity variations among the composite samples have been shown in Fig. 1. It was observed that the density of the composites was inversely related to the increasing amount of CTLT. Decreased density behavior occurs due to the gypsum particles' unstable bonding structure and the interfacial air gap to the adjacent collagen fibers of CTLTs (6). On the other hand, thermal conductivity also decreased with the increased amount of CTLT with G. Here, it was observed that a 15% CTLT-containing composite panel showed approximately 70% increased thermal insulation properties. In that case, further investigations, such as FTIR, TGA, and SEM, were conducted with only 15% CTLT containing composite panels.

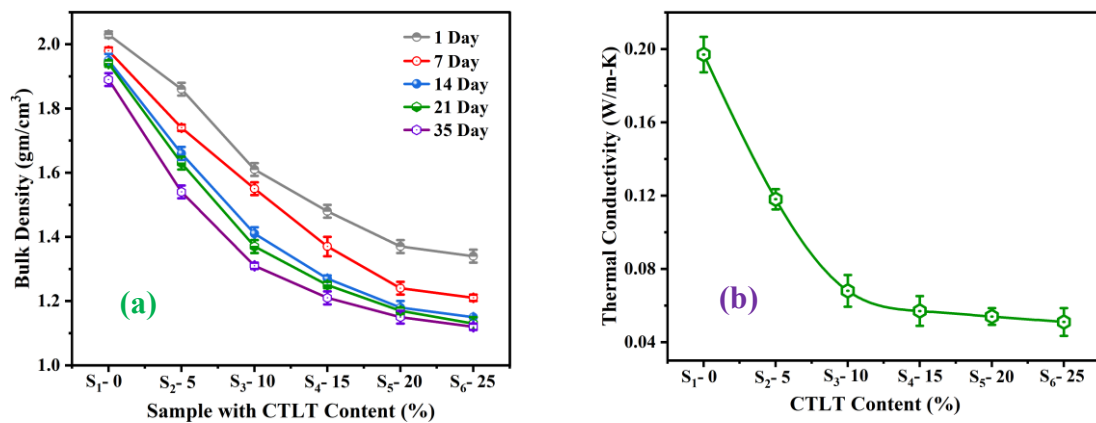


Fig. 1 Density (a) and thermal conductivity (b) of CTLT-G biocomposites

Acknowledgment

The authors are thankful for the financial support of IGA project IGA/CPS/2024/005 and Tomas Bata University in Zlin, Czech Republic and for allowing to participate in the MoDeSt 2024 Conference. The first author and his research team are also acknowledging the Leather Engineering Department, Khulna University of Engineering and Technology (KUET), Khulna-9203, Bangladesh, as performed this research activity at the Department premises.

References

- 1) FAO. World statistical compendium for raw hides and skins, leather and leather footwear 1998-2014, (2015)
- 2) S. Basak, A. Mita, D.M.J Alam, Journal of Scientific and Engineering Research, **7**, 124-130 (2020)
- 3) A. Islam, Y. Molla, T.K. Dey, M. Jamal, M.E. Uddin, Journal of Polymer Research, **28**, 322 (2021)
- 4) M.A. Hashem, M.E.H. Zahin, M.S. Haque, M.S. Milu, M.A. Hasan, S. Payel, Construction and Building Materials, **400**, 132769 (2023)
- 5) M.A. Hasan, M.A. Hashem, S Payel, Construction and Building Materials, **314**, 125702 (2022)
- 6) W. Hittini, A.H.I. Mourad, Journal of cleaner production, **236**, 117603 (2019)

SULFONATED POLYETHER ETHER KETONE-BASED PROTON EXCHANGE MEMBRANES FOR SEMI-ORGANIC REDOX FLOW BATTERIES

F. Niccolai,^{1,2} L. Calzolari,¹ Z. El Koura,² I. Pucher,² E. Martinelli¹

¹Department of Chemistry and Industrial Chemistry, University of Pisa, Italy

²Green Energy Storage, via Sommarive 18 c/o Fondazione Bruno Kessler, Italy

francesca.niccolai@phd.unipi.it, francescaniccolai@greenenergystorage.eu

INTRODUCTION

Redox flow batteries (RFBs) are considered enticing devices for the storage of energy.[1] The membrane is a crucial component for RFBs, determining charge and discharge performance and thus efficiency as well as economic feasibility,[2] its function being to limit the crossover of active species while permitting the passage of supporting electrolyte ions. An ideal membrane should possess high ionic conductivity and selectivity in order to achieve high efficiency. Moreover, it should be chemically stable, mechanically durable, cost-effective, and capable of withstanding high-power densities. Nafion-based proton exchange membranes (PEMs) can be regarded as the main benchmark for RFBs because of their high ionic conductivity and high stability in chemically aggressive environments. The present work focuses on the design and development of new efficient PEMs for semi-organic RFBs based on 9,10-anthraquinone-2,6-disulfonic acid disodium salt (AQDS)/bromine (Br₂) (Figure 1). In particular, our approach focuses on the chemical post-modification of polyether ether ketone (PEEK), commercially available specialty polymer. PEEK was directly subjected to a sulfonation reaction to obtain a sulfonated PEEK (S-PEEK) and used alone or blended with polyvinylidene fluoride (PVDF) for the preparation of PEMs.

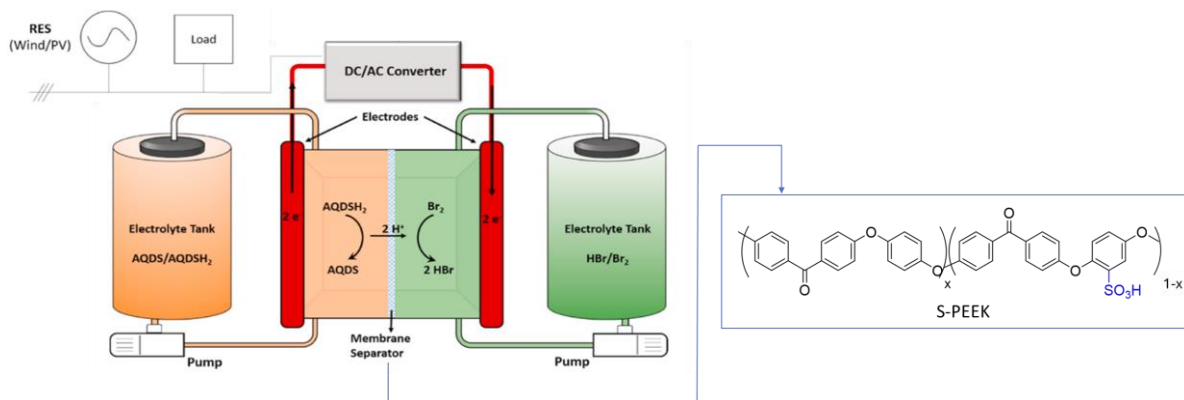


Figure 1. Representation of a semi-organic RFB [3] and chemical structure of the synthesized polymer used for PEM preparation.

EXPERIMENTAL

Materials

Dimethylformamide (DMF), Sulfuric acid (H₂SO₄) (96 wt% purity), PEEK (density = 1.30 g/cm³ and a melt viscosity of 350 Pa s) and PVDF (M_n = 850,000 – 1,050,000 g/mol).

Method

The sulfonation reaction of PEEK was performed in concentrated sulfuric acid (H₂SO₄, 96 wt%). The reaction was carried out at 70 °C for 24 hours. The reaction mixture was

precipitated in cold water. The crude polymer was rinsed with deionised water, until neutrality. The functionalized polymer powder was then dried at 50 °C for 12 h under vacuum. Degree of sulfonation (DS) was determined by $^1\text{H-NMR}$ analysis. Moreover, SPEEK was used either alone or blended with PVDF for the preparation of PEMs. The membranes were prepared by solution casting from DMF solution. The solution was poured into a glass Petri dish (9 cm in diameter), which was left at room temperature for 24 h in the fume hood and afterward heated to 50 °C under vacuum overnight to promote the evaporation of the solvent. The obtained films appeared to be free from macroscopic defects and homogeneous in thickness (70–100 μm).

Physico-chemical and electrochemical characterization

Thermal analyses were performed using thermal gravimetric analysis (TGA) and differential scanning calorimetry (DSC).

Mechanical analysis was carried out performing tensile-strain stress tests.

Electrochemical analysis was evaluated by a multi-channel potentiostat/galvanostat.

RESULTS AND DISCUSSION

S-PEEK with different DS were obtained by varying the time of sulfonation reaction. The properties of the final PEMs were modulated by changing both the DS of the S-PEEK and the weight ratio between S-PEEK and PVDF for the blended membranes. The membranes were extensively characterized to assess their chemical, thermal, mechanical, and electrochemical properties and structure-property correlations were highlighted. Selected membranes subjected to tests in 1 W AQDS/ Br_2 single cell showed good performance in terms of energy and coulombic efficiency (Figure 2), having electrochemical properties at least comparable to those of Nafion benchmark, thus indicating the actual potential of such materials for the envisaged final use.

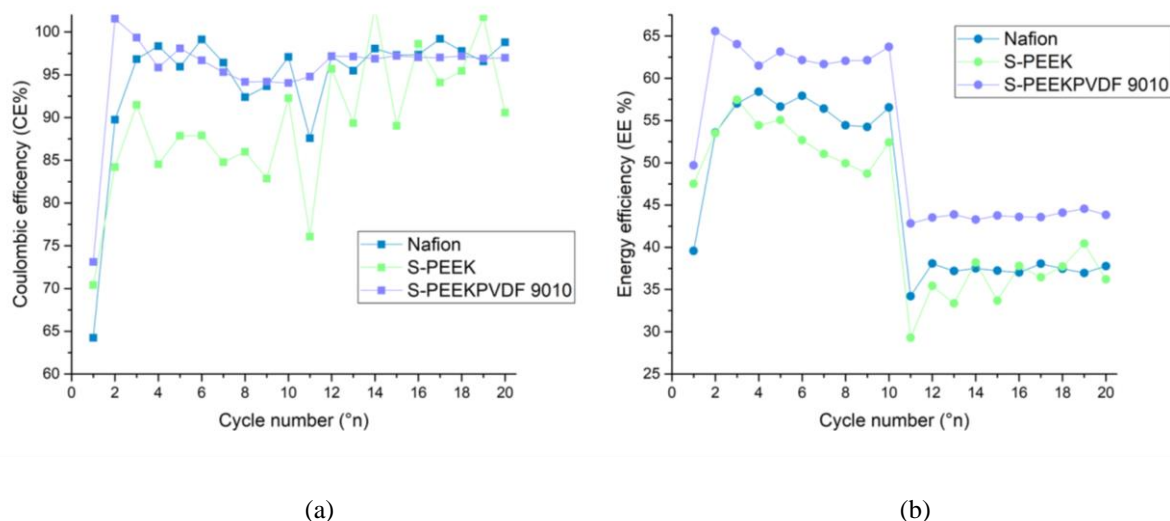


Figure 2. Comparison of (a) coulombic efficiency (CE) and (b) energy efficiency (EE) for Nafion, S-PEEK and S-PEEK/PVDF membranes by performing 10 cycles at 50 mA/cm^2 followed by 10 cycles at 100 mA/cm^2 .

Acknowledgments

The Authors of the University of Pisa thank GES s.r.l. for the financial support.

References

- [1] P. Arevalo-Cid, P. Dias, A. Mendes, and J. Azevedo, *Sustain. Energy Fuels*, 5, 5366–5419, (2021).
- [2] C.A. MacHado, G.O. Brown, R. Yang, T.E. Hopki-ns, J.G. Pribyl, T.H. Epps, *ACS Energy Lett.*, 6, 158–176, (2021).
- [3] G. Di Florio, I. Pucher, P. Todeschi, M. C. Baratto, R. Basosi, E. Busi, *J. Clean. Prod.*, 343, 130899 (2021).

How POSS in intumescent flame-retardant systems can contribute to the improvement of the fire behavior of virgin and recycled HDPE?

M. Combeau, M. Batistella, A. Breuillac^a, A. Impola^b, D. Perrin, J.M. Lopez-Cuesta

Polymers Composites and Hybrids (PCH), IMT Mines Ales, 7 rue Jules Renard, Alès, France

^aEnvironment Massif Central, 20-22 rue de la Draine ZAE du Causse d'Auge, Mende, France

^bBioenvision Technology, Herøya Industripark, Hydrovegen 67 B92, 3936 Porsgrunn, Norway
marie.combeau@mines-ales.fr

INTRODUCTION

The circular economy's requirements are now driving up the use of recycled polymers. Nevertheless, these recycled polymers are often used through downgraded applications (1). This work aims to design high-performance recycled HDPE to replace virgin polymers in technical applications (e.g. housing, cables, urban furniture) which need highly fire-resistant materials. Various flame-retardant systems have been studied in literature. In particular, intumescent flame-retardant (IFR) system combining ammonium polyphosphate (APP) and polyamide 6 (PA 6) is known to be very effective for polyolefins (2). Furthermore, a variety of nanoparticles were assessed as synergistic agents in IFR systems (3).

The current study examined the effects of an IFR system combining APP and PA6 on the fire behavior and mechanical properties of virgin and recycled PE. In addition, the effect of POSS nanoparticles as a synergistic agent (4) was also evaluated.

EXPERIMENTAL

Materials

The raw materials used in this work were: virgin HDPE granulates (vPE RIGIDEX HD5502S, Ineos), two recycled HDPE flakes (HDPE from milk bottles (rPE-b1) and from white bottles such as detergents or household products (rPE-b2) provided by EMC), APP (EXOLIT AP423, Clariant), PA 6 (TECHNYL C206, Domo Chemicals), maleic anhydride grafted polyethylene (PE-g-MA OREVAC OE825, Arkema) and antioxidant (IRGANOX B225, BASF) were used. POSS nanoparticles devoted to polyolefins were kindly supplied by Bioenvision Technology (POSS D-Pyre[®] S400).

Preparation

First, APP, was dried at 100°C and PA6 and PE-g-MA at 80°C under vacuum for 12h. Then, all formulations were prepared using a co-rotating twin screw extruder (Cleextral BC 21, 250 rpm, 230°C and a total flow of 4 kg/h). Finally, the pellets were processed into square sheet specimens (100x100x4mm³), for fire testing, and into standard testing bars (ISO 527), for mechanical and rheological tests, using an injection molding machine (Krauss Maffei 50T, 240°C, and a mold temperature of 40°C). Samples compositions are given in Table 1.

Sample names	vPE / rPE-b1 / rPE-b2	PE-g-MA	PA 6	APP	POSS
F0	99	–	–	–	–
F1	78	1	5.25	15.75	–
F2	78	1	5.125	15.375	0.5
F3	78	1	5	15	1
F4	78	1	4.75	14.25	2

Table 1 Formulation names and compositions in wt% (1wt% of antioxidant were added to all blends).

Fire testing, rheological, and mechanical characterization.

Fire tests were performed using a FTT cone calorimeter with an irradiance of 35, 50 and 75 kW/m². Mechanical measurements were conducted according to ISO 527 standard using a Zwick Z010 equipment.

RESULTS AND DISCUSSION

Cone calorimeter results show that the addition of POSS nanoparticles increase the fire reaction of all blends. Indeed, as reported in Fig. 1, the peak of HRR (heat release rate) is lower for F3 (1% POSS) than for F1 (without POSS). Results also shows a plateau for F3, indicating that POSS promotes the creation of a more cohesive protective layer, regardless of the nature of PE. On the other hand, some differences were observed for rPE-b1 formulations, which have resulted in the formation of an expanded charring layer that was not observed for the other two HDPEs.

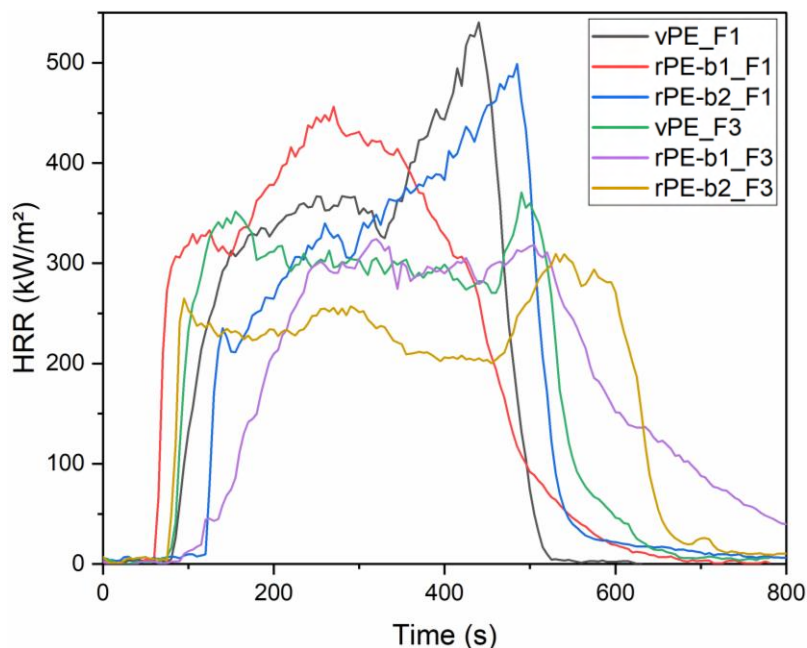


Fig. 1 Heat Release Rate plots of the composites. Heat flux: $50 \text{ kW}\cdot\text{m}^{-2}$

It appears that the three types of HDPEs exhibit different viscosities and show different fire behaviour. It is expected that rheological measurements in progress will allow viscosity and the fire properties of the blends to be correlated. Finally, mechanical properties of the blends reveal that the addition of IFR system in recycled HDPE does not degrade the mechanical properties of the recycled HDPE, which are similar to virgin ones.

The originality of this work lay in the use of POSS combined with an APP/PA6 system to achieve a clear improvement in the fire properties of HDPE formulations. Particularly for recycled HDPE and at low POSS levels (1%).

Acknowledgment

This work has been financially supported by Environment Massif Central company and IMT Mines Alès.

References

- 1) Jubinville, D. *et al.* A comprehensive review of global production and recycling methods of polyolefin (PO) based products and their post-recycling applications. *Sustainable Materials and Technologies* **25**, (2020).
- 2) Lim, K. S. *et al.* A review of application of ammonium polyphosphate as intumescent flame retardant in thermoplastic composites. *Compos B Eng* **84**, 155–174 (2016).
- 3) Lopez-Cuesta J.M., Laoutid F. Multicomponent FR systems: polymer nanocomposites combined with additional materials. *Fire Retardancy of Polymeric Materials Chap 12*, 309-313, C. Wilkie, A. Morgan, Eds., CRC Press (2010).
- 4) Turgut, G. *et al.* The effects of POSS particles on the flame retardancy of intumescent polypropylene composites and the structure-property relationship. *Polym Degrad Stab* **149**, 96–111 (2018).

Performance Bioplastic Synthesis Utilizing Platform Molecules Derived from Renewable Feedstocks

A. Nag and T. Kaneko

Green Chemistry Centre of Excellence, Department of Chemistry, University of York, York, YO10 5DD, United Kingdom

School of Chemical and Material Engineering, Jiangnan University, Wuxi 214122 China

INTRODUCTION

Biomass, a renewable carbon source which can be processed using biorefinery system as a substitute of conventional fossil-based refineries. Aromatic precursor molecule synthesis involves chemical synthesis of fossil-fuel-based starting materials, such as benzene and xylene. These energy-intensive processes usually produce many by-products along with the desired molecule. Microbial fermentation of the lignocellulosic derivatives is a solution to this issue where aromatic molecules can be extracted from natural resources involving minimum energy conversion.^{1,2} Aromatic polybenzimidazoles (PBI) are considered as high-performance plastics due to their outstanding thermal and mechanical stabilities owing to strong π - π stacking interaction among aromatic and imidazole rings, and H-bonding between N-H and N of the imidazole ring.^{3,4} In another aspect, high-performance water-soluble polymers have a wide range of applications from engineering materials to biomedical plastics. However, existing materials are either natural polymers that lack high thermostability or rigid synthetic polymers. Polyimide samples prepared from renewable resources simply converted into water-soluble polymers by ion-exchanging is interesting for various water-borne applications.⁵

EXPERIMENTAL

In this regard, 3-amino-4-hydroxybenzoic acid (AHBA) and 4-aminobenzoic acid (ABA) were produced from kraft pulp, an inedible cellulosic feedstock, using metabolically engineered bacteria. AHBA is chemically converted to 3,4-diaminobenzoic acid (DABA); subsequently, poly(2,5-benzimidazole) (ABPBI) was obtained by the polycondensation of DABA and processed into an ultrahigh thermoresistant film. Copolymer polybenzimidazole / polyamide (PBI / PA) was prepared using 4-aminobenzoic acid (PABA) which has high environmental occurrence, and they were characterized and compared with respect to existing high-performance polymers.

In another research, *Escherichia coli* derived 4-aminocinnamic acid (4-ACA) was employed for dimerization to obtain diamino truxillic acid by simple UV-irradiation which was further used as diamine moieties for biobased polyimide synthesis along with dianhydrides. Basically, an amino acid-derived building block, 4,4'-diamino- α -truxillate dianion (4ATA²⁻), that induces water solubility in high-performance polymers. Polyimides containing 4ATA²⁻ units are intrinsically water-soluble and are processed into films cast from an aqueous solution.

RESULTS AND DISCUSSION

Thermal degradation stability of all PBI / PA copolymers was measured in inert and air atmosphere; Unexpectedly all of them show very high thermal stability. One of these compounds (PBI / PA 85/15) shows ultrahigh values of 10% weight loss temp. (T_{d10}), 743 °C at max in N₂ and 689 °C at max in air. The PBI / PA films were cast over trifluoroacetic acid (TFA) solution on a glass plate. Mechanical properties for all those compounds were measured as the tensile strength of 90 MPa and Young's modulus of 7.7 GPa at maximum. All the PBI / PAs consisted of high crystallinity 41% at max. These values are as high as some of the metal oxides and being organic material with high thermal stability. Thus, the PBI / PA would be hopefully applied as organic-inorganic hybrid materials because of its ultrahigh heat resistance and chemical resistance properties. PBI/PA showed a high thermoresistance while maintaining a lower density than most of the conventional high-performance plastics, including Kevlar,

Kapton, and Zylon, among others. Considering glass-fiber-reinforced polyphenylenesulfide (density: 1.66 g cm^{-3}) and liquid crystalline polymers (density: 1.61 g cm^{-3}), the ultrahigh thermoresistance and lightweight of Ami-PBI (density: 1.36 g cm^{-3}) means it could be used in the manufacture of engine components to improve energy efficiency for hybrid electric vehicles sensitive to weight. Computational study confirmed that, incorporation of small amount of PA unit in PBI chain strengthens the interchain H-bonding and the resulting PBI/PA with 15% amide unit showed higher thermostability than the PBI homopolymer and infact highest among any of the reported biomass or petroleum-derived plastics in terms of thermogravimetric analysis.

On the other hand, the resulting polyimide films starting from biomass exhibit exceptional transparency and extremely high thermal stability. The carboxyl side chains of the polyimides were ionized by aqueous solutions of metal hydroxide such as KOH. The polyimide potassium salts were dissolved in water and the film was cast from this aqueous solution to obtain an optically clear film. In addition, the films can be made insoluble in water by simple post-treatment using weak acid or multivalent metal ions such as calcium. The films of polyimide salts produced with alkaline metals showed high T_{d10} values of $366 \text{ }^\circ\text{C}$. Furthermore, the polyimide salt films made with heavier alkaline ions those were found to be more ductile. Alkaline metal counter ions can be replaced with the multivalent metal ions and there by resulting the formation of water insoluble polyimide. The synthesized polyimide's derived from bio-based resources are useful for yielding waterborne polymeric high-performance applications.

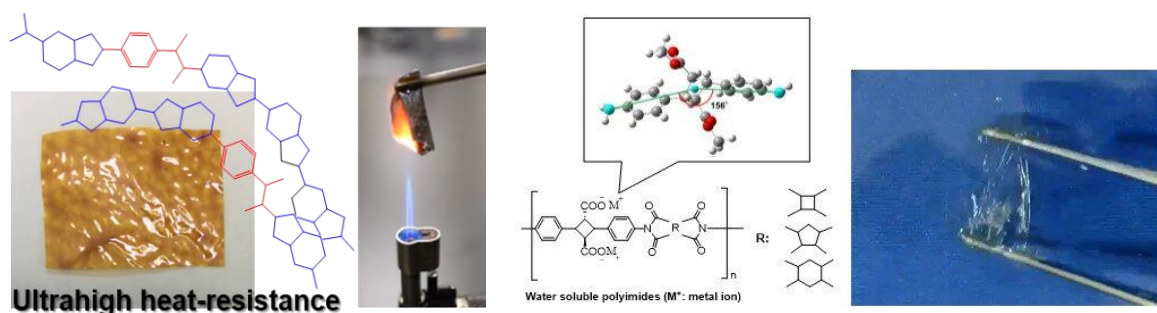


Fig. 1 Schematic representation of biobased polybenzimidazole and polyimide with their structure-property relationships

Acknowledgment

This work was supported by Japan Science and Technology Agency (CREST, Grant No. JPMJCR13B3

References

- 1) H. Suzuki, Y. Ohnishi, Y. Furusho, S. Sakuda, S. Horinouchi J. Biol. Chem. 281, 36944 (2006).
- 2) H. Kawaguchi, K. Sasaki, K. Uematsu, Y. Tsuge, H. Teramura, N. Okai, S. Nakamura-Tsuruta, Y. Katsuyama, Y. Sugai, Y. Ohnishi, K. Hirano, T. Sazuka, C. Ogino, A. Kondo Bioresour. Technol. 198, 410 (2015).
- 3) V. V. Korshak, M. M. Teplyakov, J. Macromol. Sci., Part C: Polym. Rev. 5, 409. (1971)
- 4) A. Nag, M. A. Ali, H. Kawaguchi, S. Saito, Y. Kawasaki, S. Miyazaki, H. Kawamoto, D. T. N. Adi, K. Yoshihara, S. Masuo, Y. Katayama, A. Kondo, C. Ogino, N. Takaya, T. Kaneko, Y. Ohnishi Adv. Sus. Sys. 5(1), 2000193 (2021).
- 5) S. Dwivedi, A. Nag, S. Sakamoto, Y. Funahashi, T. Hiramaoto, K. Takada, T. Kaneko RSC Adv., 2020, 10, 38069

EFFECT OF FILLERS ON THE SPINODAL DECOMPOSITION AND ELECTRICAL CONDUCTIVITY OF POLYMER BLENDS AND DIBLOCK COPOLYMERS

A.I. Chervanyov

Institute of Theoretical Physics, University of Münster, Wilhelm-Klemm Str. 9,
48169 Münster, Germany, chervany@uni-muenster.de.

INTRODUCTION

We demonstrate that adding a relatively small volume fraction of solid fillers significantly changes the thermodynamic and electrical properties of the polymer composites based on polymer blends (PB) and diblock copolymers (DBC). A key role in the described changes is played by the two relevant effects, i.e. the formation of the polymer-filler inter-phases (wetting) and the polymer-mediated interaction (1) between fillers. By developing and making use of the liquid state theory of multi-component filled polymer systems, we quantitatively analyze these effects in detail. The obtained results make it possible to elucidate the effect of fillers on the stability and miscibility of PB, as well as the conductivity of filled PB and DBC.

Based on our findings, we show that nano-fillers can be effectively used to improve the miscibility of PB that show the low critical solution temperature (LCST) behavior. Recall that improving the miscibility (compatibilization) of PB is of great importance for their use in automotive industry, electronic devices, and packaging technology (2). In addition, we demonstrate that the localization of fillers in PB and DBC, determined by the above effects of wetting and polymer-mediated interactions, is the main factor affecting the conductivity of these composites. Our theoretical predictions pave the path towards the use of PB and DBC filled with conductive fillers as electrical sensors (3).

THEORETICAL

Liquid state theory of filled polymer blends

We developed liquid state (integral equation) theory to study the effect of hard fillers on the thermodynamics, phase behaviour and electrical properties of PB. The developed theory relies on the Sanchez-Lacombe equation of state of compressible filled PB implemented in the calculation of the correlation functions between the blend species and fillers. The developed approach makes it possible to obtain the excess thermodynamic functions caused by the presence of fillers, as well as the polymer-mediated interactions between fillers. The excess thermodynamic functions are used to calculate the shift of the spinodal of PB caused by the presence of fillers. The calculated local excess chemical potential of a filler in PB is employed to determine the preferential localization of fillers in PB and calculate the conductivity of the composite.

Phase-field theory of filled diblock copolymers

The performed work has progressed through three stages as follows. In the first stage we have thoroughly investigated the interactions between fillers mediated by DBC. The described first stage also includes the calculation of the immersion energy of a filler that has different affinities for dissimilar DBC blocks. The obtained polymer-mediated interactions between fillers and the immersion energy have been used in the second stage of the present work to study the localization of fillers in the DBC system depending on the involved factors, as follows: i) affinity of fillers for copolymer blocks; (ii) interaction between fillers; (iii) temperature-dependent microstructure of DBC. The mathematical development in this stage relies on the formulation and solution of the phase-field model describing the microstructure of a filled DBC system. The third stage of the reported work involves the calculation of the conductivity of the composite comprised of the insulating DBC system and conductive fillers.

The described calculation of the conductivity has been performed by combining the developed phase-field model, Monte-Carlo simulations and the resistor network model.

RESULTS AND DISCUSSION

As one of the key results of the study, we proved that the correlations imposed by the variations of the composition of PB cause a significant non-osmotic contribution to the polymer-mediated interaction between fillers immersed in this blend. Interestingly, this contribution proves to dominate over the conventional osmotic contribution in the case of dense PBs. Based on the above results obtained for the polymer-mediated interaction between fillers, the stability and miscibility of compressible PB are studied in detail. We show that the presence of non-adsorbing fillers can be used to enhance the stability of PB that shows LCST behavior. In particular, the calculated effect of fillers explains the experimentally observed filler-induced change in the LCST (see Figure 1). As an additional important practical application of the developed theory, we investigated the electrical response of an insulating PB filled with conductive fillers.

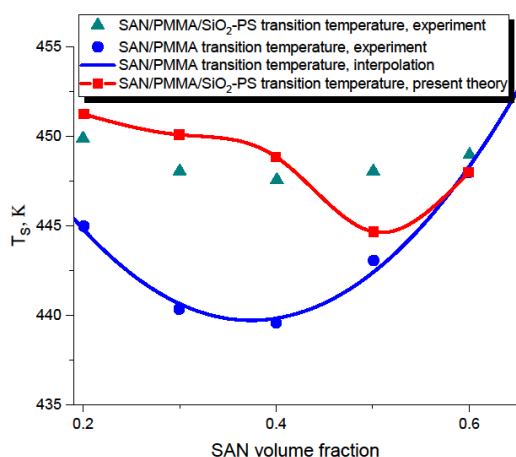


Fig. 1 Spinodal temperature T_s of *SAN/PMMA* blend filled with silica fillers: present theory vs. experiment in [C. Huang *et al.*, *Macromolecules* **45**, 8420 (2012)].

By using the method outlined in the preceding section, we calculated the distribution of fillers in DBC and the conductivity of a filled DBC system. The obtained simulation results perfectly agree, without using adjustable parameters, with the experimentally determined distribution of golden fillers in the lamella domain of PS-*b*-P2VP DBC (4). The investigated distribution of filler particles, in turn, proves to be directly related to the electrical response of the DBC-filler composite calculated by the developed model. In particular, the order-disorder transition in DBC system is found to co-occur with the insulator-conductor transition in the filler network provided a sufficient difference between the affinities of fillers for dissimilar DBC blocks. The order-order transition between the lamella and cylindrical morphologies of DBC is found to cause a spike in the composite conductivity.

Acknowledgment

Financial support of DFG through Grant No. CH 845/2-3, is gratefully acknowledged.

References

- 1) A. I. Chervanyov, *J. Coll. Inter. Sci.* **563**, 156 (2020).
- 2) C. Sarath *et al.*, *Nanostructured Polymer Blends*, William Andrew Publishing, 2014.
- 3) A. I. Chervanyov, *J. Polym. Sci.* **60**, 221 (2022).
- 4) A. I. Chervanyov, *Phys. Rev. E* **10**, 052504 (2020).

RADICAL SCAVENGING AND PROCESSING STABILITY OF NOVEL BIOBASED STABILIZERS IN POLYPROPYLENE

K. Markus, Elke Metzsch-Zilligen, Rudolf Pfaendner

Fraunhofer Institute for Structural Durability and System Reliability LBF, Division Plastics
Schlossgartenstr. 6, 64289 Darmstadt, Germany

Katrin.markus@lbf.fraunhofer.de; Elke.metzsch-zilligen@lbf.fraunhofer.de;

Rudolf.pfaendner@lbf.fraunhofer.de

INTRODUCTION

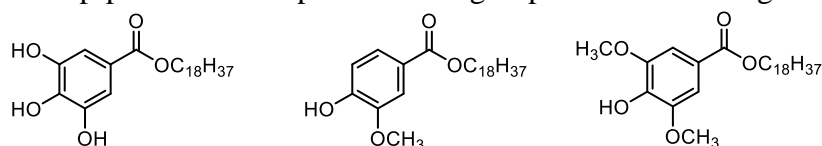
In the early days of plastic use, materials derived from natural resources were the predominant choice. However, as industry progressed, the focus shifted to petrochemicals, leading to an increase in the production of petroleum-based plastics. Recently, with rising environmental awareness and higher energy prices, there has been a rethinking of the use of plastics and additives, with a greater focus on developing alternatives derived from renewable raw materials. The motivation to investigate biobased alternatives is increasing due to bans and regulations, as well as health risks associated with suspected toxicity and potentially harmful interactions with the human metabolism. [1, 6, 7].

The objective of using stabilisers is to slow down the ageing processes that occur in the polymer during processing and use. This work focuses on elucidating the structure-property relationships of different structures based on natural phenolic derivatives. Furthermore, the radical scavenging activity in 2,2-diphenyl-1-picrylhydrazyl (DPPH) assays and the process stabilising ability of the synthesised additives are investigated. Finally, the aim is to ascertain whether there is a correlation between performance in real applications and whether the DPPH assay can be used as a valid characterisation method of the stabilisers without actually compounding them.

EXPERIMENTAL

Synthesis

The lauryl and stearyl esters of differently substituted 4-hydroxybenzoates were prepared by means of an esterification reaction. In addition, the influence of the alkyl chain length in the p-position to the phenolic OH group on the stabilizing effect was investigated.



Scheme 1: Exemplary synthesized stearyl esters. From left to right: gallate, vanillate, syringate.

Methods

To determine the radical efficiency, DPPH assays were conducted. This is a spectroscopic method in which the reduction in the absorbance of an DPPH radical solution is monitored. The faster the synthesised stabilisers release a hydrogen radical to the DPPH, the greater the reduction in absorbance and the more effective the stabiliser.

To check the behaviour of the additives during processing, prolonged extrusion experiments were conducted in a Xplore Micro Compounder MC 15 HT (Xplore Instruments B.V.; 200 °C, 200 rpm, 30 min). 1.17 mmol% stabiliser is mixed with polypropylene (Moplen HF 501N) and introduced into the compounder, which has a channel through which the polymer melt can be circulated while the screw torque is measured. During the degradation of a polypropylene, decomposition occurs with a decrease in molecular weight and screw torque. Therefore, good antioxidants differ from less good ones in a smaller drop of screw torque values. Consequently, the quality of the synthesised stabilisers can be evaluated by their ability to prevent molecular degradation.

RESULTS AND DISCUSSION

The results presented in Figure 1 demonstrate that the steric hindrance present in the ortho-position of the phenolic OH-group exerts a significant influence on the radical efficiency and the stabilisation capacity. Hydroxy groups exhibit a faster and more efficient stabilisation compared to methoxy groups in the DPPH assay as well as in the extrusion experiments. The structures containing two methoxy groups exhibit greater steric hindrance and additional stability. The methoxy groups of the vanillate or syringate structures exert a mesomeric, electron-pushing effect, which leads to an improvement in the stability of the resulting aryloxy radical. Consequently, the latter have a better radical efficiency than the single methoxy-substituted vanillate [10,11].

The influence of the chain length in the para-position was additionally evaluated using a design of experiment (DoE), which confirmed the previously suspected insignificance of chain length on the stabilising effect, at least in the investigated range between 12 and 18 carbon atoms (Figure not shown here).

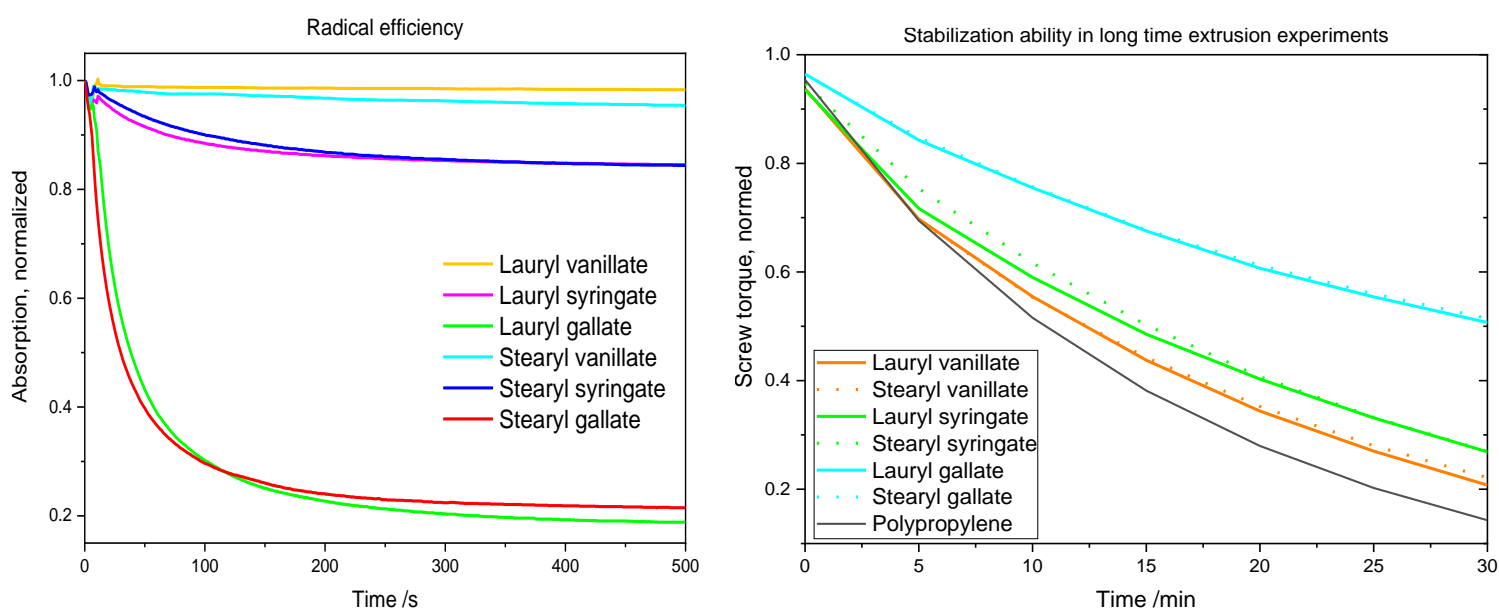


Figure 1: Results of the DPPH Assay and the stabilization ability in long time extrusion experiments.

In conclusion, it can be stated that the synthesized biogenic structures demonstrate satisfactory results within a relatively short observation period. Nevertheless, long-term stabilization still requires further improvement. In addition to investigating the synthesized substances, the objective was to ascertain whether the rapid and straightforward DPPH assay is capable of accurately representing reality and simulating the stabilizing effect during processing. The test is conducted in solution, rather than on the polymer itself. Nevertheless, it has been demonstrated that the synthetic structures that exhibited the greatest efficacy in the real-world application also demonstrated a high radical efficiency in the DPPH assay. Consequently, the results can be extrapolated to real polymer processing applications.

Acknowledgment

The authors acknowledge financial support by the Fraunhofer- Gesellschaft e.V., which supported this work as Fraunhofer Cluster of Excellence “Circular Plastics Economy”.

References

- [1] K. Schmidt, P. Schmidt, M. Lang, and A. Rusam, "Einsatz und Potential biobasierter Additive in Kunststoffen: Abschlussbericht Az.: 123-02.05-20.0328/17-II-K," Apr. 2018-Jan. 2020.
- [2] P. Eyerer, H. Domininghaus, P. Elsner, and T. Hirth, Eds., *Die Kunststoffe und ihre Eigenschaften*, 6th ed. Berlin, Heidelberg: Springer, 2005.

- [3] R. Pfaendner, "How will additives shape the future of plastics?," *Polymer Degradation and Stability*, vol. 91, no. 9, pp. 2249–2256, 2006, doi: 10.1016/j.polyimdegradstab.2005.10.017.
- [4] R. Prof. Dr. Pfaendner and T. Prof. Dr. Melz, "Biogene Kunststoff-Additive: Hochwertige Additive für Kunststoffe aus natürlichen Rohstoffen begünstigen die Kreislaufwirtschaft," in *Biologische Transformation*, p. 165. [Online]. Available: 182
- [5] M. A. de Paoli and W. R. Waldman, "Bio-based additives for thermoplastics," *Polímeros: Ciência e Tecnologia*, vol. 29, no. 2, 2019, doi: 10.1590/0104-1428.06318.
- [6] J. Hernández - Fernández, E. Rayón, J. López, and M. P. Arrieta, "Enhancing the Thermal Stability of Polypropylene by Blending with Low Amounts of Natural Antioxidants," *Macromol. Mater. Eng.*, vol. 304, 2019, doi: 10.1002/mame.201900379.
- [7] B. Mbatia, S. S. Kaki, B. Mattiasson, F. Mulaa, and P. Adlercreutz, "Enzymatic synthesis of lipophilic rutin and vanillyl esters from fish byproducts," *Journal of agricultural and food chemistry*, vol. 59, pp. 7021–7027, 2011, doi: 10.1021/jf200867r.
- [8] C. A. Rice-Evans, N. J. Miller, and G. Paganga, "Structure-antioxidant activity relationships of flavonoids and phenolic acids," *Free Radical Biology and Medicine*, 20, 7, pp. 933–956, 1996.
- [9] M.-E. Cuvelier, H. Richard, and C. Berset, "Comparison of the Antioxidative Activity of Some Acid-phenols: Structure-Activity Relationship," *Bioscience, Biotechnology, and Biochemistry*, vol. 56, no. 2, pp. 324–325, 1992, doi: 10.1271/bbb.56.324.
- [10] F. Diot-Néant, L. Migeot, L. Hollande, F. A. Reano, S. Domenek, and F. Allais, "Biocatalytic Synthesis and Polymerization via ROMP of New Biobased Phenolic Monomers: A Greener Process toward Sustainable Antioxidant Polymers," *Frontiers in chemistry*, vol. 5, p. 126, 2017, doi: 10.3389/fchem.2017.00126.
- [11] A. F. Reano *et al.*, "Structure–Activity Relationships and Structural Design Optimization of a Series of p-Hydroxycinnamic Acids-Based Bis- and Trisphenols as Novel Sustainable Antiradical/Antioxidant Additives," *ACS Sustainable Chem. Eng.*, vol. 3, no. 12, pp. 3486–3496, 2015, doi: 10.1021/acssuschemeng.5b01281.

ENHANCING THE HYDROLYTIC STABILITY OF POLY(LACTIC ACID) USING NOVEL STABILIZER COMBINATIONS

J. Hallstein, E. Metzsch-Zilligen and R. Pfaendner

Fraunhofer Institute for Structural Durability and System Reliability LBF, Division Plastics
Schlossgartenstr. 6, 64289 Darmstadt, Germany
jannik.hallstein@lbf.fraunhofer.de; elke.metzsch-zilligen@lbf.fraunhofer.de,
rudolf.pfaendner@lbf.fraunhofer.de

INTRODUCTION

To make the plastics industry more sustainable and replace petro-based plastics, there is growing interest in bio-based plastics, such as polylactic acid (PLA), with improved long-term stability. However, due to their chemical structure, the polymer chains are susceptible to acid-catalyzed hydrolytic degradation (1) and must be stabilized with additives.

Carbodiimides are commonly used here, but they are expensive and have a negative effect on some material properties (2). In this work, therefore, a novel combination of hydrolysis inhibitor and acid scavenger as a co-stabilizer is being investigated to compensate for these effects and make them economically viable (3).

EXPERIMENTAL

Materials

A commercially available PLA grade (Luminy L130, TotalEnergies Corbion, NL) was used. A polymeric carbodiimide (pCDI) (Stabaxol P, Lanxess, DE) was tested as a reference for the state-of-the-art. As a novel hydrolysis inhibitor, a bifunctional aziridine derivate (PolyU) (PolyU, Menadiona, ESP) was used. An acid scavenger, an uncoated calcium hydroxalate (HTC) (Actilox CAH EXP 0213, Nabaltec, DE) was added as a synergist to the PolyU.

Compounding and hydrolytic aging

Compounding was performed on a co-rotating parallel twin-screw extruder (Process 11, Thermo Fisher Scientific, DE) with a screw diameter of 11 mm and an L/D ratio of 40. Milled PLA was vacuum-dried for 16 h at 80 °C to a moisture content of below 250 ppm and premixed with the additives. The polymer/additive premix was fed in the extruder and compounded at a temperature of up to 200 °C. The polymer strands were then cooled in a water bath and pelletized.

The granulates obtained were subsequently stored in glass jars filled with deionized water. The jars were placed in a heating chamber with forced convection (Binder M115, Binder GmbH, DE), which was set to an aging temperature of 60 °C. The granules were removed at different time intervals and after each removal dried in a vacuum oven and vacuum sealed until further testing.

Characterization

To assess the aging condition of the granules, the melt flow index (MVR) of the aged granules was measured on a mi2 melt flow indexer (Göttfert Werkstoff-Prüfmaschinen GmbH, DE) according to DIN EN ISO 1133-2. To verify the MVR results, the molecular weights of selected samples were also determined by using size exclusion chromatography.

RESULTS AND DISCUSSION

The hydrolytic degradation of the polymer chains during water storage leads to a decrease in melt viscosity with storage time, which is reflected in an increased MVR value. The MVR curve is shown in Figure 1 for unstabilised PLA, PLA with a commercial

hydrolysis stabiliser (pCDI), the new stabilisers (PolyU and HTC) and the synergistic combination of the two.

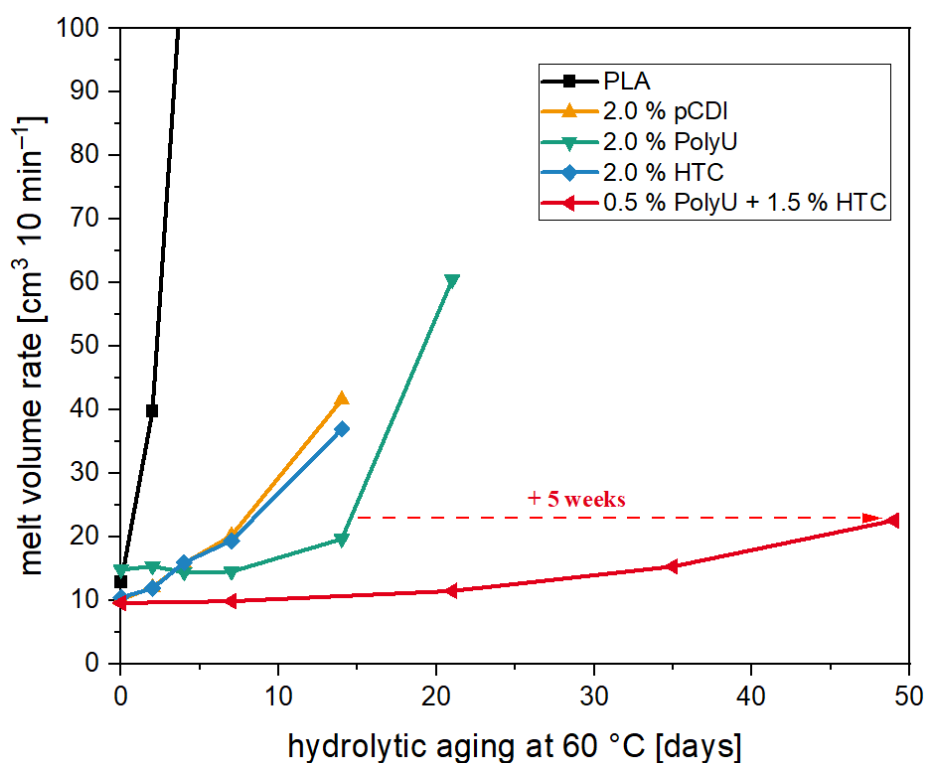


Fig. 1 MVR values of aged PLA samples unstabilized (black) and stabilized with a novel stabilizer composition over the course of 49 days at a temperature of 60 °C.

While the unstabilized PLA exhibits a marked increase in MVR after less than two days, while the addition of the hydrolysis stabilizers has a significant impact. The commercial reference (pCDI) provides a stabilizing effect for approx. 14 days. A similar level of stabilization is achieved by addition of the acid scavenger (HTC). The new hydrolysis inhibitor (PolyU) provides an even more prolonged stabilizing effect of around 21 days.

The combination of the new hydrolysis inhibitor (PolyU) and the acid scavenger (HTC), results in a synergistic effect that markedly enhance the stabilizing efficiency. For instance, with a constant additive content of 2 %, the increase in MVR during water storage is delayed by a period of another five weeks.

The stabilizing effect is based on a direct reaction of the PolyU with the moisture migrating into the PLA. This inhibits the moisture and protects the polymer chains. In contrast, the acid scavenger regulates the pH value of the moisture in the polymer, which in turn influences the rate of the degradation reactions. By combining both mechanisms, the reaction of the PolyU with the moisture and thus the additive consumption is also delayed, prolonging the stabilizing effect.

Acknowledgment

This research was funded by Fraunhofer-Gesellschaft e.V, which supported this work within the Fraunhofer Cluster of Excellence Circular Plastics Economy.

References

- 1) E. Castro-Aguirre et al., *Adv. Drug Deliv. Rev.* **107**, 333–366 (2016)
- 2) A. Porfyrus et al., *Polym. Test.* **68**, 315–332 (2018)
- 3) J. Hallstein et al., *Polymers* **16**, 506 (2024)

Microstructural Changes of XPS Foamed Plastic Adding Graphite Fillers

Y. Leem*, and R.Kitagaki

*Division of Human Environmental System, Hokkaido University, Sapporo 060-8613, Japan
lyoubin12@eis.hokudai.ac.jp

INTRODUCTION

Insulation is crucial for improving the energy efficiency of buildings, as it effectively reduces heat transfer and optimizes energy usage (1). Insulations are challenging to replace due to their installation within the walls, necessitating long-term durability.

The demand for insulation with enhanced performance for sustainability is driving the development of high-performance insulations. One approach to improving the thermal performance of insulation is to add graphite filler. It has been reported to reduce the radiation rate using graphite filler in insulation (2). However, the effect of graphite filler on insulation in the long term needs to be clarified.

In this work, two internal insulation structures were measured and compared: the initial state and the state stored for extended periods for extruded polystyrene foam (XPS) and XPS containing graphite filler (graph XPS) to explain the effect of graphite filler on insulation.

EXPERIMENTAL

Materials

Extruded polystyrene foam (XPS) and XPS with added graphite (graph XPS) were chosen as the samples. Each sample, produced in board form with a closed cell structure, was manufactured by Japanese companies. Measurements were taken in the initial state of the product approximately three months after manufacture. They were labeled as “New-” . Other samples, stored for over 1.5 years in a laboratory at 23°C and 60±10% relative humidity. They were labeled as “Old-” . Each board insulation sample was prepared in the form of a cylinder (5mm diameter and 5mm height) to facilitate measuring with X-ray CT.

Morphological characterization

We measured X-ray CT images of the “New-” and “Old-” samples to observe changes in the foamed plastic insulation by time. The settings for the X-ray CT scanner are detailed in Table 1. The X-ray CT results were converted into three-dimensional data using image analysis software (Dragonfly, ORS).

Table 1. X-ray scanner setting

Parameter (Unit)	Value
X-ray source voltage applied (kV)	100
X-ray source resulting current (μ A)	40
Scan type	Step
Geometry	Long
Field of view (mm)	5
Filters	Not activated
Voxel size (μ m)	1.93
Use 360 rotation	Activated
Scan mode	High resolution 1000ms
Integration times	8
Series description	With ring reduction
Exposure time (ms)	1000

RESULTS AND DISCUSSION

Sectional images of samples measured with X-ray CT are shown in Figure 1.

Figure 2 explains the changes in the distribution of strut thickness in each sample. Briefly, the struts exhibit an increase in thickness over time, regardless of the presence of fillers. Furthermore, the graphite-filled samples demonstrate more thickness increases than those without fillers.

Figure 3 explains the changes in the pore size distribution in each sample. Similar to the strut distribution, all types of samples show an increase in pore sizes over time. However, the sample with fillers stands out with its homogeneous pore size, while the sample without fillers displays a more varied, heterogeneous pore distribution.

XPS with graphite filler does not show a greater rate of structural change than the XPS without graphite filler. This result indicates that graphite may stabilize the structural changes in the insulation.

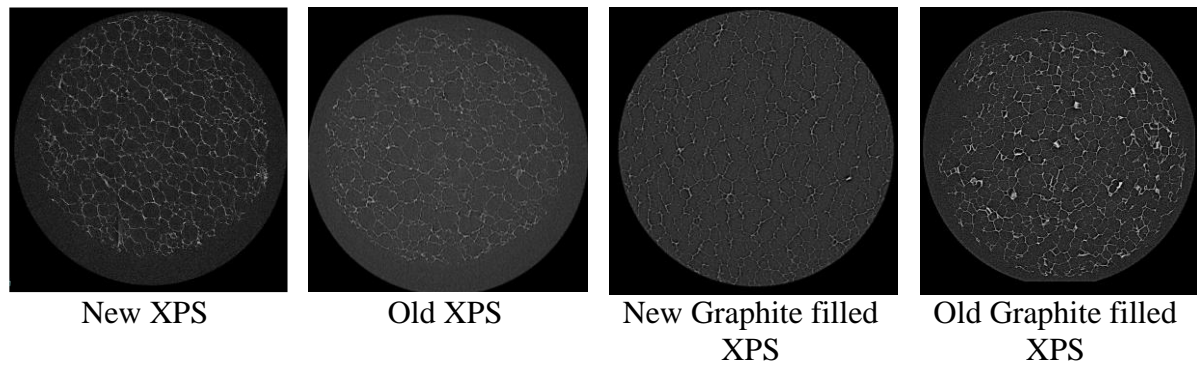


Figure 1. Sectional images of graphite filled XPS

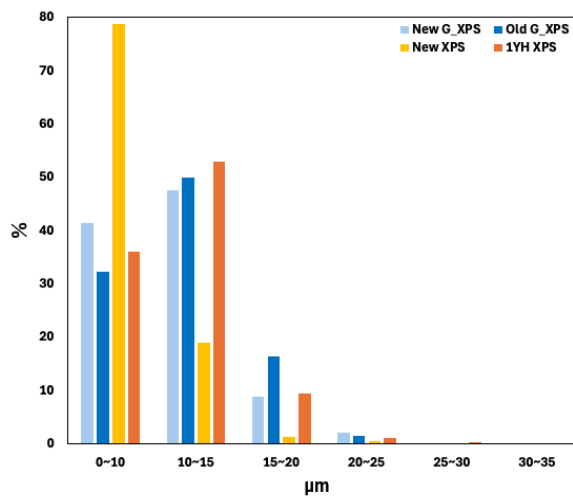


Figure 2. Strut thickness distribution of samples

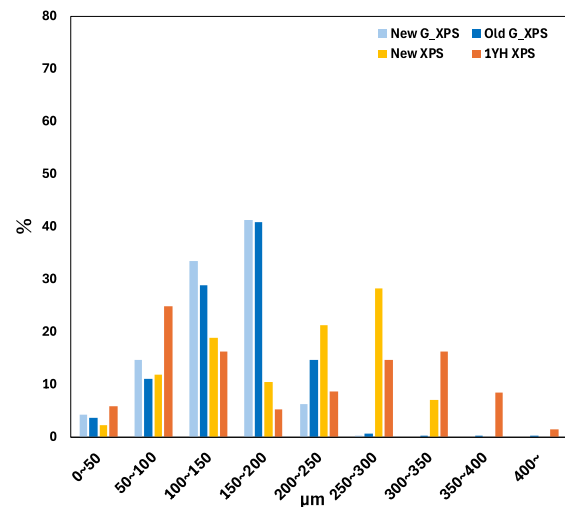


Figure 3. Pore size distribution of samples

Acknowledgment

This work has been financially supported by the JST Sakigake “Secure Bonding and Gentle Degradation for Sustainable Material Design”

References

- 1) MS AI-Homoud, Building and environment, 40, 3 (2005)
- 2) Gong P., Carbon, 93 (2015)

RESTABILIZING PVB INTERLAYER AGAINST HEAT DEGRADATION FOR CLOSED-LOOP RECYCLING IN LAMINATED GLASS

V. Nikitakos¹, A.D. Porfyris¹, K. Beltsios², R. Pfaendner³, A. Perez⁴ and C. D. Papaspyrides^{1,*}

¹Laboratory of Polymer Technology, School of Chemical Engineering, Zographou Campus, National Technical University of Athens, 15780 Athens, Greece

²Laboratory of Materials Science & Engineering, School of Chemical Engineering, Zographou Campus, National Technical University of Athens, 15780 Athens, Greece

³Fraunhofer Institute for Structural Durability and System Reliability LBF, Darmstadt, 64289 Germany

⁴LUREDERRA Technological Centre, Perguita Industrial Area, 31210 Los Arcos, Spain;

* Correspondence: *kp@cs.ntua.gr* (C.D. P.), *adporfyris@mail.ntua.gr* (A.D.P.)

INTRODUCTION

Laminated glass, created by bonding two glass layers with a polymeric interlayer (PVB), finds diverse applications such as car windshields, construction, photovoltaics, coatings, and adhesives. Its utilization is on the rise, with approximately 120 million kg of PVB sheets produced annually for automotive and architectural purposes. However, the disposal of laminated glass waste presents a significant challenge as it is typically landfilled. Yet, PVB holds considerable value, priced at an average of €5.24/kg, making its revalorization an attractive prospect within the circular economy framework. Effective recycling processes can yield PVB material with acceptable mechanical properties suitable for transparent applications. Nevertheless, original use and high-temperature reprocessing contribute to degradation, primarily through chain scission and yellowing.

This study aims to mitigate subsequent degradation of PVB caused by reprocessing and its future service life by incorporating suitable additives, such as antioxidants (AOs), into PVB. Various PVB-AO formulations were developed, through melt blending in an internal mixer apparatus. Subsequent investigations included studying different heating times (5, 10 & 15 min) and AO concentrations at 150 °C while monitoring molecular weight indirectly via melt flow rate determination (MFR) and directly through gas permeation chromatography (GPC). Additionally, PVB-AO films were produced via compression molding, and their yellowness index was assessed per ASTM E313 standards.

The most effective AO formulation, demonstrating retention of MFR and minimized yellowness, will be selected for industrial-scale reprocessing trials of post-consumed PVB waste. These trials aim to facilitate reuse within the interlayer film sector, thereby establishing a closed-loop recycling pathway.

EXPERIMENTAL

Materials

A plasticized polyvinyl butyral (p-PVB) grade was supplied by Eastman Chemical Company. Various Antioxidants (AO-1, AO-2, AO-3, AO-4, AO-5, & AO-6) were provided by BASF.

Preparation – Dry blending – Internal mixer

The incorporation of the AOs was performed in an internal mixer (Brabender T300B, Banbury type) at 150 °C and 40 rpm. The variation of AO concentration and of residence times (5,10 & 15min) was studied.

Characterization

Melt Flow Rate (MFR) was determined at 190 °C and 2.16 kg, according to ISO1133-1.

Yellowness index (YI) was calculated according to standard ASTM E313-20.

RESULTS AND DISCUSSION

The main degradation mechanism of PVB is chain scission, as indicated by the increase of the melt flow rate with residence time (Fig. 1(a)). The AO-3 & AO-5 added at 0.3% w/w concentration are the best performing additives on the basis of both MFR (Fig. 1(a)) and YI data (Fig. 1b)), even for high residence times.

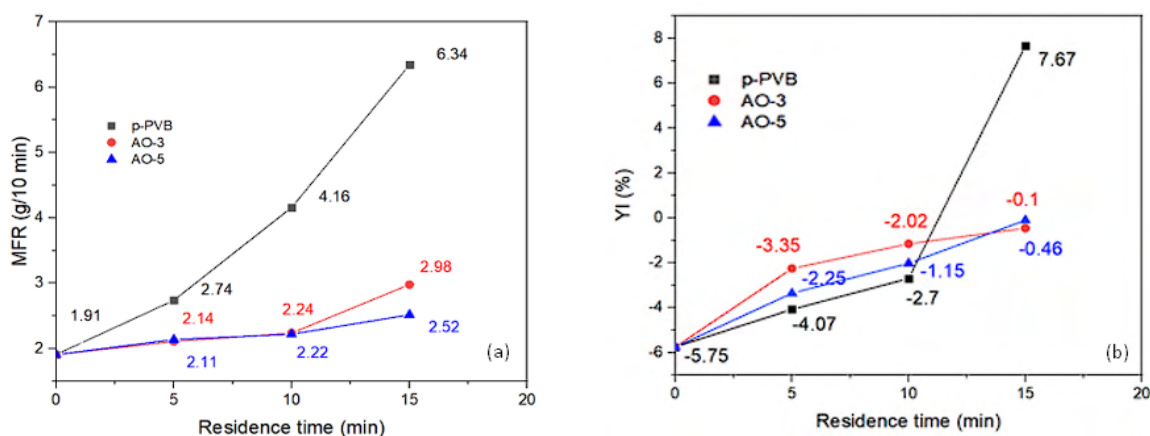


Figure 1: (a) MFR & (b) YI for non-stabilized p-PVB and re-stabilized p-PVB with AO-3 and AO-5

Acknowledgment

The results of this publication were generated in the SUNRISE project that has received funding from the European Union's Horizon 2020 Research and Innovation Program under grant agreement No 958243.

References

1. V. Nikitakos, A.D. Porfyrus, K. Beltsios, C. D. Papaspyrides, C. S. Bordignon, M.R. Chierotti, S. Nejrotti, M. Bonomo, C. Barolo, A. Piovano, R. Pfaendner, B. Yecora and A. Perez, *Polymers*, **16**, 10 (2023)
2. N. M. Safy El-Din and M. W. Sabaa Nabil, *Polym. Degrad. Stab*, **47**, 283-288 (1995)
3. H. Zweifel, *Plastics Additives Handbook*, Hanser Publication, Munich (2001)
4. L. Šooš, M. Matus, M. Pokusova, V. Cacko and J.Babics L et al., *Recycling*, **6**, 26 (2021)

MECHANICAL RECYCLING OF POLYPROPYLENE: EFFECT OF A REPAIR ADDITIVE ON FLOW CHARACTERISTICS AND PROCESSABILITY

R. Arrigo, G. Bernagozzi and A. Frache

Department of Applied Science and Technology, Polytechnic of Turin, Viale Teresa Michel
5, Alessandria, Italy

rossella.arrigo@polito.it, giulia.bernagozzi@polito.it, alberto.frache@polito.it

INTRODUCTION

Plastic recycling is a key aspect to achieve effective polymer circularity, especially for polyolefins for which usually the mechanical recycling is considered a downcycling process. The last, due to the progressive deterioration of the polymer microstructure during the reprocessing that involves a gradual loss of processability and properties and compromises the added value of r-polyolefins. In this work, the effects of the thermomechanical degradation on the microstructure of polypropylene (PP) were assessed by subjecting the polymer to multiple extrusion cycles, aiming at investigating the evolution of the molecular weight and of the macromolecular architecture of PP typically occurring in a mechanical recycling process. Furthermore, a commercially available additive capable of restoring the PP molecular weight was introduced and its effects were evaluated following two different strategies that simulate pre-consumer or post-consumer mechanical recycling. The additive-induced microstructural modifications of PP during the reprocessing cycles were monitored through rheological, thermal, and spectroscopic analyses. The obtained results allowed correlating the achieved microstructural evolutions to the processability of the recycled PP, demonstrated the possibility of achieving r-PP with different macromolecular architectures and, hence, flow characteristics, endowed with tunable and adaptable processability.

EXPERIMENTAL

Materials

A homopolymer PP (Moplen HP500N supplied by Lyondellbasell) was used. The commercially available additive NEXAMITE® R201 (hereinafter named NEX) was provided by Nexam Chemical. The additive was introduced in PP at 5 wt.%.

Preparation

The mechanical recycling of PP, with and without NEX, was simulated by subjecting the material up to 9 reprocessing cycles performed using a Process 11 (Thermo Fisher Scientific) twin screw extruder. NEX was introduced during the first reprocessing cycle of PP (rPP+NEX@n1) or in PP already subjected to 8 reprocessing cycles (rPP+NEX@n9).

Characterizations

The rheological behavior of the investigated materials was assessed using a strain-controlled rheometer ARES from TA Instruments.

RESULTS AND DISCUSSION

The rheological characterization of PP with and without NEX subjected up to 9 reprocessing cycles showed that the introduction of the additive is beneficial in mitigating the loss of PP molecular weight and in maintaining unmodified the polymer processability. In fact, as observable from Fig. 1 reporting the variation of the zero-shear viscosity η_0 (hence, of the molecular weight) as a function of the reprocessing cycle, pristine PP shows a dramatic drop of η_0 passing from the virgin material to the one reprocessed 9 times. Otherwise, for the sample rPP+NEX@n1 the decreasing rate of the viscosity is remarkably lower, indicating that the introduction of the additive was beneficial in mitigating the loss of PP molecular weight.

Furthermore, the analysis of the complex viscosity curves highlighted a progressive amplification of the Newtonian behavior as a function of the re-processing cycles for pristine PP, while for the sample containing NEX the trend of the complex viscosity as a function of the frequency is almost unmodified as a function of the reprocessing cycles. Besides, the results reported in Fig.1 indicate a significant recover of the polymer molecular weight also when NEX is introduced in a heavily degraded PP (rPP+NEX@n9), hence suggesting its possible application for the recovery of the molecular weight of post-consumer recycled PP.

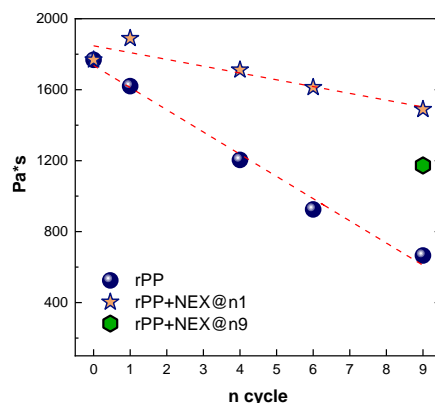


Fig. 1 Zero-shear viscosity (η_0) as a function of the number of reprocessing cycles for virgin and multi-extruded rPP, rPP+NEX@n1 and rPP+NEX@n9

Furthermore, it was also showed that NEX can induce some melt structuring phenomena (as observable for the relaxation spectra depicted in Fig.2), involving the obtainment of branched structures or crosslink points, especially if the melt processing is carried out for long residence times.

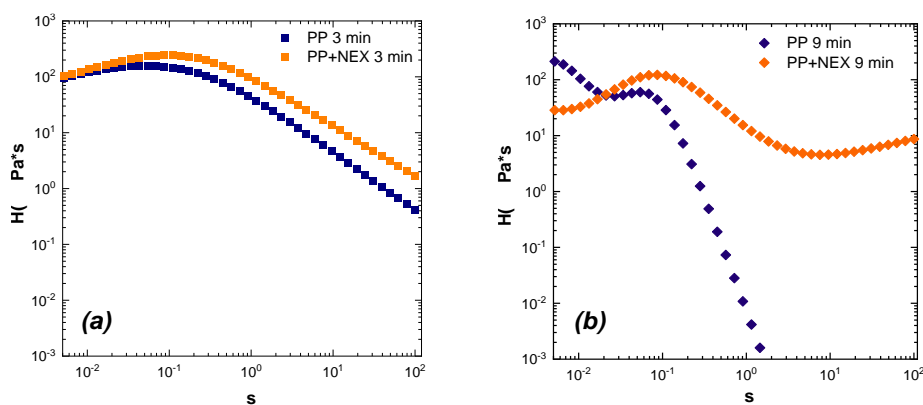


Fig. 2 Weighted relaxation spectra of PP processed for (a) 3 minutes and (b) 9 minutes with and without NEX

Acknowledgment

This study was carried out within the MICS (Made in Italy – Circular and Sustainable) Extended Partnership and received funding from the European Union Next-GenerationEU (PIANO NAZIONALE DI RIPRESA E RESILIENZA (PNRR) – MISSIONE 4 COMPONENTE 2, INVESTIMENTO 1.3 – D.D. 1551.11-10-2022, PE00000004). This manuscript reflects only the authors' views and opinions, neither the European Union nor the European Commission can be considered responsible for them.

References

G. Bernagozzi, R. Arrigo, G. Ponzielli, A. Frache, *Polym. Degrad. Stab.*, **223**, 110714 (2024)

RIGID POLYURETHANE FOAMS WITH LIMITED FLAMMABILITY AND BIOCIDAL PROPERTIES

Piotr Jankowski, Irena Grzywa-Niksińska

Łukasiewicz Research Network – Professor Ignacy Mościcki Industrial Chemistry Institute, 8 Rydygiera str., 01-793 Warszawa, Poland, piotr.jankowski@ichp.lukasiewicz.gov.pl

INTRODUCTION

Rigid polyurethane-polyisocyanurate (PUR/PIR) foams are used as insulating materials in the construction industry. Limited flammability is a crucial characteristic of PUR/PIR foams for their practical application. Currently, halogen flame retardants (FR) such as tris(1-chloro-2-propyl) phosphate (TCPP) are still used in the industry for this purpose [1]. However, European Union regulations are gradually decreasing the usage of halogen compounds due to their particularly harmful combustion products. Halogen-free additives are being used as a substitute, but they are often less effective in reducing flammability [2]. The aim of this studies was to develop halogen-free flame retardant systems (HFFRS) effective enough to be used in minimal amounts in PUR/PIR foam compositions. Additionally, a special hybrid biocidal additive (HBA) was used to prevent the growth of microorganisms on the PUR/PIR foams. Such properties are particularly important in the modular building industry.

In this work, we present our concept for obtaining flame-retardant, microorganism-resistant PUR/PIR foams modified by HFFRS and HBA along with the results related to their main properties.

EXPERIMENTAL

Materials

Plant extract obtained by PL Pat. 223494 and PL Pat. 230429. Stearic acid. TCPP. HFFRS for modification of PUR/PIR foam: APP(K) compositions based on ammonium polyphosphate, DIPER(K) compositions containing di or tri-pentaerythritol, MC(S) additives obtained by synthesis of melamine cyanurate, from melamine and cyanuric acid in the presence of other components, mFF(K) compositions containing modified phenol formaldehyde resin.

Preparation and characterization

The HFFRS were obtained through synthesis or physical mixing of nitrogen and phosphorus compounds [3,4]. The (HBA) was obtained by encapsulating a plant extract with stearic acid. A method for modifying PUR/PIR foams during their preparation with HFFRS and BA was developed [5]. The flammability properties were examined by using vertical (VBT) and horizontal burning test (HBT) (UL 94) - PN-EN 60695-11-10, limiting oxygen index (LOI) - ISO 4589-2 and ignitability of products subjected to direct flame impingement method (PN-EN ISO 11925-2). Additionally, fire resistance tests were carried out on a larger scale. The construction of an artificial wall, simulating real conditions, was necessary. The wall was subjected to one-sided heating, and the increase in temperature on the outside was measured. The combustion behaviours of the samples were analysed using the cone calorimeter at an external heat flux of 50 kW/m² (ISO 5660-2002). The effectiveness of HBA against microorganisms in PUR/PIR foams was evaluated. (ASTME2180, PN-EN ISO 846 2002). All results were compared with the reference sample made in the same way but without any additives. PUR/PIR structure analysis by scanning electron microscope (SEM).

RESULTS AND DISCUSSION

PUR/PIR foams containing approximately 5_{wt}% of HFFRS achieved higher oxygen index values compared to foams without additives or with TCPP, and maximum values of

vertical (V0) and horizontal (HB40) combustion parameters. The antimicrobial activity of foams was assessed. All modified foams showed resistance to molds (*aspergillus versicolor*, *penicillium chrysogenum*, *cladosporium herbarum*), fungi (*rhodotorula rubra*), and bacteria (*escherichia coli*, *bacillus cereus*). Data are reported in Table 1.

Nr	FR in PUR/PIR composition	LOI (%)*	LOI ¹ (%)*	VBT	HBT	resistance to microorganisms	HRR _{max} (kW/m ²)
1	-	20,6	-	fails	fails	no	135,7
2	TCPP	24,7	-	V0	HB40	yes	-
3	APP(K)	25,2-26,8	23,9-25,8	V0	HB40	yes	72,4
4	DIPER(K)	25,6-27,0	-	V0	HB40	yes	108,5
5	MC(S)	25,5-27,8	24,6-25,3	V0	HB40	yes	95,3
6	mFF(K)	24,4-26,7	-	V0	HB40	yes	-

* range of results depending on different proportions of each component in HFFRS

LOI¹ – the limiting oxygen index for PUR/PIR compositions with HFFRS and HBA combined

Table 1. The fundamental properties of modified PUR/PIR foams.

Introducing HFFRS along with HBA into PUR/PIR foams required optimization of their incorporation method. The lesser increase in the oxygen index of PUR/PIR foams when HFFRS was used together with HBA, stems from its influence on foam expansion (uniform distribution of the HFFRS within the polymer matrix) rather than a direct impact on the mechanism of reducing flammability (SEM analysis). The most effective additive turned out to be MC(S), APP(K). The hybrid encapsulated biopreparation has less impact on the oxygen index of the foams, compared to the unencapsulated form.

Analysing the results of fire resistance tests (larger scale), there is clearly a positive effect of modifying of PUR/PIR foam with HFFRS. The results of the modified foam are much better than reference sample and are better or comparable to PUR/PIR modified with halogen flame retardant. (details in the presentation)

In the cone calorimetry studies, flame-retardant modified PUR/PIR foams exhibit reduced maximum heat release rate (HRR_{max}) and lower average heat release rate. They also have lower total smoke emission, which is crucial during rescue operations in case of fire. In this study, the most effective additive was found to be flame retardant composition based on ammonium polyphosphate. (details in the presentation)

Our work has resulted in the development of halogen-free PUR/PIR foams with reduced flammability and protected against fungal and bacterial growth (a problem in modular buildings). These innovative solutions are competitive with other PUR/PIR foams on the market - used for insulating buildings - particularly those modified with halogen compounds.

Acknowledgment

The project was carried out by Łukasiewicz Research Network – Professor Ignacy Mościcki Industrial Chemistry Institute (Poland) and was supported by the National Centre for Research and Development in Poland within the framework of the European program - Operational Programme Smart Growth 2014-2020 (Application Projects).

References

1. D. Xu, K. Yu, K. Qian, *Polymer Testing* **67**, 159–168 (2018)
2. P. Jankowski, D. Kijowska, *Polimery*, **61(5)**, 327-333 (2016)
3. P. Jankowski, I. Legocka, D. Kijowska, E. Górecka, PL Pat. 230035 (2018)
4. P. Jankowski, E. Górecka, W. Pietruszka, I. Legocka, PL Pat. Appl. 445009 (2023)
5. P. Jankowski, E. Górecka, W. Pietruszka, K. Bieniek, I. Legocka, I. Grzywa-Niksińska, B. Szczepaniak, PL Pat. Appl. 445005 (2023)

SUSTAINABLE BIOCOMPOSITES BASED ON MATER-BI AND GRAPE POMACE FOR A CIRCULAR ECONOMY: PERFORMANCE EVALUATION AND DEGRADATION IN COMPOST

V. Titone^{1,2}, M. Rapisarda³, L. Pulvirenti⁴, E. Napoli⁴, G. Impallomeni³, L. Botta^{1,2}, M.C. Mistretta^{1,2*} and P. Rizzarelli^{3**}

¹*Department of Engineering, University of Palermo, Viale delle Scienze, Palermo, Italy

²National Interuniversity Consortium of Materials Science and Technology (INSTM), Florence, Italy

^{3**}Institute for Polymers, Composites and Biomaterials - National Research Council (IPCBCNR), Via Paolo Gaifami 18, Catania, Italy

⁴Institute of Biomolecular Chemistry – National Research Council (ICB-CNR), Via Paolo Gaifami 18, Catania, Italy

**paola.rizzarelli@cnr.it, *mariachiara.mistretta@unipa.it

INTRODUCTION

Biodegradable polymers often exhibit inferior properties compared to their fossil-derived counterparts. Plant wastes and by-products can improve the performances, providing in the meantime functional activity. Degradation occurs to plastic materials during processing as well the useful lifetime. Several environmental factors (e.g., sunlight UV radiation, oxygen, and heat) prompt and accelerate polymer degradation (1). Additives, selected for a particular use and the predicted life prospect of the plastic items, limit or delay the degradation processes. Waste filler can provide “natural additives” and in the meantime increase the mechanical properties. However, they can also influence the polymer matrix biodegradability.

In this work, we summarize the preparation of different biocomposites (BioCs) incorporating two diverse amounts (10% and 20%) of grape pomace (GP) in a Mater-Bi (MB) sample. The influence of the addition of the GP on the properties and degradation in compost of the biocomposites was evaluated in comparison with the neat MB.

EXPERIMENTAL

Materials

The raw materials used were: Mater-Bi® EI51N0 (density: 1.23 g/cm³; melt flow index (MFI): 19g/10min (230°C, 2.16 kg), melting temperature: 167°C), purchased by Novamont (NO, Italy), and GP, from cultivation on the Etna Mountain, were kindly provided by Al-Cantàra Srl (Randazzo, CT, Italy). Compost was supplied by Biofactory SpA (Calcinatè, BG, Italy). All solvents and reagents used were high purity laboratory grade. Water and acetonitrile were acquired from Carlo Erba (MI, Italy), caffeic acid, malvidin chloride, ellagic acid and quercetin from Sigma-Aldrich (MI, Italy), folin-ciocalteau reagent from Fluka (MI, Italy).

Preparation

BioCs were prepared in a corotating twin-screw extruder (OMC, screw diameter=19 mm, length/diameter ratio=35 mm; temperature profile: 145-150-155-160-165-170-180°C). Before the extrusion, MB was dried under vacuum at 60°C for 4 h, while the filler at 80°C overnight. The film samples were prepared by compression molding (180°C, 3min). GP (freeze-dried), MB and BioCs were milled. Then, the powders were suspended in EtOH-H₂O (70:30) with a concentration of about 130 and 200 mg/mL in the extraction solvent for GP and polymer samples, respectively. The suspensions were left in the shaker (400 rpm) in the dark for 24 h at room temperature and then the extracts were recovered by centrifugation and a subsequently filtration, in order to freshly analyze the supernatant.

Biocomposites characterization and degradation

Viscosity was measured by a rotational rheometer with 25 mm plate at T=180°C. Tensile tests were carried out by an Instron universal testing machine mod. 3365 (rate=1 mm/min until

3% strain, then at 100 mm/min until failure). Morphological analyses were conducted using a scanning electron microscopy (SEM), Phenom ProX microscope. GP extracts were analyzed by HPLC-UV at 280, 330, 350 and 520 nm that are the wavelengths characteristics of four different class of polyphenol family, namely cinnamic acids (HCA), flavonoids, anthocyanins and ellagic acid derivatives. Besides, to monitor the degradation of secondary metabolites the extracts were exposed to the folin ciocalteau assay. Nuclear magnetic resonance (^1H NMR, 500 MHz) experiments were performed at 27 °C in CDCl_3 (0.03% TMS). Surface wettability was measured by a contact angle goniometer at room temperature after samples have been equilibrated at 40°C for 30 min, with at least five values recorded. Compost burial test was performed up to 45 days at $58.0 \pm 0.1^\circ\text{C}$ and degradation monitored through weight loss (WL).

RESULTS AND DISCUSSION

GP analysis (particle size 50 μm , Fig 1a) showed a slight decrease of antioxidant potency, despite the heat treatment simulating the BioC processing (Fig 1b). The filler was distributed homogeneously in the matrix (Fig 1c). The introduction of the GP in the polymer matrix induced a proportional increase of antioxidant property in the BioCs (Fig 1d) as well as in complex viscosity at low frequencies but at higher frequency the viscosity decreased compared to that of the matrix. This behavior could be due to a degradative effect caused by the filler during the processing (Fig 1e). Degradation in compost produced a contact angle decrease (Fig 1f), whereas WL increased with the filler content and degradation time (Fig 1g). Moreover, NMR (Fig 1h) showed that, in the recovered sample after 45 days, the composition of PBAT was changed and the terephthalic percentage increased, similarly with previous results (2).

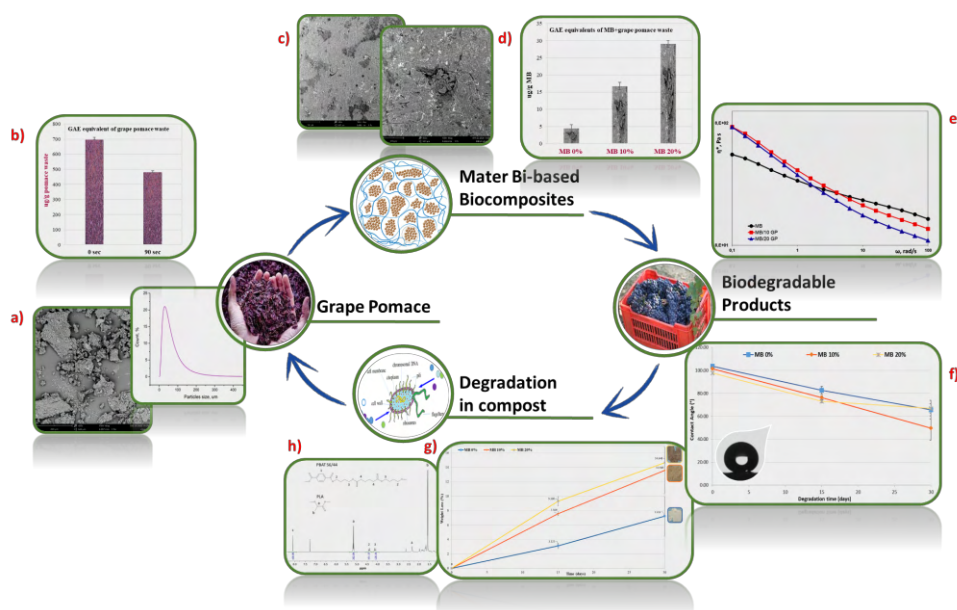


Fig. 1 Overview of the results and the circular model approach applied.

Acknowledgment

Funded by the Next Generation EU - PNRR M4 - C2 -investimento 1.1: PRIN 2022PNRR cod. P2022M3FTM, “Sustainable routes to high Performance and Recycling of Biodegradable plastics for a circular economy – SuperBio” CUP B53D23027640001. Dr L. Pulvirenti gratefully acknowledge to the PNRR project SAMOTHRACE (CUP B63C22000620005).

References

- 1) P. Rizzarelli, M. Rapisarda, L. Ascione, F. Degli Innocenti, F.P. La Mantia. *Polym. Degrad. Stab.*, **188**, 109578 (2021).
- 2) M. Rapisarda, M.C. Mistretta, M. Scopelliti, M. Leanza, F.P. La Mantia, P. Rizzarelli. *Nanomaterials*, **12**, (2022).

Degradation of rigid polyurethane foam in district heating pipes - accelerated vs natural ageing

I. Jakubowicz and N. Yarahmadi (O1)

RISE research Institutes of Sweden, Division Built Environment
ignacy.jakubowicz@ri.se, nazdaneh.yarahmadi@ri.se

INTRODUCTION

District heating (DH) pipes comprise an inner pipe (service pipe), which is normally made of steel, surrounded by rigid polyurethane (PUR) foam insulation and an outer high-density polyethylene (HDPE) casing for protection. This design requires satisfactory adhesion between the components to achieve good long-term mechanical and thermal performance. The PUR's surface that is in direct contact with the hot steel pipe is the part of the pipe most exposed to degradation because the temperature and the shear forces between the steel pipe and the PUR foam are at their maximum.

Use of polymeric materials in long-term applications requires understanding of degradation mechanisms and the use of carefully selected accelerated ageing conditions for reliable prediction of lifetime. The results from naturally aged materials are usually a primary reference for any approach to the lifetime prediction of polymeric materials.

In this presentation we summarize and discuss the results of accelerated thermal, and thermo-mechanical ageing as well as results of several naturally aged, commercially used DH supply pipes (S-pipes), at various locations, operating conditions, and for various periods.

EXPERIMENTAL

Test objects

Pre-insulated DH pipes DN50/160 produced by Powerpipe Systems AB were used in accelerated ageing tests. Different naturally aged DH pipes were tested in the field under real conditions or sent to RISE by municipal energy suppliers in connection with changes in their DH networks and maintenance.

Adhesion strength

The adhesion strength between PUR and service pipe was measured using the RISE plug method by applying a torque that was recorded by a static torque sensor until the test specimen became loose or broken (1).

Chemical characterization

Changes in the chemical structure of the PUR material were identified using FTIR spectroscopy. The reduction of the carbonyl peak in the urethane linkage at around 1712 cm^{-1} and the bending vibration peak N-H in the amide II band at 1512 cm^{-1} was a measure of the degradation.

RESULTS AND DISCUSSION

It was clearly demonstrated using measurements of adhesion strength, and changes in chemical structure by FTIR spectroscopy after various periods of accelerated ageing that the results of ageing at 170 and 150°C significantly diverges from those obtained from the ageing tests at 130 and 140°C. It was therefore concluded that accelerated ageing at commonly used, high temperatures ($\geq 150^\circ\text{C}$) does not create an acceleration of degradation processes but rather a significant alteration.

It was also shown that the pipes subjected to repetitive mechanical tensile stress during thermal ageing show significantly faster degradation compared to the unstressed pipes aged at the same temperature. The FTIR study revealed also a significantly faster chemical degradation of PUR foam when the pipes were mechanically stressed during the thermal

ageing, which indicates that the effect of thermo-mechanical ageing is not an effect of fatigue but of faster chemical degradation of PUR foam (2).

To be able to compare naturally aged pipes operated at different temperatures, the original temperature records from these pipes were compiled as average annual periods at various temperature intervals and recalculated to an equivalent service life at a common reference temperature (95 °C). Our study demonstrated that the residual adhesion strength in supply pipes was roughly at the same level (between 70 and 90 % of the return-pipe value which was regarded as a reference) regardless of their age, confirming the result from the accelerated ageing test at ≤ 140 °C, which suggested that the adhesion strength remains unchanged for a very long period.

In an ongoing project we try to add new pieces of the puzzle to support the selective exchange of parts, by finding out whether DH lines in the sliding zones, where mechanical stress is assumed to be greatest, show a greater degradation than other parts. The information would be useful for determining where status assessments should be made in the field and, in general, which parts of the DH networks degrade the fastest. The first preliminary results suggest a more advanced degradation in sliding zones.

Acknowledgment

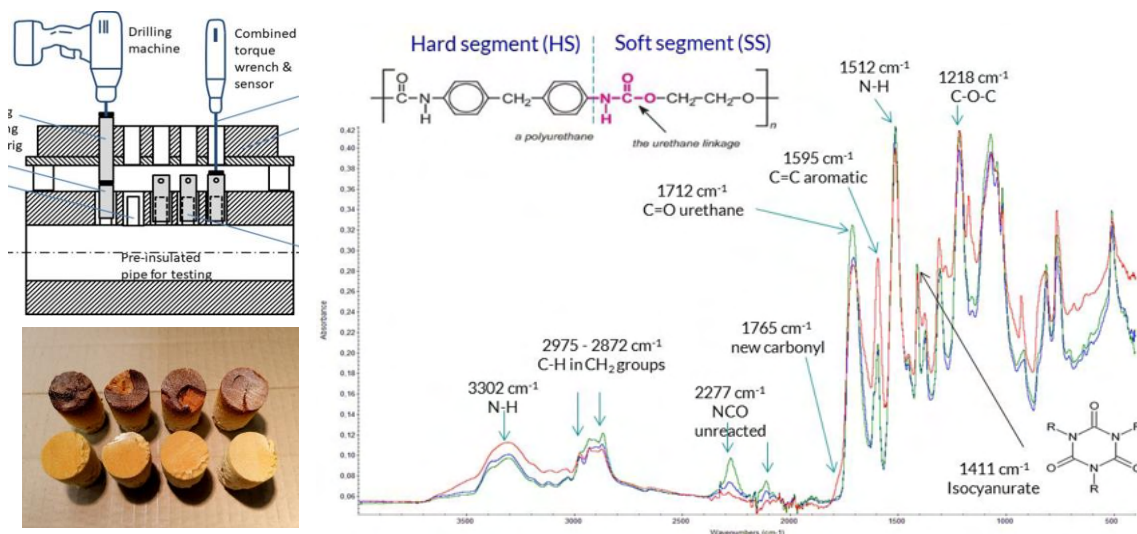
We would like to extend a big thank you to our co-workers Alberto Vega and Jan-Henrik Sällström for their great efforts and commitment.

This work has been financially supported by the Swedish Energy Agency.

The authors would like to thank Powerpipe Systems AB and the Swedish energy companies for valuable support and discussions.

References

- (1) Vega, N. Yarahmadi, I. Jakubowicz, Determination of the long-term performance of district heating pipes through accelerated ageing, *Polym. Degrad. Stab.* (2018)
- (2) A. Vega, N. Yarahmadi, J- H. Sällström, I. Jakubowicz, Effects of cyclic mechanical loads and thermal ageing on district heating pipes, *Polymer Degradation and Stability* 182 (2020) 109385



IN-PROCESS CHARACTERIZATION OF POLYMER COMPOSITES USING SMALL-SCALE EXTRUDERS

Paulo F. Teixeira, Loic Hilliou and José A. Covas

Institute for Polymers and Composites, University of Minho, 4800-058 Guimarães, Portugal
p.teixeira@dep.uminho.pt; loic@dep.uminho.pt; jcovas@dep.uminho.pt

INTRODUCTION

Lab-scale extruders are widely used for the development of novel polymer systems, since they require less amount of material than equivalent production machines and facilitate measurements and characterization. In-process measuring techniques are particularly advantageous as they: i) minimize the time delay between the need of a measurement and the result; ii) evade the need to subject the material to additional thermal/flow cycles in order to prepare samples for the measurements, which may affect its initial characteristics. This work uses a prototype small-scale extruder coupled to in-process measuring devices that were used to characterize the dispersion of organoclay in a polymer matrix.

EXPERIMENTAL

Materials

The polymer matrix was a polydimethylsiloxane (PDMS) AK 1,000,000 (Wacker-Chemie GmbH, München, Germany) with a dynamic viscosity of 970 Pa.s at 25 °C. An organo-modified montmorillonite clay (Dellite 72 T, Laviosa Chi. Mine., Livorno, Italy) was selected as filler.

Compounding and In-Process Characterization

As illustrated in Fig.1, a prototype modular small-scale co-rotating twin-screw extruder was coupled to a rheo-optical die which contains two flow channels for the extrusion of tapes. Both are fitted with valves at their entrance, to allow for the independent control of material outputs under constant total pressure drop, while maintaining extruder screw speed and feed rate. One of the channels is fitted with melt pressure transducers to enable the measurement of flow curves. Also, the existence of optical windows give access to small-angle light scattering (SALS) and turbidity measurements for the calculation of the radius R and volume fraction ϕ of particles scattering the light [1].

RESULTS AND DISCUSSION

Fig 2 (left) displays the flow curves of the composites measured in-line during extrusion at four different screw speeds. As expected, all curves are above that of the matrix, but they are shifted downwards as the screw speed increases, which contradicts the expected trend of larger yield stresses and shear thinning exponents for the linear rheological response of CPNC processed at larger screw speeds. However, it is known that composites do not follow the Cox-Merz rule, hence inferring dispersion levels from this rheological data should be made cautiously. Fig. 2 (right) presents morphological information (i.e., R) retrieved from SALS patterns. As the screw speed increases, particles with a smaller size are generated (also more particles are present, as determined from turbidity data).

The dispersion of the clay tactoids assessed in the rheo-optical slit should result from the thermomechanical history accumulated along the extruder, i.e., with the level of stresses and the time during which they were applied, with an eventual contribution of the die itself.

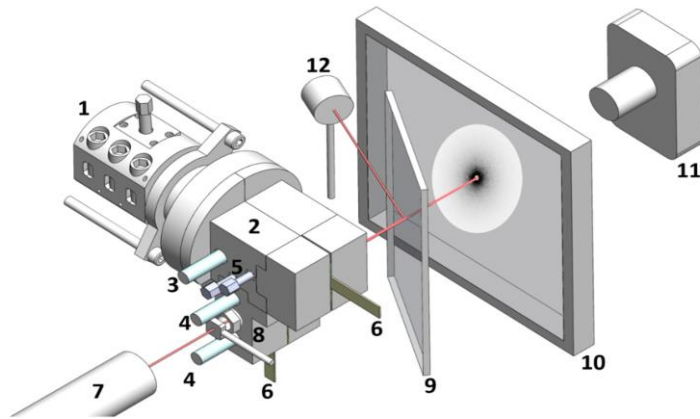


Fig. 1 Rheo-optical slit and optical train for the in-situ measurement of flow curves, SALS patterns, and turbidity. (1) Extruder; (2) rheo-optical die; (3) pressure transducer at die entry; (4) pressure transducers along the measuring channel; (5) valves for control of material output; (6) extrudate; (7) HeNe laser; (8) pinhole; (9) beam splitter; (10) screen; (11) CDD camera; (12) Photodetector.

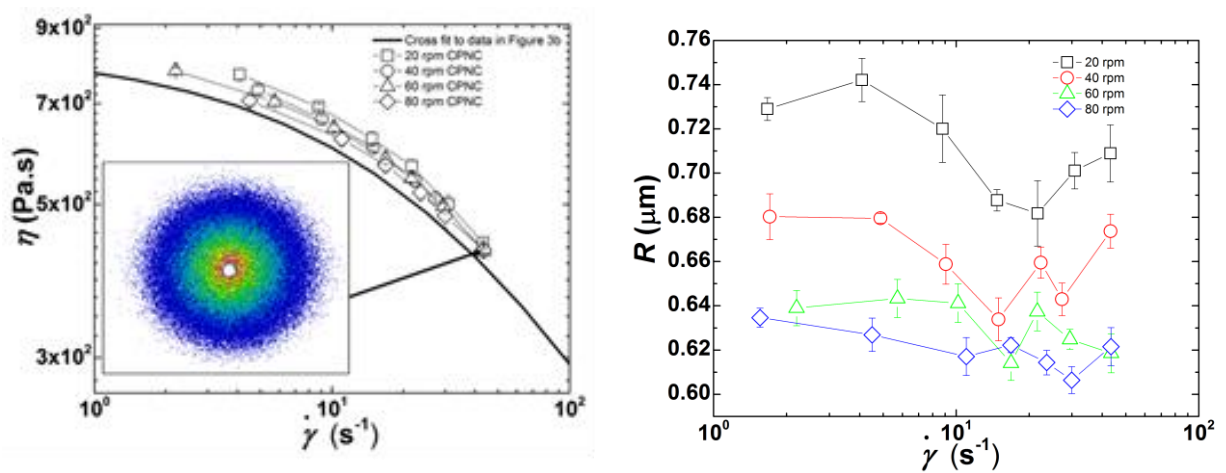


Fig. 2 *Left*: Flow curves measured in-line at different screw speeds. The line is the Cross equation fit to the PDMS flow curve. Inset: SALS pattern (at a shear rate of 44 s⁻¹ in the rheo-optical slit). *Right*: Clay particle radius R computed from the analysis of SALS patterns

Acknowledgment

The authors thank the FCT (Fundação para a Ciência e Tecnologia) for financial support under the framework of Strategic Funding grant UID/CTM/50025/2020.

References

[1] Teixeira, P.F.; Ferrás, L.L.; Hilliou, L.; Covas, J.A. A new double-slit rheometrical die for in-process characterization and extrusion of thermo-mechanically sensitive polymer systems. *Polym. Test.* **2018**, *66*, 137–145

MACROMOLECULAR MOBILITY IN AGED AND VIRGIN EPOXIES

Emmanuel Richaud

Laboratoire PIMM, Arts et Metiers Institute of Technology, CNRS, Cnam, 151 boulevard de l'Hopital, 75013 Paris, France
emmanuel.richaud@ensam.eu

INTRODUCTION

Several researches aim address the ageing of epoxies. The final aim of this research field is to predict the changes in engineering (mechanical, barrier...) properties. These latter depend on the macromolecular architecture and visco-elastic properties, which are addressed in this paper. Usually, DSC is used for monitoring glass transition and its changes, that are further related to chain scissions or crosslinking (1). Here, DMA will be used to investigate the changes in macromolecular mobility and its changes with ageing.

EXPERIMENTAL

Epoxy amine obtained from DGEBA cured with 4,7,10-Trioxa-1,13-tridecanediamine (TTDA) where thermally aged at 110°C. Ageing was mainly monitored by Dynamic Mechanical Analysis in multi frequency multi temperature sweeps.

RESULTS AND DISCUSSION

Two transitions were studied:

① The glass transition temperature. In the case of DGEBA-TTDA unaged network, this value is close to 70°C. This value was justified from the DiMarzio equation in which parameters were determined by the semi empirical method proposed by Bellenger and Verdu (2).

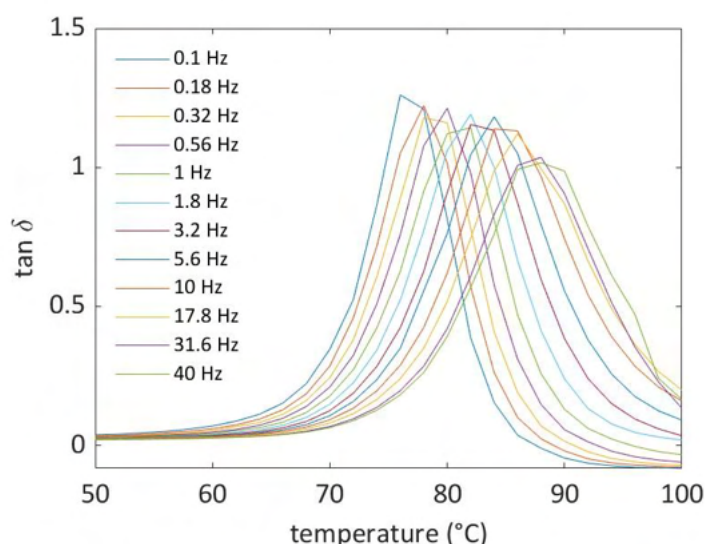


Fig. 1 Typical temperature frequency sweeps for unaged DGEBA TTDA.

During thermal oxidation under air, T_g was shown to increase, which can be explained by a predominant crosslinking mechanism. A comparison with the case of two other epoxy network where chain scissions predominate (DGEBA cured with either hexamethylene diamine or triethylene tetramine) suggests that crosslinking is due to the linear nature and the flexibility of TTDA hardener together with the reactivity of alkyl radicals in position of ether links.

DMA sweeps were exploited by two approaches:
 - relaxation maps (ln frequency vs 1/T) in which T_g can be described by the Vogel-Fulcher-Tammann-Hesse equation:

$$f = f_0 \cdot \exp\left(-\frac{DT_0}{T - T_0}\right) \quad (1)$$

- WLF equation for shifting curves

$$\log a_{T/T_g} = \frac{c_1(T - T_g)}{c_2 + T - T_g} \quad (2)$$

Both are consistent with

$$c_2 = T_g - T_0 \quad (3) \quad B = D \cdot T_0 = c_1 c_2 \ln 10 \quad (4)$$

Both approaches can allow to identify molecular parameters linked to free volume :

$$f_g = \frac{B}{\ln 10 \cdot c_1^g} \quad (5) \quad \alpha_f = \frac{B}{\ln 10 \cdot c_1^g \cdot c_2^g} \quad (6)$$

The applications were done in the case of unaged and aged DGEBA TTDA networks. It was observed in particular that C_2^g increases with ageing meanwhile C_1^g remains almost constant. This will be discussed in terms of free volume parameters.

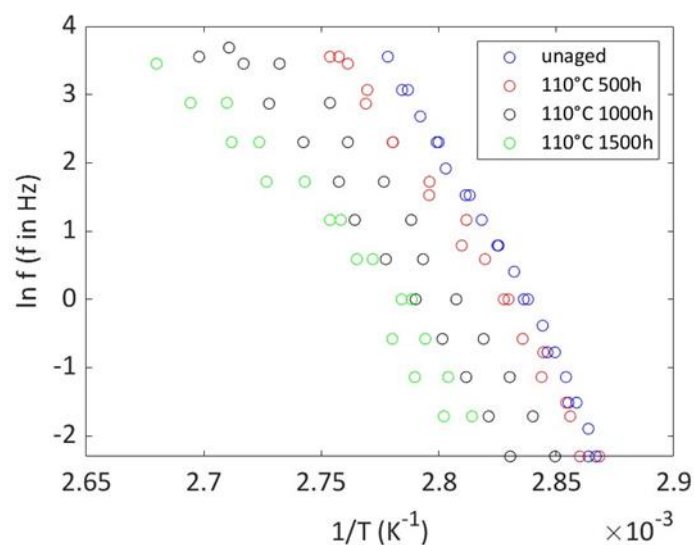


Fig. 2 Relaxation map of virgin and aged DGEBA TTDA systems for the alpha transition.

② The subglassy relaxation, observed at around -60°C and ascribed to the motion of hydroxypropylether groups (3). The temperature frequency sweeps confirm that maximum temperature of the peak and frequency are linked by an Arrhenius equation. The effect of thermal ageing on maximal temperature and relaxation amplitude will be discussed.

References

- 1) E. Ernault, E. Richaud, B. Fayolle, Polym. Degrad. Stab., 138, 82 (2017).
- 2) V. Bellenger, J. Verdu, E. Morel, J. Polym. Sci. Part B Polym. Phys., 25, 1219 (1987)
- 3) L. Heux, J.L. Halary, F. Lauprêtre, L. Monnerie, Polymer, 38, 1767 (1997)

Biopolymeric fluorescent materials dedicated to packaging perishable products

D. Bajer*

Faculty of Chemistry, Department of Biomedical and Polymer Chemistry, Nicolaus Copernicus University in Torun, Gagarina 7, Poland

* dagmara@umk.pl

INTRODUCTION

Perishable food quality and shelf life (e.g., fresh fruit, vegetables, raw meat) may be a partially controlled process by employing intelligent packaging, contributing to the sustainable development of food and agriculture. Protecting food from light plays a crucial role in packaging functions. Light quickly initiates food spoilage, prompting its chemical, enzymatic, and physical modification. Intermediate products formed during lipid peroxidation (e.g., fatty acid peroxides, aldehydes, and others) give products an unpleasant taste and harm health. Therefore, using a UV absorber in packaging can delay lipid oxidation processes. Protecting radiation-sensitive vitamins, such as C and E, is also essential.

The subject of the work was to obtain environmentally safe starch-chitosan films enriched with dialdehyde starch and fluorescein, exhibiting UV radiation absorption properties. Starch and chitosan are commonly available polysaccharides; however, they require modifications to improve their processing and functional properties. Their chemical modification is possible due to hydroxyl and amine functional groups. Dialdehyde starch enhances mechanical strength and has antimicrobial and antioxidant properties. Fluorescein, a member of the triarylmethine dye family, is a highly fluorescent molecule commonly used to label membranes and proteins. The network formed of biopolymers and fluorescein may limit direct $^1\text{O}_2$ attacks. Such coatings used in long-term exposure to visible light can be used in food packaging (coatings for meat, fruit, vegetables) to protect against UV radiation and the influence of microorganisms. Moreover, they can be applied to encapsulate drugs in medicine and pharmacy.

EXPERIMENTAL

Materials and Preparation

Dialdehyde starch was obtained from potato starch by NaIO_4 oxidation and aldehyde groups were determined (13%). Starch (S), starch-chitosan (SCh), and SCh cross-linked with dialdehyde starch (SChDs), plasticized with glycerin (Gl), were obtained by the solution casting method (S:Gl:Ch:DS = 16:5:1:4). 10 ml of 0.17% fluorescein solution was added to each bio-composite solution and subjected to 5-day dialysis in distilled water to wash out excess dye. The solution was then poured onto dishes and dried at room temperature (22°C) until the solvent evaporated completely. The following compositions were prepared: FS–starch-fluorescein, FSCh–starch-chitosan-fluorescein, FSChDs–starch-chitosan-dialdehyde starch-fluorescein. Each composite was irradiated with a UV lamp at a wavelength of $\lambda = 254$ nm for 5, 10, 15, 20, 40, 60 and 120 min. (until no significant changes were observed in the UV–Vis and FTIR-ATR spectra). The radiation intensity was 24 W/m^2 , in an air atmosphere and at room temperature. Spectroscopic studies of samples (UV-Vis, FTIR-ATR, Raman, XRD) were used to determine the chemical structure and interaction between blend components and to observe the effect of UV irradiation. XRD spectroscopy allowed to determine the crystallinity degree changes.

RESULTS AND DISCUSSION

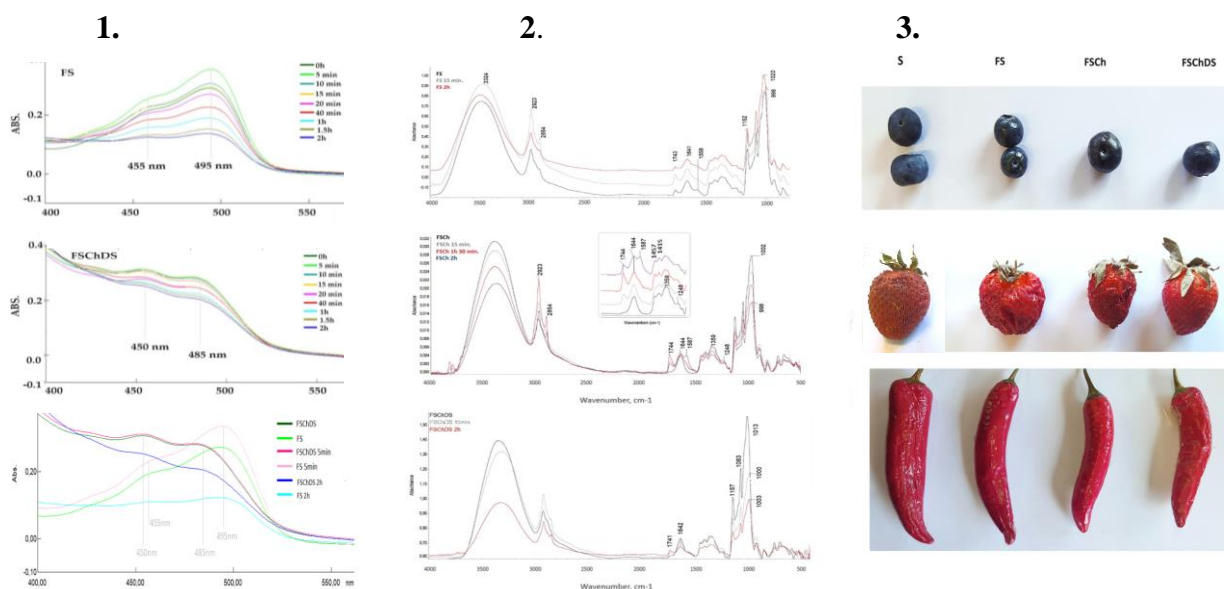


Fig. 1. UV-vis spectra of FS, FSChDS before and after UV-irradiation (5 min.-2 h.)

Fig. 2. FTIR-ATR spectra of FS, FSCh and FSChDS before UV irradiation and after 15 min. and 2 hours of UV-irradiation.

Fig. 3. Blueberry, strawberry and chili pepper covered with the followed coatings: S-starch film, FS-fluorescein-starch coating, FSCh – starch/chitosan/fluorescein coating, FSChDS- starch/chitosan/DS/fluoresceine-after 24 hours of sun-light exposure (day/night).

The fluorescein influenced the photochemical stability of the composites. FS film appeared susceptible to UV light. The modification of FS with chitosan and dialdehyde starch (FSChDS) resulted in a shift in fluorescein absorbance maximum from 495 nm to 485 nm, respectively (Figure 1). Light absorption is limited by irradiation time, wherein the FSChDS film is the most stable. FSCh sample did not show fluorescein excitation maxima on the UV-Vis spectrum, which confirms its high photo-stabilization.

The changes in the FTIR-ATR spectra confirmed that the fluorescein was attached to the chitosan and starch chains (Fig. 2). The spectra of FSCh and FSChDs films showed a drop in intensity of bands associated with protonated glucosamine residues of chitosan at around 1415 cm^{-1} , 1457 cm^{-1} , and at 1360 cm^{-1} (C-N stretching of amide III) indicating a loss of $-\text{NH}_3^+$ groups and covalent linking between the hydroxyl of dye and the amino-groups of chitosan. Irradiation affected the conformational changes of starch as well as dye photolysis (confirmed with mode fluctuations in the $900\text{-}1300\text{ cm}^{-1}$ spectral range attributed to glycosidic stretching vibration of C-O-C bonds, and the skeletal vibrations of the xanthotene moiety in fluorescein) (Fig. 2). The main changes in the spectra are also associated with competitive oxidation reactions and chromophore formation resulting from exposure to UV light. The intensity of the C=O peak rose with increasing irradiation time, which was most pronounced for FSCh sample (Fig. 1). In parallel, a decrease in hydroxyl intensity (maximum at 3324 cm^{-1}) might be related to new band formation with -OH participation as well as strongly-bonded water evolving during UV irradiation. UV-irradiation affected the new polymorphic transitions, recrystallization and the formation of a new multicomponent crystal phase of chitosan and starch/DS chains. The crystallinity degree (Xc) increased as follows: 16% for starch film, 19.6% for starch-chitosan (SCh) film, and 26.4% for SChDS film. The crystallinity degree of starch in composites containing fluorescein changed after 2 hours of irradiation: from 19.8% (sample non-irradiated) to 21.1% (2 hours of UV-action) for FSCh, and from 24% to 25.5% for FSChDS.

“3D PRINTING OF ACRYLATE EPOXIDIZED SOYBEAN OIL (AESO)-BASED COMPOSITES CONTAINING LIGNIN”

G. Colucci^{1,2*}, F. Sacchi^{1,2}, F. Bondioli^{1,2} and M. Messori^{1,2}

¹ Department of Applied Science and Technology, Politecnico di Torino, Corso Duca degli Abruzzi 24, 10129, Torino, Italy

² National Interuniversity Consortium of Materials Science and Technology (INSTM), Via G. Giusti 9, 50121 Firenze, Italy

*giovanna.colucci@polito.it

INTRODUCTION

Lignin can be considered an excellent filler to be incorporated within polymeric matrices giving rise to high mechanical and thermal properties. It has low density and low cost, which consequently reduces cost and weight of the final composites. In addition, lignin could improve flowability and processing performance of polymer matrices due to presence of active groups, such as hydroxyl groups, which made the interaction between matrix and lignin desirable, and thus the system useful to be processed by 3D printing.

For this reason, among the bio-based polymers, polymeric composites obtained by dispersing lignin as reinforcing agent can play a crucial role for additive manufacturing (AM), in particular for vat photopolymerization processes. This kind of AM technique represents an easy method for obtaining small and accurate objects by 3D printing specific geometries starting from liquid photopolymers. It is a light-based technology, which allows to obtain high printing resolution and good level of shape complexity of the printed parts. During the process, the build platform is dipped into the liquid resin and, thanks to the UV light, the resin in the vat can be photocured and transformed in a uniform layer of solid material according to the previously designed CAD model. The process goes on until the desired object is complete.

The present research work aims to prepare lignin-based composites by dispersing different amounts of lignin powder within a renewable acrylate epoxidized soybean oil (AESO) photocurable resin and to realize 3D printed parts by using LCD as vat photopolymerization 3D printing technique.

EXPERIMENTAL

Materials

The raw materials used in the work were: acrylate epoxidized soybean oil (AESO) as photocurable resin, tetrahydrofurfuryl acrylate (THFA) as reactive diluent, and phenyl bis (2,4,6-trimethylbenzoyl) phosphine oxide (BAPO) as radical photo-initiator, all purchased from Merck. UPM BioPiva™ 395 was the kraft softwood lignin used as natural filler to prepare the composites.

Preparation

Photocurable AESO-based formulations were firstly prepared by mixing the resin with THFA (60:40), in the presence of 2 wt.% of BAPO. Bio-based composites were then prepared by adding lignin to the liquid AESO-THFA resin at 5 and 7.5 phr. The unfilled and filled formulations were photocured by using a Phrozen Sonic Mini 8K vat polymerization 3D printer, LCD type, equipped with Linear Projection LED Module.

Characterization

The viscosity of the photocurable AESO-based resins was measured at room temperature to determine the best flowability and processability of the resin within the vat during the photopolymerization. Morphological investigations were also carried out using a Scanning Electron Microscope (SEM) to study the morphology of the AESO-based composites filled with lignin.

The thermal and viscoelastic properties were investigated by means of TGA, DSC, and DMTA analyses to study the changes induced to the presence of lignin on the final properties of the AESO-THFA system. Tensile properties of 3D printed samples were also tested to study the effect of lignin on mechanical properties.

RESULTS AND DISCUSSION

After the characterization of the pure lignin powder, AESO-based photocurable formulations were prepared, and their viscosity tested to study the effect of the presence of lignin on the resin flowability and printability. The values of viscosity obtained for composites containing THFA are considered suitable for printable resin in vat polymerization 3D printing process.

Several printing tests were carried out to investigate the optimal printing parameters of the AESO-based resins by LCD. Different 3D printed objects were successfully realized by LCD showing different complex structures and good level of details definition.

Morphological investigation revealed that lignin particles are dispersed and uniformly distributed within the polymer matrix, with an average particle diameter of 4.5 microns. Thermal analyses performed by TG and DSC tests underline that lignin addition does not have significant effects on the final thermal stability but lead to an increase of the glass transition temperature values. Moreover, DMTA measurements evidence that lignin dispersed within the AESO-THFA matrix induced an increase of the storage modulus, and of the maximum of tan delta curves, and put in evidence the reinforcing effect of lignin. Cytotoxicity tests were also carried out to evaluate the cytocompatibility of the novel lignin-based samples prepared.

To conclude lignin-based composites were successfully realized by LCD 3D printing with improved final properties induced to the presence of lignin particles well-dispersed within the AESO resin.

Acknowledgment

The present work was supported by MICS (Made in Italy – Circular and Sustainable) Extended Partnership and the European Union Next-Generation EU (PIANO NAZIONALE DI RIPRESA E RESILIENZA (PNRR) – MISSIONE 4 COMPONENTE 2, INVESTIMENTO 1.3 – D.D. 1551.11-10-2022, PE00000004).

References

- 1) J. Anketa, C. Ikshita, W. Ishika, R. Ankush, Mir Irfan Ul Haq, 3D printing –A review of processes, materials and applications in industry 4.0, *Sustainable Operations and Computers* **3** 33–4 (2022). doi.org/10.1016/j.susoc.2021.09.004.
- 2) M. Lebedevaite, V. Talacka, J. Ostrauskaite, High biorenewable content acrylate photocurable resins for DLP 3D printing, *J Appl Polym Sci.* **138**, 50233, (2021). doi.org/10.1002/app.50233.
- 3) L.S. Ebers, A. Arya, C.C. Bowland, W.G. Glasser, S.C. Chmely, A.K. Naskar, *M.P.* **112**, 23431 (2021). <https://doi.org/10.1002/bip.23431>.

LEWIS PAIR-CATALYZED DEPOLYMERIZATION OF POST-CONSUMER PET WASTE

L. Killinger^{1,2}, R. Hanich-Spahn¹ and A. Stephen K. Hashmi²

¹Fraunhofer Institute of Chemical Technology ICT, Pfinztal, Germany

²Organic-Chemical Institute, Heidelberg University, Heidelberg, Germany

lukas.killinger@ict.fraunhofer.de

INTRODUCTION

Plastics are ubiquitous in our daily life. Their outstanding properties like low weight, high mechanical strength, and good modifiability has led to an increasing demand throughout the past years. On the other side the high production rates, littering and their persistence in the environment has led to the accumulation of plastic waste on our planet. To achieve the goal of climate protection as undertaken in the Paris Agreement and the goal of greenhouse gas neutrality, strategies for a circular plastics economy must be identified. Mechanical recycling can be used to recycle homogeneous post-industrial plastic waste, but it suffers from some drawbacks with regards to heterogeneous post-consumer plastic waste. The recyclate obtained from such waste streams often suffers from a deterioration of properties, thereby, rendering it incapable of competing with virgin plastic. Chemical recycling represents a promising technology to valorize such plastic waste into its constituent monomers and/or other valuable chemicals and thus, complements mechanical recycling.[1] So far, chemical recycling often proceeds at a slow rate and results in a negligible product yield. Therefore, chemical recycling often requires high amounts of energy, which remains one of the major challenges for the application of chemical recycling on an industrial scale. Catalysis, as one of the green principles in chemistry, can be a key factor to enable faster, more efficient and less energy intensive processes. Catalysis is therefore a great opportunity to improve the industrial viability of chemical recycling methods.

EXPERIMENTAL

Materials

Within this work different catalytic methods for the chemical recycling of PET were investigated. For the experiments different PET waste streams were used. The initial trials were conducted using homogeneous waste material from PET bottles. Further investigations were run on heterogeneous post-consumer waste streams with PET fractions of 90 % and 70 %. The PET materials were washed and shredded into smaller particles before the subjecting it to the recycling process. For the optimization of this recycling process different commercially available and non-available catalysts were investigated.

Methods

This worked was focused on the depolymerization of PET using glycolysis. In this process ethylene glycol is used to cleave the polymeric bond of PET and degrade the polymer towards its constituent monomer BHET. For the optimization of the process different catalysts and combinations of those catalysts were applied, compared and the ideal catalyst combination was selected for further optimization. The obtained BHET was purified by crystallization and characterized using advanced analytical methods like NMR spectroscopy, HPLC, DSC and ICP-OES analysis. In the next step the recycled BHET was repolymerized to obtain recycled PET with virgin-like properties. These properties were characterized and compared to the virgin PET material.

RESULTS AND DISCUSSION

Throughout this work different catalysts were investigated in the glycolysis of PET. It was observed that by combining Lewis-basic catalysts with Lewis-acidic catalysts the conversion and yield of the depolymerization process can be increased.[2] In consequence different Lewis pairs were investigated. Beneficial effects were particularly seen in the combination of guanidine-based organobases and zinc salts. To understand the reactivity and evaluate the catalyst selection, computational simulations were conducted using the software Orca.[3] The activation energy for the transesterification of a model substrate and in the presence of the different experimentally investigated catalyst combinations were calculated. The calculated values for the activation energies can be correlated with the experimental results for the conversion of the glycolysis (Figure 1). The data reveals that the computational calculations can give a good estimation for the reactivity of a catalyst in the experimental process and can simplify the catalyst selection for the glycolysis of PET.

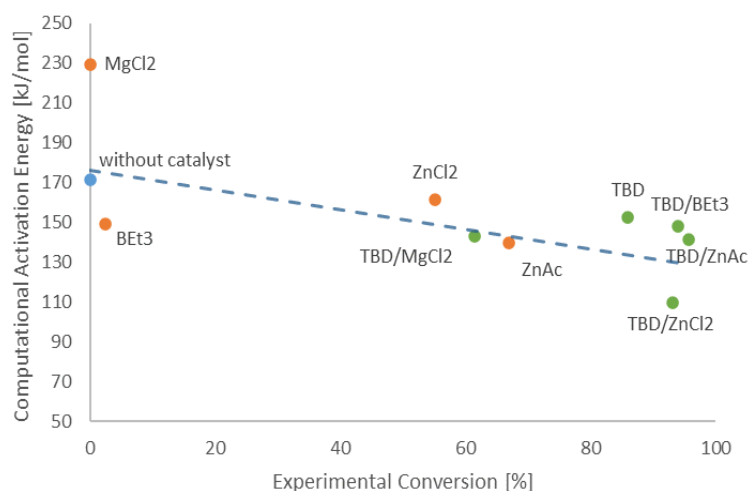


Fig. 1 Correlation of experimental results and theoretically calculated activation energy for some of the investigated catalysts in the glycolysis of PET.

Using the results from the computational and experimental analysis, the glycolysis process for PET could be optimized by selecting an ideal catalyst system. The optimized process was scaled up to obtain large quantities of pure BHET. This BHET was then repolymerized to recycled PET materials. The observations throughout the polymerization process and the quality of the recycled PET were comparable to virgin materials.

Acknowledgment

This work has been financially supported by the Fraunhofer Cluster of Excellence Circular Plastics Economy CCPE

References

- [1] A. Bardow et al., *Resources, Conservation & Recycling* **2020**, 162, 105010.
- [2] L. Killinger et al., *Poster Makromolekulares Kolloquium Freiburg* **2024**, 10.24406/publica-2799.
- [3] F. Neese, *Comput. Mol. Sci.* **2012**, 2, 73 – 78; F. Neese, *Comput. Mol. Sci.* **2017**, 8, e1327; F. Neese, *J. Chem. Phys.* **2020**, 152, 224108

Development of Low Dielectric Polysaccharide Esters for Electrical Insulating Resins

Yuya Fukata, Satoshi Kimura and Tadahisa Iwata

Department of Biomaterial Sciences, Graduate School of Agriculture and Life Sciences, The University of Tokyo, 1-1-1 Yayoi, Bunkyo-ku, Tokyo, Japan
 fukata-yuya096@g.ecc.u-tokyo.ac.jp, skimura@g.ecc.u-tokyo.ac.jp, atiwata@g.ecc.u-tokyo.ac.jp

INTRODUCTION

All electrical devices include metals and petroleum-based plastics represented by printed circuit boards (PCB). Recently, PCB waste has come to be recognized as urban mines, where valuable metals can be found. However, in the recovery process, the plastic components are often dissolved in strong acids and/or incinerated, contributing to carbon dioxide emissions, and exacerbating the climate crisis. To mitigate carbon dioxide emissions, one solution is to use biomass-based plastics derived from renewable sources.

The plastic used in PCB requires two crucial properties. First, high thermal stability is essential to prevent distortion during high-temperature manufacturing processes, such as soldering. In general, a glass transition temperature (T_g) of over 200°C is required.

Second, low hindrance to electrical signals flowing through adjacent metal circuits (low transmission loss) is vital. The degree of transmission loss depends on the dielectric constant (Dk). Lower Dk (<3.0) polymers are preferred for upcoming high-speed and large-scale communication society.

In this study, we synthesized two concept of polysaccharide ester derivatives applicable to PCB. One is the thermo-plastic, which could be used as like polyimide in flexible printed circuit. The other is thermoset plastic, which could be used as like epoxy resins in interlayer insulator.

EXPERIMENTAL

Two types of polysaccharides, cellulose and α -1,3-glucan, were utilized. α -1,3-glucan was synthesized from sucrose using enzyme (GtfJ) in water system (Fig. 2).

The linear and cycloalkane sidechain was respectively introduced into cellulose and α -1,3-glucan to realize thermo-plastic properties.

The unsaturated sidechain of 2-butenate and hexanoate were combinedly introduced into α -1,3-glucan for obtaining thermoset property. Subsequently, we evaluated thermal, mechanical, and dielectric property of each ester derivative.

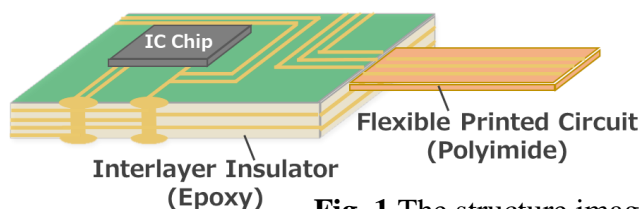


Fig. 1 The structure image of a printed circuit board.

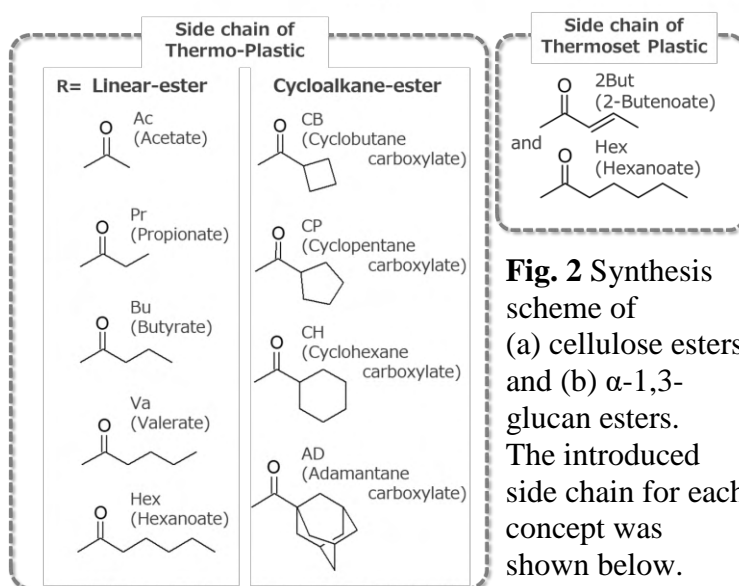
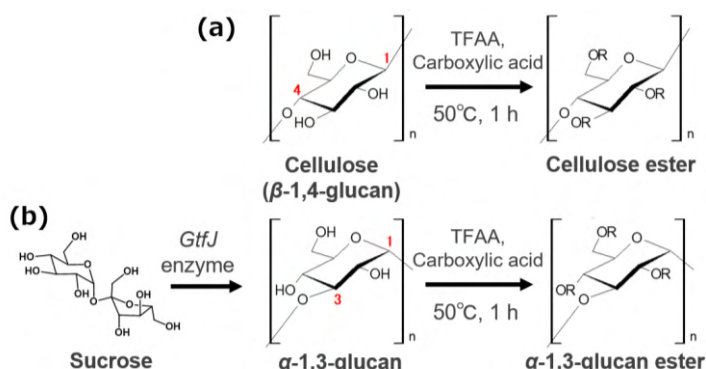


Fig. 2 Synthesis scheme of (a) cellulose esters and (b) α -1,3-glucan esters. The introduced side chain for each concept was shown below.

RESULTS AND DISCUSSION

① Thermo-Plastic

In the case of cellulose, all the carboxylic acids except for adamantane carboxylic acid were introduced. The T_g of cellulose linear esters decreased with the increase of sidechain length (Fig. 3). However, the T_g s of cellulose cyclic alkane esters (CH, CP, and CB) were almost the same ($\sim 130^\circ\text{C}$), which were comparable to the cellulose-Pr, but the value did not satisfy the demanded T_g ($>200^\circ\text{C}$).

The Dk values of cellulose ester were not dependent on the side chain structure but on the carbon number of sidechains. The derivatives of carbon number over 5, the Dk value was below 3.0, which is superior to conventional polyimides. Therefore, cellulose cycloalkane esters could be used as electrical insulators that do not require high-temperature soldering.

α -1,3-glucan linear esters showed the similar trend of T_g and Dk to those of cellulose esters. On the other hand, α -1,3-glucan cyclic alkane esters (CH and AD) showed higher T_g over 200°C which could be durable to soldering. Furthermore, the Dk of α -1,3-glucan-CH reached 2.6, which was superior to that of polyimides. Therefore, α -1,3-glucan-CH showed potential for high performance electrical insulation resins in PCB.

② Thermoset Plastic

In the case of 2-Butenoate (2But) was homogeneously introduced into α -1,3-glucan, the derivative formed highly brittle film. To address this problem, 2But and hexanoate (Hex) as internal plasticizer were introduced at the ratio of 1:2 (α -1,3-glucan-BH). α -1,3-glucan-BH started to soften at 72°C (Fig. 4). Therefore, α -1,3-glucan-BH powder was easily hot-pressed at 150°C and the transparent and flexible film was obtained (Fig. 5).

The hot-pressed film was further annealed at 220°C for 1 h, leading to crosslinking of unsaturated groups (determined by FT-IR). The T_g of crosslinked film reached 235°C , comparable to conventional epoxy resins. Furthermore, the Dk reached 2.57, significantly exceeding the conventional epoxy resins (~ 3.5).

In summary, α -1,3-glucan-BH realized fine-moldability before crosslinking and high T_g and low Dk after crosslinking. It is highly promising as interlayer insulators.

Acknowledgment

This work was supported by JSPS KAKENHI (JP23KJ0700).

[1] S. Puanglek, T. Iwata, et. al, In Vitro Synthesis of linear α -1,3-Glucan and Chemical Modification to Ester Derivatives Exhibiting Outstanding Thermal Properties. *Sci. Rep.* 2016, 6

[2] Y. Fukata, S. Kimura, T. Iwata, Manufacturing Low Dielectric Polysaccharide Esters with High

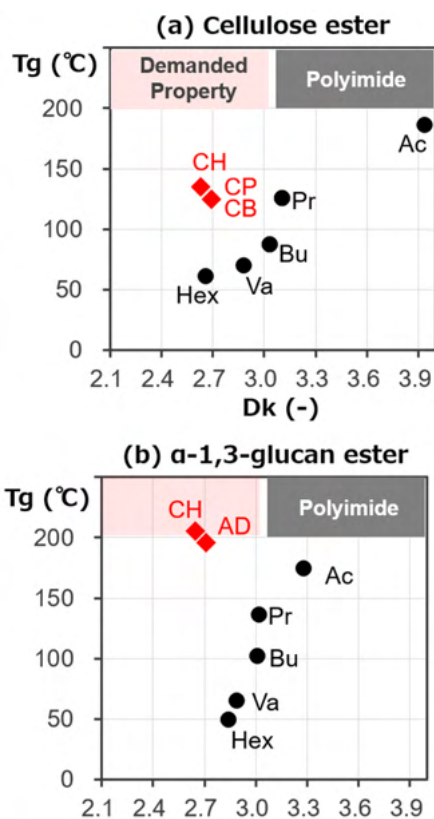


Fig. 3 T_g and Dk of (a) cellulose esters and (b) α -1,3-glucan esters.

●: Linear, ◆: Cycloalkane

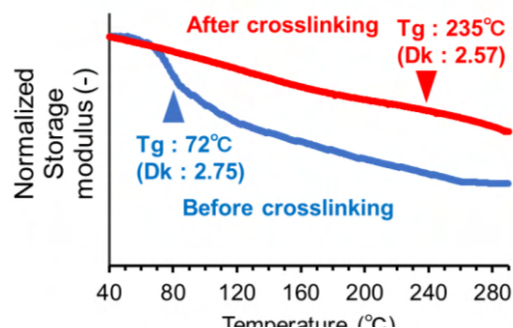


Fig. 4 DMA curves of α -1,3-glucan-BH before and after crosslinking. T_g and Dk were also shown.



Fig. 5 The hot-pressed film and the crosslinked film of α -1,3-glucan-BH

HOW TO ENHANCE IMPACT PROPERTIES OF POLYETHYLENE TEREPHTHALATE IN A MECHANICAL RECYCLING CONTEXT

G. Goncalves Marques,^{1,2} V. Bounor-Legaré,¹ R. Fulchiron,^{1*} R. Inoubli,² P. Hajji², A. Couffin³

¹ Université Claude Bernard Lyon 1, INSA Lyon, Université Jean Monnet, CNRS

UMR 5223, Ingénierie des Matériaux Polymères F-69622 Villeurbanne Cédex, France

² Arkema – Centre de Recherche Rhône-Alpes – CS42063, F-69491 Pierre Benite, France

³ Arkema – Groupement de recherches de Lacq (GRL) – BP 34, 64170 Lacq, France

*rene.fulchiron@univ-lyon1.fr

INTRODUCTION

One striking example of the environmental stress is the plastic pollution. (1) Besides reducing the plastic consumption, recycling is today one of the applicable approaches (2). In this context, polyethylene terephthalate (PET) is in the spotlight. With unique properties, PET occupies the podium of the recycled polymers worldwide (2,3). However, despite the effort spent on its recycling, many challenges still restrain its reintroduction in a wide range of industrial applications. One of the reasons for this is a lack of understanding of the structural modifications caused by successive processing steps and the effect on the final product properties, especially the impact strength.

The traditional strategies of formulating a polymer for modifying its properties becomes a greater challenge in a recycling scenario. Specially for a notch sensitive material as PET, the existing solutions are few and with numerous drawbacks. The development of additives with long-lasting toughening ability specifically adapted for multiple processing steps is still lacking. Finding an economically viable alternative capable of maintaining an ecological balance can help reducing the barriers for the recycling development (1,2).

The present research study focuses on the effect of an acrylic impact modifier additive on a mechanical recycling process of PET. Molar mass, rheological behavior and mechanical properties were compared before and after compounding, considering the accelerated physical aging of the matrix before testing. The influence of a compatibilizer on the processing cycles was studied.

EXPERIMENTAL

Materials

A bottle-grade PET pellets (IV = 0.85 dL/g) was purchased by Far Eastern New Century Corporation. Successive extrusion cycles were used to simulate a mechanical recycling process of PET. Acrylic impact modifier (AIM) was supplied by Arkema. Random terpolymer ethylene-methyl acrylate-glycidyl methacrylate Lotader AX8900 (68/24/8 wt%) was purchased by SK functional polymers and used as a compatibilizer.

Preparation

PET pellets were dried at 140°C for 4h and were left in the vacuum oven till the temperature reaches 50°C. Impact modifier was dried at 95°C overnight. Compounding was performed in a twin-screw extruder (27.5 L/D, D = 16 mm, temperature set at 45°C-270°C, screw speed at 200 rpm). Injection molding was used for the preparation of mechanical test specimens (275°C, 130 rpm, 20°C mold). Dumbbell specimens (ISO 527-2, type 5a) were milled from injected plates (milling speed 13500 mm/s). Physical aging of mechanical test samples was accelerated in an oven set at 50°C for 7 days.

Characterization

Triple detection size exclusion chromatography (SEC WYATT Technology) was used to measure the chain scission. Pellets dynamic flow properties (25 mm diameter parallel plate) were determined with a DHR-2 rheometer at 280°C, under nitrogen atmosphere (2 L/min). Differential scanning calorimetry (DSC Q1000, TA Instruments) was used to characterize

thermal and crystallinity behavior. Uniaxial tensile test was performed on dumbbell specimens and impact resistance was characterized on an Izod test (5.5J, room temperature, V-notched type A 25 mm). The morphology of compounded samples was characterized via Scanning Electron microscopy (SEM, LFD detector) and confirmed with an Atomic Force Microscope (AFM Nano-observer by CSInstruments) tapping mode (ultramicrotomy at -100°C).

RESULTS AND DISCUSSION

By successive cycles of extrusion and injection molding, the recycling process of PET was successfully simulated at a laboratory scale. The produced recycled PET (rPET) was characterized, and several structural modifications could be observed such as chain scission, aspect changes and crystallinity increase. Despite the different effects on the matrix, mechanical characterization showed a stable response of a ductile material in a uniaxial tensile test but fragile in a notched Izod test.

Both the impact sensitivity and the challenging processing of PET could be improved via compounding with additives. With chosen extrusion parameters, the use of a core-shell structured AIM showed promising results with PET even after a physical aging. The impact resistance was doubled with AIM only (10 wt%). Difficulties related to the dispersion and weak interaction with the matrix were answered by a reactive compatibilizer addition, allowing to reach a super-toughness of 57 kJ/m².

The better understanding on the relationship between structural modification and final properties may allow a fine tuning of the additive structure. Increasing rPET applications without the need of compatibilization or post-treatments can wide the upcycling possibilities for this material.

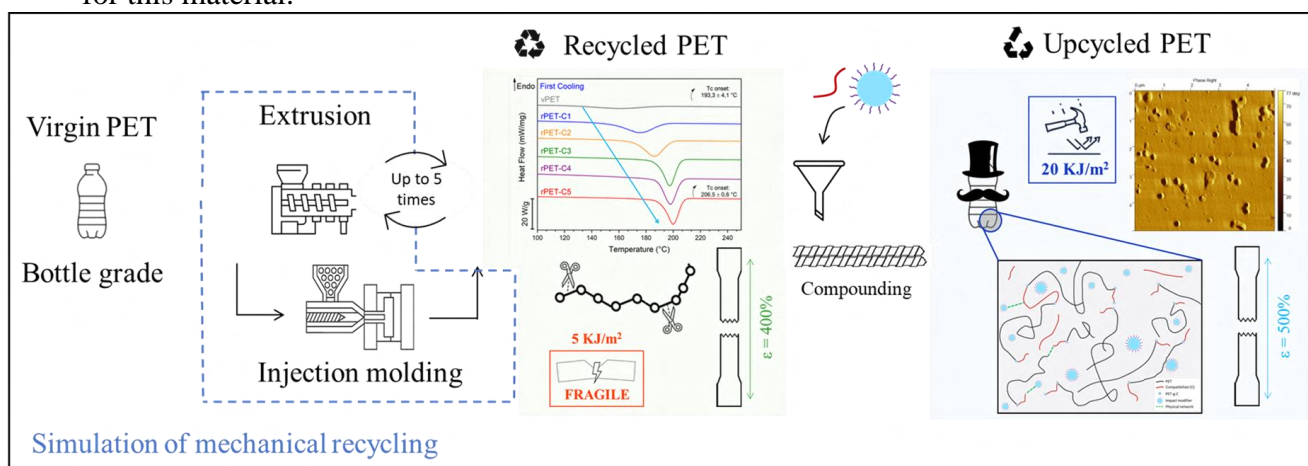


Figure 1 – Schematic representation of PET’s mechanical recycling in the presence of impact modifiers.

Acknowledgment

The authors gratefully acknowledge the "Association Nationale de la Recherche et de la Technologie" (France) for funding the PhD thesis of Gabriela Gonçalves Marques (CIFRE# 2021/1131).

References

- (1) R. Geyer, J.R. Jambeck and K. L. Law. “Production; use and fate of all plastics ever made”. *ci. Adv.* **3.7** **2017**, e1700782.
- (2) W. Damayanti, H.-S. “Strategic Possibility Routes of Recycled PET”. *Polymers* **2021**, *13*, 1475.
- (3) F. Welle. “Twenty years of PET bottle to bottle recycling—An overview”. *Resources Conservation and Recycling - RESOUR CONSERV RECYCL*, **2011**, *55*. 865-875.

Effect of High-Speed Airflow on Polymer Thermo-Oxidation

**A. Doriat^{1*}, M. Gigliotti¹, M. Beringhier¹, G. Lalizel¹, E. Dorignac¹,
P. Berterretche¹, M. Minervino²**

¹Institut Pprime, Chasseneuil Futuroscope, France

²Safran Aircraft Engine, France

aurelien.doriat@ensma.fr

INTRODUCTION

Carbon fiber-reinforced epoxy composites are used in warm aero-engine parts to reduce weight and allow of more complex and efficient shapes. In these parts, the surrounding aero-thermal environment may promote high temperatures (over 100°C in an aircraft engine) leading to thermo-oxidation phenomena [1]. Nevertheless, the laboratory aging studies have been carried out in oven only (in atmospheric condition or under oxygen pressure [2]), but the parts in real conditions are exposed to temperature but also to air flow. In the case of oven aging, the oxygen boundary condition is well known with the Henry's law as long as the oxygen partial pressure is not too high [3]. The aim of this study is to understand the effect of the airflow and the influence of the aero-thermal boundary conditions on thermo-oxidative aging of the epoxy resin. As a first step, the polymer matrix was studied by comparing oven and wind tunnel aged samples. As the experimental study shows a faster aging for the samples aged in the wind tunnel, the oxygen boundary condition should be estimated to understand the effect of the airflow.

In this work, we summarize the thermo-oxidation modeling process and more particularly the coupling between the chemical model and the experimental data in order to make oxygen boundary condition identification to understand the effect of the airflow on thermo-oxidation.

EXPERIMENTAL

Materials and aging

An aromatic diamine epoxy resin was employed, exhibiting chemical similarities to both the DGEBF-CAF resin and the PR520 resin manufactured by Syensqo, which are commonly utilized in the aerospace industry.

To understand the effect of the airflow, reference samples were exposed to atmospheric air conditions at 150°C in an oven for durations ranging from 20h to 80h. Another set of samples have been aged in the BATH (Banc AéroThermique) wind tunnel (for the detail of the bench, see [4]). A test section has been designed to put the sample inside the airflow (at 150°C, atmospheric pressure and Mach 1 on each side of the sample) and avoid temperature gradient inside a sample.

Thermo-oxidation characterization

In order to characterize the oxidized layer, classical indentation tests have been achieved [2] [5]. Also, color based measurements have also been done by measuring the color difference ΔE_{ab}^* between a virgin sample and an aged one. The color change is correlated to the mechanical elastic modulus representative of aging. This last method is faster and has a higher spatial resolution [6].

RESULTS AND DISCUSSION

The idea is to set a model to correlate in input the oxygen quantity at the interface and in the output, a measured quantity: indentation modulus or color difference. We used the mechanistic scheme developed by Colin's team [7] to couple the chemistry model and experimental data such as no analytical model exists and basic correlations are not relevant with

our material. Then, we used Physics Informed Neural Network (PINN) [8] to make the coupling. This model has been set on samples aged in oven under different oxygen pressure conditions. In addition of the data, we used physic equation to help the training process such as the decrease of our output with the space or increase with the time.

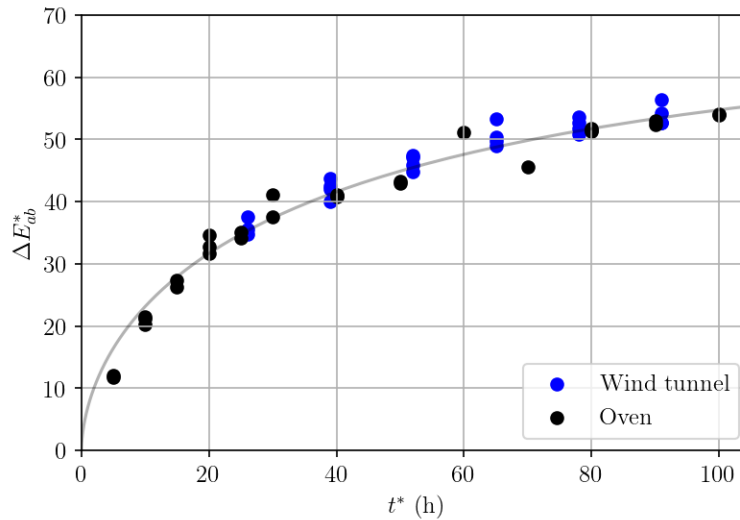


Fig. 1 : Color change comparison between oven and wind tunnel aging considering pressure effect.

Once the model is set, we used it to make boundary condition identification for the sample aged inside the wind tunnel.

With the airflow, the velocity and the pressure field at the interface seem to modify the boundary layer increasing the exchange. Then, the boundary condition identification aims to understand the effect of the airflow. The local pressure is correlated to the flow velocity throwing the compressible effect. Therefore, the aging is accelerated as the pressure is

higher at the interface. Fig. 1 shows the evolution of the color change ΔE_{ab}^* over the equivalent time t^* . For samples aged in oven, the equivalent time is equal to the exposure duration as aging is done under reference conditions (150°C, 0,21bar). For the samples aged in wind tunnel, the accelerating factor a_T is adjusted: $t^* = a_T t = 1.3 t$. As the measurements are made on the surface, there is no diffusion effect and the Henry's law gives a linear dependency with oxygen pressure. The accelerating factor is equal to the increase of pressure which validated the faster aging under high-speed flow of polymer.

Acknowledgment

This work was supported by the French government program "Investissements d'Avenir" (EUR INTREE, reference ANR-18-EURE-0010). This work was supported by Safran Aircraft Engine. This work pertains to the French government program "Investissements d'Avenir" (LABEX INTERACTIFS, reference ANR-11-LABX-0017-01). The authors thank SAFRAN Aircraft Engines for providing the polymer material.

References

- 1) P.-S. Shin, J.-H. Kim, H.-S. Park, Y.-M. Baek, S.-I. Lee, K.L. DeVries, J.-M. Park, *Fibers and Polymers*, **21**, 2 (2020)
- 2) M. Pecora, O. Smerdova, M. Gigliotti, *Composite Structures*, **244** 112268 (2020)
- 3) J. C. Grandidier, L. Olivier, M. C. Lafarie-Frenot, M. Gigliotti, *Mechanics of Materials*, **84**, 44 (2015)
- 4) A. Subramanian, E. Dornnac, G. Lalizel, PhD Thesis (2022)
- 5) P.B. Stickler, M. Ramulu, *Compsite Structures*, **52**, 3 (2001)
- 6) M. Spencer, W. Fuchs, Y. Ni, D. Li, M. R. Pallaka, A. Arteaga, L. S. Fifield, *Materials Today Chemistry*, **29**, 101417 (2023)
- 7) X. Colin, F. Essatbi, J. Delozanne, G. Moreau, *Polymer Degradation and Stability*, **181**, 109314 (2020)
- 8) M. Raissi, P. Perdikaris, G. E. Karniadakis, *Journal of Computational Physics*, **378**, 686 (2019)

ABOUT THE DEGRADATION MECHANISM OF EPOXY RESIN EXPOSED TO PARTIAL DISCHARGES

G. Buccella*[§], **A. S. Basso Peressut**[#], **L. Brambilla**[#], **A. Villa***, **L. Barbieri***, **D. Palladini***, **G. D'Avanzo*** and **S. Venturini***

*Ricerca sul Sistema Energetico (RSE S.p.A.) – Via R. Rubattino 54, 20134 Milan;

[#]Department of Chemistry, Materials and Chemical Engineering “G. Natta”, Politecnico di Milano, P.zza L. da Vinci 32-20133, Milan, Italy;

[§]giacomo.buccella@rse-web.it

INTRODUCTION

The degradation of polymeric insulating materials in electrical components may cause sudden and unexpected failures. In such a framework, partial discharges (PDs) are one of the main phenomena that contribute to the aging of insulating components, such as epoxy resin (ER)-based dielectrics [1]. PDs produce oxidizing environment in the gas, i.e. a plasma. Plasma-polymer interactions are the driving force behind the synthesis of specific chemical groups (peroxides, oxalates, etc..) on the surface of ER. These groups are associated with ER degradation, causing the decrease of its insulating strength [2]. Moreover, the abrasion of ER itself is observed as a long-term effect.

We aim at building an effective model able to predict the degradation process and provide an estimate of the remaining life of electrical components. With the aid of molecular dynamics (MD) simulations, we discuss some possible chemical mechanisms leading to ER aging.

COMPUTATIONAL

Two possible reaction paths were reproduced with MD simulations. Both mechanisms involved the species $O\cdot/OH\cdot$, which are abundant in an air-plasma, and the molecule A (Figure 1), representative of a simplified anhydride-cured ER monomer.

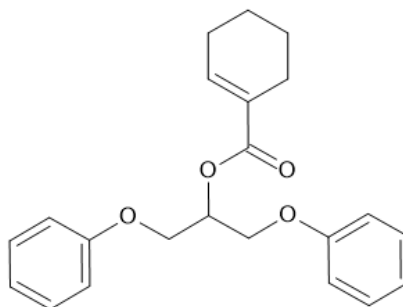


Figure 1: molecule A.

RESULTS AND DISCUSSION

The first mechanism starts with an intramolecular reaction that involves the rupture of two bonds and the formation of a new C-C bond, obtaining products B and C (Step 1, Figure 2). According to free-energy estimates obtained with metadynamics, the reaction in Step 1 needs to overcome a barrier equal to $2.4 \cdot 10^2$ kJ/mol; the energy gain associated with the formation of products B and C is estimated to be $8.7 \cdot 10^3$ kJ/mol. Product B, then, oxidizes easily to give phenol and glyoxal (Step 2, Figure 2). Some past works reported the detection of glycolic acid, glyoxylic acid and oxalic acid on the surface of ER samples exposed to PDs [3]. Glyoxal can be considered a precursor of such species.

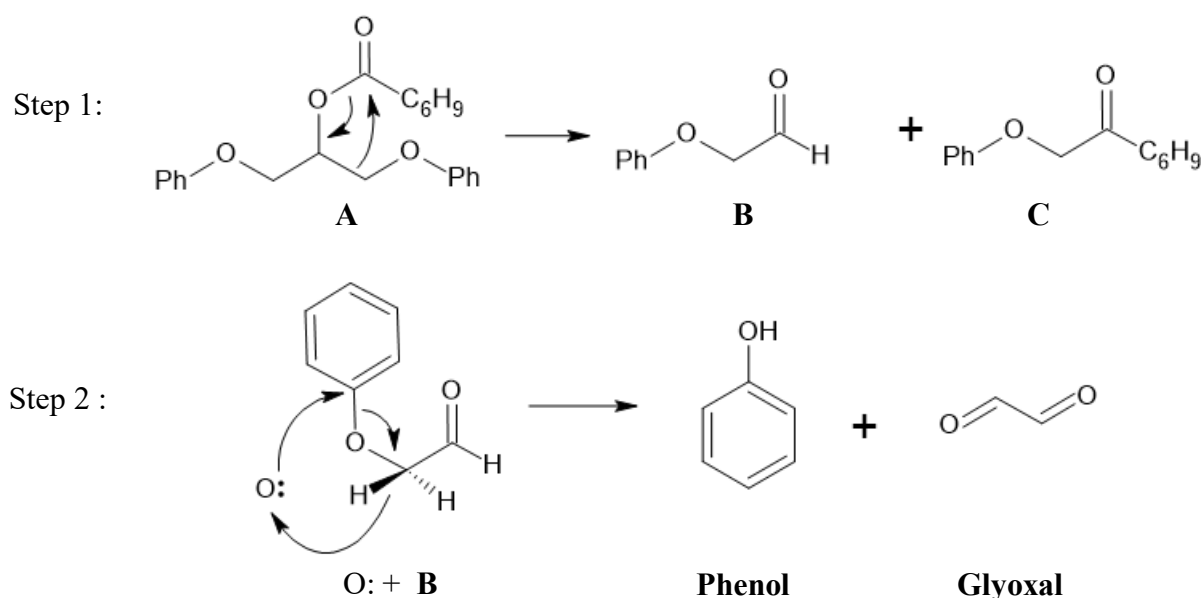


Figure 2: first mechanism, reaction path for glyoxal synthesis.

The second mechanism starts with the reaction of molecule A with $\text{OH}\cdot$ and $\text{O}\cdot$, and subsequently involves further reactions between the same oxidizing species and the product obtained at the previous step. $\text{OH}\cdot$ tends to abstract H atoms to form water molecules, while $\text{O}\cdot$ reacts with polymer backbone forming hydroxyl and peroxy groups. After 7 reaction steps, molecule A was completely degraded into smaller molecules like CO, CO_2 , CH_2O and peracids like percarbonic acid (Figure 3).

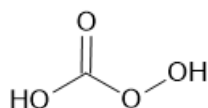


Figure 3: percarbonic acid.

With MD calculations it was possible to model the formation of possible precursors of oxalic acid and other products associated with ER degradation. Future developments may lead to the outlining of oxalic acid synthesis, starting from the further oxidation of such precursors.

Acknowledgment

This work has been financed by the Research Fund for the Italian Electrical System under the Contract Agreement between RSE S.p.A. and the Ministry of Economic Development—General Directorate for the Electricity Market, Renewable Energy and Energy Efficiency, Nuclear Energy in compliance with the decree of April 16th 2018.

References

- [1] C. Hudon, R. Bartnikas, e M. R. Wertheimer, «Effect of physico-chemical degradation of epoxy resin on partial discharge behavior», *IEEE Trans. Dielectr. Electr. Insul.*, vol. 2, fasc. 6, pp. 1083–1094, 1995, doi: 10.1109/tdei.1995.8881923.
- [2] C. Hudon, R. Bartnikas, e M. R. Wertheimer, «Surface conductivity of epoxy specimens subjected to partial discharges», in *IEEE International Symposium on Electrical Insulation*, Toronto, Ont., Canada: IEEE, 1990, pp. 153–155. doi: 10.1109/ELINSL.1990.109729.
- [3] X. Zhang, Y. Wu, H. Wen, G. Hu, Z. Yang, e J. Tao, «The influence of oxygen on thermal decomposition characteristics of epoxy resins cured by anhydride», *Polym. Degrad. Stab.*, vol. 156, pp. 125–131, 2018, doi: 10.1016/j.polymdegradstab.2018.08.006.

Enhancing Self-healing and Recycling capabilities in Unsaturated Polyester Resin: A way to introduce transesterification catalysts

Giuliana Rizzo^{*1}, Sandro Dattilo², Lorena Saitta¹, Claudio Tosto¹, Ignazio Blanco¹, and Gianluca Cicala¹.

¹Department of Civil Engineering and Architecture, University of Catania, Catania 95125, Italy, giuliana.rizzo@phd.unict.it.

²CNR Institute of Polymers, Composites and Biomaterials, Catania 95126, Italy;

INTRODUCTION

Unsaturated polyester resin (UPR) is a commercially thermosetting material renowned for its favorable thermomechanical properties and exceptional chemical resistance. These characteristics are typically attributed to the use of styrene as a curing agent. However, the high toxicity of styrene has inspired research and industry to investigate friendly alternatives. In this study, unsaturated polyester (UP) was synthesized and cured with a blend of acrylated epoxidized soybean oil (AESO), 2-hydroxyethyl methacrylate (HEMA), and styrene in low content. Notably, styrene was reduced from 40% to 26%. A catalyst was introduced into the blend to promote dissolution and recycling capabilities. Following a comprehensive characterization, the resulting resins were employed in composite manufacturing with subsequent comparison to counterparts made of commercial UPR cured with 40% of styrene¹.

EXPERIMENTAL

Materials

Phthalic anhydride, maleic anhydrides and propylene glycol were purchased from Sigma-Aldrich (St. Louis, MO, USA) and used for the synthesis of unsaturated polyester resin as reported by Korbar et al². The curing agents such as styrene, 2-hydroxyethyl methacrylate and the epoxidized acrylate soybean oil were purchased as well from Sigma-Aldrich. Zn acetylacetonate was exploited as transesterification promoters and purchased from Sigma-Aldrich as well. Commercial unsaturated polyester (UP) and correspondent catalysts for a “fast-curing” were supplied by the NTET Group. Flax fibers with an areal density of 290 gsm and a thickness of 0.75 mm were purchased from Easy Composites Ltd. UK.

Preparation

Once the UP was synthesized, two different formulations were prepared. In different vials, the UP was mixed with 25% of styrene (Sty) w/w, 10% of acrylated epoxidized soybean oil (AESO) w/w, and 20% of 2-hydroxyethyl methacrylate (HEMA) w/w. To assess the influence of the transesterification catalyst on both chemical and mechanical properties, zinc acetylacetonate was incorporated into each blend at varying mol percentages (1% and 5.0%) relative to the hydroxyl groups supplied by both AESO and HEMA reagents. Each formulation was then cured at 140 °C for 2 h and 150 °C for 1 h. The final products were identified as UPRb_Zn1% and UPRb_Zn5% to indicate the different contents of zinc catalyst.

Chemical, Mechanical and Calorimetric characterization

Chemical properties were measured with a Fourier-transforms infrared spectroscopy, and by a swelling test on different solvents. Recycling test was also performed to introduce potential recycling ability. Mechanical properties were investigated by Flexural test and DMA analysis, while calorimetric behavior was studied by DSC and TGA analysis.

RESULTS AND DISCUSSION

In this work, comprehensive characterization of unsaturated polyester resin was carried out after its full curing with biobased vegetable oil, 2-hydroxymethyl methacrylate, and reduced content of styrene. Investigation by chemical and thermomechanical analyses highlights the potential of biobased precursor as sustainable and greener alternatives to petroleum counterpart. The exploitation of developed resins in composite manufacturing provides laminates with excellent flexural modulus (around 4.8 GPa) and high glass transition temperatures (108 °C), Figure 1.a. Moreover, the thermal stability of the green laminates was preserved showing a T_s equal to 168 and 160 °C. Due to the introduction of zinc catalyst, the transesterification process promotes outstanding healing of the composites when subjected to high temperatures.

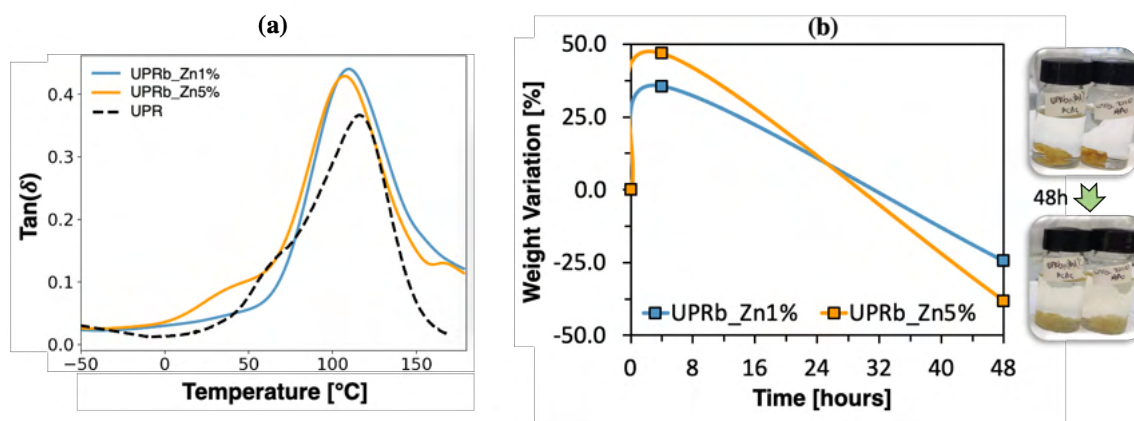


Fig. 1 Content of saturated fats as a function of the month

Recovery of more than 100% for flexural properties were reported for damaged and then healed composites. A further influence of zinc acetylacetonate was the provided degradation in acid solvents (Figure 1.b) enhancing a recyclability of UPRb resins. From a chemical recycling test, a dissolution was observed in acetic acid solution with residual part characterized by segments of polystyrene and AESO moieties. Fully dissolving was instead reported for green composites infused with UPRb resins, after which the fibers were collected and dried for potential reuse. From this result, a major investigation will be focused on the full recycling process of biobased UPR and its composites. The products will be collected, purified, eventually functionalized, and reused as precursors for a sustainable thermoset.

Acknowledgment

Professor Gianluca Cicala and Dott. Sandro Dattilo acknowledge the MIMIT within the project RE-COMP, Grant Numbers CUP B69J24001400005 and B89J24002600005. The authors acknowledge Eng. Giuseppe Cirrone (NTET Group) for commercial UPR.

References

- 1) Giuliana Rizzo, Sandro Dattilo, Vishnu Prasad, Miray Yasar, Alojz Ivankovic, Alberta Latteri, and Gianluca Cicala ACS Applied Polymer Materials 2024 6 (10), 5714-5725 DOI: 10.1021/acsapm.4c00388
- 2) Korbar, J.; Golob, J.; šebenik, A. Process of unsaturated polyester resin synthesis on a laboratory and industrial scale. Polym. Eng. Sci. 1993, 33, 1212–1216.

CONSUMPTION AND BIODEGRADATION OF POLYMERS BY INSECT LARVAE

E.A. Di Liberto^{1*}, G. Battaglia¹, R. Pellerito², G. Curcuruto³ and N.T. Dintcheva^{1,3}

¹*Department of Engineering, University of Palermo, Viale delle Scienze, Palermo, Italy

²Istituto Comprensivo Statale “Luigi Capuana”, Via A. Narbone, Palermo, Italy

³Institute for Polymers, Composites and Biomaterials (IPCB)—CNR, Via Paolo Gaifami, Catania, Italy

erikaalessia.diliberto@unipa.it, giuseppe.battaglia03@unipa.it, rosannapellerito@libero.it, giusy.curcuruto@cnr.it, nadka.dintcheva@unipa.it.

INTRODUCTION

Most plastics are non-biodegradable polymers obtained from petroleum and typically consist of long-chain polymer molecules with a high molecular mass (1). These materials have characteristics that give them stable chemical properties and high resistance to various environmental factors, such as photochemical or microbiological influence, thus making their natural degradation in the environment extremely difficult, resulting in the accumulation of plastic waste that poses a serious environmental threat (2,3).

The main approaches employed for the management of plastic waste have considerable disadvantages and limitations. In the last years, a series of studies have explored the uncommon ability of some insect such as mealworms, meal beetles, weevils or wax moths, to consume and degrade a wide range of synthetic polymers such as polyethylene, polypropylene, polyurethane, polystyrene or polyvinyl chloride into lower-molecular-weight, simple and nontoxic molecules, which are eventually excreted as frass (4,5).

In this work, polyolefins were subjected to biodegradation tests using two types of larvae and different experimental diets were compared. The degradation of polystyrene treated with hydrogen peroxide and subjected to microwave irradiation was also studied. Plastic biodegradation was monitored and characterized by measuring the mass change of the larvae and the survival rate, spectroscopy, spectrometry, microscopy and thermogravimetric analysis.

EXPERIMENTAL

Materials

Two species of Coleopterans Tenebrionidae larvae, the larvae of the yellow mealworm *Tenebrio Molitor* (TM) and superworm *Zophobas Morio* (ZM), were chosen for the degradation tests. Expanded PS and LDPE waste from electronic equipment boxes was collected and used as a feedstock for the larvae of both species.

Preparation

To compare the biodegradation ability of the larvae of the two species, different experimental tests were conducted based on feeding conditions for 30 days. A group of *T. Molitor* and *Z. Morio* larvae were reared on PS foam and PS foam treated with H₂O₂ and LDPE as their exclusive diet in a polypropylene plastic container. As a control, other groups of larvae were reared on a normal diet of wheat bran.

For microwave oxidation, a block of PS was placed in a beaker with hydrogen peroxide H₂O₂ for 5 min and then microwaved into a commercial microwave oven for 3 min, which caused the initial breakage of the polystyrene chains.

Characterization

Frass samples were collected from the container 15 and 30 days after the start of the experiment and subjected to characterization. The weight of the larvae was monitored by

weighing them periodically every 5 days and ended on day 30. Spectroscopy analysis was performed using Fourier Transform Infrared Spectrometer (Spectrum One, Perkin Elmer, USA). Morphological investigations were carried out using SEM analysis (SEM FEI, USA, Quanta 200 FEG). The changes in molecular weight of the polymers were followed by SEC (Azura GPC Knauer apparatus equipped with four TSKgel Guard Super columns). The detection was carried out using a differential refractometer. The thermal stability of the entire sample series was confirmed by thermogravimetric analysis (TGA 8000, Perkin Elmer, Italy).

RESULTS AND DISCUSSION

This work aims to evaluate the biodegradation ability of two species of Tenebrionidae larvae. All tests and experimental results show that both larvae (*Tenebrio Molitor* and *Zophobas Morio*) were able to feed on polyolefins and their mass changes and survival rate were comparable to those of bran-fed larvae.

Although not strongly pronounced, the results of spectrometry analysis of larvae frass after 15 and 30 days (Figure 1) show that the polydispersity index increased while M_w and M_n of both larvae decreased over 30 days, indicating a decrease in weight and chain length.

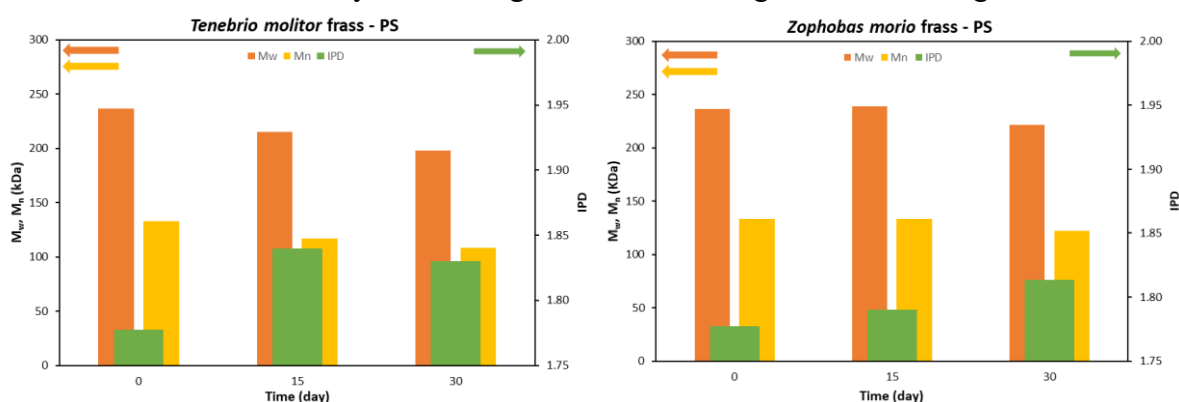


Fig. 1 Data related to the changes in ponderal molecular weight (M_w), numerical molecular weight (M_n), polydispersity index (IPD) of polystyrene (0 days) and frass of TM and ZM after 15 and 30 days.

The results of spectroscopic and thermal analysis support this thesis by showing changes in polymer composition after digestion. Morphological analysis of the polymers in the frass shows completely different structures compared to the materials before the test.

References

- 1) Shah, A.A., Hasan, F., Hameed, A., Ahmed, S., Biological degradation of plastics: a comprehensive review. *Biotechnology Advances*, 26 (2008) 246–265.
- 2) A.F. Pivato, G.M. Miranda, J. Prichula, J.E.A. Lima, R.A. Ligabue, A. Seixas, D.S. Trentin, Hydrocarbon-based plastics: Progress and perspectives on consumption and biodegradation by insect larvae, *Chemosphere* 293 (2022) 133600.
- 3) S.A. Siddiqui, A.S.A. Manap, S.D. Kolobe, M. Monnye, B. Yudhistira, I. Fernando, Insects for plastic biodegradation – A review, *Process Safety and Environmental Protection*, 186 (2024) 833–849.
- 4) B. Mitra, A. Das, The Ability of Insects to Degrade Complex Synthetic Polymers, *Arthropods—New Advances and Perspectives* (2023) IntechOpen.
- 5) R. An, C. Liu, J. Wang, P. Jia, Recent Advances in Degradation of Polymer Plastics by Insects Inhabiting Microorganisms, *Polymers*, 15 (2023) 1307.

TAILORING THE FUNCTIONALITY OF POLYMER BASED BIOMATERIALS FOR HEALTH

L. Ambrosio¹ U. D'Amora¹, Paola Manini², A. Pezzella^{1,2}, M.G. Raucci¹, A. Ronca¹, S. Scialla¹, A. Soriente¹

¹Institute of Polymers, Composites and Biomaterials, National Research Council, Viale J.F. Kennedy, 54, Mostra d'Oltremare, Pad.20, 80125 Naples, Italy.

²Department of Chemical Sciences and Department of Physics "E. Pancini", University of Naples Federico II, 80126 Naples, Italy.

luigi.ambrosio@cnr.it

INTRODUCTION

The current challenge is to design materials with specific behaviours for mimicking the natural structures and delivering appropriate signals to external interfaces defined by their specific applications.

Selection of a suitable solution is often based on material characteristics (including mechanical properties, drug release kinetics and degradation) that serve for the specific function. Micro or nano-structured materials in the form of gels, nanoparticles, nano-fibers and nano-composites have gained increasing interest in regenerative medicine because they are able to mimic the physical features of natural extracellular matrix (ECM) at the sub-micro and nano-scale levels. The same have to respond to the approach of circular economy and sustainability.

By a careful selection of materials and processing conditions it is possible to finely control characteristic shapes and sizes from micro to sub-micrometric scale and to incorporate bioactive molecules such as proteins or growth factor to develop active platforms to support the repair/regeneration of tissues as well as additives for other applications

Personalised approach is also used to design and prepare of tissue analogues by bioprinting. In this context, a proper bioink is designed to: i) confer a shear thinning behaviour for the extrusion-based process and ii) improve the mechanical properties, (iii) control the biosensing properties.

In this work materials such as hyaluronic acid, gellan gum, are investigated to define their behaviours for specific tissue repair/regeneration applications.

EXPERIMENTAL

Materials and Methods

Hyaluronic acid sodium salt (HAs) was chemically modified in order to obtain a photocrosslinkable hydrogel with tailored mechanical properties for osteochondral application such as for meniscus regeneration. Within this aims natural polymer-based double network hydrogels (DNs) were developed by a two-step network-formation procedure to obtain photocrosslinkable methacrylated hyaluronic acid (MEHA) and maleated hyaluronic acid (MAHA) while controlling viability/proliferation of cells.

In addition, methacrylated gellan gum (GGMA) is proposed as a biomaterial-based ink for three-dimensional (3D) printing applications through: i) the functionalization of GG by introducing methacrylic moieties to obtain GGMA, ii) the bioactivation of the hydrogel ink by using a naturally-derived eumelanin isolated from the Black Soldier Fly (BSF-Eumel) and/or by hydroxyapatite nanoparticles (HAp).

Different ink formulations based on GGMA (2 and 4% (w/v)), BSF-Eumel, at a selected concentration (0.3125 mg/mL), or HAp (10 and 30% $w_{\text{HAp}}/w_{\text{GGMA}}$) were developed and processed by 3D printing. All the functionalized GGMA-based ink formulations allowed obtaining 3D-printed GGMA-based scaffolds with a well-organized structure. Physicochemical, mechanical, morphological and *in vitro* biological investigations were performed to define the best formulation.

RESULTS AND DISCUSSION

By optimizing the reaction conditions, it has been possible to obtain MEHA and MAHA with high DS of 79.96 ± 2.49 and 85.49 ± 4.86 , respectively. The functionalized HA with higher DS represented the best compromise in terms of physico-chemical and mechanical properties. However, even though MAHA samples were characterized by lower structural properties, compared to MEHA hydrogels, they tended to maintain their shape over time. The biological study showed that MEHA significantly promoted HAD-MSCs and HUVECs proliferation compared to MAHA. Additionally, both MAHA and MEHA showed anti-inflammation ability on *in vitro* cell culture.

Scaffolds composed of GGMA/BSF-Eumel displayed greater stability due to the presence of negatively charged groups along the eumelanin backbone. GGMA/BSF-Eumel scaffolds showed storage modulus values that were comparable to those of GGMA, but the addition of HAp at 30w/w% resulted in a storage modulus of 32.5 kPa, which was 3.5 times higher than that of neat GGMA. *In vitro* investigations demonstrated the capability of bioactive 3D-printed scaffolds to support osteoblasts cells growth and differentiation. Notably, BSF-Eumel induced a higher cell proliferation, with a maximum at 14 days, while HAp led to a higher expression of ALP activity. Overall, the results offer interesting indications about the potential uses of these 3D-printed scaffolds for bone tissue repair/regeneration.

Acknowledgment

The authors acknowledge the financial support of the project MEFISTO — H2020-NMBP-TR-IND-2018-2020/2018, MEFISTO, GA, N. 814444 and PRIN 2017 SAPIENT-2017CBHCW.

References

- [1] Petta, D., D'Amora, U., Ambrosio, L., Grijpma, D. W., Eglin, D., D'este, M. *Biofabrication*, 2020, 12(3), 032001.
- [2] U. D'Amora, A. Ronca, M.G. Raucci, S. M. Dozio, H. Lin, Y. Fan, X. Zhang, L. Ambrosio. *Regenerative Biomaterials*. 2019, 6, 249-258.
- [3] U. D'Amora, A. Ronca, S. Scialla, A. Soriente, P. Manini, J. W. Phua, Ch. Ottenheim, A. Pezzella, G. Calabrese, M. G. Raucci and L. Ambrosio, *Nanomaterials*, 2023, 13, 772

A PRELIMINARY STUDY ON THE EXTRUSION FOAMING OF MIXED RECYCLED POLYOLEFIN WASTE WITH A CHEMICAL BLOWING AGENT

Emilia Garofalo¹, Luciano Di Maio¹, Carmelo Di Costanzo² and Loredana Incarnato¹

¹Department of Industrial Engineering, University of Salerno, Via Giovanni Paolo II, Fisciano (SA), Italy

²CONSTAB Polyolefin Additives GmbH, Industriestrasse Moehnetal, 59602 Ruethen, Germany

egarofal@unisa.it, ldimaio@unisa.it, c.dicostanzo@constab.com, lincarnato@unisa.it

INTRODUCTION

In the context of sustainable management of plastic waste, the objective of this work was to evaluate the potential use of mixed recycled polyolefins, obtained from the mechanical recycling of post-consumer flexible packaging and denoted as HW Fil-s (1-2), for foam extrusion. The experimental plan included several steps:

- chemical, thermal and rheological characterization of the recycled material before and after modification through reactive extrusion with maleic anhydride (HW Fil-s_RE) to enhance its foaming ability;
- characterization of the foamed systems, produced at different extrusion conditions; this involved evaluating the density reductions, foams' morphology, in terms of cell size and shape, and measuring the mechanical performance of both the bulk and foamed systems.

The density reductions, as well as the performances, of the foams obtained from the recycled material were compared with those of a virgin linear low-density polyethylene (LDPE), that has a good propensity to be foamed.

EXPERIMENTAL

Materials

The recycled material HW Fil-s was supplied as pellets by COREPLA, the Italian consortium for the Collection and Recycling of Plastic Packaging.

For HW Fil-s functionalization dicumyl peroxide (DCP, analysis grade 98%), as the initiator (supplied by Sigma Aldrich), and the maleic anhydride (MAH, analysis grade 99%), as the grafting agent (supplied by Sigma Aldrich), were selected.

The chemical foaming agent Ecocell® P was kindly supplied by CONSTAB (Polyolefin Additives GmbH, Germany). This company belongs to the KAFRIT Group (M.P. Negev, 8514200, Israel) together with POLYFIL USA (Rockaway, NJ 07866, USA), that developed Ecocell®.

Preparation

A constant amount (2 wt%) of Ecocell was added during the processing of the virgin and recycled materials by means of a single screw extruder at different operative conditions. In particular, the temperature of the extruder die, T_{die} , was set at 190°C and 200°C, while maintaining constant the temperatures of the feed (190°C) and transition (215°C) zones. Two different extrusion rates ($V_{ext}=30$ rpm and 40 rpm) were also tested.

Characterization techniques

Rheological tests were conducted in shear dynamic and transient extensional modes. Density measurements were carried out as stated in ASTM D792 standard, using an analytical balance. Morphological investigations were performed with SEM.

RESULTS AND DISCUSSION

The density reductions, obtained for the virgin LDPE and for both the recycled materials at the different extrusion conditions, are summarized in Table 1.

Table 1 – Density reductions for the virgin LDPE and the recycled materials

	Density reduction [%]			
	$T_{die} = 190^{\circ}\text{C}$		$T_{die} = 200^{\circ}\text{C}$	
	$V_{ext} = 30 \text{ rpm}$	$V_{ext} = 40 \text{ rpm}$	$V_{ext} = 30 \text{ rpm}$	$V_{ext} = 40 \text{ rpm}$
LDPE + 2% ECOCELL	6%	44%	12%	39%
HW FIL-s + 2% ECOCELL	27%	23%	19%	20%
HW FIL-s RE + 2% ECOCELL	37%	32%	28%	31%

For virgin LDPE, the extrusion speed had the greatest impact on the effectiveness of the foaming process. In particular, the largest density reduction (equal to 44%), was obtained at 40 rpm and $T_{die}=190^{\circ}\text{C}$. The higher extrusion speed and the lower die temperature led to a pressure increase, which enhanced the foaming process. For the recycled material, the best density reduction was 27% and was obtained at $T_{die}=190^{\circ}\text{C}$ and $V_{ext}= 30 \text{ rpm}$. These operative conditions determined, respectively, higher pressure and longer residence time within the extruder, promoting the dissolution, within the molten polymer, of the gas phase released by the blowing agent.

Since the effectiveness of the foaming process for HW Fil-s was significantly lower than for virgin LDPE, the recycled material was functionalized with maleic anhydride through reactive extrusion (3) (HW Fil-s_RE) to enhance its melt strength and drawability. These rheological characteristics, in fact, are of primary concern during the cell growth phase in order to obtain a low-density foam with uniform morphology. At all the tested processing conditions, the HW FIL-s_RE sample exhibited higher density reductions than HW FIL-s. In particular, at $T_{die}=190^{\circ}\text{C}$ and $V_{ext}= 30 \text{ rpm}$ the best density reduction (equal to 37%) was achieved.

As evidenced by the SEM images in Figure 1, HW Fil-s_RE predominantly exhibits a closed-cell structure with circular cavities, which are, on average, smaller than the ones in LDPE foam. However, larger and irregularly shaped cells can also be observed, probably resulting from the collapse of adjacent cell walls. The obtained morphology is consistent with the extensional rheological properties of HW Fil-s_RE, which showed higher draw resistance, but also lower deformability.

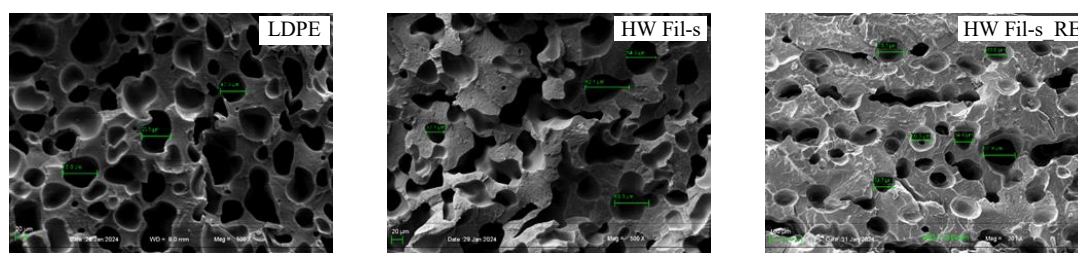


Figure 1 – SEM images of LDPE, HW Fil-s and HW Fil-s_RE foams

References

- 1) E. Garofalo, L. Di Maio, P. Scarfato, A. Apicella, A. Protopapa, L. Incarnato, *Nanomaterials* **11**, 2128 (2021)
- 2) E. Garofalo, L. Di Maio, P. Scarfato, A. Protopapa, L. Incarnato, *J. Cleaner Production* **295**, 126379 (2021)
- 3) E. Garofalo, L. Di Maio, P. Scarfato, F. Di Gregorio, L. Incarnato, *Polymer Degradation and Stability*, **152**, 52 (2018)

THE USE OF PACKAGING INDUSTRY WASTE FOR THE MODIFICATION OF POLYPROPYLENE

D. Dziadowiec, P. Szymczak, J. Andrzejewski* and M. Szostak*

EUROCAST Sp. z o. o. Strzebielino, Poland

*Institute of Materials Technology, Mechanical Engineering Department, Poznan University of Technology, Poznan, Poland

marek.szostak@put.poznan.pl, damiandziadowiec@eurocast.pl

INTRODUCTION

The current global trend in the plastics processing industry is towards greater use of recycled raw materials, which significantly contributes to reducing the consumption of virgin materials. The PP film recycling process is relatively simple and does not require complicated technologies or significant financial outlays. A variety of solutions are available on the market for manufacturers, including dedicated recycling lines that can be adapted to specific needs. Initially, foil waste is processed into flakes or scraps and then subjected to subsequent stages to obtain regranulate that can be used to produce new foils. In 2021, approximately 85 thousand tons of foil were processed for recycling purposes [1-2]. However, there are some challenges in the recycling process, especially related to the composition of waste. Film in the packaging industry is often modified in various ways, for example containing multiple layers of materials or additives to facilitate sealing or improve the barrier to oxygen and flavors. Additionally, the presence of contaminants in the waste may also pose a problem.

Biaxially oriented polypropylene films account for approximately 10% of global production of this material. These are special foils that are characterized by high transparency, mechanical strength and low permeability to water vapor and gases. The orientation process of the PP film improves its barrier properties, which means that the amount of penetrating water vapor is reduced. Thanks to this, these films are characterized by dimensional stability and good optical properties. PP films are widely used as packaging material, especially in the food industry. They are often used as multi-layer foils, where they are combined with paper, aluminum foil or other polymer foils. Additionally, metallized oriented PP foils show even better oxygen barrier properties. It is worth noting that the use of biaxially oriented foils contributes to increasing the efficiency of packaging, protecting the contents against moisture and oxidation, which is particularly important in the case of food products and other products susceptible to these factors [3].

The aim of our research was to assess the possibility of using packaging industry waste to modify polypropylene products. The conducted research showed that the foil waste analyzed in this work can be successfully used to produce new materials, both extruded and injection molded.

EXPERIMENTAL

Materials

The total of six different types of materials were used to carry out the tests: PP granulate as a base material, three different types of foil waste and two types of modifiers (MAPP, POE). The study mainly covered foil waste delivered in the form of ground foil: (Foil 1) Castopol PP MSHM - a type of polypropylene (PP) foil with an additional metal layer placed on one side, (Foil 2) LidFol BOPP/met2.2/PP is a foil consisting of two polypropylene layers (BOPP), between which there is an additional layer of metal, (Foil 3) LidFol S PET/met2.2/PP is a foil with a metal layer inside, surrounded by a polypropylene (PP) and polyester (PET) layer.

In order to improve the properties of the manufactured PP-based composites, it was decided to introduce two modifiers offered by Fine-Blend: CMG-5701 (MAPP compatibilizer) a low-emission polypropylene modified with maleic anhydride and SOG-02 - acting as an impact resistance modifier. It is a POE-g-GMA copolymer, i.e. an elastomer based on polyolefins (POE) with additional functional groups (GMA).

Preparation of samples

The foil waste was first pressed than ground in a knife mill. Before mixing they were dried 4 hours at 80°C and additionally modified adding MAPP and POE modifiers. A total of nine different mixtures (50%rPP/50%PP; 50%rPP/35%PP/15%MAPP; 50%rPP/30%PP/15%MAPP/5%POE) using 3 types of waste foil were obtained, which were then subjected to the regranulation process. Samples for mechanical testing were made in both foil extrusion and injection processes.

Mechanical properties characterization and color examination

The research tests included impact strength measurements of injected samples in accordance with the PN-EN ISO 179 standard, static tensile tests of injected samples and the produced foil, in accordance with the PN-EN ISO 527:2020 standard, and a comprehensive analysis of color differences in the pattern and the tested foil samples and injected samples. using an EnviSense calorimeter.

RESULTS AND CONCLUSIONS

- Based on the conducted experimental research, the following conclusions can be drawn:
- The technology of pressing, grinding and regranulation of foil waste is an effective method of recovering polymer material, which can be successfully used to modify polypropylene products shaped by either injection or extrusion molding.
 - The use of the MAPP modifier based on maleic anhydride and the POE impact modifier had a positive effect on the improvement of mechanical properties, such as impact and tensile strength of the produced samples.
 - The highest values of tensile strength (27.1 MPa) and Young's modulus (1110 MPa) were recorded for injected samples made from 1b blend (50% rPP, 35% PP, 15% MAPP).
 - The highest Charpy notched impact strength value (18,43 kJ/m²) was recorded for injected samples from 2c blend (50% rPP, 30% PP, 15% MAPP and 5% POE). This confirms the beneficial effect of the addition of the MAPP and POE modifiers on the impact strength.
 - During the conducted tests, the lowest properties were recorded for products based on LidFol S PET/met2.2/PP film regranulate.
 - The greatest impact on the color of products was noted for materials modified with the addition of MAPP, which caused a slightly bluish tint of the manufactured samples.

Acknowledgment

This work has been financially supported by the Ministry of Education and Science under the "Implementation Doctorate" program, project no. DWD/4/22/2020.

References

- 1) Grant A., Lahme V., Connock T.,Lugal, „How circular is PET?”, Eunomia/Zero Waste Europe, 02.2022 (Report).
- 2) Plastics Europe, EPRO: “Plastics - Facts 2022”, 10.2022 (Report)
- 3) Dziadowiec, D.; Matykiewicz, D.; Szostak, M.; Andrzejewski, J. Overview of the Cast Polyolefin Film Extrusion Technology for Multi-Layer Packaging Applications. *Materials* **16**, 1071, 2023. <https://doi.org/10.3390/ma16031071>

FULLY BIOBASED FLAME RETARDANTS FOR POLYAMIDE 11 COMPATIBLE WITH THE MELT SPINNING PROCESS

J. Regnier¹, S. Giraud¹, J.-J. Flat², B. Mulot², S. Bourbigot^{3,4}, G. Fontaine³, A. Cayla¹

¹Univ. Lille, ENSAIT, ULR 2461 - GEMTEX - Génie et Matériaux Textiles, F-59000 Lille, France

²ARKEMA, Centre d'Etude de Recherche et de Développement, 27470 Serquigny, France

³Univ. Lille, CNRS, INRAE, Centrale Lille Institut, UMR 8207 - UMET - Unité Matériaux et Transformations, F-59000 Lille, France

⁴Institut Universitaire de France, Paris, France

julie.regnier@ensait.fr

INTRODUCTION

Due to environmental concerns, the thermoplastic polymer polyamide 11 (PA 11) is attracting interest, because it is made from renewable materials such as castor oil, and because of its good properties, such as high mechanical strength. However, few studies have been conducted to improve the fire resistance properties of PA 11 with biobased flame retardants. For instance, a flame retardant system has been developed in a PA 11 based on lignin as a carbon source and non-biobased phosphinate additives to mainly inhibit the flame by releasing PO radicals (1).

The incorporation of additives especially flame retardants into a thermoplastic polymer, modifies its rheology properties and does not always allow it to be processed by melt spinning. Therefore, this work discriminates between different flame retardants: protein, phospholipid, acid, and phenolic type (2). They are incorporated in different ratios, in a PA 11, to develop a fully biobased multifilament with good flame-retardant properties. Additive screening is based on various tests: the Melt Flow Index (MFI) for rheological properties, the thermogravimetric analysis (TGA) for thermal properties and the UL94 test for fire properties (3). Blends are discriminated based on their melt-spinnability and flame-retardant efficacy, to figure out the best proportion.

EXPERIMENTAL

Materials

The polyamide 11 (PA 11) is supplied by Arkema (FMNO TLD). A protein type (FR1), a phospholipid type (FR2), two acid types (FR3 and FR4) of additive are supplied by Sigma-Aldrich. The three phenolic types of additives (FR5, FR6 and FR7) are supplied by Silva Team.

Preparation

The blends were prepared using a twin-screw corotating extruder. The flame retardants were incorporated into the PA 11 at different loadings: 5, 10 and 20 wt.%. The blends were named by codes such as "FR1-5", writing down a blend with 95 wt.% PA11 and 5 wt.% of the biobased flame retardant 1. The blends were studied in pellets form to analyse their viscosity and thermal properties. In accordance with the UL94 standard, the pellets are pressed using a thermal press to form plates measuring 127 x 13 x 2 mm³ to conduct the flammability tests.

Rheological and thermal characterization

Blends fluidity was studied using a flow tester at a temperature of 193°C and a pressure of 2.16 kg. The MFI corresponds to the fluidity (g/10 min) of a polymer or blend at a defined temperature for ten minutes. This index was used to drop blends that were less suitable for melt spinning process.

Thermal properties were assessed by TGA, figuring out the degradation temperature at 5 % mass loss, the maximum degradation temperature, and the percentage of residues at 600 °C. The samples were subjected to a temperature rise from 25 to 800 °C, at a rate of 10 °C/min, in alumina pans, in an atmosphere of nitrogen or air.

The flame-retardant properties of the blends were characterised by the UL94 vertical test according to IEC 60695-11-10. The samples were classified on the basis of the ignition times and combustion results of the cotton.

RESULTS AND DISCUSSION

To improve the flame retardancy of PA 11, additives were incorporated into the polymer. Measurements were conducted to determine the best compromise between the blend's spinnability and its flame-retardant properties. During extrusion processing, the PA 11 viscosity is impacted by the nature (chemical, shape...) and incorporated ratio of the additives (Figure 1).

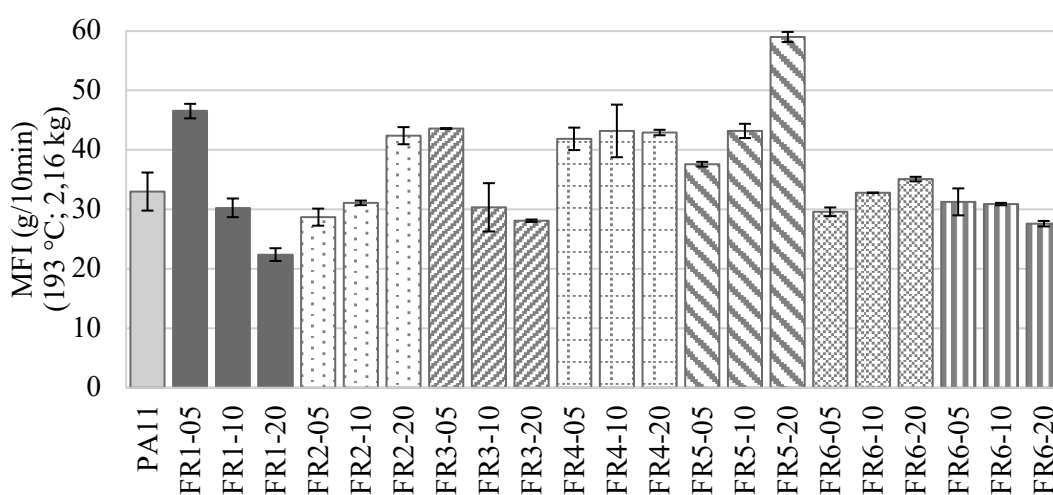


Fig. 1 Melt Flow index as a function of the additive's nature and its proportion in the PA11.

The FR2 or FR3 and FR4, increase fluidity with their proportion (like plasticizer effect). Others, have the opposite effect: their fluidity decreases with their incorporation into the PA 11 (reduced mobility of macromolecular chains by the fillers network). Therefore, they make the blend less spinnable when they are added in large quantities in the polymer.

To discriminate between additives, data is also collected on the effectiveness of their flame-retardant properties with UL94 Test and the thermal properties in PA 11 with the TGA. This test reveals, for example, better residues at 600 °C for lecithin and acid phytic with the TGA. This presentation will fully detail the results of tests conducted on all the additives used.

Acknowledgment

This work has been financially supported by Région Haut-de-France (STIMULE project: TREFLE).

References

- 1) N. Mandlekar, A. Cayla, F. Rault, S. Giraud, F. Salaün, J. Guan, **11**, 180, (2019)
- 2) S. H. Jeong, C. H. Park, H. Song, J. H. Heo, J. H. Lee, **368**, 133241 (2022)
- 3) T. C. Mokhena, E. R. Sadiku, S. S. Ray, M. J. Mochane, K. P. Matabola, M. Motloug, **139**, 36 (2022)

AGING OF MEDIUM VOLTAGE JOINTS UNDER COMBINED AGEING CONDITIONS AT LOW TEMPERATURE

**T. Vaytet^{1,2}, O. Gain¹, F. Gouanvé¹, E. Espuche¹, C. Moreau², M. Broudin²,
H. Tanzeghti³**

¹ Université Claude Bernard Lyon 1, INSA Lyon, Université Jean Monnet, CNRS UMR 5223, Ingénierie des Matériaux Polymères F-69622 Villeurbanne Cédex, France

² EDF lab Les Renardières, F-77250 Écuellen

³ Enedis, Département Expertise et Relation Fournisseurs Matériels, F-92079 Paris La Défense

INTRODUCTION

The electric power distribution network is made up of a large number of underground lines, designed to ensure reliable power delivery with minimum interruption for the customer. The joints, which allow two cables to be connected, are identified as the weak points of the lines. In medium voltage (MV) power network in France, these joints are made with "Cold Shrink" (CS) technology, which uses elastomers such as Ethylene-Propylene-Diene-Monomer (EPDM) or Ethylene-Propylene-Rubber (EPR). The formulation of these materials as well as the environment and conditions in which they operate are complex [1]. Underground lines may indeed be in contact with wet ground or water. It is therefore essential to understand the consequences of water diffusion on aging as well as the impact of additional parameters coupled to those of water, such as temperature, polymer expansion or the applied electrical voltage and this in close relation with the material formulation [2]. This work was focused on the effect of both temperature and relative humidity on aging for two industrial outer shields.

EXPERIMENTAL

Materials

Two types of industrial cold shrink joints (named A and B) were investigated. Both are composed of two distinct parts, an outer shield, and an electrical body. The outer shield (thickness around 4.6 mm) which is in contact with the external environment is under investigation in this work. Moreover, some characterizations were performed on thin layers (thickness around 600 μ m) taken from the outer surface of the outer shield.

Aging

Selected aging conditions to be representative of real aging atmospheres were applied by coupling temperature (70, 80 and 90 °C) and relative humidity (0, 75, 90 and 100 %RH). Aging durations were chosen in the range from 0 to 9000 hours with the aim of obtaining regular points at which the evolution of physico-chemical properties could be monitored.

Characterization

Fourier-transform infrared spectroscopy (FTIR), with Germanium ATR module, was used to calculate an oxidation degree on the external surface of the material, by the ratio of the oxidation band at 1575 cm^{-1} to a reference band set at 720 cm^{-1} [3]. Swelling, in cyclohexane, was used to investigate the matrix modification on total material thickness. Swelling rate Q is calculated by the Equation 1, with w_s the dry weight and w_a the weight at sorption equilibrium. Dynamic mechanical analysis (DMA) was performed to determine stress relaxation on the inner and outer side of the outer shield. To complete, designed permeation cells were used to measure water diffusion and sorption on thin layers representative of the external face of the outer shield.

$$Q = 1 + \frac{\rho_{EPDM}}{w_d} \times \frac{(w_s - w_d)}{\rho_{solv}} \quad (1)$$

RESULTS AND DISCUSSION

Comparisons between the properties of joints A and B aged at 80 °C and 90 %RH have highlighted some differences. Infrared spectroscopy reveals an oxidation for both materials, with an oxidation degree higher for joint A with respect to joint B (Fig 1). Swelling experiments show a different swelling ability of the two neat joints. However, aging leads to a decrease of Q in both materials (Fig 2), related to a crosslinking phenomenon. DMA analysis indicates that the static force required for 14 % deformation remains constant over the 12 months of aging. Furthermore, recovery also remains similar. Changes observed by infrared spectroscopy and swelling have no significant impact on the material's mechanical properties.

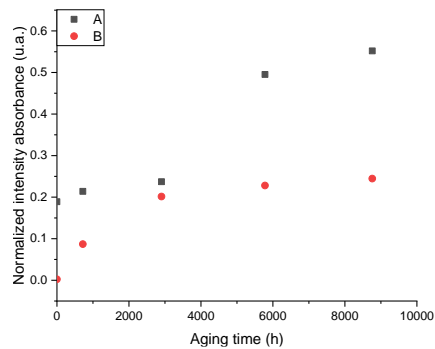


Fig. 1 Evolution of normalized carbonyl absorbance for A and B with ageing time at 80 °C and 90 %RH

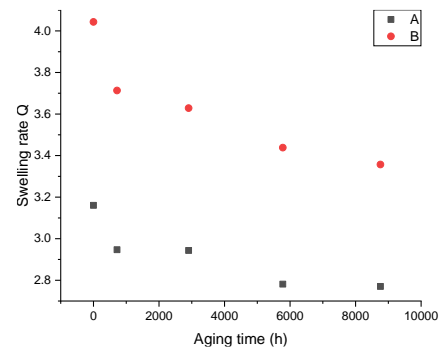


Fig. 2 Evolution of swelling rate Q for A and B with ageing time at 80 °C and 90 %RH

Acknowledgment

The authors gratefully acknowledge the "Association Nationale de la Recherche et de la Technologie" (France) for funding the PhD thesis of Théo Vaytet.

References

1. C. Canaud et al. EPDM Formulations for Electric Wires and Cables, Elastomers and Plastics, 2001
2. M. Lacuve et al. Investing and modelling of the water transport properties in unfilled EPDM elastomers, Polymer Degradation and Stability, 2019
3. C. Li et al. Compressive stress-thermo oxidative ageing behaviour and mechanism of EPDM rubber gaskets for sealing resilience assessment, Polymer Testing, 2020

SOFT ACTUATORS BASED ON THERMOPLASTIC POLYURETHANE COMPOSITES WITH YTTRIUM IRON GARNET

M. C. Paiva^{*}, M M. da Silva^{*}, J. A. Covas^{*}, and M. P. Proença[‡]

^{*} Institute for Polymers and Composites, Department of Polymer Engineering, University of Minho, Guimarães, Portugal

[‡] ISOM and Departamento de Electrónica Física, Universidad Politécnica de Madrid, Madrid, Spain

mcpaiva@dep.uminho.pt, mmsilva@dep.uminho.pt, jcovas@dep.uminho.pt,
mariana.proenca@upm.es.

INTRODUCTION

Shape-memory polymers (SMP) are a class of materials that are responsive to external stimuli. Their response manifests through significant deformations in their physical structure, making them versatile for various applications. Due to their low density, exceptional flexibility, simple fabrication, and the possibility of compounding, SMP offer abundant design possibilities. Polyurethane (PU) has been actively researched as an SMP owing to the presence of soft and hard polymer segments¹. On its own, PU can deform either by direct heat stimuli, through the thermal activation of dynamic covalent bonds, or in response to a solvent. Adding fillers to produce PU composites can benefit actuation triggered by other stimuli such as electrical,² optical,^{2,3} or magnetic.

The present work explores the soft magnet behavior of thermoplastic PU (TPU) composites with sol-gel synthesized YIG particles. The composites are analyzed, and the magnetomechanical behavior of TPU composites with YIG (mTPU), with different thicknesses and shapes, is evaluated with the application of a magnetic field using permanent magnets.

EXPERIMENTAL

Materials

TPU (Desmopan 3360A, Covestro, Leverkusen, GER), with a density of 1.154 g·cm⁻³, a shore hardness of 62, a ultimate tensile strength of 29 MPa, and a strain at break of 754%, was used in this work. TPU pellets were dried for 4 h at 80°C, in a vacuum oven. The YIG powder was synthesized by sol-gel at pH 2, and calcinated at 1000°C for 3 h.

Preparation

A micro compounder (Xplore MC 15, Xplore Instruments, Sittard, NL) containing partially intermeshing co-rotating screws and a recirculating channel, was used to melt mix TPU with YIG powder fed in a 90:10 (w/w) ratio (TPU:YIG). The melt was recirculated for 10 min, at 150 rpm and 190°C. A TPU/YIG (mTPU) filament was collected and pelletized. Sheets of mTPU, with 500 and 150 μm thickness, were obtained by compression molding, at 190°C, under a pressure of 20 tons, for 10 min.

Morphological, thermal and mechanical characterization

The morphology and elemental composition of the YIG powder were analyzed by scanning electron microscopy (SEM, FEI Inspect F50 microscope) and energy dispersive X-ray spectroscopy (EDS, Oxford instruments).

Thermograms of composites and neat TPU were collected with a TGA Q500 (T.A. Instruments) at a heating rate of 10°C · min⁻¹, from 40 °C to 700 °C, under N₂ atmosphere in a platinum crucible. A TTDMA (Triton Technology, Grantham, UK) equipped with a 1 L Dewar and a TTDMA AutoCryo Type 2 for cooling with liquid nitrogen were used to perform dynamic mechanical analysis (DMA) in tensile mode, with a 5 mm gauge length. The

frequency was set to 1 Hz with a displacement amplitude of 0.02 mm, in the temperature range from - 80°C to 150°C, at a heating rate of 2°C·min⁻¹. Values presented for glass transition temperature (T_g) were collected from the maximum of the tangent of delta curve (tan δ).

mTPU samples were cut into two different shapes: a flower-like shape, 30 mm wide, and a 5 mm × 20 mm rectangular tape (Fig. 1). Flowers and tapes were cut from compression molded sheets with two different thicknesses (500 μm and 150 μm). The applied magnetic field values (H) were measured with a gaussmeter (FH-43, Magnet-Physik Dr. Steingroever GmbH), placed at the sample position, varying the distance of the permanent magnets.

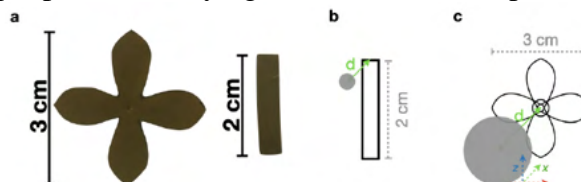


Fig. 1 a) 500 μm thick mTPU samples. Schematic representations of the shape-memory performance tests, where *d* is the distance between the tip of the magnet and the sample, for two different magnet configurations: b) aligned with the top of the tape sample; and c) aligned with the center of the flower-like sample.

RESULTS AND DISCUSSION

The storage modulus (E') of mTPU composites is higher than that of TPU (Figure 2a, Table 1) above T_g and up to 70°C. T_g, measured at the peak of tan δ (Figure 2b), is about 4 °C lower for mTPU samples. Tan δ < 1 in the range of -80°C to 150°C, indicating a predominant elastic behavior of the composite. At T_g tan δ reaches its maximum. Maximum damping is higher for TPU than mTPU since the latter has a higher content of rigid domains of YIG powder in the composite.

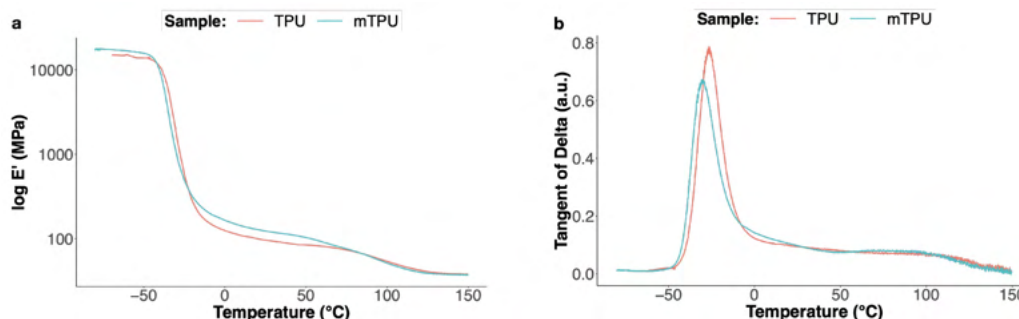


Fig. 2 Representative DMA curves of the a) storage modulus (E') and b) tan δ of neat TPU and mTPU.

The mTPU composites produced are soft magnets, and were capable of bending with the approach of a permanent magnet and returning to their original shape upon removal of the magnetic field, with reversible actuation capability. The magnetic shape-memory effect was observed demonstrating the ability of mTPU composites for controlled displacement.

Acknowledgment

The authors acknowledge: Portuguese FCT for funding: PhD grant 2020.05311.BD, National Funds UIDB/05256/2020 and UIDP/05256/2020; Spanish Ministerio de Ciencia e Innovación under the project PID2020-117024GB-C42 and ICTS Network MICRONANOFABS.

References

- 1) X. Y. Wang, H. W. Ruan, et al., *Polymer Chemistry* 2022, 13, 2420–2441.
- 2) A. Kausar, *Journal of Plastic Film & Sheeting* 2020, 36, 151–166.
- 3) M. Herath, J. Epaarachchi, M. Islam, L. Fang, J.S. Leng, *European Polymer Journal* 2020, 136.

PET NANOPLASTIC PRODUCTION AND THEIR EFFECT ON MODEL LIVING SYSTEMS

A. Maffezzoli¹, G. Polo, M. G. Lionetto², C. Mele¹, C. Esposito Corcione¹, F. Lionetto¹

¹Department of Engineering for Innovation, University of Salento, Via per Monteroni, 73100 Lecce, Italy

²Department of Biological and Environmental Sciences and Technologies (DISTEBA), University of Salento, Via per Monteroni, 73100 Lecce, Italy
alfonso.maffezzoli@unisalento.it, giulia.lionetto@unisalento.it, claudio.mele@unisalento.it, carola.corcione@unisalento.it, francesca.lionetto@unisalento.it

INTRODUCTION

The increasing nanoplastic (NP) pollution in aquatic environments has raised concerns about their potential toxicity to water organisms and risk to human health. Detection and characterization of NPs is very difficult and requires labor-intensive separation from environmental matrices which can lead to the creation of artifacts. Most of the available toxicity studies use commercial polystyrene nanospheres with results not easily correlated with real conditions. It is thus imperative to produce representative nanoplastics, obtained from the degradation of plastic objects in laboratory conditions for toxicological studies on different organisms and ecosystems.

In this work, a reliable method has been set up to produce polyethylene terephthalate (PET) nanoparticles from post-consumed bottles. The proposed top-down approach is based on mechanical fragmentation, a process close to the mechanical abrasion of microplastics occurring in the environment [1-2]. The size, morphology and chemical-physical properties of these lab-made NPs have been characterized by laser diffraction, scanning electron microscopy (SEM), X-ray diffraction (XRD), differential scanning calorimetry (DSC), spectrofluorimetry and optical fluorescence imaging to optimize the process parameters.

The environmental relevance of the produced NPs for laboratory studies on living systems has been assessed by *in vivo* exposure experiments on *Daphnia magna*. This zooplankton is a keystone species in freshwater food webs and is a widely used model organism in ecotoxicology, showing high sensitivity to changes in environmental conditions and pollution exposure [3].

EXPERIMENTAL

Materials and characterization

PET nanoparticles were produced starting from post-consumed PET bottles, cut into small pieces and finely milled with several steps in a ball mill at ambient atmosphere. The obtained PET nanoparticles were characterized by laser diffraction with a CILAS 1190 multi-laser particle size analyzer and by atomic force microscopy (AFM), employing a Bruker MultiMode 8 AFM system.

In vivo experiments

Daphnia magna organisms were cultured in ASTM hard synthetic water at 16 h light: 8 h dark cycle and temperature at 21±1°C. The distribution of PET nanoplastics in the body of organisms was detected by fluorescence microscopy after 24h of PET NP exposure at the concentration of 5 mg/L.

RESULTS AND DISCUSSION

Fig. 1a-b reveals a poly-disperse size distribution of the label-free nanoplastics. A significant nanometric fraction is centered at about 200 nm, while a sub-micrometric and micrometric fraction are centered, respectively, at about 0.8 µm and 10 µm. The observed size

heterogeneity makes the produced model NPs more similar to the sampled NPs in the aquatic environment.

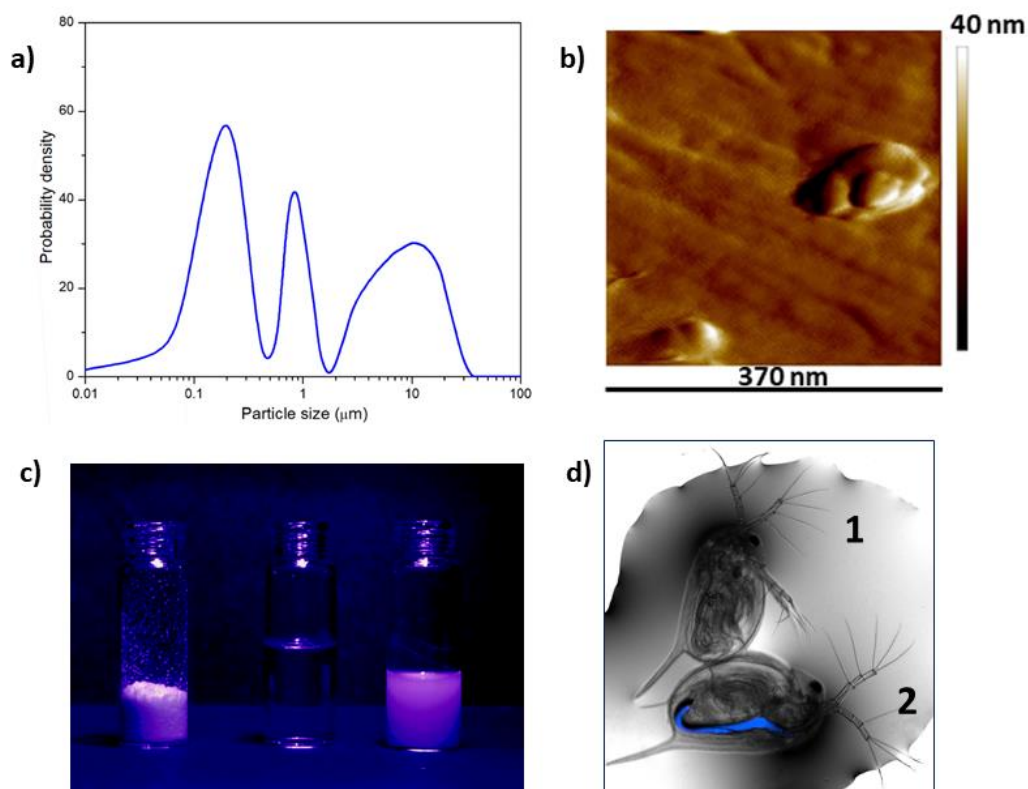


Fig. 1 PET nanoplastics: a) particle size distribution; b) AFM image; c) fluorescence under UV irradiation; d) *Daphnia magna* control (1) and after 24h exposure to 5mg/L model PET NPs (2).

Irradiation of model PET-NPs by a medium-pressure Hg UV lamp at 365 nm (Fig. 1c) confirms their autofluorescence making easy the visualization of NPs in the body of the studied organism without the use of fluorescent labeling. This possibility overcomes several disadvantages commonly associated with some fluorescent dyes such as eventual additional toxicity and leakage. The distribution of PET-NPs in the body of *Daphnia magna* has been detected by fluorescence microscopy. A prevalent accumulation in the gastrointestinal tract is evident from Fig. 1d.

The results obtained in the present study with label-free PET nanoplastics, similar to those found in the marine environment, open the perspective for future in vitro and in vivo studies addressing the absorption, tissue distribution, and the potentially toxic effects of PET nanoparticles on aquatic organisms and humans in the framework of environmental risk assessment.

References

- [1] F. Lionetto, C. Esposito Corcione, A. Rizzo, A. Maffezzoli, *Polymers* **13**, 3745 (2021).
- [2] F. Lionetto, M. G. Lionetto, C. Mele, C. Esposito Corcione, S. Bagheri, G. Udayan, A. Maffezzoli, *Nanomaterials* **12**, 1560 (2022)
- [3] D. Ebert, *EvoDevo* **13**, 1, (2022)

A CHARACTERIZATION METHOD FOR EVALUATING ADDITIVES SUITABLE FOR ODOR CONTROL IN PLASTICS

R. Grömmer^a, E. Metzsch-Zilligen^b, M. Großhauser^b, R. Pfaendner^b, H. Haug^c and C.-C. Höhne^a

^a Fraunhofer Institute for Chemical Technology ICT, Joseph-von-Fraunhofer Str. 7, 76327 Pfinztal, Germany

^b Fraunhofer Institute for Structural Durability and System Reliability LBF, Schlossgartenstr. 6, 64289 Darmstadt, Germany

^c Fraunhofer Institute for Process Engineering and Packaging IVV, Giggenhauser Str. 35, 85354 Freising, Germany

roxana.groemmer@ict.fraunhofer.de

INTRODUCTION

Recycling is a key element in achieving a sustainable circular plastics economy, which is necessary to combat climate change and pollution. However, many challenges remain.

One major challenge is the insufficient quality of recycled materials, which limits their use to low-value applications (1). One factor with considerable impact on the quality is the presence of an unpleasant odor caused by absorbed impurities, decomposition of the plastic during the use phase, and the recycling process (2).

Unpleasant odors in plastics can be addressed by different technologies, such as washing and extraction processes during recycle processing, or the incorporation of plastic additives for odor control. However, the effectiveness of an additive for odor control depends highly on the odorant and the polymer type of the recycle (3). Finding an additive which meets the requirements is currently a time-consuming and costly process, which involves the preparation of test specimens and an olfactory evaluation. There is consequently a high interest in developing a simple and fast process to measure the effectiveness and efficiency of additives for odor control.

In this study, we present a straightforward and rapid characterization method to measure the effectiveness of a substance in absorbing specific volatile organic compounds (VOCs) released from a recycle, in order to pre-evaluate its suitability as an odor absorber.

EXPERIMENTAL

Materials

The odor-contaminated material used in this study was a polypropylene (PP) recycle. The absorbing abilities of a hydrophobic zeolite were tested. A porous polymer based on 2,6-diphenylphenylene oxide with a specific surface of 35 m²/g (Tenax TA® from GERSTEL GmbH & Co.KG, Mülheim an der Ruhr) was used for emission collection.

Preparation

In the developed process, sample enrichment takes place in an oven containing a sample container and a glass tube with a frit. The container and the glass tube are connected by a gas line. A glass tube with Tenax TA® is installed outside the oven to absorb the emitted gases. A gas line leads into the oven to the sample container, the glass tube and subsequently to the Tenax TA® tube.

The PP recycle is weighed into the sample container and the zeolite into the glass tube with the frit. Both vessels are placed in the oven, connected to the gas line, and a stream of N₂ is applied. The emissions of the sample are collected at an oven temperature of 80 °C over 30 minutes. Reference values are measured by installing an empty glass tube in the oven. The Tenax TA® tubes containing the emission samples are stored in a freezer until analysis.

Thermal desorption analysis of organic emissions

The emission samples are analyzed by thermal desorption-gas chromatography/mass spectrometry (TD-GC/MS) to characterize them based on the organic substances they release. The analysis and evaluation are conducted in accordance with VDA 278, a method used within the automotive industry to examine organic emissions from non-metallic vehicle materials.

RESULTS AND DISCUSSION

To evaluate the emissions, the VOC value was determined. The VOC value is the sum of VOCs that can be emitted from the sample. This value is expressed as a toluene equivalent relative to the sample volume and is given in $\mu\text{g}/\text{m}^3$ (4).

As an example, the average VOC values from eight PP recyclate samples in combination with and without the absorber (zeolite) are shown in Figure 1.

The data show an 83 % decrease in the VOC value for the measurements containing the zeolite. This means that the amount of VOCs, and therefore possible odorants, emitted by the PP recyclate can be significantly reduced when using the tested zeolite as an absorber.

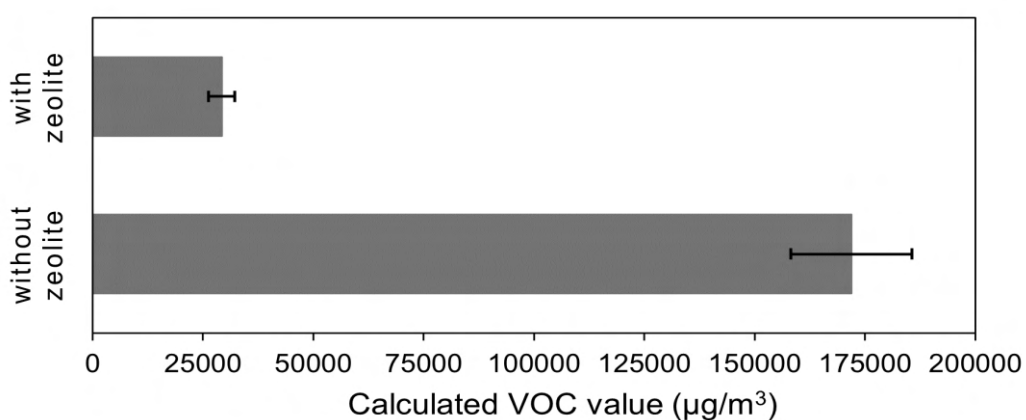


Figure 1: Determined VOC values for a PP recyclate tested with and without zeolite as an odor absorber.

CONCLUSION

A straight-forward and rapid characterization method was developed for evaluating substances suitable for the absorption of VOCs. It can be used to pre-evaluate additives for odor control in various odor-contaminated materials.

Sandwich structures containing the tested PP recyclate as a core and an odor barrier layer containing the tested zeolite as additive were studied. Sensory evaluation of these test specimens showed a significant reduction in the odor release (5).

Acknowledgment

The authors would like to thank Sonja Lauinger from Fraunhofer ICT, Pfinzthal for analytical support. This work was funded by the Fraunhofer Cluster of Excellence Circular Plastics Economy CCPE.

References

- 1) *Plastic waste and recycling in the EU: facts and figures* | Topics | European Parliament, (2018). europa.eu
- 2) S. Fischer, *So wird der Geruch von Rezyklat gebunden*, PLASTVERARBEITER, (2023). plastverarbeiter.de
- 3) R. Pfaendner, *Kunststoffe Werkst. Verarb. Anwend.*, 94–100, (2023).
- 4) Verband der Automobilindustrie e. V., *VDA Recommendation 278*, (2011).
- 5) C.-C. Höhne, A. Menrath, R. Pfaendner, E. Metzsch-Zilligen, B. Lok, *KUNSTSTOFFE Int.*, 28–31, (2022).

THE LATEST RESEARCH FOR IMPROVING INTUMESCENT COATING FOR PROTECTION AGAINST FIRE

K. Pyrzynski

DELTA Innovative Company, Krupczyn 5, 63-140 Dolsk, Poland, biuro@delta-dolsk.pl

INTRODUCTION

Intumescent coatings covering textiles, wood, and composites swell under influence of heat and form porous, non-flammable charred layer. They cut oxygen supply and cut heat penetration from flammable surfaces e.g. textiles, nonwoven, wood and lignocellulosic composites. They are effective and not expensive barriers which protect flammable materials. There are mainly two types of barriers: modified resins, carbonizing agents, foam forming agents, dehydrating agents and according to area of application with different modifiers, including nano-modifiers. Another types of intumescent materials were developed on the base of alkali silicates (not emitting toxic gases) which also can be used as a coat on textiles, nonwoven, wood, composites and even metals. They start swelling in 100 °C, or in contact with flame due to endothermic process and is associated with an emission of water vapor. The solid foam is rigid and consists of hydrated silica and some products of decomposed mineral endothermic fillers. The fire proofing efficiency of protected surface is determined by: heat release rate, the effectiveness of combustion heat, the mass loss rate and specific swelling ability of this coating.

Fire protecting coatings with intumescent properties were used for about 50-60 years, whereas the process of incorporating intumescent additives intrinsically in different polymer structures e.g. by using especially modified dendrimers and special zeolites and is relatively new.

EXPERIMENTAL

Tested polycondensation product is an intumescent fire retardant agent based on condensed amine-formaldehyde resins and phosphorus compounds. Can be added a modifiers in the form of nanoscale silica molecules in an amount 1.21-5% of total condensate mass introduced during condensation of the amine-formaldehyde resin in solid or colloidal form. A new effective intumescent coating – transparent system based on modified nano-scale silica is presented below.

To check the fire protection efficiency of the condensate, the surfaces of the chipboard samples were covered by tested polycondensation product coating 350g/m² as a ground coat and 80-100 g/m² primer varnish as a surface coat. The condensate without and with the nanomodifiers additive (Aerosil 200, Evonik, hydrophilic fumed silica with a specific surface area of 200 m²/g, 99,8 % SiO₂) in an amount 1.5% based on the weight of the condensate, was used for the tests. Preliminary research has shown that the 3% addition improves the efficiency of creating the porous insulating layer, but unfortunately it significantly increases the price of the product.

For comparison, a reference sample without a fire retardant coating was also subjected.

Combustibility measurements were performed on a cone calorimeter CONE2A made by Atlas Electric Devices . The measurements were carried out in accordance with the ISO 5660-1:2002

standard Reaction-to-fire tests—heat release, smoke production and mass loss rate—part 1: heat release rate (cone calorimeter method).

The SBI test according to PN-EN 13823:2010 (Reaction to fire tests for building products - Building products excluding floorings exposed to the thermal attack by a single burning item) simulates a single burning item burning in a corner of a room.

Based on the recorded data, the values of the main classification parameters are determined: fire growth rate indicator - FIGRA, total heat released from the sample during the first 600 seconds of exposure to the flames of the THR600s main burner, total smoke emission from the test piece during the first 600 seconds of exposure to the main burner flames - TSP600s, smoke emission rate indicator – SMOGRA.

After some modifications of this type of barrier coating was also developed another type as sealant for fire barrier doors and for protective coat of chassis and rubber tires of military vehicles, resistant to napalm conditions. They can be formulated as rigid and flexible fire barriers.

RESULTS AND DISCUSSION

As result obtained in perfect insulation of covered flammable materials (wood, composites) from the excessive rise of temperature and oxygen penetration. Intumescent coating protects flammable materials against thermal decomposition. In case of polymers and polymer composites the temperature of burning surface of polymer is close to the temperature at which extensive thermal degradation occur (300 – 600 ° C). The bottom layer of char, near the protected surface, has similar temperature below 300 ° C whereas the upper surface is exposed to almost 1500 ° C.

There is strong correlation between char yield and fire resistance because char is formed and are emitted non-combustible gases and water vapor. The presence of formed char inhibits spread of the flame, acting as a thermal barrier around the unburned material.

Summing up developed formulation is effective thanks to proper selection of: carbonizing agents, foam forming agents, dehydrating agents and special modifiers agents including very effective high dispersion endothermic fillers.

References

- E. M. Bulewicz, R. Kozłowski, A. Miciukiewicz. Fire Mater. 9(4) (1985) 171
- R. Kozłowski, B. Mieleniak, A. Przepiera, K. Bujnowicz. Progress in fire Barriers. In Composite in Construction. Ed. D. Bruno, G. Spadea, N. Swamy, International conference University of Calabria (Sept. 16-19, 2003)
- G. Fontaine et al. International symposium on Flame Retardant Materials and Technologies, Sichuan University, China (Sept. 17-20, 2010)
- Pat. USA 903 422 1B2 (2015) “Intumescent fire retardant and the method of its manufacture”, Inventor:Kozłowski R., Wesolek D., Władyka-Przybylak M., <https://patents.google.com/patent/CN101052662>
- Alongi J., Han Z., Bourbigot S.: “ Intumescence: Tradition versus novelty. A comprehensive review”, Progress in Polymer Science 2015, Elsevier vol.51, 28-7
- Pyrzynski K., Kozłowski R., Intumescent rigid and flexible fire barrier coatings on the base of textiles and nonwovens; 2023 Spring International Conference on Textile Science and Engineering (CTSE-S), April 21-23, 2023, Kunming, China
- Pyrzynski K., Michalska A., Progress intumescent coating for wood protection and wooden product against fire, WOOD – SCIENCE – ECONOMY 4th International Scientific Conference, September 14-16, 2022, Poznań, Poland

Recyclable and reusable bio-epoxy resins for composites: the approach of the Re-Comp project

G.Cicala*, L.Saitta*, A. Latteri*, S.Dattilo, G.Rizzo* and C.Tosto***

*Department of Civil Engineering and Architecture (DICAR), University of Catania, Via Santa Sofia 64, Catania, Italy, gianluca.cicala@unict.it

**ICPB, National Research Council, Via Paolo Gaifami 17, Catania, Italy

INTRODUCTION

Thermoset resins are widely used because of their easy processability and very good thermomechanical properties once fully cured. However, due to the stability of the cured network, their end-of-life (EOL) treatment is challenging. Nowadays, few alternatives exist at TRL 9 to recycle EOL thermoset resins: mechanical recycling and incineration. Both these approaches pose limitations in terms of their environmental impacts, and they do not allow for the recovery of valuable reinforcement fibers. A viable alternative is chemical recycling using tailored chemistry to drive depolymerization under mild conditions. This paper reports on the findings of the project RE-COMP, which focuses on the development of bio-epoxy resins with full recyclability.

EXPERIMENTAL

Materials

The epoxy resins studied were all cured using Recyclamine series reactants. The Recyclamines are acetal-based amines that, under specific conditions, allows to depolymerise cured epoxy thermosets in a controlled manner. Different grades Recyclamines were used as provided by Aditya Birla. The epoxy monomers were obtained from R*Concept with a maximum bio-carbon content of 20%. Some experiments were carried out using Cardanol resins and for comparison purposes Ampro resins were obtained from Gurit.

Preparation

All the resins were prepared by simple mixing procedure at room temperature being all liquid at this temperature. Resin cured samples were cured in silicone moulds after simple pouring. Different curing cycles from room temperature at 24 h and curing at 100-120 °C for 3 h were attempted. Cured resins were also recycled using the optimized procedure [1] and the recycled product (rTP) was added to the uncured formulations and the systems were tested.

Thermomechanical characterization

Thermomechanical characterization was performed using DMA and flexural test. A DMA was used to measure the T_g for each formulation. These analyses were run using a TRITEC 2000 dynamic mechanical thermal analyzer (Triton Technology, Leicestershire, UK) on samples with size of (10 × 6 × 4) mm³. Each analysis was performed in single cantilever deformation mode, since this is a well-known mode for characterization through glass transitions [49]. Each analysis was run in the temperature range between 25 °C and 150 °C with a heating rate equal to 2 °C/min. The displacement was set at 200 μm, and the frequency was 1 Hz. Five samples were tested for each investigated scenario. Next, the average and the standard deviation were evaluated for the T_g using the following approach: tanδ versus temperature curves were plotted for each investigated formulation, and the T_g was measured as the tanδ peak temperature.

The flexural properties of each thermoset formulation containing varying contents of rTP were measured according to the ASTM D790 standard. The characterized samples had a size of (80 × 10 × 4) mm³. They were mechanically tested using an Instron 5985 universal testing

machine (Instron, Milan, Italy) equipped with a load cell of 10 kN, in strain control mode, with a span length of 60 mm and a speed of 2.0 mm min⁻¹. Five samples were tested for each investigated scenario measuring the flexural strength, the flexural modulus, and the deformation at break; next, the average and the standard deviation were evaluated for each of them

RESULTS AND DISCUSSION

The cured samples, created by mixing various quantities of rTPs, were analyzed for their thermo-mechanical properties. This analysis aimed to assess their potential range of applications from a cradle-to-cradle perspective. The $\tan\delta$ versus temperature plots are shown in Figure 1. According to the results, it can be assumed that the additional post-curing step at 100°C for 3 hours resulted in the highest overall T_g value, indicating a higher cross-linking density for the epoxy resin system with an rTP content ranging from 15 to 27% wt. This finding aligns with previously observed cross-linking density behavior in virgin epoxy matrices. However, as the rTP content increased, the T_g initially decreased sharply by about 18%, from 0% wt to 15% wt. Further increases in rTP content led to a continued but less pronounced decrease in T_g, approximately 3%. This trend is consistent with literature reports on the addition of plasticizers to epoxy systems. The decrease in T_g with higher rTP content can be attributed to the lower reactivity of recycled thermoplastic compared to commercial recyclable amine and the dilution effect seen in thermoplastic/thermoset blends. The linear chemical structure of the recycled thermoplastic increases intermolecular mobility within the epoxy network, resulting in a decreased T_g

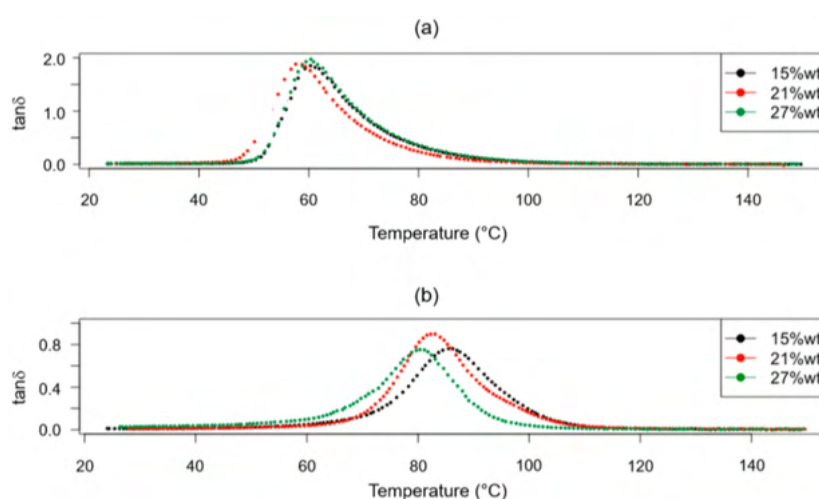


Fig. 1 DMA Test on cured specimens with different content of rTP

The data clearly explain that rTP can be used back mixing it with virgin resins obtaining epoxy formulations with an increased environmental beneficial effect.

Acknowledgment

This work has been financially supported by the project Sistemi innovativi di fabbricazione flessibile per materiali compositi ecocompatibili totalmente riciclabili- ReCOMP (CUP B69J24001400005)

References

- 1) L.Saitta et al Polymers 2023, 15(13), 2809; <https://doi.org/10.3390/polym15132809>

CHARACTERIZATION OF WATER TRANSPORT PROPERTIES OF ACRYLIC URETHANE CLEARCOAT AND UV AGEING EFFECT

Hiba LAZEREGUE^{1,2}, **Bruno FAYOLLE**¹, **Cyrille SOLLOGOUB**¹, **Stéphane DELALANDE**¹, **Jean-Charles MENETRIER**², **Raynald BOUGNOT**²

1. Laboratoire PIMM, Arts et Métiers Institute of Technology, CNRS, Cnam, ENSAM, 151 boulevard de l'Hôpital, 75013 Paris (France)
2. Stellantis, Technical center, 78140 Vélizy-Villacoublay (France)

INTRODUCTION

Automotive paint systems are complex systems that consist of several layers: electrodeposited epoxy coat (i.e., anti-corrosion coating), basecoat, and clearcoat which is the upper layer that is exposed to different ageing factors including UV [1]. One of the roles of coating layers is to limit water content in contact with galvanized steel. The quantity of water within these layers must be assessed as a function of relative humidity and temperature to predict long term durability as protective coatings against corrosion.

In this work we will present a full characterization of water transport properties of clearcoat acrylic-urethane and its associated multilayer. Furthermore, water transport properties of UV aged acrylic-urethane will be shown, in the aim of better understanding the effect of photo-oxidation on water transport properties and factors governing these later. UV-ageing is limited to clearcoat because the underlying layers are not exposed to UV and sunlight only affects the upper surface of clearcoat [1].

EXPERIMENTAL

Materials

The materials used in this work are clearcoat stand-alone films which is an acrylic matrix with urethan hardener and thickness ranging from 40 to 60 μm . The associated multilayer, as shown in **Fig. 1**, consist of electrocoat, basecoat and clearcoat.

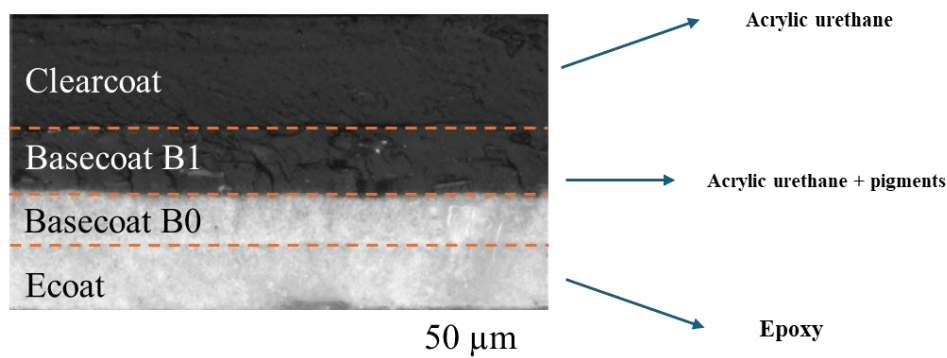


Fig. 1 Cross-section of the multilayer system, after cryofracture, observed with an optical microscope, composed of electrocoat (Ecoat) in epoxy, basecoats (B0 and B1) and clearcoat (2K)

Preparation

Clearcoat standalone films were prepared by applying liquid varnish on Tedlar[®] films using a spray gun, then cured at 140 °C for 20 minutes which allows crosslinking (T_g around 70 °C). The electrocoat standalone films were cured at 150°C for 15 minutes, and characterized as received (T_g around 105 °C and filler content of 35%). Basecoat is applied directly on the received electrocoat films, followed by clearcoat using a spray gun, multilayer is then cured at 140°C for 20 minutes (filler content of 14%). Glass transition temperatures and filler content were measured using Q800 TA DMA and Q500 TA TGA, respectively.

UV ageing was done using a weather-ometer (WOM CI4000), at 15% of relative humidity, during 250, 500, 1008 and 2016 hours.

Physico-chemical characterization

Prepared and received materials were characterized using PerkinElmer FTIR spectrometer, to follow oxidation products formation during UV exposure.

Water transport properties are measured at 30 °C, 50 °C and 70 °C using a dynamic vapor sorption analyzer (Igasorp XT DVS) for unaged clearcoat, associated multilayer and aged clearcoat with several levels of oxidation.

RESULTS AND DISCUSSION

Water sorption characterization was conducted at 30°C, investigated relative humidities range from 10% to 90%. Clearcoat water uptake is plotted against time at 30°C in **Fig.2a**. Since water uptake reaches a plateau for all the films (unaged clearcoat, aged clearcoat after 1008 hours and unaged multilayer), water concentration at saturation is then calculated and plotted against relative humidity as shown in **Fig.2b**.

As shown in **Fig.2b**, sorption isotherm for all films shows a linear behavior up to 50% RH respecting Henry's law, and then a deviation from this linear model, as an evidence of water cluster formation [2]. Same assessments were conducted on the multilayer, and it showed similar behavior and same values of water concentration at saturation.

In terms of water content whatever RH value, we can witness that water concentrations of clearcoat are surprisingly close to those of multilayer despite the polymer nature difference shown in **Fig. 1**.

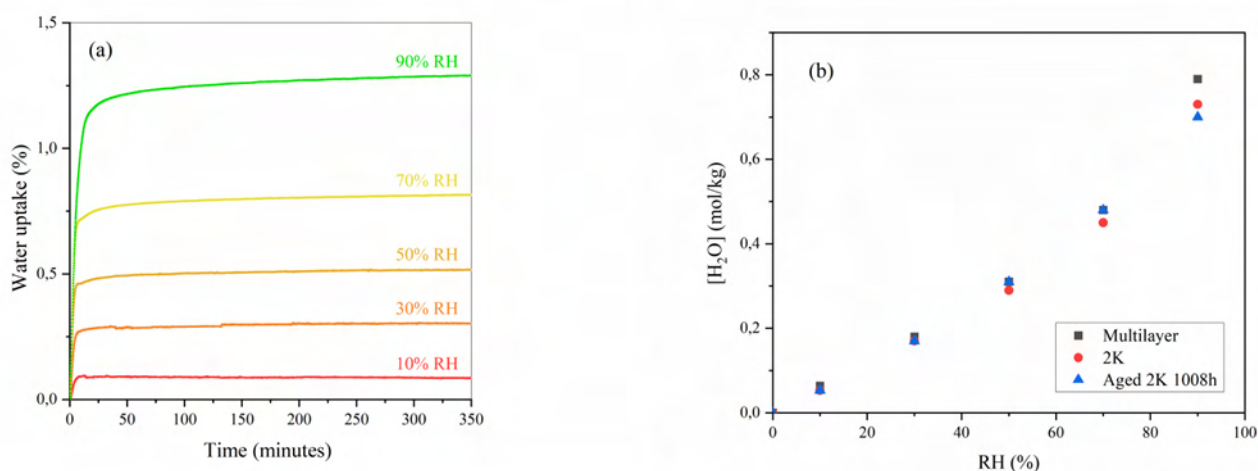


Fig. 2 (a) Sorption curves of clearcoat at 30°C and at different relative humidity rates (b) Sorption isotherms of clearcoat, multilayer and 1008 h UV aged clearcoat at 30°C

Acknowledgment

This PhD program was subsidized by ANRT (N° 2022/0485) and funded by Stellantis.

References

1. Larché J.-F, Bussiere P.-O, J.-L. Polymer Degradation and Stability, 8, 1438-1444 (2011)
2. Lesimple G, Illiopoulos I, Marijon J.-B, Fayolle B. ACS Applied Polymer Materials, 5 (1), 302-310 (2023)

3D Composite Scaffold Based on PLLA and Natural Antioxidant Molecules

Veronica Schiera¹, Francesco La Monica², Francesco Carfi Pavia¹, Paola Poma², Giulio Gherzi², Vincenzo La Carrubba¹, Valerio Brucato¹, Nadka Tz. Dintcheva¹

¹Department of Engineering, University of Palermo, Viale delle Scienze, Palermo, Italy
veronica.schiera01@unipa.it, francesco.carfi@unipa.it, vincenzo.lacarrubba@unipa.it,
valerio.brucato@unipa.it, nadka.dintcheva@unipa.it.

²Department of Biological, Chemical and Pharmaceutical Sciences and Technologies (STEBICEF), University of Palermo, Viale delle Scienze, Palermo, Italy
francesco.lamonica03@unipa.it, paola.poma@unipa.it, giulio.ghersi@unipa.it.

INTRODUCTION

Regardless of the use of biocompatible materials, implanting a scaffold will always trigger an immune response, causing inflammation and possible scarring that may affect the success of the implant (1). Antioxidant molecules have various biological effects that can help regulate oxidative stress and inflammation caused by scaffold implantation (2). Rosmarinic acid (RA) and curcumin (CU) act as antioxidants, as well as anti-inflammatory and antibacterial agents. This study concerns the possibility of incorporating natural antioxidant molecules into a polymeric structure to create composite scaffolds through a specific additive protocol.

EXPERIMENTAL

Materials

Poly-L-lactic-acid (PLLA, Resomer, L 209 S, Evonik Industries, Essen, Germany; Inherent Viscosity = 2.6–3.2 dL/g) and 1,4-dioxane (Sigma-Aldrich, Munich, Germany) were used for scaffold preparation. Rosmarinic acid (RA, 96% pure, Sigma Aldrich), Curcumin (CU, Sigma-Aldrich, 80%) and Ethanol absolute anhydrous (Carlo Erba Reagents, Cornaredo, Italy) were used for ethanol/RA and ethanol/CU solution preparation.

Composite scaffold preparation

PLLA was dissolved in 1,4-dioxane (4% wt/wt) at 120°C. Distilled water was added to achieve a dioxane/water ratio of 87/13. Five mL of the solution, maintained at 60°C, was poured into a cylindrical polyethylene sample holder and immersed in a 20°C water bath for 15 minutes. A PTFE coating, pre-cooled to -20°C, was then used to ensure uniform temperature distribution. The sample holder was placed in the PTFE cylinder and quenched in a -20°C ethyl alcohol bath for at least 15 minutes. The samples were washed with deionized water and dried at 60°C to remove solvent traces. The cylindrical scaffolds were cut into 2 mm discs and then shaped into cylinders of 4 mm diameter and 2 mm height using a biopsy punch. The PLLA scaffolds were placed in a 96-well plate and immersed in pure ethanol under vacuum for 2 min to ensure complete solvent penetration into the pores. After removing the ethanol, solutions containing ethanol and RA or CU at different concentrations were prepared. Then 200 µl of these solutions were added to each well containing a scaffold. After at least 24 hours of ethanol evaporation, the dried samples were removed from the wells for further analysis.

Characterization

FTIR-ATR spectroscopy and gravimetric analyses were carried out in order to determine the presence and the weight percentage of natural antioxidants into the polymer structure, respectively. SEM analyses complemented these analyses to examine the scaffolds' morphology before and after adding the biomolecules. Finally, water contact angle tests were carried out to assess the hydrophilicity of the composite scaffolds

RESULTS AND DISCUSSION

This study successfully incorporated rosmarinic acid or curcumin into PLLA scaffolds. As shown in **Fig 1**, a novel protocol incorporates a natural biomolecule, soluble in organic solvents, in the polymeric scaffolds produced through Thermal Induced Phase Separation (TIPS).

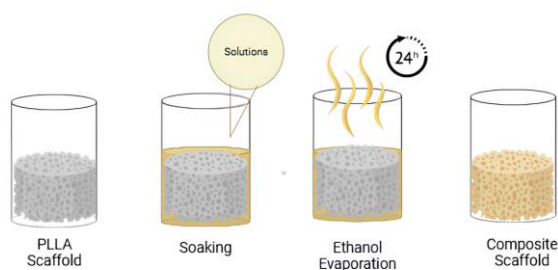


Fig 1: Experimental protocol schematics.

This approach is both cost-effective and customizable with different biomolecules. The presence of these molecules in the whole scaffold structures was confirmed by ATR-FTIR analysis in **Fig 2**.

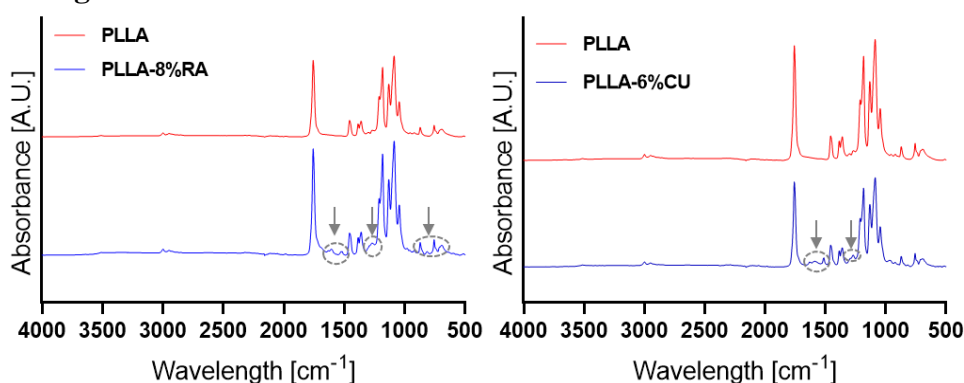


Fig 2: ATR-FTIR spectra of PLLA, PLLA-8% RA, and PLLA-6% CU samples.

Gravimetric analyses allowed to determine the weight percentages of RA and CU in PLLA scaffolds to be 8% and 6%, respectively. SEM micrographs revealed an interconnected porous network with a pore size, ranging from 50 to 70 μm . Moreover, the presence and incorporation of these biomolecules into the samples revealed an enhancement of the hydrophilic behaviour of the composite scaffold (data not shown). In conclusion, our focus on composite scaffolds based on PLLA and natural antioxidant biomolecules yielded promising results, opening a new avenue for future development in this field.

Acknowledgment

This work has been financially supported by the University of Palermo. The authors acknowledge Ms. E. Inzerillo and Ms. M. C. Sciabica for their precious help in the preparation and characterization of the samples.

References

- 1) S. Franz, S. Rammelt, D. Scharnweber, J. C. Simon, “Immune responses to implants – A review of the implications for the design of immunomodulatory biomaterials,” *Biomaterials*, **32**, 6692–6709, (2011).
- 2) X. Gao, Z. Xu, G. Liu, and J. Wu, “Polyphenols as a versatile component in tissue engineering,” *Acta Biomaterialia* **119**, 57-74, (2021).

Enhancing Rheological and Mechanical Properties of BioSourced Poly(butylene succinate-co-butylene adipate) through Green Reactive Extrusion

*Michele Gammino¹, Claudio Gioia², Roberto Scaffaro*¹, Giada Lo Re*³.*

¹*Department of Engineering, University of Palermo, Viale delle Scienze, ed. 6, 90128, Palermo, Italy*

²*Department - Department of Physics, University of Trento, via Sommarive 14, 38123 Povo (TN), Italy– CG*

³*Department of Industrial and Materials Science, Chalmers University of Technology, Rannvagen 2A, SE-412 96 Gothenburg, Sweden*

* giadal@chalmers.se, *roberto.scaffaro@unipa.it

INTRODUCTION

The PBSA copolymer is increasingly popular in the market due to its sustainability and biodegradability, as well as its mechanical properties, which are similar to low-density polyethylene but with higher deformability than PHAs and PLA. However, prolonged and/or repeated melt processing at elevated temperatures during the manufacturing and mechanical recycling of biodegradable polyesters such as PBSA is challenging due to their thermo-mechanical sensitivity, leading to a rapid loss of properties caused by degradation. This study explores the potential for controlling the thermomechanical degradation of poly(butylene succinate-co-butylene adipate) (PBSA) to design a green reactive extrusion approach that improves PBSA's rheological and mechanical properties without requiring additional additives. Various mixing protocols (temperature profile and screw rotation speed) were employed to evaluate their influence on the material's thermomechanical degradation. The impact on the online PBSA rheological assessment was studied by varying three different mixing speeds (30, 60, 120 rpm) and four different processing temperatures (150, 180, 200, 220 °C). The torque curves recorded during the different PBSA melt mixing processes at temperatures above 150 °C and 30 rpm exhibited consecutive minimum and maximum points, suggesting degradative reactions such as depolymerization followed by branching/recombination. These observations allowed the design of a reactive extrusion process based on controlling the thermomechanical degradation pathways of PBSA through the careful selection of processing conditions. The resulting reactive extrusion significantly enhanced the mechanical, rheological, and viscoelastic properties of PBSA, offering a promising avenue for the sustainable processing of biodegradable polyesters.

EXPERIMENTAL

Materials

PTT MCC Biochem provided a commercial-grade biobased PBSA copolymer, identified as BioPBS FD92PM, which has a recommended processing temperature range of 130–150 °C and is certified for home composting by Vinçotte (European Union). Chloroform (ACS grade) was purchased from Sigma-Aldrich and used without any further treatment.

Preparation

Melt Processing Conditions. The initial evaluation of reactive processing conditions was investigated on 40 g of PBSA, which was fed into a Brabender batch mixer operating at a predetermined temperature. The mixing speed was increased to the desired value within 10–15 s and kept constant for the test duration, which lasted for 60 min. Various temperatures

and mixing speeds were used (Table 1, Figure 1). The test temperatures were 150, 180, 200, and 220 °C, and the mixing speeds were 30, 60, or 120 rpm (rpm). The experiments were carried out with the mixing bowl exposed to air with a relative humidity of 50–60%. During the mixing process, samples were taken from the mixing chamber according to established parameters and monitored throughout the torque curve. The samples collected from the mixer were immediately cooled in liquid nitrogen to prevent potential recombination and to inhibit any other reaction. Reactive melt processing (RP) of PBSAC1, PBSAC2, PBSAC3, and PBSAC4 was then carried out by varying the processing time, under constant processing parameters, selected after the initial evaluation by inline rheological analysis ($T = 200\text{ °C}$ and $v = 60\text{ rpm}$) (Table 2).

Rheological and physico-chemical characterization

The viscoelastic properties of the materials were evaluated via dynamic oscillatory rheometry in the molten state. A DHR-2 rheometer (TA Instruments) with a 25 mm parallel plate geometry was used for the tests at a temperature of 120 °C and a gap distance of 1.5–2 mm in a nitrogen environment. Amplitude stress and strain sweep test were first fulfilled, with an initial stress of 10 Pa and a strain of 1×10^{-5} , up to a final strain of 2 at 0.628 rad/s. The complex modulus (G^*), storage modulus (G'), and loss modulus (G'') were recorded as a function of stress (τ) and shear strain (γ), while a minor oscillatory amplitude strain ($\gamma = \gamma_0 \sin(\omega t)$) was applied at a stress of 200 Pa and a strain of 0.1 rad. The moduli (G^* , G'), complex viscosity (η^*), and phase angle (δ) were then measured as a function of angular frequency (ω) between 0.01 and 100 rad/s.

RESULTS AND DISCUSSION

The thermomechanical degradation of PBSA at high temperatures and shear stresses can be monitored by viscosity decrease during melt processing. We investigated the influence of screw speed and temperature on PBSA degradation using in-line torque assessment during 60 minutes of melt processing in an internal mixer Figure 1. Various screw speeds (30, 60, 120 rpm) were tested at a constant temperature of 180 °C, while different temperatures (150, 180, 200, 220 °C) were assessed at a constant screw speed of 60 rpm. Reference conditions (150 °C and 60 rpm) showed constant torque values, aligning with supplier recommendations to process below 160 °C to prevent thermal degradation. Above 150 °C, torque trends varied with processing conditions Figure 1. All torque curves above 160 °C showed minimum (m) and maximum (M) points, with maxima shifting to lower residence times as temperature or screw speed increased. Torque decreases after maxima indicated reduced viscosity until a plateau was reached, suggesting reduced reaction kinetics for RP development and varying PBSA architectures Figure 1. At 220 °C, a rapid torque change was observed, with steep increases followed by swift declines, reaching plateaus after 30 minutes at the lowest recorded values ($<1.5\text{ N m}$). A 10 °C increase significantly impacted degradation kinetics more than doubling screw speed from 60 to 120 rpm, indicating similar initial chain scission kinetics but faster recombination and degradation at 220 °C. Four distinct intermediates were identified during melt processing at 200 °C and 60 rpm to explore RP reaction times. Four PBSA batches were prepared by stopping processing after 1, 2, 12, and 45 minutes. The structural, thermomechanical, and viscoelastic properties of reactively melt-processed PBSA were analyzed and compared with those of commercial PBSA processed under nonreactive conditions.

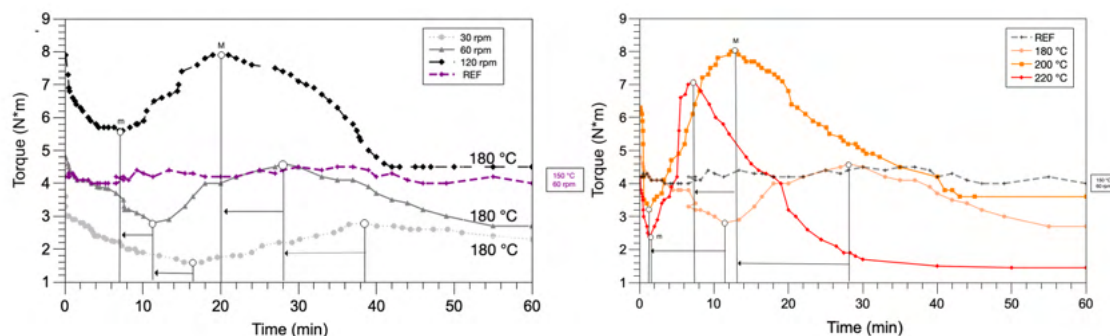


Fig. 1 Time-dependent evolution of the torque recorded during PBSA processing in an internal mixer under different processing conditions. In particular, (A) at $T = 180\text{ }^{\circ}\text{C}$ and different screw speeds and (B) at 60 rpm and different processing temperatures.

Acknowledgment

Knut and Alice Wallenberg Biocomposites [grant number V- 2019-0041, Dnr. KAW 2018.0551] and the Wallenberg Wood Science Centre (WWSC) 3.0 program are acknowledged for financial support. This study was carried out within the MICS (Made in Italy – Circular and Sustainable) Extended Partnership and received funding from the European Union Next-GenerationEU (PIANO NAZIONALE DI RIPRESA E RESILIENZA (PNRR) – MISSIONE 4 COMPONENTE 2, INVESTIMENTO 1.3 – D.D. 1551.11-10-2022, PE00000004).

Good morning, with the following I attach my oral abstract contribution for the ModeSt 2024 conference which will be held in Palermo from 1 to 4 September

Development of high-performance biodegradable bacterial polyester materials based on polymer alloy techniques

Hideki Abe^{1*}, Iffa Farahin Jeeper^{1,2}, and Kumar Sudesh²

¹ Bioplastic Research Team, RIKEN CSRS, Japan

² Ecobiomaterial Laboratory, School of Biological Sciences, Universiti Sains Malaysia, Malaysia

*Corresponding Author: habe@riken.jp

INTRODUCTION

Polyhydroxyalkanoates (PHAs) are bio-based and biodegradable polymers synthesized as an energy source by bacteria. Although it appears that PHAs have a future in the plastic industry, there are still downsides to implementing PHAs as ideal bio-based materials. These include their poor mechanical properties, susceptibility to thermal degradation, and limited functional applications. Polymer blending is an easy approach to improve the material performance and widen the material applications. Since poly(3-hydroxybutyrate-*co*-3-hydroxyhexanoate) (PHBH), one of copolymer variations of PHA, has a lot to offer in the polymer industry, many studies have been done which focus on PHBH as a polymer blend matrix in a blend, mainly contributing its flexible feature to reduce the rigidity of other blend components.

In this work, we investigated the miscibility and enzymatic degradability of PHBH-based blends by being combined with several biodegradable polymers have been investigated. In addition, in dependent on their miscibility, we synthesized the block copolymers and used as a compatibilizer for the immiscible blends and as a blend component for PHBH copolymers. The influence of the blend morphologies on the mechanical properties and biodegradability were examined.

EXPERIMENTAL

PHBH copolymers containing 5 mol% (Kaneka) and 17 mol% 3HH (lab-synthesized) monomer were used. Atactic poly(3-hydroxybutyrate) (atactic PHB), poly(ϵ -caprolactone) (PCL), and atactic PHB-*b*-PCL diblock copolymer were synthesized in laboratory by the ring-opening polymerizations of racemic β -butyrolactone (β -BL) and ϵ -caprolactone (ϵ -CL).

Blend films of 0.1 mm thickness were prepared by using a solvent-cast technique from chloroform solutions of polymers.

Molecular weight data of the samples were obtained by SEC measurements. Differential scanning calorimetry (DSC) measurements were carried out to determine the melting and glass transition temperatures. Morphologies of blends were observed by using polarizing microscope and scanning electron microscope.

Enzymatic degradation tests were done to evaluate the effect of different polymer compositions on the blends' degradability by using PHB depolymerase purified from *Ralstonia pickettii* T1 or lipase from *Burkholderia cepacia*. In addition, biochemical oxygen demand (BOD) tests for blends were performed to estimate the biodegradability in natural waters according to ISO 17556:2019.

RESULTS AND DISCUSSION

PHBH/ PCL blends have been studied to be an excellent pair of biodegradable polyesters. However, when the PCL content went over 5.0 wt%, the blend exhibited heterogeneous macro-phase separation which resulted in poor mechanical properties. It means that PHBH is immiscible with PCL. On the other hands, PHBH/atactic PHB blends showed a single glass-transition temperature (T_g), indicating miscibility in the amorphous state. The

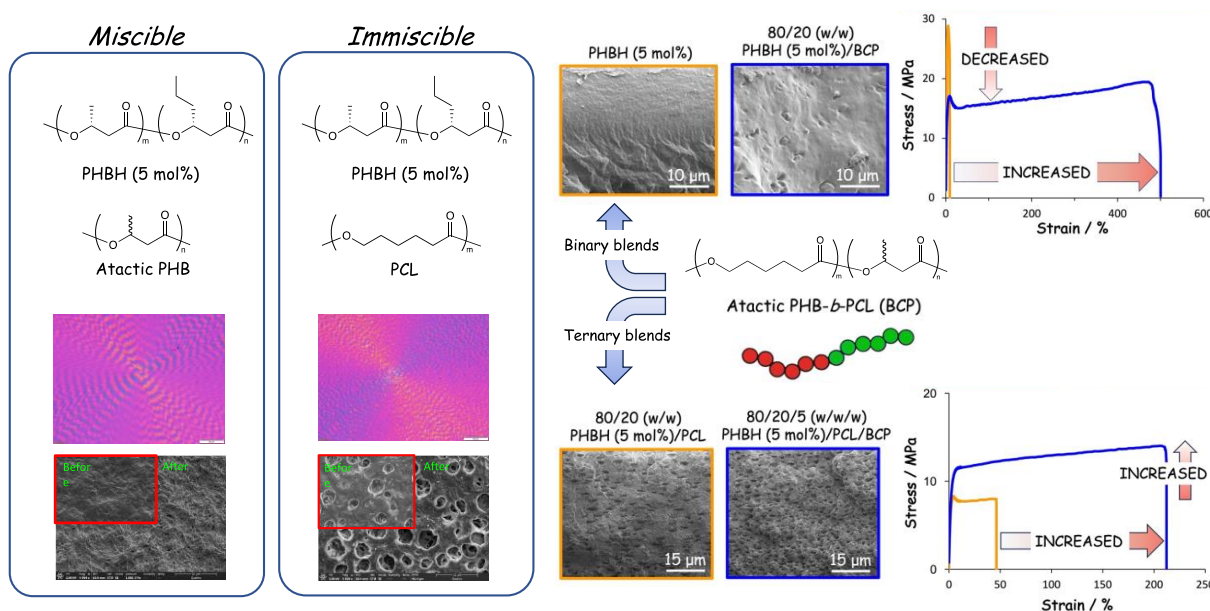
thermal properties and crystal morphology indicated that the miscibility of the PHBH-based blends is dependent on the chemical structure of the added polyesters and the copolymer composition of PHBH. Depending on the enzyme–substrate specificity, miscibility, and phase structure of the blend, the variation of the enzymatic degradation rate with the blend ratio was different among the blends.

To improve the physical properties and regulate the biodegradation rate of PHBH/PCL immiscible blends, atactic PHB-*b*-PCL diblock copolymer, a type of biodegradable block copolymer (BCP) was synthesized and used as a compatibilizer. The addition of a small amount of BCP induced changes in the size of the dispersion of PCL domains in the PHBH matrices, and the mechanical properties of PHBH/PCL/BCP ternary blends were enhanced compared to the BCP-free PHBH/PCL blends. These results demonstrate that BCP acts as an effective compatibilizer.

When the BCP was blended with PHBH as one of binary blend components, the blends exhibited improved mechanical properties, with an impressive 65 to 100-fold increase in elongation at break. The elongation at break, tensile strength and Young’s modulus were found to be influenced by the dispersion size of blend components. PHBH/BCP blends also showed promising improvement in terms of mechanical performance.

From the enzymatic degradation tests, it was found that the presence of BCP in the ternary and binary blend systems decreased the enzymatic degradation rate by PHB depolymerase.

Furthermore, the biodegradation profiles of PHBH based blends in natural waters were evaluated by monitoring the BOD values.



References

- 1) I.F. Jeepery, K. Sudesh, H. Abe, *Polym. Degrad. Stab.*, **192**, 109692 (2021)
- 2) I.F. Jeepery, T. Goto, K. Sudesh, H. Abe, *Eur. Polym. J.*, **196**, 112314 (2023)

ON THE EFFECT OF THE THERMAL HISTORY ON PORE SIZE ARCHITECTURE IN POLYMERIC SCAFFOLDS PREPARED VIA TIPS

Camilla Carbone^{1,2}, Dario Davì², Vincenzo La Carrubba², Valerio Brucato,² Francesco Carfi Pavia²

¹Department of Biomedicine Neuroscience and Advanced Diagnostic, University of Palermo, Via del Vespro 137, Palermo 90128, Italy

²Department of Engineering, University of Palermo, Viale delle Scienze Building 6, Palermo 90128, Italy

* camilla.carbone@unipa.it

INTRODUCTION

Osteochondral defects represent a challenge in clinical research due to the tissue anatomical complexity[1]. Tissue Engineering has evolved to mimic osteochondral anisotropy, for example scaffolds with two different pore size have been developed but they struggle to replicate the osteochondral junction's complexity. Continuous gradient pore scaffolds are promising as they better mimic natural tissue with a gradual transition, reducing interface instability [2]. In this work we present a detailed study of the heat transfer using MATLAB with the aim to predict the system's temperature profiles and obtain gradient architectures. Subsequently, to validate the mathematical model, several scaffolds were produced with different parameters and characterized from a morphological, topographical, and structural analysis point of view.

EXPERIMENTAL

Mathematical modeling

MATLAB's PDE Toolbox and FEM were used to model thermal transients and analyze temperature distributions in a cylindrical setup. The heat equation was solved under the assumption of conduction-dominant heat transfer, ignoring convective heat transfer due to an infinite Biot number.

Scaffold preparation and characterization

Scaffold were produced from a ternary solution of PLLA 4% and a dioxane-water ratio of 87:13. w/w. The solution, initially kept at 60 °C was poured into a cylindrical sample holder and immersed into a thermostatic water bath at a well-defined temperature, for a specific time interval (first cooling). Then the sample holder was suddenly quenched by pool immersion in an ethyl alcohol bath at a temperature of -20 °C for 10 minutes (second cooling). Four different protocols were experimented due to the presence or the absence of a teflon shell as a thermal resistance during the first and/or second cooling; they were called as follow: N-N (No Teflon-No Teflon), N-T (No Teflon-Teflon), T-T (Teflon-Teflon), T-N (Teflon-No Teflon). All the samples were characterized by Micro-Computed Tomography (μ -CT), Scanning Electron Microscopy (SEM), Differential Scanning Calorimetry (DSC) and Picnometry. In addition, software like MATLAB and Image J were used to determine, from SEM micrographs, the pore size distribution and the porosity of the samples.

RESULTS AND DISCUSSION

In the fig. 1A and 1B we reported the radial temperature profile of the solution at different times for the N-N condition during both cooling. Fig. 1C shows the temperatures of the center and border of the solution as a function of the time, whereas Fig.1D reports the temperature differences between center and border. For the conditions that during the second cooling did not present the thermal insulation (e.g., *-N), it was possible to observe an evident T (about 8°C) during the first 5 minutes. Consequently, the cooling rate of the border is remarkably faster than the center one, thus giving rise to a pore gradient. Conversely, in terms of T_{CB} , the T-T and N-T scaffolds are those with the smaller gradient of temperature. Indeed, they cooled slowly

with a very similar temperature at the border and at the center. For that reason, during the quench, the pores have more time to grow quite homogeneously.

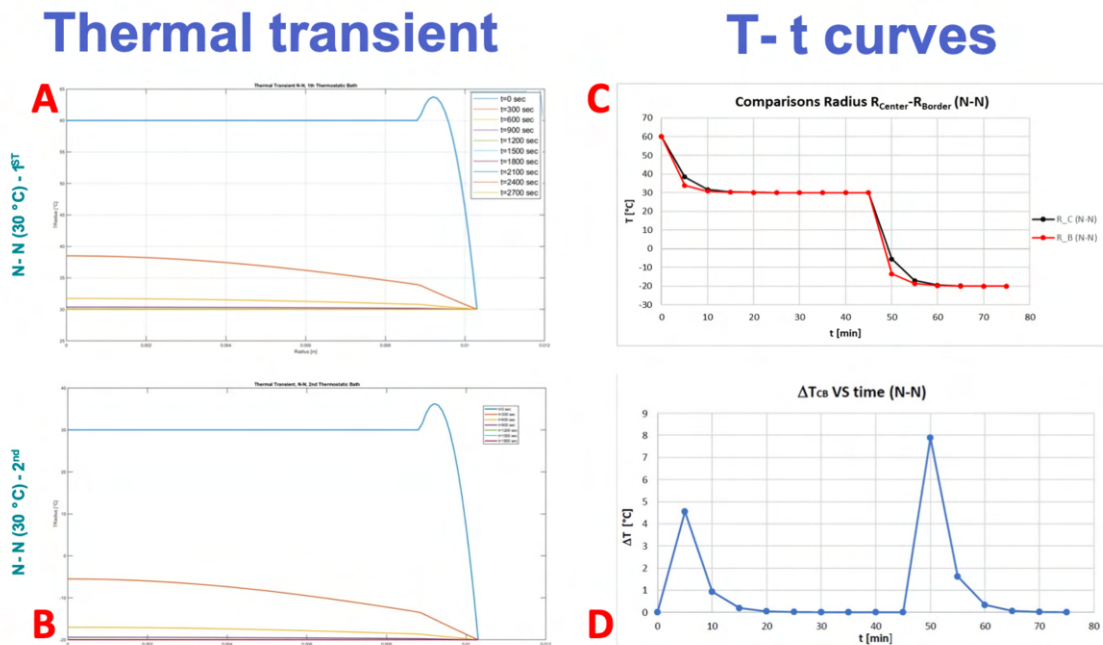


Figure 1: Thermal transient and T-t curves

Morphological characterization, reported in Fig. 2, seems to confirm the model. As a matter of fact, N-N and T-N conditions exhibit a noticeable pore size gradient, whereas the N-T and T-T scaffolds are characterized by a more homogeneous pore size.

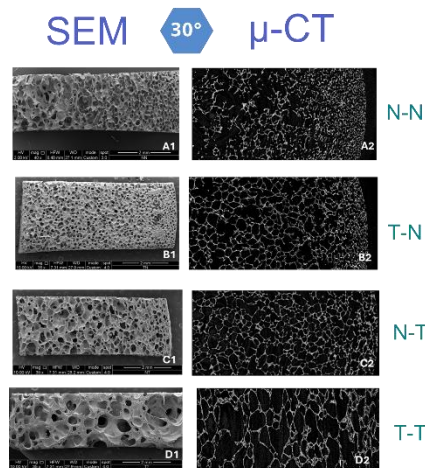


Figure 2: SEM and Micro-CT images of scaffold produced via TIPS at different conditions.

From these results it is evident that the first thermostatic bath is the key factor for pore dimension while quenching process is crucial to create the gradient structures. Controlling finely these parameters would allow the production of scaffold with a tunable gradient architecture.

References

- 1) L. Chen et al., *Bioengineering*, **10**, 2, (2023).
- 2) X. Niu, N. Li, Z. Du, and X. Li, *Bioactive Materials*, **20**, 574 (2023)

Development of Phosphonate-(Co-)Polymer-Functionalized Silica Nanoparticles as Alternative Flame Retardants for Transparent Thermoplastic Polymers

F. A. Watt¹, D. Frosien², W. Ali³, R. Weberskirch², T. Mayer-Gall³, S. Fuchs^{1*}

¹ Hamm-Lippstadt University of Applied Sciences
Marker Allee 76-78, 59063 Hamm, Germany

² Faculty of Chemistry and Chemical Biology, TU Dortmund University
Otto-Hahn-Straße 6, 44227 Dortmund, Germany

³ German Textile Research Center Nord-West GmbH
Adlerstraße 1, 47798 Krefeld, Germany

* Phone: +49 2381 8789-841; Email: Sabine.Fuchs@hshl.de

INTRODUCTION

Due to their low density and high impact resistance, transparent thermoplastic polymers such as poly(methylmethacrylate) (PMMA) represent important alternatives for glass in the electronics, construction and mobility sectors (1). However, finding suitable flame retardants which maintain the materials' optical properties remains a challenge (2). Common flame retardants can pose ecological risks and often impair the mechanical and especially the optical properties of the polymers. For economical and ecological reasons, silica nanoparticles (NPs) were identified as potentially suitable carrier materials for the immobilization of flame retardants based on phosphorus, which could be used in transparent thermoplastics (2, 3).

In this talk the incorporation of phosphonate-(co-)polymers as well as the corresponding functionalized silica NPs into PMMA via lab-scale mini extrusion will be presented. The PMMA compounds are characterized with respect to their optical (clarity, haze), thermal, and flammability properties. Furthermore, the analyses of the gas phase products during thermal degradation and the condensed phase after UL-94 vertical burning test are discussed to provide insights into a potential flame retardation mechanism.

EXPERIMENTAL

Materials

PMMA (Diakon[®] CMG 302, Lucite International Alpha B.V.) was used as powder made from commercial granulate. The RAFT-polymers (RP) and RP-functionalized silica NPs (example shown in Fig. 1) with phosphonate units were synthesized and characterized in the group of Weberskirch at TU Dortmund University.

Preparation of PMMA–RP and PMMA–RP-silica NP compounds

Finely ground PMMA was mixed with 20 wt.% of RP or RP-silica NP additive and compounded at 230 °C and 45 rpm using a lab-scale mini twin-screw extruder. Mini injection molding was performed using a cylinder temperature of 265 °C, a mold temperature of 100 °C, and a pressure of $p = 500$ bar (optical disk; $d = 20$ mm, $h = 1.5$ mm) or $p = 800$ bar (UL-94 vertical test bar; 120 mm x 12.7 mm x 1.6 mm).

Physico-chemical characterization of PMMA–RP and PMMA–RP-silica NP compounds

Clarity was evaluated qualitatively using 3D-printed disk holders with different heights ($d = 1, 2, 3, 4$ and 5 mm) placed on a checkered mat. Transmittance measurements were carried out using a UV-vis spectrometer with and without integration sphere (for haze index).

Thermal stability was determined by TGA. Flammability tests were carried out according to DIN EN 60695-11-10 (UL-94 vertical test). Pyrolysis- and EGA-GC-MS were

employed for gas phase analyses of the thermal degradation products. Burned UL-94 vertical test bars were characterized by microscopy, REM, IR, XPS, SEC and elemental analysis.

RESULTS AND DISCUSSION

Selected RP(-silica NP) additives show good compatibility with PMMA. The resulting compounds with RP-silica NPs exhibit drastically reduced haze and better clarity at 20 wt.% additive loading (Fig. 1) compared to PMMA with 5 wt.% unfunctionalized silica NPs.

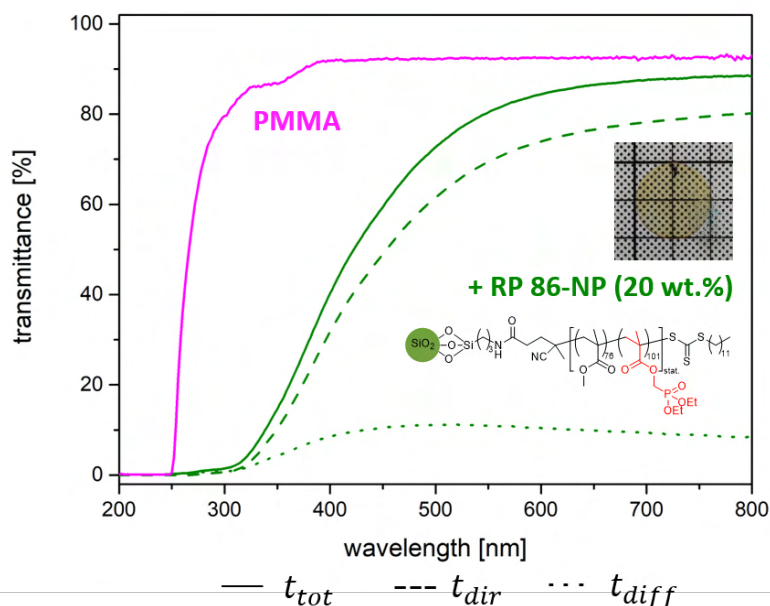


Fig. 1 Transmittance curves of PMMA and a PMMA–RP-silica NP compound (with 20 wt.% RP 86-NP). Photo: Optical disk made of the PMMA–RP 86-NP compound (d = 20 mm, h = 1.5 mm). t_{tot} : total transmittance, t_{dir} : direct transmittance, t_{diff} : diffuse transmittance.

All investigated PMMA–RP and PMMA–RP-silica NP compounds with esterified diethylphosphonate show a common behavior during UL-94 vertical burning test at 20 wt.% additive loading (< 10 s afterburning times; burning dripping during first burning; V-2 classified). GC-MS analyses under pyrolysis and EGA conditions suggest a gas phase activity due to esterified diethylphosphonate. The characterization of the condensed phase of different burned materials points to the formation of a thin phosphorus- and oxygen-rich protective layer. The results show that the investigated PMMA–RP-silica NP compounds could be potentially suitable for optical applications, under the condition that the flame retardant efficiency of these novel phosphonate-based additives can be enhanced.

Acknowledgment

This work is funded by the German Federal Ministry of Economics and Climate Protection (BMWK) through AiF as part of the Industrial Cooperative Research (IGF) program (No 22352 N).

References

- 1) N. Deka, A. Bera, D. Roy, P. De, ACS Omega, **7**, 36929 (2022)
- 2) C. Yi, C. Xu, N. Sun, J. Xu, M. Ma, Y. Shi, H. He, S. Chen, X. Wang, ACS Appl. Polym. Mater., **5**, 846 (2023)
- 3) A. Dang, S. Ojha, C.M. Hui, C. Mahoney, K. Matyjaszewski, M.R. Bockstaller, Langmuir, **30**, 14434 (2014)

Mechanistic studies on processing and fire behavior of a new cellulose-based flame retardant in polypropylene

A. Polster¹, M. Kaplan², M. Ciesielski², C. Getterle¹, S. Fuchs¹, H.-O. Fabritius^{1*}

¹ Hamm-Lippstadt University of Applied Sciences

Marker Allee 76-78, 59063 Hamm, Germany

² Fraunhofer Institute for Structural Durability and System Reliability LBF

Schlossgartenstraße 6, 64289 Darmstadt, Germany

* Phone: +49 2381 8789-850; Email: helge.fabritius@hshl.de

INTRODUCTION

Current flame-retardant solutions for plastics are either achieved by addition of low-molecular, halogenated or phosphorus-containing flame retardants. These additives can migrate in the polymer and are persistent, bioaccumulative and sometimes even toxic in the environment. Additionally, they are regarded as non-sustainable since they are mostly synthesized from fossil raw materials. As a result, environmentally friendly, toxicologically harmless and more sustainable alternatives are under investigation to find functional and safe replacements for problematic flame retardant additives. Such an example is a recently developed new phosphorus containing flame retardant based on renewable cellulose and sugar alcohols, which is environmentally compatible and toxicologically harmless, while maintaining a high flame retardancy efficiency (1,2). In this study, we investigate the distribution and structural morphology of this flame retardant in polypropylene with and without addition of compatibilizers and synergists before and after flame testing using scanning electron microscopy (SEM) combined with elemental mapping (EDX). The results are correlated with the fire behavior obtained by UL 94 V-testing to elucidate the compounding behavior and the basic mechanisms of fire retardancy

EXPERIMENTAL

Materials

Commercially available PP-co-PE (Moplen[®] RP 320 M, LyondellBasell) was used as matrix polymer for the compounds prepared for this study. The flame retardant (CeAcBu-PAHE) was synthesized at the Fraunhofer LBF in Darmstadt, Germany. Licocene[®] PP MA 7452 powder (Clariant Plastics & Coatings GmbH, Hürth, Germany) was used as compatibilizer and poly-tert-butylphenol disulfide (PDBS Vultac[®] TB 7, Arcema Inc.) was used as synergist.

Preparation of the PP-co-PE compounds

Eight sets of PP-co-PE compounds were prepared. Where applicable, 1 wt.% of compatibilizer and synergist were used, respectively. The concentration of the flame retardant was 4 wt.%. All formulations were compounded at 190 °C and 90 rpm using a lab-scale mini twin-screw extruder. UL-94 test bars (120 mm x 12.7 mm x 1.6 mm) were injection molded at a pressure of $p = 500$ bar with a cylinder temperature of 190 °C and a mold temperature of 75 °C.

Characterization of the CeAcBu-PAHE/PP-co-PE compounds

Flammability tests were carried out according to DIN EN 60695-11-10 (UL-94 vertical test). Unburned and burned UL-94 vertical test bars were both fractured and polished using a microtome equipped with a diamond knife to expose their cross sections. The obtained surfaces were analysed using SEM and EDX.

RESULTS AND DISCUSSION

SEM analysis showed that the flame retardant consists of mostly spherical particles with average diameters of 30-50 μm . In compounds with compatibilizer, the original particle size is retained with a uniform distribution and good adherence to the matrix (Fig. 1A). Without compatibilizer, large (>100 μm) rounded particles occur that adhere badly to the matrix, probably by fusion of the original particles during processing caused by different polarities (Fig. 1B). After flame exposure, the flame retardant particles processed with and without compatibilizer are smaller (Fig. 1C,D) and sometimes completely dispersed (Fig. 1C), indicating a mass loss possibly caused by migration of phosphorus into the PP matrix. Flame testing shows a synergistic effect of the flame retardant and PDBS. These combinations achieve a V-2 classification with the used low loading variations due to burning dripping. In conclusion, our results provide a detailed insight into the solid phase activity of the bio-based flame retardant CeAcBu-PAHE and open the path to a knowledge-based optimization of compound composition towards better performance.

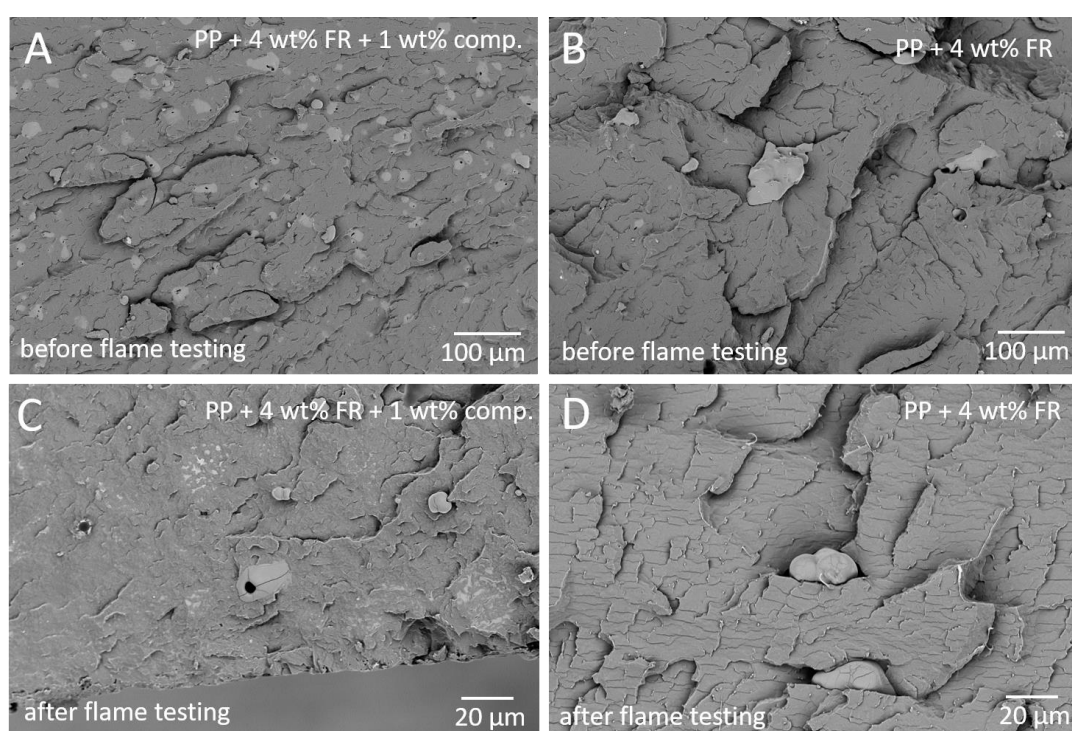


Fig. 1 Cross fracture surfaces of compounds before (A,B) and after the UL 94 V test (C,D) recorded using material sensitive backscattered electron contrast. The presence of compatibilizer (A,C) strongly influences distribution and morphology of the flame retardant in the compound both before and after burning.

Acknowledgment

This work was supported by the Federal Ministry of Education and Research (031B0719) and the *Fachagentur Nachwachsende Rohstoffe e.V.* (220NR032), Germany.

References

- 1) M. Ciesielski, E. Chalwatzis, R. Nezami, WO 20201/048335A1, (2021)
- 2) M. Kaplan, et al., *Polymers*, **15**, 3195, (2023)

EXPLORING BIODEGRADATION PROCESS TO ADVANCE BIOPLASTIC SUSTAINABILITY

**A. Marín^a, P. Feijoo^a, A. Jáuregui^a, E. Ventura^a, E. Sánchez-Safont^{ab}, J. Gámez-Pérez^{ab},
L.Cabedo^{ab} ***

^aGrupo de Polímeros y Materiales Avanzados (PIMA), Universitat Jaume I, 12071 Castelló (Spain) lcabedo@uji.es

^bCEBIMAT LAB S.L, ESPAITEC, Universitat Jaume I, Av. Vicent Sos Baynat s/n, 12071, Castelló (Spain)

The phenomenon of biodegradation refers to a natural process where materials are broken down into simpler molecules through the activity of living organisms. When it comes to polymeric materials, this involves transforming the carbon in the polymer into carbon dioxide in aerobic conditions and methane in anaerobic conditions, a process termed carbon mineralization.

This biodegradation only takes place in specific plastic materials that are chemically sensitive to the enzymatic activities of various microorganisms. Most plastic materials, however, do not possess this sensitivity, resulting in a much slower carbon transformation process that can take decades or even centuries in nature. This prolonged degradation rate poses a significant problem, as it causes plastic waste to linger in the environment and contribute to pollution. Conversely, biodegradable polymers, which degrade more rapidly and serve as a food source for microorganisms, present a significant technological opportunity for managing the end-of-life of plastic products, thereby reducing the pollution caused by plastic waste accumulation.

Despite the potential benefits, employing biodegradable polymers in plastic applications comes with significant challenges. These challenges include not only improving the performance of biodegradable polymers, which necessitates the development of new commercial materials and grades to meet market requirements, but also understanding and controlling the complexity of the biodegradation process itself. This process occurs inconsistently and is not yet fully understood or managed, making the handling of biodegradable polymer waste difficult, and the prediction of the time required for complete biodegradation in natural environments challenging.

The presentation will emphasize various studies on the biodegradation process applied to bioplastics, particularly those from the polyhydroxyalkanoates family. These studies will illustrate the technological importance of controlling this process for both waste treatment scenarios and plastic applications where no subsequent recovery is planned, such as plastics designed for direct environmental exposure.

The presentation will cover the variables that influence the biodegradation process and how these factors impact the end-of-life of plastics. Additionally, it will showcase results from biodegradation studies of plastic materials in different environments, highlighting the significance of both material type and environmental conditions. The ultimate goal is to improve the prediction of plastic biodegradation. Finally, the presentation will explore technological opportunities that arise from a better understanding and control of the biodegradation process.

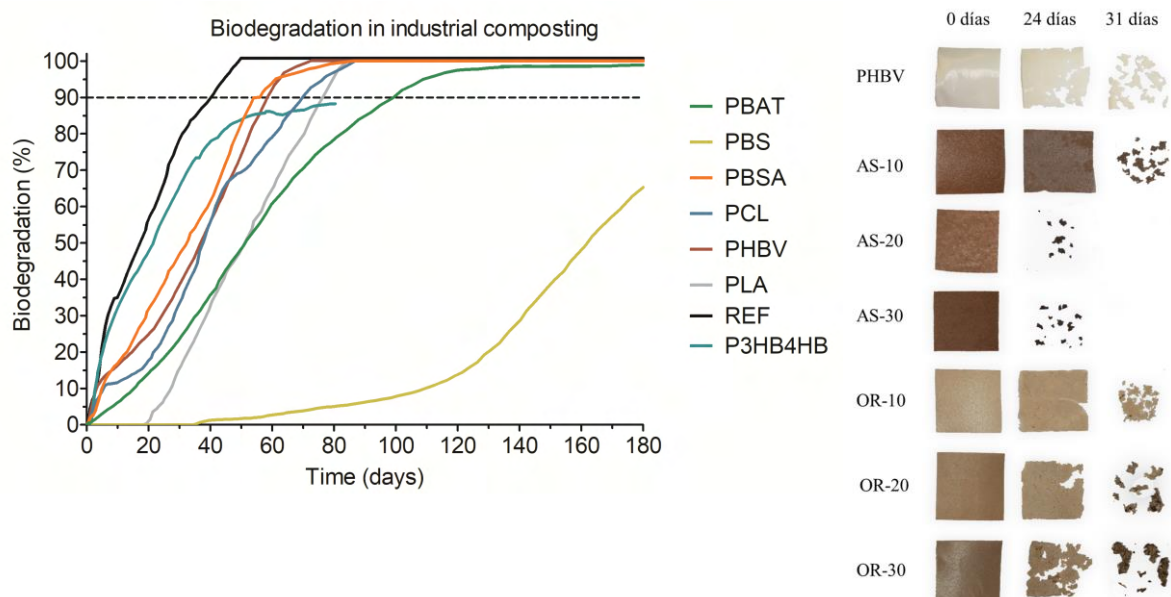


Fig. 1 Biodegradation kinetics of several commercial biopolyesters in industrial composting conditions according to ISO14855 (left). Disintegration of PHBV with and without lignocellulosic fillers (right).

Acknowledgment

This work presents results from several projects: TED2021-130211B-C31 funded by MCIN/AEI /10.13039/501100011033 and by the European Union NextGenerationEU/ PRTR, PID2021-128749OB-C32 funded by MCIN/AEI /10.13039/501100011033/ and by ERDF A Way of Making Europe, project INNEST/2023/69 AVI-COMBOOST funded by the Valencian Innovation Agency (AVI) and ERDF funds of the European Union, and UJI-2022-34 from Universitat Jaume I.

CARBONATATION OF [ETHYLENE-GLYCIDYL METHACRYLATE]-BASED COPOLYMERS WITH CARBON DIOXIDE AS REAGENT BY REACTIVE EXTRUSION: IMPACT ON POLYMERS BLENDS COMPATIBILIZATION

Bruno Guerdener,^{1,2,3} Virgile Ayzac,^{2,3} Paul Besognet,¹ Sébastien Norsic,¹ Vincent Monteil,³ Véronique Dufaud,³ Jean Raynaud,³ Yvan Chalamet¹ and **Véronique Bounor-Legaré**^{2*}

1. Université de Lyon, CNRS, Université Claude Bernard Lyon 1, INSA Lyon, Université Jean Monnet, UMR 5223, Ingénierie des Matériaux Polymères, F-42023 Saint-Etienne Cedex 2, France

*2. Université Claude Bernard Lyon 1, CNRS, INSA Lyon, Université Jean Monnet, UMR 5223, Ingénierie des Matériaux Polymères, F-69622 Villeurbanne Cedex, France

3. Univ Lyon, Université Claude Bernard Lyon 1, CPE Lyon, CNRS, UMR 5128, Catalyse, Polymérisation, Procédés & Matériaux (CP2M), 43 Bd du 11 novembre 1918, 69616 Villeurbanne, France.

bounor@univ-lyon1.fr

INTRODUCTION

The aim of the present study is to introduce CO₂ – containing moieties (e.g. cyclic carbonate functions), via carbonatation reactions, on polymers to modify their physicochemical characteristics. The carbonatation of semi-crystalline [ethylene-glycidyl methacrylate]-based polymers was achieved using carbon dioxide as a reagent and quaternary ammonium salts as organocatalysts to transform the polymers' epoxide pendant groups into cyclic carbonate moieties. A batch reactor allowed us to assess the kinetics, dependence on a catalyst and overall potential of this carbonatation. Subsequently, the reaction was transposed, for the 1st time, to reactive extrusion under CO₂ using a dedicated co-rotating twin-screw extruder to allow for CO₂ containment within the polymer melt. Finally, the in situ compatibilization of a HDPE/PC blend was performed through reactive extrusion by comparing the efficiency of three different [ethylene – glycidyl methacrylate] (E-GMA) based terpolymers and their carbonated derivatives (epoxide pendant group from glycidyl methacrylate partially converted to its cyclic carbonate derivative).

EXPERIMENTAL

Materials

Several organocatalysts (from onium salts with ammonium or phosphonium halides, ionic liquids to organic bases) were tested in the carbonatation reaction in batch and in extruder. The six different [ethylene – glycidyl methacrylate] based initial and obtained polymers structures are reported in figure 1.

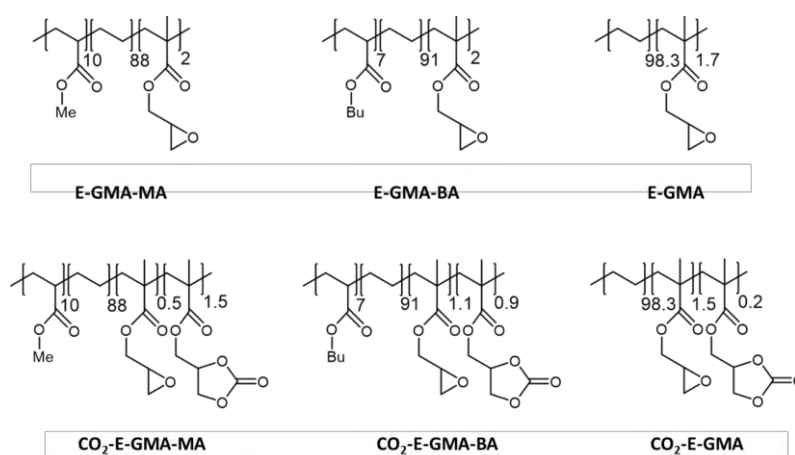


Figure 1. Initial and carbonated polymers created and used as compatibilizers.

Preparation and characterization

The E-GMA copolymer and the catalyst were feed at a throughput of 2 kg/h (1.1 mol/h of glycidyl methacrylate) and 0.083 mol/h (7.5 mol%) respectively in the first barrel. Under optimal conditions, the temperatures profile were 60, 120, 150, 150, 150, 150, 150, 150 and 150 °C, respectively. The die was also heated to 150°C. The screw speed was 150 rpm. When the flow of the extruded polymer was stabilized, the CO₂ was continuously injected in the third barrel by a Linde pump (DSD 500). The pressure and the throughput were regulated by the pump.

Mechanical properties, morphologies and spectroscopic characterization of the HDPE/PC blends compatibilized with non-carbonated and carbonated compatibilizer was used to determine the influence of the compatibilizers structure and to identify the nature of the interaction at the interface of the HDPE and PC phases.

RESULTS AND DISCUSSION

Among the results, the influence of extrusion temperature and CO₂ pressure were studied on the carbonation of E-GMA-MA (Figure 2). An increase in temperature led to an increase in carbonate yield. The optimum pressure was 4.0 MPa, which is probably a good compromise between maximal CO₂ solubilization/availability for reaction and avoidance of phase separation in the melt. At this pressure, an increase of 10 °C led to an average yield increase of 15%.

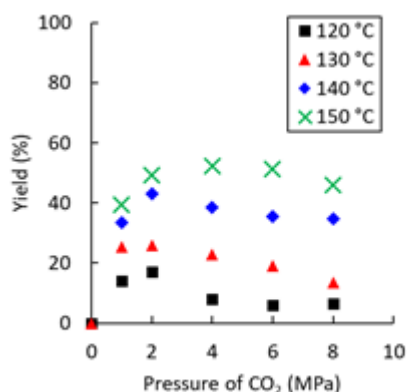


Figure 2 : Influence of temperature and CO₂ pressure. reaction conditions: 2 kg/h of E-GMA-MA, 18 g/h of TBAB (5 mol%), 150 °C, 150 rpm. Yield determined by IR-ATR using a calibration curve

The addition of a carbonated compatibilizer lead to a significant improvement of the compatibilization of the HDPE/PC blend (figure 3).

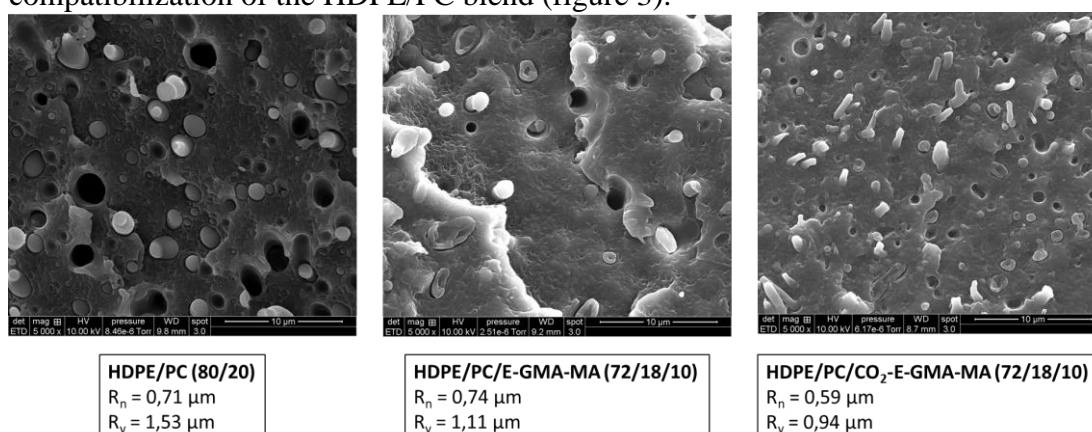


Figure 3: Morphologies of the HDPE/PC blend with different compatibilizer.

Acknowledgment

The authors would like to thank the Institut Carnot Ingénierie@Lyon for financial support, , Axel'One Campus for the NMR analyses and "La plateforme lyonnaise de caractérisation des Polymères" for the SEC analyses.

Thermal degradation of an aromatic amine cured epoxidized linseed oil vitrimer

S. Serrano^{a*}, S. Berlioz^a, H. Hajjoul^b, E. Richaud^c, P. Carriere^a,

^a*Université de Toulon, Laboratoire MATériaux, Polymères, Interfaces et Environnement Marin (MAPIEM), CS 60584, 83 041 Toulon Cedex 9, France.*

^b*Université de Toulon, Institut Méditerranéen d'Océanographie (MIO), CS 60584, 83 041 Toulon Cedex 9, France.*

^c*Laboratoire PIMM, Arts et Métiers ParisTech, CNRS, Cnam, 151 boulevard de l'Hôpital, 75013, Paris, France.*

INTRODUCTION

The study and utilization of bio-based epoxy materials, particularly those derived from epoxidized vegetable oils, are gaining increasing interest[1]. However, the adoption of these types of epoxy resins is limited by the lack of understanding regarding their aging resistance. This is particularly true for their use with aromatic diamines, a case that is not well-documented, in contrast to their use with anhydride hardeners[2]. To address this issue, various networks were cross-linked based on epoxidized linseed oil (ELO) combined with a vitrimeric aromatic diamine: 4,4'-dithiodianiline (AFD).

Fluorescence spectroscopy is an emerging characterization technique for the study of polymer materials, both for the characterization of cross-linking and for the monitoring of aging[3-4]. This presentation will focus on its application for monitoring the thermo-oxidative aging of epoxy-amine films and will highlight the specific conditions required for its effective use in this context.

EXPERIMENTAL

Materials

This study focused on monitoring the thermo-oxidative aging of free-standing thin films of aromatic epoxy-diamines (20 to 40 μm thick) that were cross-linked at stoichiometry according to an optimized curing cycle and obtained through a compression molding process.

Physico-chemical caractérisation & fluorescence measurement.

The evolution of the physicochemical properties of the films was measured using various characterization techniques:

The chemical properties of the films were monitored using transmission FTIR spectroscopy on a Bruker Invenio R system equipped with a nitrogen cooled high sensitivity MCT detector. The collected infrared spectra were processed by a decomposition method using Origin software.

The glass transition temperature (T_g) of the systems was monitored in parallel using a DSC 25(TAinstrument) in modulated mode and the mass loss of these systems was monitored using TGA-550 (TAinstrument).

The fluorescence of these thin films was measured using a Horiba Fluoromax spectrofluorometer equipped with a quartz lens holder to ensure the flatness of the thin layers.

The absorbance and reflectance of the thin films were measured with a Shimadzu UV-Vis 2600 spectrometer equipped with an integrating sphere to determine the refractive index spectra.

A model for correcting internal filter effects was then applied to the fluorescence data obtained.

RESULTS AND DISCUSSION

The aging studies revealed a distinct behaviour of these bio-based resins compared to traditional aromatic epoxy-amines based on DGEBA, induced by the presence of specific weak points in these resins. A notable difference is the presence of a methine group resulting from the reaction of non-glycidyl epoxies carried by the epoxidized vegetable oils.

Fluorescence spectroscopy experiments demonstrated that the application of this analytical method is subject to significant experimental biases that need to be controlled during aging: film flatness, water content, and, most importantly, the intrinsic absorbance of the films. The evolution of this absorbance, induced by aging, strongly influences the observed fluorescence. A method to correct this bias, often overlooked in published works on the subject, is proposed. However, it is limited by the technical capability to measure high absorbances in the UV range.

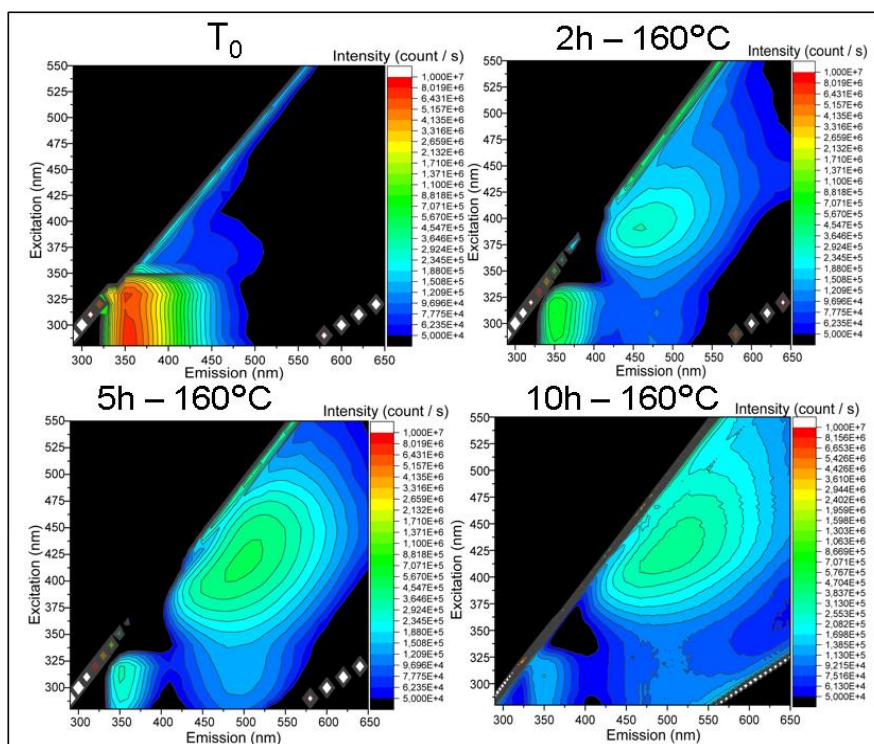


Fig. 1 – example of fluorescence and absorbance signal change of an epoxy-aromatic diamine during ageing under air at 160°C

These constraints limit the study of the intrinsic fluorescence of these systems and necessitate the use of specific fluorescence probes with excitations and emissions shifted towards the red, a region where the absorbance of epoxy-amines systems remains limited during aging.

References

- 1) Y.-Y. Liu, J. He, Y.-D. Li et al., “Biobased, reprocessible and weldable epoxy vitrimers from epoxidized soybean oil,” *Industrial Crops and Products*, vol. 153, p. 112576, 2020.
- 2) E. Richaud, A. Guinault, S. Baiz et al., “Epoxidized linseed oils based networks. Case of thermal degradation,” *Polymer Degradation and Stability*, vol. 166, pp. 121–134, 2019.
- 3) J. M. Nölle, C. Jüngst, A. Zumbusch et al., “Monitoring of viscosity changes during free radical polymerization using fluorescence lifetime measurements,” *Polymer Chemistry*, vol. 5, no. 8, pp. 2700–2703, 2014.
- 4) B. Hervé, G. Rapp, P.-O. Bussiere et al., “Use of fluorescent probes in supporting functional group analysis resulting from polymer ageing,” *Polymer Degradation and Stability*, vol. 177, p. 109167, 2020.

LIFETIME PREDICTION OF POLY (BUTYLENE ADIPATE/ TEREPHTHALATE) UNDER VARIOUS CLIMATE CONDITIONS

Yan Ye, Guoshuo Tang, Xiangze Meng and Rui Yang*

*Department of Chemical Engineering, Tsinghua University, Beijing 100084
yeyan23@mails.tsinghua.edu.cn

INTRODUCTION

As a biodegradable polymer, poly (butylene adipate/ terephthalate) (PBAT) has been widely used as mulch film. Accurately accessing the outdoor lifetime of mulch is critical for mulch-covering agriculture. Natural ageing and lab accelerated ageing are the two main approaches to estimate outdoor lifetime. The lifetime of PBAT varies under different climate conditions (1), while current lifetime prediction method takes great time and effort, and is incapable to work under various climate conditions (2).

In this work we proposed a quick and precise lifetime prediction method of PBATs under different climatic condition.

EXPERIMENTAL

Material preparation

PBAT were hot pressed into films with a thickness of $300 \pm 50 \mu\text{m}$. Dumbbell specimens were cut from the film and then experienced accelerated or natural ageing.

Ageing process

The accelerated ageing of PBAT samples was performed in a Xenon ageing chamber (Q-Sun Xe-3, Q-Lab, USA). Xenon lamps with a wavelength range of 295–800 nm were applied at the irradiance of 0.35 W/m^2 at 340 nm. The black panel temperature was 55°C and the air temperature was 40°C . The total ageing time was 30 days.

The outdoor natural ageing were performed in Beijing, China (116°E , 39°N) during July to September in 2021 and 2022.

Characterization

The tensile tests of PBAT during ageing were carried out using a universal testing machine at 50 mm/min . The average of five tests was reported.

The gel content was tested by Soxhlet extraction in chloroform.

Molecular weights were determined using gel permeation chromatography.

The CO_2 generation rate of PBAT under various combinations of solar light, temperature, and humidity was determined using the Comprehensive Ageing Evaluation System (CAES) developed in our lab (3).

Lifetime prediction model development

Since CO_2 is the final degradation product of PBAT, the CO_2 generation rate v_E was tested in CAES under different combinations of temperature T , solar irradiance I and humidity H . The ***environmental condition equation*** to show the response of PBAT to environmental factors were thus established:

$$v_E = A \cdot e^{\frac{E_a \times 10^3}{R \cdot T}} \cdot I^m \cdot H^n$$

Then, the ***ageing status correlation*** between the CO_2 generation rate and the tensile strength of PBAT during the ageing process was established:

$$\ln\left(\frac{TS_t}{TS_0}\right) = -\frac{k_1}{k_2} \cdot (v_t - v_0)$$
$$v_t - v_0 = k_3 \cdot (v_E \cdot t)$$

Finally, the *lifetime prediction model* was established to show how the tensile strength of PBAT decrease with time at a given environmental condition:

$$\ln\left(\frac{TS_t}{TS_0}\right) = -c \cdot \left[\exp\left(-\frac{E_a \times 10^3}{R \cdot T}\right) \cdot I^m \cdot H^n \right] \cdot t$$

RESULTS AND DISCUSSION

Based on the lifetime prediction model, we can calculate the space and time distribution of ageing rate of PBAT in China. Among all the capital cities, the highest PBAT ageing rate was in Urumqi, Xinjiang Province, nearly twice (191%) than that of Chongqing, which was the city with the lowest ageing rate in the map.

These results facilitated a site-specific prediction of the service life of PBAT, and enables quantitative prediction of the space and time distribution on ageing rates of PBAT in China with corresponding meteorological data, as well as quantitative comparison between any accelerated and natural ageing.

This work cut down the time and money cost of lifetime prediction of PBAT greatly and enables a timely response to mulch film deployments in various climate regions. Moreover, this lifetime prediction method is a common strategy and can be used to other polymer materials for outdoor applications.

Acknowledgment

This study was funded by National Key Research and Development Programs of China (nos. 2021YFD1700700 and 2021YFC2103603).

References

- 1) Hayes, D. G. *et al.*, Effect of diverse weathering conditions on the physicochemical properties of biodegradable plastic mulches. *POLYM TEST* **62** 454 (2017).
- 2) Xie, J. *et al.*, Prediction Model of Photodegradation for PBAT/PLA Mulch Films: Strategy to Fast Evaluate Service Life. *ENVIRON SCI TECHNOL* **56** 9041 (2022).
- 3) An, Z., Xu, Z., Ye, Y. & Yang, R., A rapid and highly sensitive evaluation of polymer composite aging with linear correlation to real-time aging. *ANAL CHIM ACTA* **1169** 338632 (2021).

WASP NEST INSPIRED BIO-BASED FLAME-RETARDANT

B. Schwind, J. Stahlmecke, M.-J. Wesemann, T. Rust, S. Fuchs and H.-O. Fabritius

Hamm-Lippstadt University of Applied Sciences, Marker Allee 76-78, 59063 Hamm, Germany

bertram.schwind@hshl.de

INTRODUCTION

Evolution has brought forth a lot of archetypes that adapted to fire prone habitats and survive forest fires. This is not limited to pyrophytes like e.g. *Quercus suber*, which is also widespread in Sicily, but even animals have notable fire-adaptive traits (1). For example, *Vespula germanica* produces a paper-like composite of their saliva and chewed wood particles to build its nests. The paper-like nest material shows low flammability and a good structural integrity of the charred material, which can mainly be attributed to the protein-rich saliva. This makes wasp nests an interesting material in terms of flame retardancy, since biomolecules are in the focus as flame retardant additives for polymers (2).

Therefore, we mimicked wasp paper for systematic analyses of the influence of protein content on the flame retardancy. Additionally, we investigated phosphorous as a possible synergist and phosphorylated gluten to enhance the found flame retardancy, since reactive flame retardants containing phosphorus are increasingly successful as halogen-free alternatives for various polymeric materials and applications (3).

EXPERIMENTAL

Materials

Wasp nests were collected in the surroundings of our Campus after the wasps abandoned them. Wood particles were kindly provided by JELU-WERK J. Ehrler GmbH & Co. KG. Commercial gluten, phytic acid and phenyl phosphonic acid, for the phosphorylation were obtained from commercial sources.

Preparation

The wasp nest paper was cleaned from dust and residues and dried before flame testing. Biomimetic wasp papers were prepared from a gluten dispersion, which was used to mimic the protein-rich ant saliva. The wasp chewed wood particles were substituted by wood particles from JELU-WERK. The phosphorylation of gluten was accomplished via multiple synthesis routes with two different sources of phosphorous: phytic acid and phenyl phosphonic acid. Also, from the phosphorylated gluten biomimetic papers were crafted.

Characterization

All samples (biological and synthetic) were flame tested and investigated by thermo gravimetric analysis coupled to a Fourier transform infrared spectrometer (TG-FTIR) to classify the combustion behavior, analyze the evolving gases, and find possible synergies. Additionally, the samples as well as their burnt residues were structurally characterized by light-microscopy as well as scanning electron microscopy. The gluten phosphorylation was verified by ATR absorption spectroscopy.

RESULTS AND DISCUSSION

The burning behavior of wasp paper of *Vespula germanica* was successfully reproduced with synthetic wasp papers based on gluten and wood particles. Figure 1a and b shows the thermal decomposition of the biomimetic paper, depending on gluten content. TG-FTIR (Fig. 1c) shows the release of non-combustive gases H₂O, CO₂ and NH₃, depending on gluten amount. The release of non-combustive gases and charring are also typical

mechanisms used for the flame protection of polymeric materials (2) and wood plastic composites (WPC), where developing halogen-free flame retardancy is still a challenge (4). Unfortunately, for achieving a self-extinguishing behavior of our biomimetic paper, large amounts of gluten were necessary, which would be unsuitable for technical applications. However, this amount could be strongly reduced by a modification of the gluten with phosphorus, which is also a strong indication for synergistic effects between protein and phosphorous.

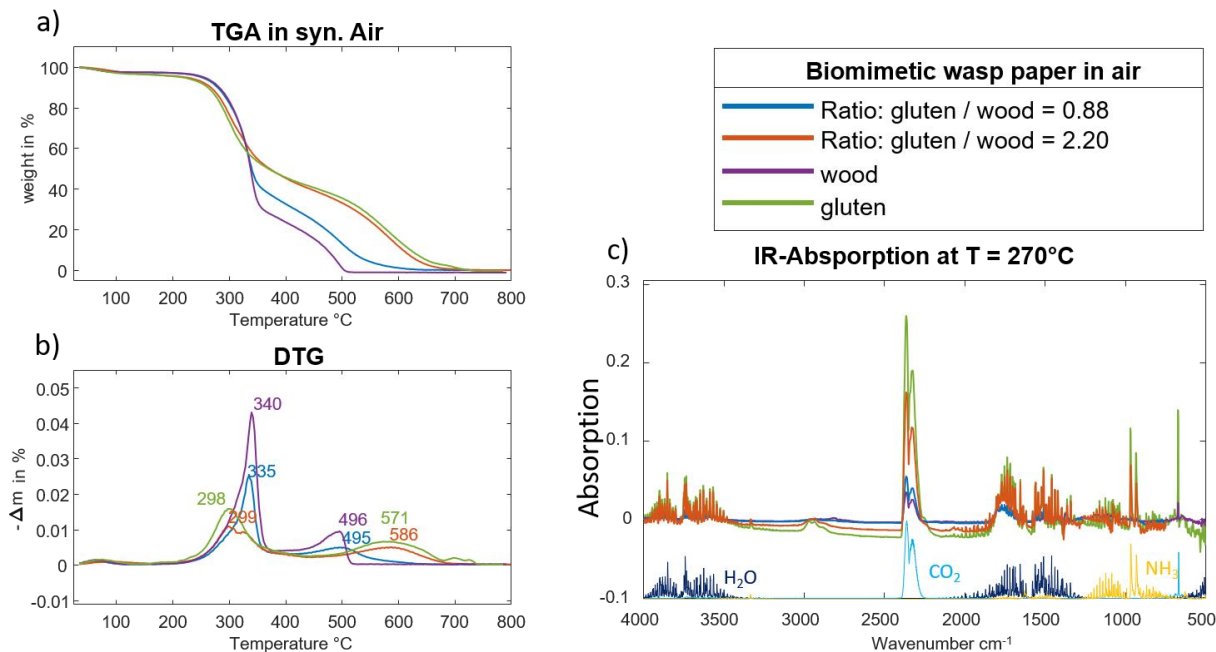


Figure 1: TGA and FT-IR analysis of biomimetic wasp paper with different amounts of gluten in comparison to the pure materials. (a) normalized TGA curves, (b) corresponding numerical derived DTG curve, with inserted peak temperatures (c) FTIR spectra at 270°C normalized to the weight change Δm of the corresponding TGA; CO₂, NH₃ and H₂O spectra are inserted as references at the bottom.

In conclusion the wasp nest material inspired a bio-based flame-retardant. The phosphorylation of gluten could be an interesting approach incorporating synergistic effects between protein and phosphorous into one flame retardant. Further development could bring forth a sustainable flame retardant, which might be applicable in WPCs and other polymers.

Acknowledgment

This project is funded within the “FF-HAW Kooperation” program by the Ministry of Culture and Science NRW

References

- 1) McGranahan, D.A., Wonkka, C.L. *Ecology of Fire-Dependent Ecosystems: Wildland Fire Science, Policy, and Management* (1st ed.). CRC Press. **2020**.
- 2) Villamil Watson, D.A., Schiraldi, D.A. *Biomolecules as Flame Retardant Additives for Polymers: A Review*. *Polymers* **2020**, 12, 849.
- 3) Schartel, B. *Phosphorus-based Flame Retardancy Mechanisms—Old Hat or a Starting Point for Future Development?* *Materials* **2010**, 3, 4710-4745.
- 4) Yin, H, Sypaseuth, FD, Schubert, M, Schoch, R, Bastian, M, Schartel, B. *Routes to halogen-free flame-retardant polypropylene wood plastic composites*. *Polym Adv Technol*. **2019**; 30: 187-202.

Radical Ring-Opening Copolymerization of Cyclic Ketene Acetals: A New Route for the Synthesis of Degradable and Functional Polymers for Cancer Therapy

**Theo Pesenti^{1,2}, Chen Zhu¹, Daniel Domingo-Lopez¹, Seika Ishii¹, Matthew I. Gibson³,
Samir Messaoudi⁴, Julien Nicolas¹**

¹ Université Paris-Saclay, CNRS, Institut Galien Paris-Saclay, 92296 Châtenay-Malabry, France

² Université Claude Bernard Lyon 1, INSA Lyon, Université Jean Monnet, CNRS UMR 5223, Ingénierie des Matériaux Polymères, Lyon, France

³ Department of Chemistry, Division of Biomedical Sciences, Warwick Medical School, University of Warwick, Gibbet Hill Road, CV4 7AL, Coventry, U.K.

⁴ Université Paris-Saclay, CNRS, BioCIS, 92296 Châtenay-Malabry, France

theo.pesenti@insa-lyon.fr ; julien.nicolas@universite-paris-saclay.fr

INTRODUCTION

Vinyl polymers represent more than half of the polymers produced in Europe. Their wide range of composition has made them indispensable materials in many daily and specialty applications. Although their high chemical and physical resistance can be a real advantage in some applications, their full carbon skeleton also makes them non-degradable. To meet environmental challenges and to allow their use in the biomedical field, it is urgent to find solutions to make them (bio)degradable. By their great versatility, vinyl polymers could then diversify the arsenal of degradable polymer materials in the field of polymer nanoparticles used in cancer therapy.

For several decades, cyclic ketene acetals (CKAs) have enjoyed tremendous success in making vinyl polymers degradable. Due to their ability to form labile ester bonds by radical ring-opening copolymerization (rROP) with numerous vinyl monomers, a wide spectrum of copolymers has been synthesized and studied. Recently, the copolymerization between 2-methylene-1,3-dioxepane (MDO) and vinyl ethers (VE) has allowed for the first time to obtain polyester-like P(CKA-*co*-VE) copolymers (*i.e.*, with >70 mol.% MDO in the final copolymer). These polymers are of great interest because of their degradation under mild conditions, due to their structure close to the traditional gold standard polyesters, while being easily functionalized via VE monomer units. In this work, we aimed at extensively describing this new class of copolymers to fully exploit their potential for biomedical applications, in particular through the problematic of synthesizing glycosylated CKA-based copolymers. Indeed, such copolymers have been scarcely described so far, due to the inherent challenges of using CKAs with nucleophilic moieties. That's why, we have also focused on developing solutions to overcome some CKAs limitations (*e.g.*, hydrophobicity, nucleophilic- and acid-sensitivity) in order to expend the scope of possibilities offered by these monomers.

EXPERIMENTAL

Synthesis of copolymers and preparation of nanoparticles

The three CKAs used in this study (MDO, BMDO, MTC) were synthesized as reported.^{1,2,3} P(MDO-*co*-VE) and P(MTC-*co*-VE) copolymers were synthesized by free-radical copolymerization (FRP) of the CKA with a VE derivative (typical initial feed ratios: $f_{\text{CKA},0} = 0.9$; $f_{\text{VE},0} = 0.1$) in bulk, initiated by diethylazobisisobutyrate at 70-90 °C for 8-24 h. P(CKA-*co*-MI) copolymers were synthesized by FRP of the CKA with a maleimide (MI) derivative (typical initial feed ratios: $f_{\text{CKA},0} = f_{\text{MI},0} = 0.5$) in toluene, initiated by azobisisobutyronitrile (AIBN) at 85 °C for 6 h. BMDO-based terpolymers were synthesized by RAFT polymerization in toluene, using CPADB as the chain-transfer agent, initiated by AIBN at 70 °C for 16 h.

In a typical preparation of nanoparticles, copolymer was dissolved in THF then added dropwise in Milli-Q water under high magnetic stirring. THF was then evaporated.

Degradation studies

For enzymatic degradation study, nanoparticles aqueous suspensions were reacted with lipases at 37 °C for 1 day under orbital shaking. For accelerated degradation study, copolymers were solubilized in THF then mixed with a mixture of NaOH in methanol for 1 day under magnetic stirring. For long-term hydrolytic degradation study, copolymers were dispersed in phosphate buffered saline (pH 7.4) at 37 °C under orbital shaking for 1 year.

RESULTS AND DISCUSSION

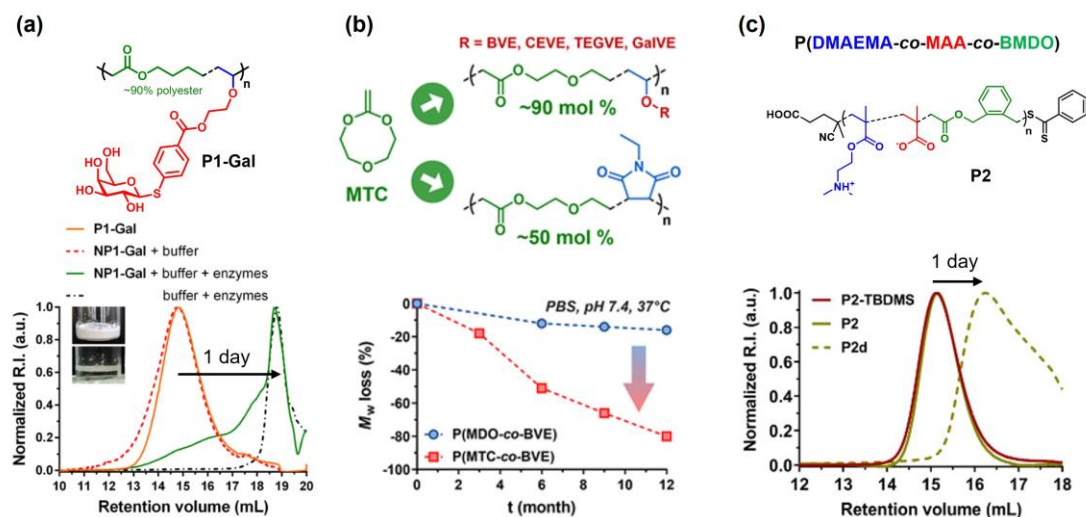


Figure 1. Schematic representation of synthesized CKA-based polymers in this study and their associate SEC traces (or mass loss) upon degradation ((a) enzymatic degradation, (b) long-term hydrolytic degradation, (c) accelerated degradation).

Glycosylated P(CKA-co-VE) copolymers¹ (Fig. 1a) were readily formulated into surfactant-free nanoparticles which are stable for months. The nanoparticles can be significantly degraded by the action of enzymes (lipases) upon 1-day incubation (mass loss > 90 %) unlike the majority of other reported CKA-based systems. With anticancer drug delivery applications in mind, we have showed that both nanoparticles and their degradation products exhibited limited cytotoxicity toward two healthy cell lines.

The degradation kinetics of P(CKA-co-VE) and P(CKA-co-MI) copolymers could be easily tuned by substituting hydrophobic CKAs (MDO or BMDO) by the less hydrophobic MTC². The newly synthesized MTC-based copolymers have been demonstrated to undergo significant hydrolysis unlike their hydrophobic counterparts (or other reported CKA-based systems) which may exhibit low-to-no hydrolysis in such mild conditions (Fig. 1b).

Finally, we have successfully synthesized degradable P(DMAEMA-co-MAA-co-BMDO) terpolymers³ (Fig. 1c). In addition to their cryoprotective properties, they are one of the very few examples of polymers composed of both CKA and carboxylic acids. Our strategy relied on using a silyl ester-protected methacrylic acid to circumvent the acid-sensitivity of BMDO while preventing any degradation of the main polymer chains upon deprotection yielding to the degradable polyelectrolyte.

Acknowledgment

This work has been financially supported by the ANR NanoCardioROP (ANR-15-CE08-0019) and the French Ministry of Research.

References

- 1) Pesenti, Théo, *et al. Biomacromolecules* 23.9 (2022): 4015
- 2) Pesenti, Théo, *et al. Biomacromolecules* 24.2 (2023): 991
- 3) Pesenti, Théo, *et al. ACS Macro Letters* 11.7 (2022): 889

Poly(isopropylacrylamide) homopolymer, copolymer and aerogel: thermosensitive behavior and ageing effect

Camille MATHIEU^{1,2} ; Samar ISSA¹ and Emmanuel RICHAUD²

¹ Ecole de Biologie Industrielle - EBI, UPR EBInnov®, 49 Avenue des Genottes CS90009 95895, Cergy-Pontoise, France, camille.mathieu@hubebi.com and s.issa@hubebi.com

² Laboratoire PIMM, Arts et Métiers Institute of Technology, CNRS, Cnam, HESAM Université, 151 boulevard de l'Hôpital, 75013 Paris, France, camille.mathieu@ensam.eu and emmanuel.richaud@ensam.eu

INTRODUCTION

Poly(N-isopropylacrylamide) (PNIPAm) is a widely developed with biomedical applications including drug delivery system (DDS) due to its thermoresponsive properties close to body's temperature [1]. In aqueous medium, PNIPAm thermosensitive behavior is related to the equilibrium between hydrophobic (isopropyl) and hydrophilic (amide) groups in interaction with water molecules through hydrogen bonding. It is widely reported that typical degradation process of polyacrylamide derivatives follows a conversion into smaller units by chains scissions and then degradation into monomers or dimers. To our knowledge, only few reports describe PNIPAm's thermal degradation [2], [3]. With increased research in pharmaceutical applications, it is quite interesting to explore the thermal and chemical stability of these polymers because of the well-known neurotoxicity of N-isopropylacrylamide (NIPAm) monomers [4]. The purpose of this study is to explore the thermal ageing of PNIPAm at different stages, long term stability at 120°C under air and short term stability at 250°C under N₂. Since addition of acrylic acid (AAc) and N,N'-methylene diacrylamide (BIS) are widely described in order to obtain DDS [5], the effect of including co-monomers is also analyzed.

EXPERIMENTAL

Materials

PNIPAm and Poly(NIPAm-co-AAc) (15mol%) are purchased from Sigma-Aldrich and used as received. Hydrogels are synthesized by free-radical polymerization of NIPAm using 1.5mol% and 0.5mol% BIS as cross-linking agent, ammonium peroxydisulfate and N,N',N'-Tetra-methyl ethylene - diamine (TEMED) as initiators in aqueous medium [5] adapted.

Preparation of samples

Following the synthesis, all samples are immersed in deionized water for 7 days with daily renewed water to remove unreacted starting materials. Aerogels are obtained with drying samples in ventilated oven at 40°C for 48 hours. Before all characterizations on PNIPAm, Poly(NIPAm-co-AAc) and PNIPAm's aerogel samples are dried at 120°C for 3 hours and at 80°C under vacuum-bell with silica gel desiccant overnight.

Characterizations

Spectra of solid polymer samples are collected on a Fourier Transform Infrared Spectrometer (FTIR Frontier, Perkin Elmer) in a range of 4000 - 650 cm⁻¹. Weight average molecular weight (M_w) estimation are analyzed by GPC (GPC, Malvern Corporation, Viscotek T3000 - T6000) using 2 mg.mL⁻¹ in tetrahydrofuran (THF). Thermal degradation is achieved on 5 mg solid polymers at 250°C under N₂ and under O₂ with thermogravimetric analysis (ATG Q500, TA Instruments). Cloud point temperature (T_{cp}) of solutions or Volume phase transition temperature (VPTT) are studied in water with a UV-Spectrometer (UV-Vis Lambda 35, Perkin Elmer) equipped with a heating device. The utilized wavelength was 651 nm, and the heating rate is 0.3°C.min⁻¹ or 0.015°C.min⁻¹.

RESULTS AND DISCUSSION

In preliminary approach, aged PNIPAm's at 120°C (until 120 days) under air are stable with slight chemical vibration modifications are observed by FTIR. However, macromolecular modifications, such as chain scission, are revealed by Gel Permeation Chromatography (GPC).

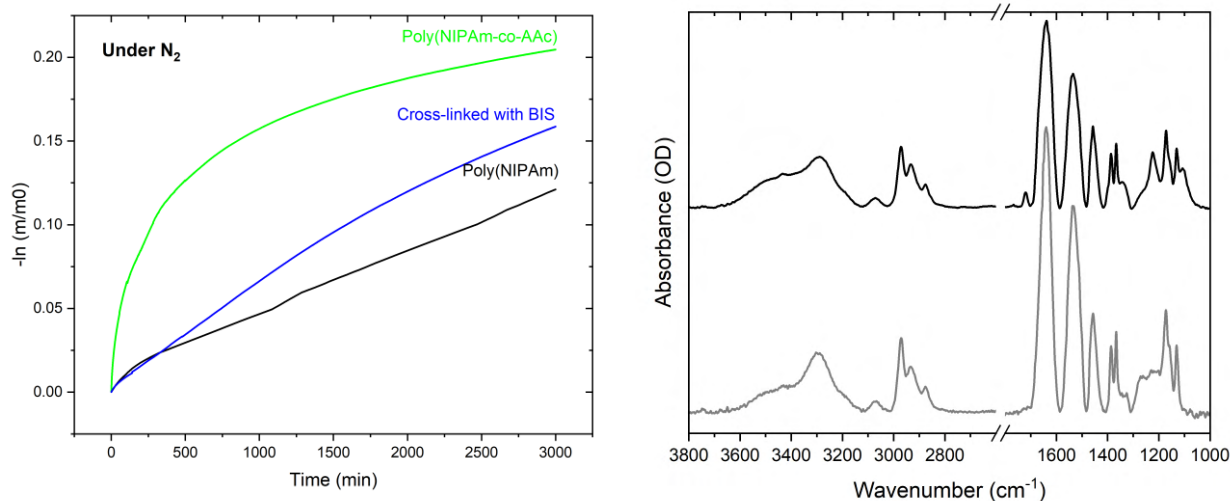


Fig. 1a) Stability of PNIPAm-based polymers under 250°C for 50 hours; b) FTIR Spectra of PNIPAm without any ageing (grey) and PNIPAm (black) after an ageing at 250°C for 50 hours under N₂.

TGA was then used for the evaluation of thermal stability as well as the effect of either the BIS-crosslinking or AAc co-monomer addition to the PNIPAm's. Fig 1a. shows that the homopolymer PNIPAm as well as the cross-linked PNIPAm samples follow first order kinetics probably due to a unique reaction mechanism. Different kinetics are observed with the copolymer, where the addition of AAc co-monomer may have induced additional mechanisms (Fig. 1a).

After 50 hours-ageing under a higher temperature, at 250°C (Fig. 1b), new FTIR absorption peaks appear at 1720 cm⁻¹, 1070 cm⁻¹ and 1110 cm⁻¹ corresponding to products of PNIPAm's thermal oxidation. A clear -C=O function stretching vibration at 1720 cm⁻¹ is observed and can be explained in terms of degradation mechanism. The effect of co-monomer on the T_{cp} responsiveness is also analyzed and appears at 29.5°C, 34°C and 35.5°C for Poly(NIPAm), cross-linked PNIPAm and Poly(NIPAm-co-AAc) respectively. Ageing seems to shift T_{cp} towards higher temperatures. The research will present a possible explanation correlating the chemical and macromolecular properties to the PNIPAm homo and copolymer macroscopic thermosensitive behavior.

REFERENCES

- [1] A. Halperin, M. Kröger, and F. M. Winnik, "Poly(*N* -isopropylacrylamide) Phase Diagrams: Fifty Years of Research," Dec. 2015, doi: 10.1002/anie.201506663.
- [2] H. G. Schild, "Thermal decomposition of PNIPAAm: TGA–FTIR analysis," 1996, doi: 10.1002/(SICI)1099-0518(199608)34:11<2259::AID-POLA21>3.0.CO;2-D.
- [3] F. Biryán, A. M. Abubakar, and K. Demirelli, "Product analysis, electrical and dielectric properties depending on thermal influence of poly(N-isopropyl acrylamide)/graphite-filled composite," 2018, doi: 10.1016/j.tca.2018.09.009.
- [4] M. A. Cooperstein and H. E. Canavan, "Assessment of cytotoxicity of (N-isopropyl acrylamide) and Poly(N-isopropyl acrylamide)-coated surfaces," Dec. 2013, doi: 10.1186/1559-4106-8-19.
- [5] Jacinthe Lapointe, "Fabrication et caractérisation d'hydrogels thermosensibles pour des applications de livraison ciblée de médicament et d'embolisation," Ecole polytechnique de Montréal, 2012.

THE SIMULATION METHOD AND APPLICATION OF PHOTO-OXIDATIVE DEGRADATION/AGING OF POLYMERS

Xiangze Meng, Yan Ye and Rui Yang*

*Department of Chemical Engineering, Tsinghua University, Beijing 100084
mengxz21@mails.tsinghua.edu.cn

INTRODUCTION

Polymer materials have been widely used in contemporary society. Their properties are vulnerable to service conditions, especially when they are exposed to photo-oxidative environments (1). The photo-oxidative reaction mechanisms and the kinetics plays a key role on the lifetime prediction and the controllable degradation strategies. In addition to experimental study, theoretical simulation is a good way to give deep understanding. There were numerous researches focus on thermo-oxidative and hydro-thermal aging by molecular dynamics (MD) simulations (including normal MD simulations and reactive MD simulations) MD and normal density functional theory (DFT) calculations. However, how to reveal photo-oxidative mechanism of polymer materials by simulation is still a challenge.

Herein, a multi-scale simulation method was proposed to theoretically investigate the photo-oxidative aging/degradation based on the time-dependent DFT (TDDFT) and MD simulations. This method was applied to the infectious ageing (2), photo-oxidative degradation of PBAT (3), and PE (4).

EXPERIMENTAL

TDDFT calculations

The nature of photons interaction with the polymer chain is alternating the electron state of the segment from the ground state to the excited state. As a result, the photo-oxidative aging involves the excited state. The TDDFT calculations were applied in the reactions with photons (5). The wavefunction ($\phi(\mathbf{r}, t)$) of a electron in a molecule can be calculated by the following differential equation:

$$i\hbar \frac{\partial}{\partial t} \phi(\mathbf{r}, t) = \left(-\frac{1}{2} \nabla^2 + V(\mathbf{r}, t) \right) \phi(\mathbf{r}, t)$$

$V(\mathbf{r}, t)$ is the potential energy operator.

$$V(\mathbf{r}, t) = V_0(\mathbf{r}, t) + \int \frac{\rho}{|\mathbf{r} - \mathbf{r}'|} d\mathbf{r}' + V_{xc}[\rho](\mathbf{r}, t)$$

V_0 is the external potential. In TDDFT, photons can be input as a alternating electric field. V_{xc} is the exchange-correlation functional. ρ is the electron density.

$$\rho(\mathbf{r}, t) = \|\phi(\mathbf{r}, t)\|^2$$

Therefore, the chemical mechanism of photo-oxidative aging can be obtained by modeling polymer segments and TDDFT calculations.

MD simulations

The MD simulations were applied for the transportation of the small molecules and the polymer segments. For the photo-oxidative reactions, the transportation of the oxygen plays a key role. The transportation of oxygen includes permeation, diffusion, and dissolution. The models of amorphous and crystalline phases were constructed respectively to investigate the effect of the aggregation state on the photo-oxidative reactions.

RESULTS AND DISCUSSION

The reason why the crystalline region is more difficult to degrade than the amorphous region is not because of a lower diffusion coefficient but because of lower permeability and solubility.

The real effect of photon absorbance is to change the electron structure of the segments, but not directly breaks the bonds with low dissociation energy.

The C–H activation plays a key role during the degradation/ageing. There exist a photo-oxidative initiation hydrogen atom transfer (HAT) to start the whole process. The oxygen, carbonyl group and other molecules or groups can act as an HAT acceptor.

The carbonyl group can react with the radicals to form a C(sp³) radical. The C(sp³) radical is vulnerable to β-scission, leading to the breakage of the polymer and the formation of ketones, aldehydes, esters, carboxylic acids and other relevant groups. However, the Norrish reactions in traditional common senses are not critical to the whole degradation because of the relative low possibility of twice-excitation and low photon molar absorptivity.

The above results are different from the traditional interpretation, but they do not contradict the experimental phenomenon. Through the above discussion, we can get closer to the essence of the polymer degradation/aging.

Acknowledgment

This study was funded by National Key Research and Development Program of China (no. 2021YFC2103603).

References

- 1) Celina, M. C., Review of polymer oxidation and its relationship with materials performance and lifetime prediction. *POLYM DEGRAD STABIL* **98** 2419 (2013).
- 2) Meng, X. & Yang, R., How formaldehyde affects the thermo-oxidative and photo-oxidative mechanism of polypropylene: A DFT/TD-DFT study. *POLYM DEGRAD STABIL* **205** 110131 (2022).
- 3) Meng, X., Ye, Y. & Yang, R., Computational and experimental study on the mechanism of CO₂ production during photo-oxidative degradation of poly(butylene adipate-co-terephthalate): Differences between PBA and PBT segments. *MACROMOLECULES* **56** 7749 (2023).
- 4) Meng, X., Jin, G. & Yang, R., A quantum chemical and molecular dynamics simulation study on photo-oxidative aging of polyethylene: Mechanism and differences between crystalline and amorphous Phases. *POLYM DEGRAD STABIL* **217** 110536 (2023).
- 5) Abedi, A., Maitra, N. T., Gross, E. K. U., Exact factorization of the time-dependent electron-nuclear wave function. *PHYS REV LETT* **105** 123002 (2010).

RecyClass, a value-chain approach to boost a circular use of plastics

Paolo GLEREAN

RecyClass (www.recyclclass.eu) Chairman, Head of Sales&Marketing at Aliplast spa (www.aliplastspa.com), Board Member of Plastics Recyclers Europe Association (www.plasticsrecyclers.eu) and Italian Plastics Recyclers Association Assorimap (www.assorimap.it)

INTRODUCTION

A circular use of plastics has become an high priority topic in the common debate, pushed from the European Commission and followed by the plastics industry. RecyClass idea came out in 2011 with the aim of creating a common understanding of recyclability in plastic items.

In the presentation I am going to share, I would like to explain how this idea has now developed in a cross value-chain initiative which embraces more than 100 members from the entire plastic value chain, from virgin resin producers, to plastics converters, plastics recyclers and technology providers.

EXPERIMENTAL

The RecyClass platform is covering today two main pillars:

- Plastics packaging recyclability;
- Traceability of recycled content in plastic items.

Plastic Packaging Recyclability: the platform consists of some specific Technical Committees with the scope of creating Testing Protocols which are simulating on lab scale what happens in a real recycling and converting plant. With such Protocols performed by authorized labs, the Technical Committee can assess the recyclability level of some specific packaging, technology or part of packaging. These assessments results are used to maintain Design for Recycling Guidelines that are a key tool for packaging designers.

RecyClass published in 2014 an online tool – available for free since then – that helps non-experts in assessing the recyclability of a plastic packaging. The tool is an user-friendly interface that has the updated Design for Recycling Guidelines behind it.

Traceability of recycled content in plastic items: RecyClass owns two Certification Schemes to certify 1. the Recycling Processes which are creating plastics recyclates and 2. The share of recycled content in the plastic items, following a chain of custody concept. Both schemes are accredited ISO 17065 and widely used across the industry worldwide.

DURABILITY AND PERFORMANCE OF SUSTAINABLE COMPOSITE FILM BY ALIPHATIC-AROMATIC POLYESTER AND CARBON-BASED PARTICLES PRODUCED BY SLOW PYROLYSIS AND HYDROTHERMAL CARBONIZATION

Nadka Tz. Dintcheva¹, Giulia Infurna¹, Maurizio Volpe², Antonino Messineo²

¹Dipartimento di Ingegneria, Università di Palermo, Viale delle Scienze, ed.6, 90128 Palermo, Italy

²Dipartimento di Ingegneria e Architettura, Università di Enna, Kore, cittadella Universitaria, 94100, Enna, Italia

Corresponding author: nadka.dintcheva@unipa.it

INTRODUCTION

The transition from a linear to a circular economy requires the implementation of new approaches to how we produce, use and dispose of all goods and materials. It is necessary to understand and implement new real production pathways in relation to the efficient implementation of the “waste-to-materials” concept. [1-2] Therefore, the implementation of new approaches towards a circular economy requires the design of durable and reusable materials, appropriate material selection and production, recycling and reuse, and the correct management of these materials at the end of their life. The innovative design, production and end-of-life management of materials play an important role in advancing the circular economy at the large-scale industrial level. [3-4]

However, as known, polymer additives are usually added to enhance the properties and performance of polymers and biopolymers, but most additives have environmental or performance concerns that limit their use. In this context, the recovery and use of bio-waste and biomass for sustainable biocomposite formulations is a challenging issue for the transition from a linear to a more sustainable and circular economy. Currently, the replacement of carbon-based fillers in polymers and biopolymers with biochar particles derived from biomass waste has become an attractive and challenging issue.

EXPERIMENTAL

In this work, sustainable biocomposite films based on poly(butylene adipate-co-terephthalate), PBAT, and biochar fillers such as Slow Pyrolysis Biochar (SP-BC) produced by slow pyrolysis (at 280, 340 and 400 °C) or Hydrothermal Carbonization Biochar (HTC-BC) produced by hydrothermal carbonization (at 220, 250 and 280 °C) were prepared by melt blending. In this study carob fruit waste obtained after syrup extraction, was subjected to dry and wet thermochemical processes, i.e. slow pyrolysis and hydrothermal carbonisation, and the resulting solid residue was characterised by elemental analysis, calorimetry, FTIR for their physico-chemical properties and SEM to investigate their morphology. PBAT and the formulated biocomposites, obtained by the addition of 10 wt. % of SP-BC and HTC-BC particles were characterised by thermal, mechanical, morphological and rheological analyses. Particular attention was paid to the photo-oxidation behaviour under accelerated artificial weathering conditions, considering the potential application of these biocomposites as sustainable packaging materials and mulch agricultural films.

RESULTS AND DISCUSSION

First of all, the carob-waste has been subjected to two different thermal-degradation treatments, *i.e.* slow pyrolysis (SP) and hydrothermal carbonization (HTC), at different temperature, to produce sustainable carbon-based particles. Then, to formulate sustainable composite films, the SP-BC and HTC-BC were added by melt mixing to PBAT.

Accurate characterization of SP-BC and HTC-BC particles through elemental analysis (e.g., CHN test) and ATR-FTIR analysis suggest that both BC particles are mainly composed of carbon atoms, and this increases with increasing the treatment temperatures. As expected, the HTC treatment leads to the production of particles enriched with organic compounds, as revealed by ATR-FTIR analysis. The SEM observations on the particle surfaces reveal that the SP-BC appears more like carbonaceous particles, while the HTC-BC have a sponge-like morphology.

The rheological and mechanical characterizations of PBAT-based composites suggest that both SP-BC and HTC-BC exert a reinforcement action for PBAT and the interactions between polymer-fillers and filler-fillers are more pronounced for PBAT/HTC-BC rather than for PBAT/SP-BC. Further, the presence of both SP-BC and HTC-BC has no significant effect on the PBAT crystallinity. Interestingly, both SP-BC and HTC-BC can slow down the photo-oxidation degradation of PBAT exerting, although not very strong, protection action for PBAT films.

Acknowledgments

This study was carried out within the MICS (Made in Italy - Circular and Sustainable) Extended Partnership and received funding from the European Union Next-Generation EU (Piano Nazionale di Ripresa e Resilienza (PNRR) - Missione 4 Componente 2, Investimento 1.3 - D.D. 1551.11-10-2022, PE00000004). This manuscript reflects only the authors' views and opinions, neither the European Union nor the European Commission can be considered responsible for them.

References

1. EU Commission - "European Green Deal" 2019.
2. European Commission *Communication From The Commission To The European Parliament, The Council, The European Economic And Social Committee And The Committee Of The Regions Closing the Loop -An EU Action Plan for the Circular Economy*; Brussels, 2018;
3. Di Bartolo A, Infurna G, Dintcheva NT. A review of bioplastics and their adoption in the circular economy. *Polymers*. 2021;13(8). doi:10.3390/polym13081229
4. Yaashikaa PR, Kumar PS, Varjani S, Saravanan A. A critical review on the biochar production techniques, characterization, stability and applications for circular bioeconomy. *Biotechnology Reports*. 2020;28. doi:10.1016/j.btre.2020.e00570

Surface micro-cracking on NBR/PVC/carbon black blends: Influence of the environmental stresses

Clara Thoral^{1,2}, Gerald Soulagnet², Pierre-Olivier Bussiere^{1*}, Sandrine Therias¹

¹Université Clermont Auvergne, CNRS, INP Sigma Clermont, ICCF, F-63000 Clermont-Ferrand, France

²Trelleborg Industrie SAS, ZI La Combaude, Rue de Chantemerle, F-63050 Clermont-Ferrand, France

*E-mail : pierre-olivier.bussiere@sigma-clermont.fr

INTRODUCTION

Blends of Nitrile butadiene Rubber/Poly(vinyl chloride) (NBR/PVC) are used by Trelleborg Industrie SAS (Clermont-ferrand) for the fabrication of hoses transporting fluids, as fuel for the automobile sector. This particular application is due to NBR good resistance to oils and solvents. To improve its properties, NBR is blended with PVC, to add thermal resistance but also a higher stiffness. However, as the majority of unsaturated polymers, the presence of double bonds in the backbone of the NBR (because of butadiene units) makes it particularly sensitive to thermo- and photoageing (1,2).

EXPERIMENTAL

Materials

A commercial nitrile butadiene rubber (NBR) with a 33% acrylonitrile content and a Mooney viscosity of 45 and poly(vinyl chloride) (PVC) with kwert $K > 60$ were used. Curing agents were also added: sulfur and an accelerator, CBS (N-cyclohexyl-2-benzothiazolesulfenamide). Carbon black (N550) and additives were also added. All products were provided by Trelleborg Industrie SAS. The blends were prepared at Trelleborg in a Banbury-type mixer at 160°C for 10 minutes, then passed through a cylinder tool at 60°C for 12 minutes. 2mm plates were prepared by moulding under an electric press and thin films (115 and 50 μm) were made by compression moulding at 155°C for 30 min to allow crosslinking.

Photoageing and Thermal ageing

Films were irradiated under artificial ageing conditions in a SEPAP 12/24 unit from Atlas (Ametek). Films were thermooxidized in a forced air venting oven Memmert UF30 at a temperature of 120 °C. The oven temperature was controlled with a tolerance of ± 1 °C.

FTIR spectroscopy

Infrared spectra were recorded in transmission mode using a Thermo Scientific Nicolet 6700 spectrometer with Omnic Software. Spectra were obtained with 32 scans and a 4 cm^{-1} resolution. A minimum of three samples were analysed to obtain good reproducibility.

Atomic force microscopy

The peak force QNM mode in AFM was used to determine the mechanical properties of the NBR/PVC blend. Measurements were performed with a Bruker multimode 8 model with a nanoscope 9.20 in tapping mode. Modulus measurement was performed on the exposed surface to monitor the stiffness evolution between aged and unaged material. Images of 5 μm x 5 μm at a scan rate of 0.5 Hz, and 512 scans were recorded. The stiffness was evaluated thanks to the reduced Young's modulus E^* obtained with DMT modulus images. The Derjaguin-Muller-Toporov model was used to determine the mechanical modulus.

RESULTS AND DISCUSSION

NBR/PVC hoses have shown a loss of their usual properties during use and in particular cracks at the surface can appear with the time (3). The aim of this study was to realise a multi-scale study of the materials in thermo- and photoageing in order to determine the main factor leading to cracks

formation. In addition, we also tried to determine how the addition of carbon black could influence the appearance of cracks, in particular through the analysis of degradation products, oxidation profiles and modulus profiles. The results obtained show significant differences between the effect of photooxidation, occurring only at the extreme surface of blends and leads to micro-cracking with stress and the thermooxidation which tends to make the whole material brittle (4).

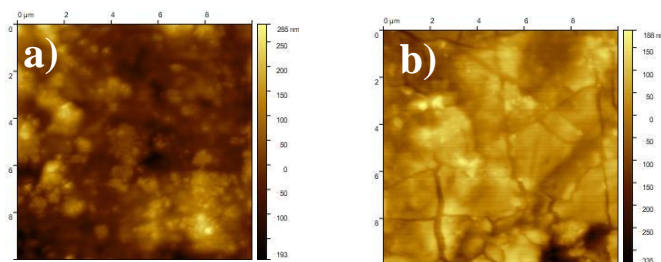


Fig. 1. AFM Images of a NBR/PVC (66/33) blend a) at 0h et b) after 100h of irradiation

To reach this objective, different analytical techniques were used from the molecular-scale, to characterize modifications corresponding to the formation of oxidation products monitored by infrared spectroscopy, to the macromolecular scale where the crosslinking reactions were characterized by Differential Scanning Calorimetry (DSC) and Dynamic Mechanical Thermal (DMTA) analyses. As shown in Figure 1, Atomic Force Microscopy was used to follow not only the modulus at the surface but also cracks formation and the degradation profile with the ageing time. This approach allows us to explain why crosslinking reactions, taking place in both photo- and thermoageing can be at the origin of a cracking effect in one case and to a material embrittlement in the second.

References

- 1) C. Adam, J. Lacoste, J. Lemaire, *Polymer Degradation and Stability*, **27**, 85 (1990)
- 2) J.-L.; Gardette, J.Lemaire, *Polymer Degradation and Stability*, **34**, 135 (1991)
- 3) N.R.Manoj, P.P DE, *Polymer Degradation and Stability*, **44**, 43 (1994)
- 4) C. Thorat, G. Soulagnet, PO. Bussiere, S.Therias, *Polymer Degradation and Stability*, **220**,110633, (2024)

Geopolymers Beyond Construction: Enhanced Adsorption and Flame Retardancy in Nanocomposite Systems.

Alessandro Lo Bianco^{a*}, Martina Maria Calvino^a, Giuseppe Cavallaro^a, Pooria Pasbakhsh^b, Giuseppe Lazzara^a, Stefana Milioto^a

^a Department of Physics and Chemistry “E. Segrè”, University of Palermo, Viale delle Scienze, Ed.17, Palermo 90128, Italy. alessandro.lobianco02@unipa.it*

^b Department of Mechanical Engineering, School of Engineering, Monash University Sunway Campus, Bandar Sunway 47500, Selangor, Malaysia

INTRODUCTION

Geopolymers, inorganic materials formed by the polymerization of silicates and aluminates, resulting in a three-dimensional structure composed of bonds between silicon (Si), aluminum (Al), and oxygen (O), have garnered significant attention due to their excellent mechanical strength, with the potential to replace Portland cement, whose production accounts for 5-7% of global CO₂ emission^{1 2}. However, geopolymers can be more than just construction materials and can be exploited to create composite systems with diverse properties. These include providing flame-retardant properties to highly flammable polymers like cellulose³ and enhancing pollutant absorption due to their increased porosity compared to the starting material. In this study, two nanocomposite systems exhibiting these characteristics are presented and compared with a pure inorganic clay-based film that was geopolymerized to assess its morphological and CO₂ adsorption properties.

EXPERIMENTAL

Materials

Gel Beads. The alginic acid sodium salt ($M_w=70-100$ kDa), Halloysite nanotubes and Sodium Hydroxide (CAS 1310-73-2) were Sigma Aldrich products. Calcium Chloride ($\text{CaCl}_2 \cdot 2\text{H}_2\text{O}$) was a Merck product. **HPC/HNTs composite geopolymers.** Ultra HaloPure Halloysite was a gift by I-Minerals Inc. mined in the geological deposit of Latah County. Hydroxypropyl cellulose (HPC) ($M_w = 80\text{kg} \cdot \text{mol}^{-1}$ CAS 9004-64-2) and Sodium Hydroxide (CAS 1310-73-2) were Sigma Aldrich products. **Halloysite Inorganic Films.** Patch Halloysite (Kalgoorie, Western Australia) is a kind donation provided by Dr. Keith Norrish from his collection and research on Patch (CSIRO Soils, Adelaide). Sodium Hydroxide (CAS 1310-73-2) was Sigma Aldrich product.

Preparation

Gel Beads. Gel beads were prepared by dissolving 2% sodium alginate in distilled water at 60°C. HNTs were added to achieve a 1:1 Alg ratio. The beads were formed by dropping the solution into a 0.1 M CaCl_2 solution, then washing and vacuum drying. Geopolymerized gel beads were treated in 12 M NaOH at various times and then cured at 50°C. **HPC/HNTs composite geopolymers.** The composite film of HPC and HNTs was prepared by dissolving 2% by weight of HPC in water at 70°C. Halloysite was added to the polymer solution to achieve 30% HPC. The dispersion was stirred overnight, poured into a glass Petri dish, and kept at 80°C until the solvent evaporated. Geopolymerized samples were prepared by immersing the composite film in a 12 M NaOH solution for varying times (5 seconds or 2 hours). **Halloysite Inorganic Film.** Patch Halloysite was dispersed in water with different concentrations (0.5%, 1.5%, 3.33%, 5%). The dispersions were stirred for 20 minutes, poured into a plastic dish (LDPE), and placed in an oven at 50°C overnight. The film was recovered by overturning the dish. PT_Hal was treated by immersing it in a 12 M NaOH solution, followed by another night in the oven at 50°C.

Structural and morphological characterizations

For structural characterization, XRD was used. TGA was employed to investigate the geopolymerization process, and SEM was used for morphological characterization.

Other measurements

Contact angle measurements, transmittance measurements, CO₂ and dodecane adsorption measurements, flame resistance tests, and DMA (dynamic mechanical analysis) were conducted.

RESULTS AND DISCUSSION

XRD, TGA, and SEM measurements were conducted to characterize the structure of all samples and confirm the occurrence of geopolymerization. Adsorption tests were performed on Gel Beads and inorganic films before and after geopolymerization. The latter, being non-composite, provides insights into the direct effect of geopolymerization. In all cases, the samples absorbed more CO₂ at equilibrium compared to non-geopolymerized samples (Fig. 1a), attributed to the increased porosity, qualitatively evaluated through SEM measurements. This trend is also confirmed by dodecane adsorption tests on the beads (Fig. 1b), showing that geopolymerized samples absorb more hydrocarbons than non-geopolymerized ones. The flame-retardant effect was evaluated on geopolymerized HPC/HNTs composite samples (Fig. 1c), which demonstrated excellent properties in this regard compared to both the HPC film and the non-geopolymerized composite, extinguishing the flame approximately 0.5 seconds after the ignition source was removed.

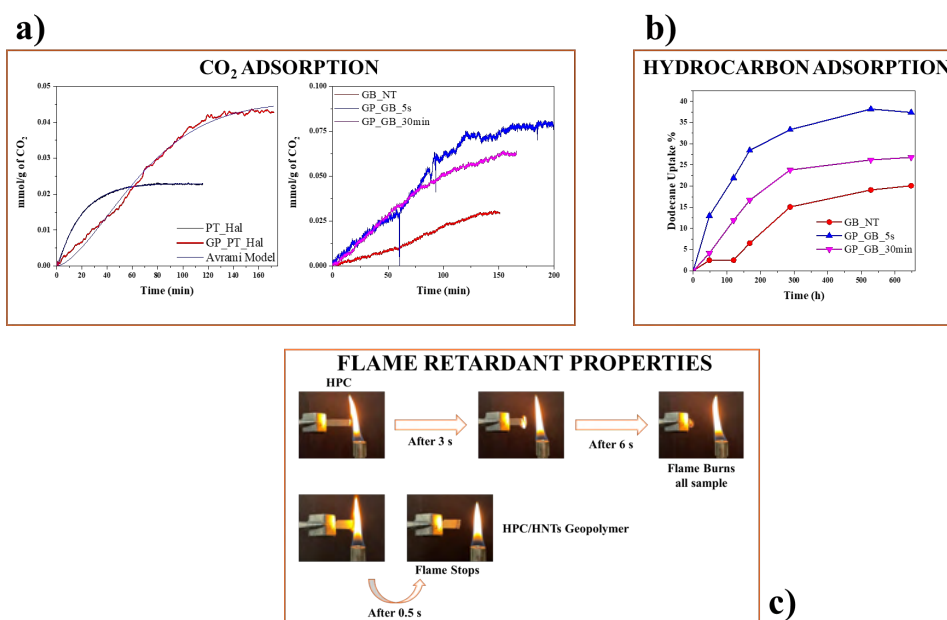


Fig. 1 CO₂ adsorption properties of Inorganic Films and Gel Beads (a), Dodecane uptake of Gel Beads samples (b) and flame-retardant properties of HPC/HNTs composites (c).

References

- (1) Benhelal, E.; Zahedi, G.; Shamsaei, E.; Bahadori, A. Global Strategies and Potentials to Curb CO₂ Emissions in Cement Industry. *J. Clean. Prod.* **2013**, *51*, 142–161. <https://doi.org/10.1016/j.jclepro.2012.10.049>.
- (2) Schneider, M.; Romer, M.; Tschudin, M.; Bolio, H. Sustainable Cement Production—Present and Future. *Cem. Concr. Res.* **2011**, *41* (7), 642–650. <https://doi.org/10.1016/j.cemconres.2011.03.019>.
- (3) Calvino, M. M.; Cavallaro, G.; Milioto, S.; Lazzara, G. Composite Materials Based on Halloysite Clay Nanotubes and Cellulose from Posidonia Oceanica Sea Balls: From Films to Geopolymers. *Environ. Sci. Nano* **2024**, *11* (4), 1508–1520. <https://doi.org/10.1039/d3en00879g>.

UV-C/H₂O-DRIVEN ABIOTIC DEGRADATION OF PBAT/TPS-BASED COMMERCIAL FILMS

K. Gutiérrez-Silva, O. Gil-Castell, J.D. Badia*

Materials Technology and Sustainability (MATS). Department of Chemical Engineering. Av. de la Universitat, s/n 46100 Burjassot, València, España.

karen.gutierrez@uv.es, oscar.gil@uv.es, jose.badia@uv.es

INTRODUCTION

Poly(butylene adipate-co-terephthalate) (PBAT) is a fully biodegradable aliphatic-aromatic co-polyester extensively utilized in agriculture, textile, and food packaging applications. Despite its biodegradability, the intrinsic degradation rate of PBAT is relatively slow, resulting in substantial waste accumulation and presenting significant environmental challenges [1]. The degradation rate can be modulated through the combination of PBAT with other polymers, such as thermoplastic starch (TPS). This work evaluates the consequences of the exposure of PBAT/TPS commercial films to UV-C radiation in combination with water. In particular, UV-C was used because of its higher energy and capacity to excite photons in a short time and therefore accelerate degradation.

EXPERIMENTAL

Materials

PBAT/TPS-based extruded commercial films with 100 μm thickness were supplied by Prime Biopolymers SL (Paterna, Spain). These films included formulations with different additive percentages, identified as PT, PT10, and PT20.

UV-C/H₂O exposure

Films were exposed to UV-C radiation in a dark chamber with four 15W UV-C lamps, which provided irradiation of 0.90 mW/cm² at 254 nm wavelength. Films were subjected to irradiation at both dry and wet conditions with exposure times of 24, 48, 72, and 96 h. For the wet environment, films were immersed in 20 mL of distilled water in petri dishes. After the selected times, samples were washed in distilled water, dried under vacuum at 40 °C until constant mass, and stored for further analyses.

Characterization

The changes in the bulk and surface properties were evaluated through different perspectives, involving the evaluation of the macroscopic appearance, and color changes, together with SEM, FTIR-ATR and DSC studies.

RESULTS AND DISCUSSION

Exposure to UV-C caused slight changes in the L*a*b* indexes of the films, as shown in Figure 1. Chain scission after UV pretreatment leads to a decrease in optical properties, expressed as an increase in yellowing in dry conditions. Besides the combination of UV-C and immersion in water causes an inversion of the colouring tendency, from a predominantly yellowing during dry conditions to a bluish process when immersed in water.

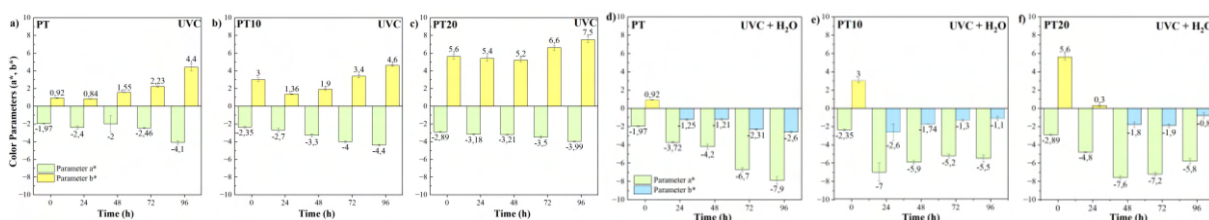


Figure 1. Colour parameters (a*, b*) variation of (a) PT, (b) PT10, (c) PT20 films after UV-C irradiation in dry conditions and (d) PT, (e) PT10, (f) PT20 films after UV-C irradiation in wet conditions.

Figure 2 presents the FTIR spectrum for treated films. The peak at 1709 cm^{-1} was reduced, indicating the reduction of contribution of the carbonyl group and therefore the formation of low molecular weight ester bonds. Additionally, a decrease in the methylene ($-\text{CH}_2-$) group corresponding to 727 cm^{-1} could be attributed mainly to the chain scission as a result of photo-oxidation processes [2]. The perceived reduction was more prominent as the percentage of additives increased in the films.

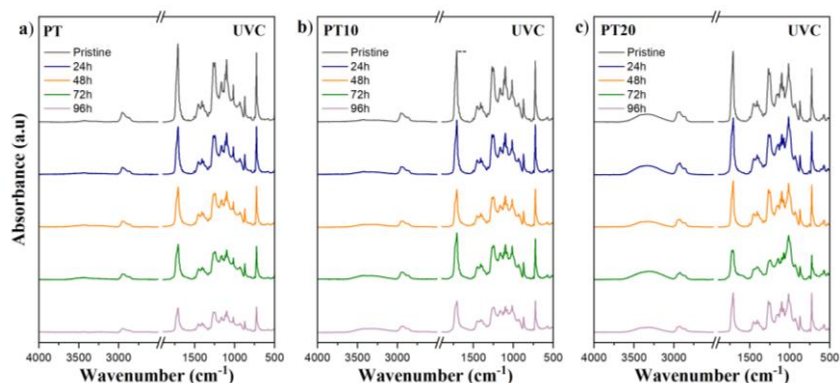


Figure 2. FTIR spectra of PBAT/TPS films exposed to UV-C.

UV-C radiation attacked the granular domains on the surface of the films, generating areas of microcracks. The combination of UV-C and water promoted the generation of holes, which became more pronounced with a higher percentage of additives, as shown in Figure 3. In general, the combination of UV-C and water was demonstrated as a driving force for the degradation of PBAT/TPS-based commercial films.

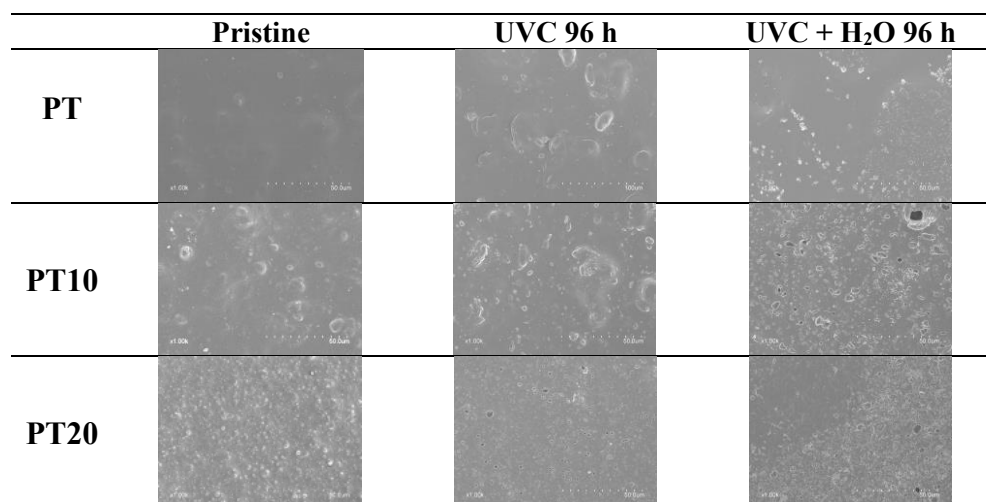


Figure 3. Electron surface micrographs of films after UV-C and UV-C/H₂O exposure for 96 h.

Acknowledgements

The authors would like to acknowledge funding from the Agència Valenciana de la Innovació (AVI) through the INNEST/2022/295 project (BIOFAST-Methodological strategies for the accelerated biodegradation of bioplastics in compost medium).

References

- [1] Yang, Y., Min, J., Xue, T. et al. Complete bio-degradation of poly(butylene adipate-co-terephthalate) via engineered cutinases. *Nat Commun.* **2023**, 14, 1645.
- [2] Kijchavengkul, T., Auras, R., Rubino, M. et al. Assessment of aliphatic–aromatic copolyester biodegradable mulch films. Part II: Laboratory simulated conditions. *Chemosphere.* **2008**, 71, 1607–1616.

RECYCLING OF PERSONAL PROTECTION EQUIPMENT: SANITISATION, DEGRADATION AND POLYMER BLEND FORMULATIONS

Giulia Infurna¹, Alessia Romani², Maria Chiara Riccelli³, Marinella Levi², Loredana Incarnato³, Nadka Tz. Dintcheva¹,

¹Department of Engineering, University of Palermo, Palermo, Italy

²Department of Chemistry, Materials, and Chemical Engineering “Giulio Natta”, Politecnico di Milano, Milano, Italy

³Department of Industrial Engineering, University of Salerno, Fisciano (SA), Italy

Corresponding author: giulia.infurna@unipa.it

INTRODUCTION

The linear model of the global economy, which follows the 'take, make, use, and dispose' pattern, is causing significant environmental issues. A necessary shift towards circularity is outlined in the EU's Green Deal and Italy's National Recovery and Resilience Plan[1–3]. With the planet's limited resources and waste absorption capacity, transitioning to a circular economy is urgent. This means treating end-of-life products as opportunities for resource recovery, which is especially crucial for plastics to address waste accumulation and meet the rising global demand [4]. Despite being the most commonly used polymer in the EU, polypropylene (PP) has a low recycling rate of about 5%, compared to polyethylene terephthalate (21%) and polyethylene (9%) [5]. This low rate is due to the challenges in separating PP from other polyolefins, the presence of various additives in PP products, and its rapid thermo- and photo-degradation during reprocessing and use. Given that the polypropylene used in disposable facial masks has a naturally short lifespan and lacks other polyolefins or additives in its composition, this study focuses on sanitizing and recycling PP nonwoven textiles through extrusion reprocessing for additive manufacturing.

EXPERIMENTAL

In this study, polypropylene was recycled through melt blending, a common mechanical recycling method for plastic waste. The material used was 3-ply facemasks, each weighing 4.41 ± 0.05 grams, with the polypropylene filter layers accounting for 3.41 ± 0.02 grams (77% of the total weight). The facemasks underwent simulated sanitization processes using steam [6,7], aqueous sodium hypochlorite [8], and ultrasound treatments [8].

To facilitate processing and stabilize material feeding, both untreated and sanitized facemasks were hot-pressed to form PP sheets. These sheets were then ground, extruded, and pelletized. Hot pressing was conducted at 190°C for 5 minutes under a pressure of 6000 Pa. Extrusion was performed at a temperature profile of 165–170–170°C, at 30 rpm, with a torque of 10 Nm.

The resulting pellets were subjected to thermal, rheological, and mechanical characterization. Additionally, spectrometric and calorimetric analyses were conducted to assess degradation phenomena and pathways resulting from the sanitization and melt blending processes.

RESULTS AND DISCUSSION

This study aims to transform waste into secondary raw materials by employing a circular economy and waste-to-materials approach. After processing, both with and without a

sanitization process, the resulting pellets were thermally, rheologically, and mechanically characterized. Spectrometric and calorimetric analyses were also conducted to assess the degradation phenomena and pathways induced by the sanitization and melt blending processes.

The analyses revealed that different sanitization methods led to varying degrees of polymer chain degradation. This was evidenced by the formation of distinct crystalline forms of polypropylene in the calorimetry curves and the increased amplitude of degradation peaks in the spectroscopic analyses. Despite the degradation associated with the mechanical recycling processes, the use of masks as a secondary raw material remains viable, especially when mixed with virgin materials.

Acknowledgment

Finanziato dall'Unione europea – “Next Generation EU” - PNRR M4 - C2 -investimento 1.1: Fondo per il Programma Nazionale di Ricerca e Progetti di Rilevante Interesse Nazionale (PRIN) - PRIN 2022 cod. 20229BHA75 dal titolo “FUnctional Technology Unlocking Recycling and VALorization of Personal Protective Equipment production scrap and waste” (FUTUREVAL-PPE). CUP B53D23005690006.

References

1. EU Commission European Green Deal 2019.
2. European Commission: *Communication from The Commission to The European Parliament, The Council, The European Economic and Social Committee and The Committee Of The Regions Closing the Loop -An EU Action Plan for the Circular Economy*; Brussels, 2018;
3. Alessandro D'ALFONSO Italy's National Recovery and Resilience Plan. **2021**.
4. Michael, F.A. *Materials and Sustainable Development*; 1st edition.; Elsevier: Waltham, MS, 2015; ISBN 978-0-08-100176-9.
5. Plastic Europe Plastics - The Facts 2021 2021.
6. De Man, P.; Van Straten, B.; Van Den Dobbelen, J.; Van Der Eijk, A.; Horeman, T.; Koeleman, H. Sterilization of Disposable Face Masks by Means of Standardized Dry and Steam Sterilization Processes; an Alternative in the Fight against Mask Shortages Due to COVID-19. *Journal of Hospital Infection* **2020**, *105*, 356–357, doi:10.1016/j.jhin.2020.04.001.
7. Ma, Q.; Shan, H.; Zhang, C.; Zhang, H.; Li, G.; Yang, R.; Chen, J. Decontamination of Face Masks with Steam for Mask Reuse in Fighting the Pandemic COVID-19: Experimental Supports. *Journal of Medical Virology* **2020**, *92*, 1971–1974, doi:10.1002/jmv.25921.
8. Francisco, C.A.I.; Araújo Naves, E.A.; Ferreira, D.C.; Rosário, D.K.A.D.; Cunha, M.F.; Bernardes, P.C. Synergistic Effect of Sodium Hypochlorite and Ultrasound Bath in the Decontamination of Fresh Arugulas. *Journal of Food Safety* **2018**, *38*, e12391, doi:10.1111/jfs.12391.

Characterization and flame retardant properties of a set of styrenic copolymers containing (meth-)acrylate phosphates and organic sulfides

S. Fuchs^{1*}, M. Andruschko¹, P. Frank², U. Jonas²

¹ Chemistry and Materials Science, Hamm-Lippstadt University of Applied Sciences, Marker Allee 76-78, 59063 Hamm, Germany

² Macromolecular Chemistry, University of Siegen, Adolf-Reichwein-Strasse 2, 57076, Siegen, Germany

* Sabine.Fuchs@hshl.de

INTRODUCTION

Polystyrene (PS) and related copolymers are usually compounded with effective and widely-used halogenated flame-retardants like e. g. a polybrominated styrene-butadiene-styrene (SBS) copolymer in PS foams (1, 2), or decabromodiphenyl ethane, often applied in combination with antimony(III) oxide, in HIPS. (3, 4) Despite of their efficiency and economic advantages those brominated flame retardants are often highly persistent in the environment, bio-accumulative, and sometimes toxic.^[5] Therefore demands to replace these flame-retardants with non-migrating halogen-free alternatives are increasing.

In this work, a unique set of intrinsically flame-retardant, styrenic copolymers synthesized from styrene, various acrylate and methacrylate phosphate comonomers, and elemental sulfur via free radical bulk polymerization, is presented. Deeper insights into their chemistry, polymer characteristics, and flame retardant properties will be provided.

EXPERIMENTAL

Materials

Chemicals used in this work: Styrene, elemental sulfur (sublimed), tetrahydrofuran, methanol, dichloromethane, and UV-grade tetrahydrofuran were purchased from Alfa Aesar (Germany), Carl Roth GmbH (Germany), Chemsolute (Germany), and VWR (Germany), and used as received. Acrylates and methacrylates were extracted, distilled, and stored at 4 °C prior to use. Polystyrene 158K (PS) was obtained from BASF SE (Germany).

Synthesis of the copolymers

In a general procedure, styrene (94 – 98 wt.%), elemental sulfur (1 wt.%), and the acrylate or methacrylate phosphate comonomers (1 – 5 wt.%) were mixed, and subsequently degassed by three freeze-thaw-cycles. The monomer mixture was then heated to 130 °C under vigorous stirring for 64 – 72 h. The crude copolymer mixture was dissolved in THF, precipitated into methanol, and subsequently dried *in vacuo*. The copolymers were obtained as colorless solids in overall yields of 64 – 87 %.

SEC and UV-Vis analyses

SEC experiments were performed on a Prominence LC-20AD liquid chromatograph (Shimadzu, Duisburg, Germany) with degassing unit (DGU-20A3R), auto sampler (SIL-20AHT), column oven (CTO-20AC), refractive index detector (RID-20A), diode array detector (SPD-M20A, 30 °C), and SDV columns (PSS Polymer Standard Services GmbH, Mainz). Calibration with PS standards (PSS Polymer Standards Service, Mainz, Germany). UV-Vis analyses were performed on a UV-2600 spectrometer (Shimadzu, Duisburg, Germany). Quartz cuvettes were used with UV-grade unstabilized THF as solvent.

UL 94 vertical flame testing

UL 94 vertical flame tests were performed in a HVUL2 flame chamber (Atlas Material Testing Technology GmbH, Linsengericht, Germany). The flame energy was 50 W.

RESULTS AND DISCUSSION

The obtained copolymers consisting of styrene, phosphorous comonomers, and sulfur, were characterized by SEC, elemental analysis, and NMR spectroscopy. Their thermal properties were analyzed by DSC and TGA, and their flame-retardant properties evaluated by UL-94 vertical flame testing.

SEC experiments with an refractive index (RI) and a photodiode array (PDA) detector revealed that the prevalence of sulfur was unevenly distributed over the different obtained molar mass fractions of CP-1b and CP-3, being predominantly present in the lower mass polymers.

The chemical structures of two selected copolymers (CP-1b and CP-3) and their UL 94 vertical test results are presented in Fig. 1.

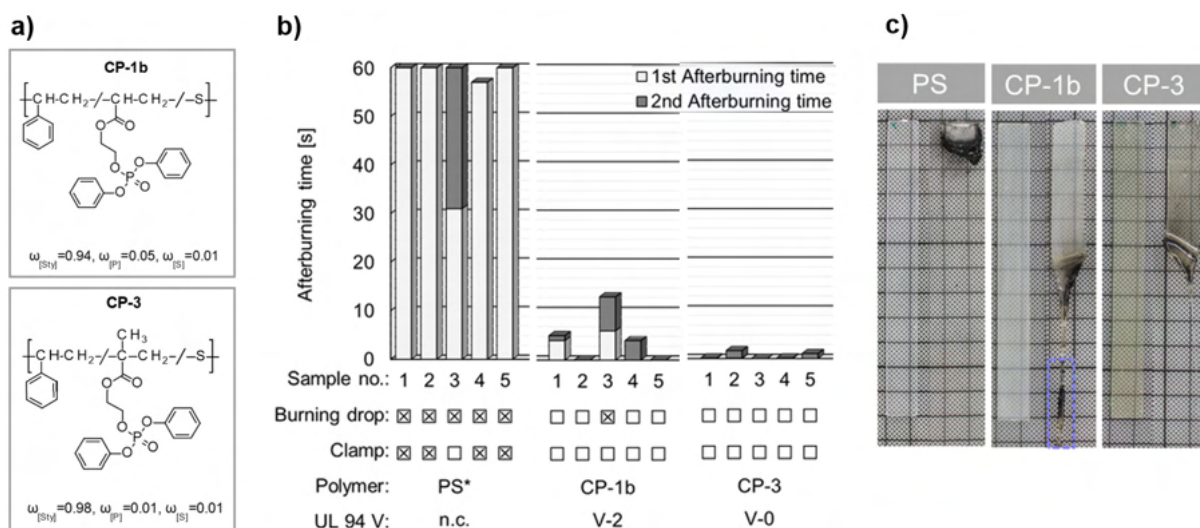


Fig. 1 Styrenic copolymers CP-1b and CP-3: a) Chemical structures, b) UL 94 V (1.6 mm) results, and c) Injection molded UL 94 test bars (1.6 mm). (*) Commercial PS 158K as reference.

Despite of their rather low phosphorus (CP-1b: 0.4 %, CP-3: 0.1 %) and sulfur contents (CP-1b: 0.4 %, CP-3: 0.1 %) the presented copolymers exhibit very short afterburning times in the UL 94 test, and CP-3 even achieves an UL 94 V-0 classification (Fig. 1 b). In addition to their self-extinguishing fire behavior originating from the incorporated phosphorus and sulfur moieties, copolymers CP-1b and CP-3 exhibit a strongly enhanced melt flow during combustion, which leads to a rapid withdrawal of the polymer melt from the flame. (Fig. 1 c).

Acknowledgment

This work has been financially supported by the Zentrum für Forschungsförderung of Hamm-Lippstadt University of Applied Sciences, Germany, which is gratefully acknowledged.

References

- 1) M. W. Beach, J. W. Hull, B. A. King, I. Beulich, W. G. Stobby, S. L. Kram, D. B. Gorman, *Polymer Degradation and Stability*, 135, 99 (2017).
- 2) B. A. King, W. G. Stobby, D. J. Murray, A. Z. Worku, I. Beulich, S. M. Tinetti, et al. (Dow Global Technologies Inc., USA.). WO2007058736 A1, 2007.
- 3) J. Troitzsch, Ed., *Plastics flammability handbook*, 3rd edition, München, Cincinnati, Hanser; Hanser Gardener. 2004
- 4) E. D. Weil, *Flame retardants for plastics and textiles*, 2nd edition, Munich, Hanser. 2016.

BIOMEDICAL POTENTIAL OF ELECTROSPUN MATS BASED ON FURANOATE POLYESTERS

Sofia Santi¹, Giulia Fredi¹, Nadia Lotti^{2,3,4}, Michelina Soccio^{2,3}, Andrea Dorigato¹

¹ Department of Industrial Engineering and INSTM Research Unit, University of Trento, Via Sommarive 9, 38123 Trento, Italy

(sofia.santi@unitn.it; giulia.fredi@unitn.it; andrea.dorigato@unitn.it)

² Department of Civil, Chemical, Environmental, and Materials Engineering, University of Bologna, Via Terracini 28, 40131, Bologna, Italy

(nadia.lotti@unibo.it; michelina.soccio@unibo.it)

³ Interdepartmental Center for Industrial Research on Advanced Applications in Mechanical Engineering and Materials Technology, CIRI-MAM, University of Bologna, Bologna, Italy

⁴ Interdepartmental Center for Agro-Food Research, CIRI-AGRO, University of Bologna, Bologna, Italy

INTRODUCTION

Bioderived furanoate polyesters are emerging as promising substitutes for petrochemical-derived polyesters in diverse applications including packaging, textiles, and biomedicine. This work presents the successful production of electrospun nanofibrous mats using two furan-based polyesters - poly(butylene 2,5-furanoate) (PBF) and poly(pentamethylene 2,5-furanoate) (PPeF). While PBF and PPeF have very similar chemical structures, they exhibit remarkably different physical and mechanical properties. This work focuses on the evaluation of the potential of these mats to be applied in the biomedical field, especially as drug delivery systems. In fact, controllable drug delivery through nanostructured systems can enhance treatment efficacy, safety, compliance, and quality of life. While traditional methods have bioavailability and release limitations, biobased nanocarriers like PBF and PPeF nanofibers would offer high loading efficiency, precise distribution, and tunable release kinetics.

EXPERIMENTAL

Materials

Dimethyl 2,5-furandicarboxylate (2,5-DMF) (Sarchem labs, CAS 4282-32-0), 1,4-butanediol (1,4-BDO) (Sigma-Aldrich, 99% pur, CAS 110-63-4), 1,5-pentanediol (1,5-PD) (Fluka, ~97% pur, CAS 111-29-5), Hexafluoroisopropanol (Carlo Erba/Cas 920-66-1, Hexafluoro-2-propanol, HFIP), Chloroform (Carlo Erba/Cas 67-66-3, Chloroform, CHCl₃), dimethylformamide (Sigma/Cas 68-12-2, DMF).

Sample preparation

PBF and PPeF were synthesized at the lab scale through a solvent-free polycondensation process, according to the procedure described in a previous work [1] starting from dimethyl 2,5-furandicarboxylate and 1,4-BDO for PBF and 1,5-PD for PPeF. Titanium tetrabutoxide (TBT) and titanium isopropoxide (TIP) used as catalysts.

The feasibility of electrospinning these polymers into non-woven mats was systematically investigated by optimizing the solvent type (HFIP, CHCl₃, DMF) and mixture and polymer concentration (0.1-0.2 g/mL), which affected the polymer solubility and solution viscosity. The spinning rate (0.01-0.2 ml/min), applied voltage (18-24 kV), and environmental temperature (20 °C) and moisture (RH = 45%) were also controlled.

Characterization

A detailed morphological analysis using field-emission scanning electron microscopy identified optimal processing conditions for generating electrospun PBF and PPeF mats. Subsequently, the optimized mats were characterized from the thermal (differential scanning calorimetry) and mechanical (tensile test) point of view. Tensile tests were performed before and after a treatment in physiological conditions (NaCl 0.9%, pH 7.5, 37 °C). Finally, the potential of electrospun mats to administer anti-inflammatory dexamethasone treatments was evaluated using UV-Vis spectroscopy to monitor release over 7 days.

RESULTS AND DISCUSSION

The morphological characterization of the electrospun mats revealed that, for PBF, the optimal conditions for producing smooth, homogeneous submicron fibers with a diameter of $0.7 \pm 0.3 \mu\text{m}$ were identified as a 0.11 g/mL polymer concentration in a HFIP/ CHCl_3 (1:1) solvent mixture, subjected to a voltage of 24 kV and a spinning rate of 0.01 mL/min. In contrast, the electrospinning of PPeF solutions in HFIP resulted in partially fused and interconnected fibers due to the proximity of the processing conditions to the polymer's T_g (19 °C). However, the incorporation of DMF as a co-solvent facilitated improved fiber formation, yielding mats with an average fiber diameter of $1.3 \pm 0.6 \mu\text{m}$ from a 0.2 g/mL PPeF solution in DMF/ CHCl_3 (1:5) at 24 kV and 0.1 mL/min. The wettability of the optimized PBF and PPeF mats was assessed through contact angle measurements, revealing a highly hydrophobic nature with water contact angles of approximately 130° after complete solvent removal [2].

The optimized mats were subjected to mechanical characterization through quasi-static tensile tests before and after a treatment in physiological conditions. PBF mats exhibited high stiffness, with an elastic modulus of around 352 MPa/(g/cm³) before treatment and 359 MPa/(g/cm³) after treatment, indicating minimal alterations in mechanical performance. PBF mats displayed a limited plastic region, suggesting brittleness and a tendency to break with minimal deformation. In contrast, PPeF mats exhibited a more ductile behavior, with an extended plastic region, reaching a strain at break exceeding 600%.

Biological evaluations, including cytotoxicity assays and cell adhesion tests, yielded promising results for the potential biomedical applications of PBF and PPeF mats. Lactate dehydrogenase (LDH) assays indicated that neither PBF nor PPeF mats exhibited cytotoxic effects on human lung fibroblast cells (MRC5). SEM imaging further revealed good cell adhesion and the formation of long-shaped cytoskeletons on PBF and PPeF mats, highlighting their suitability as substrates for cell adhesion without surface functionalization.

For the drug delivery properties, energy Dispersive X-ray Spectroscopy (EDS) coupled with SEM revealed a homogeneous distribution of DX within PBF mats when dissolved in methanol, compared to dissolution in CHCl_3 /HFIP. UV-Vis analysis demonstrated the efficacy of vacuum treatment over oven treatment for solvent removal, as evidenced by higher DX concentrations released from vacuum-treated PBF mats. UV-Vis measurements indicated approximately 50% DX release from PBF mats within 3 days of incubation, highlighting their potential for controlled drug release applications.

References

- [1] G. Guidotti, M. Soccio, M.-C. García-Gutiérrez, E. Gutiérrez-Fernández, T.A. Ezquerro, V. Siracusa, A. Munari, N. Lotti, Evidence of a 2D-Ordered Structure in Biobased Poly(pentamethylene furanoate) Responsible for Its Outstanding Barrier and Mechanical Properties, *ACS Sustainable Chemistry & Engineering* 7(21) (2019) 17863-17871. DOI: 10.1021/acssuschemeng.9b04407
- [2] S. Santi, M. Soccio, G. Fredi, N. Lotti, A. Dorigato, Uncharted development of electrospun mats based on bioderived poly(butylene 2,5-furanoate) and poly(pentamethylene 2,5-furanoate), *Polymer* 279 (2023) 126021. DOI: 10.1016/j.polymer.2023.126021

INVESTING THERMAL OXIDATIVE AGING MECHANISMS IN EPDM

C. Jost¹, J. Sahyoun², M. Lacuve², X. Colin³ and E. Espuche¹

¹ Université Claude Bernard Lyon 1, CNRS UMR 5223, Ingénierie des Matériaux Polymères F-69622 Villeurbanne Cedex, France chloe.jost@univ-lyon1.fr

² Nexans Research Center, 69353 Lyon Cedex 07, France

³ Arts et Métiers Institute of Technology, PIMM, CNRS UMR 8006, 75013 Paris, France

INTRODUCTION

The terpolymer Ethylene Propylene Diene Monomer (EPDM) is particularly used in the field of electrical wiring as insulating materials, for accessories, due to its excellent dielectric properties and thermomechanical stability. The environmental solicitations endured by underground electric power distribution lines in service can be diverse: heat, oxygen, humidity, mechanical stress, and can lead to irreversible degradation of their functional properties, thus potentially leading to premature failures [1]. One of the main stresses to which insulating materials are exposed in service is temperature, generally in the 50-70 °C range. Thermal oxidation causes a reduction of the material's lifetime. Understanding this reaction is therefore a major challenge for the electrical wiring industry.

Two cross-linking modes are possible for this polymer: sulphur and peroxide cross-linking [2]. Sulfur-crosslinked EPDMs (denoted EPDMs XL-S) are generally employed when looking for materials with higher mechanical strength [3], whereas peroxide-crosslinked EPDMs (EPDMs XL-P) are used when needing for materials that maintain high mechanical properties throughout aging processes. In this study, two EPDMs crosslinked according to these two modes were manufactured then subjected to thermal aging in air in order to examine the impact of the cross-linking route on the thermal oxidation mechanisms and kinetics.

EXPERIMENTAL

Materials preparation and thermal aging

The starting linear EPDM is composed of 50 wt% in ethylene, 45 wt% in propylene and 5 wt% in ethylidene norbornene (ENB) as diene monomer. EPDM plates of about 0.6-0.8 mm thick were press-moulded and crosslinked under a compression of 2.0 MPa. EPDM XL-S was crosslinked using 0.40 phr of sulfur compounds at 170 °C for 15 min, whereas EPDM XL-P was crosslinked with 0.56 phr of dicumyl peroxide at 180 °C for 11 min. In both cases, the optimal crosslinking conditions (temperature and duration) were previously determined using rheometry according standard ISO 3417 [4]. The duration is defined as the time required for the torque to reach 90% of its maximum value plus 5 min. A lower temperature was chosen for EPDM XL-S in order to avoid reversion.

Before the aging experiments, rectangular samples of size 12x38 mm were degassed for 72h to remove moisture and residual vulcanization products. The samples are then thermally aged in an air-ventilated oven at 90, 110 and 130 °C for defined periods of time. The temperatures were chosen in order to accelerate the thermal oxidation without changing the mechanism involved in this reaction [5].

Characterization

Oxidized chemical functions were observed in a reflexion mode with a Spectrometer IR-TF Nicolet™ iS™10 equipped with a diamond crystal. Density measurements were performed through hydrostatic weighing at room temperature using a high-precision balance from Mettler Toledo. The samples were first weighed in air, then in immersion in ethanol, and their density was determined by applying the Archimedes' principle. Swelling measurements were performed in cyclohexane at room temperature to determine the crosslinking density

using the common Flory-Rehner's equation. Finally, changes in hydrophilicity through thermal aging were determined on few carefully chosen samples by dynamic water sorption (DVS).

RESULTS AND DISCUSSION

Monitoring the formation of oxidized functions by IRTF spectroscopy highlights the different mechanisms involved during thermal aging. At 130 °C for both EPDMs, two major bands are observed at 1730 and 1710 cm^{-1} , corresponding to the formation of carbonyl groups. In addition, in the case of EPDM XL-S (Fig. 1a), double bonds are formed during thermal aging, as shown by the shoulder at around 1640 cm^{-1} . In the case of EPDM XL-P (Fig. 1c), however, very few double bonds are formed. The presence of polysulfide junctions in an EPDM has clearly a protective effect against thermal oxidation.

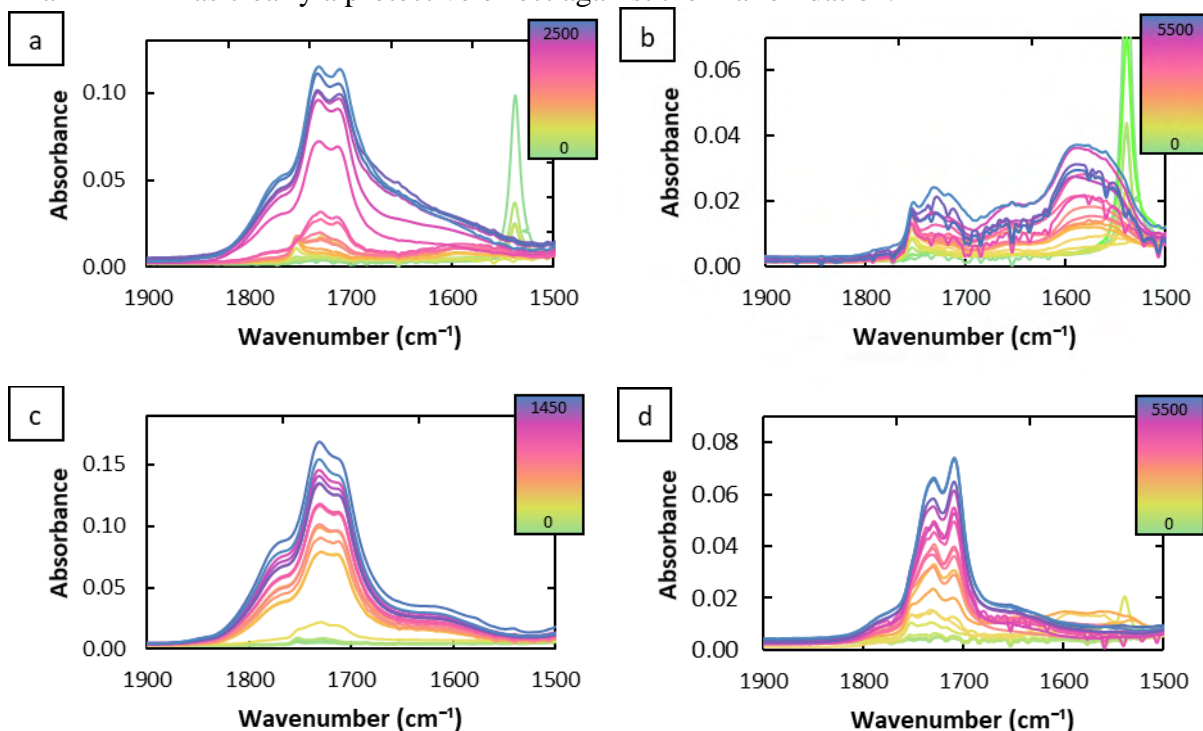


Fig. 1 Changes in the ATR spectrum during thermal aging (in hours) of EPDM XL-S in air at 130 °C (a) and 90 °C (b), and EPDM XL-P in air at 130 °C (c) and 90 °C (d)

The comparison of the agings at 130 °C (Fig. 1a) and 90 °C (Fig. 1b) for EPDM XL-S reveals that the double bonds band (at 1590 cm^{-1}) becomes more intense than the carbonyl band (at 1730 cm^{-1}) when decreasing the temperature. There is thus a competition between the thermal oxidation mechanisms, which is clearly temperature dependent. In light of these findings, one may question the reliability of lifetime predictions for industrial applications, knowing that accelerated aging tests are generally conducted at temperatures above 90 °C [6].

References

- [1] S. Hettal, S.V. Suraci, S. Roland, D. Fabiani and X. Colin, *Polymers*, 13:24, 4427 (2021)
- [2] M. Akiba, *Progress in Polymer Science*, 22:13, 475-521 (1997)
- [3] C. M. Kok and V. Yee, *European Polymer Journal*, 22:14, 341-345 (1986)
- [4] ISO 3417, Rubber - Measurement of vulcanization characteristics with the oscillating disc curemeter
- [5] M. Gardette, A. Perthue, J.-L. Gardette, T. Janecska, E. Földes, B. Pukánszky and S. Therias, *Polymer Degradation and Stability*, 98:111, 2383-2390 (2013)
- [6] Camille Blivet, Jean-François Larché, Yaël Israëlï and Pierre-Olivier Bussi re, *Polymer Degradation and Stability*, 201, 109978 (2022)

Fabrication and Characterization of Piezoelectric Polyhydroxybutyrate/Barium Titanate Nanocomposite Materials and Scaffolds for Bone Tissue Applications

M. Milazzo^{1*}, Massimiliano Labardi², Maurizia Seggiani¹, Giuseppe Gallone¹, Serena Danti¹

¹ Department of Civil and Industrial Engineering, University of Pisa, Largo L. Lazzarino 2, Pisa, Italy. ²CNR-IPCF, Pisa Unit, Largo Pontecorvo 3, 56127 Pisa, Italy.

*mario.milazzo@unipi.it, labardi@df.unipi.it, maurizia.seggiani@unipi.it, giuseppe.gallone@unipi.it, serena.danti@unipi.it

INTRODUCTION

Bone possesses an inherent ability for self-healing, enhancing a complex sequence of physiological processes involving cellular and molecular activities. Bone regeneration can face obstacles in some contexts, such as large defects also from pathological conditions. Bone replacements, independently of their nature (i.e., autografts, allografts, or xenografts) possess evident disadvantages, including little availability and donor-compatibility. Consequently, scaffolds developed with synthetic and/or natural biomaterials have been developed for favoring growth and differentiation of bone cells and, thus, tissue regeneration. A large portfolio of biomaterials, which includes polymers, ceramics, and composites, has been used in tissue engineering applications. Ideally, the replacement should: i) mimic the mechanical properties of the bone tissue; ii) be able to be easily fabricated with three-dimensional porous morphologies; iii) be able to dispatch signals to promote bone regeneration [1].

Recent attention has been drawn to the piezoelectric materials, like the bone constituents – hydroxyapatite and collagen [2]. Among polymers exhibiting a significant piezoelectric response and biodegradability also in physiological conditions, the polyhydroxyalkanoate (PHA) family, and in particular Polyhydroxybutyrate (PHB), stands out as an emerging class based on their crystalline properties for bone tissue engineering applications [3]. In view of fabricating piezoelectric nanocomposites, perovskite ceramics usually possess higher piezoelectric constants with respect to other types of materials. Among them, barium titanate (BaTiO_3) has been considered one of the first choices for making polymeric nanocomposites because of its intrinsic properties of biocompatibility, a high dielectric constant and piezoelectric coefficient, which has been demonstrated having a potential positive influence on bone cellular proliferation [4].

This work aims to develop and characterize piezoelectric nanocomposite materials in the form of 3D-printed scaffolds for bone tissue applications.

EXPERIMENTAL

Nanocomposite preparation and scaffold fabrication

Polyhydroxybutyrate (PHB) was purchased from Biomer® (Krailling, Germany) while Barium titanate powder (particle size < 3.0 μm) was supplied by Sigma-Aldrich (Steinheim, Germany). PHB pellets were dried for 24 h at 60 °C to remove residual humidity. Then, four nanocomposite classes, made by adding PHB with 5%, 10%, 15% and 20% w% of BaTiO_3 , were prepared by mixing and extrusion. Fused deposition modelling was employed to fabricate scaffolds with an alternated filling pattern of 0° - 90° layers using a nozzle diameter of 0.4 mm, a printing speed of 50 mm/s, and an extrusion temperature of 190 °C.

Physico-chemical, mechanical, and piezoelectric characterization

Differential Scanning Calorimetry and Thermogravimetric analysis were employed to investigate the thermal properties of the produced samples in the form of granules. Tensile and compression tests were performed to evaluate the main mechanical properties (i.e.,

Young's Modulus, Compressive strength) using dog bone specimens and the produced scaffolds, respectively.

The piezoelectric characterization was conducted by means of a custom-made experimental setup, on the materials samples in the form of films, through an electric potential that was applied along the transverse direction (z -axis, across the sample thickness) through a pair of planar electrodes, positioned as close as possible to the sample without touching it. The transverse electric field produces a longitudinal deformation (along the x -axis, along the sample length direction) proportional to the transverse, converse piezoelectric coefficient d_{31} of the material.

Finally, mass loss over time was assessed by putting the scaffolds in 8-mL of saline solution (pH 7.4, 0.9% NaCl) at 37 °C in a time frame of 8 weeks.

RESULTS AND DISCUSSION

We successfully produced PHB-based nanocomposites containing 5%, 10%, 15% and 20% (w%) BaTiO₃, through mixing and extrusion in the form of filaments, which were later 3D printed in porous cubic shapes, showing pore size in 600 -770 μm range and porosity in 54% - 62% range. The filler resulted finely dispersed in all the nanocomposites. The thermal and mechanical properties of the bulk samples were evaluated, the latter demonstrating a stiffening effect rising

with BaTiO₃ concentration, as well as a drop in the elongation at break even with the lowest amount of filler (5% w%). In our findings, PHB films had moderate piezoelectric properties ($d_{31} = 4.15 \text{ pm/V}$; $g_{31} = 0.113 \text{ Vm/N}$); on the other hand, an enhanced piezoelectric performance was achieved in the nanocomposites, which increased with the BaTiO₃ content. Indeed, the highest piezoelectric response was observed in the 20% (w%) barium titanate nano-composite ($d_{31} = 37 \text{ pm/V}$ and $g_{31} 0.67 \text{ Vm/N}$) (Fig.1). Overall, the 20/80 (w/w%) BaTiO₃/PHB displayed the best mechanical and piezoelectric properties, beside its filaments were difficult to print. The 20/80 (w/w%) BaTiO₃/PHB scaffold also showed 3.3% mass loss in saline solution at 37°C after 2 months, which indicated a long-lasting material in biological environment. All these outcomes support the investigated nanocomposites for further biological studies to provide new strategies for vascularized bone tissue engineering.

Acknowledgment

This study was funded by PRA project "New strategies for regenerating autologous vascularized bone substitutes (ANGIOSS)" (CUP: I56J20001060005). The authors acknowledge Prof. Andrea Lazzeri for making available some of the pieces of equipment used in this work.

References

1. M. Bahraminasab, M. Janmohammadi, S. Arab, A. Talebi, V. T. Nooshabadi, P. Koohsarian, and M. S. Nourbakhsh, *ACS Biomater. Sci. Eng.* **7**, 5397 (2021)
2. C. C. Silva, A. G. Pinheiro, S. D. Figueiró, J. C. Góes, J. M. Sasaki, M. A. R. Miranda, and A. S. B. Sombra, *J. Mater. Sci.* **37**, 2061 (2002)
3. G. Strangis, M. Labardi, G. Gallone, M. Milazzo, S. Capaccioli, F. Forli, P. Cinelli, S. Berrettini, M. Seggiani, S. Danti, and others, *Bioengineering* **11**, 193 (2024)
4. L. J. Bakhtar, H. Abdoos, and S. Rashidi, *J. Taiwan Inst. Chem. Eng.* **148**, 104651 (2023)

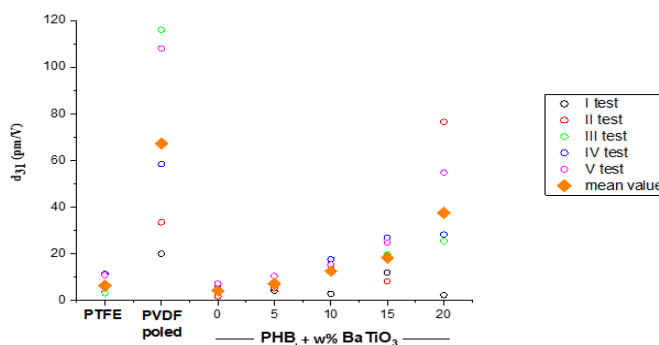


Fig. 1 Graph showing the converse piezoelectric coefficient d_{31} results obtained for PHB and BaTiO₃/PHB nanocomposites.

Chitin and chitosan materials from black soldier fly (*Hermetia illucens*): an insight onto new perspectives of circularity

M. B. Coltelli*, V. Gigante*, L. Panariello*, L. Aliotta, C. Scieuzo**,***P. Falabella**** and A. Lazzeri*

*Department of Civil and Industrial Engineering, University of Pisa, Via Diotisalvi 2, Pisa, Italy

**Department of Sciences, University of Basilicata – Via dell'Ateneo Lucano 10, 85100 Potenza, Italy

***Spinoff XFlies s.r.l, University of Basilicata, Via dell'Ateneo Lucano 10, 85100 Potenza, Italy

maria.beatrice.coltelli@unipi.it

INTRODUCTION

Functional materials obtained from chitin, like chitin nanofibrils and chitosan, were demonstrated to show anti-microbial and anti-inflammatory activities [1], thus their use in packaging, hygiene, personal care, cosmetic and biomedical application is rapidly increasing. In this contest, obtaining chitin and chitosan from different sources to grant their availability can be convenient. In the last years, valuable protein sources, necessary for aquaculture, were identified in biotechnological processes like the rearing of insects. Some insects behave as bioconverters, since they transform agro-food waste into proteins (useful for development of feeds), chitin (present in their exoskeletons) and other valuable compounds. In this chain chitin can be considered a by-product.

Chitin can be obtained from black soldier fly (*Hermetia illucens*) by demineralization and deproteination. Then chitin can be converted in chitosan by deacetylation. Chitin consists mainly of poly(N-acetyl-glucosamine), whereas chitosan consists mainly of poly(glucosamine). Actually, they can be considered copolymers of these two repeating units. Despite of several aspects of the functional properties of chitin and chitosan were widely explored, the correlation between their chemical structure and properties deserves to be more investigated for exploiting these interesting materials in biocircular industrial chains.

In the present work an ATR-IR methodology was adopted to compare the degree of acetylation of chitin and chitosan obtained in the different vegetative steps (larvae, pupal exuviae, adult) of the black soldier fly insect to distinguish N-acetyl glucosamine (chitin) from acetyl glucosamine (chitosan) copolymers. Commercial samples of chitin and chitosan from shrimp and mushrooms were also considered for comparison.

EXPERIMENTAL

Materials

H. illucens larvae, pupal exuviae and dead adults were provided by Xflies s.r.l (Potenza, Italy).

Preparation

The preparation of chitin by demineralization and deacetylation as well as the successive deacetylation to obtain chitosan were carried out as described in a previous work [2]. Decolorized samples, identified with the letter “D” were also prepared [2].

Infrared characterization

Infrared spectra were recorded by using an infrared spectrometer Nicolet 380 (Thermo Fisher Scientific, Carlsbad, CA, USA) equipped with an attenuated total reflection (ATR) smart ItX accessory (Thermo Fisher Scientific, Carlsbad, CA, USA). Spectra were recorded in the range 550–4000 cm^{-1} collecting 256 scans with a resolution of 4 cm^{-1} . ONMIC software was used to elaborate the spectra and to compare different spectra profiles.

The Rac ratio, that can be correlated to the acetylation degree of the sample, was determined by calculating Rac value defined as the ratio between A_{1620} and A_{1020} , where A_{1620} is the area of the band obtained by integrating the peak at 1620 cm^{-1} , attributed the amide group, in the range $1695\text{-}1618\text{ cm}^{-1}$ and A_{1020} is the area of the reference band in the range $1186\text{-}1026\text{ cm}^{-1}$. The integrations were carried out after tracing a baseline passing through the minima present in all the spectra at about 1735 cm^{-1} and 1185 cm^{-1} . The measurements were done in triplicates onto the chitin (CHITI) and chitosan (CHITO) samples obtained from adult (A), larvae (L) and pupal exuviae (EP), in order to calculate the standard deviation. Chitin from shrimp and fungi and chitosan from shrimps were also tested for comparison.

RESULTS AND DISCUSSION

The determination of Rac values allowed to observe that the acetylation degree was, as we could expect, higher for chitin samples (green bars in Fig.1) than for chitosan (yellow bars). Moreover, the preparation of chitin result in copolymers with a higher N-acetyl glucosamine content for adult insect with respect to chitin extracted from larvae or pupal exuviae

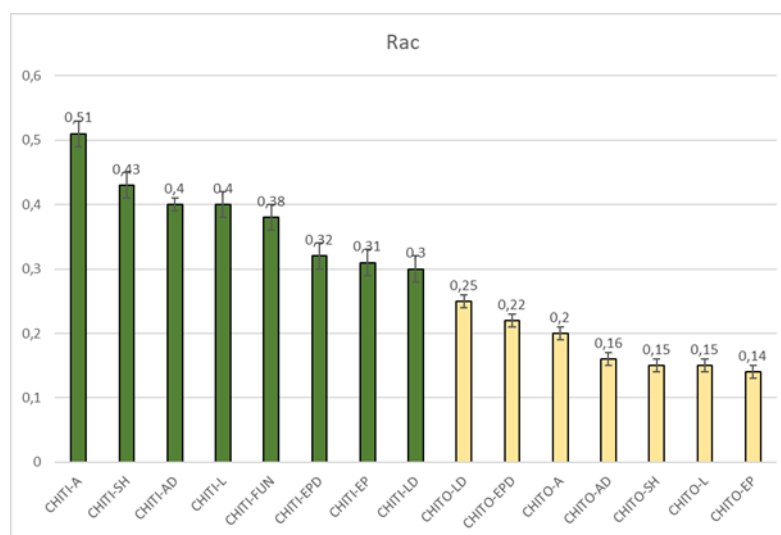


Fig. 1 Rac value calculated from infrared spectra for samples of chitin (green) and chitosan (yellow)

Decolorized chitin samples showed a lower Rac than corresponding not bleached ones. The deacetylation of chitin from pupal exuviae or larvae resulted in chitosan with the lowest value of Rac. This value resulted similar to the value observed for a commercial chitosan obtained by shrimps, indicated by SH in Fig.1.

Acknowledgment

This work has been partially supported by “PLAnt-based antiMicrobial aNd circular PACKaging for plant products” (PLAMINPACK) project under the PRIMA2023-section2 program, with italian entities funded by Ministero dell’Università e della Ricerca (MUR).

References

- 1) A. Guarnieri, M. Triunfo, C. Scieuzo, D. Ianniciello, E.Tafi, T. Hahn, S. Zibek, R. Salvia, A. DeBonis, P. Falabella. Scientific reports Rep, **12**, 8084 (2022)
- 2) M. Triunfo, E. Tafi, A. Guarnieri, R. Salvia, C. Scieuzo, T. Hahn, S. Zibek, A.Gagliardini, L. Panariello, M.B. Coltelli, A. De Bonis, P. Falabella. Scientific reports, **12(1)**, 6613 (2022)

Kinetic models for a hydrolysis reaction with marine degradable biopolymers based on the water sorption behavior

T. Koike, Y. Muranaka*, and T. Maki

Department of Chemical Engineering, Kyoto University, Kyoto, Japan

*muranaka@cheme.kyoto-u.ac.jp

INTRODUCTION

Biodegradable polymers, including polyhydroxyalkanoate (PHA), have attracted attention because plastic waste is entering the ocean and causing problems. Controlling the rate of PHA degradation is essential for expanding its application, and fundamental studies on the reaction mechanisms are needed. This study focused on the nonenzymatic hydrolysis reaction of poly(3-hydroxybutyrate-co-3-hydroxyhexanoate) (PHBH), which involves a two-step kinetic process which are water sorption and hydrolysis within biodegradable polymers. Previous studies have examined the characteristics of the hydrolysis reaction of polyesters, but no reaction-kinetic model has yet been developed to predict polymer hydrolysis reactions that considers water sorption processes. In this study, the mechanisms of water sorption and hydrolysis reactions within PHBH were experimentally verified, and the kinetic models were constructed.

EXPERIMENTAL

PHBH (X131A, Kaneka, Japan), with an hydroxyhexanoate (HHx) content of 6 % and a weight average molecular weight of 450K-479K, was provided as pellets and used as received. PHBH plates with four different thicknesses, 0.5, 2.8, 5.5 and 8.2 mm, were prepared by melting the pellets on a hot-press machine at 160 °C. The plates were then cooled and held at 40 °C for another 10 minutes to solidify. A prepared PHBH plate was immersed in deionized water at a designated temperature ranging from 40 to 80 °C using a drying oven.

The following two measurements were performed on 0.5 mm thick PHBH plates. A plate immersed in deionized water was removed occasionally from the bath, and its near-infrared (NIR) transmission spectrum was measured after water was wiped off the plate surface. After the measurement, the plate was returned to deionized water in a temperature-controlled thermostat bath. This procedure was repeated until the plate was saturated with water. The plate's water concentration averaged in the plate thickness direction was obtained from the transmission NIR spectrum using the NIR spectrometer (Spectrum 100, PerkinElmer, USA).

The plate was removed from the bath and dried in vacuum. The average molecular weight (M_n) of PHBH plates were measured by a high-performance liquid chromatography system (Shimadzu, Japan) equipped with a UV spectrometer (SPD-20A, Shimadzu, Japan). The oven was set at 40 °C, and the column used was GPC K-806 L (Resonac Holding Corporation, Japan).

RESULTS AND DISCUSSION

Fig. 1 shows the normalized water sorption curves on the PHBH plates with a thickness of 0.5 mm measured by near-infrared spectroscopy. The amount of water sorption on the PHBH plate increased with time, and the water sorption rate increased with increasing sorption temperature. Furthermore, the normalized water sorption curves into PHBH did not follow Fick's law of diffusion. Therefore, the water sorption behavior into PHBH by using the adsorption and diffusion two modes model was expressed with two equations (Eqs. (1) and (2)), where C is the water concentration in a polymer [mol/m^3], x is the distance from the center of the polymer plate thickness direction [m], t is the time [s], D is the diffusion coefficient of water in the polymer [$\text{m}^2 \text{s}^{-1}$], q is the molar adsorption quantity of water [mol/m^3], γ is the adsorption rate constant [s^{-1}], and β is the desorption rate constant [s^{-1}].

$$\frac{\partial C}{\partial t} = D \frac{\partial^2 C}{\partial x^2} - \frac{\partial q}{\partial t} \quad \text{Eq. (1)}$$

$$\frac{\partial q}{\partial t} = \gamma C - \beta q \quad \text{Eq. (2)}$$

As shown in Fig. 1, the model estimates agreed with the experimental data. This result demonstrated that water sorption on PHBH proceeded by two kinetic processes involving adsorption and diffusion.

Fig. 2 shows the experimental data of M_n of the PHBH plates with a thickness of 0.5 mm carried out at reaction temperature within 40-80 °C. The hydrolysis reaction progressed, and M_n decreased with increasing reaction time. Since the hydrolysis reaction of polyesters is an autocatalytic reaction of carboxy groups, the model equation was constructed in which the hydrolysis reaction depends on the concentration of both ester bonds and carboxy groups, as expressed in Eq. (3). n is degree of polymerization [-], $[P_n]$ is molar density of polymer [mol/m^3], $[\text{COOH}]$ is molar density of carboxy group [mol/m^3], k is reaction rate constant [$\text{m}^3/(\text{mol s})$]. Eq. (4) expresses the change in M_n over time derived from Eq. (3).

$$d(\sum_{n=1}^{\infty} [P_n])/dt = k\{\sum_{n=1}^{\infty} (n-1)[P_n]\}[\text{COOH}] \quad \text{Eq. (3)}$$

$$\ln(M_n) = \ln(M_{n0}) - k(\sum_{n=1}^{\infty} n[P_n])t \quad \text{Eq. (4)}$$

The experimental data and Eq. (4) estimates are in good agreement (Fig. 2), indicating that this model is valid and can predict the degradation rate of PHBH.

For the plate with a thickness of 0.5 mm, the water sorption rate was extremely fast compared to the hydrolysis rate and could be regarded as a reaction-controlled process. However, when the thickness of the PHBH plate increases, longer time is needed for water sorption to reach saturation, and the sorption rate may affect the hydrolysis reaction (degradation) rate. Here, the hydrolysis reaction model was extended by modifying the reaction rate constant (k) while considering water sorption (change in concentration during hydrolysis) as Eq. (5).

$$dM_n/dt = -k'(\sum_{n=1}^{\infty} n[P_n])M_n \quad \text{Eq. (5)}$$

$$k' = \int \{C(x,t) + q(x,t)\} dx / 2(C_{\infty} + q_{\infty})L$$

Fig. 3 shows the experimental data and the calculation results obtained by the change in M_n of PHBH plates with three different thicknesses, 2.8, 5.5, and 8.2 mm, soaked at 80 °C. The calculation was performed using D , γ , β , and k values obtained from the experiments of the 0.5 mm thick plate and solving Eqs. (1), (2), and (5). As shown in Fig. 3, the larger the thickness was, the slower the hydrolysis reaction progressed because time was needed for water to penetrate and achieve saturation. The proposed model can predict the degradation of PHBH plates of different thicknesses.

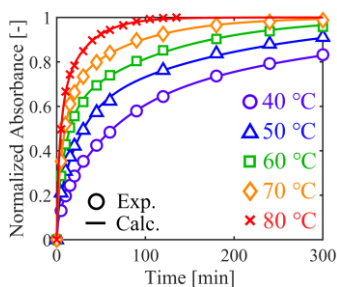


Fig. 1 Water sorption rates of the PHBH plate with a thickness of 0.5 mm and Eq. (1) and (2) estimates

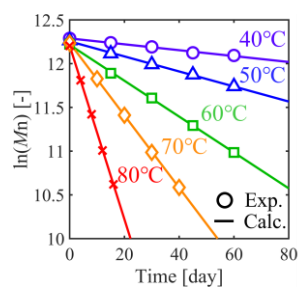


Fig. 2 The experimental data and Eq. (4) estimates of M_n of the PHBH plate with a thickness of 0.5 mm

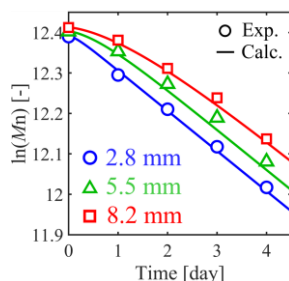


Fig. 3 The experimental data and Eq. (5) estimates of M_n of PHBH plates with thicknesses of 2.8 mm, 5.5 mm, and 8.2 mm carried out at 80 °C

Acknowledgment

The authors appreciate Kaneka Corporation for providing PHBH resin.

Nanocomposite gellan gum based injectable and printable hydrogel with antimicrobial properties

C.Fiorica^a, G. Barberi^a, G. Pitarresi^a, F.S. Palumbo^a, V. Catania^b, D. Schillaci^a and

G. Giammona^a

^a Department STEBICEF, University of Palermo, Via Archirafi 32, Palermo, Italy

^b Department DISTeM., University of Palermo, Viale delle Scienze, Palermo, Italy

INTRODUCTION

Managing skin ulcers typically involves local antibiotics or antimicrobials and hydrogels, which maintain tissue hydration and resemble the extracellular matrix [1]. However, excessive antibiotic use in topical treatments can lead to microbial adaptation and the emergence of resistant strains. Silver nanoparticles (AgNPs) offer a promising alternative, effectively combating resistant bacteria [2]. In our study, we developed a novel cationic derivative of gellan gum (named GG-EDA-GTMAC) as a precursor for producing injectable hydrogels. We demonstrated that AgNPs can be synthesized and stabilized within the hydrogel without the need for toxic reducing agents. This nanocomposite system can be conveniently injected or printed to achieve specific shapes and dimensions. Hydrogels exhibit the characteristic ionic strength sensitivity of gellan gum, and the presence of AgNPs confers effective antimicrobial properties against both Gram-negative and Gram-positive bacteria.

EXPERIMENTAL

Materials

Gellan gum, ethylenediamine (EDA), diethylamine (DEA), Glycidyltrimethylammonium chloride (GTMAC), 2,4,6-Trinitrobenzenesulfonic acid (TNBS), AgNO₃, were purchased from Sigma-Aldrich.

Production of GG-EDA-GTMAC

GG-EDA [3], was dissolved in water at 50°C in the presence of DEA, and reacted with GTMAC at this temperature for 24 h. The functionalization of the obtained product, purified via dialysis and recovered by freeze dried, was investigated through ¹H-NMR, and confirmed by TNBS assay.

Production and characterization of nanocomposite injectable hydrogel

GG-EDA-GTMAC was dissolved in water at 70°C and cooled at 40°C prior to add AgNO₃ solution. The obtained *sol* was irradiated for 30 min with UV light at 366nm. The rheological investigation of nanocomposite hydrogel was investigated to analyze its viscoelastic properties. The presence of reduced silver (nanoparticles) was investigated by means of UV-Vis, SEM-EDX and XPS analyses.

Cytocompatibility and antimicrobial assessment

Cytocompatibility was investigated by MTS test by culturing the hydrogel, containing or not silver nanoparticles, with human dermal fibroblasts. The antimicrobial properties against *P. Aeruginosa* and *S. Aureus* were investigated by colony forming unit (CFU) assay.

RESULTS AND DISCUSSION

Spectroscopic (NMR) (Fig.1) and colorimetric (TNBS) analysis confirm that the functionalization degree of GG-EDA in GTMAC moieties is 20±5mol%. AgNPs can be readily produced via UV in situ photoreduction. Before UV irradiation, GG carboxyl groups

adsorb silver ions, and after irradiation, the permanent cations and residual free amine groups of the derivatives stabilize the AgNPs, preventing aggregation.

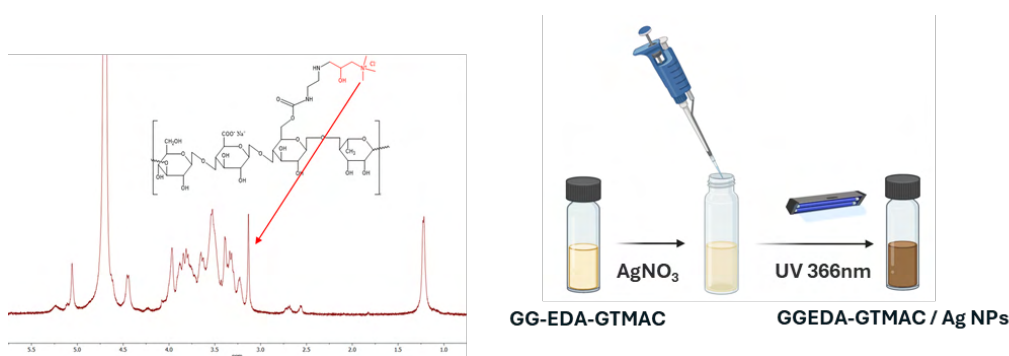


Figure1: Chemical structure and ¹H-NMR spectrum of GG-EDA-GTMAC. Schematic illustration of the UV photoreduction and production of AgNPs

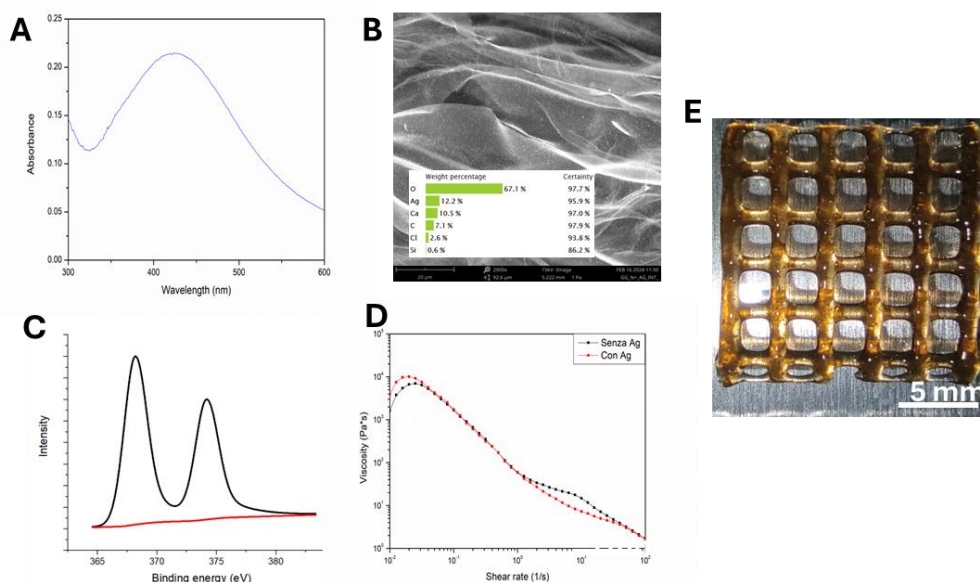


Figure1: UV-Vis of AgNPs produced inside the hydrogel(A), SEM-EDX (B), XPS (C) and shear thinning (D) analysis of nanocomposite hydrogel. 3D printed grid of nanocomposite hydrogel (E)

UV-Vis and XPS analysis confirmed the presence of AgNPs inside the hydrogel while rheological studies demonstrated the injectability of the systems that makes it easily administrable and suitable for 3D printing.

In vitro biological studies demonstrated that the cytocompatibility as well as the antimicrobial activity of the nanocomposite hydrogel depend on the amount of silver payload.

On the whole, these results demonstrated that the proposed nanocomposite hydrogel can be an optimal candidate to treat infected skin wounds.

Acknowledgment

Funded by the European Union - NextGenerationEU through the Italian Ministry of University and Research under PNRR - M4C2-I1.3 Project PE_00000019: " Health Extended Alliance for Innovative Therapies, Advanced Lab-research, and Integrated Approaches of Precision Medicine - HEAL ITALIA" to Giovanna Pitarresi, CUP B73C22001250006

References

- 1) Pranantyo, D., Yeo, C.K., Wu, Y. et al. Nature Communication, **15**, 954 (2024)
- 2) Autumn, S., Dominika, I., Wren, R. et al. Frontiers in Microbiology, **13**, (2023)
- 3) Fiorica, C., Pitarresi, G., Palumbo, F.S., et al. Carbohydrate Polymers, **15**, 236 (2020)

HUMID/DRY CYCLES IN NATURAL FIBER REINFORCED COMPOSITES ARE A REAL AGING ISSUE?

A. Valenza^{1*}, V. Fiore¹, L. Calabrese² and E. Proverbio²

¹Department of Engineering, University of Palermo, Viale delle Scienze, Palermo, Italy

²Department of Engineering, University of Messina, Contrada Di Dio, Messina, Italy

*antonino.valenza@unipa.it

INTRODUCTION

Natural fibers are increasingly replacing traditional materials in composite design due to their sustainability benefits. NFRCs (Natural Fiber-Reinforced Composites) offer a suitable combination of lightweight, good mechanical strength, and eco-friendly credentials. From automotive parts to building materials, these composites have the potential to enhance sustainability and green design in various industries. However, a significant problem remains in realizing their full potential: the durability in outdoor applications.

Unlike their synthetic counterparts, NFRCs face a particular challenge when exposed to the elements - humid/dry cycles. These cycles, characterized by repeated fluctuations in temperature and moisture levels, affect the long-term performance of NFRCs. As environmental conditions swing between wet and dry, hot and cold, natural fibers and related composites undergo dimensional and chemo-physical changes.

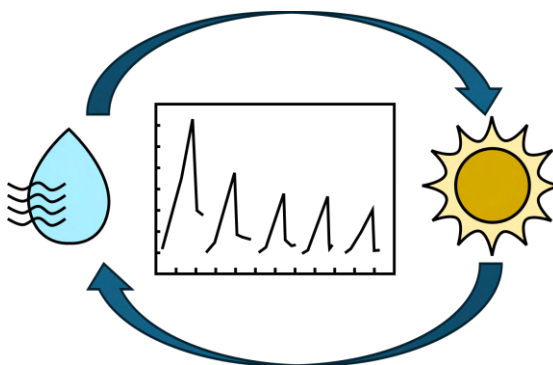


Fig. 1 Graphical schematization of humid/dry cycles aging

Understanding how alternate humid/dry cycles degrade NFRCs is crucial to unlocking their true potential for outdoor applications. This introduction will delve into the mechanisms by which alternate humid cycles accelerate material degradation.

In this work, we are going to investigate whether, and if so, how, moisture absorption, fiber-matrix interface breakdown, and mechanical weakening combine to limit, either reversibly or permanently, the durability of NFRCs (1)-(5). Furthermore, a wide and detailed discussion will be held on ongoing research efforts aimed at mitigating these challenges (6)-(7). By exploring potential solutions such as improved surface treatments (Fig. 2), targeted fiber modification techniques and the development of hybrid composites that combine natural and synthetic fibers (Fig. 3), we can pave the way for a new generation of NFRCs that can truly withstand the rigors of the outdoors.

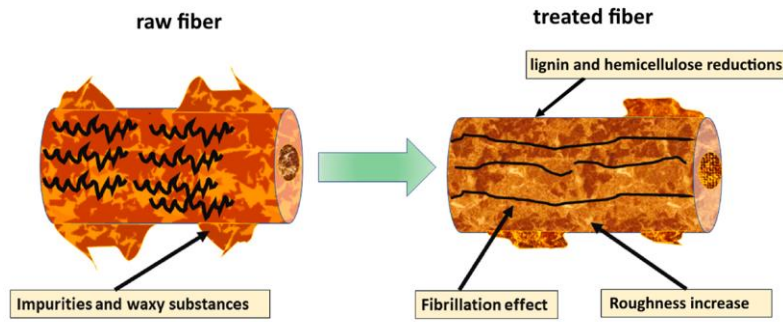


Fig. 2 Main effects of chemical treatment on natural fibers

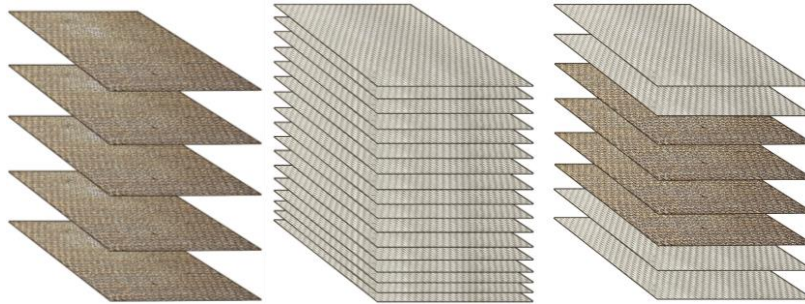


Fig. 3 Staking sequences of different composite laminates

This quest for improved durability opens a scientific discussion for NFRCs' future use, where these materials could truly be identified as sustainable and high-performance materials for a wide range of outdoor applications. By overcoming this key hurdle, we can unlock the full potential of these eco-friendly composites, contributing to a more sustainable future for our built environment.

References

- 1) V. Fiore, L. Calabrese, R. Miranda, D. Badagliacco, C. Sanfilippo, D. Palamara, A. Valenza, E. Proverbio. *Composites Part B*, **230**, 109535 (2022)
- 2) V. Fiore, L. Calabrese, R. Miranda, D. Badagliacco, C. Sanfilippo, D. Palamara, A. Valenza, E. Proverbio. *Composites Part B*, **238**, 109897 (2022)
- 3) V. Fiore, L. Calabrese, R. Miranda, D. Badagliacco, C. Sanfilippo, D. Palamara, A. Valenza, E. Proverbio. *Composites Part B*, **257**, 110693 (2023)
- 4) L. Calabrese, V. Fiore A., Valenza, E. Proverbio. *Polymer Testing*, **127**, 108186 (2023)
- 5) Fiore A., L. Calabrese, C. Sanfilippo, E. Proverbio, V. Valenza. *Polymer Testing*, **135**, 108472 (2024)
- 6) Q. Wang, T. Chen, X. Wang, Y. Zheng, J. Zheng and G. Song., *Polymers*, **15**, 4121 (2023)
- 7) K. Mak, A. Fam, *Composites Part B* 183 (2020) 107645

IONIC LIQUIDS AS MULTIFUNCTIONAL POLYMER ADDITIVES

(this is a sample, Times New Roman, 12 single line))

J.F. Gérard, J. Duchet-Rumeau, S. Livi

Ingénierie des Matériaux Polymères UMR CNRS 5223, Université de Lyon-INSA Lyon, F-69621 Villeurbanne

jean-francois.gerard@insa-lyon.fr

Using polymers in the design of the new products of the future will of course mean rethinking the design of products to enable them to be dismantled to allow materials to be separated, but it will also mean going back to macromolecular design and the formulation of plastics. Often, in fact, several polymers are combined, as in polymer blends or multilayers, to take advantage of the intrinsic properties of each of the polymers (e.g. combining rigidity and toughness). Furthermore, polymers cannot be shaped and used in a wide range of applications without the addition of a number of additives to ensure their stability during formulation and/or shaping, under a variety of environments (e.g. UV exposure, humidity), and under extreme conditions (e.g. fire resistance). In the latter case, for example, to simplify recycling, the aim is to avoid multiplying the number of additives by substituting a cocktail of additives with, ideally, a single additive. Also, adding additive to a polymer to give it the multifunctional character so often sought is a challenge that needs to be addressed. The present lecture illustrates the integration of ionic liquids of different natures (imidazolium or phosphonium -based, combinations of cations and anions) and forms (dispersed, nanostructured, encapsulated, at phase boundaries) in various types of thermoset or thermoplastic polymers (1,2).

The first case involves the integration of ionic liquids of different kinds in reactive systems, leading to epoxy networks (3-6). Ionic liquids introduced in very low concentrations (<10 wt. %) can *i/* catalyze polymerization kinetics (fast-cure formulations have been proposed for carbon-fiber-based composites for hyperbaric hydrogen tanks); *ii/* lead to ionic nanostructures which leads to networks having enhanced elastic and fracture properties; *iii/* confer higher fire resistance than modified networks; *iv/* add new functionalities to coatings prepared from these formulations: corrosion protection, superhydrophobic surfaces, antibacterial properties, etc. The fire properties of thermosetting resins are essential for many applications of these high-value-added materials, such as aerospace and railways transportation. In previous works, it was shown that the addition of organic/inorganic (nano)clusters such as metal-oxo clusters of the PolyOligomericSilSesquioxane (POSS[®]) type could help to partially replace conventional flame retardants such as halogens. In this presentation, we present an approach combining POSS and ionic liquids by preparing ionic liquid-functionalized POSS[®] (7,8). The benefits of such ionic liquids supported by O/I nanoclusters are demonstrated in terms of the fire-retardant properties of modified epoxy networks.

In the second part of the lecture, we describe at the addition of ionic liquids to a conventional thermoplastic polymer, polyvinyl chloride (PVC)(9). In a sector such as construction, the use of flame-retardant additives is required, but these compounds present significant toxicities and are in the process of being progressively banned. The use of LIs as flame retardants is therefore proposed for plastisol formulations. LIs are compared alone or in combination with different families of more conventional flame retardants such as metal oxides, phosphorus compounds, nitrogen compounds, and biosourced flame retardants. The chosen strategy was to combine several flame retardants including ILs with different but complementary flame retardant mechanisms.

In conclusion, ionic liquids are compounds of interest because they are multifunctional, making it possible *i/* either to replace or partially substitute thermoplastic or thermoset polymer additives, in particular to meet new environmental or toxicity requirements, or *ii/* to impart different types of behavior to the final formulated polymer. Other research works were

done on other combinations of polymers with ionic liquids: IL-nanostructured thermoplastics (10) including polyolefins (11,12) and fluorinated TPs (13), IL-microcapsules as healing agents of thermosets (14,15), ILs as interfacial agents in blends (16) or sizing of carbon fibers in composites (17), ILs for tailoring biodegradation of polymer blends (18), ILs inserted in the monomer architecture (19,20), etc.

Acknowledgments

These works have been financially supported by the French Ministry of Higher Education & research (MESR), the Agency for Research (ANR), and MERMET Co. sponsored by the ANRT Agency. The authors would thank Dr. C. Michelin, Dr. H. Chabane, and Dr. T. Shi who contributed with their PhD works to these researches.

References

- (1) S. Livi, J. Duchet-Rumeau, J.F. Gérard, T.N. Pham, *Macromol. Chem. Phys.*, **216**, 4, doi 10.1002/macp.201400425 (2015)
- (2) A.A. Silva, S. Livi, D.B. Netto, B.G. Soares, J. Duchet, J.F. Gérard, *Polymer*, **54**, 8, doi 10.1016/j.polymer.2013.02.021 (2013)
- (3) B.G. Soares, A.A. Silva, S. Livi, J.F. Duchet-Rumeau, J.F. Gérard, *J. Appl. Polym. Sci.*, **131**, 3, doi 10.1002/app.39834 (2014)
- (4) S. Livi, A.A. Silva, Y. Thimont, T.K.L. Nguyen, B.G. Soares, J.F. Gérard, *J. Duchet-Rumeau, RSC Adv.*, **4**, 53, doi 10.1039/c4ra03643c (2014)
- (5) B.G. Soares, A.A. Silva, S. Livi, J. Duchet-Rumeau, J.F. Gérard, *J. Appl. Polym. Sci.*, **131**, 3, doi 10.1002/app.39834 (2014)
- (6) T.K.L. Nguyen, S. Livi, B.G. Soares, S. Pruvost, J. Duchet-Rumeau, J.F. Gérard, *ACS Sustain. Chem. & Engng.*, **4**, 2, doi 10.1021/acssuschemeng.5b00953 (2016)
- (7) H. Chabane, S. Livi, H. Benes, C. Ladavière, P. Ecorchard, J. Duchet-Rumeau, J.F. Gérard, *Europ. Polym. J.*, **114**, doi 10.1016/j.eurpolymj.2019.03.005 (2019)
- (8) H. Chabane, S. Livi, X.P. Morelle, R. Sonnier, L. Dumazert, S. Duchet-Rumeau, J.F. Gérard, *Polymer*, **224**, doi 10.1016/j.polymer.2021.123721 (2021)
- (9) C. Michelin, PhD Dissertation INSA Lyon (2024)* T. Shi, S. Livi, J. Duchet-Rumeau, J.F. Gérard, *Nanomaterials*, **10**, 5, doi 10.3390/nano10050881 (2020)
- (10) C.F. Zornio, S. Livi, J. Duchet-Rumeau, J.F. Gérard, *Nanomaterials*, **9**, 10, doi 10.3390/nano9101376 (2019)
- (11) L.T. Hou, S. Livi, J.F. Gérard, J. Duchet-Rumeau, *Europ. Polym. J.*, **210**, doi 10.1016/j.eurpolymj.2024.112928 (2024)
- (12) L.T. Hou, S. Livi, J.F. Gérard, J. Duchet-Rumeau, *Polymers*, **15**, 2, 370 doi 10.3390/polym15020370 (2023)
- (13) L.C. Lins, S. Livi, M. Maréchal, J. Duchet-Rumeau, J.F. Gérard, *Europ. Polym. J.*, **107**, doi 10.1016/j.eurpolymj.2018.08.022 (2018) PVDF
- (14) T. Shi, S. Livi, J. Duchet-Rumeau, J.F. Gérard, *Polymer*, **233**, doi 10.1016/j.polymer.2021.124182 (2021)
- (15) T. Shi, S. Livi, J. Duchet-Rumeau, J.F. Gérard, *Europ. Polym. J.*, **215**, doi 10.1016/j.eurpolymj.2024.113233 (2024) capsules
- (16) L.C. Lins, S. Livi, J. Duchet-Rumeau, J.F. Gérard, *RSC Adv.*, **5**, 73, doi 10.1039/c5ra10241c (2015)
- (17) B. Gaumond, S. Livi, J.F. Gérard, J. Duchet-Rumeau, *Polymers*, **14**, 7, doi 10.3390/polym14173692 (2022)
- (18) E. Delamarche, A. Mattlet, S. Livi, J.F. Gérard, R. Bayard, V. Massardier, *Frontiers in Materials*, **9**, doi 10.3389/fmats.2022.975438 (2022)

- (19) A.V. Radchenko, J. Duchet-Rumeau, J.F. Gérard, J. Baudoux, S. Livi, *Polym. Chem.*, **11**, 34, doi 10.1039/d0py00704h (2020)
- (20) G. Perli, L. Wylie, B. Demir, J.F. Gérard, A.A.H. Pádua, M.C. Gomes, J. Duchet-Rumeau, J. Baudoux, S. Livi, *ACS Sustainable Chem. & Engng.*, **10**, 47, 15450-15466, doi 10.1021/acssuschemeng.2c04499 (2022)

Study of the Abiotic Degradation of Elastomers (Vulcanised or Not) for their Biodegradation

Mbaye Dieng^a, Laurie Calarnou^a, Sandrine Therias^a, Jean-Luc Gardette^a,
Pierre-Olivier Bussière^a, Lucie Malosse^b, Séverin Dronet^b,
Pascale Besse-Hoggan^a, Boris Eyheraguibel^a

^a Université Clermont Auvergne, Clermont Auvergne INP, CNRS, Institut de Chimie (ICCF),
F-63000 Clermont– Ferrand, France

^b Manufacture Française des Pneumatiques MICHELIN, Centre de Technologies Ladoux,
63040 Clermont-Ferrand, France

Auteur correspondant : sandrine.therias@uca.fr

INTRODUCTION

The emission of wear particles is the main mechanism of tire mass loss for passenger cars and heavy goods vehicles and represents approximately 1 kg of tread per year per inhabitant in Europe [1]. To document the fate of these particles in the environment, we investigated the abiotic and biotic degradation of elastomers widely used in the formulation of tire treads, such as polystyrene-co-butadiene (SBR: Styrene Butadiene Rubber).

This presentation will focus on characterizing the degradation of SBR, whether vulcanised or not, via abiotic processes including photooxidation, to identify the resulting degradation products with the aim to subsequently studying their biodegradation. The results highlight the impact of abiotic degradation on the subsequent biodegradation of SBR, identifying oxidised short chains as the carbon substrates degraded by bacteria [2].

EXPERIMENTAL

Materials

Two elastomers supplied by Michelin were studied: SBR or vulcanised SBR formulations. Elastomer films (50 µm thick) were prepared by compression molding between silicone-coated polyester sheets: SBR films at 110°C for 30 s, then pressed at 50 bar for 1 min at 110°C, and vulcanised SBR films at 150 °C for 20 min.

Abiotic degradation

Photoaging experiments were carried out either using an Atlas Suntest CPS/XLS for SBR or using a SEPAP 12/24 for vulcanised SBR.

Characterisation techniques

Characterisation techniques included infrared analysis, UV-visible spectroscopy, gel fraction, steric exclusion chromatography, and mass spectrometry.

Biotic degradation

For biotic degradation, two bacterial strains, *Rhodococcus ruber* ATCC 29672 and *Gordonia polyisoprenivorans* VH2 (DSMZ 44266), were selected. The strains were inoculated with 100±5

mg of SBR film as a carbon source. The films, sterilized with ethanol, were cultured with different bacterial strains and control materials. Incubations lasted 30 days at 27°C and 130 rpm.

RESULTS AND DISCUSSION

The FTIR spectrum of an SBR film revealed bands characteristic of styrene and butadiene units, with specific vibrations at 966 cm^{-1} and 912 cm^{-1} . Significant spectral changes were observed in the hydroxyl and carbonyl regions upon irradiation (Fig.1), confirming the formation of oxidation products from butadiene part.

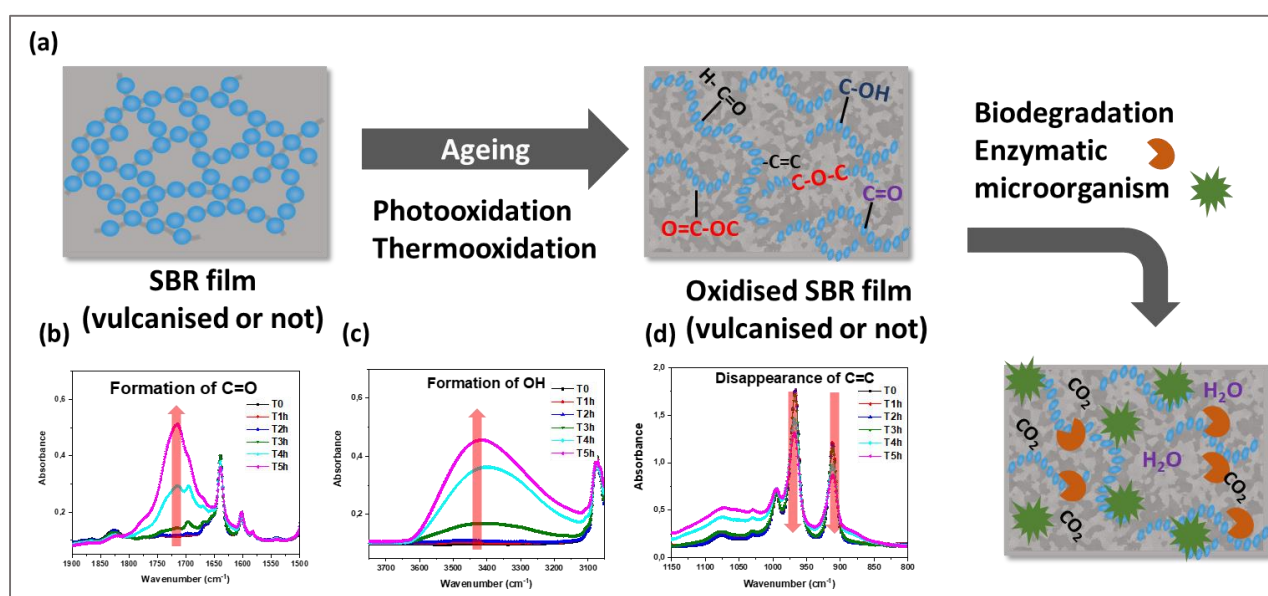


Figure 1: (a) Aging of SBR films by photooxidation or thermooxidation. Characterization by FTIR: (b) carbonyl zone, (c) OH bond zone, and (d) double bond zone.

The results show that *Rhodococcus ruber* and *Gordonia polyisoprenivorans* strains can degrade oxidized SBR samples, highlighting the positive impact of abiotic degradation on biodegradation.

References

- [1] Unice et al., "Characterizing export of land-based microplastics to the estuary - Part I: Application of integrated geospatial microplastic transport models to assess tire and road wear particles in the Seine watershed," *Sci. Total Environ.*, 2019, 646, 1639-1649, <https://doi.org/10.1016/j.scitotenv.2018.07.368>.
- [2] Calarnou et al., "Study of sequential abiotic and biotic degradation of styrene butadiene rubber," *Sci. Total Environ.*, 2024, 926, 171928, <https://doi.org/10.1016/j.scitotenv.2024.171928>.

Effect of the incorporation of recycled materials on the durability of polyethylene films

A. Duchamp^{a,b}, J. Christmann^a, J-L. Gardette^a, J. Charbonnier^b, B. Bouchut^b, S. Therias^a

^aUniversité Clermont Auvergne, CNRS, Clermont Auvergne INP, ICCF, F-63000 Clermont-Ferrand, France

^bGroupe Barbier, F-43600 Sainte Sigolène, France

INTRODUCTION

Recycled Plastic Materials (RPM) are used in a growing number of applications in order to reduce their environmental impact. Among the numerous issues arising from the use of RPM, their durability in use conditions under environmental stress factors (light, heat...) is of great interest because raw RPM are very irregular in terms of chemical composition and stability.

To tackle these issues, Barbier Group (French company leader of PE film producer) and POPPI (Polymers, Photochemistry, Properties and Interfaces) group are working in close collaboration in the frame of a Common Laboratory on the durability of polyethylene (PE) films including recycled polymers. This work aims to understand the photochemical behaviour of PE films containing RPM, especially the impact of contaminants and additives resulting from the first life of the materials, in order to develop innovative stabilization strategies to increase their durability [1].

EXPERIMENTAL

Materials

Various films (100 μm thick) were produced by Barbier group, either from recycled PE (r-PE) or virgin PE (v-PE). These films contained, or not, HALS and/or acid scavengers.

FTIR (Fourier-transform infrared spectroscopy)

FTIR spectra were obtained using a ThermoNicolet 6700 spectrometer in transmission mode. (2 cm^{-1} , 32 scans, 4000 – 400 cm^{-1}). The kinetics of photooxidation were determined from the

A values at 1713 cm^{-1} , calculated by subtracting spectra prior to ageing to those after photooxidation time.

Photoageing

Artificial accelerated photooxidation was performed in SEPAP MHE devices in High Energy (HE) mode (300W/m² in the 290-420 nm range, T_{CH} = 60°C / T_{BST} = 80°C).

RESULTS AND DISCUSSION

Upon photooxidation, the FTIR spectra of both recycled PE (r-PE) and virgin PE (v-PE) show growing bands in the carbonyl region (1900-1500 cm^{-1}), with a maximum at 1713 cm^{-1} (C=O stretching of carboxylic acids [2]).

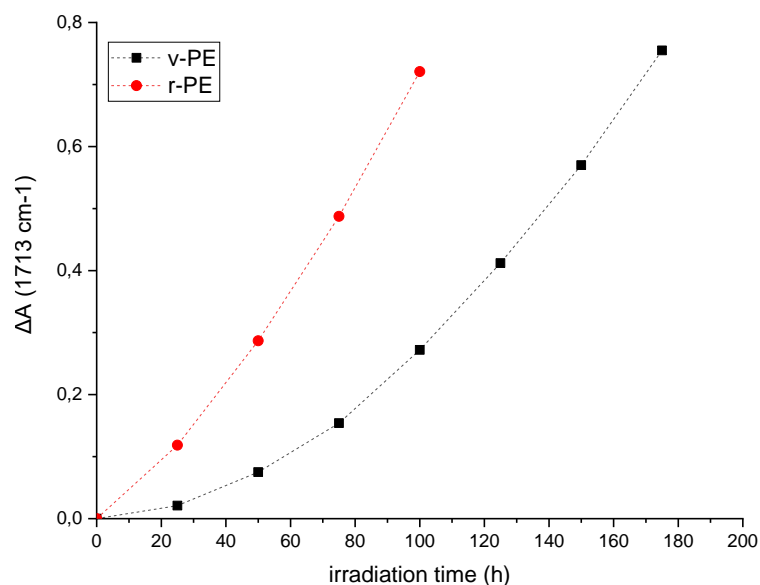


Figure 1: Photooxidation kinetics of v-PE and r-PE.

Figure 1 compares the photooxidation rates of v-PE and r-PE by plotting the increase of absorbance at 1713 cm^{-1} as a function of irradiation time. This figure shows that r-PE degrades faster than v-PE.

The efficiency of different HALS stabilizers commonly used for v-PE or specially designed for recycled materials will then be tested. The influence of contaminants and oxidation products that can be present in post-use materials will be evaluated.

The ultimate goal is the proposal of stabilization strategies to prevent early degradation of RPM-containing films.

References

- [1] R. Pfaendner, « Restabilization – 30 years of research for quality improvement of recycled plastics review », *Polymer Degradation and Stability*, 2022, 203, 110082, doi: [10.1016/j.polymdegradstab.2022.110082](https://doi.org/10.1016/j.polymdegradstab.2022.110082).
- [2] M. Gardette *et al.*, « Photo- and thermal-oxidation of polyethylene: Comparison of mechanisms and influence of unsaturation content », *Polymer Degradation and Stability*, 2013, 98, 2383, doi: [10.1016/j.polymdegradstab.2013.07.017](https://doi.org/10.1016/j.polymdegradstab.2013.07.017).

Elucidate Intrinsic Origin of Heterogeneous Oxidative Aging using Coarse-Grained Molecular Dynamics Simulation

Takato Ishida

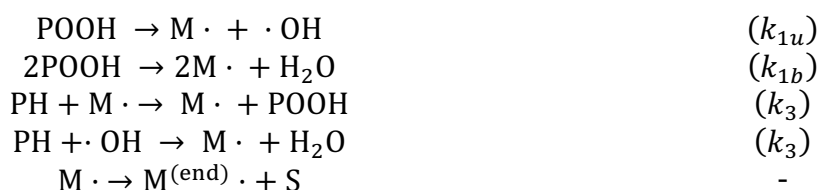
Institute for Advanced Research, Nagoya University, Furo-cho, Chikusa, Nagoya, Japan
ishida@mp.pse.nagoya-u.ac.jp

INTRODUCTION

Heterogeneous aging has been often reported in the field of polymer aging. Previously reported origins are such as the diffusion-limited oxidation (i.e., DLO effect), the spreading of small radical species, and the localized consumption of stabilizers at sample edges. Here, we present results elucidating another intrinsic origin of heterogeneity that occurs even in bulk polymer melts, using the framework of coarse-grained molecular dynamics. This origin is attributed to the transport of radical species, arising from the competition between the mobility of molecular chains and the timescale of oxidative aging reactions.

MODELS AND SIMULATIONS

In this model, polymer chains are represented by the standard Kremer-Grest (KG) model with a chain length of $N = 100$ [1]. The system consists of 256000 beads (2560 chains). We refer to the scheme of polypropylene thermal oxidation in the oxygen excess regime (OER) and adopted the kinetic model constructed by Richaud et al. [2], extrapolated to 180 °C.



where POOH is the hydroperoxide, PH is the oxidative site (substrate), S is the chain scission event, and $\text{M}\cdot$ is the chain radical. We assume that the β -scission process, for which the reaction rate constant is left blank, occurs more rapidly compared to other reactions.

The selected reaction rate constants in this study are $k_{1u}/k_3 = 1.6 \times 10^{-4}$ and $k_{1b}/k_3 = 5.8 \times 10^{-3}$. The rate parameter governing the oxidation kinetics is expressed as the product with the longest relaxation time $\tau_{R_0} = 20000\tau$ (in LJ time unit) for $N = 100$ KG chain. In this study, the selected values for $k_3\tau_{R_0}$ were 60, 120, 240, 1200. In this framework, we modeled that beads within the reaction radius ($r_c = 2^{1/6}\sigma$ in LJ length unit) are stochastically reacted by the Monte Carlo method. The simulation can reproduce the reaction kinetics while finding the spatial heterogeneity of radicals and scission sites, as shown in Figure 1 [3, 4].

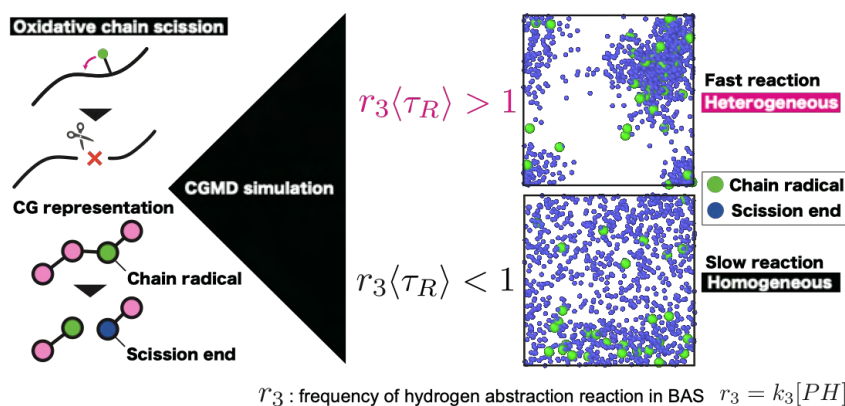


Fig. 1 Coarse-grained modeling and snapshots with fast and slow oxidation systems

RESULTS AND DISCUSSION

As shown in Fig. 1, this oxidative aging simulation reveals that the threshold for heterogeneous aging is determined by whether the dimensionless quantity $r_3\langle\tau_R\rangle$ is greater than or less than unity, where r_3 is the frequency of the characteristic hydrogen abstraction reaction ($r_3 = k_3[\text{PH}]$) and $\langle\tau_R\rangle$ is the average relaxation time of polymer chains. In other words, when the frequency of hydrogen abstraction is higher compared to chain relaxation, reactions progress locally with remaining spatial correlations, resulting in heterogeneity.

When heterogeneous aging occurs, the spatial fluctuations in the local conversion increase significantly (Fig. 2). The results in Fig. 2 were obtained by dividing the simulation box into 8000 meshes with 20 meshes along each side, and calculating the fluctuations in the number of remaining reaction sites (N_{PH}) within each mesh. Additionally, such fluctuations in local conversion lead to a retardation of oxidation reactions due to the local depletion of $[\text{PH}]$, as shown in Fig. 3. Furthermore, since the progression of the oxidation aging region is governed by local mobility (dynamic heterogeneity), in cases of heterogeneous aging, the spatial distribution of short chains resulting from scission will also be heterogeneous (Fig. 4).

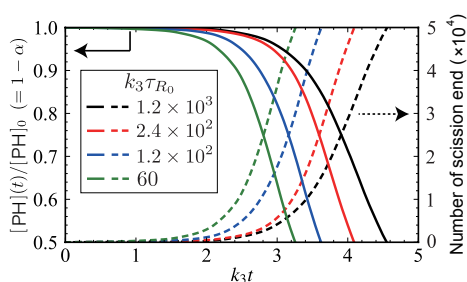
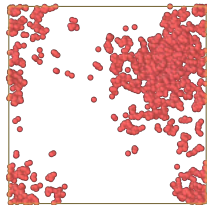


Fig. 2 Oxidation kinetics of PH and scission sites (normalized by k_3).

(a) $k_3\tau_{R_0} = 1.2 \times 10^3$



(b) $k_3\tau_{R_0} = 2.4 \times 10^2$

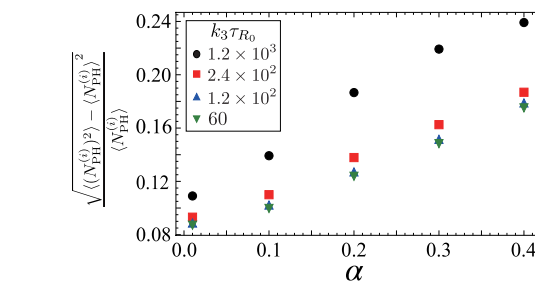
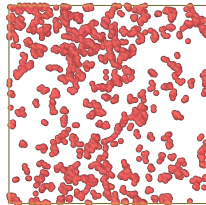
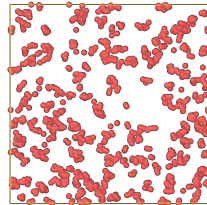


Fig. 3 Fluctuations in the number of PH beads within each mesh (N_{PH} from the i -th mesh).

(c) $k_3\tau_{R_0} = 1.2 \times 10^2$



(d) $k_3\tau_{R_0} = 60$

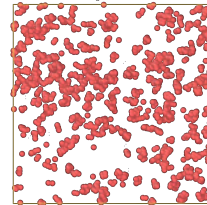


Fig. 4 Snapshots of $N < 10$ short chain beads at $[\text{PH}]/[\text{PH}]_0 = 0.99$ in the oxidative aging simulation for the cases of $k_3\tau_{R_0}$

Acknowledgment

This work was supported by JSPS KAKENHI Grant Numbers 24K20949, 22KJ1543, "Nagoya University High Performance Computing Research Project for Joint Computational Science" in Japan.

References

- 1) K. Kremer and G. S. Grest, Dynamics of entangled linear polymer melts: A molecular-dynamics simulation, *The Journal of Chemical Physics*, 92(8), 5057–5086, 1990.
- 2) E. Richaud, F. Farcas, B. Fayolle, L. Audouin, J. Verdu, Hydroperoxide Build-up in the Thermal Oxidation of Polypropylene A Kinetic Study. *Polymer Degradation and Stability*, 92(1), 118 – 124 (2007).
- 3) T. Ishida, Y. Doi, T. Uneyama, and Y. Masubuchi, "Modeling for Heterogeneous Oxidative Aging of Polymers Using Coarse-Grained Molecular Dynamics", *Macromolecules*, 56(21), 8474–8483 (2023).
- 4) T. Ishida, Y. Doi, T. Uneyama, and Y. Masubuchi, "Coarse-grained Molecular Dynamics Simulation of Oxidative Aging of Polymers -Effect of free radical diffusivity-", *Polymer Journal*, accepted.

A STUDY ON BIOPLASTIC OBTAINED FROM RENEWABLE SOURCES: MATERIAL'S CHARACTERIZATION AND BIODEGRADATION IN SOIL

Annamaria Visco^{a,b,*}, Cristina Scolaro^a, Salim Brahimi^a,
Noemi Bardella^c, Valentina Beghetto^{c,d,e}

^a Department of Engineering, University of Messina, C.da Di Dio, 98166 Messina, Italy

^b Institute for Polymers, Composites and Biomaterials - CNR IPCB, Via Paolo Gaifami 18, 9-95126-Catania, Italy

^c Crossing S.r.l., Viale della Repubblica 193/b, 31100 Treviso, Italy

^d Department of Molecular Sciences and Nanosystems, University Ca' Foscari of Venice, Via Torino 5 155, 30172 Mestre, Italy. Tel. +390412348928.

^e Consorzio Interuniversitario per le Reattività Chimiche e la Catalisi (CIRCC), via C. Ulpiani 27, 701268 Bari, Italy

avisco@unime.it, cscolaro@unime.it, salim.brahimi@studenti.unime.it,
noemi.bardella@crossing-srl.com, valentina.beghetto@crossing-srl.com

INTRODUCTION

Plastic from Fossil Source (FSP) has been commonly used for decades to produce disposable objects and components present in all industrial sectors, from automotive to biomedical, from electronics to the clothing one ^[1]. Bioplastic produced from Renewable Sources (RSB) is a valid alternative to FSP since it biodegrades quickly in the soil compared to PFS which requires hundreds - thousands of years, restricting the problem of plastic pollution. Biodegradation, therefore, favors the ecological transition of these materials which are conceived in the spirit of a circular economy and no longer linear as in the past ^[2].

In addition, the millions of tons of agri-food waste (AFW) produced annually represent a major disposal problem due to their cost. Therefore, the production of RSB with AFW is a good way to reuse waste products and, at the same time, allows the use of less bioplastic. In this study, brewer spent grain (BSG) has been processed as AFW.

EXPERIMENTAL

Materials

New RSBs were formulated by mixing bioplastics with properly pre-treated BSG and with appropriate additives, by using a melt mixing machine (Brabender Plasticorder PL2100) at 140°C for 15 minutes. Different chemical formulations have been obtained by changing the chemical composition (quantity of BSG ranging between 5 wt.% and 45 wt.%).

Physico-chemical characterization and work-ability test

Both surface (roughness, water contact angle, shore D hardness) and bulk (torque and static tensile test) investigations were carried out on all the blends. It has also been verified that these blends are workable with normal thermoplastic polymer processing technologies, including extrusion and injection molding. A commercial sample of bioplastic polymer has been used as Control Sample (CS).

Biodegradation test

The soil biodegradation tests were carried out according to the ASTM D5988-18 standard. Carbon dioxide monitoring, according to ISO 17556:2019, was performed together with a thermo-mechanical characterization, wettability, roughness analysis, and shore-D hardness of the surfaces, during 3-6 months of degradation in soil.

RESULTS AND DISCUSSION

The experimental results indicated the best chemical composition of bioplastics to have optimal mechanical performance was around 25-30 wt.% of BSG.

Stress reduction data suggested that the higher the BSG amount, the higher the degradation rate. Besides, RSB with high BSG amount degrades in 3 months, while the control (CS) requires higher times (> 6 months), see fig.1.

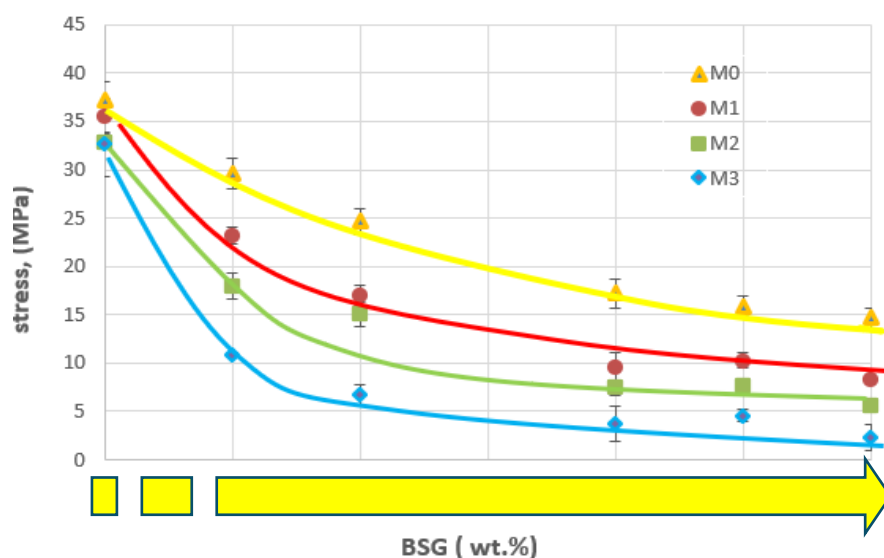


Fig. 1. Tensile strength of the CS and of the RSB with different BSG load during the degradation period in soil (0-1-2-3 months)

The results suggest that it is possible to control the biodegradation time by changing the composition of the mixture. Furthermore, the first prototype plant pots, made with our RSB blend and extrusion/injection molding technologies, have the right potential to replace the millions of pots currently produced in FSP.

Acknowledgment

Authors thanks LIFE project for the Environment and Climate Action” Project LIFE2021-SAP-ENV-101074314 LIFE-Reuse of bEer SpenT grAin foR bioplasTics – RESTART, co funded by European Community.

References

- 1) A.Visco, C. Scolaro, M. Facchin, S. Brahimi, H. Belhamdi, V.Gatto, V. Beghetto. *Polymers* , 14, 2022.
- 2) Beghetto, V.; Gatto, V.; Samiolo, R.; Scolaro, C.; Brahimi, S.; Facchin, M.; Visco, A.. *Environmental Pollution* 2023, 334, 122102,

SYNTHESIS OF BIOBASED COMPATIBILISER FOR MODIFICATION OF RECYCLED POLYPROPYLENE COMPOSITES WITH BUCKWHEAT STRAW

S. Motrončiks, R. Bērziņš, R. Merijs-Meri, A. Ābele, J. Zicāns

Institute of Chemistry and Chemical Technology, Faculty of Natural Sciences and Technology, Riga Technical University, Riga, Latvia

remo.merijs-meri@rtu.lv

INTRODUCTION

To ensure sustainable development, there is a necessity to change prevalent consumption patterns in global scale. Hence, it is extremely important to transform existing fossil-based production routes towards biobased and circular technologies complying with UN Sustainability Goals and EU Green Deal. In the light of these findings the current research is devoted to valorisation of post-consumer polypropylene containing admixtures of polyethylene (rPPPE) by developing its composites with buckwheat residue biomass derived fibrous reinforcement (BWR). Use of BWR instead of wood flour offer some advantages in respects of sustainability, considering shorter growth-harvesting cycle of agricultural crop biomass. It was aimed to increase bio-based content of the composites up to 40 wt.% still allowing their processability by injection molding. It was expected that addition of BWR could improve stiffness and strength of the developed composite material. To ensure this, pre-treatment of hydrophilic BWR with tannic acid or catechin modified stearyl chloride (SCTA and SCCA respectively) was performed to increase its hydrophobicity and hence compatibility with rPPPE matrix. It was expected that such modification could improve not only compatibility between of the polar reinforcement and the non-polar polymer matrix, but also could improve thermal and ageing resistance of the composite because of antioxidant properties of tannin and catechin.

EXPERIMENTAL

Compatibiliser synthesis

Synthesis of biobased compatibilizer was performed using tannic acid (TA) or catechin hydrate (CA) and stearyl chloride (SC) to obtain SCTA or SCCA compatibilizer respectively. After synthesis of SCTA and SCCA, they were combined with silane treated BWR before melt compounding. The efficiency of the synthesized biobased compatibilizers was assessed in comparison to commonly used additive package for natural fiber reinforced polymers, containing from maleic anhydride grafted polypropylene (MAH) and commercial antioxidant (IRGA).

Development of rPPPE composites

rPPPE composites with various amounts of BWR (10-40 wt.%) have been obtained by melt compounding. 4 different series of composites have been obtained, including 1) the composites with alkali treated BWR, MAH and IRGA, 2) the composites with silane treated BWR, MAH and IRGA, 3) the composites with silane treated BWR and SCTA instead of MAH and IRGA and 4) the composites with silane treated BWR and SCCA instead of MAH and IRGA.

Characterization of properties

The obtained rPPPE composites have been characterized in respect to their rheological, tensile, flexural, impact and thermal properties using oscillating parallel plate rheometer, universal testing machine, Charpy impact strength apparatus, TGA and DSC. DSC

was used for both, characterization of crystallinity changes of the polymer matrix upon its modification and determination of oxidation induction time, characterizing thermal stability of the obtained rPPPE composites.

RESULTS AND DISCUSSION

The obtained research results testify that after sylanization BWR surface becomes more hydrophobic, denoting to improved interaction with hydrophobic rPPPE matrix. After melt compounding of rPPPE with BWR increment of modulus of elasticity and strength while decrement of ultimate elongation and impact strength were observed disregarding whether the BWR is modified or not. However, in the case of compatibilized and silane treated fibers containing compositions higher impact strength and ultimate elongation at break values are observed. In addition, it is important to mention that silane treated fibers containing rPPPE/BWR composites demonstrated considerably higher oxidation induction time values in comparison to alkali treated fibers containing systems (Fig.1).

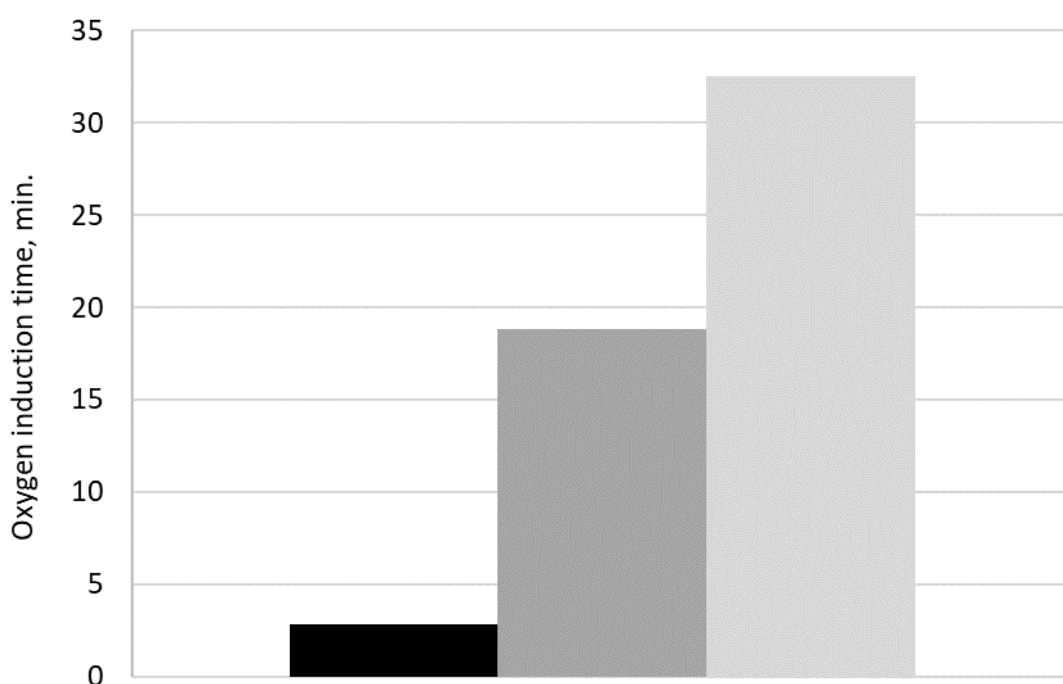


Fig. 1 Oxidation induction time values of rPPPE/BWR composites
(■ rPPPE, ■ rPPPE+10%BWR_alkali+3%MAH+1%IRGA,
■ rPPPE+10%BWR_sil+3%MAH+1%IRGA)

Acknowledgment

This research is funded by the Latvian Council of Science, project This research was funded by The Latvian Science Council, grant number LZP 2021/1-0347

CHAR FORMATION IN POLYETHYLENE: EFFECT OF THE MACROMOLECULAR ARCHITECTURE

A. Frache*, R. Arrigo, G. Malucelli, G. Camino

Department of Applied Science and Technology, Politecnico di Torino, viale Teresa Michel 5, Alessandria, Italy *alberto.frache@polito.it

INTRODUCTION

Organic polymers ignite following a very complex mechanism, which involves the occurrence of several physical and chemical events [1,2]. From a general point of view, the typical involvement of polymers in fires occurs through their chemical degradation taking place in three steps: ignition, combustion, and smouldering. The ignition process is bound to be kinetically controlled because it involves a heterophasic reaction between oxygen of air and the solid or liquid polymer material [2]. The degree of kinetic control and therefore the dependence of ignition on irradiation is related to the polymer chemical reactivity with oxygen and oxygen diffusion rate into the polymer phase. In this work, the charring ability of polyethylenes (PEs) having different macromolecular architectures, in terms of molecular weight and presence of short- or long-branching structures, is thoroughly investigated.

EXPERIMENTAL

Materials

Different grades of commercial LDPEs and HDPEs were studied namely HDPE_HV (Lupolen 5021DX), HDPE_LV (Eraclene MP90U), LDPE_HV (Lupolen 2420F) and LDPE_LV (Alcudia PE02).

Characterization

FTIR-ATR measurements were performed both on the pristine and degraded materials in order to have a chemical characterization of the materials. Differential Scanning Calorimetry (DSC) characterization was performed in order to evaluate the crystallization temperature (T_c), crystallization enthalpy (ΔH_c), melting temperature (T_m), and melting enthalpy (ΔH_m). Rheological analyses were carried out using a parallel plate-plate instrument to evaluate the complex viscosity as a function of frequency. The obtained experimental data were fitted using the Cross model. The thermal and thermoxidative behavior of the materials were assessed using Thermogravimetric analysis both in dynamic heating and isothermal conditions. Finally the time to ignition (TTI) of the polymers were evaluated through cone calorimetry tests and the temperatures involved before combustion were recorded using thermocouples in contact with the upper surface of the specimens.

RESULTS AND DISCUSSION

Preliminary spectroscopic, thermal and rheological characterizations were carried out on the different PEs in order to determine their physico-chemical behavior. The results of TGA performed in oxidative atmosphere have highlighted different behaviours between the samples, in terms of both thermo-oxidative stability and degradation temperatures. In Figure 1 the isothermal TG curves are reported in which is possible to see different residual weight after 60 min of treatment in oxidative atmosphere at 320°C. This phenomena was connected to the different char formation on the surface of the samples and FTIR-ATR spectroscopy confirmed the presence in large amount of C=C aromatic stretching for HDPE_HV. The chemical/physical modifications occurring in the PEs preignition step were studied on the samples exposed to 20 kW/m² in the Cone Calorimeter also monitoring the temperature on the surface of the samples. The TTI was correlated with the char stability and for the HDPE_HV was 240s instead 170-180s that was found for the other samples.

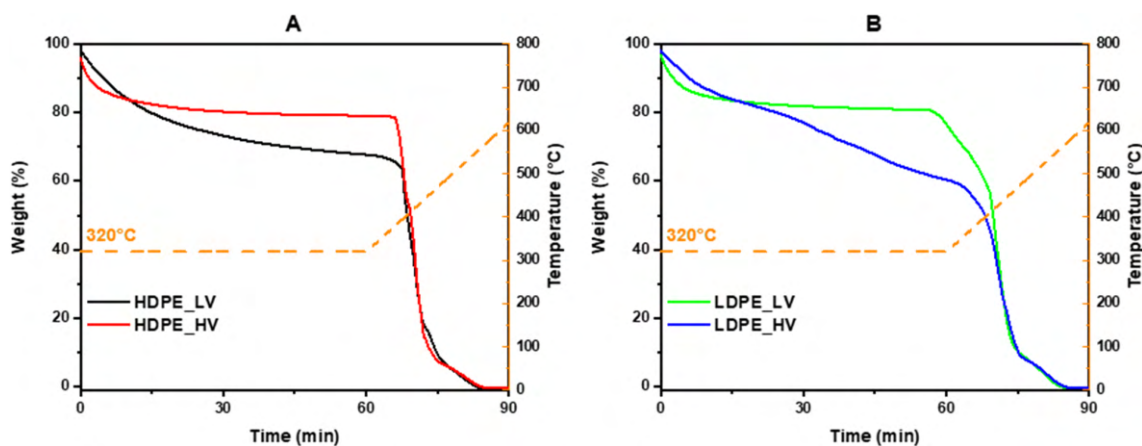


Fig. 1 Isothermal TG curves for 60 min at 320°C, then heated to 650°C (10°C/min) for HDPEs (A) and LDPEs (B) samples.

The mechanism of char formation in polyethylene proceeds through oxidative dehydrogenation reactions resulting in conjugated polyenes, which further undergo crosslinking, until the formation of char. Therefore, the kinetics of the charring mechanism and the stability of the formed char are strongly affected by the promptness of the polymer macromolecules in interacting with the surrounding chains to form crosslinked structures, representing the precursors of the carbonaceous residue. Aiming at verifying the possible different tendency of the chains of the different PE samples in establishing polymer-polymer interactions when subjected at high-temperature treatments, time sweep tests were performed on all the investigated materials.

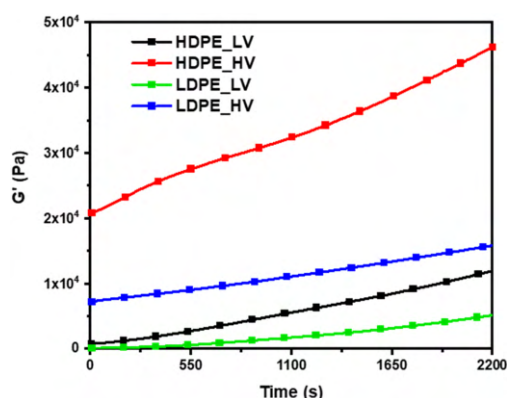


Fig. 2 Storage modulus (G') as a function of time for all investigated materials.

These tests (Figure 2) have been demonstrated that the linear chain structure of HDPE (especially in the case of high molecular weight polymers) leads to the establishment of strong interactions between the macromolecules (due to their close proximity), enabling the formation of a well-developed crosslinking network, which is likely able to further evolve into a stable char. Conversely, the presence of long-chain branched structures increases the distance between the polymer backbones, making more difficult the establishment of strong and durable interactions, notwithstanding the formation of a highly entangled structure. This issue might compromise the formation of a stable char for long-chain branched LDPE, which, indeed, showed a lower charring ability [3].

References

- 1) A.B. Morgan, J.W. Gilman, *Fire. Mater.* **37** 259 (2013)
- 2) A. Fina, G. Camino, *Polym. Adv. Technol* **22** 1147 (2011)
- 3) A. Frache, R. Arrigo, G. Malucelli, G. Camino, *Polym. Degr. Stab.* **216** 110476 (2023)

A NOVEL ROUTE FOR OBTAINING HIGH MELT STRENGTH RECYCLED HIGH-DENSITY POLYETHYLENE

G. Bernagozzi, R. Arrigo and A. Frache

Department of Applied Science and Technology, Polytechnic of Turin,
Viale Teresa Michel 5, Alessandria, Italy

giulia.bernagozzi@polito.it, rossella.arrigo@polito.it, alberto.frache@polito.it

INTRODUCTION

The thermo-mechanical degradation of high-density polyethylene (HDPE), typically occurring during mechanical recycling processes, involves several concurrent phenomena, such as chain scission, branching formation and crosslinking [1], resulting in the achievement of a heterogeneous microstructure. This last, and the consequent poor mechanical properties of recycled HDPE, limit the final application of this material towards low added-value products. Therefore, to effectively accomplish a circular economy model aiming at reuse and recycle the plastic products already in circulation, the degradation-induced microstructural modification should be in some way controlled, in order to drive it towards the achievement of a specific microstructure enabling recycled HDPE utilization in valuable applications. In this work, an effective strategy for obtaining recycled HDPE with increased melt strength, hence improved processability upon elongational flow, was proposed. To this aim, a commercially available additive (Nexamite® R305, NEX) was introduced in a degraded HDPE sample, and the so-obtained material was subjected to further reprocessing. The recycled materials with and without NEX were subjected to non-isothermal elongational flow for obtaining fibers at different draw ratios which were further characterized through tensile tests.

EXPERIMENTAL

Materials

The materials used in this work were:

- High-density polyethylene (HDPE) Eraclene MS80U supplied by Versalis having a melt flow rate of 27 g/10 min (190 °C/2.16 kg);
- Nexamite® R305 (NEX) supplied by Nexam Chemical.

Processing

The melt processing (190°C) was carried out by means of a twin-screw extruder Process 11 (Thermo Fisher Scientific) equipped with a screw profile with alternance of conveying and kneading screw elements.

Rheological and physico-chemical characterization

The spectroscopic characterization was carried out on thin films (thickness = 50 µm) by means of attenuated total reflectance infrared spectroscopy, using a Frontier spectrophotometer (Perkin Elmer).

Rheological measurements were performed using a strain-controlled parallel plate rheometer ARES (TA Instrument) at 190°C under nitrogen atmosphere. The melt strength was calculated in non-isothermal elongational flow by using a RheoSpin apparatus and fibers with different draw ratios ($DR = \frac{\text{diameter}_{\text{extrudate}}^2}{\text{diameter}_{\text{fiber}}^2}$), were collected.

The mechanical characterization was performed through tensile tests with an Instron® 5966 machine. The measurement parameters for testing ISO 527-5A specimens were an initial strain rate of 1 mm/min that increased up to 10 mm/min once a deformation of 0.25% was exceeded. The tests on fibers were performed with a crosshead speed of 20 mm/min.

RESULTS AND DISCUSSION

The preliminary tensile characterization of recycled HDPE showed that, due to the thermo-mechanical degradation underwent by the polymer, the tensile modulus slightly decreases as compared to the virgin material, while the elongation at break suffers a drastic reduction passing from HDPE (114 %) to its degraded counterpart (5 %).

The rheological and spectroscopic characterizations demonstrated that the observed dramatic decrease of the material ductility can be ascribed to the heterogeneous microstructure resulting from the different phenomena (namely, chain scission, branching formation, crosslinking) concurrently occurring during the HDPE reprocessing.

Aiming at solving this issue, a commercially available additive (NEX) was introduced in an already degraded HDPE. The obtained results demonstrated that the additive is capable of selectively directing the thermo-mechanical degradation pathway of HDPE towards the achievement of long-chain branching microstructure, as can be inferred from the analysis of the Cole-Cole plot reported in figure 1A. Interestingly, long-chain branched recycled HDPE (containing NEX) exhibits remarkably higher values of melt strength values as compared to recycled HDPE (without NEX), hence allowing the further processing of the so-obtained materials through technologies dominated by the elongational flow.

Finally, fibers based on recycled HDPE containing NEX were collected and characterized through tensile tests, showing a striking increase of the elongation at break as compared to the pristine recycled HDPE fibers (Fig 1B).

In all, this work demonstrates the possibility of obtaining recycled HDPE materials potentially suitable for future applications characterized by high-engineering requirements, opening new perspectives towards an effective upcycling of HDPE-based wastes.

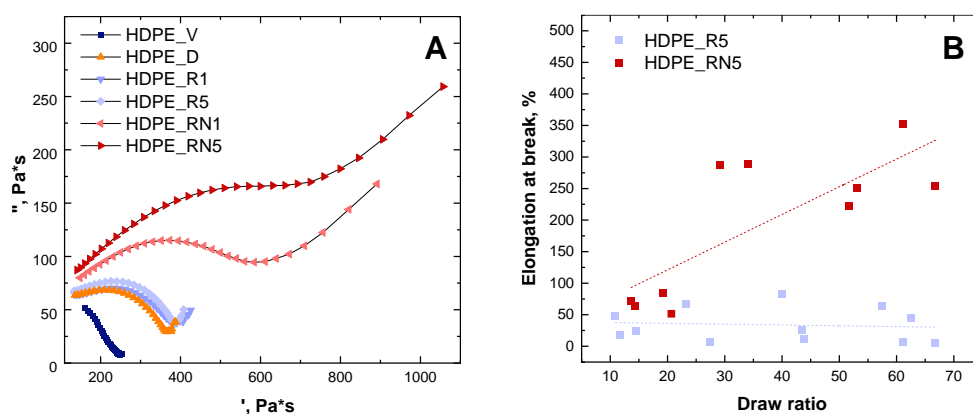


Figure 1. Cole-Cole plot (A) and elongation at break as a function of the DR (B).

Acknowledgment

This study was carried out within the MICS (Made in Italy – Circular and Sustainable) Extended Partnership and received funding from the European Union Next-GenerationEU (PIANO NAZIONALE DI RIPRESA E RESILIENZA (PNRR) – MISSIONE 4 COMPONENTE 2, INVESTIMENTO 1.3 – D.D. 1551.11-10-2022, PE00000004). This study reflects only the authors' views and opinions, neither the European Union nor the European Commission can be considered responsible for them.

References

- 1) J. Zhang, V. Hirschberg, A. Goecke, M. Wilhelm, W. Yu, M. Orfgen, D. Rodrigue, *Polymer*, 297, 126866 (2024)

DESIGN OF TAILOR-MADE POLYHYDROXYALKANOATES: FROM BIOSYNTHESIS TO BIODEGRADATION

G. Derippe¹, G. Brouchon¹, P. Lemechko², S. Bruzaud¹

¹ Université Bretagne Sud, Institut de Recherche Dupuy de Lôme, UMR CNRS 6027, 56100 Lorient, France

² Institut Régional des Matériaux Avancés, allée Copernic, 56270 Ploemeur, France
stephane.bruzaud@univ-ubs.fr

INTRODUCTION

Polyhydroxyalkanoates (PHA) are bacterial polyesters, which constitute a very promising family of polymers both from the point of view of their properties of use and that of their environmental impact. The PHA biosynthesis is particularly relevant since it avoids the traditional chemical processes, by using some of the most energy-efficient industrial biotechnology processes. For a large number of marine or terrestrial bacteria, PHA are an ideal carbon and energy storage material, due to their low solubility and high molar mass [1]. The chemical composition (nature of the monomer units constituting the PHA and their proportion in the chain) and therefore the PHA physico-chemical properties are closely dependent on the bacterial strain and the carbon sources available.

RESULTS AND DISCUSSION

The conference will present different examples of PHA production in order to show how the choice of substrates integrated at the start of the biosynthesis process makes it possible to influence the chemical structure and the morphology of the PHA produced and thus to adjust the physico-chemical characteristics and the functional properties (thermal stability, mechanical behavior, viscosity, barrier properties, etc.) [2]. PHA can be divided into two subgroups: short chain-length PHA (*scl*-PHA) composed of monomers of 3-5 carbon atoms, and medium chain-length PHA (*mcl*-PHA) composed of monomers of 6-14 carbon atoms. The physico-chemical properties differ between the *scl*-PHA, that are rigid and brittle polymers and the *mcl*-PHA that are usually more rubbery and ductile. Due to their limited commercial availabilities, no studies have ever reported microbial activity and diversity on *mcl*-PHA, thus resulting in a lack of comparison between the environmental end of life of polymers coming from *scl*- or *mcl*-PHA families.

Some results that we have recently obtained by different approaches illustrate the ability of certain PHA, mainly *scl*-PHA, to biodegrade in a very spectacular way in the marine environment [3-7]. However, significant differences in behavior are observed with regard to the composition and morphology of the *scl*-PHA [3]. The main factors intrinsic to PHA (chemical structure, molar mass, free volume, glass transition, mobility, crystallinity, solubility, hydrophilic/hydrophobic balance, etc.) play a determining role in their degradation [4,5]. Additionally, in marine environment, understanding the mechanisms of biofouling is also a key issue for assessing the ecological impacts and the future of plastics. Assessments of polymer surface physical properties (hydrophobicity and roughness) combined with microbiological characterization of the biofilm (cell counts, taxonomy, composition and heterotrophic activity) can be performed using a wide range of techniques [6-8].

This study compares the marine biodegradation behavior between different *scl*-PHA and *mcl*-PHA and shows that *mcl*-PHA biodegradation takes longer than *scl*-PHA (Fig. 1). The results point out that the chemical nature of the polymer (*scl*- vs *mcl*-PHA) together with the diversity of microorganisms living on the polymer films (and probably the associated enzymes, i.e. PHA depolymerases) are the main drivers of the PHA biodegradability in the marine environment [9,10]. Although some microorganisms are capable of degrading *scl*-PHA and *mcl*-PHA, the majority of PHA degraders are for *scl*-PHA (*scl*-PHA

depolymerases), that can be easily found in seawater, soil and compost. The *mcl*-PHA depolymerases are much less numerous in these environments and less active.

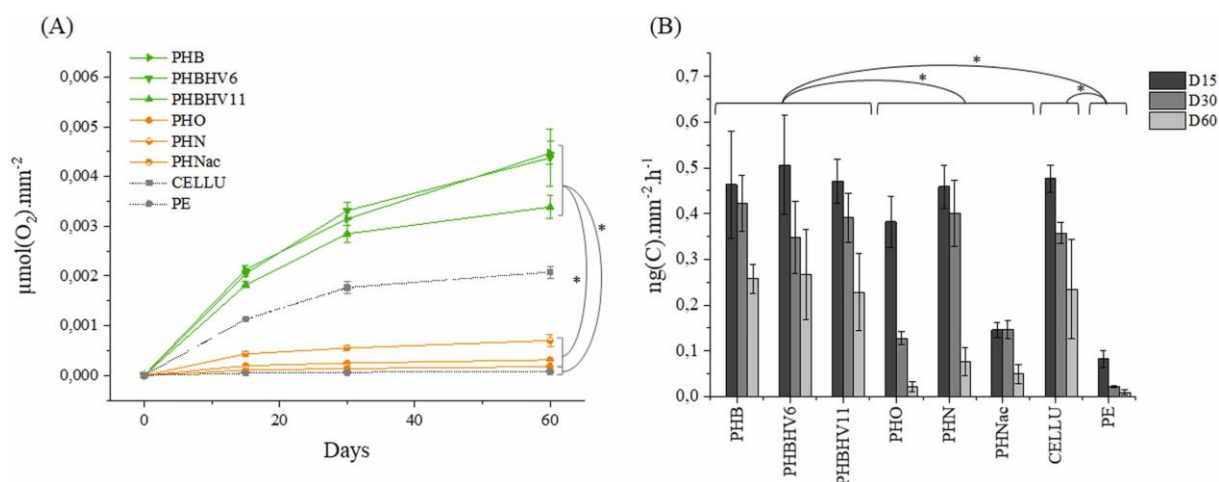


Fig. 1. (A): Cumulative oxygen consumption (*scl*-PHA in green and *mcl*-PHA in orange) and (B): Bacterial heterotrophic production on the different polymers in minimum media for 15, 30, 60 and 90 days [9]

All of this work provides original data and new insights into the colonization of PHA by marine microorganisms. The results already obtained and those to come aim to develop models to help design tailor-made (bio)degradable polymers. Their (bio)degradation could be controlled, or even programmed, by acting on the physical and chemical factors previously identified and intrinsic to the PHA, as well as on the extrinsic factors, relating to the environment.

References

1. T. Thomas, K. Sudesh, A. Bazire, A. Elain, H.T. Tan, H. Lim, S. Bruzard, *Bioengineering* **2020**, *7*, 1-22
2. P. Lemechko, M. Le Fellic, S. Bruzard, *Int. J. Biol. Macromol.* **2019**, *128*, 429-434
3. C. Volant, E. Balnois, A. Magueresse, G. Vignaud, S. Bruzard, *J. Polym. Env.* **2022**, *30*, 2254-2269
4. M. Deroiné, A. Le Duigou, Y.M. Corre, P.Y. Le Gac, P. Davies, G. César, S. Bruzard, *Polym. Degrad. Stab.* **2014**, *105*, 237-247
5. M. Deroiné, G. César, A. Le Duigou, P. Davies, S. Bruzard, *J. Polym. Environ.* **2015**, *23*, 493-505
6. C. Dussud, C. Hudec, M. George, P. Fabre, P. Higgs, A.M. Delort, B. Eyheraguibel, A.L. Meistertzheim, J. Jacquin, J. Cheng, N. Callac, C. Odobel, S. Rabouille, S. Bruzard, J.F. Ghiglione, *Front. Microbiol.* **2018**, *9*, 1571
7. J. Jacquin, N. Callac, J. Cheng, C. Giraud, Y. Gorand, C. Denoual, M. Pujo-Pay, P. Conan, A.L. Meistertzheim, V. Barbe, S. Bruzard, J.F. Ghiglione, *Front. Microbiol.* **2021**, *12*, 604395
8. J. Cheng, B. Eyheraguibel, J. Jacquin, M. Pujo-Pay, P. Conan, V. Barbe, J. Hoypierres, G. Deligey, A. Ter Halle, J.F. Ghiglione, A.L. Meistertzheim, S. Bruzard, *Polym. Degrad. Stab.* **2022**, *206*, 110159
9. G. Derippe, L. Philip, P. Lemechko, B. Eyheraguibel, A.L. Meistertzheim, M. Pujo-Pay, P. Conan, V. Barbe, S. Bruzard, J.F. Ghiglione, *J. Hazard. Mater.* **2024**, *462*, 132782
10. V. Barbe, J. Jacquin, M. Bouzon, A. Wolinski, G. Derippe, J. Cheng, C. Cruaud, D. Roche, J.L. Petit, P. Conan, M. Pujo-Pay, S. Bruzard, J.F. Ghiglione, *J. Hazard. Mater.* **2024**, *466*, 133573

Preparation and functionality of microbial-produced polyester porous material by liquid phase deposition method

T. Kabe R. Suzuki and T. Iwata*

*Department of Biomaterial Sciences, Graduate School of Agriculture and Life, University of Tokyo, Japan, The University of Tokyo, 1-1-1 Yayoi, Bunkyo-ku, Tokyo 113-8657, Japan
taizo-kabe@g.ecc.u-tokyo.ac.jp, atiwata@g.ecc.u-tokyo.ac.jp

INTRODUCTION

In recent years, as pollution from plastics spilled into the environment has become increasingly serious, attention has been focused on biodegradable plastics. Biodegradable plastics are starting to be used widely, including disposable containers and packaging bags. It is believed that exploring new ways to use biodegradable plastics will lead to further widespread use. In this study, we focused on poly[(R)-3-hydroxybutyrate-co-(R)-3-hydroxyhexanoate)] (PHBH), which is a microbially produced polyester produced from biomass and has biodegradability.

Recently, our laboratory has developed a method to fabricate PHBH porous materials by mixing three components, PHBH-chloroform solution, pure water, and hexane, in a predetermined ratio. However, the relationship between the production conditions and the structure of the obtained PHBH porous material and its functionality are not clear.

The purpose of this study was to identify the parameters that affect the bulk volume, bulk specific volume, and pore diameter of the PHBH porous material, and to evaluate the functionality of the prepared PHBH porous material. As for functionality, we focused on oil absorption and use as slow release fertilizer.

EXPERIMENTAL

Preparation of the PHBH porous material

The PHBH porous material was prepared according to the following procedure (Figure 1). First, a 100 mg/mL PHBH-chloroform solution (PHBH solution), pure water, and hexane were prepared in a certain ratio, and placed in a sample tube and shaken for 15 seconds. When the shaken sample tube was allowed to stand for 1 minute, it separated into a gel-like solid phase and a liquid phase, and the upper liquid phase was removed using a decanter. A PHBH porous material was obtained by leaving the lower solid phase to stand for 24 hours and drying it. In addition, samples with different pore diameters and pore densities were created by changing the preparation temperature and amount of water.

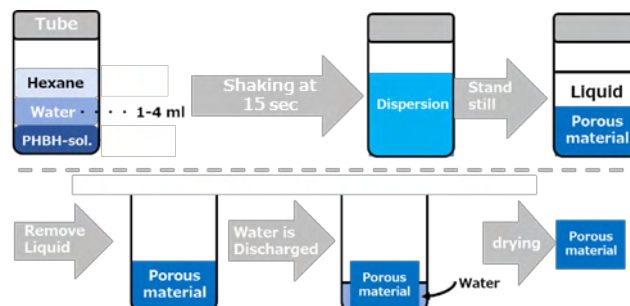


Figure 1 Preparation method of PHBH porous material

A cross section of the prepared PHBH porous material was observed using a scanning electron microscope (SEM). A part of the PHBH porous material was cut out, and the internal structure was observed using an X-ray CT scan.

Oil Absorption Experiment with PHBH Porous Material

An oil absorption experiment was conducted to evaluate the performance of PHBH porous material. PHBH porous materials with different bulk specific volumes were prepared by varying the preparation temperature and the amount of pure water. After the weight was measured, it was immersed in colored vegetable oil for 60 minutes. The weight was measured

again, and the "oil absorption magnification" and "oil absorption rate" were obtained from the difference in weight before and after immersion.

RESULTS AND DISCUSSION

Preparation of PHBH porous material

Figure 2 shows the prepared PHBH porous material. From cross-sectional observation using SEM, it was observed that the PHBH porous material consisted of spherical and ellipsoidal pores with a diameter of approximately 500-1000 μm . Furthermore, observation of the internal structure using X-ray CT scanning confirmed that holes (connecting pores) were formed on the surface of the pores, and that the pores were connected through the connecting pores.

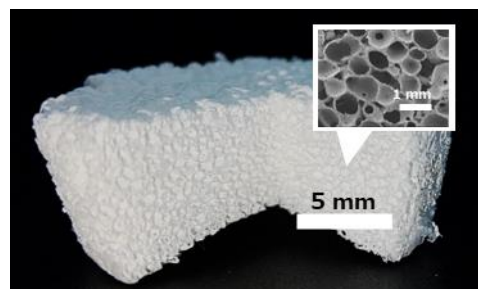


Figure 2 Overall image of PHBH porous material. The upper right is a SEM image.

Effects of preparation parameters on bulk volume and pore diameter of PHBH porous material

When the amount of pure water used to prepare the PHBH porous material was increased from 1 mL to 4 mL, the bulk specific volume increased from 3.7 cm^3/g to 11.5 cm^3/g and the pore diameter increased from 154 μm to 473 μm (Figure 3). When the preparation temperature was increased to a higher temperature (50 $^{\circ}\text{C}$), the bulk specific volume decreased from 11.5 cm^3/g to 8.5 cm^3/g , and the pore diameter increased from 473 μm to 956 μm . With increasing shaking time, the bulk specific volume increased from 8.3 cm^3/g to 9.4 cm^3/g , and the pore diameter decreased from 334 μm to 193 μm . In other words, it was found that the bulk specific volume and pore diameter can be controlled by changing these parameters.

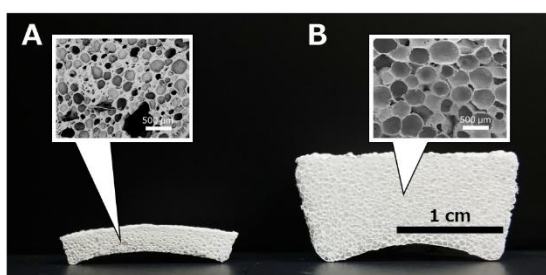


Figure 3 Cross-sectional view and SEM images of PHBH porous material (A) prepared using 1 mL of pure water, (B) prepared using 4 mL of pure water

Oil absorption experiment of PHBH porous material

Oil absorption experiments were conducted using PHBH porous materials, which were prepared with varying amounts of pure water. As a result of oil absorption experiments, the PHBH porous material was found to have oil absorption capability (top photo in Figure 4). Its oil absorption capacity increased linearly as the bulk specific volume of the PHBH porous material increased, up to 12 times (Fig. 4).

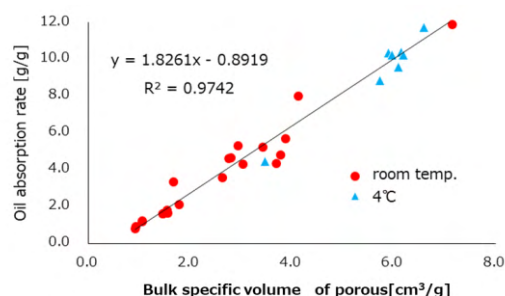
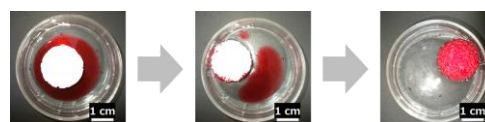


Figure 4 Bulk specific volume and oil absorption capacity of the prepared porous material. The preparation temperature was (●) room temperature and (▲) 4 $^{\circ}\text{C}$.

In addition, the amount of oil absorbed after 1 minute of oil immersion reached 96% of the maximum oil absorption, indicating that the prepared PHBH porous material had a high oil absorption rate. On the other hand, this porous material did not absorb any water. From the above results, this porous material is biodegradable and is a material that selectively absorbs oil.

Acknowledgment

This work was supported by the KAKENHI, from the Japan Society for the Promotion of Science, with Grant Numbers JP19H00908.

EFFECT OF GAMMA RADIATION ON THE THERMOMECHANICAL BEHAVIOUR OF POLYBUTYLENE FURANOATE

Debora Puglia¹, Franco Dominici¹, Alessandro Coatti², Marco Giannetto², Michelina Soccio², Nadia Lotti², Elena Macerata³, Maddalena Negrin³, Mario Mariani³, Andrea Soldini⁴, Ignacio Solaberrieta⁵, María Carmen Garrigós⁵, Alfonso Jimenez⁵

¹ Department of Civil and Environmental Engineering, University of Perugia, Italy

² Civil, Chemical, Environmental and Materials Engineering Department, University of Bologna, Italy

³ Department of Energy, Politecnico di Milano, Italy

⁴ Gammatom srl, 22070 Guanzate CO, Italy

⁵ Analytical Chemistry, Nutrition and Food Sciences Department, University of Alicante, San Vicente del Raspeig, Alicante, Spain.

debora.puglia@unipg.it

INTRODUCTION

Polymers are widespread used in packaging for healthcare products, such as single-use medical devices, implants, drug delivery and packaging systems, because of their versatility and economic advantages, including low weight and ability to withstand sterilization processes^{1,2}. Around 50% of all single-use polymer-based medical devices manufactured worldwide are sterilized using ionizing radiation from ⁶⁰Co sources in gamma irradiation, or high energy electrons by an electron beam accelerator or, less commonly, X-rays. Degradation due to radiation of these polymers generates poor resistance to aging with loss in mechanical properties, crosslinking phenomena and discoloration. Further, in the case of applications requiring high barrier properties, double packaging is performed, with workability issues and related cost increase. The main limitations of traditional polymers are the critical selection of non-renewable sources and the complicated recyclability. It is well recognized that aromatic materials are more resistant to radiation and with higher gas barrier than aliphatic materials, even if aliphatic polymers exhibit degrees of resistance depending upon their levels of unsaturation and substitution, density, presence of small pendant (side) groups, crystallinity, which can greatly affect the response of a plastic to external sources. 2,5-FDCA based polyesters, such as PBF (polybutylene furanoate), are expected to withstand higher barrier properties to gases and radiation.

EXPERIMENTAL

Poly (butylene 2,5-furanoate) (PBF) was prepared from 2,5-furandicarboxylic acid dimethyl ester (DMF) by two-stage melt polycondensation. Irradiation experiments have been performed, with the main objective to evaluate the impact of radiation on the polymer's properties, by means of gamma sources of ⁶⁰Co present in the irradiation facilities of Gammatom srl. Total absorbed doses ranging from 25 to 100 kGy were applied. Despite the high precision and uniformity in distributing the dose at the Gammatom facility, the highest and lowest absorbed doses delivered during the sterilization treatment were checked by treating some samples in the hot and cold point, respectively. Molecular changes due to irradiation were assessed by GPC and chemical modifications analysed through spectroscopic measurements (NMR and FTIR). DSC was also considered to follow changes in crystallinity degree. Water contact angle as well as tensile tests were also performed.

RESULTS AND DISCUSSION

In this study, we investigated the overall behaviour of PBF under different conditions of γ -irradiation, with the main aim of exploring the factors influencing critical aspects of plastic degradation depending on the received radiation dose (**Figure 1**). The FTIR results showed

limited degradation via irradiation, deduced from unmodified intensities of most of the PBF original infrared bands. The DSC results indicated the reduction of glass transition temperature (from 42 to 37 °C, respectively, for untrated and 100 kGy treated PBF fim) upon irradiation. Conversely, no variations in terms of crystallinity were observed at high doses compared with low doses. In the plastic film, no pinholes were induced by radiation and the effects on the tensile strength were not significant. Results confirmed the importance of taking furan-based biopolymers into consideration for safety guarantees in radiation processing for healthcare products packaging, especially for sterilization of products on large scale commercial plants. This study contributes to the development of a strategy for the sustainable management of plastic. Future research should continue to focus on the impact of tuning gamma radiation dosages for the depolymerization of furan based biopolymers.

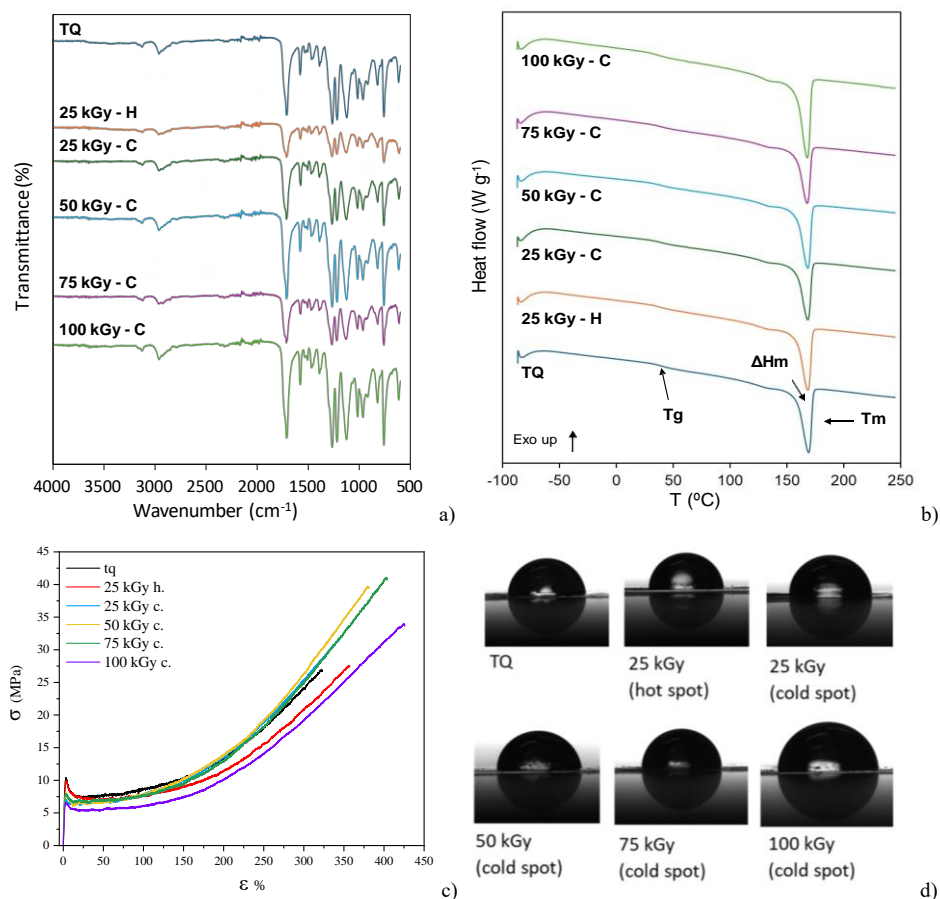


Figure 1. FTIR spectra (a), DSC curves for 2nd heating scan (b), curves of tensile test (c) and contact angle measurements of PBF after irradiation at different total absorbed doses (25, 50, 75 and 100 kGy. H = hot point, C = cold point)

Acknowledgement

This project is supported by the Circular Bio-based Europe Joint Undertaking and its members under grant agreement GA101112541 – FURIOUS (Call: HORIZON-JU-CBE-2022).

References

- 1) Jamalzadeh M, Sobkowicz MJ, Review of the effects of irradiation treatments on poly(ethylene terephthalate), *Polymer Degradation and Stability*, 206, 2022, 110191, doi: 10.1016/j.polymdegradstab.2022.110191.
- 2) Naikwadi AT, Sharma BK, Bhatt KD, Mahanwar PA (2022) Gamma Radiation Processed Polymeric Materials for High Performance Applications: A Review. *Front. Chem.* 10:837111. doi: 10.3389/fchem.2022.837111

IRRIGATION DRIPLINES WITH REDUCED CARBON FOOTPRINT

E.G.Rodi, A. Oliveri, S. Corviseri, C. Giuffré, M. Baiamonte**, F.P.LaMantia **

*Irritec SpA, Via Gambitta Conforto, 98071 Capo d'Orlando, Messina

** Università degli studi di Palermo, INSTM Interuniversity Consortium of Science and Technology of Materials

INTRODUCTION

Agriculture is responsible for the consumption of a large number of polymeric materials. Consumption of greenhouse films and silage films in Europe amount to 72,000 and 75,000 t/year respectively. In Italy, compared to an average annual consumption of over 350,000 t of agricultural plastic products, a corresponding flow of post-consumer material of about 200,000 t/year is estimated and about 55% of this amount comes from protected crops such as greenhouse linings, tunnels, soil mulching, vineyard nets (1,2). All these materials can constitute a starting waste for mechanical recycling valid for reuse. Having a fossil origin, these plastic materials are perfectly compatible with polyethylene, that is, with the most widely used material in agriculture and in Irritec to produce driplines (2,3). The complex nature of plastic waste in terms of polymer composition and presence of impurities requires extensive pre-treatments of cleaning and separation before reprocessing. Sometimes the cost of producing virgin materials is considered lower than the cost of collecting, cleaning, sorting, and processing post-consumer plastics. Another reason explaining the difficulty of reprocessing agricultural plastic waste (APW) (4) is the fact that plastic is sensitive to heat and handling. It is now clear that global environmental pollution is directly linked to the production of plastics from fossil sources, such as polypropylene (PP) and polyethylene (PE). It is therefore essential to increase the use of recycled materials or those produced from renewable sources. Despite the development of advanced synthetic methods and the application of biofilms in agriculture or for food packaging, the commercial production of biopolymers is limited by the cost, the relatively short useful life linked to biodegradation problems and by the availability of suitable agricultural waste (5). In this study Irritec used both wastes from mechanical recycling and biodegradable/compostable materials to create a complete irrigation system consisting of a light dripline and connected fittings. The recycling of biodegradable waste at the end of its life and post-processing has also been studied in order to evaluate the degradation undergone by the pipe during installation and the possibility of using the recycled polymer mixed with virgin polymer for the production of the same product.

EXPERIMENTAL

Materials

The materials used in the study for the realization of a complete irrigation system are of two different categories. First, the waste of driplines collected from the field. The biodegradable and compostable materials chosen will be renamed with A, B, C and D, where the A and B products are film grade commercially available, C is a product made for Irritec for this purpose and D is an injection molding product. All products are TUV certified. These materials were compared to standard polyolefins used in the agricultural world such as FB506 polyethylene supplied by Versalis and Capilene E50E polypropylene supplied by Carmel Olefins.

Preparation

The end-of-life driplines were recovered, shredded, washed and extruded in a regeneration plant. The waste in the form of granules was reused to make new seasonal and multi-seasonal driplines. The biodegradable and compostable film grade polymers were extruded at a maximum speed of 100 m/min with a Ø45 L/D=40 extruder usually used for

polyethylene. The molding material was instead molded on a 32-cavity injection press with 120 ton to make the internal dripper. The Irritec biodegradable tape made with materials A (used for the pipe) and B (used for the continuous dripper) were placed in the field for 5 months on a tomato crop and collected at the end of their life to be recycled in percentages of 20, 30 and 80% in a mixture with virgin polymer A.

Rheological and physico-chemical characterization

Viscosity properties were measured with an ARES G-2 rotational rheometer and a CEAST Rheologic 1000 capillary viscometer at 180 °C. To produce the samples for all mechanical tests, the materials were subjected to a compression molding using a Carver laboratory hydraulic press at 180 °C for 5 min.

Tensile tests were performed using a Universal Testing Machine (Instron model 3365, UK) on rectangular samples obtained from the platelets. The tests were performed using a tensile speed of 1 mm/min for 1 min, to evaluate the Young's Modulus and, subsequently, the speed was increased to 100 mm/min until the sample broke, using a 1 kN load cell.

RESULTS AND DISCUSSION

Post-production dripline waste and end-of-life product from the field were both used to produce lightweight, thin-gauge dripline. The regranulation process of the internal waste does not seem to have a significant effect on the degradation of the polymer and its subsequent use to obtain the same product, while the waste at the end of its life shows variegated impurities and the presence of cross-linked polyethylene which prevents its use on thin products.

The recycling of post-consumer biodegradable/compostable driplines in the conditions adopted in this research allows us to obtain a material that can be used mixed with virgin polymer to produce thin wall pipes. Both rheological properties and processing are little affected even with recycled polymer content greater than 30%.

Mechanical properties are also little affected except elongation at break. Since the burst characteristics could decrease due to the decrease in deformability, it is advisable not to exceed 20% in the mixture.

Acknowledgment

Azienda agricola Gianguzzi-dall'orto alla tavola

References

- 1) Scarascia Mugnozza G et al, The optimization of the management of agricultural plastic waste in Italy using a geographical information system. Act Horti 2008;801(1)
- 2) Picuno, Pietro, et al. Experimental tests and technical characteristics of regenerated films from agricultural plastics. Polymer degradation and stability 97.9 (2012): 1654-1661
- 3) Korol, Jerzy, et al. Wastes from agricultural silage film recycling line as a potential polymer materials. Polymers 13.9 (2021): 1383
- 4) Mariansky, G., 2006. Plastics – Solution or pollution, Cal Engineering & Geology (CalEng), pp. 12–15. <<http://www.caleng.com/>> (date of last access 19.10.12)
- 5) Production of Sustainable and Biodegradable Polymers from Agricultural Waste. Chrysanthos Maraveas. Polymers 2020, 12, 1127

Comparing additive vs conventional manufacturing via LCA

A. Latteri, G. Cicala, C. Tosto

Department of Civil Engineering and Architecture, DICAR, University of Catania, Viale Andrea Doria, Catania, Italy

INTRODUCTION

Life Cycle Assessment (LCA) is a powerful tool to evaluate the environmental impacts of any activity, including at the industrial level for the consumption of goods and services. Clean production and sustainability are fundamental in the field of production processes, where large amounts of energy and materials are consumed. In this study, the authors present a comparative analysis of the environmental impacts between two production techniques for high-performance polymeric components. The material used in the two production processes, Injection Moulding (IM) and Fusion Deposition Modelling (FDM) 3D printing, is pelletized Polycarbonate (PC) defined as the model material. The LCA study was conducted from cradle to gate, including the impacts from raw material extraction, transportation, energy used during production, waste materials, wastewater treatment, and all impacts from final product finishing, i.e., post-processing, but excluding the end-of-life of the final product. A batch of 12 parts was selected as the industrial production order; therefore, the functional unit of the study is set to the production of 12 parts using the two investigated technologies.

EXPERIMENTAL

The material used for the production of the final products in both processes is pelletized Polycarbonate (defined as the model material), while the support material for FDM printing is the proprietary, soluble SR100 pellet, distributed by Stratasys (defined as the support material)(1). To compare the two types of processes, IM and FDM, the same geometry was chosen, an air flow sensor mount.

The IM process is data taken from the Ecoinvent database. For FDM, it was necessary to produce the filament with SR100 using an extruder located in our laboratories (Brabender GmbH & Co. Compounding KETSE 20/40 twin-screw extruder). The geometry was designed in Autodesk Fusion360 software, and the printing parameters were chosen using the proprietary software Insight (Stratasys, Los Angeles, USA), considering a 100% infill. The printer model is a Fortus 400mc (Stratasys, Los Angeles, CA, USA), also located in our laboratories.

The studied system is schematized in Figure 1, a simple diagram that helps us describe each process in the two cases.

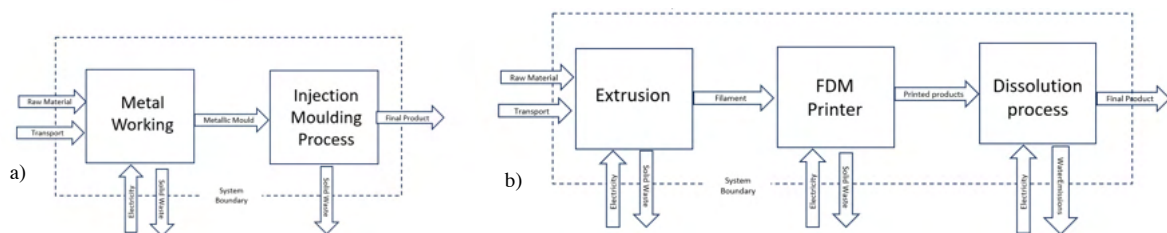


Figure 1 a) System boundary for CM; b) System boundary for AM

- a) For the conventional process, the input is considered to be metal and polymer. The metal is processed to produce a mold specifically designed for our final product, as we are at an industrial level and therefore not bound to a mold. The IM process is repeated several times until a batch of 12 parts is produced. The main inputs for this process are energy consumption, PC, and metal for the mold.
- b) For the AM process, the inputs considered are the two types of polymer pellets (model and support materials). Another input is the consumption of the extruder to create the filament for printing, considering a 5% waste that will go into the recycling scenario. The printed product, after eliminating 10% waste of the model material, requires post-processing to remove the soluble support polymer. This is treated in a bath of Waterwax Solution (distributed by Stratasys) where the polymer dissolves. The main inputs for this process are electrical consumption, model and support materials, and the Waterwax solution. The study was conducted in the same location to ensure the consistency of the acquired real data.

RESULTS AND DISCUSSION

This study provided a life cycle assessment from cradle to gate of two production processes for polymeric products using two technologies: Injection Moulding and FDM printing. An exhaustive analysis was carried out using various methods: Ecoindicator 99, Impact 2002+, Recipe, Cumulative Energy Demand (CED).

With the various selected methods, it was verified that the FDM production process has excessively long production times, especially for high-performance components, which limits its practical application to rapid prototyping.

However, using the Ecoindicator 99 method, which evaluates impact based on different categories, the worst environmental performance is observed with IM (Injection Moulding).

While the results obtained with other methods, more specific to energy consumption, indicate a lower environmental impact with the conventional process, generating lower cumulative impact, reduced global warming potential, and lower CED (Cumulative Energy Demand). To improve the impact of the entire production chain using IM, one could use the mold for the production of multiple parts, thereby increasing the reference flow, distributing the environmental impact across more pieces. On the other hand, to decrease the impact of the production chain using AM technology, the post-processing could be changed by considering other types of techniques to eliminate the support material, thereby avoiding the impact of water treatment. These proposals could be the subject of future studies.

Acknowledgment

C. Tosto acknowledges the European Union (NextGeneration EU) and MUR-PNRR project Sicilian MicronanoTech Research And Innovation Center – SAMOTHRACE (CUP E63C22000900006), Spoke 1.

A. Latteri acknowledges the MUR PRIN project TARGET “addiTive mAnufactuRing for liGhtwEight joinTs” (grant number 2020E3XL47_003, CUP E63C20011220001).

References

- 1) Additive manufacturing of plastics: an efficient approach for composite tooling <https://doi.org/10.1002/masy.201900069>

DURABILITY OF FLAX FIBER REINFORCED COMPOSITES UNDER ALTERNATE SALT-FOG AND DRYING CYCLES

L. Calabrese^{1*}, V. Fiore², C. Sanfilippo², E. Proverbio¹ and A. Valenza²

1 Department of Engineering, University of Messina, Contrada Di Dio, 98166 Messina, Italy

2 Department of Engineering, University of Palermo, Viale delle Scienze, 90128 Palermo, Italy

* lcalabrese@unime.it

INTRODUCTION

While extensive research activities focus on the durability of natural fiber-reinforced composites (NFRCs) under constant humidity conditions [1], their behavior in outdoor environments with fluctuating humidity/dry cycles requires further investigation to improve our understanding. Additionally, their recovery during drying remains poorly understood. To address this knowledge gap, studies [2, 3] examined the impact of humidity exposure and subsequent drying on the performance of glass, flax, and combined fiber composites in simulated marine environments. These research works identified the composites' ability to regain their physical and mechanical properties after a single cycle of salt-fog (humid) exposure and drying. Based on these promising results, the present study investigates the reversibility of performance in flax fiber-reinforced composites under alternating humid/dry conditions for semi-structural applications. NFRCs were subjected to simulated exposure cycles consisting of three alternating phases: 10 days of humid salt-fog spray followed by 18 days of dry conditions (22°C, 50% RH). Mechanical properties were assessed through three-point bending tests conducted during each dry phase (after 0, 5, 10, and 18 drying days). Water absorption and desorption were monitored by tracking composite weight changes throughout the aging process.

EXPERIMENTAL

Epoxy composites were made with five layers of 318 g/m² twill weave flax fabric using a vacuum-assisted resin infusion process. The composites underwent initial curing at 25 °C for 24 hours, followed by post-curing at 50 °C for 15 hours, using a DEGBA epoxy resin (SX8 EVO) mixed with its amine-based hardener (100:30 weight ratio).

The aging process took 3 months (12 weeks) consisting of three cycles, each lasting 4 weeks. Each cycle had a 10-day wet phase in a corrosion chamber (model CC1000IP by Ascott) at 35°C and 100% humidity with a salt spray fog (5% sodium chloride solution) as per ASTM B 117. This initial step was followed by an 18-day dry phase at 22°C and 50% humidity.

Throughout a 10-day degradation test, weights of three (100 x 100 mm²) square samples from a salt-fog chamber were regularly measured to track water absorption and release. The samples were wiped dry daily, and their weights were measured using a high-precision scale (model AX 224 by Sartorius), following ASTM D570 standard.

Five 13 mm x 64 mm samples underwent quasi-static three-point bending tests after drying for 0, 5, 10, and 18 days. A Zwick-Roell UTM (model Z005, 5 kN load cell) according to ASTM D790 standards, was used for testing (1.4 mm/min crosshead speed; 54 mm support span).

RESULTS AND DISCUSSION

The composites underwent weight gain during humid exposure, followed by weight loss during drying. This pattern held true across all cycles. Notably, the maximum water uptake

increased with each cycle, while the residual weight after drying decreased, leading to a growing difference between these values as the cycles progressed.

This behavior can be justified considering that the material degrades during the wet part of each cycle because water gets absorbed and spreads throughout it. This weakens the material's structure by creating and growing microcracks and debonding phenomena. The more cycles the material goes through, the worse this damage becomes.

As shown in Figure 1, the flexural modulus histogram reveals a decrease in stiffness for the composite during the humid phase (0D samples). This is followed by a recovery in stiffness during the subsequent dry phase. The results demonstrate that drying times significantly impact mechanical performance, with substantial recovery achievable after only a few days in a dry environment.

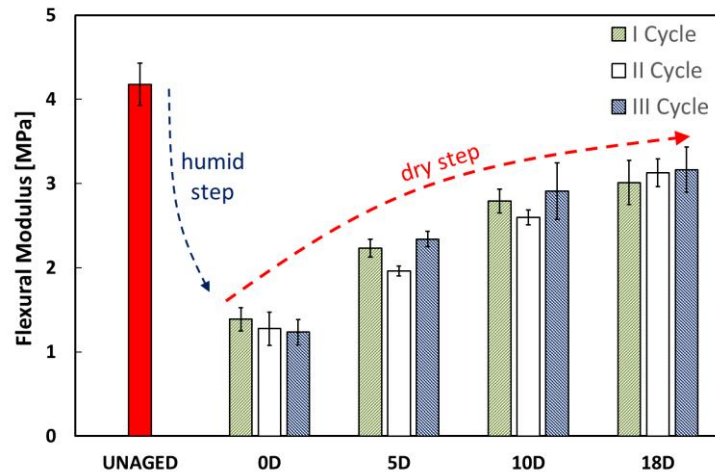


Fig. 1 Flexural modulus of FFRCs at increasing drying time at varying aging cycle

Even though the stiffness (modulus) of the FFRCs increases at increasing drying time, it's consistently much lower than the stiffness of the unaged material. After aging, the average stiffness of the FFRCs is 3.16 GPa, which is roughly 25% less than the unaged one (4.18 GPa).

Multiple ways composites degrade hurt their performance. These include fibers absorbing water and swelling, microcracks forming in the matrix, and interfacial stresses. This can start damaging phenomena, but the limited salt-fog exposure (10 days) might not cause significant damage. If the composite is removed from the wet environment, some damage could be reversible, explaining why bending strength seems to hold up. Wet NFRCs lose stiffness cause of combined softening in both fibers and matrix. Dry flax fibers are stiff due to cellulose fibrils, but water weakens them by forming hydrogen bonds, increasing its flexibility. Water also affects the epoxy, making it more flexible. Additionally, repeated cycles of wetting and drying favor loss of adhesion at the fiber-matrix interface. Preferential water pathways form at this interface, further weakening adhesion. These weakening phenomena, occurred during the wet phase, could persist even when the composite is dried. This reduces permanently the stiffness of NFRCs limiting its durability during aging.

References

- 1) Q. Wang, T. Chen, X. Wang, Y. Zheng, J. Zheng and G. Song., *Polymers*, 15, 4121 (2023)
- 2) V. Fiore, L. Calabrese, R. Miranda, D. Badagliacco, C. Sanfilippo, D. Palamara, A. Valenza, E. Proverbio. *Composites Part B*, 230(1), 109535 (2022).
- 3) L. Calabrese, V. Fiore A. Valenza and E. Proverbio. *Polymer Testing*, 127, 108186 (2023)

Poster presentations

Phosphorus pentoxide (P2O5) catalyst for Ring Opening Polymerization of ϵ -Caprolactone (ϵ -CL)

I. Adoumaz^{a,b,*}, M. Save^a, M. Lahcini^b

^a Universite de Pau et des Pays de l'Adour, E2S UPPA, CNRS, IPREM, Pau, France.

^b IMED-Lab, Cadi Ayyad University, Marrakech 40000, Morocco

* adoumaz91@gmail.com

INTRODUCTION

poly(ϵ -caprolactone) (PCL) is a semi-crystalline aliphatic polyester. Its thermal ($T_g = -65^\circ\text{C}$ and $T_m = 60^\circ\text{C}$) and mechanical properties, as well as its high miscibility with many polymers such as poly(vinylchloride) or poly(bisphenol-A), make it as polymer with a very good processability for a large number of industrial applications (1). Its biodegradability has also been a great success for more than 30 years especially in the biomedical field. For example, poly(ϵ -caprolactone) is promoted as a homopolymer or as an encapsulation matrix for Levogestrel, a contraceptive, under the trademark Capronor (2). Mechanical properties could be modulated by preparing copolymers containing caprolactone and other monomers, the rate of degradation could be also accelerated, as in the case of the poly(ϵ -caprolactone-coglycolide) copolymers used for producing resorbable sutures, Monocryl (3). In this context, it was the purpose of this work to provide first-hand data on the usefulness of phosphorous pentoxide (P2O5) as catalysts for the ROP of ϵ -caprolactone (ϵ -CL) under solvent-free condition. Indeed, phosphorous pentoxide is of particular interest, because it presents numerous advantages due to its green character, low price, ease of handling and experimental simplicity. It should be noted, that the phosphorous pentoxide has already been extensively used as catalyst for several organic reactions such as Beckmann rearrangement, dimerization of olefin,²¹ but to the best of our of knowledge its application as catalyst for ring-opening polymerizations of cyclic esters has never been reported before.

EXPERIMENTAL

Materials

P2O5, iPrOH and ϵ -caprolactone were purchased from Aldrich. ϵ -Caprolactone (ϵ CL) was refluxed and distilled in vacuo over freshly powdered calcium hydride. The P2O5 was used without any farther purification, iPrOH was distilled over CaH2.

Preparation

ROP of ϵ -caprolactone: ϵ -CL (10 mmol) was weighed under dry argon into a Schenck having silanized glass walls. The P2O5 was injected in the form of a powder. The closed reaction vessel was placed into an oil bath preheated to an adequate temperature.

Characterization:

NMR: For the determination of time conversion curves, small samples were removed from time to time under an atmosphere of argon. After cooling, the virgin reaction product was characterized by NMR. The NMR spectra were recorded in CDCl3 on Bruker Avance 400 MHz spectrometers at 25 °C.

Size exclusion chromatography (SEC): The average molar masses and the number average molecular weight and dispersity indices (D) of the PCL polymers were determined by exclusion chromatography (SEC).

Mass spectrometry: Matrix-assisted laser desorption, time-of-flight ionization (MALDI-TOF) MS spectra were recorded on the Bruker Daltonics flexAnalysis.

RESULTS AND DISCUSSION

In this study, we succeeded in synthesizing various poly (ϵ -Caprolactone) (PCL) with well-defined structures by ring opening polymerization (ROP) of ϵ -Caprolactone (ϵ -CL) using phosphorus pentoxide (P₂O₅), as organocatalyst and isopropanol (iPrOH) as initiator (Fig 1). P₂O₅ activated the carbonate group of ϵ -CL, an alcohol molecule reacted as an initiator with the activated ϵ -CL to give the carbonated adduct of ϵ -CL and alcohol (iPrOH), and the process was repeated to produce PCL without side reactions, such as transesterification reactions; that is, the P₂O₅ catalyzed ROP of ϵ -CL passes through the activated monomer mechanism to produce the PCL having the iPrOH group as the end of the chain. In addition, P₂O₅ acted as a ROP catalyst and was inactive with respect to the initiator and monomer functional groups to give well-defined poly (ϵ - Caprolactone) (PCL) with functional groups in the side chain and the end of it.

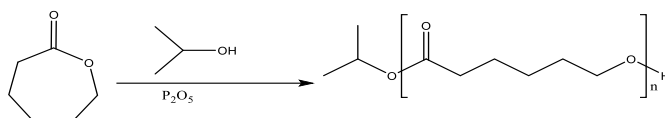


Fig. 1 Synthesis of poly(ϵ -caprolactone) by Ring-Opening Polymerization with ϵ -caprolactone (ϵ -CL) of iPrOH catalyst by P₂O₅.

Acknowledgment

We thank the PHC Toubkal program for the scholarship and Campus France / CNRST, the program for its financial and academic support during my thesis.

References

- 1) J. W. B. J. J. Ziska, and D. R. Paul, *POLYMER*, **22** (1981).
- 2) S. J. Ory, C. B. Hammond, S. G. Yancy, R. Wayne Hendren and C. G. Pitt, *American Journal of Obstetrics and Gynecology*, **145**, 600-605 (1983).
- 3) U. Piotrowska and M. Sobczak, *Molecules*, **20**, 1-23 (2014).

PVA-PVP-lignin-sodium oleate films for cationic dye degradation

Y. Aleeva and D.F. Chillura Martino*

*Department of Biological, Chemical and Pharmaceutical Sciences and Technologies, University of Palermo, Bld.17, Viale delle Scienze, Palermo, Italy
yana.aleeva@unipa.it, delia.chilluramartino@unipa.it

INTRODUCTION

Efficient removal of dyes by adsorption from industrial waters before their discharge into the environment remains a challenge that could improve the habitat of aquatic organisms and reduce risks to human health. Therefore, there is a growing need for new efficient adsorbents based on biopolymers. Since lignin has an abundance of chemical bonds, hydroxyl, methoxyl and carboxyl functional groups, it can be used as an adsorbent for the removal of various pollutants. However, due to its heterogeneity, recalcitrance and the lack of a solvent system for lignin, it is difficult to use it as a polymeric material.

In this study, we investigate the preparation of polyvinyl alcohol (PVA)-polyvinyl pyrrolidone (PVP)-lignin (L) films with and without the addition of sodium oleate for the purification of cationic dyes. Chemical cross-linking and surfactant loading were carried out to improve the chemical-physical properties of the films in an aqueous environment.

EXPERIMENTAL

Materials

Alkali lignin (L), PVP ($M_w = 1,300,000$), glutaraldehyde (25 % in H₂O, Grade II), methylene blue hydrate (MB, Bioreagent grade) were purchased from Merck/Sigma Aldrich. PVA (98-99 % hydrolyzed, high molecular weight) was acquired from Alfa Aesar and sodium oleate (SO, purum) from Riedel-de Haen respectively. All reagents were used as received and without further purification

Preparation

A PVA solution was prepared by dissolving 1 g of PVA in 25 mL of water and heating at 85 °C with continuous stirring until complete dissolution. Then 0.25 g PVP was added to the PVA solution and mixed until complete dissolution. A lignin solution was prepared by dissolving lignin (0.100, 0.020 and 0.010 g) in 1 mL of PEG-200 solution by ultrasonication for 1 hour. These two solutions were then mixed to prepare the PVA-PVP-L solution, the temperature was adjusted to 65 °C and 0.020 g of sodium oleate was added to the reaction mixture as required. Glutaraldehyde (0.100 mL) was added to the PVA-PVP-L solution to initiate the cross-linking reaction, which was carried out for 30 min. After the reaction, the solutions were poured into Petri dishes and air dried at room temperature for 5 days. The hydrogels were named according to the concentration of lignin used: PVA-PVP-L0.1, PVA-PVP-L0.1-SO, PVA-PVP-L0.02-SO, PVA-PVP-L0.01-SO, also PVA-PVP (without lignin and sodium oleate added) and PVA-PVP-SO (film without lignin added) were prepared as control samples.

Physico-chemical characterization

Methylene blue (2.5×10^{-5} M, 40 mL) was mixed with approximately 0.35 g of film to monitor MB degradation over time. Absorbance spectra were collected every 30 minutes using a UV-Vis spectrophotometer (DU 800 spectrophotometer, Beckman Coulter, USA). ATR-FTIR spectra of the films were collected using an FTIR Bruker Vertex Advanced Research Fourier Transform Infrared Spectrometer (Bruker, Billerica, MA, USA) equipped with a platinum ATR and a diamond crystal in the 400-4000 cm⁻¹ range (lateral resolution of 2 cm⁻¹ and 120 scans). ATR-FTIR measurements of films after MB degradation were

performed on dried films after soaking in MB solution (2.5×10^{-5} M, 40 mL) for 3 h and desorption in 40 mL H₂O for 20 h.

RESULTS AND DISCUSSION

The effect of the lignin to sodium oleate ratio and the physicochemical properties of the PVA-PVP-L films were evaluated. Fig. 1a shows that the introduction of lignin and/or SO into the PVA-PVP matrix resulted in 50 to 87% MB degradation within 2 h, the highest degradation for lignin containing films was achieved in the presence of PVA-PVP-L0.01-SO film.

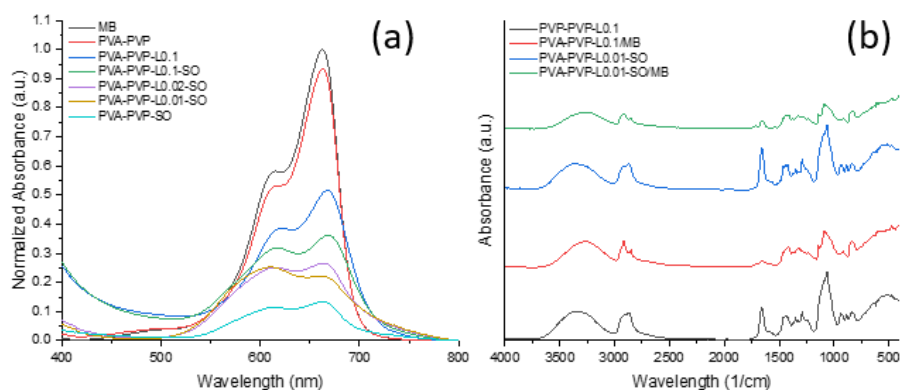


Fig. 1 a) UV-vis absorption spectra of MB reduction in the presence of as deposited films after 2 hrs, b) FTIR spectra of PVA-PVP-L0.1 and PVA-PVP-L0.01-SO before and after methylene blue adsorption.

Figure 1b shows the FTIR spectra of PVA-PVP-L films before and after methylene blue adsorption. The results of the FTIR spectra analysis of the pristine films and after dye adsorption show changes due to the attachment of MB, revealing characteristic IR adsorption bands of MB at 1390 and 1330 cm^{-1} , corresponding to $-\text{CH}_3$ symmetric deformation and $\text{C}=\text{N}$ bond, respectively (1). Furthermore, for both PVA-PVP-L0.1/MB and PVA-PVP-L0.01-SO/MB, the peak at 3500-3100 cm^{-1} was shifted to a lower wavelength, indicating that the phenolic hydroxyl group is the main reaction site for MB adsorption (2). These phenolic hydroxyl groups can form active hydrogen bonds with MB molecules. These observations suggest that the methylene blue molecules were preferentially adsorbed on the surface of the PVA-PVP-L films by electrostatic interaction, but additional hydrogen bonding also took place.

Acknowledgment

This work has been financially supported by the Project MICS - “Made in Italy Circolare e Sostenibile - MICS”, tematica “11. Circular and sustainable Made-in-Italy”, Spoke 3 (CUP B73C22001270006)

References

- 1) T.M. Budnyak, S.Aminzadeh, I.V.Pylypchuk, D.Sternik, V.A. Tertykh, M.E.Lindstrom, O. Sevastyanova, *J. Env. Chem. Eng.*, **6**, 4997 (2018)
- 2) S. Jung, H. Yun, J. Kim, J. Kim, H. Yeo, I. Choi, H.W. Kwak, *Int. J. Biol. Macromol.*, **257**, 128810 (2024)

THERMAL BEHAVIOR OF POLYSACCHARIDES MODIFIED CASEIN

M.R.Ricciardi¹; V.Antonucci^{1*}; L.Affatato²; A.Langella³

¹ Institute for Polymers, Composites and Biomaterials, National Research of Council, P.le E.Fermi, Portici, Italy

² Institute for Polymers, Composites and Biomaterials, National Research of Council, Via Campi Flegrei 34 Comprensorio "A. Olivetti" Pozzuoli (Na)

³ Department of Chemical, Materials and Production Engineering, University of Naples "Federico II", P.le Tecchio 80, 80125 Naples, Italy

Corresponding author *: vincenza.antonucci@cnr.it

INTRODUCTION

The use of healthier, safer, and more environmentally friendly materials throughout their entire life cycle has become a priority for scientists and producers. In particular, the use of bio-based adhesives and resins, as a replacement for synthetic ones, is interesting to address some of the main issues: toxicity and disposal.

Biopolymers are polymeric materials made from bio-based and/or biodegradable raw materials, and they have intrinsic properties such as biodegradability, biocompatibility, non-toxicity, and sustainability. In general, biopolymers can be classified into three main groups: nucleic acids and nucleotides; proteins and amino acids; carbohydrates [1].

Within this context, the use of casein, which is a biopolymer derived from milk proteins, is relevant due to the solubility of casein in alkaline solutions. The formation of caseinates, such as Calcium caseinate, also known as "casein glue" enables the preparation of strong, resistant, and insoluble adhesives. However, the effective use of these natural adhesive needs to reduce the overall volume loss, that occurs during the drying phase due to the water evaporation and leads to undesired thermal shrinkage. The adoption of polysaccharides during the casein glue preparation can slow down the evaporation process. In fact, thanks to the presence of amine and hydroxyl functional groups, polysaccharides are able to absorb and retain water, allowing for a more gradual drying and consequently reducing shrinkage.

In this work, the thermal behaviour of a casein glue, properly modified by the addition of chitosan and dextrose, two sugars with long and short chains, respectively, at different weight concentration levels, has been investigated. In particular, the thermal decomposition and degradation kinetic of prepared sugar based casein glues have been analysed by performing thermogravimetric TGA characterization at different heating rates (5, 10, 15, and 20°C/min). Experimental results and the evaluation of thermal degradation activation energy by Kissinger analysis evidenced that the chitosan and dextrose could be efficient and sustainable additives to control and mitigate the degradation mechanisms of casein glue.

EXPERIMENTAL

Materials

The lactic casein used is from AN.T.A.RES srl. It is obtained from fresh milk through acid precipitation and drying. Casein is the main family of phosphoproteins present in the milk of mammals [2]. It is a globular protein, consisting of tightly coiled chains of amino acids. The chitosan and dextrose used as fillers in the production of natural composites are those produced by ALDRICH Chemistry.

The lime putty from the Stilema line produced by Sestriere Vernici is a ready-to-use mixture containing 50.4% CaO, 17.4% MgO, 23.2% H₂O, and the remaining portion of other oxides. It has a density of 1.6 g/cm³.

Preparation

The formulation of casein glue is: 30 g of casein, 60 g of water, and 22.5 g of lime putty, with the addition of chitosan and dextrose from 10% to 50% by weight.

The solution is first mixed mechanically until a homogeneous mixture is obtained and, then, sonicated in an ultrasonic bath at a frequency of 59 kHz for 10 minutes. Sonication promotes the dissolution of aggregates, such as casein micelles, overcoming the cohesive forces between protein molecules and realizing a solution with a network of protein material aggregates. After sonication, the samples are cured at 60°C for 24 hr.

RESULTS AND DISCUSSION

Thermogravimetric TGA tests have been performed for all prepared formulations at different heating rates at 5, 10, 15, and 20°C/min under nitrogen atmosphere. Figure 1 shows the degradation stages for casein and chitosan and dextrose (20%w/w) formulations under nitrogen atmosphere at 10°C/min. Experimental results evidence the influence of both sugars on the degradation mechanisms of casein by significantly lowering the rate of the thermal degradation. This effect is confirmed by the evaluation of activation energy for all different stages by Kissinger kinetic analysis. In fact, the activation energy for dextrose formulation increases up to 92% respect to that of casein, demonstrating the efficiency of sugars for the casein thermal degradation mitigation.

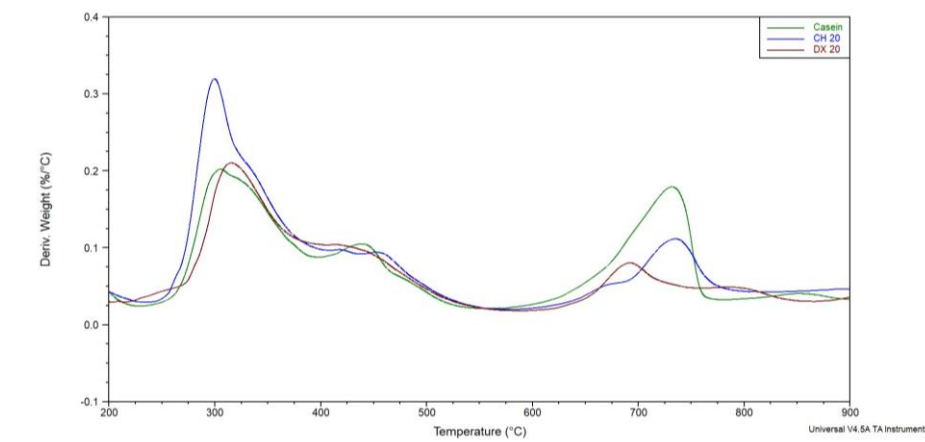


Fig. 1 DTG curves of casein, chitosan and dextrose (20%w/w) formulations under nitrogen atmosphere at 10°C/min.

Acknowledgment

This work has been financially supported by the Ministry of Research under the PRIN 2022 PNRR: "Manufacturing of composite materials casein-based: New frontiers for sustainability - MaCoSu" with the identification code: P2022KYCY9.

References

- [1] O. Smidsrød, S. Moe, and S. T. Moe, Tapir Academic Press, 2008.
- [2] I. Chang, J. Im, M. K. Chung, and G. C. Cho, *Constr Build Mater*, vol. 160, pp. 1–9, 2018, doi: 10.1016/j.conbuildmat.2017.11.009.

PROTECTIVE NANOSTRUCTURED FLAME RETARDANT COATINGS FOR CABLE INDUSTRY APPLICATIONS

R. Arrigo, F. Cravero, E. Lorenzi and A. Frache

Department of Applied Science and Technology, Polytechnic of Turin, Viale Teresa Michel
5, Alessandria, Italy

rossella.arrigo@polito.it, fulvia.cravero@polito.it, leonora.lorenzi@polito.it,
alberto.frache@polito.it

INTRODUCTION

This work deals with the formulation of nanocomposites based on ethylene butyl acrylate (EBA) copolymer and nanoclays potentially suitable as halogen-free flame retardant materials for applications in wire and cable industry. In particular, two different strategies were exploited: the first dealt with the incorporation of the nanofillers into the bulk copolymer; the second involved the utilization of a pre-prepared EBA/nanoclay film that was applied, as a surface coating, onto unfilled EBA specimens. This latter approach has been already proposed and discussed in the literature, showing its suitability in providing protection to an underlying polymer matrix [1].

Furthermore, since the morphology of the coating film, in terms of dispersion, distribution or orientation of the embedded nanofillers, can affect its effectiveness as protective layer, the surface films were prepared through cast extrusion or compression molding, aiming at gaining important insights into the processing/microstructure relationships of nanostructured materials endowed with flame retardant properties.

EXPERIMENTAL

Materials

EBA Lucofin® 1400MN (content of butyl acrylate 17%, MFI 7.0 (190 °C, 2.16 kg)) was used as matrix while the nanoclays were introduced at 4 wt% (referred to the inorganic content) starting from a commercially available masterbatch Lucofin 7500.

Preparation

EBA/nanoclay nanocomposite was prepared through a melt compounding step in a twin-screw extruder and further processed through: (i) cast extrusion or compression molding for obtaining films having a thickness of about 300 µm; (ii) injection molding for obtaining EBA/nanoclay_bulk specimens. The films were then applied on unfilled EBA specimens, pre-prepared through an injection molding step.

Characterizations

Cone calorimetry tests were carried out with a Noselab Ats (Nova Milanese, Italy) instrument, following the ISO 5660 standard. Each sample (size: 50 × 50 × 3 mm³) was tested under a 35 kW/m² irradiative heat flux. The morphology of the different samples and of the residues at the end of the cone calorimeter tests was assessed through SEM (EVO15, Zeiss) observations.

RESULTS AND DISCUSSION

The preliminary evaluation of the morphology of the cast extruded and compression molded films demonstrated the achievement of a uniform microstructure in both materials; in fact, the embedded nanofillers appear homogeneously dispersed and distributed within the host EBA matrix, and no agglomerates or clusters are observable. As expected, a preferential orientation of the nanoclays along the extrusion direction is clearly noticeable in the EBA/nanoclay_CE film.

The combustion behavior of all formulated EBA-based systems was evaluated through cone calorimeter tests (Figure 1). From an overall point of view, it is worthy to note that, regardless the exploited strategy (namely, bulk or surface approach), the incorporation of the nanoclays lowers the pHRR of the unfilled EBA, likely due to the well documented action of nanoclays [2]. In brief, the acidic sites on the silicate layers resulting from the thermal degradation of the organomodifier are able to catalyze the formation of a coat-like char on the specimen surface (that serves as a potential barrier to both mass and energy transport) and the oxidative dehydrogenation of the polymer chains, leading to the formation of double bonds and consequent aromatization and charring. Lastly, a minor contribution could be also provided by the barrier created through the ablative reassembly of the silicate layers on the polymer surface. Obviously, the more pronounced effect in the EBA/nanoclay_bulk system can be ascribed to the higher amount of nanoclays contained in this sample as compared to the surface-coated ones.

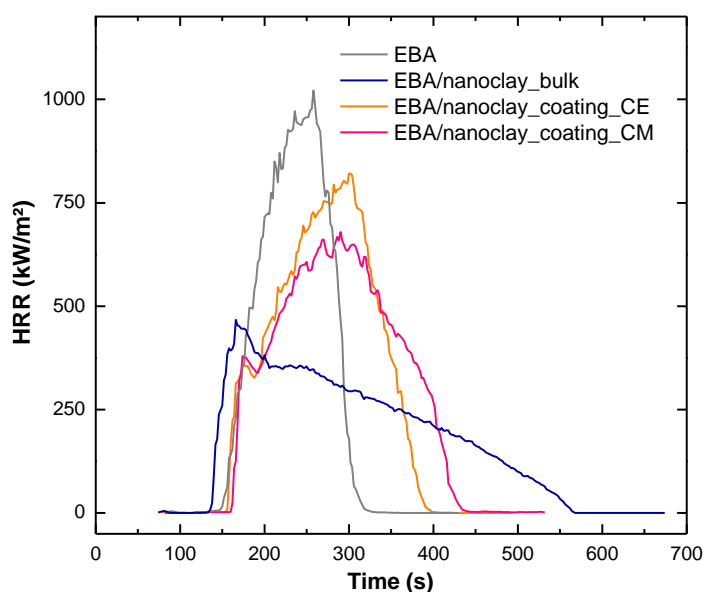


Fig. 1 HRR curves for pristine EBA and all investigated nanoclay-containing systems

Furthermore, looking at the HRR curves of the samples prepared following the two approaches, important differences emerge when comparing bulk incorporation and surface coating. In particular, in the first case the nanofillers anticipate both time to ignition and time to peak as compared to unfilled EBA, while an opposite behavior is observed for the surface-coated samples. In particular, the delayed time to peak of both systems obtained through the surface approach is a clear indication of the thermal shielding effect provided by the presence of the nanofillers on the surface of the sample exposed to the irradiative heat flux. Concerning the effect of the processing adopted for the formulation of the protective layer, the differences observed between the HRR curves of the two specimens can be ascribed to the different microstructure of the residues at the end of the cone calorimeter test, resulting from the different state of dispersion and orientation of the nanoclays in the original cast-extruded or compression molded films.

In all, the obtained results demonstrated the effectiveness of the proposed surface approach, capable to concentrate the flame retardant action on the surface of a polymer system, where the combustion specifically takes place, thereby preserving the required features of the polymer bulk and minimizing the amount of flame retardant.

References

- 1) S. Matta, M. Bartoli, R. Arrigo, A. Frache, G. Malucelli, *Comp. Part C*, **8**, 100252 (2022).
- 2) M. Zanetti, T. Kashiwagi, L. Falqui, G. Camino, *Chem. Mater.*, **14**, 881 (2002).

EVALUATION OF BIODEGRADATION OF CROSSLINKED SERICIN-BASED MEMBRANES

M.C. Arango^{a,b}, K. Gutiérrez-Silva^a, O. Gil-Castell^a, J.D. Badia^a, C. Alvarez-López^b, J.P. Cerisuelo^a, and A. Cháfer^{a*}

^a Material Technology and Sustainability (MATS). Department of Chemical Engineering, Universitat de València. València, España. karen.gutierrez@uv.es, oscar.gil@uv.es, jose.badia@uv.es josep.cerisuelo@uv.es amparo.chafer@uv.es

^b Agroindustrial Research Group (GRAIN). Universidad Pontificia Bolivariana. Medellín, Colombia. maria.arangosa@upb.edu.co, catalina.alvarezl@upb.edu.co

INTRODUCTION

Biodegradable polymers have received considerable attention and interest for biomedical applications, specifically wound healing, owing to their high biocompatibility [1]. These polymers can be used to create materials that can be loaded with drugs, which are gradually released as polymers degrade. In addition, they reduce the environmental impact compared with non-biodegradable polymers. Among the materials made with biodegradable polymers, hydrogel-type membranes stand out because of their ability to control humidity and absorb fluids such as exudates present in the wound, which helps promote wound healing [2]. A mixture of synthetic and natural polymers, as well as green cross-linking methods, are presented as an alternative to improve stability in humid environments while controlling the rate of degradation. In this study, a new porous membrane was developed using a polymeric mixture process comprising silk sericin (SS), a protein easily isolated from silk cocoons, gelatin (G), and poly (vinyl alcohol) (PVA), followed by a physical cross-linking process. The chemical structure, swelling capacity, and degradation in phosphate-buffered saline (PBS) were evaluated. Thermogravimetric analysis was performed before and after immersion in PBS.

EXPERIMENTAL

Materials

Defective silkworm cocoons (SC) were provided by the Corporation for the Development of Cauca Sericulture in Colombia. The PVA used in this study was a commercial product purchased from Sigma–Aldrich with a degree of hydrolysis higher than 98-99% and a molecular weight of 146–186 kDa. Porcine skin gelatin from Sigma–Aldrich (gel strength: 300 g Bloom) was used. PBS with pH 7.4 and 1X was purchased from Gibco.

Preparation

A high-temperature and high-pressure degumming method and a spray drying process were used to extract SS from SC and obtain SS powder, respectively. Subsequently, aqueous solutions of SS, G, and PVA (each at 2% w/v) were mixed in a 1:1:2 v/v ratio (SS/G/PVA) at 80 °C. The mixture was concentrated by evaporation of the solvent to 6% w/v and glycerol (Gly) was added to the solution (1.5% Gly v/solution v). The obtained solutions were stabilized overnight and dried in an oven at 40 °C for 24 h, followed by lyophilization to obtain the porous SS/G/PVA membranes. Cross-linking with water vapor was performed at 60 °C and -0.6 bar for 3.5 h. Following the same procedure, the pristine SS, PVA, and G membranes were developed. The samples were stored in a desiccator until further characterization.

Physical and structural characterization

The chemical structures of all membranes were determined using Fourier transform infrared spectroscopy (FTIR). The spectral range was fixed at 4000–400 cm⁻¹.

The swelling capacities of SS/G/PVA, pristine SS, G, and PVA membranes were evaluated by immersion in PBS for 24 h at 37°C. After immersion, the wet samples were dried at 60 °C in a forced-convection oven for 24 h and subsequently weighed to evaluate their degradation in PBS. The thermal behavior of the samples was analyzed using thermogravimetric analysis (TGA), both before and after immersion in PBS. For this analysis, dry samples (10 mg each) were processed under an inert nitrogen (N₂) atmosphere to avoid oxidation at a flow rate of 50 mL/min and a heating ramp of 10°C/min. From the TGA results, the first mass derivative (DTG) was calculated with respect to time to obtain decomposition profiles and characteristic temperatures.

RESULTS AND DISCUSSION

Fig. 1.a shows the swelling capacity and degradation of SS/G/PVA membranes and their components in PBS. SS exhibited the highest swelling capacity owing to its highly hydrophilic structure, allowing it to absorb large amounts of fluid and moderate degradation while maintaining its structure during the test. In contrast, G could not be quantified because of its rapid degradation in an aqueous medium, which was accelerated by the addition of glycerol, a plasticizer that reduces rigidity and increases solubility. PVA, which is known for its lower hydrophilicity than proteins, has the lowest swelling capacity but offers greater structural stability. The SS/G/PVA membrane exhibited a high swelling capacity with moderate degradation (26%), likely because of the combination of the hydrophilic properties of proteins with the structural stability provided by PVA and the occurrence of hydrogen bond interactions between the polymers.

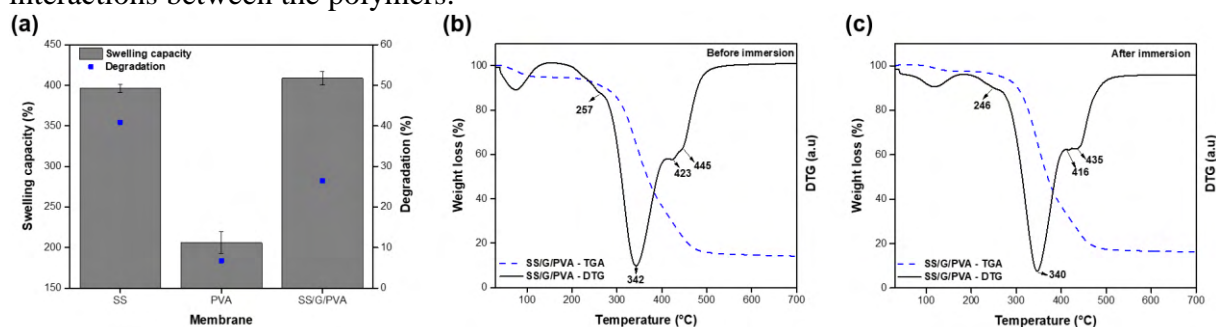


Fig. 1 (a) Percentage of swelling capacity after 24 h of immersion in PBS and degradation test for pristine SS, pristine PVA, and SS/G/PVA membranes (n = 3). TGA and DTG curves of dried SS/G/PVA membranes (a) before and (b) after immersion in PBS.

The TGA and DTG results for the SS/G/PVA membrane before and after immersion in PBS are shown in Fig. 1. b and c, respectively. A lower decomposition temperature was observed for the membranes after immersion, which was attributed to swelling in PBS. Membranes absorb fluids, which can cause partial hydrolysis of the bonds in the polymer chains, particularly in components such as G, which is known for its rapid degradation in aqueous media. This hydrolysis and possible rearrangement of the polymer chains resulted in a more disordered and less thermally stable structure.

Acknowledgment

This work has been financially supported by Ministerio de Ciencia, Tecnología e Innovación 852, 2019.

References

- 1) Sonjan S, Ross GM, Mahasaranon S, et al. *J Polym Environ*, **29**, 334 (2021)
- 2) Bakadia BM, Zhong A, Li X, et al. *Adv Compos Hybrid Mater* (2022)

DEVELOPMENT OF BIOFORMULATIONS BASED ON NATURAL CARRIERS AND ESSENTIAL OILS FOR AGRICULTURAL APPLICATIONS: PRELIMINARY RESULTS

M. Baiamonte¹, H. Tsolakis², G. Lo Verde², E. Ragusa², R. Rizzo³, E. Spinozzi⁴, F. Maggi⁴ and L. Botta^{1*}

¹Department of Engineering, University of Palermo, Viale delle Scienze, Palermo, Italy

²Department of Agricultural, Food and Forest Sciences, University of Palermo, Viale delle Scienze, Palermo, Italy

³CREA - Research Centre for Plant Protection and Certification, Palermo, Italy

⁴Chemistry Interdisciplinary Project (ChIP) Research Center, School of Pharmacy, University of Camerino, Via Madonna delle Carceri, Camerino, Italy

*luigi.botta@unipa.it, marilena.baiamonte@unipa.it

INTRODUCTION

The overuse of synthetic pesticides has driven research and experimentation with new natural substances for sustainable agriculture. Currently, useful bioformulations are being developed to control plant parasites, reducing dependence on synthetic pesticides and minimizing harmful impacts on humans and the environment. Botanical pesticides, such as essential oils (EOs) and plant extracts, offer an environmentally friendly and sustainable alternative to synthetic pesticides. However, their use is often limited by high volatility, rapid oxidation, and degradation upon exposure to air. To address these issues, the development of formulations based on carriers that provide physical stability and protection from evaporation and degradation is necessary. EOs are particularly unstable and susceptible to degradation or loss (1). Carriers can prevent the loss of the antioxidant and biocidal properties of EOs, ensuring their effectiveness in various applications (2). Additionally, carriers allow for controlled release of these active substances. Common carriers include coal, calcined clays, and plant waste materials (agricultural waste) (3). The selection of botanical pesticides and carriers is crucial for developing effective bioformulations. This study focuses on carvacrol, a phenolic monoterpene occurring in several Lamiaceae EOs, known for its antibacterial, antimicrobial, and antioxidant properties (1, 4, 5), chosen as a model molecule, and evaluates two natural materials—zeolite and biochar—as suitable carriers for the development of bioformulations.

EXPERIMENTAL

Materials

Two different types of carriers were utilized in this study: biochar, a powdered vegetable charcoal derived from coconut shells without additives; and micronized zeolite of natural origin, untreated and not chemically enriched, based on chabazite. These carriers were chosen for their potential to enhance the efficacy of carvacrol essential oil, selected as a potential biopesticide. Additionally, Tween80, a surfactant, was employed to optimize the final formulations.

Preparation

Two methods were used to incorporate carvacrol essential oil into the powder: firstly, by adding the oil drop by drop onto the powders; and secondly, by creating an emulsion of water and oil to which the powders were added. To prevent thickening, Tween80, a surfactant, was introduced into the formulations following established methods in the literature (6). Initially, carvacrol was mixed with Tween80 and the mixture was vortexed for 5 minutes. Subsequently, biochar or zeolite was slowly added. Distilled water was then added to the mixture, which was shaken at room temperature for 120 minutes and subsequently

sonicated for 5 minutes to ensure homogeneity and stability. The prepared formulation was stored at 4°C until use.

RESULTS AND DISCUSSION

The initial assessment of the carriers focused on their dispersibility in water. Both zeolite and biochar demonstrated good dispersibility; however, observations revealed distinct behaviors. Zeolite settled at the bottom after approximately two hours of cessation of agitation, whereas biochar exhibited greater stability, remaining suspended for up to 24 hours. When carvacrol essential oil was added drop by drop onto the powders, biochar tended to form dense agglomerates upon contact with the oil. Subsequent addition of distilled water failed to disperse the oil-soaked biochar, resulting in agglomerated sediments. In contrast, zeolite showed a different response, effectively absorbing the oil to form a cohesive mixture that dispersed well upon addition of water.

Emulsions of water and oil with added powders highlighted further differences: biochar consistently formed agglomerates, albeit smaller than those observed in the first method, while zeolite exhibited a more dispersed formulation with slight oil separation. To address these observations, Tween80 surfactant was incorporated into the final formulations as per the described methodology. The resultant formulations showed improved dispersion and stability for both carriers. This study underscores the importance of carrier selection and formulation methods in optimizing the efficacy of bioformulations containing carvacrol essential oil for agricultural applications.

Acknowledgment

Funded by the European Union – Next Generation EU - PNRR M4 - C2 -investimento 1.1: Fondo per il Programma Nazionale di Ricerca e Progetti di Rilevante Interesse Nazionale (PRIN) - PRIN 2022 cod. 202274BK9L_001 dal titolo "Bioformulations for controlled release of botanical pesticides for sustainable agriculture." CUP B53D23008570006

References

- 1) V Gandova, A Lazarov, H Fidan, M Dimov, S Stankov, P Denev, S Ercisli, A Stoyanova, H Gulen, A Assouguem, A Farah, R Ullah, M Kara, A Bari, *Open Chemistry* 21, 20220319 (2023)
- 2) AP Ferreira, C Almeida-Aguiar, SPG Costa, IC Neves, *Molecules*, 27, 23 (2022)
- 3) Tripti, A. Kumar, Z. Usmani, V. Kumar, Anshumali, *Journal of Environmental Management* 190, 20-27 (2017)
- 4) R Kotan, F Dadasoglu, S Kordali, A Cakir, N. Dikbas, and R. Cakmakci, *Journal of Agricultural Technology* (2007)
- 5) C Maes, S Bouquillon, ML Fauconnier, *Molecules*, 24, 14 (2019)
- 6) Anupama, Deepika, A K Singh, P Khare, *Industrial Crops & Products* 205, 117440 (2023)

“Nano-starch for multidirectional application in medicine, food, and cosmetic industries”

D. Bajer*

Faculty of Chemistry, Department of Biomedical and Polymer Chemistry, Nicolaus Copernicus University in Torun, Gagarina 7, Poland

* dagmara@umk.pl

INTRODUCTION

Nanotechnology enjoys tremendous interest among producers and processors, especially in food storage and packaging, medicine, pharmacy, and household chemistry. The rapid progress in the industrial application of nanomaterials requires in-depth determination of the toxicity of such materials, and understanding of the mechanisms of molecular interactions of nanoparticles (i.e. with food), as well as full knowledge of their physicochemical structure and properties. The search for ecological materials contributes to the growing interest in natural biopolymers, including readily available polysaccharides. The methods of obtaining nano-starch (for various purposes) with acid hydrolysis or sonication are used by some authors according to a fixed scheme, but rather no significant attempts are made to modify the conditions of these syntheses [1-3].

The goal of the presented studies was to develop the nano-starch synthesis procedure to shorten the exposition time to a minimum and simultaneously obtain nanoparticles of the most petite possible sizes without the broad size distribution and with limited susceptibility to agglomeration. Corn starch (CS) and waxy corn starch (WCS) differed with amylose content were subjected to acid hydrolysis, ultrasound, and a combination of both, performed at a raised temperature and short period, to obtain nanoparticles (nano-WCS and nano-CS). Aside from chemical modification, the physical influence (cavitation) was examined in the direction of nanoparticles preparation, both as exclusive effect and after prior hydrolysis.

EXPERIMENTAL

Material, Sample Preparation and Methodology

10g of Corn starch (CS) / waxy corn starch (WCS) (both from Cargill Sp. z o.o., Warsaw, Poland) were dispersed in 50 mL distilled water. After the solution temperature of 65 °C was reached, the 2 mol/L HCl solution was gradually added dropwise until the pH was 3-4. The solution was then heated in a water bath and simultaneously stirred on a magnetic stirrer for 1h at 420 rpm. Subsequently, the suspension was subjected to the sonication process using an EMAG Emmi E60 ultrasonic cleaner with a frequency of 45 kHz (EMAG AG, Mörfelden-Walldorf, Germany) for 1h at 60°C. Sonication was performed at an amplitude of 80% (frequency 36 kHz). Samples were subjected to chemical and physical modification independently, and the combination of both methods was also applied (sonication following HCl hydrolysis). The solid samples were obtained by water evaporation and thorough drying in a vacuum drier at 50 °C.

HR-TEM-STEM images of samples were collected using a microscope Tecnai 20F X-Twin (Fei Company, Hillsboro, Oregon, United States). The nano-particle sizes were estimated with TIA 4.2 SP1 software (Fei Company, US) as an average of 60 results.

Amylose content was determined by UV-VIS spectroscopy, according to procedure describe in literature [3].

X-ray diffraction analysis was performed with X'Pert PRO (Malvern Panalytical, Almelo, The Netherlands). The radiation of the CuK α lamp with the wavelength $\lambda = 1.540 \text{ \AA}$ was used. The degree of crystallinity (X_c , %) of the starch samples was calculated as the ratio of the areas of the crystalline peaks to the total area under XRD curves (i.e., to the sum of the amorphous halo and surface area of crystalline peaks) in the range of $2\Theta = 10-28^\circ$.

RESULTS AND DISCUSSION

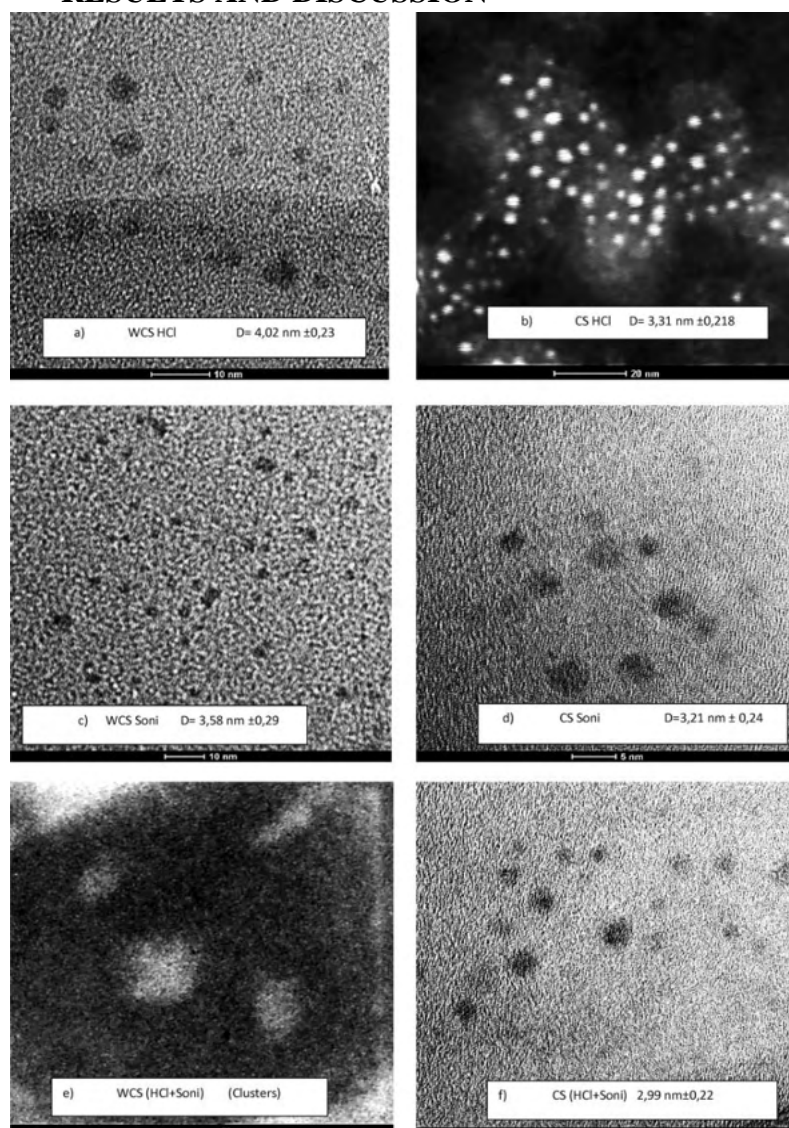


Fig. 1. Transmission electron microscopy (TEM-STEM) images: a, b – corn starch (CS) and waxy corn starch (WCS) after HCl treatment (CS HCl; WCS HCl, respectively), c, d- corn starch (CS) and waxy corn starch (WCS) after sonication (CS Soni; WCS Soni, respectively) and e, f- corn starch (CS) and waxy corn starch (WCS) after HCl and sonication (CS (HCl+Soni), WCS (HCl+Soni), respectively)).

The proposed methodology turned out to be an effective, fast, and economical way of synthesizing nanoparticles from corn and waxy corn starch. The advantages are the mild conditions (slightly acidic environment, elevated temperature not exceeding gelatinization temperature) and the short time of the modification (up to 1 h). Acid hydrolysis, sonication, and combining these methods lead to relatively homogeneous starch nanoparticles with sizes not exceeding 5 nm.

The amylose concentration in corn starch dropped from 12% to a maximum of 5%, and in waxy corn starch, its amount was 3% and lowered to 1.5% after sonication. The amylose content influences the properties of the obtained nano-starch. Amylose-rich corn starch, which is more susceptible to sonication, acid treatment, and combined methods, exhibits significant decreases in the degree of crystallinity (from 37 to 21%), contrary to waxy maize starch (Xc~52-55%). This latter sample is more resistant to cavitation and HCl hydrolysis. Modifying starches decreases their thermal stability, which is the effect of partial chain breaking. Nanoparticles are expected to be more effective for functional food and medical applications to encapsulate active ingredients, facilitating their transport or enhancing their durability, compared to native starch.

References

1. B. Airlangga, A.M. Sugianto, G. Parahita, F. Puspasari, N.E. Mayangsari, P.N. Trisanti, J.P. Sutikno, S. Sumarno, *Journal of the Science of Food and Agriculture*, 101, 6, 537 (2021). <https://doi.org/10.1002/jsfa.10864>.
2. H-Y. Kim, D.J. Park, J-Y. Kim, S.-T. Lim, *Carbohydrate Polymers*, 98, 1 (2013). <https://doi.org/10.1016/j.carbpol.2013.05.085>.
3. D.Bajer, *Food Chemistry*, 402, 134489 (2023) <https://doi.org/10.1016/j.foodchem.2022.134489>

Conceptual framework for the hazard assessment of recycled plastics

R. Becker*, M. Lukas, C. Drago and U. Braun

German Environment Agency (UBA), Berlin, Germany

*Richard.Becker@uba.de

INTRODUCTION

One of the challenges for widespread recycling of plastic products is the complex chemical composition and its implications for human health and the environment. Assessing hazards of recycled plastics is rather difficult since the chemical composition of different plastic products can vary greatly, with more than 16000 chemicals currently annotated¹ in plastics. A common way to assess the toxicological hazards is to either test extracts in bioassays² or derive them from chemicals found in these extracts. In either case the conditions typically used to perform the extraction are at best a worst-case scenario and at worst lead to an unnecessarily high barrier for materials to be deemed recyclable. The precautionary principle justifies the use of worst-case scenarios but the selectivity of the assessment can be increased by using more realistic conditions for migration, similar to how food contact materials are evaluated. The increased selectivity enables a wide spread usage of recycled plastics while not compromising on safety.

In this work a practical approach for the assessment of recycled plastic will be developed based on realistic migration scenarios using recycled plastic granules from different waste streams.

EXPERIMENTAL

Elution

Recycled plastic pellets of different plastic polymers (Polyethylene, Polypropylene, Polyethylene terephthalate and Polystyrene) from relevant waste streams will be eluted with different solvents (water, methanol, isooctane) altering the temperature (from ambient to 70°C) and the elution time (24h to 10 days). The migration behavior to water will further be tested at different pH values.

Chemical analysis

Initially, sum parameters like DOC (dissolved organic carbon), electric conductivity and AOX (absorbable organic halides) along with a metal analysis using inductively coupled plasma optical emission spectrometry (ICP-OES), will be used to evaluate the migration of chemicals during the elution. These results will be linked to different bioassays and single substance analysis by a Liquid chromatography - Mass spectrometry (LC-MS) analysis of the eluates in conjunction with a Pyrolysis - Gas chromatography - Mass spectrometry (Py-GC-MS) analysis of the plastic granules.

Bioassays

Selected bioassays will be used to evaluate the hazards of the eluates and thus of the recycled plastic granules, under the given conditions. To assess general toxicity to aquatic plants an algae growth inhibition assay will be employed. Cytotoxic effects on the organismic level will be monitored via a luminescent bacteria assay and estrogenic effects will be determined using a recombinant reporter gene assays with eukaryotic cells.



Fig. 1 Workflow for the development steps of the framework.

The approach to the investigations can be described by a structured workflow (Fig 1). The individual steps can also be chosen as endpoints for the final framework if they prove to be useful in predicting the hazards of a sample. Each step is evaluated by the following and its conditions can thus be adjusted based on the results.

RESULTS AND DISCUSSION

Identifying representative elution scenarios, that are practical, will be the essential first step to assess the hazards of recycled plastics. These scenarios can be adjusted based on the assumed application of the recycled material and its major constituents, especially the plastic polymer. The selection of suitable endpoints will also depend on both mentioned factors, the assumed application and the material from which the plastic was recycled, and need to initially be thoroughly evaluated and verified by chemical analysis. It aims to identify if organismic tests / sum parameters are sufficient to estimate the hazards of certain plastics or waste streams in a first step. This will enable selecting representative steps as shown in Figure 1 for a flexible assessment tool according to the use case and origin of the material. Through a combination of generalized parameters, we aim to reduce the number of tests needed without compromising on the safety.

Further the results of substance specific chemical analysis will provide information about blind spots which are not covered by selected screening methods. Finally, substance specific bioassays and single substance analysis should connect causality between results from biological and chemical analysis.

We plan to assess the question about the major factors determining the hazards: Do they originate from the known additives (incl. their transformations products), degradation of the polymer matrix or non-intentionally added substances (NIAS)?

Acknowledgment

We thank J. Bartz, M. Gutsche, R. Kochmann, T. Kremer and J.C. Kullwatz (all German Environment Agency) for their laboratory work, as well as the Institut für Kunststoff- und Kreislauftechnik Hannover (IKK) for the provision of the samples. We are thankful for the financing of the project under FKZ 3723653010.

References

1. Wagner, M. *et al.* *State of the Science on Plastic Chemicals - Identifying and Addressing Chemicals and Polymers of Concern*. <https://zenodo.org/doi/10.5281/zenodo.10701706> (2024) doi:10.5281/ZENODO.10701706.
2. Zimmermann, L., Dierkes, G., Ternes, T. A., Völker, C. & Wagner, M. Benchmarking the in Vitro Toxicity and Chemical Composition of Plastic Consumer Products. *Environ. Sci. Technol.* **53**, 11467–11477 (2019).

SUPER-POROUS AND SUPER-SWELLING CHITOSAN-BASED MATRICES FOR WOUND AND BURN TREATMENT

Fátima Díaz-Carrasco, Álvaro Torrecillas-Cortés, Elsa Galbis, M. Gracia García-Martín, M. Violante de-Paz, Elena Benito*

Departamento de Química Orgánica y Farmacéutica, Universidad de Sevilla, C/ Prof. García González, n.º 2, 41012-Sevilla, España.

*ebenito@us.es

INTRODUCTION

Chitosan (CTS) is a natural biopolymer with unique properties, such as its ability to improve healing, bioadhesion, cell permeation and its antimicrobial activity, as well as having excellent properties for use in humans such as biocompatibility and non-toxicity (1). These properties make it an excellent polymer in biomedical applications, however, there are still challenges to address. Thus, the physicochemical and mechanical properties of CTS hydrogels may be limited due to the different interactions within the manufactured hydrogel (2). On the other hand, there is a need to develop CTS hydrogels with rapid swelling and response kinetics, as well as improved mechanical strength, to implement their potential for use in biomedical applications (3).

The main objective of this study is the development of biocompatible materials, with improved properties for burn and wound therapies on the skin and mucous membranes, using CTS as the base polymer. To achieve this, several interpenetrating polymer networks (IPNs) were prepared generating complex 3D structures that enhance the mechanical stability of the material.

Based on the previous results obtained in the FQM-135 research group (4), the use of orthogonal cycloaddition reactions between diamines and bis- and tris(cyclic carbonate)s was proposed for the preparation of such materials.

EXPERIMENTAL

Materials

The reagents used in this work were: chitosan (CTS), 4-vinyl-1,3-dioxolan-2-one (VEC), dithioglycerol, 1,8-diazabicyclo[5.4.0]undec-7-eno (DBU), trimethylolpropane tris(3-mercaptopropionate), 2,2-dimethoxy-2-phenylacetophenone (DMPA) and mucin from porcine stomach (Type III).

Preparation

The synthesis of two crosslinker molecules with two and three cyclocarbonate groups (bis-CC and tris-CC) were carried out by a click thiol-ene reaction employing a procedure previously established for other thiol-ene combinations (4). These reactions were activated using DMPA and UV light ($\lambda = 365$ nm) for 10 min and, subsequently, they were left stirring overnight in the absence of UV light.

A pool of 1st generation IPN was synthesized by varying the concentrations of crosslinker (bis-CC or tris-CC) and CTS, and the AcOH/H₂O ratio (used as solvent). The crosslinker concentrations used were adjusted to react with 10%, 20% and 30% of the amino groups of the CTS. The CTS concentrations used were 2%, 4% and 6% (w/v), while the AcOH/H₂O ratios were 1:1, 1:2 and 1:4 (v/v).

Rheological and physico-chemical characterization

The rheological properties of the formed IPNs were studied, as well as their microstructure, mucoadhesive properties, buoyancy and swelling index, obtaining relevant

information on the relationship between the physicochemical properties of the prepared systems and their possible role in application on skin and mucous membranes.

RESULTS AND DISCUSSION

The systems that were synthesized with 2% CTS, presented a viscous character ($G'_1 < G''_1$), and had liquid behavior (liquid state like fluids). However, as the CTS concentration increased (at 4% and 6%), the elastic character predominated ($G'_1 > G''_1$) in most of the systems (Figure 1), reaching its maximum at 6% CTS. Another observed trend was that in the majority of IPNs, as the crosslinker % increased, the values of G'_1 and G''_1 , increased. Regarding the solvent concentration, no clear trend was observed in the values of G'_1 and G''_1 .

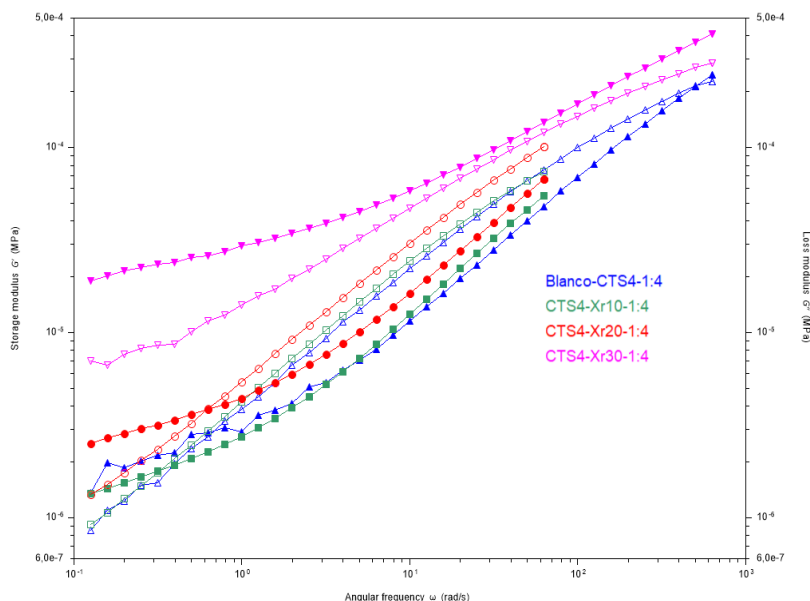


Fig. 1 Frequency sweep of systems at 4% de CTS and AcOH/H₂O 1:4. Filled symbol: G' ; Empty symbol: G'' .

Scanning electron microscopy (SEM) imaging confirmed that the IPNs were highly porous systems. Analysis of the SEM images using the Fiji image processing software revealed that the pore area of the IPNs ranged from 17% to 23%.

The samples demonstrated an exceptional fluid absorption capacity, with swelling indices ranging from 2,200% to 20,000% within 2 hours. This corresponded to a 22- to 200-fold increase in the weight of the lyophilized matrices compared to their original weights. Regarding buoyancy, it was observed that nearly all the systems remained afloat for at least 120 min.

The mucoadhesion tests revealed that all the samples exhibited positive rheological synergy, meaning they were mucoadhesive, albeit with lower adhesion force values compared to those obtained for CTS.

In subsequent studies, factors such as the degree of crosslinker and the viscous elastic character of the systems will be optimized to improve mucoadhesion properties.

Acknowledgment

This research was funded by the Ministerio de Ciencia e Innovación-Agencia Estatal de Investigación (MCIN/AEI/10.13039/501100011033), grant number PID2020-115916GB-I00.

References

- 1) I. Bano, M. Arshad, T. Yasin, M.A. Ghauri, M. Younus, *International Journal of Biological Macromolecules*, **102**, 380, (2017).
- 2) J. Fu, F. Yang, Z. Guo Z, *New Journal of Chemistry*, **42(21)**, 17162, (2018).
- 3) P. Sánchez-Cid, A. Romero, M.J. Díaz, M.-V. de-Paz, V. Perez-Puyana, *Journal of Molecular Liquids*, **379**, 121735, (2023).
- 4) A.I. Carbajo-Gordillo, E. Benito, E. Galbis, R. Grosso, N. Iglesias, C. Valencia, R. Lucas, M.G. García-Martín, M.-V. de-Paz, *Polymers*, **16(7)**, 880, (2024).

CACTUS PEAR BY-PRODUCTS AS FILLERS FOR THE DEVELOPMENT OF BIOCOMPOSITES: REINFORCEMENT OR DEGRADATION EFFECT?

M.C. Mistretta^{1,2}, G. Lamattina^{1,2}, F. Gargano³, G. Liguori³, P. Rizzarelli⁴, P. Scarfato⁵
and L. Botta^{1,2*}

¹Department of Engineering, University of Palermo, Viale delle Scienze, Palermo, Italy

²National Interuniversity Consortium of Materials Science and Technology (INSTM), Florence, Italy

³Department of Agricultural, Food and Forest Sciences, University of Palermo, Viale delle Scienze, Palermo, Italy

⁴Institute of Biomolecular Chemistry – National Research Council (ICB-CNR), Via Paolo Gaifami 18, Catania, Italy

⁵Department of Industrial Engineering, University of Salerno, Via Giovanni Paolo II 132, Fisciano (SA), Italy

* luigi.botta@unipa.it

INTRODUCTION

Food waste is a pressing global issue with significant environmental, economic, and social implications. Fruit processing generates various by-products, including undesired parts such as skins, seeds, and fleshy residues, which can constitute up to 30% of the initial mass of processed fruit. Transforming these by-products into reinforcement materials for polymeric composites is a promising way to valorize fruit waste (1). A natural and sustainable approach involves combining these fillers with biodegradable polymers as matrices. Among the various biopolymeric matrices suitable for this purpose, polylactic acid (PLA) stands out due to its chemical and physical properties, which allow it to replace conventional oil-based polymers in many applications. Additionally, PLA is widely used as a biodegradable polymeric matrix for biocomposites enriched with natural fillers (2).

In this context, the utilization of cactus pear (*Opuntia ficus-indica*) by-products presents a promising avenue. Cactus pear, a widely cultivated cactus, produces fruits with both edible flesh and seeds. The peel, rich in fibers and other bioactive components, along with glochids—tiny spines found on the fruit's surface—are typically discarded as waste. However, these components could serve as valuable natural fillers to enhance the mechanical and sustainable characteristics of polymeric materials.

Our research aims to explore the potential of cactus pear by-products as sustainable fillers in PLA-based biocomposites.

EXPERIMENTAL

Materials

The polymer used as the matrix for producing the biocomposites was a sample of Ingeo™ PLA 4032D, supplied by NatureWorks LLC. The cactus pear by-products (peels and glochids) were kindly provided by a commercial orchard (Garufa) located in Roccapalumba, Palermo, Italy (37°48' N, 13°38' E, 350 m a.s.l). Specifically, the peels were sourced from the processing stages of fruits destined for the fresh-cut industry, while the glochids were collected as a by-product of the mechanical brushing of fruits prior to marketing.

The peel was processed into micrometric particles suitable for incorporation into the biopolymeric matrix through a two-stage procedure: drying and grinding. The glochids, naturally micrometric and oblong in shape, were used as-is, with a selection process via sieving to remove larger lignocellulosic residues, preserving the smaller particles.

Preparation

The biocomposites, at 10% and 20% by weight for both fillers, were prepared using a batch mixer at 190 °C with a mixing speed of 60 rpm for 5 minutes.

Characterization

The prepared materials were characterized morphologically through scanning electron microscopy (SEM), rheologically using frequency sweep tests with a rotational rheometer, mechanically through tensile and dynamic mechanical analysis (DMA), and calorimetrically using differential scanning calorimetry (DSC). Additionally, the intrinsic viscosity $[\eta]$ was measured to evaluate the viscosity average molecular weight (M_v) using the Mark-Houwink equation.

RESULTS AND DISCUSSION

The findings revealed that biocomposites filled with peel particles exhibited reduced viscosity compared to pure PLA, while those with glochids showed higher flow curves than that of PLA (Fig. 1). Furthermore, biocomposites with glochids exhibited an increased elastic modulus proportional to filler content, surpassing both PLA and peel-filled biocomposites.

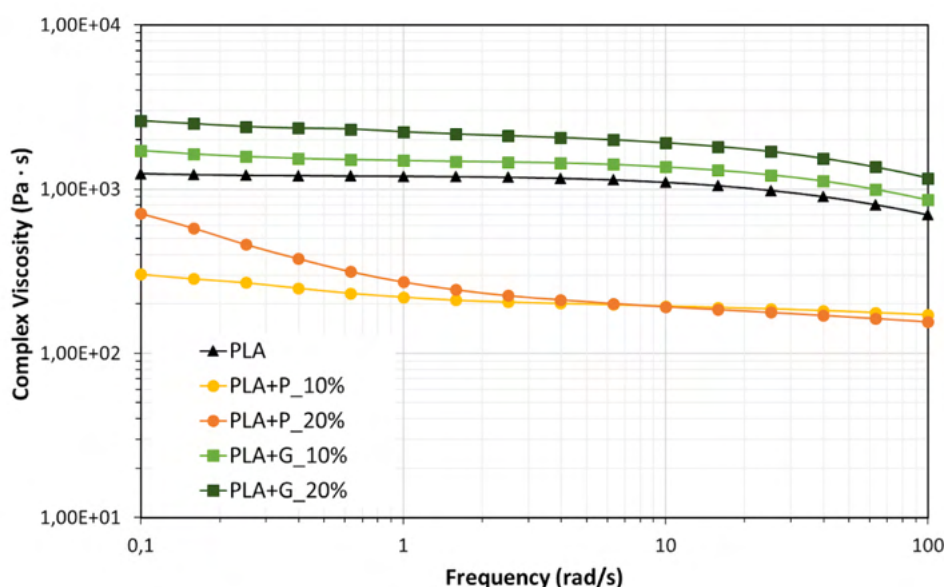


Fig. 1 Complex viscosity as a function of frequency of neat PLA and all biocomposites.

The difference between the two fillers in affecting the properties of filled PLA was attributed to the observed degradation induced by peel, contrasting with the inert nature of glochids. This underscores the potential of glochids as effective reinforcement agents for PLA-based biocomposites, offering promising applications such as food packaging.

Acknowledgment

Funded by the European Union – Next Generation EU - PNRR M4 - C2 -investimento 1.1: Fondo per il Programma Nazionale di Ricerca e Progetti di Rilevante Interesse Nazionale (PRIN) - PRIN 2022PNRR cod. P2022M3FTM_002 dal titolo " SUsustainable routes to high PErformance and Recycling of BIODegradable plastics for a circular economy - SuperBio" CUP B53D23027630001

References

- 1) L. Klaai, D. Hammiche, A. Boukerrou, J. Duchet-Rumeau, J.-F. Gerard, N. Guermazi, *Emergent Mater.*, **5**, 859 (2022).
- 2) A.K. Trivedi, M.K.Gupta, H. Singh, *Adv. Ind. Eng. Polym. Res.*, **6**, 382 (2023).

EFFECT OF ALTERNATING HUMIDITY AND DRYNESS ON THE DURABILITY OF ADSORBENT SHEETS USED IN OPEN-CYCLE ADSORPTION PROCESSES

Luigi Calabrese^{1,2*}, Emanuela Mastronardo¹, E. Piperopoulos¹, G. Scionti¹, Stefano De Antonellis³, Angelo Freni² and C. Milone¹

1 Department of Engineering, University of Messina, Messina, Italy; * lcalabrese@unime.it

2 CNR ICCOM - Institute of Chemistry of Organometallic Compounds, Pisa, Italy

3 Department of Energy, Politecnico di Milano, Milano, Italy

INTRODUCTION

Open-cycle adsorption processes offer an eco-friendly and energy-saving approach for air dehumidification humidification and energy storage [1,2]. However, loose grain adsorbents can degrade due to wear and tear during operation [3]. To address this, several research activities have been addressed toward the development of composite adsorbent materials characterized by improved performance and durability [4].

This study investigates the impact of alternate humid/dry aging tests on the stability of silica gel-based adsorbent sheets designed for open-cycle adsorption processes. These cycles simulate real-world operating conditions. The mechanical strength and water vapor adsorption capacity of the sheets were evaluated before and after aging. The results indicate that the adsorbent sheets exhibit good hydrothermal stability, maintaining their mechanical robustness and adsorption capacity even after undergoing a relevant number of aging cycles. This paves the way for further research to optimize these materials for open-cycle adsorption systems, ultimately enhancing their long-term effectiveness and reliability in this application.

EXPERIMENTAL

The composite adsorbent material is formed by combining silica gel for water absorption, sodium polyacrylate for increased capacity and workability, vinyl glue as a matrix, demineralized water for mixing, and polypropylene fibers for enhancing the composite strength. The material ratio was selected to achieve an optimal balance between mechanical properties and low binder content. After mixing, the slurry settled for 30 minutes. A 2mm layer was spread on a polypropylene board and dried in a preheated oven (45°C for 4 hours, then 75°C for 1 hour) before separating from the board. More details on the preparation, characterization and testing of the adsorbent sheets are presented in [5].

Concerning the accelerated aging tests, a homemade climatic chamber with temperature and humidity control was employed to expose the samples to repeated humid/drying cycles at varying temperatures and humidity to mimic aging system. Samples underwent cycles of humid (25°C, 90% RH, 20 min) and dry (40°C or 50°C, 30% RH, 20 min) conditions, ending with re-hydration (25°C, 90% RH, 20 min). Samples were repeatedly cycled (500-1000 times) for aging evaluation. Before aging, samples were cut and placed in the climatic chamber. Samples were subjected to tensile test at various drying times to assess aging effects (reversible vs irreversible damage). Untreated samples were tested for comparison. Composite samples of dog-bone shape were tested using a universal machine with 5 kN load cell. Drying times up to 7 days at 50% humidity and 22°C were applied to each aging condition (3 replicates, including unaged). Batches were properly coded (drying temperature-cycles-storage days). E.g., '50-1000-2' means dried at 50°C, 1000 cycles, stored 2 days.

RESULTS AND DISCUSSION

Figure 1a shows stress-strain curve changes for the 40-500 batch after humid/dry cycles. Samples (40-500-0, tested immediately) and (40-500-7, stored dry for 7 days) are compared.

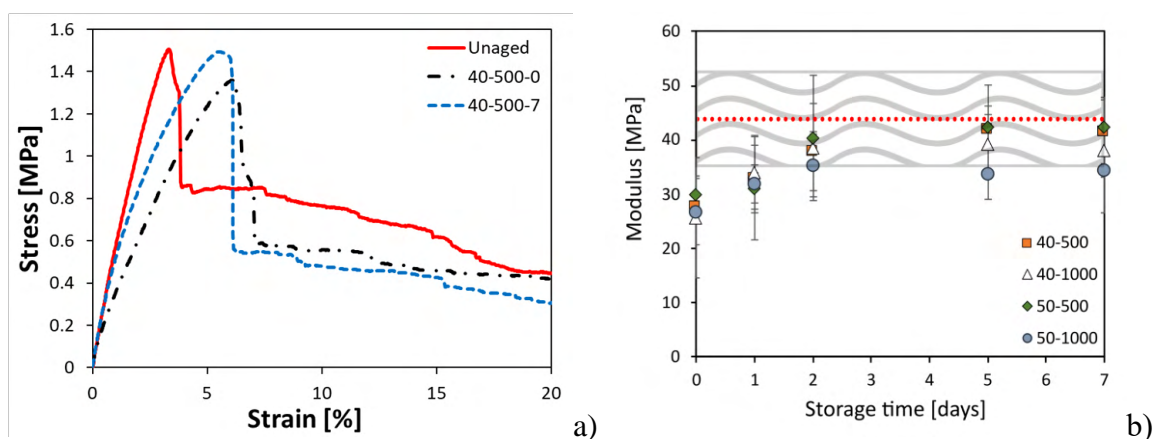


Fig. 1 a) Stress-strain curves after repeated humid/dry cycles and storage phase for 40-500 batch. Unaged sample (solid red line in the plots) was added as reference; b) Evolution of flexural modulus of the composite sheets at varying aging cycles at increasing storage time

The stress-strain curve of the unaged specimen (and others) reveals three zones: i) Elastic Zone: Low strain, linear stress-strain relation - material recovers shape, ii) Strain Hardening: Stress increases with strain until fracture; iii) Post-Fracture: Residual strength remains (about half peak) due to fiber bridging. Furthermore, it was found that humid/dry cycles (40-500-0) weaken adsorbent sheets (9.7% strength loss, +2.8% strain). Considering the hydrophilic nature of the matrix, water exposure likely causes swelling and micro-cracks, reducing strength and stiffness. Aged samples, which exhibited reduced performance in stress-strain testing post humid/dry cycles, notably regained their mechanical properties when stored in a dry environment for 7 days. This suggests that certain aging mechanisms during aging cycles have a reversible impact on composite mechanical properties, possibly due to facilitated water desorption in controlled dry storage conditions.

Analyzing flexural modulus (Figure 1b) across dry storage times reveals how tensile properties change for each batch after humid/dry aging. Samples at zero dry time represent post-aging properties. Unaged material (red line) sets the baseline for degradation/recovery. Modulus properties significantly rebound after aging, suggesting a reversible weakening mechanism. All composites recover most strength within 2 days, approaching unaged one.

This suggests that weakening is caused by reversible degradation factors, while softening is due to lasting changes that irreversibly cannot be regained after removal of critical aging conditions. Future research will validate a map predicting hydrothermal durability of adsorbent composites under humid/dry cycles. Optimization will focus on exposure time to balance reversible and irreversible damage for specific applications.

Acknowledgment

We acknowledge financial support by PRIN 2022 - National Recovery and Resilience Plan (NRRP), Mission 4, Component 2, Investment 1.1, Call for tender No. 104 published on 2.2.2022 by the Italian Ministry of University and Research (MUR), funded by the European Union – NextGenerationEU– Project Title ACE-STES – CUP J53D23002370006

References

- 1) N. Enteria, H. Yoshino, A. Mochida, *Renewable and Sustainable Energy Reviews* **28** 265–289 (2013).
- 2) Y. Zhang, R. Wang, *Energy Storage Materials* **27**, 352-369 (2020)
- 3) L. Calabrese, L. Bonaccorsi, A. Freni, E. Proverbio, *Appl Therm Eng* **124**, 1312–1318 (2017)
- 4) P. Abhishek, V. Baiju, *Desalination* **572**, 117130 (2014).
- 5) S. De Antonellis, E. Bramanti, L. Calabrese., B. Campanella, A. Freni, *Appl Therm Eng* **214**, 118857 (2022)

Study of the degradation of water soluble thermoset polymers based on Aza-Michael addition – Effects of polar/nonpolar characteristics of monomers

F. Cavodeau, J-F. Stumbe and M. Brogly

Laboratoire de Photochimie et d'Ingénierie Macromoléculaires (LPIM), 3b rue Alfred Werner, Mulhouse, France

florian.cavodeau@uha.fr

INTRODUCTION

The study of the durability of thermoset polymers often faces difficulties regarding the end of life. These materials are mostly designed for high mechanical and thermal properties and a will to last as long as possible. An application like structural adhesive systems requires to reach such properties. For this study we decided to focus on crosslinked systems based on Aza-Michael addition presenting a capacity to degrade under humid conditions. Aminoester groups could be sensitive to hydrolysis, leading to the degradation of the polymer. Crosslinked systems were prepared by mixing at room temperature with tri and tetrafunctionnal acrylates. The combination of primary and secondary amines in the same molecule increases the density of the network, and also the mechanical properties of the polymer. A structural study of the hydrolysis was carried out and showed that the breaking of chemical bond was mostly localised between the carbonyl group and the -O- of the ester, leading to carboxylic acids and alcohols. The recyclability of aminoesters was then studied from a completely degraded polymer using a catalysed esterification as a proof of concept.

This work mainly focuses on hydrolysis mechanisms and kinetics of crosslinked Aza-Michael polymers depending on the nature and the polar/nonpolar characteristics of initial monomers. These characteristics have a certain influence on the degradation mechanisms and may tailor the hydrolysis of water soluble polymers. The aim of this study is to determine the recycling capacity of Aza-Michael thermoset polymers from hydrolysis products.

EXPERIMENTAL

Materials

Neopentyl glycol diacrylate (NPGDA) was used as a reference acrylate and mixed with three different amines in bicomponents stoichiometric mixtures for the preparation of Aza-Michael thermoset polymers. The amines are isophorone diamine (IPDA), diethylenetriamine (DETA) and Priamine 1074, synthesized from castor oil. All monomers were purchased from Sigma-Aldrich except Priamine 1074, provided by Croda. Obtained polymers are relatively soft and present Tg between -40°C and 10°C.

Preparation

Thermoset polymers were prepared by mixing NPGDA with one of the amines by respecting a stoichiometry of functions. Around 15 g of mixture was prepared with a SpeedMixer DAC 150.1 FVZ apparatus at 3500 rpm during 3 minutes. A part of the mixture was analyzed by rheology to determine the gel point and the end of reaction. The remaining system was poured into a silicone mould and left to rest until the end of the crosslinking reaction.

Study of the hydrolysis of thermoset polymers

The aging was then carried out with multiple samples of the same mixture and immersed in water at 60°C during two months in order to collect and analyze samples at specific times. The hydrolysis kinetics was followed by measuring mass variation of the sample during aging, water absorption capacity, mass of the sample after drying and mass of extracted species. Structural modifications were followed by IRTF measurements and NMR ¹H. The NMR mostly focused on the analyze of extracted species of water evaporation. For samples presenting an advanced degradation in water, size exclusion chromatography (SEC) was used to determine the sample of the molecules obtained by hydrolysis.

RESULTS AND DISCUSSION

The study helped to understand the influence of some structural parameters on the hydrolysis of Aza-Michael thermoset polymers. As expected, hydrophobic chains slow down water diffusion within the system and the hydrolysis of aminoester functions. More hydrophilic systems present a faster degradation in water, even leading to a complete dissolution of the polymer, even after less than 1 week of aging. The progressive hydrolysis of the polymers led to the formation of smaller molecules with time, which was confirmed by SEC analysis. Hydrolysis indeed led to the formation of alcohols and carboxylic acids functions, which open the possibility for further studies on the recyclability of this kind of thermosets.

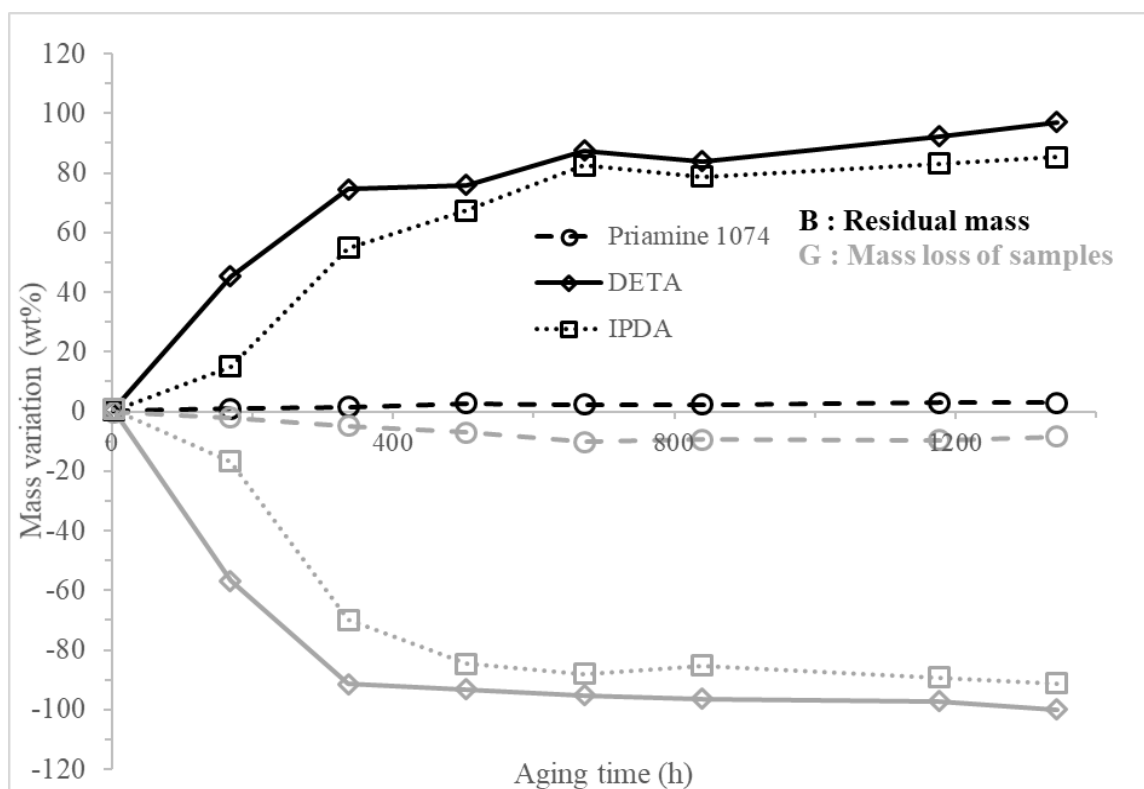


Fig. 1 Mass loss of Aza-Michael thermoset polymers and residual mass measured after water evaporation with aging time in water at 60°C

References

- 1) G. Baschek et al., *Polym.*, **40** (199)
- 2) V. Baukh et al., *Macromol.*, **44**, 4863-4871 (2011)
- 3) P. Gilormini et al., *Polym.*, **142**, 164-169 (2018)

UV aging resistance of modified bitumen: comparison of SBS and Biochar

Clara Celauro^{1a}, Rosalia Teresi^a and Nadka Tz. Dintcheva^a

¹ National Sustainable Mobility Center (Centro Nazionale per la Mobilità Sostenibile—CNMS)

^a Dipartimento di Ingegneria, Università degli Studi di Palermo, Viale delle Scienze, 90128 Palermo, Italy;

INTRODUCTION

The importance of road pavement durability must not be underestimated, as it affects road safety, reduces maintenance costs and environmental impacts. The constant exposure of wearing courses to atmospheric agents such as UV-rays or rain, and traffic-induced stresses, contribute to accelerated wear and deterioration [1,2]. The aging behaviour of the binder used plays a crucial role in the pavement’s durability during its service life. The objective of this study is to investigate the potential of more sustainable additives compared to conventional polymers in enhancing resistance to UV aging. For this purpose, the effect of two different additives (one natural and one synthetic) on the durability of bitumen was studied. Biochar was chosen as the natural additive and styrene-butadiene-styrene (SBS) as the synthetic. The experimental results obtained suggest that biochar has a positive anti-aging effect, though lower than that offered by virgin SBS polymer, and that, for selected applications, it could represent a cost-effective alternative.

EXPERIMENTAL

Materials

In this study, three bitumen binders have been used: a neat bitumen with a 50/70 penetration grade used as base for modification with polymer, and two proprietary polymer modified bitumen (PMB) obtained with it. The first PMB, named LSBS, contains a low concentration of SBS (2-4% w/w), while the second one, named HSBS, had a higher concentration of SBS (6-8% w/w). The general properties of all the binders are summarized in table 1.

For the purpose of this study, a commercial biochar derived from the pyrolysis of birch and beech wood used in the food industry was added to 50/70 penetration grade bitumen. The neat bitumen was modified in the laboratory by adding two different percentages of Biochar using a Silverson high shear mixer: 2% (named 2_BCH), and 10% (named 10_BCH). The mixer was set to 3000 rpm and a temperature of 180°C for 2 hours. For this purpose, both unaged and short-term aged binders were tested, according to the following flow chart shown in figure 1.

Table 1. Properties of the binder investigated.

Characteristics	50 70	LSBS	HSBS	Standard
Penetration at 25°C, pen [0.1*mm]	52.25	50.5	51	EN 1426
Ring and ball softening point, T _{R&B} [°C]	52.6	77.6	88.5	EN 1427
After RTOFT according to EN12607-1				
Penetration at 25°C, pen [0.1*mm]	39.3	36	40	EN 1426
Ring and ball softening point, T _{R&B} [°C]	56	84	91.25	EN 1427

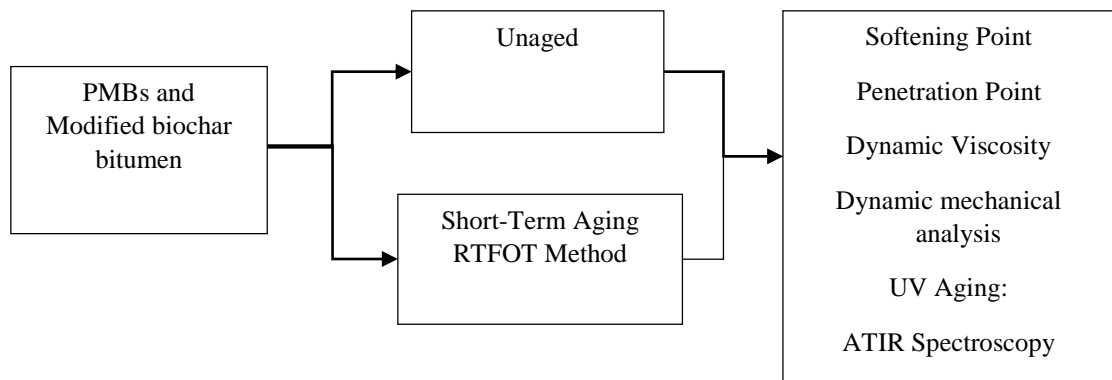


Fig.1 Experiment plan.

RESULTS AND DISCUSSION

In accordance with the literature [3,4], the structural indices of all binders under investigation are calculated as shown in equation 1 and 2.

$$\text{Carbonyl Index} = \frac{\text{Area of the carbonyl band centred at ca.1700 cm}^{-1}}{\text{Area of the CH}_2 \text{ centred at ca.1455 cm}^{-1} + \text{Area of the CH}_3 \text{ band centred at ca.1376 cm}^{-1}} \quad (1)$$

$$\text{Sulfoxide Index} = \frac{\text{Area of the carbonyl band centred at ca.965 cm}^{-1}}{\text{Area of the CH}_2 \text{ centred at ca.1455 cm}^{-1} + \text{Area of the CH}_3 \text{ band centred at ca.1376 cm}^{-1}} \quad (2)$$

The photo-oxidation behaviour of some binders studied was investigated with surface spectroscopic analysis (ATR-FTIR) in unaged condition (0h), and after 24h of artificial UVB aging. Figure 2 illustrates the spectra obtained for neat bitumen, LSBS, HSBS and 10_BCH. After 24 hours of photo-oxidation, the binder without SBS presented a higher degradation than the LSBS and HSBS samples. To better evaluate the photooxidative behaviour of modified bitumen, equation 1 and 2 were used to estimate the evolution of carbonyl and sulfoxide accumulation and the results are shown in Figure 3, along with the error bars for repeated testing.

The increase in both indices, due to the formation of new oxygen groups, suggests that oxidative degradation increases with UV irradiation. As expected, the carbonyl and sulfoxide accumulation of all the samples studied increases with prolonged UVB exposure.

Oxidative stability is improved for SBS modified bitumen compared to those without polymer. In fact, even though the samples containing biochar show a reduction in both indices compared to pure bitumen after 24 hours of photo-oxidation, the PMBs containing SBS, regardless of the percentage added, show a carbonyl index close to that of not photo-oxidized samples. As far as the biochar effect is concerned, a beneficial effect is also noticeable since the carbonyl trend of the neat aged bitumen is reduced of at least the 25% when biochar is added to binder, at different percentages.

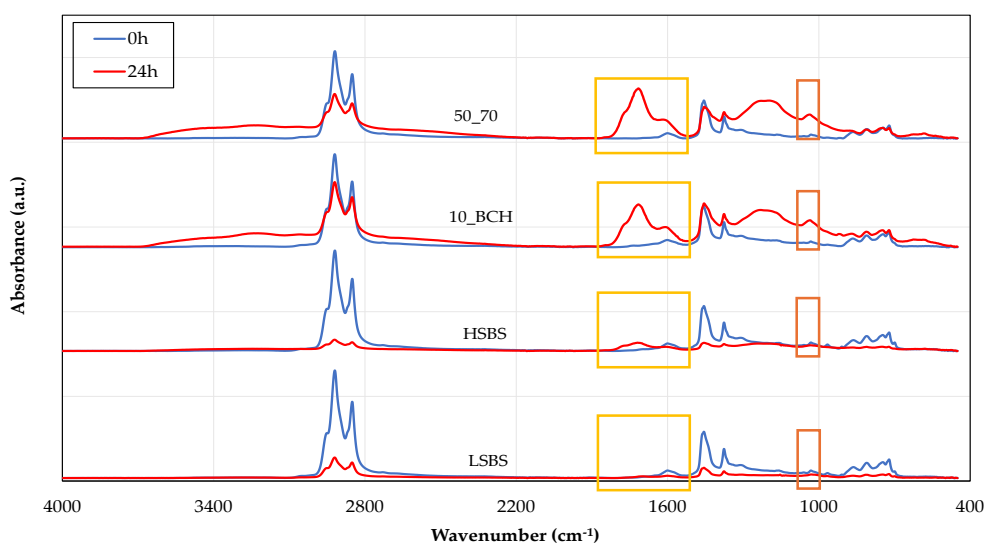


Fig. 2 ATR-FTIR spectra of LSBS, HSBS, neat bitumen and 10_BCH.

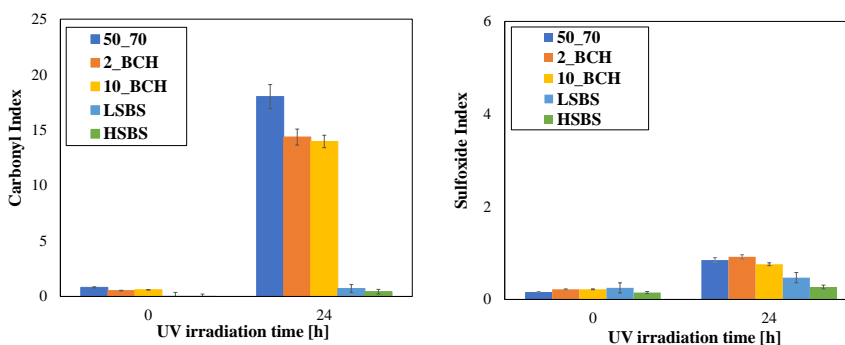


Fig. 3 Carbonyl and Sulfoxide trends of all samples investigated as a function of UVB aging time.

In order to further assess the anti-aging effect induced by the additives selected, the rheological behaviour of all binders was investigated before and after short term aging treatment; the complex modulus as a function of frequency was evaluated and the trends are shown in Figure 4. It is known [5,6] that the bitumen stiffens during the short-term aging process, leading to an increase in the complex modulus trend: specifically, after short-term aging the binder becomes stiffer, and the complex modulus curve is expected to shift towards higher viscosity values in the low frequency range.

It is noteworthy that all the modified binders show minimal alteration after RTFOT aging, when compared to what happens for the neat bitumen. This observation demonstrates that the biochar at low concentration (2% as in Fig. 4b) already has a beneficial effect, as for the addition with SBS (Fig. 4c and 4d). Furthermore, it appears that the positive effect of SBS is more evident when it is incorporated in larger quantities, as evidenced in fig. 4d: HSBS has identical values for complex modulus throughout the frequency range studied, both before and after short-term aging.

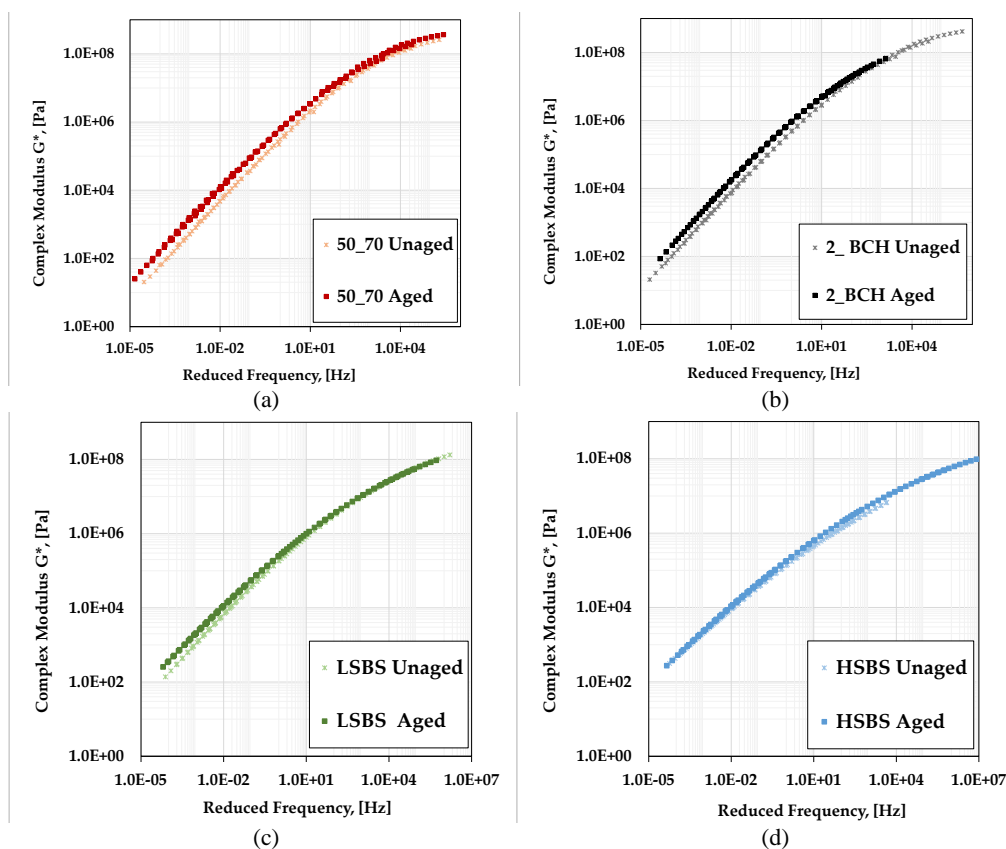


Fig.4 Complex modulus of unaged and short-term aged binders: (a) 50_70, (b) 10_BCH, (c) LSBS and (d) HSBS.

Acknowledgement

This research has been partially supported by the European Union - NextGenerationEU - National Sustainable Mobility Center CN00000023, Italian Ministry of University and Research Decree n. 1033— 17/06/2022, Spoke XX, CUP B73C22000760001

References

1. Chen, Z.; Zhang, H.; Duan, H. Investigation of Ultraviolet Radiation Aging Gradient in Asphalt Binder. *Constr Build Mater* **2020**, *246*, doi:10.1016/j.conbuildmat.2020.118501.
2. Yang, Z.; Zhang, X.; Zhang, Z.; Zou, B.; Zhu, Z.; Lu, G.; Xu, W.; Yu, J.; Yu, H. Effect of Aging on Chemical and Rheological Properties of Bitumen. *Polymers (Basel)* **2018**, *10*, doi:10.3390/polym10121345.
3. Yu, H.; Bai, X.; Qian, G.; Wei, H.; Gong, X.; Jin, J.; Li, Z. Impact of Ultraviolet Radiation on the Aging Properties of SBS-Modified Asphalt Binders. *Polymers (Basel)* **2019**, *11*, doi:10.3390/polym11071111.

4. Azimi Alamdary, Y.; Singh, S.; Baaj, H. Laboratory Simulation of the Impact of Solar Radiation and Moisture on Long-Term Age Conditioning of Asphalt Mixes. *Road Materials and Pavement Design* **2019**, *20*, S521–S532, doi:10.1080/14680629.2019.1587496.
5. McNally, T. *Polymer Modified Bitumen: Properties and Characterisation*; Elsevier.; 2011;
6. Hunter, R.N.; Self, A.; Read, J. *The Shell Bitumen Handbook*; Ice Publishing: London, UK, 2015; Vol. 514;.

INFLUENCE OF A RUBBERY COMPATIBILIZER ON GNPS NANOCOMPOSITES: ANALYSIS ON ISOTROPIC AND ANISOTROPIC SAMPLE

M. Ceraulo, V. Titone¹, M. Baiamonte¹, L. Botta^{1,2}, F. P. La Mantia^{1,2}

¹Department of Engineering, University of Palermo, V. le delle Scienze, 90128 Palermo, Italy

²INSTM, Consortium on Materials Science and Technology, via G. Giusti 9, 50125 Florence, Italy

INTRODUCTION

In recent years, nanocomposites have attracted great interest in both academia and industry because of the versatile that make them suitable for many applications.

In this respect, in this work, graphene nanocomposites (GNPs) were prepared with and without compatibilizer using a laboratory mixer. The aim of this study is to investigate influence on the elongation flow of these nanocomposites, which utilize an immiscible blend of polypropylene (PP) and polyethylene terephthalate (PET) as their matrix. More specifically, our objective was to understand whether the presence of the compatibilizer affects the fibrillation efficiency of the dispersed PET phase. To this end, the mechanical and morphological properties of melt-spun fibers obtained with different hot elongation ratios were analysed and compared with isotropic samples.

EXPERIMENTAL

Materials

- Polypropylene (PP) with the trade name Moplen RP340H was purchased by LyondellBasell (LyondellBasell, Ferrara, Italy). It is a random polypropylene copolymer having a melt flow index (MFI) of 1.8 g/10min (230 °C/2.16 kg) and a density of 0.90 g/cm³;
- Polyethylene terephthalate (PET) was obtained by grinding preforms for water bottles;
- KratonTM under the trade name KratonTM FG1901 G was supplied from North America as a dusted pellet. Is a clear, linear triblock copolymer based on styrene and ethylene/butylene with a polystyrene content of 30%.
- Graphene nanoplatelets (GNPs) under the trade name xGNP®, grade C, were supplied XG Sciences Inc (Lansing, MI, USA) with the following characteristics reported in previously paper [1]: average diameter between 1 and 2 µm; an average thickness lower than 2 nm; a specific surface area of about 750 m²/g;

Preparation

The nanocomposites were prepared by melt mixer in a Brabender mixer mod. PLE330 (Germany) operating at 270 °C at 60 rpm for 5 min. Before blending, both PET and GNPs were dried in a vacuum oven at 120 °C overnight.

Rheological and physics-chemical characterization

The rheological characterization in shear flow was conducted using a rotational rheometer ARES G2 (TA Instruments, USA). The experiments were carried out at 270 °C over a range of angular frequency from 100 to 0.1 rad/s. Furthermore, high shear flow curves were obtained using a capillary viscometer (Rheologic 1000, CEAST) with the same

temperature. Non-isothermal elongational flow tests were performed using the same instrument. A drawing module consisting of a series of pulleys was used to grab the hot filament, which gradually cooled in the air, and deliver it to an end pulley rotating at a constant speed. The melt strength (MS) was directly measured. The breaking stretching ratio (BSR) was calculated as the ratio between the drawing speed at break and the extrusion speed at the die.

Tensile tests were carried out on an Instron universal testing machine (Instron, UK). The drawing ratio (DR) was calculated as follows:

$$DR = D_0^2/D_F^2$$

where D_0 represents the capillary diameter and D_F signifies the diameter of the fibers.

RESULTS AND DISCUSSION

Elongation at break versus draw ratio is shown in Figure 1.

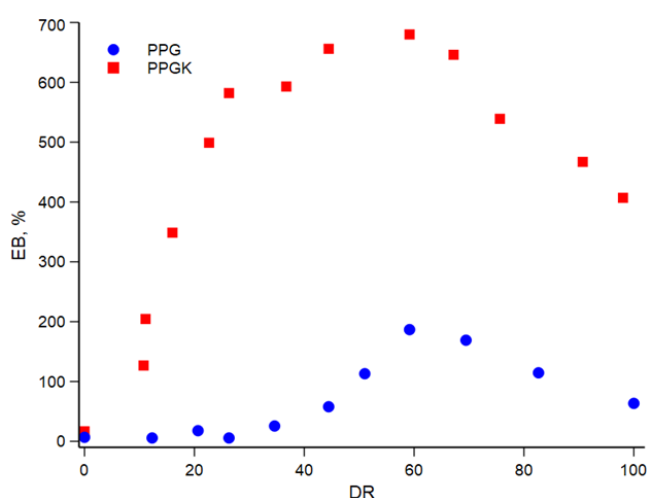


Fig. 1 Elongation at break (EB) versus draw ratio (DR).

From Figure 1, it can be seen that the elongation at break first increases with the draw ratio, reaches the maximum and then starts to decrease. This behavior can be interpreted by many factors such as: morphology ordered, absence of defects and the large contact area between the matrix and the PET fibrils which reduces the impact of poor adhesion. However, once a certain ratio of elongation, the decrease in elongation at break is probably due to the better orientation of the matrix, which makes the sample more brittle.

Interesting results from a rheological point of view were obtained, not reported for brevity.

References

- 1) F.P. La Mantia, V. Titone, A. Milazzo, M. Ceraulo, L. Botta, Morphology, Rheological and Mechanical Properties of Isotropic and Anisotropic PP/rPET/GnP Nanocomposite Samples. *Nanomaterials* 2021, 11, 3058, doi:10.3390/nano11113058.
- 2) V. Titone, M. Baiamonte, M. Ceraulo, L. Botta, F.P. la Mantia, Analysis on Isotropic and Anisotropic Sample of Polypropylene/Polyethyleneterephthalate Blend/Graphene Nanoplatelets Nanocomposites: Effects of Rubbery Compatibilizer, *Polymers* 2024

MULTIFUNCTIONAL 3D-PRINTED COMPOSITES BASED ON BIOPOLYMERIC MATRICES AND TOMATO PLANT (*SOLANUM LYCOPERSICUM*) WASTE FOR CONTEXTUAL FERTILIZER RELEASE AND CU(II) IONS REMOVAL

M.C. Citarrella¹, E.F. Gulino¹ and Roberto Scaffaro¹

¹ Department of Engineering, University of Palermo, Viale delle Scienze, ed. 6, 90128 Palermo, PA, Italy

² INSTM, Consortium for Materials Science and Technology, Via Giusti 9, 50125 Florence, Italy

INTRODUCTION

The production of tomatoes faces significant challenges, including the high amount of waste generated during the harvest stage and copper-contaminated soil due to pesticide use. To address these issues and to promote a more sustainable agriculture, innovative biodegradable green composites for contextual controlled soil fertilization and Cu removal were produced by 3D-printing technology. These composites were made by incorporating NPK fertilizer flour and tomato plant waste particles (SLP) into three different biodegradable polymeric matrices: polylactic acid (PLA); a commercial blend of biodegradable co-polyesters (Mater-Bi®, MB) and their blend (MB/PLA, 50:50). Rheological characterization suggested the potential processability of all of the composites by FDM. Morphological analysis of printed samples confirmed the good dispersion of both filler and fertilizer, which also acted as reinforcement for MB and MB/PLA composites. SLP and NPK moduli were evaluated by powder nanoindentation and, for almost composites, the theoretical Halpin-Tsai model satisfactorily fitted the actual tensile moduli. The decrease in NPK fertilizer release rate and the increase in Cu(II) removal efficiency were achieved using whole 3D-printed composites. By selecting the appropriate matrix and incorporating SLP particles, it was possible to tune the NPK release rate and achieve copper absorption efficiency. Notably, MB samples containing SLP particles displayed the fastest release and the highest Cu(II) removal efficiency.

EXPERIMENTAL

Materials

Mater-Bi® EF51L and PLA 2003D were used, both neat and in combination, to prepare green composites. *Solanum lycopersicum* plant waste (SLP) was generously provided by a local farm (Palermo, Italy). NPK fertilizer (12-12-17) purchased from Flortis, Orvital S.p.A., was used.

Preparation

Nine different formulations were prepared. An internal mixer was used to melt mix 10% of SLP and (or) 10% of NPK to all the selected matrices. The obtained formulations were then extruded. A conveyor belt system was used to draw the output extrudate aiming to obtain filaments with a diameter of ~ 1.75 mm.

Characterizations

Morphological analysis was performed before and after NPK release through scanning electron microscope (SEM). Mechanical performance of the samples was investigated by tensile tests. The elastic modulus of SLP and NPK particles were tested using a nanoindenter. Differential scanning calorimetry (DSC) analysis was performed.

Release of NPK fertilizer and Cu(II) removal

Electrolyte resistance of the obtained solution was evaluated through electrochemical impedance spectroscopy (EIS). The metal ion adsorption capability was assessed by using UV/vis spectrophotometer.

RESULTS AND DISCUSSION

All the obtained filaments were successfully printed by FDM, in agreement with morphological analysis and rheological characterization. Morphological analysis performed on the cross section of 3D printed composite samples confirmed a relatively uniform dispersion of both natural filler and fertilizer in all composite samples. Moreover, MB and MB/PLA samples displayed good adhesion between the fillers and the matrix, unlike PLA ones where imperfect adhesion was observed. NPK release tests showed the ability of all the obtained composites to slow the release rate of the fertilization up to 30 days. Moreover, it was possible to tune the release kinetics by changing the polymeric matrix and adding the natural filler (SLP). Cu(II) removal tests confirmed that all the green composites exhibited a significant increment in the removal efficiency over the neat matrices. More in detail, the Cu removal efficiency could be increased by adding SPL particles that, as expected, have been very successful in absorbing copper. MB-SLP-NPK showed 100% release of NPK after 30 days and the highest copper removal ability with 78% of Cu removed from the aqueous solution (Figure 1).

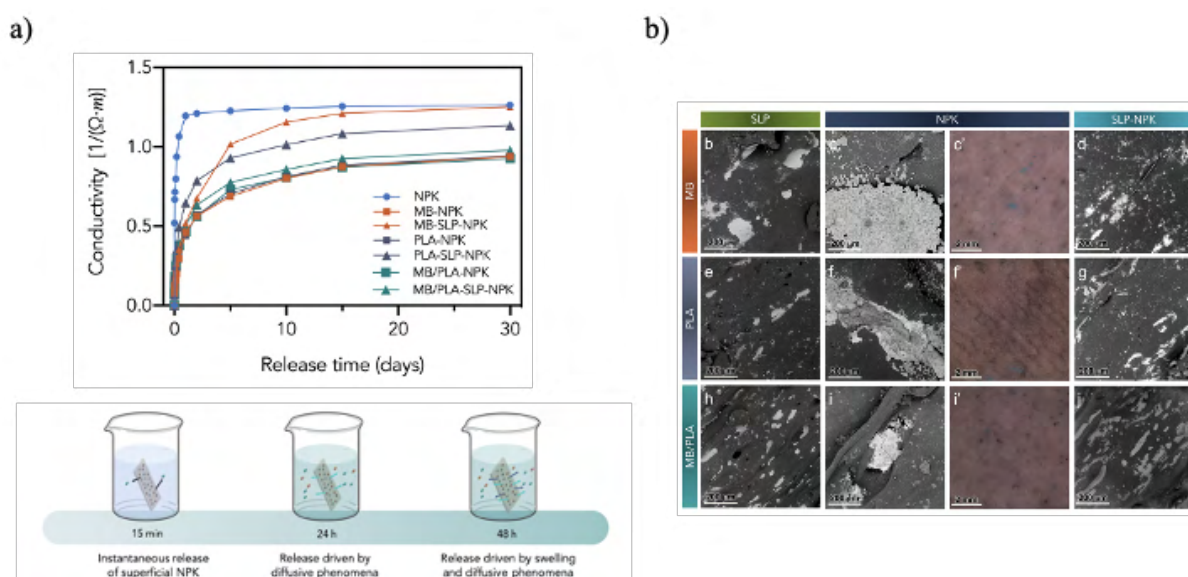


Figure 1. NPK release (a) and Cu(II) (b) removal of bio-composite.

Acknowledgment

PRIN: Green composites based on biodegradable polymers and vegetal biomasses of Mediterranean area: processing, characterization and degradability - Bando 2022 - Prot. 20228WNZ2Z.

References

- 1) Scaffaro R, Citarrella MC, Catania A, Settanni L (2022) Green composites based on biodegradable polymers and anchovy (*Engraulis Encrasicolus*) waste suitable for 3D printing applications. *Compos Sci Technol* 230:109768. <https://doi.org/10.1016/J.COMPSCITECH.2022.109768>
- 2) Scaffaro R, Citarrella MC, Gulino EF (2022) Opuntia Ficus Indica based green composites for NPK fertilizer controlled release produced by compression molding and fused deposition modeling. *Compos Part Appl Sci Manuf* 159:107030. <https://doi.org/10.1016/J.COMPOSITESA.2022.107030>

Bio-based Polymer Recycling for Food Contact: an approach of food security

R. Paiva¹, M. Aznar², M. Wrona², A.P. Lima Batista¹, C. Nerín² and S.A. Cruz^{1*}

¹Chemistry Department, Center for Exact Sciences, Federal University of Sao Carlos (UFSCar), Brazil *sandra.cruz@ufscar.br (S. A. Cruz), ²Department of Analytical Chemistry, Aragon Institute of Engineering Research I3A, CPS-University of Zaragoza, Spain

INTRODUCTION

The European Commission has issued new directives to minimize environmental impact, foster a culture of environmental responsibility, and advance the circular economy. These directives aim to reduce reliance on non-renewable resources for single-use packaging, ultimately replacing them with renewable materials. They also promote the use of recycled raw materials and biodegradable bio-based polymers in plastic packaging. In this work it was studied PLA bio-based polymer recycling, analyzing the three stages of the recycling cycle: (i) post-consumer packaging material using the FDA contamination protocol, (ii) washing process, and (iii) mechanical recycling. Unlike previous studies, this research provides a comprehensive approach to recycling bio-based polymers. The efficiency of recycling in decontaminating these materials was evaluated through migration tests in different simulants and the dissolution of pellets after the process. Contaminants were analyzed using the SPME-GC-MS technique. An in-depth evaluation of Hansen's solubility parameters and theoretical methodologies was used to assess the molecular volume and interaction energy between contaminants and PLA monomeric structures.

EXPERIMENTAL

Materials

For the FDA contamination protocol were used benzophenone, tetracosane, toluene, heptane, and chloroform. Sodium hydroxide and Triton X-100 were used for washing. Furthermore, ethanol HPLC grade and acetic acid were used to prepare food simulants with ultrapure water. The commercial bio-based polymer used in this work was PLA Ingeo 4043D, supplied by NatureWorks.

Preparation

The sample preparation was divided into three stages. First, PLA pellets underwent a forced contamination protocol (Stage 1) as per the USFDA (2006). Next, the contaminated pellets were washed (Stage 2) following the parameters set by Paiva et al. Finally, the pellets were mechanically recycled (Stage 3) using a Thermo Scientific Process 11 Parallel Twin-Screw Extruder at 200°C, with a co-rotation speed of 400 rpm and a feed rate of 3%.

Total dissolution, migration tests and analysis by SPME-GC-MS

PLA pellets were dissolved in dichloromethane in an ultrasonic bath for 1 hour, then mixed with ethanol and centrifuged. The mixture was filtered through a 0.25 µm PET filter. PLA films underwent migration tests to measure surrogate transfer to food simulants at different recycling stages. Simulants used were ethanol 10% (v/v) and acetic acid 3% (v/v) under conditions of 10 days at 40°C and 60°C. Contaminants from both total dissolution and migration tests were extracted using SPME and analyzed via GC-MS.

Theoretical Methodology

Electronic structure calculations, theoretical computational methods and the solubility model proposed by Hansen were used to discuss the polymer-solvent/non-solvent interaction. The structure of each system, heptane, chloroform, benzophenone, toluene, tetracosane, and PLA monomer was optimized at the GFN2-XTB method, as implemented in the ORCA program. All structures were confirmed as a minimum in the explored potential energy surface.

RESULTS AND DISCUSSION

Figure 1a illustrates the concentration of contaminants in PLA pellets before and after each stage of the recycling cycle. The recycling process proved efficient in decontaminating PLA samples, with each stage significantly reducing contaminant concentrations. The mechanical recycling step was more effective than the washing step, showing values above 60%. However, the combination of both steps (PLAcwr) was more effective than each individual step, as certain surrogates were more significantly decontaminated in one step than the other.

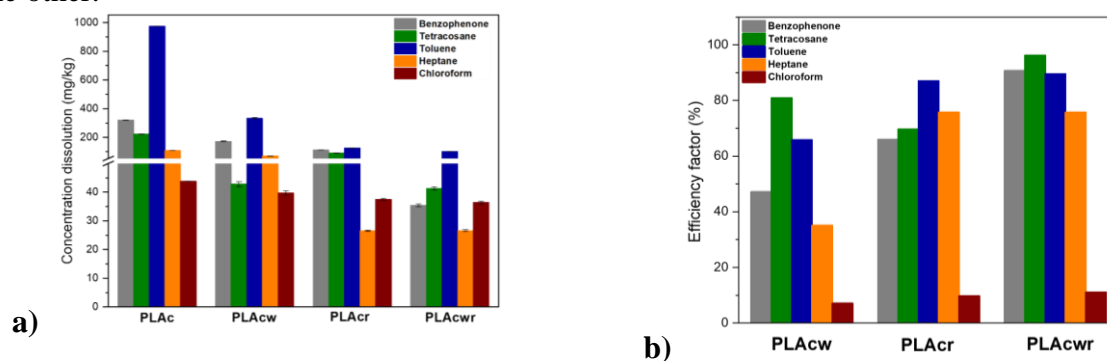


Figure 1: a) Contaminants concentration for the samples and, b) efficiency factor for PLA decontamination.

Factors such as the theoretical molecular volume of the contaminants, the type of food simulants used, the test temperature, and the interactions between polymers and surrogates influence the migration of contaminants. Interaction energy values estimated from electronic structure calculations are crucial for predicting and analyzing overall interaction trends between contaminant molecules and polymers. Notably, there is a strong consistency between the results from Hansen's sphere analysis and those derived from the theoretical approach.

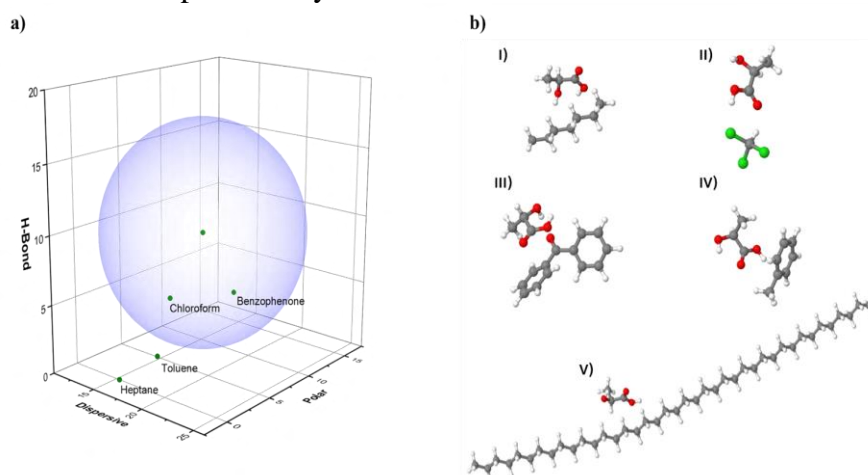


Figure 3: a) Sphere and solubility parameter components of contaminants, and b) the lowest energy aggregates formed between PLA monomer and each molecular contaminants I) heptane, II) chloroform, III) benzophenone, IV) toluene and V) tetracosane.

Acknowledgment

The authors acknowledge financial support from CAPES (Finance Code 001), CNPq (200096/2022-2), FAPESP (Grants 2021/08224-1 and 2022/12043-5), the Government of Aragon, and the European Social Fund (T-53-20R) for the GUIA Group.

References

- 1 Commission, E.; Sheet, F. Single-Use Plastics: New EU Rules to Reduce Marine Litter. **2018**, No. May
- 2 US Food and Drugs Administration (FDA). Guidance for Industry: Use of Recycled Plastics in Food Packaging (Chemistry Considerations). **2021**, No. December 1992, 1–13.

Enhancement of biodegradable food packaging films by coextrusion of PBS, PBSA and Nano-Composite PHB systems

Francesco Palmieri¹, Joseph Nii Ayi Tagoe², Luciano Di Maio¹

¹Department of Industrial Engineering, University of Salerno, Fisciano, SA, Italy

²Department of Chemistry and Biology "A. Zambelli", University of Salerno, Fisciano, SA, Italy

INTRODUCTION

Biobased and biodegradable plastics have emerged as promising alternatives to conventional plastics offering the potential to reduce environmental impacts while promoting sustainability. This study focuses on the production of multilayer blown films with enhanced functional properties suitable for food packaging applications. Films were developed through co-extrusion in a three-layer film configuration, with Polybutylene Succinate (PBS) and Polybutylene Succinate Adipate (PBSA) as the external and internal layers, respectively. The functional layer consisted of Polyhydroxybutyrate (PHB) enhanced with nanoclays Cloisite® 30B at varying weight ratios. Films were also processed by manipulating the extruder screw speed of the functional layer to investigate its impact on the functional properties. Rheology, mechanical strength, and barrier performance were characterized to establish correlations between processing conditions and functional layer blends (Cloisite® 30B/PHB) on the properties of the resultant films.

EXPERIMENTAL

Materials

In this study Pellets of bio-PBS grade FZ91PM (Density = 1.26 g/cm³, T_m = 115 °C) and bio-PBSA grade FD92PM (Density = 1.24 g/cm³, T_m = 84 °C) were supplied by PTT MCC Biochem (Chatuchak, Bangkok, Thailand). PHB grade Y3000P (Density = 1.25 g/cm³, T_m = 175-180 °C) was supplied by Tianan-ENMAT™ while Cloisite® 30B (C30B) Nanoclay provided by Southern Clay Products, Inc. (St. Louisville, KY, USA), with a basal interlayer spacing equal to d₀₀₁ = 18.5 Å and organically modified by methyl, tallow, bis-2-hydroxyethyl quaternary ammonium chloride, was used as nanofiller.

Preparation of the nanocomposites

The nanocomposite blends were prepared as follows: dry blends of PHB pellets and C30B powder were prepared according to the nomenclature and compositions reported in Table 1; the dry blends were then vacuum - dried at 80 °C overnight. The mixture was compounded by means of a co-rotating Collin ZK25 twin-screw extruder (D = 25 mm, L/D = 42) at a screw speed of 250 rpm with a thermal profile between 110 °C and 170 °C. The extruded blend filament was pelletized in a SCHEER SGS 25-E4 lab pelletizer.

Preparation of the films

Pellets of virgin polymers along with nanocomposite blends were vacuum-dried for 16 h at 80 °C before being film-blown using a laboratory co-extrusion blown film apparatus equipped with Gimac three single-screw extruders (D_{screw} = 12 mm, L = 24 D) and a take-up/cooling system (Collin Film Blowing Line Type BL 50). Three-layer films were produced with PBS and PBSA as the external and internal layers, respectively, with PHB0, PHB2, and PHB5 sandwiched as the functional layer. The films were processed at constant extruder screw speeds of 50 rpm for the internal and external layers, whereas the screw speed of the extruder for the functional layer ranged from 30 to 60 rpm.

Mixture	PHB content [% w/w]	Cloisite® 30B content [% w/w]
PHB0	100	0
PHB2	98	2
PHB5	95	5

Table1. PHB/Cloisite® 30B blend composition.

Rheological and Oxygen barrier characterization

Dynamic shear rheological experiments were performed out with an ARES rotational rheometer. Tests were performed with parallel-plate geometry ($d=25$ mm), at 180°C .

Oxygen permeability tests were performed by GTT gas apparatus (Brugger, München Germany) at 23°C and 25% R.H., with the oxygen flow rate of 80 mL/min, according to the ASTM D1434 procedure.

RESULTS AND DISCUSSION

From the graph illustrating complex viscosity versus angular frequency (Figure 1), the curve for the complex viscosity of PBS, throughout the analyzed frequency range, appears to be superimposable on the curve of PBSA pointing out that despite PBSA being a copolymer with a slightly distinct chemical structure, this may not significantly impact the rheological behavior. The viscosity values of (unprocessed) neat PHB are found to be lower than those for PBS and PBSA. PHB pellets subjected to an extrusion cycle show a marked decrease in the complex viscosity values, however, the flow curve retains the same trend as that for neat PHB. PHB2 shows no noticeable difference if compared to the neat PHB polymer. On the contrary, PHB5 shows a higher complex viscosity than that of PHB0 and PHB2 throughout the analysed frequency range. Additionally, it exhibits a more pronounced shear thinning behaviour, with significant reduction of the Newtonian plateau. The increased viscosity at higher concentrations of nanoclay proves the development of the intercalated/exfoliated structure of Cloisite 30B which hinders the flow of polymer chains.

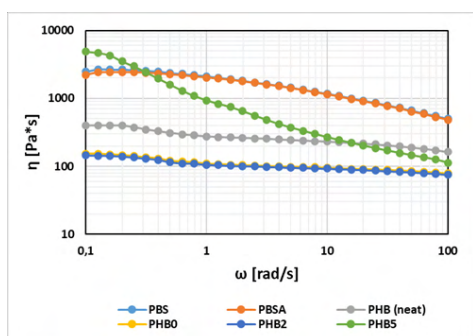


Figure 1. Complex viscosity (η^*) against angular frequency (ω).

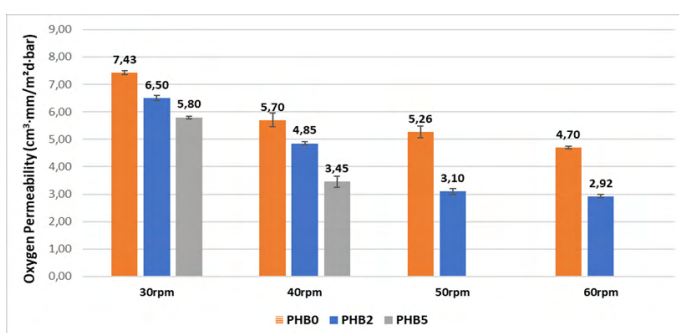


Figure 2. Oxygen permeability of multilayers films at different screw speed for functional layer.

The results of the oxygen permeability tests performed on the multilayer films are shown in Figure 2. For the same percentage of nanoclays, increasing the thickness of the nanocomposite layer a progressive decrease in oxygen permeability was observed; for example, the PHB2 multilayer films show values from 6.50 to 2.92 ($\text{mm}\cdot\text{cm}^3/(\text{m}^2\cdot\text{d}\cdot\text{bar})$), which corresponds to a percentage decrease of 55%. Similar trends can be observed as the amount of Cloisite content increases. It is worthy to point out that even if in general with the increase of a film thickness a decrease of gas transmission rate is normally achieved, in this case the results show that also the permeability coefficient of multilayers systems decreases. This is due to the positive effect given by the increase in the overall amount of nanoclay in the films as the thickness of the functionalized layer increases.

IMPROVING THE STABILITY OF GUAR GUM-BASED HYDROGELS

**Fátima Díaz-Carrasco, M.-Violante de-Paz, M.-Gracia García-Martín and
Elena Benito***

Departamento de Química Orgánica y Farmacéutica, Universidad de Sevilla, C/ Prof. García González, n.º 2, 41012-Sevilla, España.

*ebenito@us.es

INTRODUCTION

Guar gum (GG), a polysaccharide extracted from the seeds of *Cyamopsis tetragonoloba*, has gained significant attention for its potential biomedical applications [1]. GG is known to form thick, viscous solutions in water due to its ability to form hydrogen bonds, which contributes to its mucoadhesive characteristics [2]. However, the stability of such hydrogels are scant as was inferred from previous works [1,3].

In this work, we investigate the stability of guar gum (GG) hydrogels over time and temperature. Furthermore, we summarize the preparation and rheological studies of stabilized GG-based semi-interpenetrating polymer networks (semi-IPNs), which provide structural stability to GG hydrogels, a property of great importance for their potential use in biomedical and pharmaceutical fields [1,4].

EXPERIMENTAL

Materials

The chemicals used in this work were acquired from the supplier Sigma-Aldrich (Madrid, Spain): guar gum (GG), furfuryl isocyanate, dibutyltin dilaurate, and D-ribo-1,4-lactone. All products were used as received.

Preparation

The monomers difurfuryl derivative of L-tartaramide (MT) and 1,8-dimaleimide-3,6-dioxaoctane (DMDOO) were prepared according to the procedure established by Ma and Davies [5] and Galbis et al. [6], respectively. The crosslinker 2,3,5-tri-*O*-[(furan-2-ylmethyl)carbamoyl]-D-ribo-1,4-lactone (Tri-Fur) was synthesized as recorded next: A round-bottom flask charged with 0.5 g of D-ribo-1,4-lactone (3.37 mmol) was subjected to 3 vacuum/argon cycles, and 1.7 mL of dry tetrahydrofuran (THF) was added to give a solution. Subsequently, 1.14 mL of furfuryl isocyanate (10.61 mmol) and a drop of dibutyltin dilaurate as a catalyst were added. The mixture was stirred at room temperature for 5 hours, and then, the solvent was evaporated. The resulting residue was purified by column chromatography (EtOAc-Hex 1:2 → EtOAc-Hex 1:1). The crosslinker (Tri-Fur) was obtained as an orange wax (1.38 g, yield: 79.2%).

Two third-generation interpenetrating polymer networks (IPNs) were prepared, formed from two polymers in a 1:1 relative proportion and a 4% w/w concentration, where polymer 1 was synthesized from the monomers MT and DMDOO and the crosslinking agent Tri-Fur, while polymer 2 was guar gum (GG), a biocompatible polymer of great interest. The two IPNs systems varied in the degree of crosslinking of polymer 1 (4% or 10% crosslinking degree).

Rheological and physicochemical characterization

The rheological properties of the GG-X_{r10} and GG-X_{r4} IPNs were studied using strain sweeps as well as frequency sweeps (at a constant strain value within the linear viscoelastic region) to obtain significant rheological parameters of the samples. The relative stability of the samples over time and temperature was studied at constant frequency and strain values and compared with GG blank hydrogels.

RESULTS AND DISCUSSION

The stability of the GG blank hydrogel (4%) was studied by monitoring the evolution of the elastic modulus (G') and viscous modulus (G'') over time for 7 days after its preparation. It is important to highlight that systems containing only GG were unstable and deconstructed after a few days, what could be verified even with the naked eye. In the frequency sweeps shown in Figure 1a, a substantial drop in both the elastic modulus and the viscous modulus of the hydrogel can be observed over the course of days, until its complete deconstruction. However, the IPNs retained their gel structure for an extended period of time (Figure 1b). Additional thermal stability assays were conducted at constant frequency and strain values, with comparative tests at 25 °C, 37 °C and ramp of temperature from 25 °C to 70 °C and vice versa.

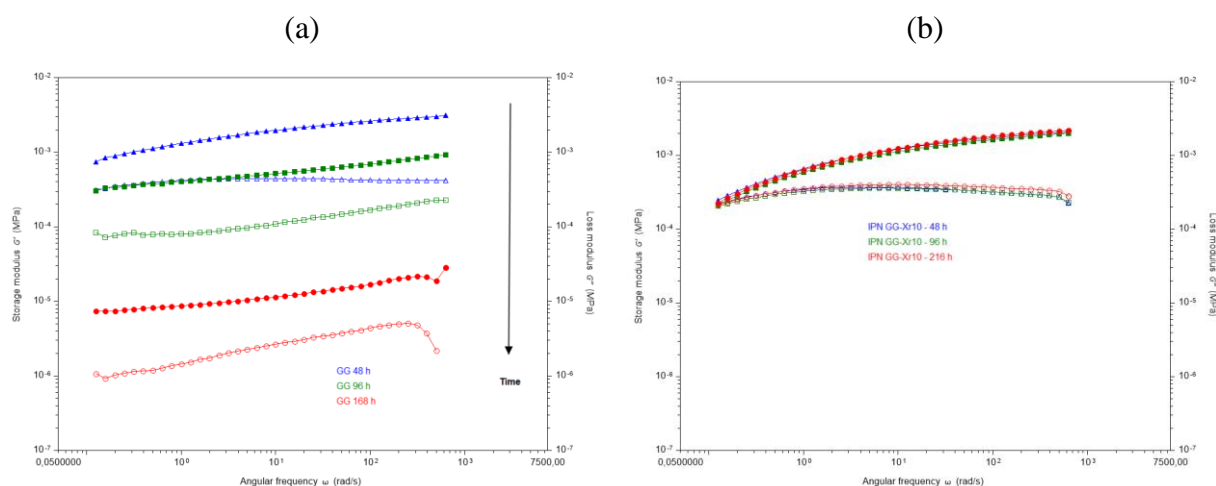


Figure 1. Evolution of G' and G'' of (a) 4% guar gum blanks and (b) IPN GG-Xr₁₀ over time. Solid symbols (G'), empty symbols (G'').

We have demonstrated the inherent instability of GG hydrogels, and how the incorporation of a synthetic polymer to form semi-IPNs with GG was found to significantly enhance the structural stability of the hydrogels, preserving their gel-like properties for months. The semi-IPN approach provides a promising strategy to improve GG-based hydrogels stability, which is a critical property for their potential use in biomedical and pharmaceutical applications.

Acknowledgment

This research was funded by the Ministerio de Ciencia e Innovación-Agencia Estatal de Investigación (MCIN/AEI/10.13039/501100011033), grant number PID2020-115916GB-I00.

References

- [1] R. Grosso, E. Benito, A.I. Carbajo-Gordillo, M.G. García-Martín, V. Perez-Puyana, P. Sánchez-Cid, M.-V. De-Paz, *International Journal of Molecular Sciences*, **24**, 2281 (2023).
- [2] M.L. Amin, T. Ahmed, M.A. Mannan, *Advanced Pharmaceutical Bulletin*, **6**, 195 (2016).
- [3] R. Grosso, E. Benito, A.I. Carbajo-Gordillo, M.J. Díaz, M.-G. García-Martín, M.-V. de-Paz, *European Journal of Pharmaceutical Sciences*, In press (2024).
- [4] P. Sánchez-Cid, A. Romero, M.J. Díaz, M. V. De-Paz, V. Perez-Puyana, *Journal of Molecular Liquids*, **379**, 121735 (2023).
- [5] X. Ma, R.P. Davies, *Tartramide Ligands for Copper-Catalyzed N-Arylation at Room Temperature*, *Advanced Synthesis and Catalysis*, **364**, 2023 (2022).
- [6] E. Galbis, M. V de Paz, K.L. McGuinness, M. Angulo, C. Valencia, J.A. Galbis, *Polymer Chemistry*, **5**, 5391–5402 (2014).

ASSESSING THE PERCOLATION THRESHOLD IN PLA/KENAF BIOCOMPOSITES FOR BIODEGRADATION PURPOSES

G. Filippone

Dipartimento di Ingegneria Chimica, dei Materiali e della Produzione Industriale, Piazzale Tecchio 80, 80125 Napoli, Italy
gfilippo@unina.it

INTRODUCTION

Biodegradable polymer composites with natural fibers are popular for their eco-friendliness. Achieving controlled biodegradation is crucial. In biopolyesters, biodegradation depends on environmental conditions (acidity and enzymatic activity) and typically starts with the hydrolysis of polyester ester groups. The inherent hygroscopic feature of natural fibers may facilitate water absorption enhancing biodegradation. In addition, poor fiber-matrix adhesion accelerates the process by allowing easier access for water and microorganisms. Key parameters affecting biodegradation include fiber composition, geometry, and volume fraction (Φ), with significant changes past the percolation threshold (Φ_c). Therefore, determining Φ_c is vital to trigger biodegradation of hydrolysable bio-matrices. Unfortunately, assessing Φ_c in biocomposites is difficult. Theoretical models often fail due to assumptions about fiber uniformity, leading to discrepancies with experimental results. Effective techniques for Φ_c determination include dielectric spectroscopy and rheology. In this work, which is part of a wider recently published study [1], a novel rheological approach adapted from polymer nanocomposites accurately pinpointed Φ_c in PLA composites with kenaf fibers, aligning with both theoretical predictions and the results of dielectric methods, which require much longer measurements to identify Φ_c due to the slow water diffusion dynamics.

EXPERIMENTAL

PLA pellets were supplied by Corbion (Luminy® LX175, density: 1.24 g/cm³, MFI: 6g/10min at 210°C/2.16 kg). Kenaf bast fibers were provided from Kenaf Eco Fibers Italia (Guastalla, Italy). Prior to compounding, the fibers were ground using a Retsch cutting mill equipped with a 0.25 mm grid. It was evaluated the water absorption capacity of the fibers through a thermogravimetric analysis (TGA Q500, TA Instruments). The fibers were soaked in tap water at approximately 15°C for 7 days, then dried at 110°C under nitrogen flow. Weight loss was monitored over time until a constant weight was achieved.

PLA/kenaf biocomposites at fiber volume fractions $\Phi = 5, 10, 15, 20, 25, 30,$ and 35 were prepared by employing a static Brabender Pantograph EC batch mixer (Brabender GmbH & Co.). Prior to compounding, the PLA pellets were dried overnight at 85°C under vacuum, while the kenaf fibers were conditioned at 25°C and 80% relative humidity (RH). The mixing process conditions were 180°C and 60 rpm mixing rate for 6 min.

The melt compounded material, after being dried overnight at 85°C under vacuum, was shaped into square panels (100×100×3 mm³) using a hydraulic press (Bench Top Hydraulic Press 20 MT, Lab Tech Engineering Company LTD). The mold, pre-heated at 180°C, allowed the material to soften for 5 minutes without pressure, followed by a compression step at about 150 bar for 4 minutes. The panels were then cooled to room temperature while maintaining pressure. After being taken out of the mold, the panels were cut into square samples (30×30×3 mm³) to use for rheological testing.

Rheological tests used stress-controlled rotational rheometer (AR-G2, TA Instruments) with 25 mm parallel plates at 180°C under nitrogen, adjusting oscillatory frequency (ω) from 6×10^2 to 6×10^{-2} rad/s and strain amplitude (0.2÷2%). Dielectric spectroscopy employed ARES rotational rheometer with 25 mm stainless-steel plates and LCR Meter (E4980A,

Agilent), measuring dielectric permittivity across frequencies (f) from 2×10^1 to 6×10^4 Hz at room temperature post water absorption tests.

RESULTS AND DISCUSSION

In this work it was evaluated the percolation threshold of short kenaf bast fibers ($<500\mu\text{m}$) in PLA-based biocomposites using three different methods: (i) theoretical calculations based on percolation theory, (ii) linear viscoelastic analysis in the molten state, and (iii) dielectric spectroscopy. We compared the accuracy and easiness of these methods. Theoretical calculations rely on knowing fiber geometry (size, shape, aspect ratio) and spatial orientation, which are challenging to estimate accurately in real-world scenarios. For our systems, theoretical calculations predict Φ_c to fall into the range 4.3-17.2%.

More accurate experimental estimates of Φ_c were achieved through simple linear viscoelastic analysis. We adapted a previously developed viscoelastic model for polymer nanocomposites to our composites, validating it by constructing a master curve of the elastic modulus above percolation. This approach narrowed down the Φ intervals relevant for finding Φ_c . Finally, we computed Φ_c using the power-law scaling of network shear elasticity predicted by percolation theory, resulting in Φ_c values of about 19.5%. The reliability of these Φ_c values was confirmed by dielectric spectroscopy analyses, which yielded Φ_c values of about 18.5%. The output of the equilibration and dielectric spectroscopy tests are shown in Fig. 1. It is important to note that dielectric tests required a more laborious and time-consuming (ca. 3 weeks) procedure due to the conditioning step needed before measurements.

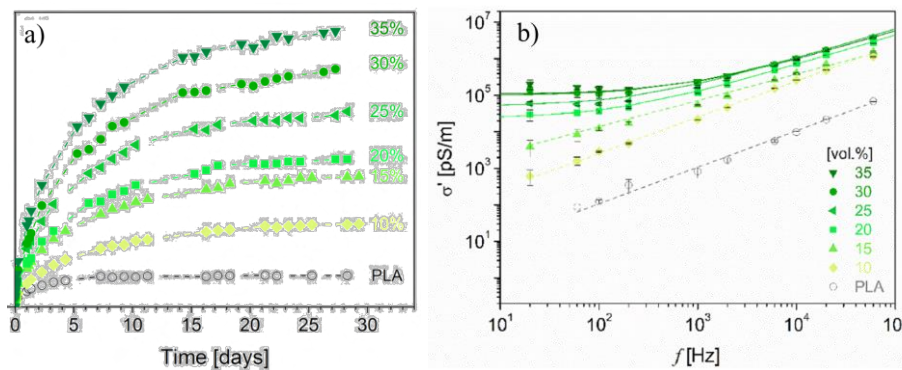


Fig. 1 a) Percentage weight gain of neat PLA and kenaf-based composites at different Φ as a function of soaking time in tap water at 30°C . Lines are guides for the eye. b) Real part of the complex conductivity for the kenaf-based composites at different fiber content. The samples were equilibrated in tap water for ~ 3 weeks. Solid lines are the fitting of the alternated current universal law to the data. Images readapted from [1].

Acknowledgment

This work has been financially supported by the PRIN-GREENCO (Bando 2022 Prot. 20223LWKTC) - Research project title: Untapping the potential of GREEN COmposites by combining performance and environmental sustainability.

References

- 1) L. Vitiello, M. Salzano de Luna, V. Ambrogi, & G. Filippone. *Composites Science and Technology*, 245, 110345 (2024).

FLAME RETARDANT PP-BASED MATERIAL: THE EFFECT OF 3D PRINTING PROCESS

A. Frache*, E. Lorenzi, R. Arrigo

Department of Applied Science and Technology, Politecnico di Torino, viale Teresa Michel 5, Alessandria, Italy *alberto.frache@polito.it

INTRODUCTION

Fused filament fabrication (FFF) is one of the most used techniques for 3D printing of thermoplastic materials. Despite the rapid development of FFF techniques, their application is still limited by the modest availability of suitable materials. In particular the use of polypropylene (PP), one of the most studied and used polymer, is still very limited and challenging in FFF process [1,2]. In addition, there is a lack of functionalized PP-based materials, including, for example, those with flame-retardant properties. In this context, a PP-based flame retardant filament suitable for FFF processing and its burning behavior were developed [3].

EXPERIMENTAL

Materials

Polypropylene ISPLEN® PB 170 G2M (named PP COPO), Cloisite®20A (C20A) and polypropylene-graft-maleic anhydride (PP-g-MA) were used as received

Nanocomposite preparation

The nanocomposite PP COPO + 5% C20A + 3% PP-g-MA was produced through melt compounding in a twin-screw extruder Thermo Fisher Scientific™ Process 11. A Felfil Evo filament making machine was used to produce filaments with a diameter of 1.75 mm and a Roboze One 3D printed was used to 3D print the cone calorimeter and UL94 test specimens.

Characterization

The thermal properties of the formulated materials were evaluated by Differential Scanning Calorimetry (DSC); the rheological properties of the unfilled PP COPO and PP-based composite were evaluated using an ARES strain-controlled rheometer in parallel plate geometry rheometer; the surface morphology and section of filaments were investigated using an EVO 15 Scanning Electron Microscope (SEM) and to evaluate the combustion behavior cone calorimeter tests were performed.

RESULTS AND DISCUSSION

In order to assess the processability and hence the FFF printability of the composite, the complex viscosity of the investigated materials was evaluated using dynamic frequency sweep tests (see Figure 1). The pristine PP COPO shows marked Newtonian behavior with a Newtonian plateau developing at low and intermediate frequencies, followed by mild shear thinning at high frequencies. The introduction of the nanoclays leads instead to an important amplification of the non-Newtonian behavior of the material, with a significant increase in complex viscosity at low frequencies and a more pronounced shear thinning at high frequencies compared to the neat PP COPO. Both the presence of yield stress and shear thinning are beneficial for the processability of polymers in extrusion printing processes.

The optimization of the extrusion process, in order to achieve a regular filament, occurred by changing three main parameters, namely the extrusion temperature, screw speed and power of the cooling fans, was performed and a regular filament was obtained (see Figure 1A). Concerning the 3D-printing process, parameter optimization trials were also carried out and specimens for combustion tests with both a $\pm 45^\circ$ and a concentric pattern were produced. In Figure 1B is reported the side view of the specimen in which it is evident how the accuracy of the deposited layers decreases when increasing the height of the specimen. Nevertheless it is possible to appreciate a good adhesion between the layers.

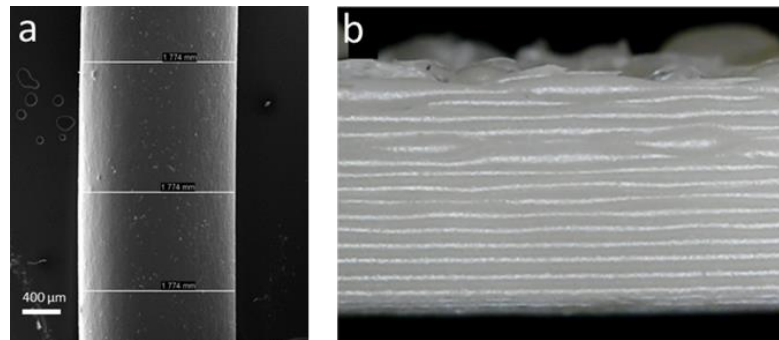


Figure 1: a) SEM images of the surface of the PP COPO/C20A filament; b) Optical micrographs of cone calorimeter sample

The cone calorimeter tests were carried out on both 3D-printed and compression-molded specimens (CM), considering either pristine PP COPO or PP COPO/C20A. The curve of the PP COPO 3D sample is characterized by a maximum HRR of 1358 kW/m². The presence of the nanoclays leads to a decrease in the value of pHRR to 978 kW/m² in the case of CM sample and to 690 kW/m² in the case of 3D sample respectively (see Figure 2A). It is clear that the processing method strongly influences the final combustion behavior of the material. First of all, it can be seen that the 3D-printed sample has a shorter ignition time (50 s) than the compression-molded sample (58 s). This is probably caused by the higher surface roughness of the 3D-printed specimen, but in terms of peak of heat release rate the 3D sample has better performances in respect to CM one. The improved performance of the 3D-printed specimen can be correlated to and explained by observing the carbonaceous residues collected at the end of the cone calorimeter tests. In Figure 2B, it is possible to observe that the char formed by the CM specimen is composed of several “islands”, while that of the 3D-printed specimen is more compact and characterized by fewer cracks. The formation of a more compact char can likely be attributed to two different phenomena. Firstly, the shear stress experienced by the material during the passage through the printing nozzle in the FFF process could favor some evolution of the composite microstructure, promoting the achievement of a better dispersion of the nanoclays’ lamellae into the polymer matrix. On the other hand, it should be considered that, due to the layer-by-layer approach for the construction of the FFF sample, the 3D-printing process allows for a much more uniform concentration of nanoclays throughout the specimen.

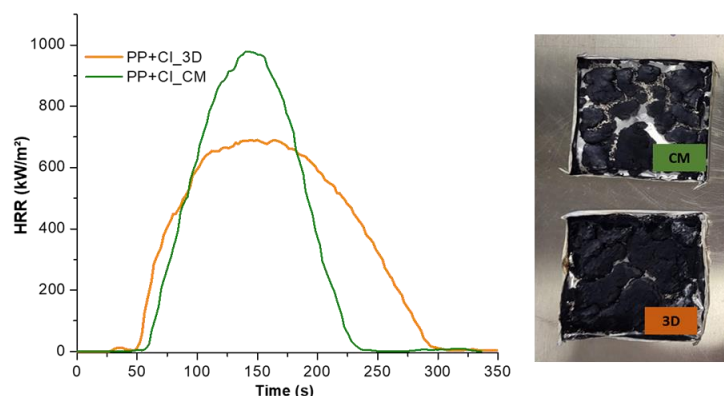


Figure 2: HRR curves and residues of compression molding and 3D printing samples

References

- 1) M. Bertolino, D. Battezzore, R. Arrigo, A. Frache, *Addit. Manuf.* **40** 101944 (2021)
- 2) G. Bernagozzi, D. Battezzore, R. Arrigo, A. Frache, *Polymers* **15** 2263 (2023)
- 3) E. Lorenzi, R. Arrigo, A. Frache, *Polymers* **16** 858 (2024)

BIODEGRADABLE POLYHYDROXYURETHANE (PHU) BIOMATERIALS DEVELOPED USING THE NIPU METHODOLOGY

Ana-I. Carbajo-Gordillo, Elsa Galbis, Elena Benito,* Fátima Díaz-Carrasco, Roberto Grosso, Nieves Iglesias, M.-Gracia García-Martín, Ricardo Lucas and M.-Violante de-Paz

Departamento de Química Orgánica y Farmacéutica, Facultad de Farmacia, Universidad de Sevilla, C/ Prof. García González, n.º 2, 41012-Sevilla, España. elsa@us.es, ebenito@us.es

INTRODUCTION

Polyurethanes (PU) are highly versatile polymeric materials that are widely used in a variety of utilities including biomedical applications: from the manufacture of medical devices (1) to smart materials useful in the preparation of responsive drug delivery systems (DDS) (2).

PU can be prepared by several methods, being the most widely used approach the reaction between di(multi)isocyanates and di(multi)alcohols (3). It is important to consider the inherent toxicity of isocyanates, due to the health risk that these chemicals represent for handlers, and also because of the environmental impact they could cause. Moreover, metal-based catalyst such as $[\text{Sn}(\text{Oct})_2]$ is generally used, which has been reported to be hazardous and very toxic to the environment (4).

We present the preparation and characterization of novel polyhydroxyurethanes (PHU) that will bear labile disulfide bonds in their structures and hence, may present interesting applications as biomaterials, especially in drug delivery under hypoxic conditions (2,5). The polymerization method to be employed will be a non-isocyanate polyurethane (NIPU) methodology, by which the aminolysis of a bis(cyclic carbonate) derived from 1-thioglycerol will take place by means of a diamine. A comparative study in the use of an aprotic polar solvent, DMSO, and a protic polar solvent, 2,2,2-trifluoroethanol (TFE) is performed emphasizing the use of low temperatures and metal-free catalyst in the production of the new materials (6).

EXPERIMENTAL

Materials

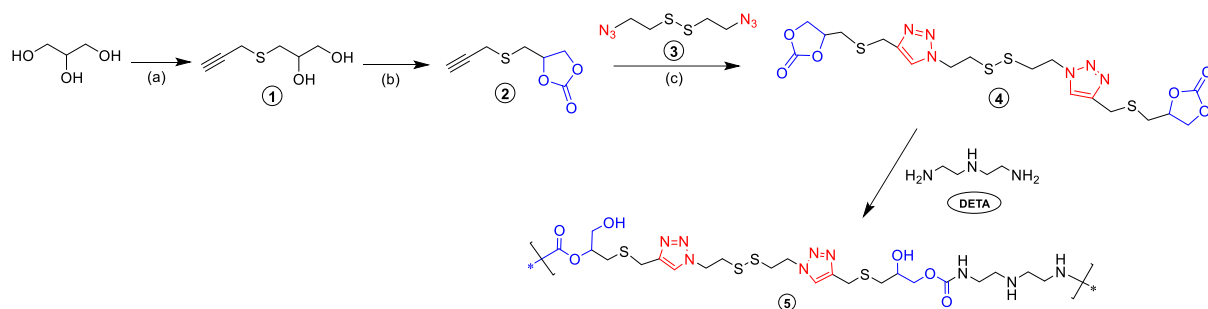
All chemicals used were from Aldrich Chemical Co (Madrid, Spain): Diethylenetriamine (DETA), tris(2-aminoethyl)amine (TAEA), and PVA [hydrolysis degree: 89%; weight average molecular weight (M_w , kDa): 32.0].

Preparation of non-isocyanate polyurethanes (NIPU)

The preparation of PHU (**5**, Polymer 1) was conducted by the aminolysis of monomer **4** (6) with DETA (Scheme 1) under a variety of polymerization conditions recorded.

As an example, the general in-solution polymerization procedure for the manufacture of PHU (**5**) was as follows: to a solution of monomer **4** (90 mg, 0.164 mmol, $[\text{monomer}] = 165 \text{ mmol/L}$) and DETA (12 μL , 0.114 mmol) in the chosen solvent [whether DMSO or 2,2,2-trifluoroethanol (TFE)], the organo-catalyst (TU, DBU, or none) was added (8.26 μmol , 10% in mol regarding monomer **4**) and the reaction stirred at the chosen temperature (25 °C or 50 °C) for 24 h.

Similarly, quasi-in-bulk polymerizations ($[\text{A}] = 1.8 \text{ mol/L}$) with the same solvents, catalysts, and selected temperatures were conducted. In every case, once the polymerization had taken place, the polymer was precipitated over cold *tert*-butyl methyl ether (*t*BME), washed with additional *t*BME, and dried under vacuum for 48 h (from 91% to quantitative yields). M_w ranged from 3.4 kDa to 16.4 kDa.



Scheme 1. Synthetic scheme for the preparation of monomer **4** and PHU (**5**). (a) Propargyl bromide, TEA, MeCN, 0°C → r.t., 5 h; (b) bis(trichloromethyl) carbonate, pyridine, CH₂Cl₂, -55 °C → r.t., overnight; (c) diazide **3**, sodium ascorbate, CuSO₄, tBuOH-H₂O 2:1, r.t., 19 h.

Preparation and characterization of a PHU/PVA-based semi-interpenetrating network

The preparation of a hybrid material, an interpenetrating network (IPN) of 3rd generation, has been addressed. This super-porous material was prepared when a crosslinked redox NIPU network (Polymer 1, **5**), was formed in a solution of PVA (Polymer 2) so that the whole system became an IPN. They could be of great interest in biomedical applications as previously demonstrated.

RESULTS AND DISCUSSION

We described an optimized method for the formation of redox-responsive PHU through the aminolysis of a functional bis(cyclic carbonate) derived from 1-thioglycerol and diethylenetriamine (DETA) by isocyanate- and phosgene-free routes, under ambient atmosphere at room temperature and mild temperatures.

Optimizing PHU formation identifies key variables, with the highest molecular weights being achieved under near-bulk polymerization conditions using TU-protic and DBU-aprotic as catalyst–solvent combinations

The best polymerization conditions were found in near-bulk conditions using TU as an organo-catalyst, at ambient temperatures in TFE ($M_w = 16.4$ kDa) and at 50 °C using DBU as an organo-catalyst, in which the polymerization solvent was DMSO.

The synthetic strategy was also validated by means of its use in the formation of a PVA-based 3rd generation IPN, a highly porous, sponge-like material with enhanced rheological properties.

The method demonstrates exceptional orthogonality, with the functional groups in Polymer 2 not interfering with Polymer 1 formation.

In summary, this innovative approach presents a versatile methodology for obtaining advanced hydrogel-PHU-based systems with potential applications in various biomedical fields.

Acknowledgment

This research was funded by the Ministerio de Ciencia e Innovación-Agencia Estatal de Investigación (MCIN/AEI/10.13039/501100011033), grant number PID2020-115916GB-I00.

References

- [1] J.P. Santerre, K. Woodhouse, G. Laroche, R.S. Labow, *Biomaterials*, **26**, 7457, (2005).
- [2] E. Benito, L. Romero-Azogil, E. Galbis, M.-V. De-Paz, M.-G. García-Martín, *Eur. Polym. J.*, **137**, 109952, (2020).
- [3] C. Ferris, M.-V. de-Paz, J.A. Galbis, *J. Polym. Sci., Part A: Polym. Chem.*, **49**, 1147, (2011).
- [4] R. Mehta, V. Kumar, H. Bhunia, S.N. Upadhyay, *J. Macromol. Sci., Part C*, **45**, 325, (2005).
- [5] M.-V. de-Paz, F. Zamora, B. Begines, C. Ferris, J.A. Galbis, *Biomacromolecules*, **11** 269, (2010).
- [6] A.I. Carbajo, E. Benito, E. Galbis, R. Grosso, N. Iglesias, C. Valencia, R. Lucas, M.-G. García-Martín, M.-V. de-Paz. *Polymers*, **16**(7), 880, (2024).

REACTIVE EXTRUSION FOR COMPATIBILIZING BIODEGRADABLE PHBV/PBSA BLENDS

E. Sánchez-Safont^{a,b}, I. Pisa Ripoll^a, K. Samaniego-Aguilar^a, L. Cabedo^{a,b},
J. Gámez-Pérez^{a,b*}

^aGrupo de Polímeros y Materiales Avanzados (PIMA), Universitat Jaume I, 12071 Castelló (Spain) lcabedo@uji.es

^bCEBIMAT LAB S.L, ESPAITEC, Universitat Jaume I, Av. Vicent Sos Baynat s/n, 12071, Castelló (Spain)

INTRODUCTION

The effective transition towards a circular economy represents a significant challenge in applications such as food packaging, where mechanical recycling is often not feasible due to the structural complexity of the packaging. Replacing conventional plastics with biodegradable polymers offers a pathway for managing these wastes through organic recycling (composting), which simplifies their disposal along with organic waste. Among the emerging alternatives, polyhydroxyalkanoates (PHAs) are gaining significant relevance. Specifically, poly(hydroxybutyrate-co-hydroxyvalerate) (PHBV) is highly biodegradable in various ecosystems and possesses properties similar to conventional polymers like polypropylene (PP). However, PHBV still presents certain limitations, primarily low toughness, a narrow processing window, and high cost.

A common strategy to improve the mechanical performance of inherently brittle polymers is the development of blends with more ductile ones. Poly(butylene succinate-co-butylene adipate) (PBSA), a biodegradable polymer that can be obtained from renewable sources, could be considered a good candidate due to its low glass transition temperature and high impact resistance. However, PHBV and PBSA exhibit limited compatibility.

EXPERIMENTAL

Materials

PHBV and PBSA polymers were used as received from their respective suppliers. Reactive agents such as diisocyanates and peroxides were used to enhance the blend compatibility.

Preparation

Reactive Extrusion: The PHBV and PBSA blends were prepared using a twin-screw extruder under specific processing conditions optimized for each reactive agent.

Characterization:

Morphological characterization was carried out using Scanning Electron Microscopy (SEM). Mechanical properties were assessed through tensile tests according to ISO 527. Biodegradability was evaluated under industrial composting conditions following the ISO 14855-1 standard.

RESULTS AND DISCUSSION

Morphological Analysis

SEM images revealed a more homogenous dispersion of PBSA within the PHBV matrix in the presence of reactive agents. This indicates improved phase compatibility which is critical for the mechanical performance of the blend.

Mechanical Properties

The tensile tests showed that the addition of diisocyanates and peroxides significantly improved the mechanical properties of the PHBV/PBSA blends. Specifically, the elongation at break increased by up to 200%, suggesting a much more ductile behavior compared to the neat PHBV.

Biodegradability

The biodegradability tests confirmed that the inclusion of reactive agents did not hinder the degradation process. All samples, including those with reactive agents, achieved complete biodegradation within the time frame established by the ISO 14855-1 standard.

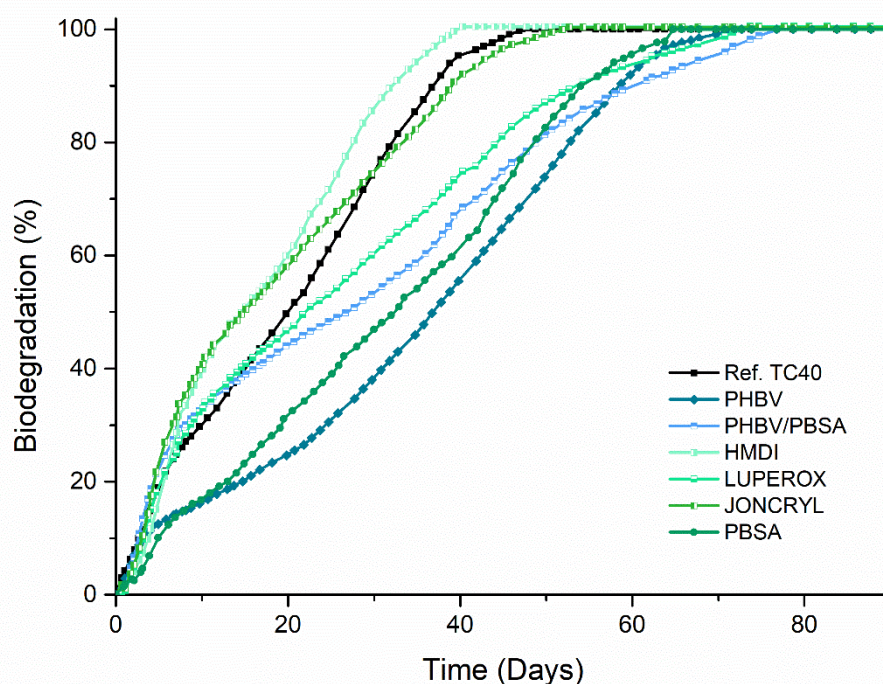


Fig. 1 Biodegradation (%) in the composting conditions as a function of time.

The results indicate that the use of reactive agents such as diisocyanates and peroxides is an effective strategy to compatibilize PHBV/PBSA blends, significantly enhancing their mechanical properties without compromising their biodegradability. This study demonstrates the potential of these blends for applications in which both mechanical performance and environmental sustainability are critical, presenting a viable solution for developing high-performance biodegradable materials suitable for a variety of applications, including food packaging.

Acknowledgments

This research was funded by MCIN/AEI/10.13039/501100011033 and by the European Union NextGenerationEU/ PRTR project number CPP2021-008973. This work also received financial support from Agencia Valenciana de la Innovación (AVI) and European Union FEDER project INNEST/2022/64 AVI-ELASTOTEX. K. Samaniego-Aguilar wishes to thank the MCIN/AEI/10.13039/501100011033 and FSE “The FSE invests in your future” for her FPI grant (PRE2019-091448).

L-TARTARAMIDE AND GUAR GUM-BASED MATRICES FOR GASTRO-RETENTIVE DRUG DELIVERY SYSTEMS

Fátima Díaz-Carrasco, Estefanía García-Pulido, Matea Katavić, M. Gracia García-Martín, M. Violante de-Paz, Elena Benito*

Departamento de Química Orgánica y Farmacéutica, Universidad de Sevilla, C/ Prof. García González, n.º 2, 41012-Sevilla, España.

*ebenito@us.es

INTRODUCTION

The synthesis of controlled Gastroretentive Drug Delivery Systems (GRDDS) to enhance the pharmacokinetics of oral formulations as antibiotics or antidiabetic drugs is nowadays a main research focus to improve therapeutic treatments (1,2).

This research presents the synthesis of multicomponent hydrogels that could be used as GRDDS for the administration of different drugs such as amoxicillin (AMOX) or metformin (MTF).

The new systems are composed by two polymers that are interpenetrated (IPNs): Polymer A is obtained by optimized Diels-Alder cycloaddition reaction (3) between a difuran monomer derived from L-tartaramide (MT) and a dimaleimide (DMDOO); Polymer B is guar gum (a natural and widely used mucoadhesive polysaccharide).

EXPERIMENTAL

Materials

The raw materials used in this work were: guar gum (GG), amoxicillin (AMOX), metformin (MTF), diethyl-L-tartrate, furfuryl amine, 1,8-diamine-3,6-dioxaoctane, maleic anhydride, furfuryl isocyanate, dibutyltin dilaurate and D-ribonic- γ -lactone.

Preparation

The monomers necessary for the preparation of the IPNs were synthesized according to the procedure established by Davies in the case of MT (4), and according to the procedure described by our research group for DMDOO (5). The synthesis of a tri-furfuryl (Tri-Fur) crosslinker was carried out as follows: to a solution of D-ribonic- γ -lactone (3.37 mmol) in THF (1,7 mL) under argon, furfuryl isocyanate (10.61 mmol) and one drop of dibutyltin dilaurate as catalyst were added. The mixture was stirred at room temperature for 5 hours, and then the solvent was removed. The resulting residue was purified by flash column chromatography on silica gel [ethyl acetate-hexane 1:2 \rightarrow ethyl acetate-hexane 1:1].

The synthesis of linear Diels-Alder polymers from difurfuryl L-tartaramide (MT) and DMDOO was carried out by stirring at 40 °C during 48 h using DMSO, AcOH-H₂O or AcOH as solvents so that [monomers] = 514 mM.

To afford the final interpenetrated systems in a single-step process, the Diels-Alder reaction took place within a colloidal solution of GG, using the crosslinker Tri-Fur (Figure 1). The corresponding drug (AMOX or MTF) was also added in the same **one-pot** process.

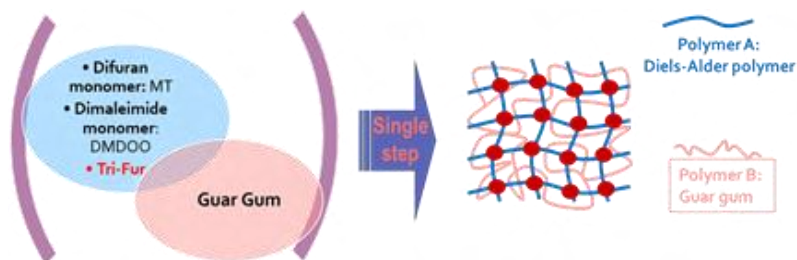


Figure. 1 Preparation of 3rd generation of superporous hydrogels by IPN methodology.

Physico-chemical characterization and in vitro drug release studies

Chemical structures of small molecules and linear polymers were confirmed by spectroscopic techniques (NMR, ATR-FTIR and ESI-MS). Molecular mass averages of linear polymers and their distributions were measured by gel permeation chromatography (GPC) and estimated against polystyrene standards.

The release studies of AMOX and MTF were conducted in simulated gastric fluid at pH 2.0 and pH 5.0 at 37 °C. The drug release was determined by UV spectroscopy, and the amount of drug released was calculated by means of the corresponding calibration curves.

RESULTS AND DISCUSSION

The novel interpenetrated systems were assessed for their porosity, swelling, and buoyancy capacity. Additionally, studies were conducted to investigate the uptake and release of MTF and AMOX at various pH values indicating their potential for controlled drug release at the gastrointestinal level.

The AMOX-loaded IPN demonstrated a sustained controlled release of the drug at both pH values, achieving 65-80% cumulative drug release within 8 hours. The release was slightly more pronounced at pH 2.0.

In contrast, IPNs loaded with the hydrophilic drug MTF exhibited an initial burst release of 60-100% of the initially loaded drug within 1 hour at both pH values, what could be attributed to MTF's high solubility.

In summary, these innovative materials offer a promising avenue for serving as controlled release systems for lipophilic drugs. Notably, their preparation in a single step presents a significant advantage for the industry, streamlining processes and enhancing efficiency.

Acknowledgment

This research was funded by the Ministerio de Ciencia e Innovación-Agencia Estatal de Investigación (MCIN/AEI/10.13039/501100011033), grant number PID2020-115916GB-I00.

References

- 1) N. Iglesias, E. Galbis E, L. Romero-Azogil, E. Benito, R. Lucas, M.G. García-Martín, M.V. de Paz. *Pharmaceutics*, **12(7)**, 636, (2020).
- 2) R. Grosso, E. Benito, A.I. Carbajo-Gordillo, M.G. García-Martín, V. Perez-Puyana, P. Sánchez-Cid, M.V. de-Paz. *International Journal of Molecular Sciences*, **24**, 2281, (2023).
- 3) N. Iglesias, E. Galbis, L. Romero-Azogil, E. Benito, M.J. Díaz-Blanco, M.G. García-Martín, M.V. de-Paz. *Polymer Chemistry*, **10**, 5473, (2019).
- 4) X. Ma, R.P. Davies. *Advanced Synthesis and Catalysis*, **364(12)**, 2023-31, (2022).
- 5) E. Galbis, M.V. de Paz, K.L. McGuinness, M. Angulo, C. Valencia, J.A. Galbis. *Polymer Chemistry*, **5(18)**, 5391-402, (2014).

SIMULATING THE MECHANICAL RECYCLING OF PET- AND HDPE-BASED PACKAGING: THE INTERACTION BETWEEN PRESENCE OF CONTAMINANTS, DEGRADATION AND REPROCESSING

C. Gnoffo, R. Arrigo, A. Frache

Dipartimento di Scienza Applicata e Tecnologia, Politecnico di Torino, Viale Teresa Michel 5, 15121, Alessandria, Italy.

chiara.gnoffo@polito.it, rossella.arrigo@polito.it, alberto.frache@polito.it

INTRODUCTION

The increasing plastic production involves a greater need of recycling polymeric end-of-life items. One of the encountered difficulties is related to the heterogeneity of composition of plastic materials, which can entail a drastic reduction of final properties and variation of processability of the recyclates [1]. As concerns polyethylene terephthalate (PET) bottles, besides PET from the central body of the container, high-density polyethylene (HDPE) in the closure system and polypropylene (PP) as label are encountered, while HDPE flacons are constituted by a polyethylenic main body, a PP-based closure and a PET-based label. During mechanical recycling, if the different polymers have different densities, separation by flotation takes place, notwithstanding this there is the presence of some contaminants in the final material that cannot be separated efficiently.

In this work, the effects of the presence of the most common contaminants and different forms of degradation on PET- and HDPE-based systems were assessed, aiming at evaluating their possible impacts on the processability and the final properties of recyclates.

EXPERIMENTAL

Materials

Regarding PET blends, bottle-grade PET (Intrinsic Viscosity 0.8 dl/g) and injection molding-grade HDPE (Melt Flow Rate 7.6 g/10 min) were used in order to obtain three systems: pristine PET, PET+0.5%HDPE and PET+2%HDPE. For HDPE systems, flacon-grade HDPE (Melt Flow Rate 5 g/10 min), PP (Melt Flow Rate 12 g/10 min) and bottle-grade PET (Intrinsic Viscosity 0.8 dl/g) were employed for formulating HDPE, HDPE+10%PP and HDPE+10%PP+2%PET.

Processing

A co-rotating twin-screw extruder has been used for the melt compounding. For PET systems, die temperature and screw rotation were set at 270°C and 50 rpm, respectively; for non-aged HDPE blends the processing parameters were chosen equal to 230°C and 100 rpm; die temperature was increased up to 250°C for aged polyethylenic systems.

Aging and characterization techniques

Photoaging was carried out through SEPAP, while thermal aging was performed in oven in presence of humidity for PET systems and surfactants for HDPE ones. Rheological, mechanical, thermal, spectroscopic and morphological properties were evaluated through rotational rheometer, dynamometer, DSC, FTIR-ATR and SEM, respectively.

RESULTS AND DISCUSSION

The present study was carried out considering the three following different aspects, which concurrently verify in a real mechanical recycling scenario: (i) presence of polymer-based contaminants deriving from ineffective separations; (ii) photo- and/or thermo-oxidative degradation (also in presence of humidity and/or other agents) underwent by the materials

during their service life; (iii) thermo-mechanical degradation occurring during the polymer reprocessing in the recycling stage. Concerning the PET systems, the presence of HDPE-based contaminants entails a significant increase of the complex viscosity as compared to pristine PET, while its effect on the mechanical properties is almost negligible. On the other hand, a remarkable decrease of the system viscosity was observed after photo- and thermoxidative-aging and reprocessing, likely due to the occurrence of chain scission and/or hydrolysis phenomena which mainly affect the molecular weight of PET (Fig. 1a). Furthermore, the mechanical properties of the reprocessed materials mostly depend on degradation. In fact, a sharp reduction of the elongation at break was observed for the samples subjected to photodegradation and thermal degradation in presence of humidity. These results can be attributed to the already mentioned reduction of the PET molecular weight, hence causing a loss of ductility.

As far as HDPE blends are concerned, their behavior is influenced not only by the aging and presence of contaminants, but also by reprocessing. In this case, the presence of PP and PET involves an increase of the complex viscosity values, due to the formation of a droplet-like morphology typical of an immiscible blend. Besides, the UV exposure promotes the occurrence of chain scission reactions (leading to a decrease of the complex viscosity), while the thermoxidative treatment in presence of surfactants does not significantly affect the rheological response. Otherwise, the thermomechanical degradation underwent by the materials during the reprocessing step induces the obtainment of branched structures and crosslinking, promoting an increase of the viscosity as compared to that of the starting polymer. These noticed alterations of the microstructure strongly affect the mechanical properties of the HDPE-based samples and, especially, the elongation at break. In particular, as observable in Figure 1b, the aging treatment and the subsequent reprocessing induce a general embrittlement of the materials, which is even more severe in presence of PP and PET contaminants.

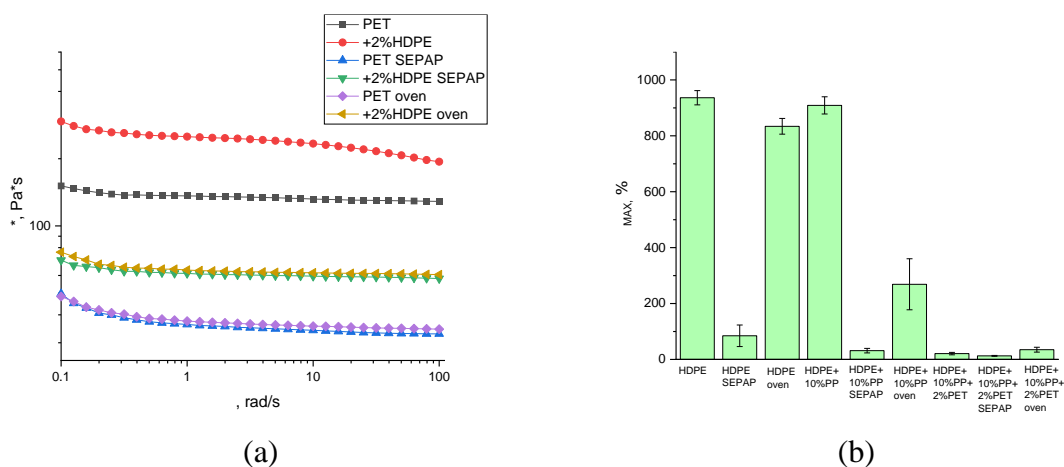


Fig. 1 (a) Complex viscosity curves for PET-based systems and (b) elongation at break for HDPE-based materials

Acknowledgment

This work is part of the project NODES which has received funding from the MUR – M4C2 1.5 of PNRR funded by the European Union - NextGenerationEU (Grant agreement no. ECS00000036).

References

- 1) Roosen et al, Environ Sci Technol, 2020, **54**, 20, 13282–13293

THE EFFECT OF PLASTICISER TYPE ON THE THERMAL DEGRADATION OF POLY(VINYL CHLORIDE): MULTIMODAL SPECTROSCOPIC ANALYSIS

Karol Górecki¹, Sonia Bujok², Łukasz Bratasz² and Krzysztof Kruczała¹

¹ Faculty of Chemistry, Jagiellonian University, Kraków, Poland

² Jerzy Haber Institute of Catalysis and Surface Chemistry, PAS, Kraków, Poland
karol.gorecki@student.uj.edu.pl

INTRODUCTION

Plastic has undeniably become an integral part of our everyday life. Due to tuneable properties and plentiful uses, it is truly omnipresent nowadays, filling every niche possible. Synthetic and semisynthetic polymer materials are the dominating ones within many of the contemporary art collections [1]. For over a century now, they have been enabling the creation of riveting new forms of art expression, bearing invaluable heritage information about our culture and society. The preservation of such a legacy is necessary, however clear guidelines for conservators are still under debate, requiring a study of processes accompanying ageing – especially since, among others, inappropriate formulation, variable storage conditions, and different mechanical stimuli can lead to accelerated degradation [2].

Poly(vinyl chloride), PVC, as it comprises even up to 13% of all contemporary art collections [3], is an important medium in e.g. sculpturing and mixed-media arts. Brittle by nature, it's usually plasticised with different compounds – mainly *ortho*-phthalates (including DBP, DEHP, DOP, and DINP) or non-phthalate plasticisers (like DEHT and DEHA). During the degradation, PVC undergoes changes resulting in the creation of double bonds and the release of chlorine. Although the degradation of PVC by itself has already been somewhat analysed, the effect of additives' degradation on the lifetime of the plastic object still is not well understood [4], hence the need for research into the processes ongoing in the system, elucidating at last the mechanistic root. Since the significant amount of plasticiser in an object usually makes it the main additive, we chose it as the target of this investigation.

In this work, we summarise the outcomes of a detailed study on artificially aged pure plasticisers and phantom samples of plasticised PVC foils by spectroscopic methods.

EXPERIMENTAL

Materials

The materials used in this study included pure suspension poly(vinyl chloride) (Polanvil provided by Anvil, Poland), tetrahydrofuran (pure for analysis, POCH, Poland), and six different plasticisers: di-*n*-butyl phthalate (DBP), bis(2-ethylhexyl) phthalate (DEHP), dioctyl phthalate (DOP), and diisononyl phthalate (DINP) were purchased from Sigma-Aldrich (Poland), bis(2-ethylhexyl) adipate (DEHA) was purchased from Supelco (Poland), and bis(2-ethylhexyl) terephthalate (DEHT) was purchased from Thermo Scientific (USA).

Preparation

Pure plasticisers were used as received, without further purification, placed in small glass vials (approx. 1 ml per vial, tightly closed). Thin, plasticised PVC films of ca. 0,2 mm thickness were prepared by solvent casting method. Briefly, the PVC powder was dissolved in THF with a certain amount (0, 20, 30, 40, and 50 wt. %) of a selected, single plasticiser added. As-prepared solutions were poured into Petri dishes and left overnight at room temperature to let the THF evaporate. The solidified films were then detached from the Petri dishes and left for at least one week under a fume hood to remove the THF residues.

Airtight closed vials with plasticisers and formerly prepared films (cut into smaller pieces) were placed in dryers for artificial ageing tests (without humidity control). Plasticised PVC films were aged at 60 and 80 °C, whereas pure plasticisers were also degraded at 120 °C.

The timescale of the degradation differed between the temperatures and for all the films ranged for up to 11 weeks, whereas for plasticisers up to 10 weeks at 60 °C, up to 20 weeks at 80 °C, and up to 16 days at 120 °C.

Physico-chemical and spectroscopic characterisation

UV-Vis-NIR measurements in the range of 200 to 3300 nm were performed on an Agilent Technologies Cary 7000 spectrophotometer. ATR-FTIR spectra were collected on a Thermo Scientific Nicolet 6700 FT-IR spectrometer in the 400 to 4000 cm^{-1} range. The Raman scattering spectra were collected in the 100 to 4000 cm^{-1} range using a Renishaw InVia spectrometer. EPR spectra were collected on a Bruker ELEXSYS 500 spectrometer and NMR spectra were done on a Jeol 400 MHz YH spectrometer.

RESULTS AND DISCUSSION

Multi-modal spectroscopic analysis of pure plasticisers suggested that in moderate temperatures, similar to those in museums, plasticisers don't undergo thermal degradation by themselves – both ATR-FTIR and NMR showed only minor differences between the samples. In plasticised plastics, so multicomponent systems, the plasticiser choice can play a role in the degradation rate though. The analysis of UV-Vis-NIR spectra proved that during the ageing, conjugated double bonds are created in the PVC chains, leading to a visible colour change in all aged samples. Further spectroscopic analysis showed that certain plasticised foils undergo faster degradation, whereas others hardly degrade at all. Two extremes were DINP samples, which showed nearly no degradation signs (Fig. 1, left), and DBP samples, which underwent the fastest changes (Fig. 1, right). Degradation, accompanied by diffusion and evaporation of plasticiser, leads to the worsening of properties of plastic (both visual and mechanical), and the effect of temperature and the starting concentration of the plasticiser was clearly visible in the analysed spectra – the rate of degradation grows rapidly with the increase of the temperature, and the higher the starting concentration of plasticiser, the faster it diminishes.

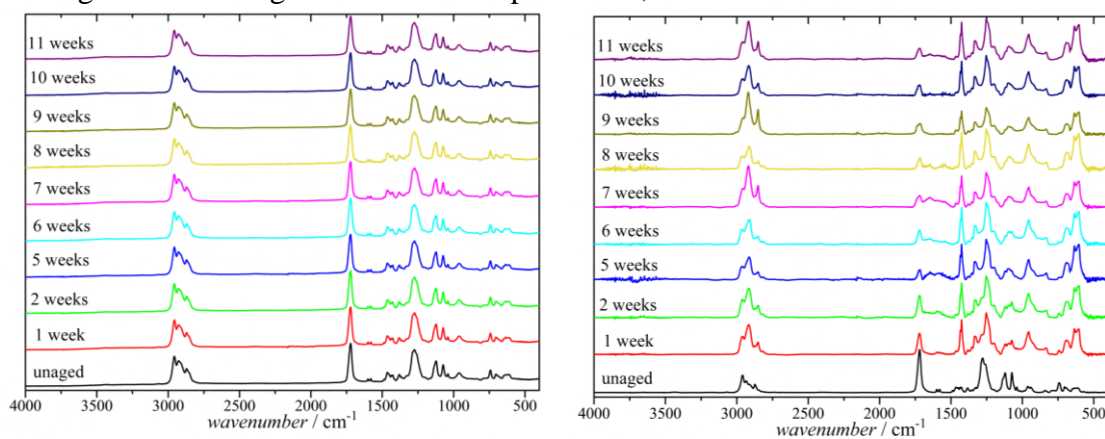


Figure 1. ATR-FTIR of aged PVC (80 °C) with 50% of DINP (left) and 50% of DBP (right).

Acknowledgement

The research is carried out within the OPUS LAP 20 (2020/39/I/HS2/00911) project, funded through the CEUS scheme as a cooperation between the NCN (National Science Centre, Poland) and ARRS (Slovenian Research Agency, N1-0241). Measurements were performed using research infrastructure funded by the European Union in the framework of the Smart Growth Operational Programme, Measure 4.2; Grant No. POIR.04.02.00-00-D001/20, “ATOMIN 2.0 – Center for materials research on ATOMIC scale for the INnovative economy”.

References

- 1) B. Lavedrine et al., Preservation of plastic artefacts [...]; CTHS, Paris, 2012.
- 2) T. Rijavec, M. Strlic, I. Kralj Cigic, Polym. Degrad. Stab., 2023, 211, 110329.
- 3) T. Rijavec, D. Pawcenis, K. Kruczała, M. Strlic, I. Kralj Cigic, Herit. Sci., 2023, 11, 155.
- 4) K. Saido et al., Macromol. Res., 2003, 11, 3, 178-182.

HYDRO/CHEMO-THERMAL PERFORMANCE OF COMMERCIAL PBAT/TPS-BASED FILMS

K. Gutiérrez-Silva, A. Jordán-Silvestre, M. Izquierdo, V. Martínez-Soria, O. Gil-Castell, J.D. Badia *

Materials Technology and Sustainability Research Group (MATS). Department of Chemical Engineering, Universitat de València. Av. de la Universitat, s/n 46100 Burjassot, València, Spain.
karen.gutierrez@uv.es, ajorsil@alumni.uv.es, marta.izquierdo-sanchis@uv.es, v.mtnez-soria@uv.es, oscar.gil@uv.es, jose.badia@uv.es

INTRODUCTION

In recent years, the use of chemical treatments for enhancing management of post-consume plastic materials has gained significant interest due to its potential to expedite the valorization process [1]. Especially in biopolymers, treatments with alkaline [2] or acid solutions can promote micro and macroscopic changes in the polymer structure. These modifications are expected to allow for a faster and more effective biodegradation.

In this work, hydro/chemothermal conditions with different pH levels were applied as a preliminary treatment to enhance the biodegradation of several commercial formulations of PBAT/TPS-based films.

EXPERIMENTAL

Materials

Commercial PBAT/TPS-based extruded films (PT) with a thickness of 100 μm were supplied by Prime Biopolymers (Paterna, Spain), with different additive percentages, labelled as PT, PT10 and PT20.

Hydro/chemo-thermal treatment

Alkaline treatment was carried out using a 1 M NaOH solution (pH 13.10 \pm 0.15); hydrothermal treatment was conducted using distilled water (pH 6.60 \pm 0.15); and acid treatment was performed using a 0.1 M HCl solution (pH 1.10 \pm 0.010).

Films were cut into pieces of 2 \times 7 cm² and immersed in glass vials with 20 mL of the above-mentioned solutions at 58 \pm 2 °C, in an orbital shaker at 100 rpm, during 1, 3, 6 and 12 h. After that, films were washed in distilled water, dried under vacuum at 40 °C until constant mass, and stored for further analyses.

Characterization

The consequences of hydro/chemo-thermal treatments were evaluated through analytical techniques such as gravimetry, colorimetry, SEM, WCA and FTIR. The goal was to observe changes in the material's morphology at both macroscopic and microscopic levels, as well as in its molecular interactions.

RESULTS AND DISCUSSION

Figure 1a shows the mass loss (Δm) as a function of the treatment time for the different media. Generally, disintegration was enhanced by the increase in pH, as the alkaline treatment reported the highest mass loss across all formulations in the early stage of the treatment, especially for higher percentage of additives.

The study of the water contact angle reported changes in the surface properties. In Figure 1b, an increase in the hydrophilicity of the films can be observed as a result of the pretreatments, again more pronounced in the alkaline pretreatment for the films with the higher percentage of additives.

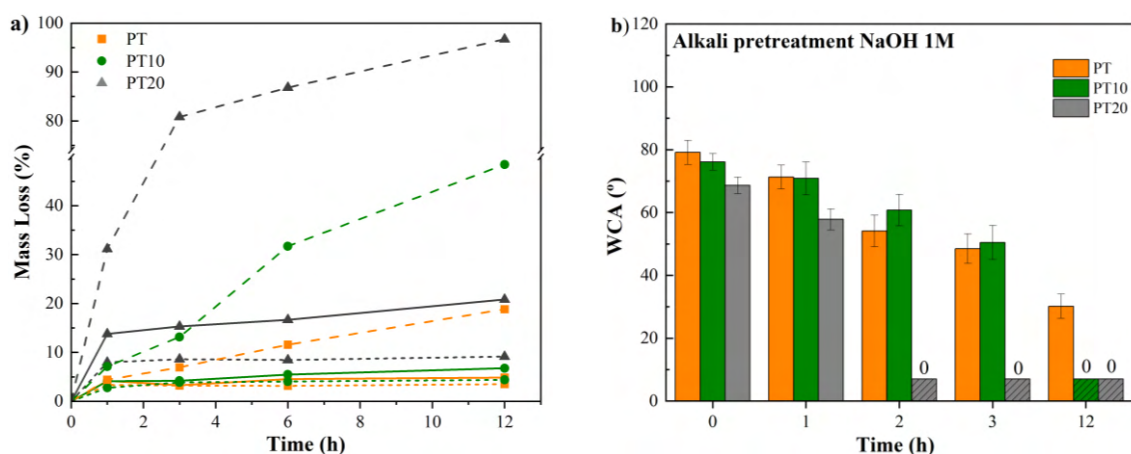


Figure 1. (a) Mass loss of PT films during alkaline (dash), aqueous (solid) and acid (short-dash) pretreatment; (b) WCA variation for films during alkali pretreatment.

Hydroxide groups in alkaline medium attacks preferably discrete starch domains dispersed within the PBAT matrix, producing microcracking on the surface of the films, as shown in Figure 2. The granular domains on the surface become planar and holes appear after the alkaline pretreatment, also making the surface rougher and more hydrophilic. Those modifications presume to enhance the biodegradation of PBAT/TPS films by increasing their vulnerability to subsequent hydrolysis and enzymatic action.

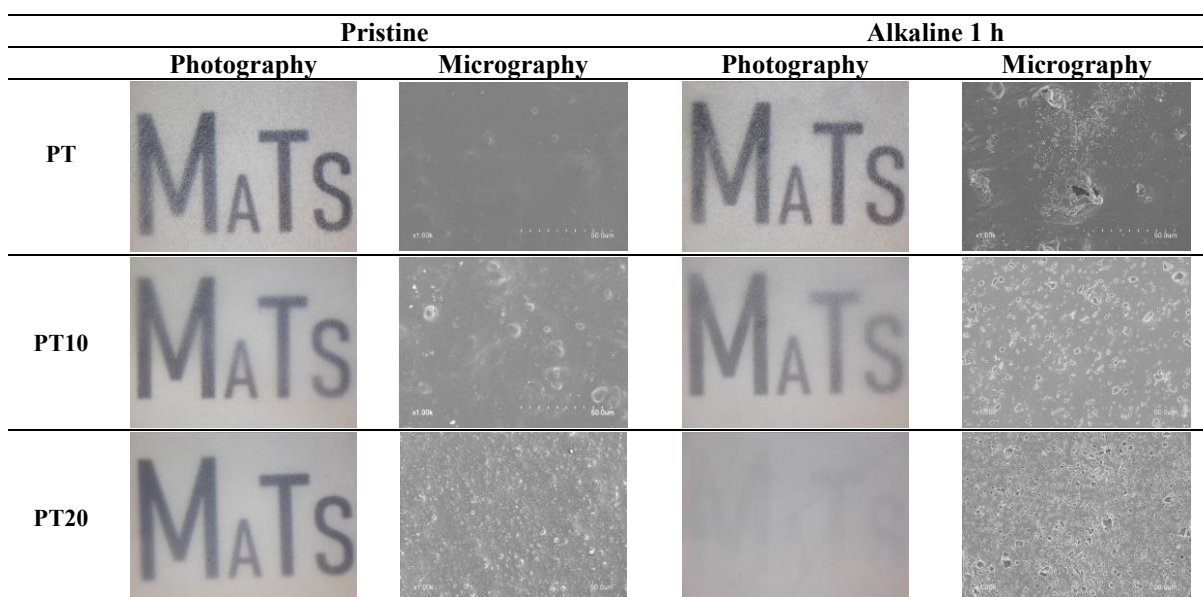


Figure 2. Macroscopic images of PT films pristine materials and SEM microscopies after alkaline pretreatment for 1 h.

Acknowledgements

Authors would like to acknowledge funding from the Agència Valenciana de la Innovació (AVI) through the INNEST/2022/295 project (BIOFAST-Methodological strategies for the accelerated biodegradation of bioplastics in compost medium).

References

- [1] B. Ciuffi, E. Fratini, and L. Rosi, Plastic pretreatment: The key for efficient enzymatic and biodegradation processes, *Polym Degrad Stab.* **2024**, 222, 110698.
- [2] Y. Jin, X. Sun, C. Song, F. Cai, G. Liu, and C. Chen, Understanding the mechanism of enhanced anaerobic biodegradation of biodegradable plastics after alkaline pretreatment *Science of the Total Environment.* **2023**, 873, 162324.

COMPOSITES FROM WASTE POLYPROPYLENE AND RECOVERED CARBON FIBRE

Ehsan Zolfaghari¹, Giulia Infurna¹, Sabina Alessi¹, Clelia Dispenza¹, Nadka Tz. Dintcheva¹

¹Dipartimento di Ingegneria, Università di Palermo, Viale delle Scienze, ed.6, 90128 Palermo, Italy
Corresponding author: nadka.dintcheva@unipa.it

INTRODUCTION

Carbon fibre reinforced plastics (CFRPs) are composite materials made from a polymer matrix (usually thermoset polymers) and carbon fibres, and their main advantages are related to the excellent mechanical performance, such as stiffness and fatigue resistance, thermal stability, corrosion resistance and a favourable strength to weight ratio. The properties of CFRPs can therefore be tailored by varying the matrix type and the type, length/diameter ratio and volume fraction of the carbon fibers. Due to these encouraging properties and performance, CFRPs have found numerous applications in many sectors, such as aerospace, automotive, sports equipment, marine equipment, wind power generation, etc. Therefore, considering the large consumption and continuous growth of CFRP applications, their end-of-life must be properly studied and designed. [1-3]

Therefore, thermoset composite waste is a serious concern in most countries due to the related environmental and health risks. Efforts are required to give this composite waste a second life, thus reducing its quantity and limiting the consumption of new resources. [1-2]

This research study aims to manufacture thermoplastic composites utilizing two type of industrial wastes of neighbor companies: waste polypropylene (wPP) from household manufacture and carbon-fiber reinforced epoxy composite scrap from a pultrusion company. This scrap is either machined into a powder or subjected to a chemical : carbon fiber reinforced plastic powder waste (pCFRP) and reclaimed carbon fibers (rCF). A micromixer was used to mix wPP with either wCFRP or rCF, added in different weight ratios. The fillers were characterised for their morphology via Scanning Electron Microscopy (SEM). Rheological studies were conducted to assess the strength of interaction between filler and matrix and the processability of these materials by injection moulding. Differential Scanning Calorimetry (DSC) was employed to investigate the thermal transitions and change in crystallinity of wPP in the composites. Finally, the systems were characterized for their mechanical properties via tensile tests.

EXPERIMENTAL

Waste polypropylene (wPP) has been supplied by Euroscope MDF srl (Italy).

Carbon fiber reinforced epoxy matrix composite waste has been supplied by K-composite srl (Italy). Recovered carbon fiber (rCF) was obtained from a chemical matrix digestion process.

wPP composites were produced using pCFRP (powder) at 1 %wt., 10 %wt. and 20 %wt. and rCF at 10 %w and 20%w by melt mixing at temperature of 190 °C.

The wPP-based composites have been characterized by rheological analysis (oscillatory test), morphological analysis (SEM observations), differential scanning calorimetry (DSC) analysis, thermo-gravimetry analysis (TGA) and tensile test.

RESULTS AND DISCUSSION

First of all, accurate SEM observations of virgin carbon fibres (vCF) and recovered carbon fibres (rCF) reveals that the recovered fibres are clean, but slightly swelled, randomly oriented, and corrugated after the digestion reaction. Further, pCFRC (powder) has included epoxy resin fragments that is partially attached to the fibres.

The DSC analysis highlights the presence of two distinct melting peaks in all investigated samples suggesting the presence of different crystalline forms or a wide range of crystal sizes for wPP. The calculation of the degree of crystallinity (X_c) shows a constant increase in crystallinity degree by increasing the filler content, however, it is 10% to 18% lower than wPP. Moreover, in equal filler content, rCF indicated higher crystallinity percentage. pCFRC (20% is excluded) and rCF show slightly higher crystallization temperatures compared to neat wPP, however, it does not indicate a noticeable nucleation due to fillers. In contrast, the addition of filler decreases the overall crystallinity of the polypropylene matrix, as evidenced by the lower enthalpy values.

The rheological analysis evidence a higher viscosity with increased filler content and as noticeable, both rCF and pCFRC fillers increase viscosity compared to wPP, indicating the formation of stronger network structures due to the polymer-filler interactions.

Carbon fibres significantly enhance the composite's stiffness through effective stress transfer from the polypropylene matrix to the stiffer carbon fibres, as revealed by the tensile test analysis. Further, the carbon fibres are inherently brittle compared to the ductile polypropylene matrix. When added to the matrix, they reduce the overall ductility of the composite, leading to a lower elongation at break. This is because the fibres restrict the polymer chains' mobility, making the composite less capable of elongating under stress

Acknowledgments

E.Z. would like to thank the Italian Ministry of University and Research (MUR), DM 352/2022 PNRR, Misura 4, comp. 2, investimento 3.3 and K-Composites srl for the financial support in the development of his PhD studies.

The authors would like to thank the Euroscope MDF srl (Mr. G. Montalto) for supplying of waste polypropylene (wPP).

References

1. A. Sarmah *et al.*, "Recycle and Reuse of Continuous Carbon Fibers from Thermoset Composites Using Joule Heating," *ChemSusChem*, vol. 15, no. 21, Nov. 2022, doi: 10.1002/cssc.202200989.
2. Y. Bai, Z. Wang, and L. Feng, "Chemical recycling of carbon fibers reinforced epoxy resin composites in oxygen in supercritical water," *Mater Des*, vol. 31, no. 2, pp. 999–1002, Feb. 2010, doi: 10.1016/j.matdes.2009.07.057.
3. C. Soutis, "Carbon fiber reinforced plastics in aircraft construction," *Materials Science and Engineering: A*, vol. 412, no. 1–2, pp. 171–176, Dec. 2005, doi: 10.1016/j.msea.2005.08.064.

A NEW CASE IN ABS POLYMER FOR NANOSTRUCTURED LEAD BATTERIES: STABILITY STUDY IN 5M SULFURIC ACID

M. Insinga, L. Oliveri, N. Moukri, B. Patella, R. Inguanta

Department of Engineering, University of Palermo, Viale delle Scienze, Palermo, Italy
rosalinda.inguanta@unipa.it

INTRODUCTION

Over the years, various studies have been carried out and many solutions have been proposed for improving the performance of lead-acid batteries aimed to increase the life cycles and energy density and also to decrease the sulfurization phenomena. The main solution is focused on adding various types of carbon additives in the positive and negative plates or adding substances into the electrolyte to delay the sulfation of both positive and negative electrodes. Another approach consists of replacing the commercial plates with nanostructured electrodes. The research activity of this project is focused on the fabrication of nanostructured electrodes, with high surface area and thus high utilization of the active material. The performance of the electrodes will be also incremented using carbonaceous additives such as reduced graphene oxide. Based on our previous results, obtained with a single 2V cell consisting of low-capacity lead oxide nanowires (1), lead nanowires (2) and rGO-lead nanowires (3) electrodes, the main activity of this research is focused on the fabrication of high-capacity 6V and 12V nanostructured lead acid battery. The research activity involves a complete characterization from a chemical-physical point of view, and validation in different charging and discharging conditions to define the optimal operating conditions and the lifetime of the prototypes obtained. To fabricate the prototype a new case was developed. In particular, the case of battery was obtained using a 3D printer and Acrylonitrile Butadiene Styrene (ABS) polymer. Since this is a new type of battery case material, the stability of this material in 5M sulfuric acid was verified through FTIR, XRD and SEM measurements made on pieces of polymer immediately after manufacturing and after immersion tests in the acid solution.

EXPERIMENTAL

Materials

A 3D printing filament in ABS (Z-ABS, Zortrax) was used to fabricate the case of the prototype of a lead acid battery. Concentrated sulfuric acid (>97%, Sigma Aldrich) was used to prepare the 5M solution. Millipore-grade water was also used.

Preparation

Small pieces of the case, with dimensions 3*3 cm, were obtained through a 3D printer (Zortrax, M300). To have samples that faithfully reproduced the case, the pieces were obtained using the CAD model of the entire case, and therefore present the grooves on the internal wall (Figure 1) intended to house the electrodes and separators. The same printing conditions used to obtain the case were also used to fabricate the small parts.

Characterization

Once obtained, the pieces were characterized using different techniques before and after immersion in 5M sulfuric acid. The samples were analyzed after different immersion times. In particular, the samples were analyzed using a scanning electron microscope (SEM) and X-ray diffraction (XRD) and Fourier Transform spectroscopy (FTIR). After immersion and before analysis the samples were simply washed with distilled water and air dried.

RESULTS AND DISCUSSION

The stability of samples of ABS polymer obtained by a 3D printer in 5M sulfuric acid was verified through different techniques. FTIR, XRD and SEM measurements were made on pieces of the case immediately after manufacturing and after immersion tests in the acid solution. Samples were characterized after different immersion times, from a few hours to several months. The tests are still ongoing, but the first analyses show a high resistance of this polymer despite the extremely acidic environment.

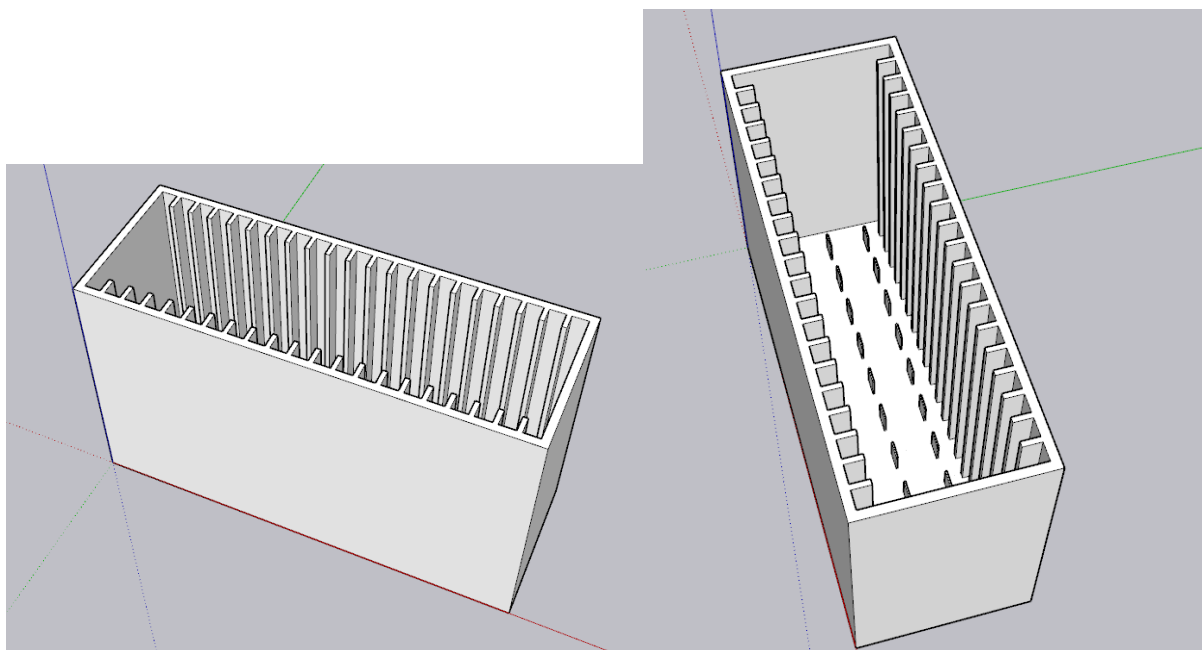


Figure 1_ Scheme of the case in ABS polymer obtained by 3D printing used for the fabrication of lead nanostructured battery prototype.

Acknowledgment

This work was partially financed by the project “SiciliAn MicronanOTecH Research And Innovation Center “SAMOTHRACE” (MUR, PNRR-M4C2, ECS_0000022), spoke 3 - Università degli Studi di Palermo “S2-COMMs - Micro and Nanotechnologies for Smart & Sustainable Communities”.

References

- 1) Moncada A., Piazza S., Sunseri C., Inguanta R. Recent improvements in PbO₂ nanowire electrodes for lead-acid battery (2015) *Journal of Power Sources*, 275, 181 - 188, 10.1016/j.jpowsour.2014.10.189
- 2) Insinga M.G., Oliveri R.L., Sunseri C., Inguanta R. Template electrodeposition and characterization of nanostructured Pb as a negative electrode for lead-acid battery (2019) *Journal of Power Sources*, 413, 107 - 116, 10.1016/j.jpowsour.2018.12.033
- 3) Rossini M., Ganci F., Zanca C., Patella B., Aiello G., Inguanta R. Nanostructured Lead Electrodes with Reduced Graphene Oxide for High-Performance Lead–Acid Batteries (2022) *Batteries*, 8 (11), art. no. 211, 10.3390/batteries8110211

MODIFICATION OF POLYMER MATRICES COMPOSED OF SODIUM ALGINATE AND STARCH BY INCORPORATION OF MICROSPHERES

J. Kozłowska

Functional Polymer Materials Team, Department of Biomaterials and Cosmetic Chemistry, Nicolaus Copernicus University in Torun, Torun, Poland
justynak@umk.pl

INTRODUCTION

Encapsulation is the process of enclosing active substances in a polymeric coating that isolates and protects them from the external environment. This enables the design of particles, such as capsules or spheres, with a controlled or triggered-release mechanism. Microencapsulation of active substances offers numerous advantages and has a wide range of applications in various industries, such as food (encapsulation of flavors, vitamins, and probiotics), pharmaceutical (controlled drug delivery systems), cosmetics (a. o. encapsulation of fragrances for long-lasting scent), textiles (temperature regulation materials), agriculture (controlled release of pesticides and herbicides).

The aim of this work was to develop new materials for potential cosmetic and dermatological purposes by modifying polymeric matrices by incorporating microspheres based on poly(vinyl alcohol) (PVA)/sodium alginate into matrices based on sodium alginate and starch, as well as to evaluate their physicochemical properties. *Calendula officinalis* flower extract was used as a model encapsulated substance.

EXPERIMENTAL

Preparation of microspheres

Two solutions were prepared to obtain the microspheres. The first was a mixture of 6% PVA solution and 0.6% sodium alginate solution in 0.1% solution of *Calendula officinalis* flower extract. The second solution contained 4% boric acid and 3% calcium chloride.

The microspheres were formed using a Büchi encapsulator. The PVA/sodium alginate mixture with calendula flower extract was taken from a pressure bottle and then dripped into the crosslinking mixture of $H_3BO_3/CaCl_2$.

Matrices preparation

Two polymeric solutions were prepared to obtain the films: 2% sodium alginate solution and 1% starch solution. Then, different mixtures were prepared, including 1) control samples without plasticizers based on sodium alginate and mixtures of sodium alginate with starch in various weight ratios; 2) matrices containing sodium alginate, starch, and plasticizers (glycerin or sorbitol), and matrices based on sodium alginate with plasticizers. Each mixture (100 ml) was poured onto surfaces of 15x20 cm and left to dry at room temperature. After drying, the matrices were crosslinked in a 0.5 M $CaCl_2$ solution by immersing them for 10 minutes, rinsing them with distilled water, and drying again.

Selected matrices were modified by adding prepared microspheres (0.35%) before drying.

Physico-chemical characterization

Swollen and dry microspheres were imaged using a Motic SMZ-171 BLED stereoscopic microscope. The shape, topography, and size of the prepared microparticles were assessed. The efficiency of extract incorporation into microspheres, as well as the in vitro release profile of plant extract, were examined by Folin-Ciocalteu assay.

The obtained materials were assessed regarding swelling ability, mechanical properties, thermal properties, and stability.

RESULTS AND DISCUSSION

The study obtained PVA/sodium alginate microspheres containing a *Calendula officinalis* flower extract (Fig. 1), which were then incorporated in polymer matrices based on starch and sodium alginate. The efficiency of incorporating the extract was 12.8 ± 3.0 mg/g. The extract release was completed after 105 minutes.

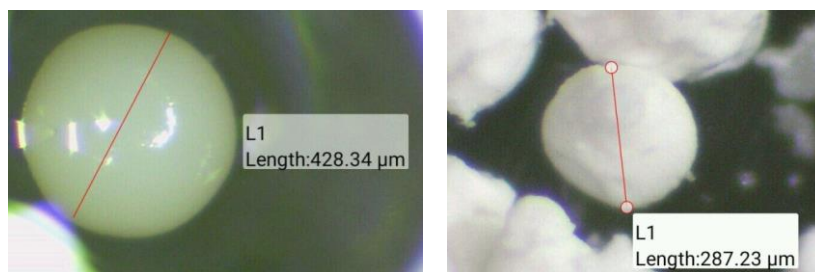


Fig. 1. Microspheres: A – swollen, B – dry

The properties of the polymer films can be modified by changing the polymer composition or by adding plasticizers and microspheres. Higher starch content caused a decrease in film thickness and reduced their durability, while plasticized films were thicker and exhibited a higher degree of swelling. Films containing microspheres had a higher degree of swelling compared to films without microspheres.

Matrices with added sorbitol were stiffer than those with glycerin, and films with glycerin were the most flexible. The addition of microspheres to the polymer materials slightly increased their stiffness, while the addition of starch reduced the water content in the samples.

Adding starch to the films increased the temperature at which the thermal degradation process proceeded at its maximum rate. Thermal degradation was accelerated in the presence of plasticizers, with matrices containing glycerin showing lower thermal stability. The degradation process in PBS buffer proceeded faster with increasing starch content, while the addition of plasticizers and microspheres did not affect the degradation in a buffer with pH 5.4 (corresponding to the pH value of the skin).

These materials can become the basis for developing new forms of cosmetic and dermatological preparations. Application tests of the obtained materials with the participation of a group of probands are planned shortly to determine their cosmetic effect, considering skin parameter tests.

Acknowledgment

This work has been financially supported by National Science Centre (NCN, Poland) Grant no. UMO-2016/21/D/ST8/01705.

References

- 1) S.S. Ayyaril, A. Shanableh, S. Bhattacharjee, M. Rawas-Qalaji, R. Cagliani et al, Results in Engineering, **18**, 101094 (2023)
- 2) G. Nelson, International Journal of Pharmaceutics, **242**, 55-62 (2002)
- 3) N. Devi, M. Sarmah, B. Khatun, T. Maji, Advances in Colloid and Interface Science, **239**, 136-145 (2017)
- 4) G.L. Zobot, F. Schaefer Rodrigues, L. Polano Ody, et al, Polymers, **14**, 4194 (2022)

EFFECT OF ACCELERATED THERMAL DEGRADATION OF POLY(VINYL CHLORIDE): THE CASE OF UNPLASTICIZED PVC

Marwa Saad¹, Marek Bucki², Sonia Bujok³, Dominika Pawcenis¹, Tjaša Rijavec⁴, Karol Górecki¹, Łukasz Bratasz³, Irena Kralj Cigič⁴, Matija Strlič⁴, Krzysztof Kruczala^{1*}

¹Faculty of Chemistry, Jagiellonian University in Krakow, Krakow, Poland

² Doctoral School of Exact and Natural Sciences, Jagiellonian University, Krakow, Poland

³ Jerzy Haber Institute of Catalysis and Surface Chemistry, PAS, Kraków, Poland

⁴ Faculty of Chemistry and Chemical Technology, University of Ljubljana, Ljubljana, Slovenia
kruczala@chemia.uj.edu.pl

INTRODUCTION

The extensive development of polymeric materials, where the main or the only ingredients are synthetic polymers, is one of the twentieth century's biggest technological and industrial achievements. Thanks to the great variety of forms, colors and textures, ease of molding and modification, commercial polymer materials have also found their way into artists' studios. However, the plastics undergo degradation, which leads to changes in chemical, physical and mechanical properties. In the case of unplasticized poly(vinyl chloride), one of the most commonly used plastics, chemical changes primarily involve dehydrochlorination, leading to polyene sequence formation and thus yellowing of PVC objects over time (1,2). Most literature related to the thermal degradation of rigid unplasticized PVC deals with the degradation mechanisms at 120-200 °C range (3), i.e. significantly different than typical environmental conditions encountered in museums. Less attention has been paid to artificial thermal degradation at moderate temperatures and relatively high relative humidity that could be more representative of the conditions of the museum environment. Therefore, in this study we focused on unplasticized PVC stabilized with organotin which was artificially degraded at lower temperatures, 60 °C and 80 °C. This study aims to establish a link between structural changes associated with discoloration with the potential risk of damage to PVC objects in heritage collections.

EXPERIMENTAL

Materials: The commercial stabilized rigid PVC samples were used.

Preparation: Accelerated degradation was performed in a climate chamber for up to 32 weeks at 60 and 80°C, relative humidity (RH) 20 and 60% and without humidity control (<7% RH).

Mechanical and physio-chemical characterization: Raman and ATR-FTIR spectroscopies were used to study chemical changes in polymer chains, whereas paramagnetic resonance spectroscopy (EPR) was used to detect the formation of the radicals. SEM and XPS were used to examine the surface compositions. Color changes and yellowing index were determined with the color analyzer ColorQuest, while UV-Vis spectrophotometry was employed to quantify the number of polyene sequences. The distribution of molar mass and change in molecular weight was determined by size exclusion chromatography (SEC). The mechanical properties of PVC samples were investigated using dynamic mechanical analysis (DMA).

RESULTS AND DISCUSSION

The unplasticized PVC was used to separate the effect of thermal degradation on PVC mechanical properties from the changes due to plasticizer migration. The investigated PVC1 samples contained 0.10% tin from the stabilizer, as determined by ICP-MS. The ATR-FTIR spectra confirmed the presence of PVC and organotin stabilizer however, no significant difference was observed during degradation at both temperatures (60°C and 80°C). Then, the color changes during thermal degradation were investigated since they are highly noticeable to the naked eye, and thus of high significance to museum objects. PVC samples degraded at

60 °C do not exhibit apparent color changes, whereas, increasing the temperature to 80 °C results in visible yellowing of the samples. Raman spectroscopy demonstrated greater sensitivity to polyene formation, with the appearance of peaks attributed to the ν_1 (C-C=C) and ν_2 (C-C=C) stretching vibrations (1100 cm^{-1} and 1514 cm^{-1}) after a six-week degradation at 80 °C in the absence of humidity control. These peaks became increasingly discernible at 80 °C and 60% RH. As indicated by the UV-Vis results, there was not only an increase in the number of carbon-carbon double bonds but also an increase in the length of polyenes. For the sample subjected to aging at 80 °C without humidity control for a duration of 22 weeks, the formation of 14 conjugated double bonds was evident (absorption at 521 nm). The SEC findings indicated that there were no statistically significant changes in the molecular weight of PVC after artificial aging for up to 22 weeks. Consequently, it can be concluded that neither chain scission nor cross-linking occurs during artificial aging under these conditions. Similarly, 22 weeks of artificial degradation, did not affect the stiffness of rigid PVC, however, rigid PVC degraded at 80 °C and 60% RH became stiffer after a prolonged time of treatment. Assuming constant average conditions of 20 °C and 60% RH, expected time to color change which is considered as damage ($\Delta b = 15$), lifetime of the unplasticized PVC is ca. 36 years and the expected increase in the material's stiffness will be only of ca 2.0%, so we conclude that even extensive discoloration of the PVC does not contribute significantly to a higher risk of mechanical damage due to large external loads (impact) during handling or transportation. The water contact angle showed an increase in of surface hydrophilicity of the rigid PVC aged due to partial oxidation and formation ionic chlorine, as confirmed by XPS results presented in **Figure 1**.

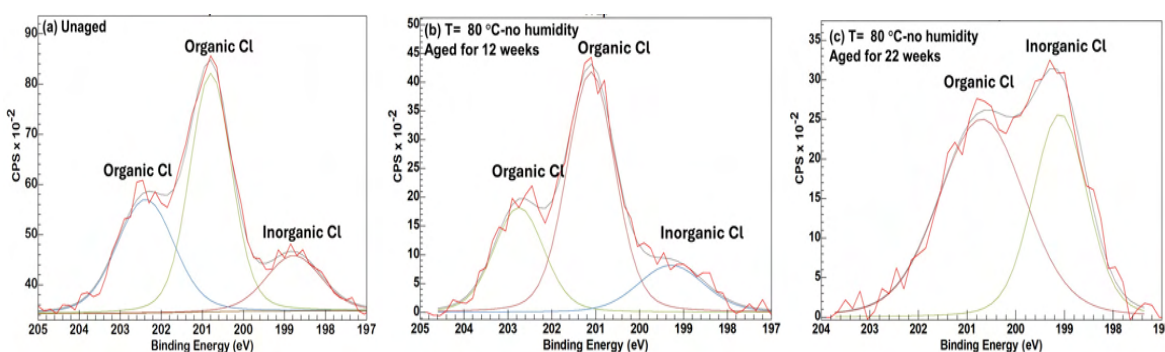


Figure 1. The Cl $2p_{3/2}$ and Cl $2p_{1/2}$ XPS spectra of PVC (a) unaged, (b) degraded for 12 weeks and (c) for 22 weeks at 80 °C without humidity control.

The EPR spectra of not degraded samples has only a broad signal around $g=2.02$, which was stable for 22 weeks, except where PVC were degraded at 80 °C at R.H=60. In this case the signal completely disappears after 18 weeks. However, the most interesting observation was appearance of the peak with $g=2.003$, which can be assigned to stable radicals formed in the sample. It was visible even in the samples degraded at 60 °C and 60% and become evident after 10 weeks degradation at 80 °C and 60%RH. This finding indicates that the radical mechanism of PVC degradation may be a factor even at relatively low temperatures.

Acknowledgment

The research is carried out within the OPUS LAP 20, National Science Centre, Poland 2020/39/I/HS2/00911 and Slovenian Research Agency, N1-0241 project, CEUS scheme. The infrastructure funded by the European Union in the framework of the Smart Growth Operational Programme, Measure 4.2; Grant No. POIR.04.02.00-00-D001/20, was used.

References

- 1) T. Rijavec, D. Pawcenis, K. Kruczala, M. Strlič, I. Kralj Cigić. *Herit, Sci.* 11, 155 (2023)
- 2) M. Saad, S. Bujok, K. Kruczala, *Spectrochimica Acta Part A*, 322 (2024) 124769
- 3) G. Wypych, *PVC degradation & stabilization*, Chemtec Publishing (2020).

INJECTION MOLDING OF POLYMER-ALUMINIUM NANOCOMPOSITES TO TUNE OPTICAL PROPERTIES

**Federica Moretti^{a*}, Matthieu Fischer^c, Stefano Fornasaro^b, Andreas Leuteritz^c,
Ines Kühnert^c, Vanni Lughi^a, Paola Posocco^a**

^a Department of Engineering and Architecture, University of Trieste, Italy

^b Department of Chemical and Pharmaceutical Sciences, University of Trieste, Italy

^c Department of Processing Technology, Leibnitz Institute of Polymer Research Dresden,
Germany

*federica.moretti@phd.units.it

INTRODUCTION

Polymeric nanocomposites are widely used to improve the properties of polymeric materials. Based on the aim of such modification, a lot of factors may come into play. Among those, the chosen process can greatly impact the results¹.

Aluminium flakes may be used as fillers to engineer the optical and mechanical properties of polymers. Despite their potential in functional applications, polymeric nanocomposites filled with aluminium are mainly used as design product to obtain polymers with a metallic finish².

A Design of Experiments (DoE) approach was implemented to study how to tune the injection molding parameters in order to reach the desired optical and mechanical properties³.

EXPERIMENTAL

Materials

All nanocomposites in this study were made of a polymeric matrix with high light transmittance (PMMA, PP, or ABS) filled with aluminium flakes. Four different types of aluminium flakes were considered, based on the combination of two possible diameters and two possible carriers (erucamide wax or Parol mineral oil). The carrier is present in the aluminium powder due to safety reasons.

Preparation

A total of thirty combinations of the chosen parameters were selected by DoE for each matrix; for each combination, platelets of fixed dimensions were produced via injection molding. The variables considered for this experiment involve both aspects of the material composition (such as concentration and dimension of the flakes) and the process parameters (such as temperature and pressure).

Characterization

Optical properties in the visible spectrum of all the produced platelets were assessed using a Cary60 UV-vis from Agilent Technologies. All samples were at first observed by optical microscopy (Nikon H550L). Their morphology was characterized by SEM (Gemini300, Zeiss) and AFM (Solver PRO, NT-MDT) in order to get a local and very refined description, as well as by profilometry to achieve a more statistical and comprehensive picture.

RESULTS AND DISCUSSION

The optical properties were considered as the response variable for the realization of the DoE data driven model. Within the range of factors considered, the estimate made by the model is optimal and enables the prediction of the optical properties of specimens produced with parameter combinations that have not been realized experimentally.

Moreover, most of the parameters considered have a relevant effect on the morphology. For example, a higher temperature of the mold may promote a reduction of the roughness. However, the effects are strongly related to the considered matrix. Therefore, there is not a unique recipe to reach the desired goal, but the process and the material composition should be tailored to the chosen matrix.

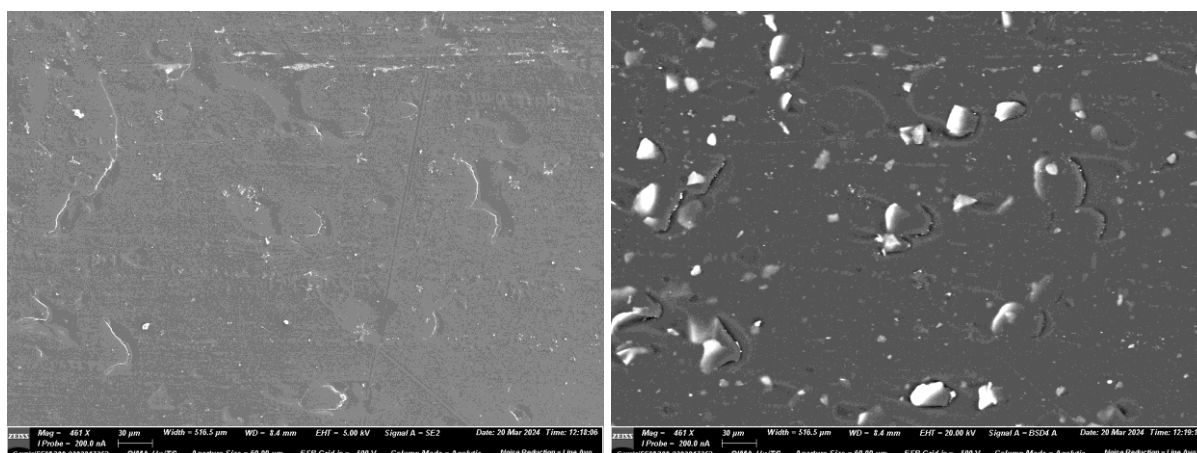


Fig. 1 SEM images of a sample prepared with a PP matrix and 1% in weight concentration of aluminum flakes with 11 microns diameters. The picture on the left was acquired using an accelerating voltage of 5kV and the signal from secondary electrons to highlight the morphology of the surface, whereas the picture on the right was acquired using an accelerating voltage of 20kV and the signal from backscattered electrons to see the aluminium flakes under the polymer.

Overall, the results underline how a fine tuning of the process is necessary to improve the optical properties of the nanocomposite. The aim should be the increase of the temperature of the mold while reducing the final warpage of the part. Indeed, the optical properties would benefit from a reduction of the surface roughness.

Furthermore, the concentration of the aluminium flakes turned out to be a key parameter. Of course, their presence is what enables to boost the optical properties of the material, however a significant increase in this parameter leads to the increase in the number of surface defects. Hence, there is an optimum value of the flakes' concentration, which establishes a tradeoff between the optical properties and the defects formation.

Acknowledgment

Fellowship co-funded by the Italian Recovery and Resilience Plan (PNRR) – NextGeneration EU. This work has also been technically and financially supported by Honeywell Pittway Tecnologica Trieste.

References

1. Omanovi, E., Badnjevi, A., Kazlagi, A. & Hajlovac, M. Nanocomposites: A Brief Review. *Health Technol. (Berl)*. **10**, 51–59 (2020).
2. Park, S. H. & Lyu, M. Y. Observation of Two-Dimensional Shaped Aluminum Flake Orientation During Injection Molding and Its Orientation Mechanism. *Macromol. Res.* **27**, 481–489 (2019).
3. Rios, P. *et al.* Impact of Injection-Molding Processing Parameters on the Electrical, Mechanical, and Thermal Properties of Thermoplastic/Carbon Nanotube Nanocomposites. *J. Appl. Polym. Sci.* **120**, 70–78 (2011).

MICROPLASTICS AND NANOPLASTICS: MAIN SOURCES AND ISSUES

M. Morreale and F.P. La Mantia*

Department of Engineering and Architecture, Kore University of Enna, Cittadella Universitaria, Enna, Italy

* National Interuniversity Consortium of Materials Science and Technology (INSTM), Via Giusti, Florence, Italy and Department of Engineering, University of Palermo, Viale delle Scienze, Palermo, Italy

marco.morreale@unikore.it, francescopaolo.lamantia@unipa.it

INTRODUCTION

The increasing utilization of polymer-based goods has been showing its downsides and threats in terms of environmental impacts. Unfortunately, due to unsatisfactory recycling procedures and rates, and the lack of biodegradability of traditional polymers, the persistence of plastics in the environment can eventually lead to the formation of microplastics (particles with size < 5 mm), having several and threatening environmental impacts on soil, fresh waters, sea waters, air. A further concern is the possible formation and/or release of smaller size particles, i.e. nanoplastics, which are potentially even more dangerous for the environment and living organisms.

Microplastics (and, to some extent, nanoplastics) can usually come from two main pathways, i.e. intentional or unintentional use/release into the environment, the first mainly involving scrubbers, additives, pellets etc., the second involving degradation phenomena of larger plastic items but also release from tear and wear of paints, tires and textiles during their life cycle.

There are, in summary, several mechanisms and sources involved, which in turn require accurate classifications and complicate the full understanding of the problems linked to the environmental release of these kinds of pollutants, and the development of adequate strategies for containment.

EXPERIMENTAL

In this work, we carried out an extensive Literature review, aimed at providing a synthetic overview of the main aspects regarding the sources of microplastics and nanoplastics release into the environment, their nature, some of the consequences for the environment (especially, marine environment) and possible mitigation pathways.

RESULTS AND DISCUSSION

The review of numerous literature sources pointed out that, in partial divergence from the public opinion's perception and despite some allegations from certain think-tanks or environmental protection groups, there is still not a sufficiently strong and accepted evidence that microplastics and, even more, nanoplastics related pollution is significantly affected by the commercial use of polymer packaging, while much more significant sources seem to be paints, tires, and textiles.

References

- 1) I.O. Musa, H.S. Auta, et al., *Int. J. Environ. Res.*, **18**, 1 (2024)
- 2) European Commission. *EU Action Against Microplastics*, Publications Office of the European Union (2023)
- 3) F. Degli Innocenti, *J. Hazard. Mater.*, **463**, 132923 (2024)

3D PRINTED AND COMPRESSION MOLDED BIO-COMPOSITES BASED ON OFI WASTE AND BIODEGRADABLE POLYMERS FOR NPK FERTILIZER CONTROLLED RELEASE

Roberto Scaffaro, Maria Clara Citarrella, Emmanuel Fortunato Gulino

Department of Engineering, University of Palermo, Viale delle Scienze, ed. 6, 90128 Palermo, PA, Italy
roberto.scaffaro@unipa.it, mariaclara.citarrella@unipa.it; emmanuelfortunato.gulino@unipa.it;

INTRODUCTION

Ecological problems arise from excessive fertilization due to leaching issues. To address this and promote agricultural sustainability, an innovative green composite for controlled release fertilizers was developed. This composite was produced by adding NPK fertilizer flour to a biodegradable polymer, with or without *Opuntia Ficus Indica* (OFI) particles. By appropriately selecting the particle size, adding OFI, and choosing the production technique, it was possible to modulate the NPK release rate: FDM samples containing fine particles of OFI and NPK showed the fastest release. Release data were modeled according to the Peppas-Korsmeyer model to understand the release mechanism.

EXPERIMENTAL

Materials

The matrix used to prepare the composites was a sample of Mater-Bi® EF51L (MB), supplied by Novamont SpA (Novara, Italy) a polymer based on blends of aromatic and aliphatic biodegradable co-polyesters which composition is proprietary. OFI cladodes, supplied by Bio Ecopuntia (Italy), were washed, ground, meshed and vacuum-dried overnight at 90 °C to remove any residual vegetation water. NPK 12-12-17 (supplied by Flortis, Orvital S.p.A.) was used as releasable fertilizer.

Preparation

OFI and NPK were separately grinded and the obtained particles were sieved selecting two different mesh sizes: under 75 µm (labeled as OFI-A and NPK-A) and from 75 µm to 300 µm (labeled as OFI-B and NPK-B). Particle size were selected to be suitable for the 3D printer preventing nozzle obstruction. The amount of filler to prepare hybrid biocomposites (ones containing both OFI and NPK) was chosen with the aim to not overcome total amount of filler of 20 wt.% [1,2]. Six formulations namely MB/OFI-A, MB/OFI-B, MB/NPK-A, MB/NPK-B, MB/OFI-A/NPK-A and MB/OFI-B/NPK-B were produced by melt mixing.

The obtained blends were then extruded using a cylindrical nozzle to obtain filaments. Plaques for further characterization tests were obtained by compression molding using a laboratory press. The samples were also printed using a Sharebot Next Generation (Italy) 3D printer.

Characterizations

Morphological analysis was performed before and after NPK release through Phenom ProX (Phenom-World, The Netherlands) scanning electron microscope (SEM). Mechanical performance of the samples was investigated by tensile tests by using an Instron 3365 machine (UK) in tensile mode and equipped with a 1kN load cell.

Release of NPK fertilizer

Electrolyte resistance of the obtained solution was evaluated through electrochemical impedance spectroscopy (EIS) using an AMETEK potentiostat/galvanostat (model PARSTAT 2273) and Power Suite software. The obtained release data were fitted according to the Peppas-Korsmeyer equation.

RESULTS AND DISCUSSION

The final devices were successfully fabricated both for compression molding and FDM using all the prepared formulation. Both filler and fertilizer displayed good dispersion in the composites, excellent adhesion with the polymeric matrix and effectively acted as reinforcement (Figure 1).

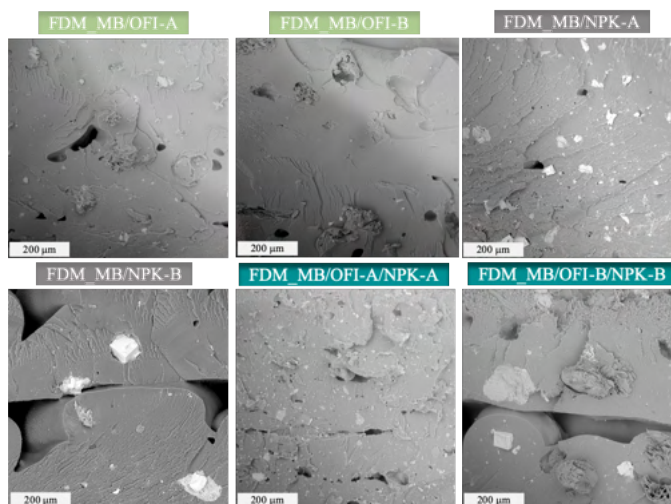


Figure 1 SEM micrograph of fractured cross-section of green composites and CRF devices fabricated for FDM.

FDM samples showed higher mechanical properties if compared with compression molded ones. Release tests of CRF devices reveal the ability of all the obtained composites to slow the release rate of NPK (up to 30 days), which proved to be tunable by modifying formulation, flours granulometry and production techniques. The porous structure of FDM samples, induced by the process itself, promote the water transport across the devices allowing the release of the NPK also from the more inner layer. In particular, FDM_MB/OFI-A/NPK-A act as the best CRF device showing a remarkable burst delivery with about 70% of NPK released in the first 24 hours and a 100% release after 30 days (Figure 2).

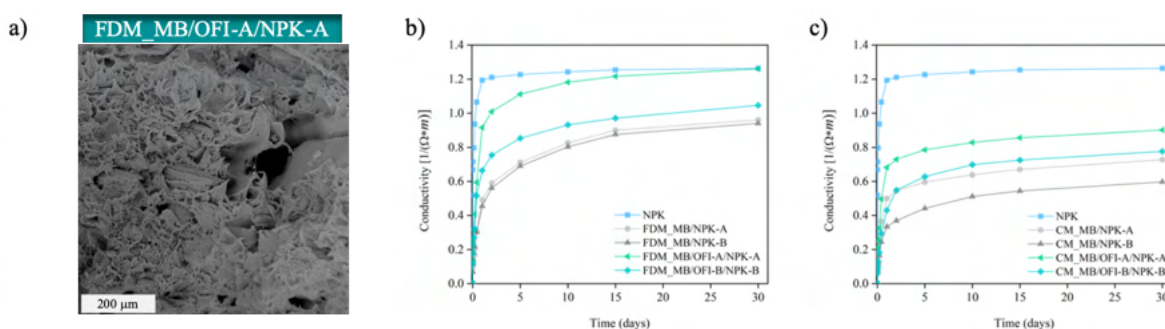


Figure 2 SEM micrograph of FDM sample after soaking in water for 30 days (a). Fertilizer release monitoring by conductivity measurements as function of time for FDM (b) and compression molded CRF devices (c).

References

- [1] Scaffaro R, Citarrella MC, Gulino EF, Morreale M. Hedysarum coronarium-Based Green Composites Prepared by Compression Molding and Fused Deposition Modeling. *Materials* 2022;15. <https://doi.org/10.3390/ma15020465>.
- [2] Scaffaro R, Gulino EF, Citarrella MC, Maio A. Green Composites Based on Hedysarum coronarium with Outstanding FDM Printability and Mechanical Performance. *Polymers* 2022, Vol 14, Page 1198 2022;14:1198. <https://doi.org/10.3390/POLYM14061198>.

Acknowledgement

PROGETTO DI RICERCA DI RILEVANTE INTERESSE NAZIONALE (PRIN) P2022K9XN3 "New recyclable thermosetting and elastomeric polymeric materials based on bio-renewable feedstocks" - Finanziato dall'Unione europea - NextGenerationEU

HYALURONIC ACID/TANNIC ACID FOR APPLICATIONS AS WOUND-DRESSINGS

L. Zasada¹, M. Wekwejt², M. Małek³, A. Ronowska⁴, A. Michno⁴, A. Pałubicka⁵, A. Klimek⁶, B. Kaczmarek-Szczepańska¹,

¹ Department of Biomaterials and Cosmetics Chemistry, Faculty of Chemistry, Nicolaus Copernicus University in Torun, Poland;

² Department of Biomaterials Technology, Faculty of Mechanical Engineering and Ship Technology, Gdansk University of Technology, Poland

³ Faculty of Civil Engineering and Geodesy, Military University of Technology, Poland

⁴ Department of Laboratory Medicine, Medical University of Gdansk, Poland

⁵ Department of Laboratory Diagnostics and Microbiology with Blood Bank, Specialist Hospital in Kościerzyna, Poland

⁶ Faculty of Mechanical Engineering, Military University of Technology, Poland
503555@doktorant.umk.pl (L.Z.); beata.kaczmarek@umk.pl (B.K-S.)

INTRODUCTION

Hyaluronic acid and tannic acid have natural origin (1) and are characterized as biocompatible and biodegradable (2), which attracts a significant scientific interest. As an extracellular matrix component, hyaluronic acid promotes cell proliferation, angiogenesis, and tissue regeneration (e.g. wound healing). Tannic acid, composed of glucose and gallic acid molecules (3), presents antibacterial and antioxidant properties, as well as biocompatibility. As evidenced, tannic acid supports skin regeneration, e.g. in the treatment of burns (4). They were selected by us as components of novel biomaterials. The aim of the study was to obtain and characterize hyaluronic acid/tannic acid films to evaluate their safety for use as wound dressings.

EXPERIMENTAL

Materials

Hyaluronic acid (HA, $M_v = 1.8 \times 10^6$ g/mol) and 2,2-Diphenyl-1-picrylhydrazyl were purchased from Sigma-Aldrich. Tannic acid (TA, $M_w = 1701.23$ g/mol) and acetic acid (98 %) were purchased from the ROTH company. MTT (3-(4,5-dimethylthiazol-2-yl)-2,5-diphenyltetrazolium bromide) and (S)-lactate: NAD + oxidoreductase (lactate dehydrogenase, LDH, EC 1.1.1.27) assays, culture medium (Ham's F12 and Dulbecco's Modified Eagle's), gentamicin disulfate salt (G418), fetal bovine serum (FBS) and Triton X-100 were purchased from the Merck company.

Preparation

Hyaluronic acid and tannic acid were dissolved in 0.1 M acetic acid at 1 % concentration, separately. The solutions were mixed in three weight ratios (HA/TA):80/20, 50/50, and 20/80. Such mixtures were placed on the magnetic stirrer and mixed for 2 h. All the mixtures were placed on the plastic holder (40 mL per 10 cm × 10 cm).

Hemocompatibility, cytocompatibility, and antibacterial activity

Hemocompatibility and cytocompatibility were tested on human RBCs and osteoblasts (hFOB 1.19), with films sterilized and tested for hemolysis and cell viability using MTT and LDH assays. Antibacterial activity was evaluated against *Staphylococcus aureus* and *Escherichia coli* by measuring bacterial growth turbidity.

RESULTS AND DISCUSSION

The results showed that films had no negative effect on human erythrocytes, with low hemolysis and LDH release. While 20HA/80TA and 80HA/20TA inhibited cell growth by ~50%, they were not cytotoxic (Fig. 1). The 50HA/50TA film was the most biocompatible. All films had antibacterial properties against *Staphylococcus aureus* and *Escherichia coli*, with 50HA/50TA most effective against *Staphylococcus aureus* and 20HA/80TA against *Escherichia coli* (Fig. 2).

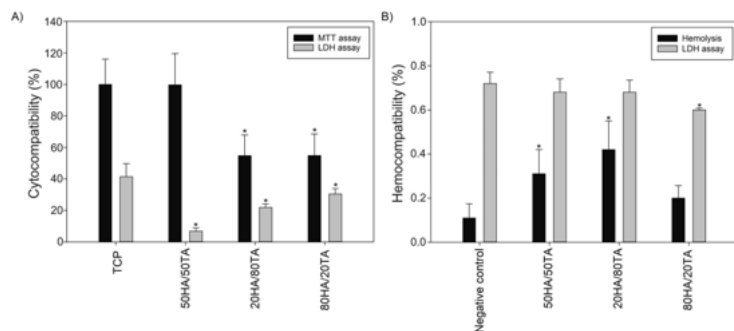


Fig. 1. The effect of the developed films on cytocompatibility after 72 h of culture and hemocompatibility after 24 h exposure to films (n = 4, * significantly different from the respective controls (p < 0.05)).

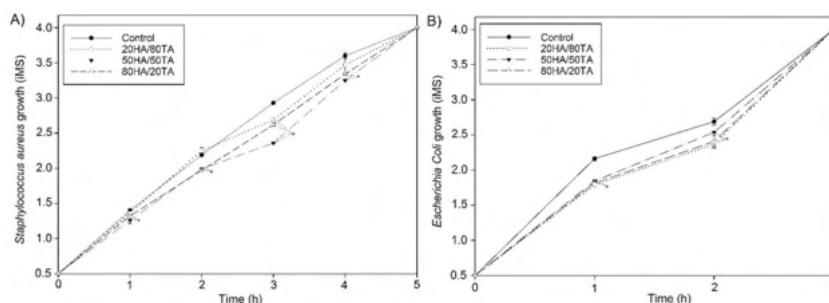


Fig. 2. Bacterial growth inhibition:
A) *Staphylococcus aureus* and B) *Escherichia coli* (n = 3; * significantly different from control (p < 0.05)).

Tannic acid (TA) inhibits MMP-2/-9 activities, aiding tissue remodeling and wound healing through interactions such as H-bonds and metal-organic coordination bonds. Hyaluronic acid (HA) and TA are biocompatible and FDA-approved, with developed films showing hemocompatibility and cytocompatibility, particularly the 50HA/50TA composition. The films also demonstrated antibacterial properties, especially against *Escherichia coli* and *Staphylococcus aureus*, likely due to TA's phenolic hydroxyl groups. The 50HA/50TA film was deemed most suitable for medical applications, offering balanced mechanical properties, biocompatibility, and effective antibacterial action.

Acknowledgment

This research was funded by Nicolaus Copernicus University in Torun (grant number 282/2021 IDUB) (B.K.S.). We wish to express our deep gratitude to Aleksandra Laska for the technical assistance in nanoindentation tests.

References

- 1) R. Bahrami, R. Zibaei, Z. Hashami, S. Hasanvand, F. Garavand, M. Rouhi, S.M. Jafari, R. Mohammadi, Crit. Rev. Food Sci. Nutr. **62**, 1936–1950 (2022)
- 2) R. Uppal, G.N. Ramaswamy, C. Arnold, R. Goodband, Y. Wang, J. Biomed. Mater. Res. B Appl. Biomater. **97B**, 20–29 (2011)
- 3) S. Grabska, A. Sionkowska, B. Kaczmarek, Mol. Cryst. Liq. Cryst. **670**, 90–96 (2018)
- 4) J. Xu, Y. Li, Y. Chen, L. Wang, M. Liao, J Biomater Sci Polym Ed. **32**, 1927–1943 (2021)

Polymer pyrolysis pathways affecting the characteristics of polymer combustion

E.Nakashima*, T. Fuji and T. Ueno

*School of Engineering, Chubu University, Kasugai, Aichi, Japan
Graduate School of Engineering, Nagoya University, Nagoya, Japan
e-nakashima@isc.chubu.ac.jp, fujii@isc.chubu.ac.jp, ueno.tomonaga@material.nagoya-u.ac.jp

INTRODUCTION

Polymeric materials have become increasingly popular in various applications due to their outstanding mechanical properties. However, their high flammability is one of their drawbacks, which can lead to fire accidents. Since the 1940s, researchers have focused on flame retardancy in polymeric materials to overcome this issue. Yet, conventional flame retardant research has been limited to qualitative evaluations based on standardized tests.

Our research team has developed an analysis program that overcomes the limitations of traditional methods for studying the combustion behavior of polymeric materials in a vertical flame test. This new analysis method provides longitudinal data on the combustion behavior of polymeric materials in time series during the vertical flame tests and extracts characteristic data to quantify the combustion behaviors of different resins quickly. Accumulating highly validated numerical data will significantly advance research on the combustion of polymeric materials and allow for a deeper understanding of the vast amount of information on the combustion state in the time series. We are expected to accelerate research on the flame retardants of polymeric materials.

EXPERIMENTAL

Materials

This study used nine different types of injection-grade resins. The polyethylene (PE) resin used was Nipolon Hard 4010 ($M_w = 76,000$), manufactured by Tosoh Corporation. The polypropylene (PP) resin used was Isotactic PP ($M_w = 250,000$) manufactured by Sigma-Aldrich. The polystyrene (PS) resin used was $M_w = 350,000$, manufactured by Sigma-Aldrich. The polymethyl methacrylate (PMMA) resin used was manufactured by Sigma-Aldrich. The polymethyl pentene (PMP) resin used was manufactured by Sigma-Aldrich. The polybutylene terephthalate (PBT) resin used was DURANEX 2000 manufactured by Polyplastics Co., Ltd. The polyacetal (POM) resin used was Tenac-C manufactured by Asahi Kasei. The polycarbonate (PC) resin used was SD POLYCA200-20 ($M_w = 23,000$) manufactured by Sumika Polycarbonate Co., Ltd. Finally, the modified polyphenylene ether (PPE) resin used was S201A manufactured by Asahi Kasei Co., Ltd.

Vertical flame test

The sample was hung vertically during the experiment and heated from the bottom until it caught fire. Afterward, the Bunsen burner was quickly separated from the specimen to examine the flame behavior at the beginning of the combustion process. The flame behavior was captured at 60 frames per second using a single-lens reflex digital camera (Z30, Nikon Corporation, Tokyo, Japan) against a black background without any light reflection. FHD video was recorded under these conditions: 1/125 s, F3.5, and ISO 2500.

Extraction of combustion behavior features and discriminant analysis

Our research group has developed an image analysis program using MATLAB to quantitatively analyze the behavior of flames of different polymers during the vertical flame test [1,2]. The analysis was performed by cutting out a frame on a 1500×370 pixel area

centered on the specimen from the FHD video. The analysis extracted the following 14 combustion state characteristics. Using the extracted data, we distinguished between polymeric materials automatically by canonical discriminant analysis using IBM's SPSS statistical software.

RESULTS AND DISCUSSION

In Figure 1, the results of the image analysis of the combustion behavior of PE and PMMA are presented. Throughout the combustion, the top flame height for PE remains below 200 mm, with a gradual shift towards the upper side. There is a high dripping frequency, and the melt is continuous for approximately 30 seconds after ignition. On the other hand, PMMA exhibits a faster rise rate at the upper flame edge (6.8 mm/s), reaching a top flame height of 200 mm in about 20 seconds after ignition. The first drip time is 20 seconds and it is longer than PE. The combustion flame for PMMA is located above the lower edge of the sample and is completely extinguished in about 60 seconds. It is evident that the combustion conditions differ significantly when comparing PE and PMMA, which is closely related to the pyrolysis of polymers.

The pyrolysis of PE occurs through two main pathways: random cleavage of the main chain and cleavage from the ends [3]. When the main chain undergoes pyrolysis, it reduces the molecular weight and produces a high frequency of drips, which then burn up in a series of melts. On the other hand, cleavage from the terminal end forms a monomer when cleavage occurs at the β -position from the radical terminal and a trimer when cleavage occurs at the β -position by 1,5-radical transfer. Meanwhile, PMMA demonstrates pyrolysis behavior that resembles depolymerization, with a prominent occurrence of end-cleavage. The flame has a tendency to spread, and the upper part of the flame moves upward more quickly. As main chain cleavage is less probable, the reduction in molecular weight loss is smaller, and the frequency of dripping is decreased because of the higher viscosity.

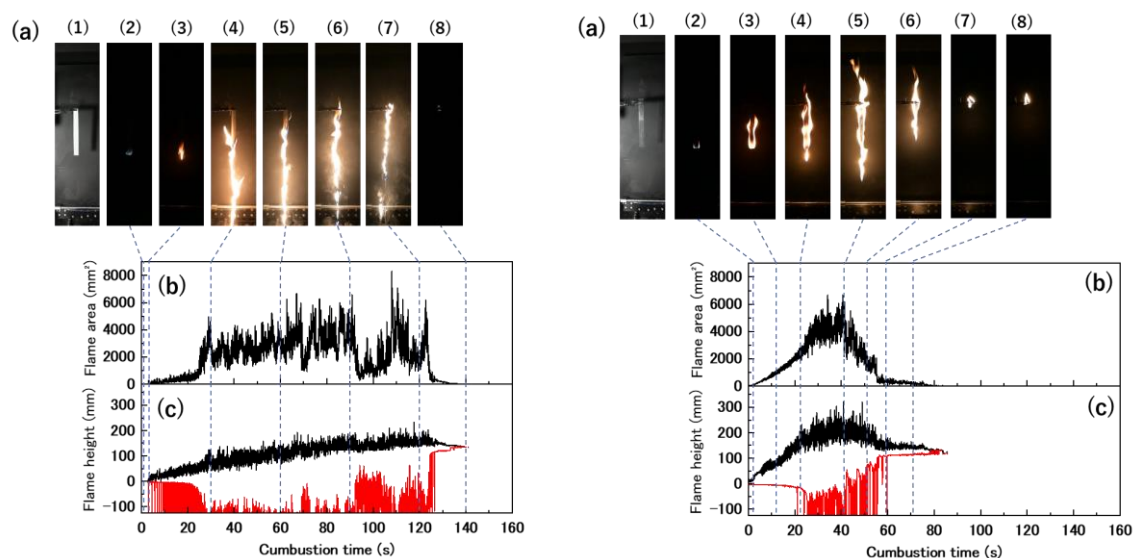


Fig 1 Digital analysis of the combustion behavior by time series (left: PE, right: PMMA)

Acknowledgment

This work is supported by JSPS KAKENHI Grant Number 22K04625. Nagoya University also partially supports it.

References

- [1] Hosokawa, Y., Nakashima, E. & Ueno, T. J. Appl. Polym. Sci. 138, (2020).
- [2] Nakashima, E., Hosokawa, Y. & Ueno, T. J. Appl. Polym. Sci. 140, e54511 (2023).
- [3] Ueno, T., Nakashima, E. & Takeda, K. Polym. Degrad. Stab., 95(9), 1862 (2010).

ULTRAVIOLET IRRADIATION EFFECT AT DRY AND WATER IMMERSION CONDITIONS ON PLA/PBAT COMMERCIAL FILMS

K. Gutiérrez-Silva¹, R. Muñoz-Espí², C.M. Gómez², M. Culebras², O. Gil-Castell¹, J.D. Badia^{1,*}

¹Materials Technology and Sustainability Research Group (MATS). Department of Chemical Engineering, Universitat de València. Av. de la Universitat, s/n 46100 Burjassot, València, Spain.

²Institute of Material Science (ICMUV). Universitat de València. Carrer del Catedràtic José Beltrán Martínez, 2, 46980 Paterna, València, Spain

karen.gutierrez@uv.es, rafael.munoz@uv.es, clara.gomez@uv.es, mario.culebras@uv.es, oscar.gil@uv.es, jose.badia@uv.es

INTRODUCTION

The search for biodegradable materials has driven the development of polymer blends based on biopolymers, such as PLA and PBAT. These blends, and particularly those of PLA/PBAT, are widely used in applications such as packaging and mulch films. However, the biodegradation times of these materials remain a challenge for end-of-life management, contributing to waste accumulation in treatment centers. This study aims to investigate the physico-chemical consequences of irradiation with ultraviolet (UV), specifically UV-C, as a strategy to enhance the degradation of commercial PLA/PBAT films [1].

EXPERIMENTAL

Materials

Commercial PLA/PBAT-based extruded films (F) with a thickness of 100 μm were supplied by Prime Biopolymers (Paterna, Spain), with different additive percentages, labelled as F, F10 and F20.

Pretreatment process

Films were exposed in a dark chamber equipped with four 15 W UV-C lamps, providing an irradiation intensity of 0.90 mW/cm² at 254 nm wavelength. The films were subjected to both dry conditions (UV-C) and immersion in 20 mL of distilled water (UV-C+H₂O), with exposure times of 24, 48, 72, and 96 h. After exposure, the films were dried until constant weight and stored in darkness for further analysis.

Characterization of morphological, thermal, and optical changes

To evaluate the consequences of the photodegradation process in bulk and surface properties, analytical techniques such as colorimetry, FTIR, and DSC were used. The goal was to observe changes in the material's morphology at both macroscopic and microscopic levels, as well as in its thermal properties.

RESULTS AND DISCUSSION

Figure 1 illustrates the evolution of the L*a*b* indexes of the films after being exposed to UV-C irradiation, both in dry conditions and during immersion. Following irradiation, presumable chain scission and oxidation reactions resulted in a reduction in the optical characteristics, which was manifested as an increase in the yellowing and greening indexes, regardless of the dry or immersion conditions. Particularly in dry conditions, the change in the color was more pronounced the lower the additive percentage. It can also be highlighted that greening was more severe when the films were irradiated in the dry state. However, when irradiated during immersion, the role of the additive percentage was unclear, with the yellowing index increase being more generally relevant.

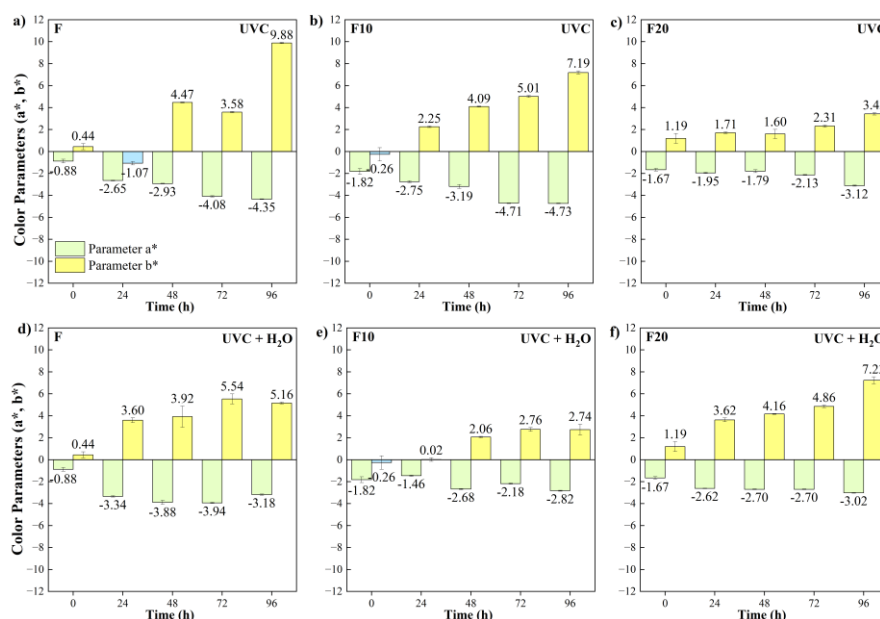


Figure 1. Variation of color parameters (a^* , b^*) for (a) F, (b) F10, (c) F20 films after UV-C irradiation in dry conditions and (d) F, (e) F10, (f) F20 films after UV-C irradiation during immersion.

The FTIR spectra for treated films are shown in Figure 2. The peak at 1709 cm^{-1} decreased, signifying a reduction in the carbonyl group's contribution and the consequent scission of the ester bonds and the creation of shorter molecules. The band at 727 cm^{-1} corresponds to the methylene ($-\text{CH}_2-$) group of PBAT and exhibited a significant decrease after 48 h of irradiation, suggesting that UV-C irradiation can speed up the breakdown of functional groups on the polymer surface [2].

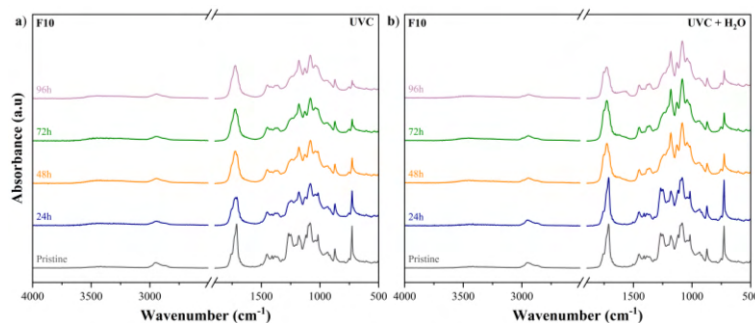


Figure 2. FTIR spectra of the F10 films irradiated after UV-C irradiation in dry conditions and during immersion.

Acknowledgement

The authors would like to acknowledge funding from the Agència Valenciana de la Innovació (AVI) through the INNEST/2022/295 project (BIOFAST-Methodological strategies for the accelerated biodegradation of bioplastics in compost medium).

References

- [1] B. Ciuffi, E. Fratini, and L. Rosi, Plastic pretreatment: The key for efficient enzymatic and biodegradation processes, *Polym Degrad Stab.* **2024**, *222*, 110698.
- [2] Z. Wang, J. Ding, X. Song, L. Zheng, J. Huang, H. Zou and Z. Wang, Aging of poly (lactic acid)/poly (butylene adipate-co-terephthalate) blends under different conditions: Environmental concerns on biodegradable plastic, *Science of The Total Environment.* **2023**, *855*, 158921.

Polysaccharide-based biodegradable polymers for medical applications

V. Ciaramitaro, F. Vitale, E. Piacenza, A. Presentato and D.F. Chillura Martino

Department of Scienze e Tecnologie Biologiche Chimiche e Farmaceutiche, University of Palermo, Viale delle Scienze, Palermo, Italy

veronicaconchetta.ciaramitaro@unipa.it, filippo.vitale02@unipa.it, elena.piacenza@unipa.it, alessandro.presentato@unipa.it, delia.chilluramartino@unipa.it

INTRODUCTION

Biofilm formation on medical devices leads to chronic infections due to antibiotic resistance and is a major challenge in healthcare (1). In this context, several studies have shown that indocyanine green (ICG), an FDA-approved dye, has photodynamic antimicrobial properties, particularly when it forms J-aggregates, which enhance NIR absorption, allowing deeper light penetration into biofilms and enhancing the photodynamic effect (2). To address this, we developed a system capable of releasing J-ICG aggregates, modulating their concentration and release through the porous structure of a polymeric film based on chitosan (CS), sodium alginate (SA) and sodium carboxymethylcellulose (CMC). We studied the interaction and structural changes of ICG within the polymer matrix by IR spectroscopy and X-ray diffraction. We evaluated the dye stability and release kinetics under physiological-like conditions. We also evaluated the swelling capacity, solubility and moisture absorption of the polymer matrix to verify its integrity during application involving contact with an aqueous medium, packaging and storage. The results demonstrated the potential of the developed polymer matrix to release the J-aggregates of ICG for infection treatment from biofilm, thereby enhancing its therapeutic efficacy.

Here, we summarise the preparation of this polymeric film enriched with different amounts of ICG and provide a detailed study of the release dynamics of dye aggregates and the chemical-physical properties of the ICG-enriched film.

EXPERIMENTAL

Materials

The raw materials used in this work were: *chitosan* (CAS 9012-76-4), *sodium alginate* (CAS 9005-38-3), *glycerin* (99.5%, CAS 56-81-5), *acetic acid* (>99.8%, CAS 64-19-2), *sodium carboxymethyl cellulose* (CAS 9004-32-4) and Indocyanine green dye purchased from SIGMA Aldrich. Demineralized water (conductivity <10 $\mu\text{S}/\text{cm}$) was used in all experiments.

Preparation

1.5% (w/v) CS/SA and CMC dispersions were mixed at a CS/SA and CMC weight ratio of 1:1 and stirred magnetically for 30 min. Subsequently, aliquots of 6 g dispersions were cast on Petri dishes (diameter 6 cm) and dried in an oven for 24 h at room temperature. Finally, the polymer films were immersed in 5 ml of a 100 μM , 200 μM and 500 μM indocyanine green dye solution respectively, dried in an oven for 24 h at 30°C, and cooled at room temperature.

Release kinetic and physico-chemical characterization

The release and kinetics mechanism of the dye were studied by UV-Vis-NIR spectroscopy. Interactions and structural investigations were carried out using ATR-FTIR spectroscopy and X-ray diffractometry. The resistance and integrity of the polymeric material in an aqueous medium mimicking physiological conditions (PBS) were determined by tests of the degree of swelling, weight loss and moisture content.

RESULTS AND DISCUSSION

In all cases, the polymer matrix showed good ability as a controlled release system for the ICG dye. At low concentrations of ICG, the dye is released predominantly in its monomeric form, as shown by the UV-Vis-NIR spectra. With increasing dye concentration and prolonged contact with the solvent medium, the system becomes more efficient in releasing J-type aggregates. Among the polymer films tested, those enriched with 200 μM ICG solution seem to mediate a finely tuned release over time, as indicated by the kinetic profiles of ICG aggregates (Fig. 1d), whose release is governed by a time-dependent diffusion. XRD analysis provides further insight into the relationship between the porous structure of the polymeric matrix and the release kinetics of ICG aggregates. The XRD patterns of dye-enriched films show diffraction peaks that are more intense and broader than the reference film, consistent with the higher degree of crystallinity (DC) for films enriched with 100 μM (31%) and 500 μM (31%) ICG. On the other hand, the DC does not change for the film enriched with 200 μM dye (21%), suggesting a different structural organisation of the dye through the porous structure of the polymeric matrix at this concentration, which could justify the immediate release of the J aggregates. In addition, a lower degree of crystallinity indicates a more amorphous structure, characterised by a higher mobility of the polymer chains, which probably allows the dye molecules to arrange themselves head-to-tail (J) rather than face-to-face (H), thus also justifying the higher capacity to inhibit the formation of *S. aureus* biofilms.

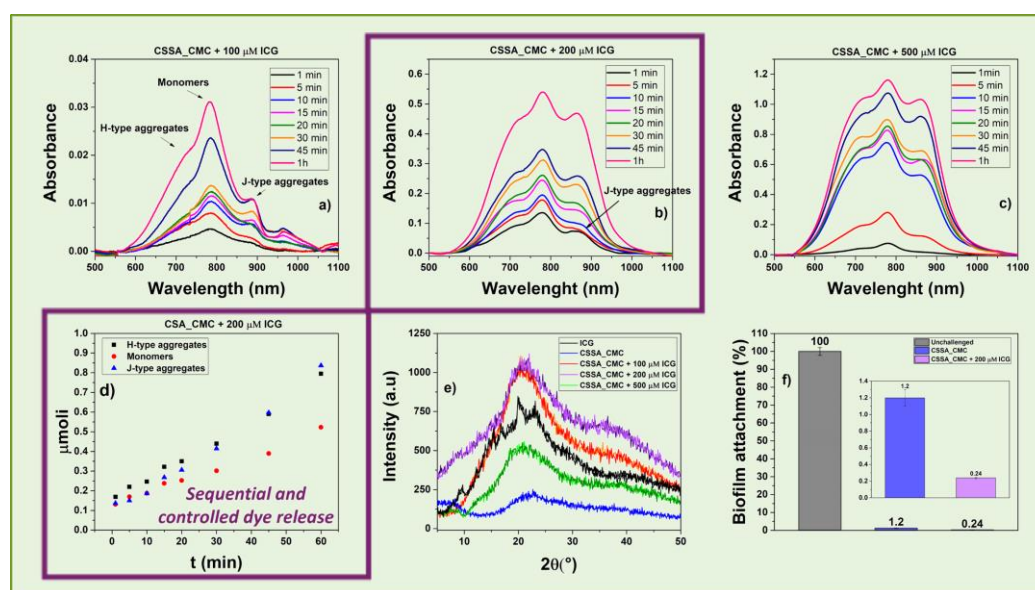


Fig. 1 UV-Vis-NIR spectra of ICG dye released from polymer matrix a) 100 μM b) 200 μM and c) 500 μM and d) release profile of 200 μM ICG from enriched film e) XRD patterns of film enriched f) inhibition of *S. aureus* biofilm formation

Further findings aimed at understanding the physical cross-linking of the polymer matrix and the interactions with the dye molecules, as well as the evaluation of the swelling capacity of the dye-loaded films (data not reported here), show how the amount of dye influences the porous structure of the polymer matrix. Thus, the present study could shed light on how the developed polymer film loaded with appropriate amounts of ICG dye could be used to improve its efficiency in the biomedical field.

References

- 1) G. Koch, et al. Cell, **158**, 1060-1071 (2014)
- 2) M. Pourhajbagher, et al. Journal of lasers in medical sciences, **11**, 187 (2020)

IMPACT OF PRINTING PROFILES ON THERMAL CONDUCTIVITY AND TENSILE STRENGTH IN METAL FUSED FILAMENT FABRICATION

C. Tosto, L. Saitta, R. Barbagallo, I. Blanco, and G. Cicala

Department of Civil Engineering and Architecture, University of Palermo, Via Santa Sofia 64, Catania, Italy

claudio.tosto@unict.it, gianluca.cicala@unict.it

INTRODUCTION

Metal Fused Filament Fabrication (metal FFF) is an emerging technique within Additive Manufacturing (AM) that has garnered significant attention in recent research (1).

Optimizations in the FFF process have led to improvements in the thermal and mechanical properties of the final products (2), which is extremely important for components in power electronics and other applications requiring efficient thermal dissipation, such as heat sinks, power modules, and thermal interface materials.

Researchers have been exploring how various AM process parameters, such as layer thickness and infill flow, affect these properties (3). Despite significant advancements in conventional metal AM techniques, there remains a gap in understanding the correlation between printing profiles and the thermal and mechanical properties of Metal FFF parts. This study aims to investigate the mechanical properties and thermal conductivity of metal parts produced via metal FFF, focusing on different printing profiles provided by the material manufacturer. By establishing a correlation between these properties, the research seeks to optimize the performance of metal FFF components.

EXPERIMENTAL

Materials

In this study, we used an Ultimaker S5 desktop 3D printer (Ultimaker, Utrecht, NL) with a 0.6 mm nozzle designed for composite and abrasive filaments. The 316L stainless steel samples were printed using metal FFF technology with Ultrafuse 316L filament (BASF, Ludwigshafen, GE). To ensure the metal parts reached full density, the green samples were sent to a debinding and sintering (D&S) service for post-processing.

3D printing manufacturing

In their Cura slicing software plugin, BASF set the printing conditions. According to BASF, the printing profiles (Table 1) are designed to deliver quality, flexibility, and reliability for a variety of products and applications using their hybrid polymer-based filament, Ultrafuse.

Table 1. Printing profiles used in this study.

Parameters	Unit	Printing profiles		
		Fast	Strong	Quality
Layer Height	mm	0.2	0.15	0.1
Infill line width	mm	0.6	0.6	0.6
Wall line count	-	2	2	3
Top/Bottom layers	-	1	1	1
Infill density	%	105	105	105

Printing temperature	°C	240	245	240
Wall flow	%	95	100	100
Top/Bottom flow	%	95	105	105
Infill flow	%	95	100	100
Print speed	mm/s	30	25	25

Each profile, detailed in Table 1, is optimized to produce sintered parts quickly (Fast profile), to create strong parts while maintaining productivity (Strong profile), and to ensure excellent quality (Quality profile). These profiles define specific sets of printing parameters that impact the mechanical and thermal properties of the printed samples. Additionally, evaluating the productivity of these three profiles is crucial for cost analysis. The printing times for creating a set of six samples are 61 minutes for the Fast profile, 80 minutes for the Strong profile, and 119 minutes for the Quality profile.

Design of Experiment and Thermo-mechanical characterization

The 3D-printed specimens were evaluated for their thermal conductivity and mechanical properties, specifically tensile strength, to determine if a correlation exists between these properties. The printing profile, referred to as factor A, was selected as the independent variable and varied across three categorical levels: Fast, Strong, and Quality. The dependent variables examined were thermal conductivity (TC) in [W/m K] and Ultimate Tensile Strength (UTS) in [MPa]. Thermal conductivity was measured using Laser Flash Analysis (LFA), and tensile strength was assessed through tensile testing (ASTM E8). Each experimental condition was replicated $n = 3$ times, resulting in a total of $N = 9$ runs per response variable. Once data for the dependent variables were collected, an Analysis of Variance (ANOVA) was performed to determine the statistical significance of the independent variable, i.e., the factor A.

RESULTS AND DISCUSSION

The impact of the selected printing settings, specifically the printing profiles (factor A), on the thermal conductivity (TC) and ultimate tensile strength (UTS) of the specimens was analyzed using ANOVA. The results are detailed in Tables 3 and 4 for TC and UTS, respectively.

The effect diagrams for thermal conductivity (Figure 1a) indicate that the printing profile significantly influences the heat conduction capability of the 3D-printed specimens. Transitioning from the Fast to the Strong profile resulted in a 17% increase in TC, and from the Strong to the Quality profile, there was an additional 14% increase. These findings are supported by the ANOVA results, which show that factor A is significant for TC (p -value < 0.0001), as presented in Table 4.

A similar trend was observed for UTS. The effect diagrams (Figure 1b) reveal that UTS is highly dependent on the printing profile used. The highest UTS, 554.44 ± 1.23 MPa, was achieved with the Quality profile. The Strong profile produced a UTS of 535.45 ± 1.92 MPa, which is about 3.5% lower than the Quality profile. The Fast profile resulted in the lowest UTS, 525.19 ± 0.54 MPa, showing a decrease of approximately 5% and 2% compared to the Quality and Strong ones, respectively. These results are consistent with the ANOVA findings, where factor A significantly affects UTS (p -value < 0.0001), as shown in Table 5.

No anomalies were detected in the model adequacy checks for both TC and UTS. The high R^2 values (0.9997 for TC and 0.9758 for UTS) and adjusted R^2 values (0.9996 for TC and 0.9677 for UTS) indicate that most of the variability in the data can be attributed to the changes in the printing profiles, as shown in Tables 3 and 4.

The equation for the developed quadratic polynomial regression model, which correlates the TC and UTS of each investigated printing profile, is given below:

$$\text{UTS} = 640.90 - 25.70 \text{ TC} + 1.61 \text{ TC}^2 \quad (1)$$

The ANOVA study results confirm the statistical significance of both the linear (p-value < 0.05) and quadratic (p-value = 0.028 < 0.05) terms, as shown in Table 4. Additionally, the overall model is significant (p-value < 0.05), and the high values of R^2 (97.80%) and R^2_{adj} (97.10%) suggest that the model is adequate, with a low noise level. This indicates that the regression model fits the observed data well, as depicted in Figure 3, which shows the fitted quadratic regression line.

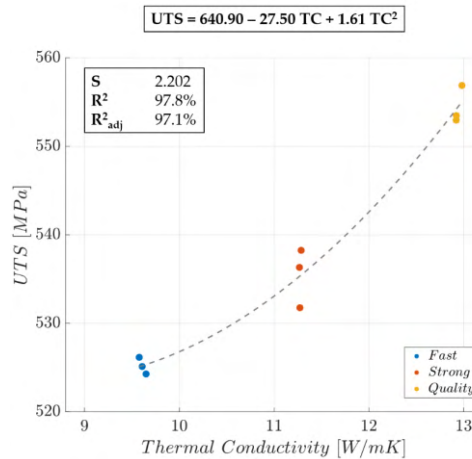


Figure 1. Fitted line plot: selected quadratic polynomial regression model fitting the collected observations (UTS values for different printing profiles). Predictor: TC=thermal conductivity; Response: UTS=Ultimate Tensile Strength.

Figure 4 includes both the residuals plotted against the fitted values for the model adequacy check and their normal probability plot, with no anomalies detected in either plot. Lastly, the model has demonstrated high predictive capabilities, as confirmed by the high value of the R^2_{adj} parameter (95.10%).

CONCLUSION

This study highlights the significant influence of printing profiles on the thermal conductivity and tensile strength of metal parts produced via metal FFF. The developed regression model effectively captures the relationship between thermal and mechanical properties, providing a guide to explore the performance of metal 3D printed components for industrial applications in thermal dissipation.

Acknowledgment

The authors acknowledge the European Union (NextGeneration EU) and MUR-PNRR project Sicilian MicronanoTech Research And Innovation Center – SAMOTHRACE (CUP E63C22000900006), Spoke 1.

References

- (1) C. Tosto, J. Tirillò, F. Sarasini, G. Cicala. *Applied Sciences*, **11**(4), 1444 (2021)
- (2) C. Tosto, J. Tirillò, F. Sarasini, C. Sergi, G. Cicala. *Polymers*, **14**(16), 3264 (2022)
- (3) C. Tosto, F. Miani, G. Cicala. *Macromolecular Symposia*, **411**(1), (2023)

FROM WASTE TO SUSTAINABLE RESOURCE: 3D-PRINTED BIOCOMPOSITE FISH CRATES BASED ON BIODEGRADABLE POLYMERS AND ANCHOVY FISHBONE SCRAPS

M.C. Citarrella¹, E.F. Gulino¹ and Roberto Scaffaro¹

¹ Department of Engineering, University of Palermo, Viale delle Scienze, ed. 6, 90128 Palermo, PA, Italy

² INSTM, Consortium for Materials Science and Technology, Via Giusti 9, 50125 Florence, Italy

INTRODUCTION

The amount of fish wastes produced and grossly discarded in markets has undergone a dramatic increase over the last years causing environmental and hygiene issue. The use of these scraps for the production of materials with higher added value would reduce waste production and solving related environmental and hygiene issue. Combining biopolymers with animal waste could be an effective strategy in the view of producing food packaging decreasing the amount of bioplastic needed creating more sustainable products.

EXPERIMENTAL

Materials

Mater-Bi® EF51L and PLA 2003D were used as biodegradable polymeric matrices to prepare green composites. Anchovy fishbone (EE), collected at Ballarò market (Palermo, Italy).

Preparation

Anchovy fishbones were ground into powder and melt mixed to biopolymeric matrices (Mater-Bi® or PLA). The obtained formulations were extruded in order to produce 3D-printable filaments. A conveyor belt system was used to draw the output extrudate aiming to obtain filaments with a diameter of ~ 1.75 mm.

Characterizations

Morphological analysis was performed through scanning electron microscope (SEM). Mechanical performance of the samples was investigated by tensile tests. Microbiological analysis was performed on the fishbone powder to verify if it is safe to handle.

RESULTS AND DISCUSSION

Microbiological analyzes revealed that anchovy fishbone powder does not contain microorganisms which, by type or quantity, may represent a risk to human health and, therefore, the filler is safe to handle. MB/EE10 and PLA/EE10 composite filament were able to be 3D printed for FDM into flat (Figure 1a) or geometrically complex products (Figure 1b). The printing process proceeded smoothly and no clogging of the nozzle was observed.

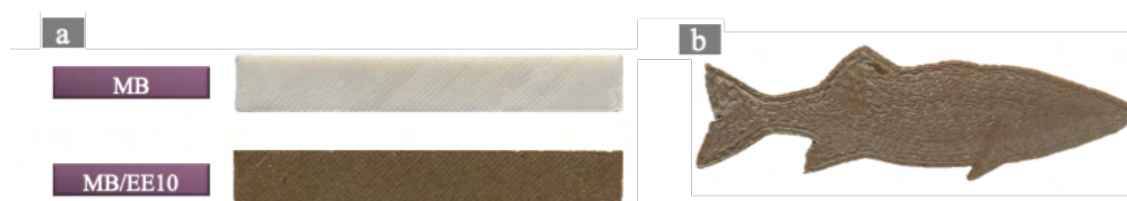


Figure 1. Specimen 3D printed (a) and product with complex geometry printed with MB/EE10 (b).

All prepared composites formulation displayed viscosity values potentially compatible for be processed by 3D printing. Good interfacial adhesion between anchovy fishbone particles and the polymeric matrices was obtained.

The addition of 10% of EE to MB lead to a decrease in E and TS but the ductility of the composite displayed a strong increase if compared with pure matrices, reasonably due to the presence of the oily phase in the filler that act as plasticizer (Figure 2). MB/EE10 and PLA/EE10 can be employed for the manufacture for 3D printing of fish crates and other similar packaging.

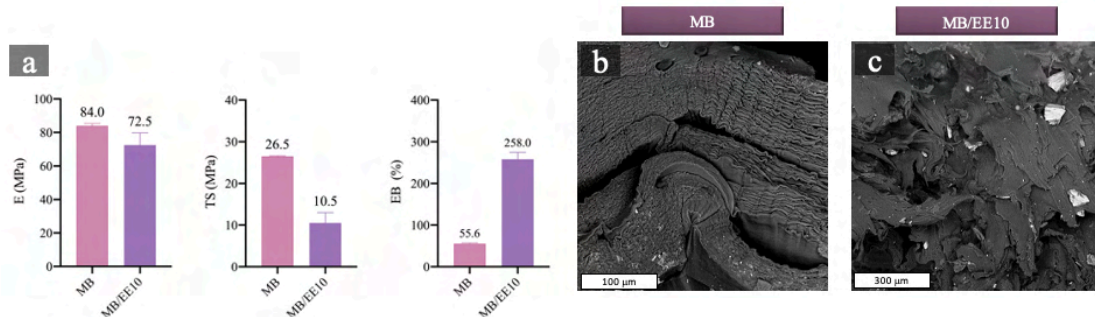


Figure 2. Elastic modulus (E), tensile strength (TS), and elongation at break (EB) of 3D-printed MB and MB/EE10 (a) and relative SEM micrograph of their fractured cross-section (b, c).

Utilizing 10% of anchovy fishbone waste to produce composite filaments for 3D printing is a feasible and value-added prospect of dispose such scraps that usually accumulate in fish markets, generating bad odors and attracting insects, with a high risk of bacterial proliferation. The produced composite filaments, in fact, can be employed for the manufacture for 3D printing (FDM) fields that need biodegradable, renewable and cost-effective raw material.

References

- 1) Scaffaro R, Citarrella MC, Catania A, Settanni L (2022) Green composites based on biodegradable polymers and anchovy (*Engraulis Encrasicolus*) waste suitable for 3D printing applications. *Compos Sci Technol* 230:109768. <https://doi.org/10.1016/J.COMPSCITECH.2022.109768>
- 2) Scaffaro R, Citarrella MC, Gulino EF (2022) Opuntia Ficus Indica based green composites for NPK fertilizer controlled release produced by compression molding and fused deposition modeling. *Compos Part Appl Sci Manuf* 159:107030. <https://doi.org/10.1016/J.COMPOSITESA.2022.107030>

ENHANCING THE THERMAL STABILITY OF GELATIN-BASED HYDROGELS AT PHYSIOLOGICAL TEMPERATURES

Fátima Díaz-Carrasco, Elena Vidal-Nogales, Álvaro Santos-Medina, Manuel J. Díaz, M.-Violante de-Paz, M.-Gracia García-Martín and Elena Benito*

Departamento de Química Orgánica y Farmacéutica, Universidad de Sevilla, C/ Prof. García González, n.º 2, 41012-Sevilla, España.

*ebenito@us.es

INTRODUCTION

Tissue engineering is a multidisciplinary field whose primary objective is the development of substitutes made with biomaterials that are capable of healing, repairing, or regenerating injured tissues and organs. Among these biomaterials is gelatin, a natural polymer derived from collagen that is notable for its multiple properties, such as biocompatibility, biodegradability, and low toxicity. However, the limitations of gelatin hydrogels in biomedical applications stem from their relatively low melting temperature, which is approximately 32 °C, a temperature range that is proximal to physiological temperatures [1]. Consequently, gelatin hydrogels can undergo structural degradation and property loss when employed at temperatures near body temperature, thereby compromising their performance in biomedical applications.

The purpose of this study is to produce interpenetrating polymer networks (IPNs) based on gelatin through a Diels-Alder reaction (DA), inducing orthogonal reticulation that could enhance the mechanical, physical-chemical, and rheological properties of the original gelatin, thereby improving its final properties for potential use in tissue engineering and three-dimensional scaffolding.

EXPERIMENTAL

Materials

The chemicals used in this work were acquired from the supplier Sigma-Aldrich (Madrid, Spain): gelatin of bovine skin, 2,2'-dithiodiethanol, furfuryl isocyanate, dibutyltin dilaurate, and D-ribo-1,4-lactone. All products were used as received.

Preparation

The monomers difurfuryl derivative of dithiodiethanol (Di-Fur) and 1,8-dimaleimide-3,6-dioxaoctane (DMDOO) were prepared according to the procedure established by Iglesias et al. [2] and Galbis et al. [3], respectively. The crosslinker 2,3,5-tri-*O*-[(furan-2-ylmethyl)carbonyl]-D-ribo-1,4-lactone (Tri-Fur) was synthesized using a dried solution of 0.5 g of D-ribo-1,4-lactone (3.37 mmol) in tetrahydrofuran (THF, 1.7 mL) at which 1.14 mL of furfuryl isocyanate (10.61 mmol) and a drop of dibutyltin dilaurate as a catalyst were added. The mixture was stirred at room temperature for 5 hours, the solvent evaporated, and the resulting residue purified by column chromatography (EtOAc-Hex 1:2 → EtOAc-Hex 1:1). The crosslinker (Tri-Fur) was obtained as an orange wax (1.38 g, yield: 79.2%).

Ten third-generation interpenetrating polymer networks (IPN) named G-Pol_x-Xr_y were formed by two polymers in a 1:1 relative proportion, where Polymer 1 was synthesized from the monomers DiT-Fur and DMDOO and the crosslinking agent Tri-Fur, while Polymer 2 was gelatin from bovine skin (G), a biocompatible polymer of great interest. The 10 IPN systems varied in the polymer concentrations (p/v) for Polymers 1 and 2 (2%, 3% or 4%) and the degree of crosslinking of Polymer 1 (2%, 3.5% or 5% crosslinking degree).

Rheological and physicochemical characterization

To determine the thermal stability of the synthesized IPN compared with gelatin hydrogels, gelatin blanks and selected IPN hydrogels were investigated using heating and cooling ramps from 25 °C to 65 °C and vice versa at a rate of 2 °C/min. The relative stability of the samples over temperature was studied at constant frequency and strain values.

RESULTS AND DISCUSSION

The thermal stability of the synthesized IPN materials was evaluated and compared to gelatin hydrogels. For illustrative purposes, the evolution of G' with temperature of gelatin blank hydrogel (3%) and the G-Pol₃-Xr₅ IPN are displayed in Figure 1. It was observed that 3% gelatin underwent a pronounced drop in its elastic modulus around physiological temperature (between 31 °C and 40 °C) without subsequent recovery of its viscoelastic properties. In contrast, the G-Pol₃-Xr₅ IPN system maintained and even improved its rheological properties between 25 °C and 37.3 °C, likely due to a curing effect on Polymer 1.

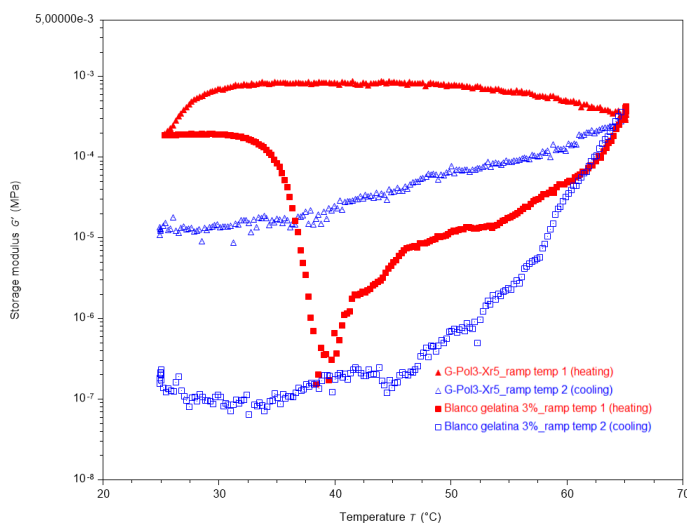


Figure 1. Variation of elastic modulus with temperature during heating (Red) and cooling (Blue) ramps at 2 °C/min for IPN G-Pol₃-Xr₅ and its Blank (3% Gelatin).

Consequently, the inherent thermal instability of gelatin hydrogels around physiological temperatures was mitigated when they were intertwined with the polymer network of Polymer 1, resulting in an IPN system. It is also worth highlighting that the IPN system was thermally stable up to 51 °C and this is consistent with our observations for the DA polymers studied by TGA [2]. On the other hand, heating the hydrogel above 50 °C can negatively impact its rheological properties, and this effect may persist even after cooling.

We can conclude that the use of these materials at physiological temperatures not only becomes feasible but also results in a significant improvement in their mechanical properties, rendering them suitable for use in tissue engineering applications.

Acknowledgment

This research was funded by the Ministerio de Ciencia e Innovación-Agencia Estatal de Investigación (MCIN/AEI/10.13039/501100011033), grant number PID2020-115916GB-I00.

References

- [1] J.H. Kang, M.H. Turabee, D.S. Lee, Y.J. Kwon, Y.T. Ko, *Biomedicine and Pharmacotherapy* (2021), **143**, 112144.
- [2] N. Iglesias, E. Galbis, L. Romero-Azogil, E. Benito, M.-J. Díaz-Blanco, M.G. García-Martín, M.V. De-Paz, *Polymer Chemistry* (2019), **10**, 5473–5486.
- [3] E. Galbis, M. V de Paz, K.L. McGuinness, M. Angulo, C. Valencia, J.A. Galbis, *Polymer Chemistry* (2014), **5**, 5391–5402.

Enhanced Mechanical and Rheological Properties of Chitosan-Based Hydrogels with Hydroxyapatite for Bone Tissue Engineering

C.Di Marco¹, M.Trapani², M.Testa¹, B. Di Stefano², V. La Carrubba¹, F. Lopresti¹

¹ Department of Engineering, University of Palermo, Viale delle Scienze, Palermo, Italy

² BIOPLAST-Laboratory of Biology and Regenerative Medicine-Plastic Surgery, Plastic and Reconstructive Surgery Section, University of Palermo, 90127 Palermo, Italy

INTRODUCTION

Chitosan, a natural polymer derived from chitin, is widely used as a scaffold hydrogel in bone tissue engineering (BTE) due to its capacity to support the attachment and proliferation of osteoblast cells [1], [2]. However, its low mechanical strength with lack of structural integrity hinder its application. This study explores the enhancement of chitosan-based hydrogels through the incorporation of hydroxyapatite (HA), a primary mineral component of bone, aiming to improve their mechanical properties and osteoinductivity for BTE applications [3]. This work compares the effect of three different HA concentrations (10, 20, and 30 wt%) on a chitosan polymer matrix to obtain pH-induced Chitosan and Chitosan/HA hydrogels by physical crosslinking.

EXPERIMENTAL

Materials

High molecular weight chitosan (Chi), commercial grade nano-hydroxyapatite (HA), acetic acid (AA) (for analysis, 99.8%), sodium hydroxide (NaOH) (ACS reagent, 97.0%, pellets) were purchased from Sigma-Aldrich, St. Louis, MO, USA. Dulbecco's Phosphate-Buffer Saline (PBS pH 7.4) was purchased from Gibco.

Preparation

The polymer solution was prepared by dissolving Chi 2 wt% in aqueous AA solution 0.5 vol%. HA was suspended in an aqueous AA solution of 0.5 vol% with different concentrations (10, 20, and 30 wt%) for 15 minutes in an ultrasonic bath. For the crosslinking agent NaOH 1 M was prepared. To obtain cylindrical scaffolds, the Chi and Chi/HA solutions were loaded into polymethyl methacrylate molds. The cross-linking procedure was reached by immersing the mold in a NaOH bath for 15 minutes. Once the crosslinking process was completed, the hydrogels were soaked in deionized water to remove any excess NaOH.

Rheological, Mechanical, and physic-chemical characterization

The presence of HA was confirmed by spectroscopic (FTIR-ATR), while its correct dispersion was evaluated through scanning electron microscopy (SEM). Compression tests evaluated the mechanical strength and stability, while rheological properties were assessed using frequency and amplitude sweep tests. Swelling tests were performed to evaluate the influence of HA on the ability of the hydrogels to absorb water, while degradation test was measured to study the stability of the hydrogels over time. Finally, the hydrogels were seeded with mesenchymal stem cells derived from adipose tissue (S-ASCs) to study their osteoinductivity potential.

RESULTS AND DISCUSSION

Figure 1 shows the stress-strain curves, that exhibit an increasing slope with an increasing concentration of HA nanofiller, indicating an enhancement in the stiffness of the hydrogel. This result is confirmed by the evaluation of the elastic modulus and compressive strength, which increased with higher HA concentrations. Figure 2 shows the flow curves of the polymeric solutions, it's noticeable that the Chi/HA solutions show higher complex viscosity at low frequencies due to the HA nanofiller, while both solutions exhibit typical shear-thinning behavior. The correct dispersion of the HA was confirmed by SEM, the nanofiller are homogeneously distributed in the polymer matrix, and their average diameter is almost uniform.

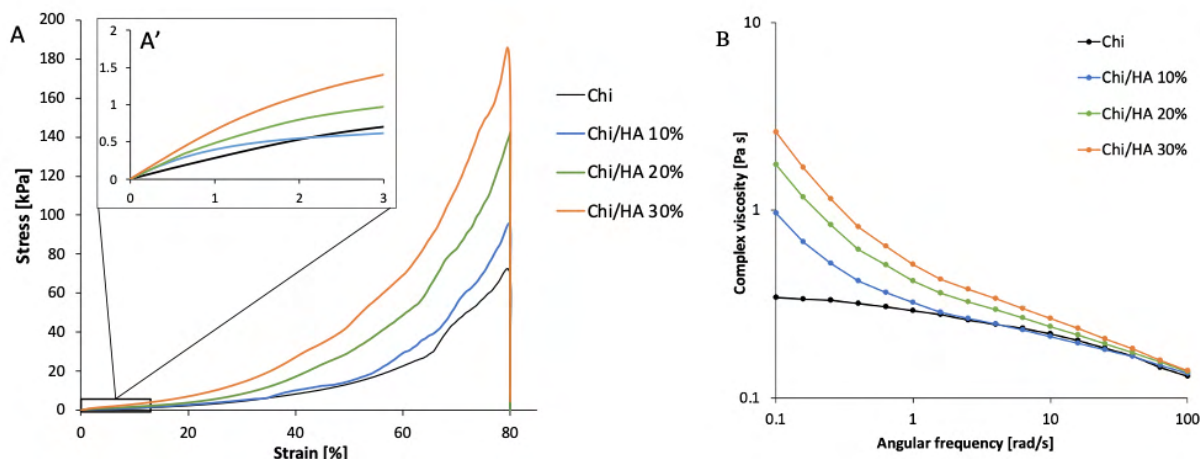


Fig. 1: **A)** Stress-strain curves of hydrogels and **(B)** Complex viscosity as a function of the angular frequency of polymeric solutions.

The study highlights that the mechanical and rheological properties of chitosan-based hydrogels can be significantly enhanced by incorporating HA. The results indicate that HA provide mechanical reinforcement and stability, making these hydrogels more suitable for BTE applications. In addition, the improved osteoinductivity also suggests the potential for promoting bone regeneration.

References

- [1] S. Maiz-Fernández, L. Pérez-álvarez, “pH-Induced 3D Printable Chitosan Hydrogels for Soft Actuation,” *Polymers (Basel)*, 14, 3 (2022)
- [2] K. Guillén-Carvajal, B. Valdez-Salas, “Chitosan, Gelatin, and Collagen Hydrogels for Bone Regeneration,” *Polymers*, 15, 13, (MDPI) (2023)
- [3] C. Xiang *et al.*, “A Porous Hydrogel with High Mechanical Strength and Biocompatibility for Bone Tissue Engineering,” *J Funct Biomater*, 13, 3, (2022)

MARINE BIODEGRADATION OF BIODEGRADABLE VS. CONVENTIONAL PLASTICS

A. Marín^a, P. Feijoo^a, A. Jáuregui^a, E. Sánchez-Safont^{a,b}, J. Tena-Medialdea^c, J.R. García-March^c, L. Cabedo^{a,b}, J. Gámez-Pérez^{a,b*}

^aGrupo de Polímeros y Materiales Avanzados (PIMA), Universitat Jaume I, 12071 Castelló (Spain) lcabedo@uji.es

^bCEBIMAT LAB S.L, ESPAITEC, Universitat Jaume I, Av. Vicent Sos Baynat s/n, 12071, Castelló (Spain)

^cIMEDMAR-UCV, Institute of Environment and Marine Science Research, Universidad Católica de Valencia, Alicante, Spain

INTRODUCTION

It is estimated that nearly 20 million tons of plastics enter our oceans each year, generating a negative impact on marine flora, fauna, and human health. Consequently, polymers labeled as biodegradable are emerging as a potential solution to replace conventional plastics, particularly in applications where there is a high risk of uncontrolled entry into the environment. However, there is considerable uncertainty about their behavior in these ecosystems due to the diversity of marine habitats.

This study monitors the marine biodegradation of biopolyesters such as poly(lactic acid) (PLA) and poly(3-hydroxybutyrate-co-3-hydroxyvalerate) (PHBV) as well as conventional plastics like polyamide (PA), polypropylene (PP), and polyethylene (PE) in terms of abiotic and biotic degradation over 12 months of immersion in the port of Calpe (Alicante, Spain).

EXPERIMENTAL

Materials and Methods

PLA, PHBV, PA, PP, and PE were used for this study. Using a hot-plate press (Carver 18 4122, USA), polymer films with a thickness of 400 μm were obtained. Pieces were inserted into slide frames which were grouped into panels containing triplicates of the materials. Six panels were deployed at the fishing port of Calpe (Alicante, Spain) at coordinates 38°38'20.5"N 0°04'15.8"E. Samples takes-outs were carried out after 2, 6, 9 and 12 months of exposure to seawater.

Scanning Electron Microscopy (SEM) was used to study the morphological changes and biofilm formation on the samples. Profilometry tests were also employed to assess the surface roughness and biofilm density and Infrared Spectroscopy (IR) was used to analyze the chemical changes during biodegradation.

RESULTS AND DISCUSSION

Marine Biodegradation of Biopolymers and Conventional Plastics

The behavior of PLA was notable as it did not differ significantly from non-biodegradable plastics, which only showed minor changes due to interactions with the marine environment. These findings challenge the application of the term "biodegradable" for PLA in marine contexts, as this definition does not guarantee its marine biodegradation.

On the other hand clear biodegradation was observed for PHBV, along with significant physical aging, resulting in a 16% mass loss during the testing period. However, a reduction in the biodegradation rate over time was noted, which could be related to the adverse conditions for microorganisms on the sample surface affected by the formation of a dense

biofilm that may limit oxygen access. Morphological studies conducted by SEM and profilometry confirmed a higher roughness and biofilm density compared to the other materials. The results obtained from infrared spectroscopy suggest that biodegradation in PHBV occurs layer by layer, starting in the amorphous regions of the polymer.

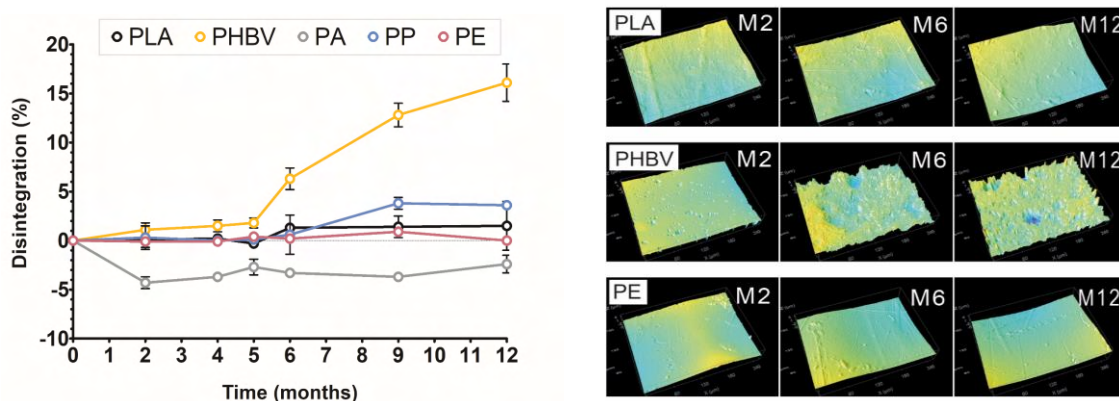


Fig. 1 Disintegration assessed by mass percentage loss (left) and profilometry analysis of the samples (right), the latter evidencing biodegradation of PHBV on the surface.

The comparative study of marine biodegradation between biodegradable and conventional plastics provides crucial insights into the performance and environmental impact of these materials in marine ecosystems. The findings highlight the need for careful consideration when labeling plastics as biodegradable, particularly for marine applications, and underscore the potential for developing advanced materials that balance functionality with environmental sustainability.

Acknowledgment

This research was supported by MCIN/AEI /10.13039/501100011033 and by the European Union NextGenerationEU/ PRTR, project TED2021-130211B-C31, by the Generalitat Valenciana (project AICO/2021/045) and by the Universitat Jaume I (project UJI-B2022-34).

One-Step Fabrication and Thermal Stabilization of PVA Nanofiber Membranes via Heat-Assisted Solution Blow Spinning

Gulino E.F.¹, Scaffaro R.¹

¹ Department of Engineering, University of Palermo, Viale delle Scienze, Palermo, Italy

INTRODUCTION

Polyvinyl alcohol (PVA) nanofibers have garnered significant interest in biomedical applications owing to their exceptional properties, including water solubility, biodegradability, and biocompatibility. Among these applications, controlled release is extensively researched. However, the highly hydrophilic nature of PVA leads to dissolution when exposed to aqueous environments, thereby restricting sustained release capabilities. Conventional techniques to address this issue typically involve expensive thermal or chemical treatments, which pose environmental and health hazards. This study presents a novel, rapid, and eco-friendly approach to stabilizing PVA nanofibers through an enhanced Solution Blow Spinning (SBS) process.

EXPERIMENTAL

Materials and method

Polyvinyl alcohol (PVA) was dissolved in distilled water at 95°C for 4 hours. Chlorhexidine (CHX) and/or graphene nanoplatelets (GNP) were subsequently added to the polymer solution at concentrations of 2 wt% and 1 wt%, respectively. Nanofiber membranes were fabricated using a heat-assisted solution blow spinning (HASBS) technique. The HASBS setup consisted of a compressed air source, a syringe, an electronic injection pump, and a spinning system equipped with concentric nozzles. The fibers were collected on an aluminum foil collector heated to 200°C. The process parameters were as follows: a polymer solution flow rate of 45 mL/h, an air pressure of 0.5 MPa, a needle-to-collector distance of 20 cm, a spinning duration of 15 minutes, and a chamber temperature of 60°C

RESULTS AND DISCUSSION

The neat PVA system (figure 1) exhibited smooth and homogeneous fibers with a unimodal diameter distribution and an average diameter of 1 μm . The incorporation of graphene nanoplatelets (GNP) in the PVA/GNP system resulted in the formation of fiber bundles and a 50% increase in the average diameter. Adding chlorhexidine (CHX) to PVA produced homogeneous fibers with some beads and a 20% decrease in the average diameter compared to neat PVA. When both CHX and GNP were present in the PVA/CHX-GNP system, the fibers formed were homogeneous and defect-free, without any fiber bundles.

The formation of fiber bundles in the PVA-GNP system may be attributed to solution instability during processing, aligning with findings from previous studies. The presence of GNP likely increased fiber diameter due to its effect of increasing polymer solution viscosity. On the other hand, chlorhexidine typically decreases viscosity, but this effect was counterbalanced by the presence of GNP. All systems produced wavy fibers, which is uncommon in conventional SBS nanofibers. This wavy pattern may result from the stabilization of PVA fibers during deposition onto the heated collector.

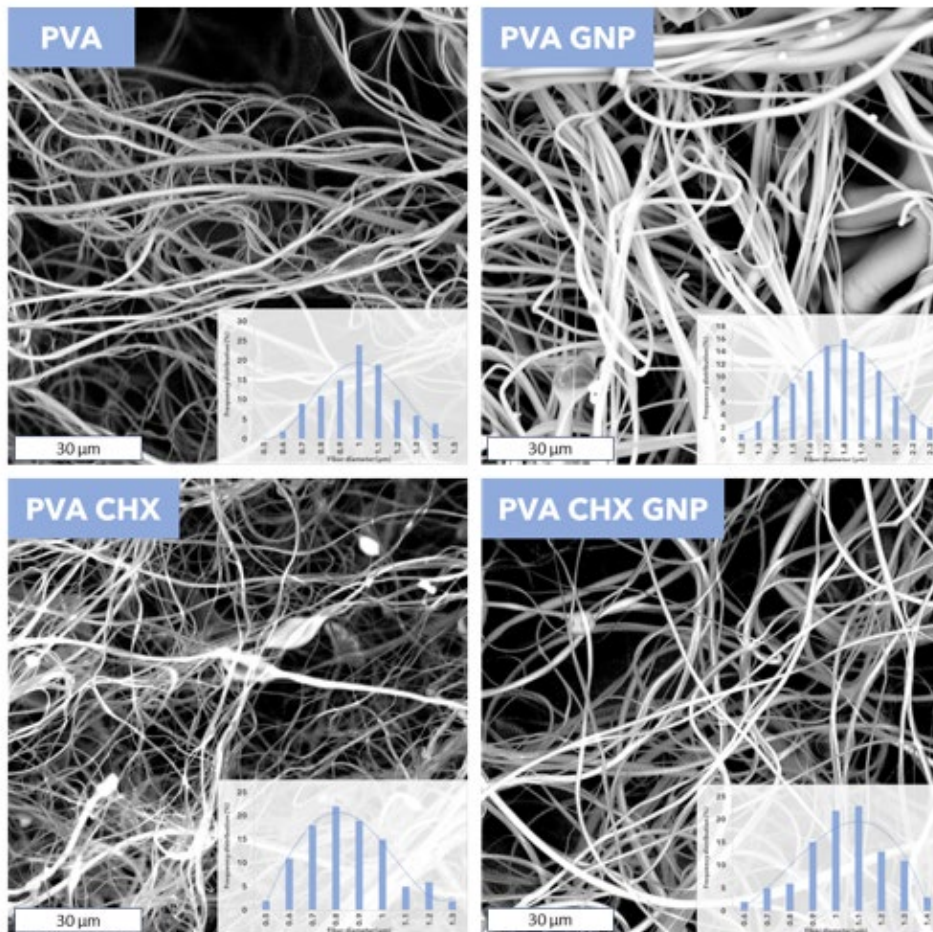


Fig. 1 membrane surface of PVA, PVA GNP, PVA CHX and PVA CHX GNP

Acknowledgment

This study was carried out within the SAMOTHRACE (Sicilian micro and nano technology research and innovation center) Extended Partnership and received funding from the European Union Next-GenerationEU (PIANO NAZIONALE DI RIPRESA E RESILIENZA (PNRR) – MISSIONE 4 COMPONENTE 2, INVESTIMENTO 1.5). This manuscript reflects only the authors' views and opinions, neither the European Union nor the European Commission can be considered responsible for them.

Flame retardant properties of *s*-triazine phosphonates in PU rigid foams

C.-C. Höhne^{a,*}, J. Limburger^a, A. König^c, T. Wagener^d, and E. Kroke^b

^a Fraunhofer Institute for Chemical Technology ICT, Joseph-von-Fraunhofer-Str. 7, 76327 Pfinztal, Germany

^b Technische Universität Bergakademie Freiberg, Institut für Anorganische Chemie, Leipziger Str. 29, 09599 Freiberg Germany

^c BASF SE, 67056 Ludwigshafen, Germany

^d BASF Polyurethanes GmbH, Elastogranstr. 60, 49448 Lemförde, Germany

* carl-christoph.hoehne@ict.fraunhofer.de

INTRODUCTION

The liquid flame retardant tris(2-chloro-isopropyl) phosphate (TCPP) is widely used in polyurethane (PUR) and polyisocyanurate rigid foams (PIR). However, TCPP is currently under assessment by the European Chemicals Agency ECHA and the National Toxicology Program NTP, USA. For this reason, new flame retardants with similarly good processing and application properties are of high interest. In this poster, the influence of *s*-triazine phosphonates on the foaming behavior and flame retardancy of PUR and PIR rigid foams for building applications is discussed. The newly developed flame retardants *s*-triazine phosphonates improve the flame retardancy of PUR and PIR rigid foams and are able to replace the flame retardant TCPP in PIR rigid foam formulations for building applications without any loss of foam properties.

EXPERIMENTAL

Materials

Polyol blends and isocyanate of the foam formulations for rigid PUR foam and rigid PIR foam were provided by BASF. Water and cyclopentane were used as blowing agents. The *s*-triazine phosphonates were synthesized as previously reported via the following reaction path [1]. Mixtures of asymmetrically substituted *s*-triazine phosphonates **mT/R/R'/R''** e.g., obtained from a reaction of 1 equiv. C₃N₃Cl₃, 1 equiv. P(OMe)₃ and 2 equiv. P(OnBu)₃ denoted **mT/Me/2nBu**.

Preparation of PU rigid foams for LOI tests

A premixed polyol blend-cyclopentane mixture and a premixed isocyanate-flame-retardant mixture containing 5 wt.% flame retardant were added to a 0.7 L paper cup and stirred at 2000 rpm for 15 s. The foam was allowed to react in the paper cup.

Preparation of rigid PUR/PIR foams for EN 13501 class E test and cone calorimeter test

The respective polyols, stabilizers, catalysts, and flame retardants were sequentially weighed into a 750 mL plastic cup and stirred at 2000 rpm for 30 s. Subsequently, chemical blowing agent was weighed and stirred at 2000 rpm for 30 s, followed by the addition of physical blowing agent via back weighing. Then, the A component was overlaid with the respective amount of isocyanate in the plastic cup and mixed for 3-5 s with increasing stirring speed. The reaction mixture was immediately poured into a 200 × 200 × 200 mm³ metal box carrying a cardboard insert for polymerization. The reaction scale was adjusted to produce a sample body weighing approximately 600 g.

RESULTS AND DISCUSSION

Low-molecular liquid *s*-triazine phosphonates improve the flame retardancy of PUR and PIR rigid foams, see Figure 1, and are able to replace the flame retardant TCPP in PIR rigid foam formulations for building applications without any loss of foam properties. PIR rigid foam containing the low amount of 3 wt.% of 2,4,6-tris(di-*n*-butylphosphonate)-1,3,5-triazine **T(nBu)₃** passes the EN 13501 class E test for building applications without any additional flame retardant. PUR rigid foam with a synergistic combination of flame retardants, which are 4.5 wt.% TCPP, 3.3 wt.% **T(nBu)₃**, and 1.6 wt.% triethyl phosphate, passes the EN 13501 class E test.

From a material point of view, *s*-triazine phosphonates are a promising class of flame retardants which are produced in a cost-efficient one-step synthesis and show the necessary flame-retardant effects in PU rigid foams even in small quantities. Current limitations in industrial processing are the subject of further investigations into the realization of next-generation flame retardants for PUR and PIR foams.

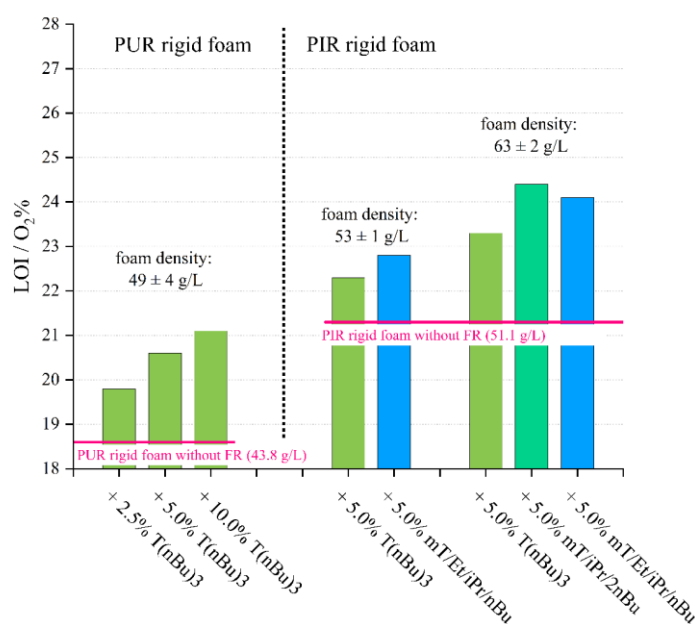


Fig. 1 Limiting oxygen index (LOI) results *s*-triazine phosphonates in PU rigid foams



Fig. 2 Flame-retardant polyisocyanurate rigid foam demonstrator containing **T(nBu)₃**

Acknowledgment

The authors would like to thank their colleagues from Fraunhofer ICT, Pfinztal: Valeria Berner, Beatrice Tübke, and Yvonne Kasimir and TU Bergakademie Freiberg: Beate Kutzner for technical and analytical support. Funding: This work was supported within the Fraunhofer and DFG transfer programme (DFG project number KR1739/35-1).

References

- 1) C. Vogt, C.-C. Höhne, J. Limburger, A. König, T. Wagener, E. Kroke, ChemistryOpen, **12** (9), e202300075 (2023).

Coarse-Grained Molecular Dynamics Simulations of Oxidative Aging in Amorphous Regions of Semi-crystalline Polymers -Decay of Stress Transmitter Content-

Institute for Advanced Research, Nagoya University, Furo-cho, Chikusa, Nagoya, Japan
ishida@mp.pse.nagoya-u.ac.jp

INTRODUCTION

Oxidative aging occurs in polymers through oxygen and radicals to cause chemical-level changes such as chain scission (β -scission) and adding oxygenated groups. Consequently, it leads to material failures (e.g., embrittlement). It is known that the oxidative aging of crystalline polymers preferentially occurs in amorphous regions between lamellae, where the penetration of oxygen molecules is facilitated. In this presentation, I present the results of oxidative aging simulations conducted on the geometry of the amorphous regions between lamellae using our previously proposed coarse-grained molecular dynamics simulation method [1, 2].

MODELS AND SIMULATIONS

Using a computational model that combines the standard Kremer-Grest (KG) model [3], which has a proven track record for long-term polymer dynamics calculations, with a kinetic model of thermal oxidative aging reactions for polypropylene (PP) at 120 °C [4] under the oxygen excess regime (OER), we calculated the molecular dynamics and chain scission of amorphous chains in crystalline polymers. The initial structure was computed in a region enclosed by two walls ($z = 0, 26.1\sigma$) representing the crystalline lamellar phase, where σ is the size of the coarse-grained beads, and the z -axis is perpendicular to the walls.

The polymer chains are composed of both long chains and short chains sampled from different statistical ensembles, with a number long chain fraction of 0.4. The long chains are sampled from a probability distribution calculated by Uneyama et al. [5] using self-consistent calculations, with an average chain length of 37. The short chains are sampled from an exponential distribution with an average degree of polymerization of 10. All generated chains are grafted at both ends to the lamellar phase, with long chains classified as either tie molecules or loose loop molecules, and short chains classified as tight loops. Appropriate topological constraints are applied as shown in Fig. 1.

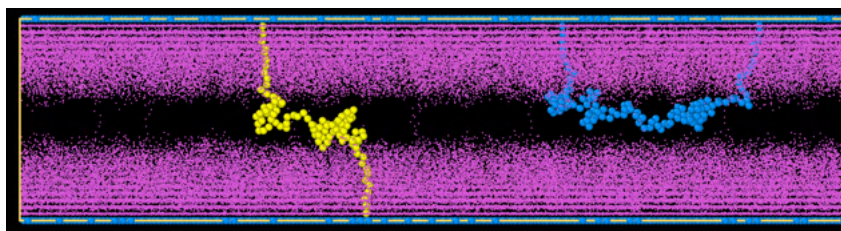


Fig. 1 2D Snapshots of the initial structure representing the amorphous region (projected onto the xz plane). Tight loop chains are shown in purple, tie molecules in yellow, and loose loop molecules in blue. For clarity, only one tie molecule and one loose loop molecule are depicted.

RESULTS AND DISCUSSION

Fig. 2 shows the spatial distribution of degradation sites for each reaction rate (conversion of undegraded beads) projected onto the xz plane. Spatially heterogeneous degradation progression can be observed, indicating that the region filled with tie chains and loose loop chains ($8.3 \leq z/\sigma \leq 16.8$) decompose preferentially compared to the areas near the lamellar walls. The characteristic hydrogen abstraction reaction corresponds to the process

of radicals hopping between chains. The movement of radicals on the chains is due to the diffusion of the polymer chains to which the radicals are attached and the hopping between polymer chains.

Fig. 3 shows the transition in the retention rates of tie chains and long/short loop chains (normalized by the initial number of chains). In the system under study, tie chains and loose loop chains, which act as stress transmitters, are preferentially broken compared to short loop chains, likely due to their higher mobility. To accurately count the number of stress transmitters and evaluate their decay, it is necessary to examine the number of tie chains and loose loop chains, as well as combinations of two loose loop chains, that possess so-called trapped entanglement topology. The results of this analysis will be presented at the poster session.

In summary, it was found that chains acting as stress transmitters are cleaved even faster than the decay of the average reaction rate (consumption of oxidative sites), which serves as a good indicator of oxidative aging in the bulk state.

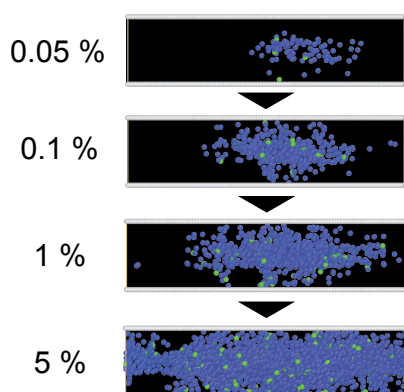


Fig. 2 Snapshots taken at conversion ratios of 0.05%, 0.1%, 1%, and 5% during aging simulation, showing only scission ends (blue) and chain radicals (green).

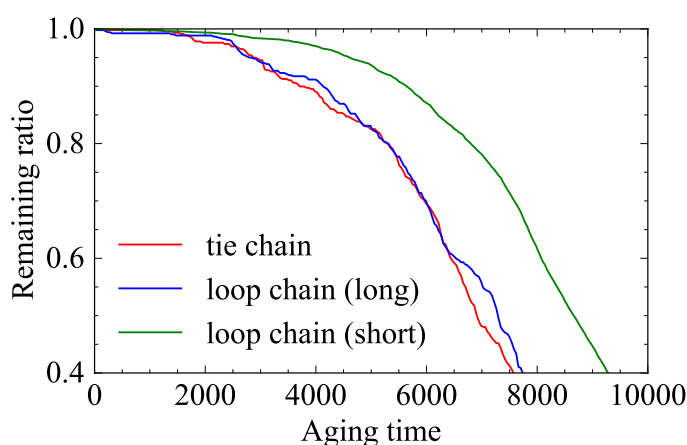


Fig. 3 Remaining ratios of tie and loop chains

Acknowledgment

This work was supported by JSPS KAKENHI Grant Numbers 24K20949, 22KJ1543, "Nagoya University High Performance Computing Research Project for Joint Computational Science" in Japan.

References

- 1) T. Ishida, Y. Doi, T. Uneyama, and Y. Masubuchi, "Modeling for Heterogeneous Oxidative Aging of Polymers Using Coarse-Grained Molecular Dynamics", *Macromolecules*, **56**(21), 8474–8483 (2023).
- 2) T. Ishida, Y. Doi, T. Uneyama, and Y. Masubuchi, "Coarse-grained Molecular Dynamics Simulation of Oxidative Aging of Polymers -Effect of free radical diffusivity-", *Polymer Journal*, accepted.
- 3) K. Kremer and G. S. Grest, Dynamics of entangled linear polymer melts: A molecular-dynamics simulation, *The Journal of Chemical Physics*, **92**(8), 5057–5086, 1990.
- 4) E. Richaud, F. Farcas, B. Fayolle, L. Audouin, J. Verdu, Hydroperoxide Build-up in the Thermal Oxidation of Polypropylene A Kinetic Study. *Polymer Degradation and Stability*, **92**(1), 118 – 124 (2007).
- 5) T. Uneyama, T. Miyata, and K. Nitta, Self-consistent field model simulations for statistics of amorphous polymer chains in crystalline lamellar structures, *The Journal of Chemical Physics*, **141**(16), 164906 (2014).

CHITOSAN AND NANOCLAY MODIFIED POLYBUTADIENE SUCCINATE COMPOSITES RHEOLOGICAL AND MECHANICAL PROPERTIES FOR ANTIMICROBIAL PACKAGING

T. Ivanova, R. Berzina, A. Lebedeva, I. Bochkovs, J. Bitenieks, R. Merijs-Meri, J. Zicans
Institute of Chemistry and Chemical Technology, Faculty of Natural Sciences and
Technology, Riga Technical University, Riga, Latvia
Tatjana.Ivanova@rtu.lv

INTRODUCTION

Packaging industry is dominant contributor for continuously growing plastic waste amounts. Besides it, reduction in food and beverage plastic packaging waste generation is restricted to some extent due to continuous necessity to ensure safety of the packed foodstuff. To tackle the challenge of the global pollution of the Earth's terrestrial and aqueous ecosystems, bio-based and biodegradable plastics have been introduced. Unfortunately, the share of biobased and biodegradable plastics continues to be low, ca 1%, from the global plastics production market (1), mainly because of higher costs and more hurdled processing. Consequently, in the light of diminishing quality and quantity of natural resources on the one hand, and increasing consumption patterns on the other hand there is an urgent need to develop novel bio-based and biodegradable composite materials, which could be obtained by low-cost mass production thermoplastics processing methods.

This initiated our research on thermoplastically processable polybutadiene succinate copolymer (PBSA) hybrid composites with nanoclay (NC) and fungal chitosan oligosaccharide (COS), which offers more sustainable manufacturing process compared to crustacean chitosan. Addition of COS was expected to endow antibacterial properties, whereas NC was believed to improve barrier properties to the developed hybrid composites, without considerably limiting its thermoplastic processability. Thus, it is expected to contribute for achievement of UN Sustainability Goal on Responsible Consumption as well as EU Green Deal.

The current research particularly focuses on the thermoplastic manufacturing of the PBSA/NC/COS hybrid composites and characterization of their mechanical properties.

EXPERIMENTAL

Materials

In the current research fungal COS (C98, ChitoLytic) and NC (Nanocor) have been used for modification of PBSA (NaturePlast) by melt compounding approach. From our previous studies the concentration of COS was fixed in the range from 7 to 10 wt.%, whereas the NC content was varied between 1 to 8 wt.%.

Preparation

PBSA/NC/COS hybrid composites have been obtained using two-roll milling. Test specimens for rheological and mechanical tests have been obtained from compression molded plates.

Rheological and physico-chemical characterization

Rheological behavior of PBSA/NC/COS nanocomposites has been measured by oscillation and rotation tests using dynamic shear rheometer (Anton Paar) with parallel plates set-up configuration at various temperatures in the range from 100°C and 160°C. Tensile mechanical properties have been measured using universal testing machine (Zwick) at room temperature.

RESULTS AND DISCUSSION

It has been concluded that melt compounding temperature during manufacturing of the composites should be below 140°C in order to prevent thermal degradation of the biopolymer and especially chitosan additive. It has been also determined that COS and NC demonstrate synergistic reinforcing effect in the case of PBSA hybrid composites.

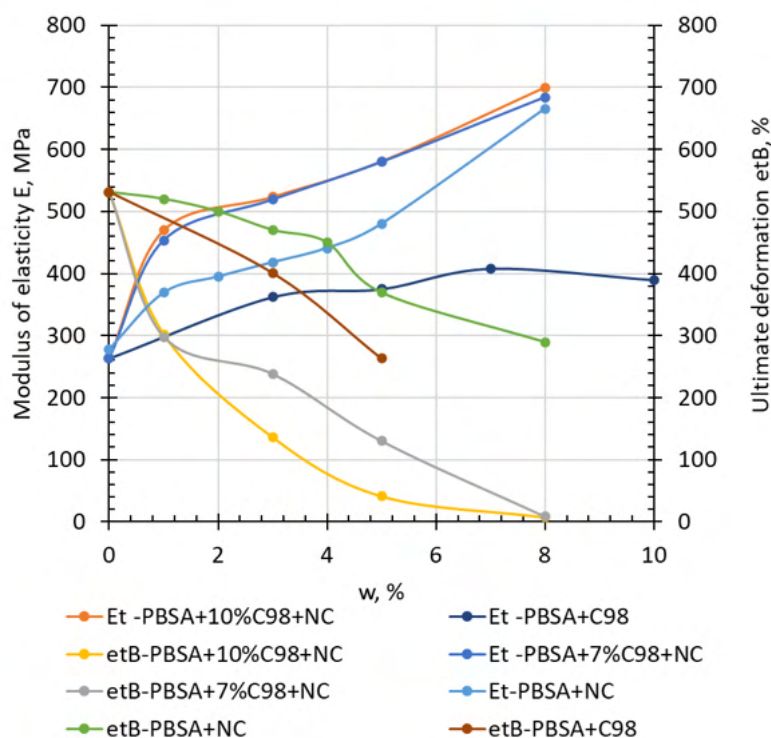


Fig. 1 Modulus of elasticity and ultimate tensile deformation of PBSA hybrid composites with COS and NC

Acknowledgment

This research is funded by the Latvian Council of Science, project “Smart Materials, Photonics, Technologies and Engineering Ecosystem” project No VPP-EM-FOTONIKA-2022/1-0001

References

- 1) F.M. Lamberti, L.A. Román-Ramírez, J. Woo, J. Polym. Environ. **28**, 2551–2571 (2020) <https://doi.org/10.1007/s10924-020-01795-8>

Pipeopsy: A novel method for status assessment of district heating pipes in operation

I. Jakubowicz and N. Yarahmadi

RISE research Institutes of Sweden, Division Built Environment
ignacy.jakubowicz@ri.se, nazdaneh.yarahmadi@ri.se

INTRODUCTION

District heating (DH) pipes comprise an inner pipe (service pipe), which is normally made of steel, surrounded by rigid polyurethane (PUR) foam insulation and an outer high-density polyethylene (HDPE) casing for protection. This design requires satisfactory adhesion between the components to achieve good long-term mechanical and thermal performance. Loss of adhesion especially between the PUR insulation and the service pipe is the most critical failure mechanism.

There are strong economic and environmental reasons to continue to use the existing 600 000 km of DH networks in Europe in a reliable and cost-effective way as long as possible, but these demands planned, efficient, and selective replacement of worn-out parts. A prerequisite to accomplish this is reliable information about the functional status and remaining service life of different parts of existing DH networks in operation. To date, there has been no field test method which has been able to provide such information and that is feasible from a practical and economic point of view.

At RISE (Research Institutes of Sweden) we have now developed a novel fast, reliable, and cost-effective field test method, Pipeopsy (a biopsy for pipes) that provides a detailed picture of the status of pipes and can be used to make prediction about the remaining lifetime and be a basis for decision for maintenance plans and asset management.

EXPERIMENTAL

Testing in field using Pipeopsy can be performed using simple, portable tools and without shutting down the operation of DH pipelines. It is based on four parts:

1. measuring adhesion strength;

Measurement of adhesion strength is based on cutting out a cylindrical PUR plug using two-hole saws. Then, an aluminum tube is glued to the plug, which is still attached to the service pipe. After a short curing period, torque is applied to each plug at a constant angular velocity. The torque and the angle of rotation are measured when the plug is loosened.

2. analyzing foam using FTIR spectroscopy;

Changes in the chemical structure due to degradation of the PUR insulation foam that was in contact with the service pipe are evaluated and quantified using FTIR. Reduction in band intensity of the carbonyl peak at around 1712 cm^{-1} and the N-H bending vibration band at 1512 cm^{-1} , which is attributed to the degradation of urethane linkage is used as a measure of degradation.

3. measuring thermal conductivity,

Measurement of thermal conductivity of PUR foam is performed using Thermtest TLS-100 A instrument which consists of a hand-held unit to which a 100 mm long, needle-shaped sensor is connected. The sensor is pushed into the PUR foam in the plug hole at an angle so that the sensor ends up at least at 5 mm distance from the steel pipe. All calculations take place directly in the instrument's accompanying software.

4. restoring pipeline

The plug method causes only minor damage to the insulation and is like a biopsy on a human body. It is nevertheless very important to restore the pipe after testing to prevent outside water from penetrating the insulation and causing rapid degradation. We therefore developed a restoration method that involves the use of new prefabricated PUR plugs that are pressed into the holes. Then, HDPE round discs are placed on top of the plugs and welded into the casing.

SUMMARY

Pipeopsy provides valuable information on whether adhesion strength between PUR foam and the steel pipe is at a satisfactory level. At the same time, FTIR analysis provides information on the degree of degradation of the PUR closest to the steel pipe. If a corresponding investigation can be carried out on a similar return pipe, conclusions can be drawn about the extent of reduction in adhesion and whether it is due to the thermo-oxidative degradation of PUR. With this information, the remaining life of the DH pipe can be estimated. In addition, information on the thermal conductivity of PUR foam can be obtained in the same field test. Using Pipeopsy, testing can be performed at a small cost, using simple mobile tools and without shutting down the operation.

Acknowledgment

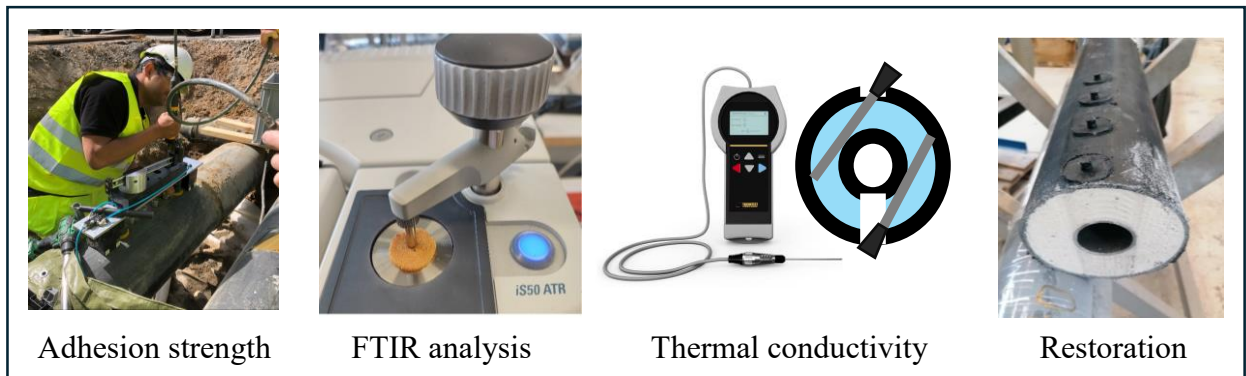
We would like to extend a big thank you to our co-workers Alberto Vega and Jan-Henrik Sällström for their great efforts and commitment.

This work has been financially supported by the Swedish Energy Agency.

The authors would like to thank Powerpipe Systems AB and the Swedish energy companies for valuable support and discussions.

References

- (1) Vega, N. Yarahmadi, I. Jakubowicz, Determination of the long-term performance of district heating pipes through accelerated ageing, *Polym. Degrad. Stab.* (2018)
- (2) A. Vega, N. Yarahmadi, J- H. Sällström, I. Jakubowicz, Effects of cyclic mechanical loads and thermal ageing on district heating pipes, *Polymer Degradation and Stability* 182 (2020) 109385



Adhesion strength

FTIR analysis

Thermal conductivity

Restoration

Zinc oxide nanoparticles and sage essential oil as active components of alginate films for food packaging

J. Kowalonek, N. Stachowiak-Trojanowska, Z. Ciecierska, A. Richert*

Department of Biomedical and Polymer Chemistry, Faculty of Chemistry, Nicolaus Copernicus University in Torun, Gagarina St. 7, 87-100 Torun, Poland

*Department of Genetics, Faculty of Biological and Veterinary Sciences, Nicolaus Copernicus University in Torun, Lwowska St. 1, 87-100 Torun, Poland

jolak@umk.pl, naat.staa@gmail.com, z.ciecierska00@gmail.com, a.richert@umk.pl

INTRODUCTION

The increasing amount of plastic waste threatens the natural environment and humans; therefore, searching for replacements for synthetic polymers is now an important topic. Among polymer products, packaging films constitute about one-third of all waste [1]. Food packaging, in particular, can be replaced with biodegradable, non-toxic biopolymers, which are abundant in nature and will degrade after usage. Besides the excellent biodegradability of food packaging, its primary role is protecting food from spoilage and preventing food waste. Therefore, the research aimed to form biodegradable and functionalized packaging film. Sodium alginate was a biopolymer used for studies. Zinc oxide nanoparticles (ZnONPs) were added to the biopolymer to make the film antibacterial, and sage essential oil (SEO) as an antioxidant was added to the film. ZnONPs were obtained by means of green synthesis using tansy (*Tanacetum Vulgare*) extract. Such active packaging protects food from spoilage, prolonging food shelf life. The obtained nanocomposite films were characterized in terms of physicochemical, mechanical, antioxidant, and antibacterial properties. There is no literature information on the influence of a combination of ZnO nanoparticles and sage essential oil on alginate films.

EXPERIMENTAL

Materials

Sodium alginate (ALG), Büchi Labortechnik AG (Flawil, Switzerland) whose $M_v = 55,800$ for $K = 0.0178 \text{ cm}^3/\text{g}$ and $a = 1$ determined in our laboratory [2]; glycerol (G) p.a. Avantor Performance Materials Poland S.A. (Gliwice, Poland); sodium hydroxide, 98%, Sigma-Aldrich (Poznań, Poland); zinc acetate dihydrate 99%, Sigma-Aldrich (Poznań, Poland); tansy, Nanga (Złotów, Poland); sage essential oil (SEO) Etja (Elbląg, Poland); surfactant – Tween 80, Greenaction Sp. z o.o. (Kielce, Poland); DPPH 95%, Sigma-Aldrich (Poznań, Poland); methanol p.a. POCh (Poland).

Film preparation

First, tansy extract in water was prepared. Next, zinc salt was dissolved in this extract, and the solution was stirred on a magnetic stirrer for an hour at 60 °C. Then, a 2M sodium hydroxide solution was added until the solution achieved pH = 10. After establishing the appropriate pH value of the solution, it was stirred for another hour at 60 °C. The formed precipitate was centrifuged at 4000 rpm and then washed with distilled water. The product was dried at 80 °C for 5 hours, then calcined in a muffle furnace for 2 hours at 400 C.

A sodium alginate of 2% (wt./v) was prepared, and glycerol was added to it at 2.5% (wt./v).

A mixture of sage essential oil and Tween 80 was prepared with a volume ratio of SEO to surfactant of 2:1.

Aqueous solutions of 40 cm³ were prepared, stirred, and finally poured onto polystyrene Petri dishes with 8 cm. The following films were obtained: sodium alginate, sodium alginate

with ZnO NPs, sodium alginate with ZnONPs and SEO, and sodium alginate with SEO. The weight ratio of these substances in the films was 0.6 g of alginate, 0.1 g ZnONPs, or 0.4 g SEO. ZnONPs were treated with ultrasounds to better dispersion.

Physico-chemical, antioxidant and antibacterial characterization

ZnONPs were characterized using XRD and SEM analysis. Spectroscopic (ATR-FTIR, UV-Vis), SEM, mechanical properties, moisture content, and antioxidant and antibacterial activity were tested for active alginate films.

RESULTS AND DISCUSSION

XRD pattern of the obtained ZnONPs showed narrow peaks at $2\theta = 31.9^\circ, 34.6^\circ, 36.4^\circ, 47.7^\circ, 56.8^\circ, 63.0^\circ, 66.5^\circ, 68.1^\circ, 69.3^\circ, 72.7^\circ$ and 77.1° assigned to (100), (002), (101), (102), (110), (103), (200), (112) (201) (004) (202) planes, which confirmed the existence of wurtzite crystalline structure of ZnO. The average particle size calculated according to the Scherrer equation was 15 nm. Similar results were obtained by other researchers [3,4].

The results of mechanical and antioxidant studies are gathered in Table 1. The mechanical properties of films are important because the packed product should be safe in packaging during storage or handling. Incorporation of ZnONPs, SEO, and both these additives simultaneously into the plasticized alginate films influenced Young's modulus (E), stress at break (σ), and strain at break (). It is seen that Young's modulus slightly decreased, whereas stress and strain at break increased for all samples, indicating greater flexibility and tensile strength in the doped films. The film with ZnONPs formed a more compact structure (the smaller thickness) and uniform particle distribution in the plasticized alginate film. Unique interactions, such as hydrogen bonding between zinc ions and the functional groups of alginate or glycerol, were probably formed, as suggested by other researchers [5]. The presence of SEO made the film more flexible, reducing the interactions between the film components as a result of film heterogeneity and the formation of free volume [5]. ZnONPs and SEO caused higher flexibility and tensile strength of the film, suggesting the changes in the film structure after adding both components. Adding both additives resulted in a significant increase in film thickness due to the increase in solid content and, consequently, thickness. [5].

The antioxidant activity of the mixed sage essential oil and ZnONPs film was stronger than that of the components separately, showing a synergistic effect between the compounds.

Tab. 1. Mechanical and antioxidant properties of the studied films.

Sample	E [MPa]	σ [MPa]	[%]	Thickness [mm]	AC μmol Trolox/100g
Alg	8.10 ± 1.03	4.75 ± 0.63	51.28 ± 5.09	0.1000 ± 0.0043	0
Alg+ZnO	7.10 ± 0.47	5.08 ± 0.76	59.69 ± 7.81	0.0936 ± 0.0037	0
Alg+SEO	6.06 ± 0.65	4.50 ± 0.76	58.17 ± 7.14	0.1144 ± 0.0051	$58,10 \pm 4,08$
Alg+ZnO+SEO	6.13 ± 0.24	7.76 ± 0.75	64.98 ± 2.27	0.1844 ± 0.0106	$91,64 \pm 3,62$

References

- 1) Z. Eslami, S. Elkoun, M. Robert, K. Adjallé, *Molecules*, **28**, 6637 (2023)
- 2) J. Kowalonek, N. Stachowiak, K. Bolczak, A. Richert, *Polymers*, **15**, 260 (2023)
- 3) K. Ali, S. Dwivedi, A. Azam, Q. Saquib, M. S. Al-Said, A. A. Alkhedhairi, J. Musarrat, *J. Colloid Interf. Sci.* **472**, 145–156 (2016)
- 4) A. Tymczewska, B. U. Furtado, J. Nowaczyk, K. Hryniewicz, A. Szydłowska-Czerniak, *Int. J. Mol. Sci.* **23**, 2734 (2022)
- 5) M. Alizadeh-Sani, E. M. Kia, Z. Ghasempour, A. Ehsani, *J. Polym. Environ.* **29**:588–598 (2021)

HDPE and PP based systems with PVP-I additive: mechanical and barrier properties

M. Leanza¹, D.C. Carbone¹, M. Baiamonte^{2,3}, M. Rapisarda¹, E.T.A. Spina¹, F.P. La Mantia^{2,3*} and P. Rizzarelli^{1}**

¹Istituto per i Polimeri, Compositi e Biomateriali (IPCB) - SS di Catania, Consiglio Nazionale delle Ricerche (CNR), via P. Gaifami 18, 95126 Catania, Italy

²Dipartimento di Ingegneria, Università di Palermo, Viale delle Scienze, 90128 Palermo, Italy

³INSTM, Consorzio Interuniversitario Nazionale per la Scienza e Tecnologia dei Materiali, Firenze, Italy

melania.leanza@ipcb.cnr.it, [*francescopaolo.lamantia@unipa.it](mailto:francescopaolo.lamantia@unipa.it), **paola.rizzarelli@cnr.it

INTRODUCTION

The complex of iodine with polyvinylpyrrolidone (PVP-I) is largely utilized in clinical settings due to its broad range of antimicrobial activity and lack of known bacterial resistance. PVP-I complex consists of PVP units linked with iodine via hydrogen bonds between two pyrroles and contains triiodide anions and a small amount of non-complexed mobile iodine (I_2 -free) that is the active bactericidal agent (1). One of the main problems faced in the pharmaceutical formulations of PVP-I, as well as other organic iodophor solutions packaged in a plastic container for medical use, is the leaching of I_2 through the packaging itself (2). Glass (not permeable to iodine) represents the more suitable material for a container to store dilute PVP-I solutions. However, the stability of dilute solutions can be affected by the presence of plastic components (e.g. dropper) in the glass containers, which may be an important source of iodine leaching. In this study, we investigated the possibility of reducing I_2 leaching through packaging by introducing small amounts of iodine via HDPE and PP blending with PVP-I.

EXPERIMENTAL

Materials

The raw materials used for the preparation of the blends were: HDPE (PHARMALENE® MP 30 PH, Versalis, Italy), PP (Purell HP371P, Lyondellbasell, Italy), PVP K30 (Sigma-Aldrich Chemical Co., Ltd., Italy), PVP-I (PVP-Iodine 30/06 BASF, Italy) and Sokalan (VA 64 P 25 K BASF, Italy), a vinyl pyrrolidone-vinyl acetate copolymer 55/45.

Preparation

Two series of samples based on HDPE (labeled as A, B, C, D, E) and PP (labeled as F, G, H, I, L) added with PVP-I, PVP and Sokalan (2% by weight) were prepared. They were made by a Dr Collin Teach Line ZK 25T twin-screw extruder adjusting the operating parameters according to the material. From the pellets obtained from the different polymeric blends, plates were made by die-casting in a PM 20/200 press (DGTS srl, Verduggio, Italy). From the plates, disks (rods) were obtained and used to evaluate the iodine barrier effect, using an accelerated test at 40°C (3).

Polymer blends characterization

The prepared mixtures based on HDPE and PP, in the form of granules or plates, were subjected to mechanical (tensile tests) characterization. Furthermore, the variation in wettability induced by the introduction of the minority, hydrophilic components was determined through static contact angle (SCA) measurements. Tests were carried out to determine the barrier properties to oxygen (OTR), water vapor (WVTR) and iodine (3).

RESULTS AND DISCUSSION

Considering the gas permeation mechanism and assuming that the loss of I_2 is the key factor for packaging in plastic material, we evaluated different approaches that could repress or reduce the diffusion of I_2 , such as the introduction into the packaging of an additional amount of iodine (3). The aim was to introduce molecular iodine into HDPE or PP-based polymeric

matrices indirectly and without the use of organic solvents. For this purpose, we mixed a polymeric complex with iodine (as in the case of PVP-I) or a second polymeric component that can complex the I₂ released from an iodophor solution (in the case of blends with PVP or Sokalan) in vapor phase or from solution. In fact, in the preparation phase the thermo-mechanical action can lead to the release of iodine, which would reasonably remain incorporated into the polymeric matrix. Furthermore, direct mixing of HDPE or PP with I₂ in the extruder would not be feasible as iodine is volatile and sublimates even at room temperature. Both PVP and Sokalan have also been added with the aim of improving the miscibility between HDPE or PP matrices and PVP-I. The data is shown in the Fig. 1.

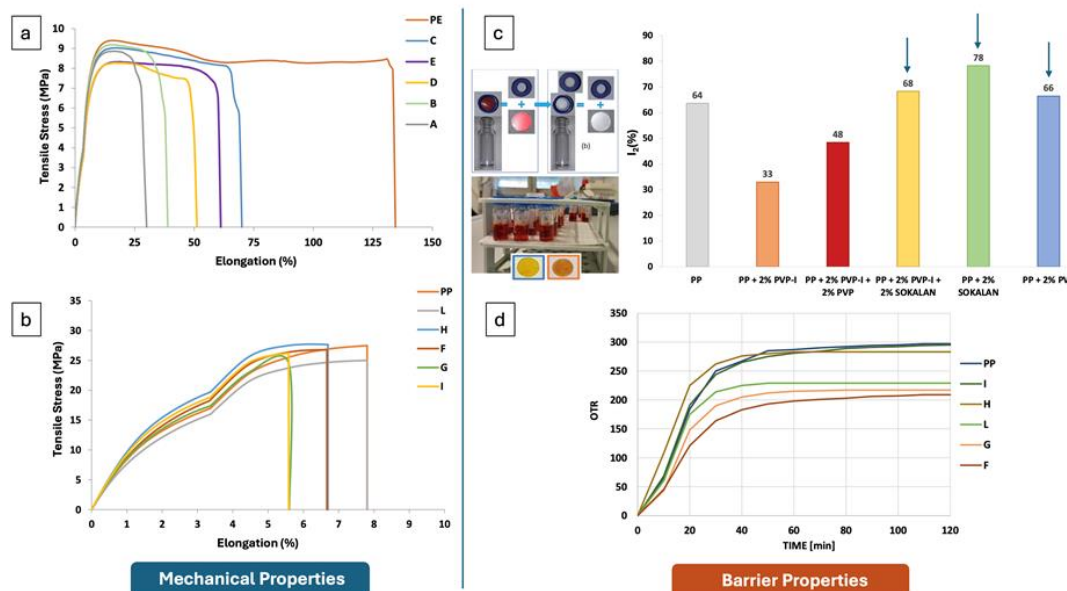


Fig. 1 Stress-strain curves of the **a)** PP and **b)** HDPE series. **c)** OTR curves of the PP matrix systems. **d)** I₂ concentration changes in PVP-I solutions stored in modified vials with PP septa.

The reported data shows that the presence of the minority components causes an increase in the value of the elastic modulus (Fig.1 a-b). This is reflected in an increase in the stiffness of the samples. Furthermore, the HDPE samples with 2% Sokalan+2% PVP-I, 2% Sokalan and 2% PVP (samples C, D and E, respectively) have higher elongation at break values and can therefore be considered as the samples with the best morphology and adherence between matrix and dispersed phase. The same can be said for the PP samples with the 2% PVP-I and 2% PVP blend (samples F and L, respectively). The barrier tests clearly show that PP samples with 2% Sokalan, 2% Sokalan + 2% PVP-I and 2% PVP (samples I, H, and L, respectively) provide a barrier to iodine (Fig. 1 c). It is likely that these systems absorb and retain the iodine, preventing it from leaching through the packaging. All blends showed a reduction in oxygen (Fig.1 d) and water vapour permeability compared to the neat matrices, resulting in a significant improvement in the barrier performance of the polymer blends.

Acknowledgment

This work has been financially supported by the by PO FESR 2014–2020, Action 1.1.5, project “New therapeutic strategies in ophthalmology: bacterial, viral and microbial infections-NUSTEO”, CUP: G68I18000700007-application code 08CT2120090065.

References

- 1) J.C. Koerner, M.J. George, D.R. Meyer, M.G. Rosco, M.M. Habib, *Surv. Ophthalmol.*, **63**, 862 (2018).
- 2) D. Bhagwat, B. Oshlack, U.S. Patent 5,126,127 (1992).
- 3) L. Ferreri, M. Rapisarda, M. Leanza, C. Munzone, N. D’Antona, G.M.L. Consoli, P. Rizzarelli, E.T.A. Spina, *Molecules*, **28**, 1869 (2023).

MECHANICAL CHARACTERIZATION AND THERMAL DEGRADATION OF SUSTAINABLE ADHESIVES BASED ON BIO-EPOXY RESINS ADDITIVATED WITH THERMOPLASTIC POLYMERS FOR SEPARABLE JOINTS

M. Luciano¹, R. Miranda¹, C. Sanfilippo¹, F. Mazzara¹, V. Fiore¹, A. Valenza¹

¹Department of Engineering, University of Palermo, Viale delle Scienze, 90128 Palermo, Italy
marco.luciano@unipa.it

INTRODUCTION

The importance of sustainability and circular economy is steadily increasing, particularly in industrial sectors such as naval, aerospace, and automation, where structural joints play a crucial role. Epoxy resin-based adhesives are an efficient solution for bonding substrates of different natures due to their lightness and high mechanical performance without compromising the structural integrity. However, traditional adhesives have significant limitations in terms of recyclability and environmental impact. This work aims to investigate possible solutions starting from a bio-based epoxy resin enhanced with thermoplastic polymers, in order to improve its workability and adhesive properties, with a focus on end-of-life recycling and resistance to different temperature environments.

EXPERIMENTAL

Materials

The recyclable epoxy resin used (commercial name Polar Bear) was provided by R*concept. This resin has a bio-content of 19%. The addition of thermoplastic polymers to the epoxy system was investigated. Two thermoplastic polymers were investigated: Polyetherimide (PEI), known for its excellent thermal stability and mechanical resistance, and Poly- ϵ -caprolactone (PCL), biodegradable and easily soluble in epoxy resins. The adhesive mixtures were prepared with different percentages of thermoplastics. The substrate on which the adhesive was applied is aluminum 6061 with a thickness of 3 mm.

Preparation of adhesive samples

Regarding the addition of PEI to the system, it was incorporated in quantities of 1%, 2%, 3%, 4%, and 5% relative to the weight of the monomer.

The PEI was added to a dichloromethane solution for two hours. Once the polymer was completely dissolved, epoxy resin was added. The solution was then heated to 90°C for 2 hours with continuous stirring to evaporate the dichloromethane. Subsequently, it was cooled to room temperature, and the curing agent was added.

Concerning PCL, it was chosen to evaluate the addition of a biodegradable thermoplastic so as not to compromise the system's bio-sustainability. The thermoplastic pellets were directly mixed with the monomer in proportions of 5%, 10%, 15%, and 20% by weight.

Once the PCL was added to the resin, the solution was maintained at 80°C with stirring for three hours to dissolve the PCL, and then cooled to room temperature.

The adhesive behavior of these mixture was studied by single lap shear test. The adhesive was placed between two 6061 aluminum sheets. The overlap measurement was 25mm x 25mm. For each joint, 0.4g of adhesive was used. Subsequently, they were subjected to a curing cycle for 24 hours at room temperature and post-cured in oven at 100°C for 3 hours.

Rheological and mechanical characterization

Rheological tests were conducted using the ARES-G2 parallel plate rheometer from TA Instruments. All tests were performed at room temperature, applying a rotational speed of 30 rad/s. The purpose of these tests was to evaluate the viscosity of the adhesives produced during the initial moments of application on the substrate of the joint. The obtained values were compared with those of commercial epoxy adhesives. Bending tests were performed on samples consisting of all types of adhesives described above to assess their mechanical performance. A

Zwick-Roell Z005 universal testing machine, equipped with a 5 kN load cell, was used. The tests were conducted according to the ASTM D790-03 standard. Furthermore, the samples were subjected to Charpy impact tests according to the ASTM D6110-10 standard. The testing machine used was an Istron Ceast 9050, equipped with a 25 J tool.

After performing the described tests, the types of adhesives that exhibited the desired characteristics in terms of mechanical strength and viscosity were selected through analysis of the experimental data obtained.

Single lap shear test was performed using a WANCE model ETM-C universal testing machine, equipped with a 50 kN load cell. For this test, the ASTM D1002 standard was used. The samples were tested at room temperature, and subsequently, the test was repeated at temperatures of 80°C and -40°C in order to investigate the adhesive's range of applicability and study its degradation.

RESULTS AND DISCUSSION

The results indicate that the addition of PEI and PCL significantly increases the viscosity of the adhesive system, with varying effects on mechanical properties depending on the concentration of the added polymer. Specifically, adhesion and mechanical resistance vary proportionally to the amount of incorporated thermoplastic, highlighting an improvement in performance in specific formulations. Additionally, the formulation of the cleavable adhesive allows for easy disassembly of adhesive components post-use, facilitating the recycling process and reducing the overall environmental impact.

The analysis demonstrates that current adhesive management strategies are not sufficient in the long term and suggests the need for an integrated and sustainable approach. The developed adhesives show great potential for industrial applications where sustainability and recyclability are fundamental criteria, thus contributing to the reduction of the environmental impact of structural joints and promoting a circular economy.

References

- 1) L. Barral, J. Cano, J. Lo´pez, I. Lo´pez-Bueno, P. Nogueira, M.J. Abad, C. Ramirez, *Polymer* **41** (2000)
- 2) Guanjun Liu, Fan Yang, Yujiao Bai, Chuang Han, Wenbo Liu, Xingkui Guo, Peipei Wang, Rongguo Wang, *Journal of Energy Storage* **42** (2021)
- 3) Shiqiang Deng, Luke Djukic, Rowan Paton, Lin Ye, *Composites: Part A* **68** (2015)
- 4) Jia-ting Wu, Wei-zhen Li, Shu-long Wang, Wen-jun Gan, *Royal Society of Chemistry* **11** (2021)

ONE-STEP FABRICATION AND MODIFICATION OF BIOPOLYMER FIBERS COATED WITH ACTIVE NANOPARTICLES FOR SUSTAINABLE TECHNOLOGIES

A. Maio*, M. Gammino, R. Scaffaro

Department of Engineering, University of Palermo, Viale delle Scienze, Palermo, Italy

andrea.maio@unipa.it, michele.gammino@unipa.it, roberto.scaffaro@unipa.it

INTRODUCTION

Surface coating of polymer fibrous materials is stimulating the latest research, aiming to develop multiphase materials with well-orchestrated morphology that could combine - possibly improving - the properties of starting constituents into a unique, high-performance material. Unfortunately, such materials are often prepared via multi-step protocols. Hence, the most urgent challenge is to develop sustainable preparation methods, such as rapid and possibly one-step pathways, in the perspective of reducing environmental and economic costs along with the use of toxic/dangerous chemicals.

EXPERIMENTAL

Materials

Polycaprolactone (PCL) and polylactic acid (PLA) were chosen as polymer substrates, graphene oxide (GO), carbon nanotubes (CNTs), nanocellulose fibers (NCF), lignin were used as coating agents. Chloroform, dichloromethane, acetone, ethanol, water were chosen as solvents (or co-solvents/non-solvents, depending on formulation). Methylene blue (MB), methyl orange (MO), phenol, dichlorobenzene, motor oil were selected as model molecules/pollutants.

Preparation and characterizations

Electrospinning in active bath was implemented to prepare 3D fibrous membranes coated with hybrid nanoparticles in one-step. A series of PLA and PCL solutions were prepared and electrospun into a coagulation bath constituted of ethanol or ethanol/water containing nanoparticles dispersed. The materials were fully characterized from a physicochemical, morphological, mechanical, electrical standpoint. Functional tests were performed to assess their sorption performance towards various pollutants.

RESULTS AND DISCUSSION

We prepared fluffy scaffolds with well-organized structure and single or hybrid coating/decorations. The microstructure of the polymer substrate was designed by adjusting the compositions and characteristics of spinning solution and coagulation bath, together with electrospinning parameters. Bulky or porous biopolymer fibers were obtained using the appropriate co-solvents/non-solvents mixture in the liquid collector. Different coatings, either uniform or discrete, were designed exploiting electrostatic interactions and self-assembly of different nanoparticles. Hybrid coatings with spider leg-like architectures were attained using 2D/1D hybrid dispersions of GO-CNTs in ethanol or ethanol/water. Longer fibers as 1D fillers (e.g., GO-Cellulose Nanofibers, CNF, dispersed in ethanol/water) led to spider web-like architectures constituted by a dual network. Introducing 0D nanoparticles like lignin, along with 2D nanoparticle dispersions, gave rise to shish kebab fibers. Changing the process parameters it was even possible to achieve discrete decorations, with the formation of branch-leaf configurations. Coating biopolymer fibers with nano-engineered surfaces, allowed tunable architecture, porosity (up to 99.5%), and modified all the surface properties, including roughness and specific surface area, with obvious repercussions on wettability, which was

varied from hydrophobic to hydrophilic and amphiphilic (Fig. 1), making them suitable for treating wastewater contaminated with (multiple) dyes, organic molecules, and oil/water emulsions. All samples demonstrated highly sensitive electrical conductivity to environmental variations, showing their potential as multifunctional materials. Moreover, the presence of a stiff armor constituted by hybrid coatings, such as GO-CNT and GO-NCF, protected the polymeric thin fibers, resulting in huge increments in mechanical properties, as well as higher thermal and chemical stability.

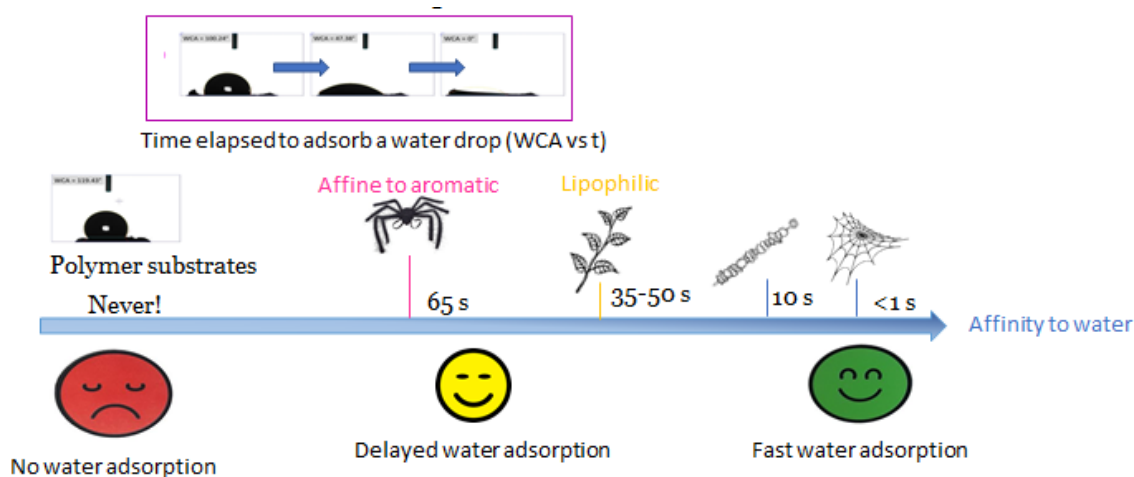


Fig. 1 Tunable affinity to water and other compounds, as a function of the chemical properties and morphology of hybrid coatings.

Acknowledgment

This study was carried out within the MICS (Made in Italy - circular and Sustainable) Extended Partnership and received funding from the European Union Next-GenerationEU (PIANO NAZIONALE DI RIPRESA E RESILIENZA (PNRR) - MISSIONE 4 COMPONENTE 2, INVESTIMENTO 1.3 - D.D. 1551.11-10-2022, PE00000004). This manuscript reflects only the authors' views and opinions, neither the European Union nor the European Commission can be considered responsible for them.

This study was carried out within the SAMOTHRACE (Sicilian micro and nano technology research and innovation center) Extended Partnership and received funding from the European Union Next-GenerationEU (PIANO NAZIONALE DI RIPRESA E RESILIENZA (PNRR) – MISSIONE 4 COMPONENTE 2, INVESTIMENTO 1.5). This manuscript reflects only the authors' views and opinions, neither the European Union nor the European Commission can be considered responsible for them.

Biodegradable polymer materials of bacterial origin

Anna Masek^{1*}, Stanisław Bielecki², Kamila Rulka¹, Valentina Brunnela³, Matilde Arese³

1 Institute of Polymer and Dye Technology, Faculty of Chemistry, Lodz University of Technology, 90-537 Lodz, Poland; 231401@edu.p.lodz.pl (D.L.)

2 International Center for Research on Innovative Biobased Materials, Lodz University of Technology, 2/22 Stefanowskiego Str., 90-537 Lodz, Poland;

3 University of Torino, Department of Chemistry, Via Verdi, 8 - 10124 Torino, Italy

Correspondence author: anna.masek@p.lodz.pl

INTRODUCTION

Bacterial cellulose (BNC) has unique physicochemical properties that are used compared to other biomaterials of bacterial and plant origin. BNC is a system with a high degree of porosity, high crystallinity and a high degree of polymerization. Due to the method of extraction, bacterial cellulose has a very high water content. The additional material has ten certificates, is biocompatible and hypoallergenic. The properties of bacterial nanocellulose are independent of the production process, therefore the use of this material may have various applications. BC samples spread in different ways, differing in particular structures, pore sizes and fiber geometries, which influence the properties of this material. Due to the fact that there are certain mechanical properties and full biodegradability of BC, they are becoming more and more popular as polymer composite products and ecological alternatives to glass and carbon fibers, and even plant cellulose fibers [1-4].

RESULTS AND DISCUSSION

Currently, many scientists are focusing on finding alternatives that will allow the production of environmentally friendly materials with properties similar to those of conventional materials. Natural biopolymers of plant origin or produced by microorganisms, such as cellulose fibers, can replace synthetic materials, ensuring the biodegradability of composites made from them. Biopolymers can be used in many fields of engineering, as textiles, biosensors and intelligent packaging, and in biomedicine. The use of natural fibers would help alleviate pollution problems such as waste, landfilling, toxic emissions and greenhouse gases. A promising raw material that can be used as reinforcement in polymer composites is bacterial cellulose, characterized by exceptional mechanical properties, biodegradability and renewability.



Fig. 2. Photo showing a dried sample of BC

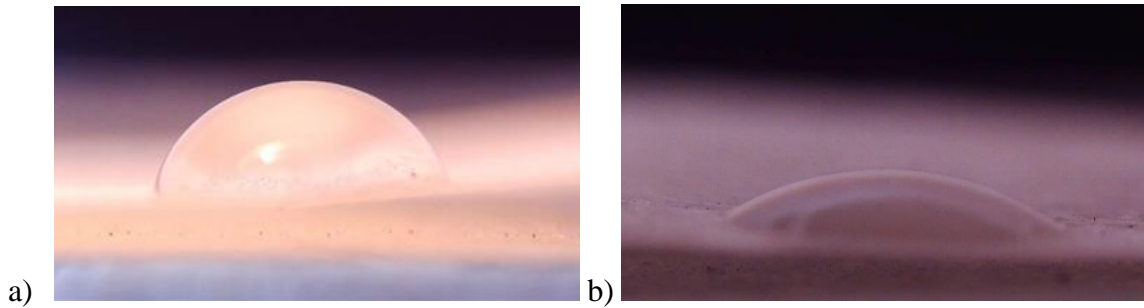


Fig.1. Photos from the assessment of BNC surface modification a) after rotation; b) before processing.

The development of new materials and technologies related to polymer processing requires analysis of their impact on the environment. Biodegradability or recyclability of manufactured products are desirable features if we want to reduce their negative impact on the environment. The above work presents a polymer composite material reinforced with natural biodegradable raw materials, which could potentially replace traditional structural composites. Bacterial cellulose has been effectively modified and the composites produced are ecological, with satisfactory thermal properties and can potentially be used in industry.

Acknowledgment

References

- 1) A. Masek, A. Kosmalska, *Front. Bioeng. Biotech.* 17, (2022).
- 2) Hickey R. J., Pelling A. E. *Front. Bioeng. Biotech.*, 7: 45-59. (2019).
- 3) Ates B., Koytepe S., Ulu A., Gurses C., Thakur V. K. *Chemical Reviews* 120, (2020).
- 4). D. Lisowski, S. Cichosz, S. Bielecki, A. Masek, *Mat.*, 17, 2783. (2024).

EFFECTS OF SALT SPRAY AGEING ON BIO-BASED EPOXY RESINS

V. Fiore¹, B. Megna¹, F. Sarasini², D. Rossano³, R. Miranda¹

¹ Department of Engineering, University of Palermo, Viale delle Scienze, 90128, Palermo, Italy

² Department of Chemical Engineering Materials Environment, Sapienza-Università di Roma, Via Eudossiana 18, 00184, Roma, Italy

³ Department of Business and Economic Studies, University of Naples “Parthenope”, Via Ammiraglio Ferdinando Acton, 38, 80133, Napoli, Italy

vincenzo.fiore@unipa.it

INTRODUCTION

Nowadays, composite materials have become a focal point in industry thanks to the synergy between the reinforcement and the matrix phase that imparts high strength, stiffness, and durability while maintaining low weight. In recent years, there has been a growing interest in sustainable and environmentally friendly materials, leading to the development and usage of eco-friendly materials such as bio-based epoxy resins as matrices of these composites. They are at least partially derived from renewable resources such as plant oils, lignin, and other natural polymers, offering a greener alternative to traditional petroleum-based epoxies. These bio-based epoxies maintain the desirable mechanical properties and chemical resistance of conventional epoxies while reducing the environmental footprint (1–5). This work investigates how exposure to a salt-fog environment can impact on the mechanical response of various bio-based epoxy resins, aiming to identify their possible use as matrix for bio-composites in harsh environments such as marine applications.

EXPERIMENTAL

Materials

Three thermoset systems, supplied by R*Concept, were investigated. The epoxy monomer Polar Bear, having a bio-based content higher than 28%, was cured with its recyclable hardener Recyclamine™ R101 that, bearing the cleavable ketal group, led to the full recyclability of the cured resin system (6). The Green Turtle epoxy with a bio-based content higher than 40% was mixed with its non-recyclable hardener. The last, named Plankton, having the highest bio content (i.e., >77%), was mixed with its non-recyclable hardener.

Preparation

The epoxy systems preparation followed the subsequent procedures:

- Polar Bear: The epoxy monomer was mixed with the recyclable hardener (100:22 by weight). Manual mixing was performed for 5 min, followed by a degassing in a vacuum chamber for 15 min.
- Green Turtle: Part A was mixed with its non-recyclable hardener in the weight ratio of 100:30. Manual mixing was performed for 3 min, followed by a degassing in a vacuum chamber for 5 min. The shorter time was due to the faster curing process of this system.
- Plankton: Part A was mixed with its non-recyclable hardener in the weight ratio of 100:30. Manual mixing was performed for 5 min, followed by a degassing in a vacuum chamber for 15 min.

All the thermoset prepared polymers were poured in the silicon mold to create the specimens for the mechanical tests.

Salt spray aging and characterizations of samples

The aging behavior of the bio-epoxy systems was evaluated by exposing them to salt-fog spray condition in a climate chamber model CC1000IP by Ascott, according to ASTM B117 standard. Each material was exposed to salt-spray fog (5 wt.% NaCl) at $35\text{ }^{\circ}\text{C} \pm 1\text{ }^{\circ}\text{C}$ for a period up to 60 days. Single set of specimens for mechanical tests were removed from the climatic chamber and tested after 15, 30, 45 and 60 days.

Mechanical tests consisted of tensile, three-point bending, and impact. Tensile tests were performed on dog-bone specimens (7 mm thickness) according to the ASTM D638, by using a universal testing machine WANCE model ETM-C, equipped with a load cell of 50 kN. The crosshead speed was set equal to 5 mm/min. The strain of the specimens was evaluated through a YYU-10/50 extensometer with a gauge length of 50 mm. Three-point bending tests were conducted following the ASTM D790 standard on prismatic specimens (3 mm x 57 mm x 12.7 mm). The crosshead speed was set to 1.3 mm/min. The Charpy impact test was carried out according to ASTM D6110 standard on prismatic samples (3 mm x 10 mm x 90 mm). Finally, FTIR and DMA techniques were used to evaluate how the salt-spray aging impact the structure of the thermoset polymers.

RESULTS AND DISCUSSION

The mechanical properties of all samples during ageing were evaluated at an interval of 15 days. Tensile strength, flexural strength and impact strength were compared between each thermosetting resin type during ageing, showing how mechanical properties were affected by salt spray exposure. The results were compared with morphological analysis using FTIR to highlight the effects of degradation on the chemical composition of the resins and link them to the mechanical test results. All bio-based thermosetting resins have responded well in aggressive environments, such as maritime salt spray, a sign of the high applicability of this type of material as a replacement for fossil-based epoxy resins, with a focus on eco-sustainability and the circular economy.

Acknowledgment

Funded by the European Union - Next Generation EU - PNRR M4 - C2 - investment 1.1: Fund for the National Research Program and Projects of Significant National Interest (PRIN) - PRIN 2022PNRR cod. P20223YBZ8_001 entitled "Recyclable biocomposites With enhanced Durability" (REWIND) CUP B53D23026710001

References

- 1) G. Mashouf Roudsari, A.K. Mohanty, M. Misra, ACS Sustain Chem Eng **5**, 9528 (2017)
- 2) R. Auvergne, S. Caillol, G. David, B. Boutevin, J.P. Pascault, Chem Rev **114**, 1082 (2014)
- 3) E. Ramon, C. Sguazzo, P.M.G.P. Moreira, Aerospace **5**, 110 (2018)
- 4) C. Ding, A.S. Matharu, ACS Sustain Chem Eng **2**, 2217 (2014)
- 5) J.M. Raquez, M. Deléglise, M.F. Lacrampe, P. Krawczak, Progress in Polymer Science, **35**, 487 (2010)
- 6) S. Dattilo, G. Macaroni, P.M. Riccobene, C. Puglisi, L. Saitta, Polymers, **14**, 4828 (2022)

PHOTO-OXIDATIVE DEGRADATION OF BIOCOMPOSITES BASED ON MATER-BI AND GRAPE POMACE: PROPERTIES AND SOIL BURIAL PERFORMANCE

M. Rapisarda¹, V. Titone^{2,3}, L. Pulvirenti⁴, E. Napoli⁴, G. Impallomeni¹, L. Botta^{2,3}, P. Rizzarelli^{1*} and M.C. Mistretta^{2,3**}

^{1**}Institute for Polymers, Composites and Biomaterials - National Research Council (IPCB-CNR), Via Paolo Gaifami 18, Catania, Italy

^{2*}Department of Engineering, University of Palermo, Viale delle Scienze, Palermo, Italy

³National Interuniversity Consortium of Materials Science and Technology (INSTM), Florence, Italy

⁴Institute of Biomolecular Chemistry – National Research Council (ICB-CNR), Via Paolo Gaifami 18, Catania, Italy

*mariachiara.mistretta@unipa.it, **paola.rizzarelli@cnr.it

INTRODUCTION

The realization of biocomposites represents an important tool with a view to a circular economy. Various food or agricultural wastes are added to biodegradable matrices in order to improve their mechanical performance while maintaining the advantage of biodegradability.

Furthermore, some of these fillers have also been found to be functional, so their use also allows improvements from other points of view (1). In this work, we highlighted how the introduction of the grape pomace (GP) induced a proportional increase of antioxidant property in biocomposites (BioC) based on Mater-Bi (MB), improving significantly their UV resistance and their biodegradability.

EXPERIMENTAL

Materials

The materials used in this work were: Mater-Bi® E151N0 (melting temperature: 167 °C, density: 1.23 g/cm³) provided by Novamont (NO, Italy), and GP from cultivation on the Etna Mountain, kindly supplied by Al-Cantàra Srl (Randazzo, CT, Italy). All solvents and reagents used were high purity laboratory grade. Water and acetonitrile were acquired from Carlo Erba (MI, Italy), CDCl₃, caffeic acid, malvidin chloride, ellagic acid and quercetin from Sigma-Aldrich (MI, Italy), folin-ciocalteau reagent from Fluka (MI, Italy).

Preparation

All materials were prepared through extrusion in a co-rotating twin-screw extruder (OMC, screw diameter = 19 mm, length/diameter ratio = 35 mm; temperature profile: 145-150-155-160-165-170-180 °C). The specimens were prepared by compression molding at 180 °C and after they were photo-oxidized for 48h and 72h. The exposure cycle conditions were 8h of UV irradiation at a temperature of 55 °C followed by 4h condensation at the temperature of 45 °C. GP (freeze-dried), MB and BioCs were milled. Then, the powders were suspended in EtOH-H₂O (70:30) considering a concentration of about 130 and 200 mg/mL in the extraction solvent for GP and polymer samples, respectively. The suspensions were left in the shaker (400 rpm) in the dark for 24 h at room temperature and then the extracts were recovered by centrifugation and a subsequently filtration, in order to freshly analyze the supernatant.

Biocomposites characterization, photodegradation and biodegradation

Viscosity was measured by a rotational rheometer with 25 mm plate at T = 180 °C. Tensile tests were carried out by an Instron universal testing machine mod. 3365 (rate = 1 mm/min until 3% strain, then at 100 mm/min until failure). Morphological analysis were conducted using a scanning electron microscopy (SEM), Phenom ProX microscope. GP extracts were analyzed

by HPLC-UV at 280, 330, 350 and 520 nm that are the wavelengths characteristics of four different class of polyphenol family, namely cinnamic acids (HCA), flavonoids, anthocyanins and ellagic acid derivatives. Furthermore, to monitor the degradation of secondary metabolites the extracts were subjected to the folin ciocalteau assay. Nuclear magnetic resonance (^1H NMR, 500 MHz) experiments were performed at 27 °C in CDCl_3 (0.03% TMS). Surface wettability was measured using a contact angle goniometer at room temperature after samples have been equilibrated at 40 °C for 30 min, with at least five values recorded. Soil burial test was performed up to 45 days at 58.0 ± 0.1 °C and degradation monitored through weight loss (WL).

RESULTS AND DISCUSSION

The analysis of GP (particle size 50 μm , Fig 1a) showed a slight decrease of antioxidant potency, despite the heat treatment simulating the BioC processing, but a relevant ones after 72h of UV irradiations and the combined action of heat and photo-oxidation (Fig 1b). However, the introduction of the GP in the polymer matrix induced a proportional increase of antioxidant property in the BioCs that improved significantly their UV resistance (Fig 1c). The comparison between the flow curves of photo-oxidized and non-photo-oxidized materials shows how the presence of GP reduces the non-Newtonian behavior of the biocomposites. This behavior could be attributed to a protective effect caused by the filler during the photo-oxidation. Both degradation in soil and photo-oxidation caused a contact angle decrease (Fig 1d) due to the formation of new end groups detected by NMR analysis. Interestingly, WL increased with the filler content and photo-oxidation for BioCs while decreased with UV irradiation time for MB (Fig 1e). These results could be related to crosslinking reactions and gel formation in MB, limited by the functional compounds of the GP filler in the BioCs.

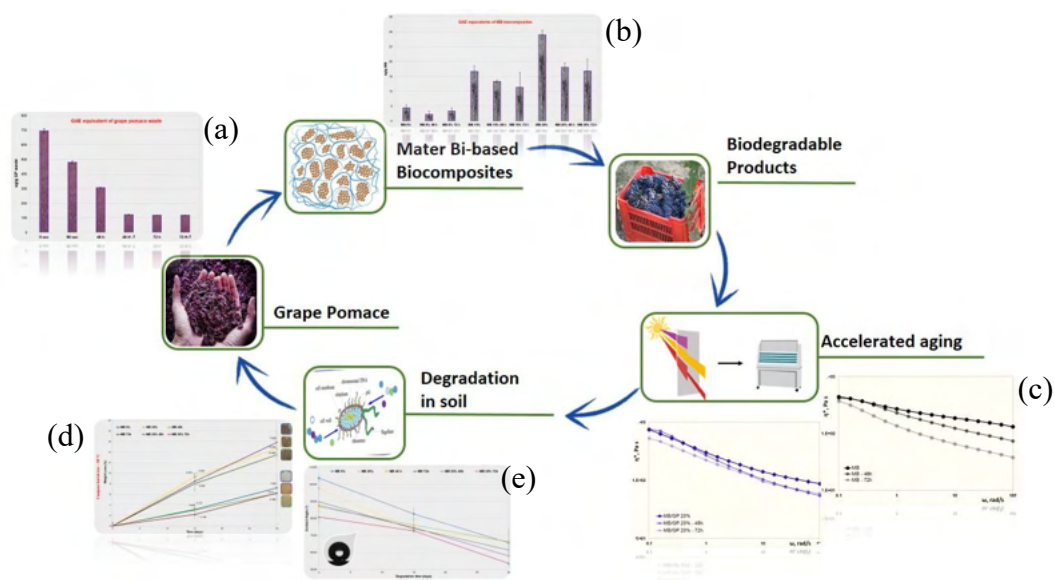


Fig. 1 Overview of the results and the circular model approach applied.

Acknowledgment

Funded by the European Union – Next Generation EU - PNRR M4 - C2 -investimento 1.1: Fondo per il Programma Nazionale di Ricerca e Progetti di Rilevante Interesse Nazionale (PRIN) - PRIN 2022PNRR cod. P2022M3FTM_002 dal titolo “Sustainable routes to high Performance and Recycling of BIOdegradable plastics for a circular economy – SuperBio” CUP B53D23027630001. Dr L. Pulvirenti gratefully acknowledge to the PNRR project SAMOTHRACE (CUP B63C22000620005).

References

1) M. Baiamonte, M. Rapisarda, M.C. Mistretta, G. Impallomeni, F.P. La Mantia, P. Rizzarelli. Polymer Composite, 2024.

Rheological and spinning behaviour of a starch-based polymer

M. Morreale, M. Baiamonte* and F.P. La Mantia*

Department of Engineering and Architecture, Kore University of Enna, Cittadella Universitaria, Enna, Italy

* National Interuniversity Consortium of Materials Science and Technology (INSTM), Via Giusti, Florence, Italy and Department of Engineering, University of Palermo, Viale delle Scienze, Palermo, Italy

marco.morreale@unikore.it, marilena.baiamonte@unipa.it, francescopaolo.lamantia@unipa.it

INTRODUCTION

Currently, increasingly stringent requirements (both in terms of public opinion and actual legislative measures) aiming at the reduction of the environmental impact related to the use of plastics coming from non-renewable sources and, more generally, without biodegradability/compostability features, have spur the focus on alternatives that are biodegradable/compostable (hereafter, referred to generically as "biopolymers"). In this regard, one of the most interesting commercial biopolymer families is certainly the one produced by Novamont under the MaterBi® name. Considering that more and more new grades of MaterBi® are being launched on the market, it is important to have a complete characterization in order to identify all the possible applications and, in particular, the most suitable. In this context, rheological characterization is fundamental to assess the actual processability of the polymer. In the present work, therefore, the rheological characterization and, more in general, the behaviour under non-isothermal elongational flow of a starch-based biopolymer coming from the MaterBi family was investigated.

EXPERIMENTAL

The starch-based biopolymer investigated in this work was a MaterBi "EF05B" grade, with proprietary composition but known to be composed by corn starch, synthetic biodegradable polyesters and plasticizers based on polyols [1].

Characterization was carried out under shear flow, both at medium/low gradients using a rotational rheometer, and at medium/high gradients using a capillary rheometer; in addition, the behavior under non-isothermal elongational flow was evaluated at two different temperatures (namely, 145 °C and 155 °C) in order to measure the Melt Strength (MS) and Breaking Stretching Ratio (BSR) of the extrudate and, in particular, its actual spinnability. Finally, mechanical characterization of the extrudates at different draw ratios (DR) was carried out.

RESULTS AND DISCUSSION

The results from the rheological tests showed that a small temperature difference led to a significant increase of the viscosity and a more non-Newtonian behaviour, thus suggesting that 155 °C should be the optimal processing temperature. This was further proven under non-isothermal elongational flow, since adequate/good values of the melt strength and the breaking stretching ratio were measured. These found a proof in the very good spinnability of the extrudates.

The obtained filaments were subjected to tensile tests, which showed adequate values of the tensile strength, and a good deformability in the investigated draw ratio range.

References

- 1) M. Barbale, S. Chinaglia, A. Gazzilli, A. Pischedda, M. Pognani, M. Tosin, F. Degli Innocenti, *Polym. Degrad. Stab.* **188**, 109592 (2021).

Exploring the impact of siloxane networks on the thermal behavior of P/N-enriched flame retardant finishes for cotton fabric

R. Otto^{1,2}, W. Ali^{1,2}, J. S. Gutmann^{1,2} and T. Mayer-Gall¹

¹ Deutsches Textilforschungszentrum Nord-West gGmbH, Krefeld (Germany)

² Department of Physical Chemistry and Center for Nanointegration (CENIDE), University of Duisburg-Essen, Essen (Germany)

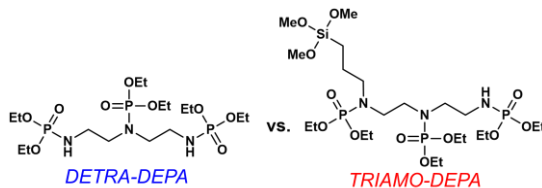
INTRODUCTION

Phosphorus/nitrogen (P/N) based flame retardants (FRs) have emerged as a promising solution for imparting fire-resistant properties to cotton fabrics due to the synergistic effects of phosphorous and nitrogen moieties.¹ A notable category of chemically bonded P/N-containing FRs is phosphoramidates, which albeit exhibiting excellent flame retardancy, face challenges related to poor washability. A widely recognized approach to ensure strong fiber adhesion and enhance wash resistance of the applied FR is the sol-gel method, utilizing either chemically functionalized silane precursors or fabricating a silicon dioxide supporting layer. Our study emphasizes on the influence of functionalized siloxane layer on the flame retardancy and thermal stability of a TRIAMO based phosphoramidate (TRIAMO-DEPA) comparing it with the corresponding silica-free diethylenetriamine derivative (DETRA-DEPA).

EXPERIMENTAL

Materials

The main materials used in this work were: woven cotton fabric (CO, plain weave, 170 g/m²), TRIAMO_DEPA and DETRA_DEPA flame retardant materials which were synthesized by nucleophilic substitution of 3-[(Trimethoxysilyl)propyl]diethylenetriamine (TRIAMO, 99%) or diethylenetriamine (DETRA, 99%) respectively and chlorophosphoric acid diethylester (97%).



Scheme 1: DETRA_DEPA and TRIAMO_DEPA flame retardant materials used in this work.

Sol-gel and wet finishing process

Sol-gel coating of cotton textile specimen was carried out by dissolving the TRIAMO_DEPA-silane in Millipore water with a fixed weight concentration β (w/v) of 0,25 g/mL. The pH of the solution was adjusted to 4-5 using concentrated HCl. The dispersion was then stirred for 72 h at room temperature. In case of DETRA_DEPA flame retardant, 20.10 g was solved in 60 mL of Millipore water to achieve a concentration of 0.25 g/mL.

Afterwards, a fixed volume of 60 mL was placed into a tray and a 15 cm² piece of cotton textile was immersed in the solution for approximately 5 min. Subsequently, the soaked fabric underwent a padding process (one dip, one nip) using a standard laboratory padding machine and horizontally cured at 130 °C for 20 min in a lab dryer. The coated specimens were stored overnight under standard atmospheric conditions (60±2 % relative humidity and 20±1 °C).

Thermal and chemical characterization

The finished specimen were subjected to thermogravimetric analysis (TGA) and dynamic scanning calorimetry (DSC) at varying heating rates (5, 10, 20, 40°C) for isoconversional kinetic analysis according to ASTM. Gaseous degradation products were analyzed by TG-IR-coupling, while residues were examined by XPS and IR-spectroscopy. Flame retardant parameters were obtained, most notably pHRR, THR and FGC, by micro-scale combustion calorimetry (MCC).

RESULTS AND DISCUSSION

Through kinetic studies, we observed that siloxane layer significantly influences the combustion mechanism of the finished textile. While both flame retardants catalyse dehydration and thus the charring of cotton, siloxane treatment leads to a higher initial activation energy by forming a protective physical barrier that supports the condensed phase activity of the phosphoramidate FR. The protective influence of the silica moiety even prohibits cotton pyrolysis (as seen in DSC) and slows down the reaction kinetics by portraying an obstacle for diffusion (as seen in DTG).

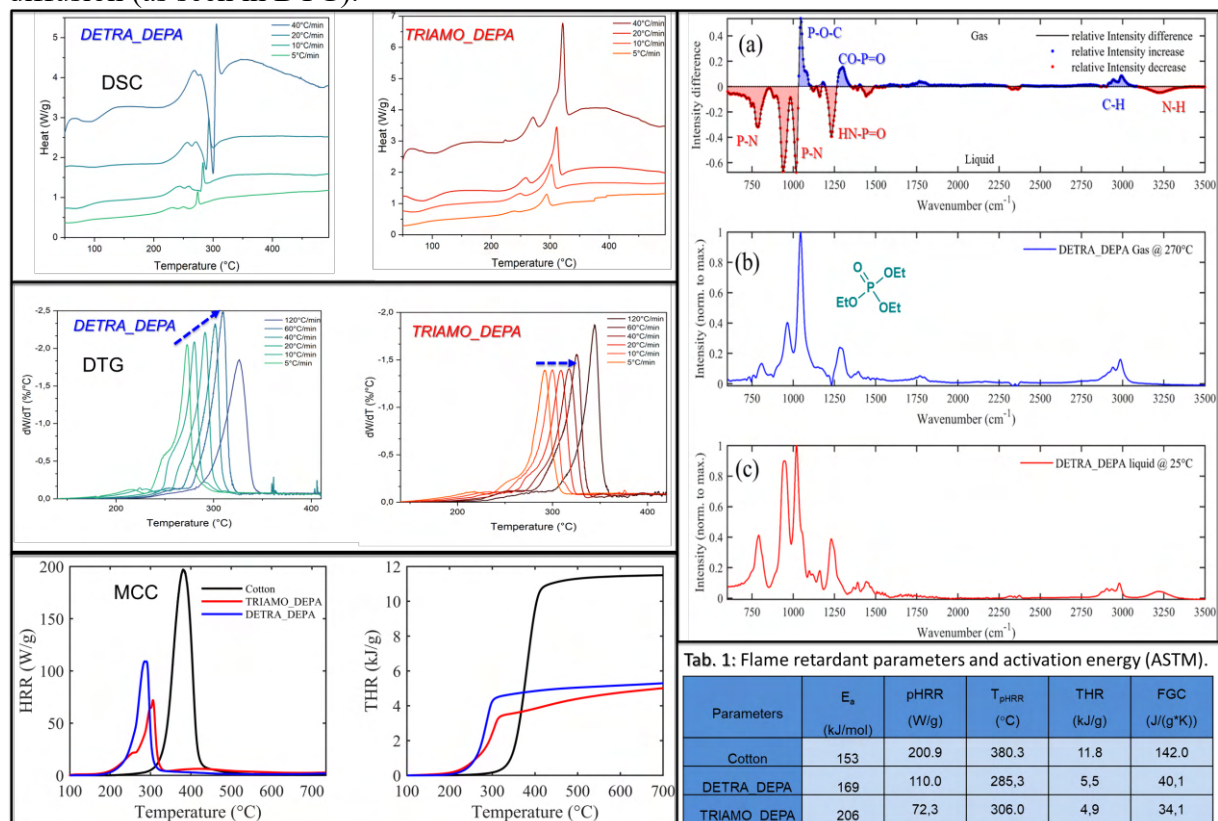


Fig. 1: Thermal analysis for both FR finished specimen. Depicted are the heating rate dependent DSC and DTG spectra on the top left, the HRR and THR as a function of applied temperature acquired by MCC in the bottom left, while on the right hand side the IR-signals of the flame retardant and the derived thermal degradation products are portrayed.

Spectroscopical and XPS data suggest a wide mix of PN-derivatives in the char for both species, where DETRA_DEPA produces mainly polyphosphazene, while TRIAMO_DEPA forms more aliphatic PN-species like phosphoramides and phosphor oxynitrides, and thus a denser network. The gas phase products seem to be identical though according to our investigations, leading us to believe that silica moieties do not intervene in the primary reaction mechanisms of phosphoramidates but rather enhancing condensed phase action by limiting gas transport.

Acknowledgment

This work was funded by the Deutsche Forschungsgemeinschaft (DFG, German Research Foundation) – 517869745

BIODEGRADABILITY OF 'POLYURATHANE SHOE SOLE': ENSUING BY THE SOIL BURIAL DEGRADATION

N. Saha^{1,2*}, A.C. Paul^{2,3}, T. Saha², N. Saha² and P. Saha²

¹Centre of Polymer Systems, University Institute, Tomas Bata University in Zlin, Trida Tomase Bati 5678, 76001 Zlin, Czech Republic

²Footwear Research Centre, University Institute, Tomas Bata University in Zlin, Nad Ovcirnou IV, 3685 Zlin, Czech Republic

³Department of Leather Engineering, Khulna University of Engineering & Technology, Khulna-9203, Bangladesh

* nabanita@utb.cz, adhir@utb.cz, tsaha@utb.cz, nibedita@utb.cz and saha@utb.cz

INTRODUCTION

Polyurethane soles are slowly replacing the natural materials: leather and natural rubber as shoe sole materials and gradually in the process, reforming the shoe industry [1]. Polyurethane (PU) prepared from a new kind of organic polymer material. The global PU sole market which was USD 5.26 billion in 2022, is expected to reach USD 8.19 billion by 2030. The continuous growth of global footwear industry, driven by fashion trends and rising consumer income, serves as a substantial driver for the PU sole market. Polyurethane soles are favoured for their durability, comfort, and versatility in footwear design. Beside this, increasing social awareness of environmental sustainability that exhilarated a shift toward the use of eco-friendly materials like PU in footwear industry [2]. It is also the responsibility of the footwear researchers to promote socially responsible production to develop sustainable footwear. Biodegradation of the PU waste is still challenging due to its complex molecular composition [3].

To confirm social awareness about biodegradability of PU sole in nature, in this work we mainly evaluate the '*biodegradability of polyurethane shoe sole*' following the soil burial degradation study on the basis of its changes in chemical, physical, morphological and rheological properties (before and after degradation). Other key properties of materials such as weight loss, hardness, density, tensile strength etc. are also will be studied.

EXPERIMENTAL

Materials

The test sample (PU shoe sole) used in this biodegradation study was supplied by EPUR spol. s.r.o., Pod Hôrkou 149/14, 95842 Brodzany, Slovakia. Polypropylene boxes (3.8 L) with the lids including two holes were used as the bioreactor with the dimensions of (H:9.0cm x L:25.0cm x W:16.5cm). Holes were made to provide fresh air while biodegradation process is going on insides of the bioreactor. Soil was collected from the landfill area managed by Technické služby Zlín, s.r.o., Zlin, Czech Republic.

Soil burial degradation test method

Soil burial test was carried out at 30 ± 0.1 °C under moisture-controlled (60%) conditions (as shown in figure 1). Soil was collected having with an extremely source of inoculum (to evaluate the biodegradability of PU shoe sole in the controlled environment and pH: 7.1). The bed for soil burial test was prepared with landfill soil: 600g; perlite: 60g (to maintain moisture content and for increasing the aeration to the soil bed); sucrose: 6g (to supply additional source of nutrient for existing microflora present in the soil) and 100 ml water. The moisture content of the soil and the mixture soil (soil + perlite) was determined by following the equation [(Weight of fresh solids—Weight of dry solids/ Weight of fresh solids) *100]. The PU sole samples were sandwiched between two layers of soil + perlite mixture (10:1). The test samples were removed after intervals of each 15 days and the preliminary

experiment was conducted until 60 days to understand the trend of degradation. Filter paper samples were used as a positive control.

The degree of biodegradation was evaluated as the weight loss divided by the initial sample weight. The chemical, physical, morphological and rheological properties including hardness, density, tensile strength etc. will be characterized following the respective methodologies.

RESULTS AND DISCUSSION

The PU shoe sole obtained from EPUR spol. s.r.o, Brodzany, Slovakia is depicted in Fig.1. The composition of PU sole are follows: polyester polyol, monoethylenglycol and commercial diisocyanate etc. which are assumed to be biodegradable. The description of test samples of PU shoe sole is depicted in Table 1 which indicated that diameter: **24 mm**, thickness: **4.5-6.5 mm** and initial weight: **1.7-2.4 g** and compressive modulus: **9.2-12.1 N/mm²**. The initial moisture content of the soil is **18:83%**; moreover, it is clearly visible from Fig 1 that enough mixed microflora (bacteria and fungi) is present in the land fill soil.

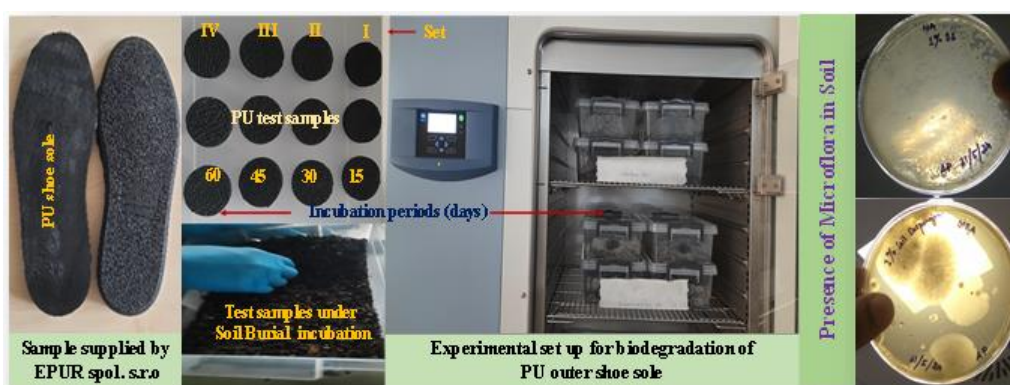


Fig. 1 A visual image of experimental set up for biodegradation of 'PU shoe sole' and presence of mixed microflora in landfill soil (used in Soil Burial Degradation).

Table 1: Brief description of PU shoe sole (before biodegradation)

Sample Index	Incubation Period (Days)	Diameter (mm)	Thickness (mm)	Weight (g)	Compressive Modulus (N/mm ²)
Set I	15	24.62 ± 0.10	4.45 ± 0.08	1.72 ± 0.14	09.17 ± 0.07
Set II	30	24.56 ± 0.12	5.46 ± 0.20	1.85 ± 0.05	10.86 ± 0.07
Set III	45	24.40 ± 0.07	6.30 ± 0.26	2.02 ± 0.12	11.71 ± 0.09
Set IV	60	24.34 ± 0.09	6.47 ± 0.73	2.38 ± 0.63	12.10 ± 0.03

*Presented values are average data of 3 samples.

The experiment on biodegradability study is in progress. The observed changes in test samples (in course of time) are recorded and will be presented during conference presentation.

Acknowledgment

This work has been financially supported by the Project Grant no: 101139988 — AEQUALIS4TCLF — ERASMUS-EDU-2023-PI-ALL-INNO "Addressing Skills Gaps in the European Textile, Clothing, Leather and Footwear Industries, Emphasizing Equality, Innovation, and Resilience." Authors are thankful to the owner EPUR spol. s.r.o., Slovakia, for providing the PU shoe sole for biodegradation study.

References

- 1) M.Mukherjee, T. Loganathan, S. Mandal, and G. Saraswathy; JALCA, VOL. 116, (2021)
- 2) <https://www.databridgemarketresearch.com/reports/global-pu-sole-market> (accessed on 12.06.2024)
- 3) T. Su, Tong Zhang, P. Liu et.al Applied Microbiology and Biotechnology, 107:1983-1985 (2023)

RECYCLING OF HDPE FROM BUSHES USED IN RAILWAYS CROSSBEAMS FASTENING AND ITS REINFORCEMENTS WITH THE SCRAPED FRACTION OF CARBON FIBERS WASTES UPCYCLING

R. Petrucci*, L. Torre*, M. Rallini

Civil and Environmental Engineering Department, University of Perugia, Strada di Pentima, 4, Terni, Italy

INTRODUCTION

Every year a wide amount concrete based railway crossbeams are disposed. Currently, their end of life deals with milling and materials separation, thus tons of HDPE bushes are produced and sent to landfill, as significantly polluted by both coarse and fine inert materials.

There are many other factors leading to a small incentive to recycle this polymer, as property degradation during the related recycling, high viscosity and poor processing ability, but also cheapness and high quality of the virgin counterpart (1).

However, the use of recycled plastic waste potentially ensures sustainable resources and the reduction of waste, whenever the mechanical properties of recycled HDPE match the performance requested for the intended applications.

The developed strategy, aimed to increase the processing ability of the recycled HDPE, deals with the related mixing with rheological additives, able to decrease the system viscosity, and other compatibilisers. To increase the related strengths and stiffness, an additional waste stream, such as carbon fiber residues produced during this waste recycling, otherwise discarded in landfill, has been introduced into the system (2). Short fibers composite materials have been obtained, whose thermal stability, mechanical and electrical performance has been investigated.

EXPERIMENTAL

Materials

The HDPE bushes have been directly provided by the company performing the crossbeams milling process (Calcestruzzi Cipiccia SPA). Scraped strips cut out from recycled mats of 30 mm to 40 mm carbon fibers (selvage), as well as short fibers clusters collected from the filters of air filtering systems, have been provided by the company Carbon Task Srl.

Erucamide (rheological additive) has been purchased by Sigma Aldrich, while coupling agent (Fusabond E226) has been provided by DuPont.

Preparation

The as received bushes have been subjected to a recycling pathway based on a preliminary dry/compressed air based cleaning, granulation by milling, subsequent gurgling water cleaning, material sieving and drying. Also a procedure aimed at water recycling through micro/nano filtration has been carried out. Also the as received carbon fibers have been subjected to a milling stage aimed at a fibers dimension homogenization.

Three kinds of matrices have been produced: rHDPE(95%)/Erucamide(5%), rHDPE(80%)/Fusabond(20%), rHDPE(76%)/Fusabond(19%)/ Erucamide(5%). Each ones has been reinforced with 0%, 10%, 20% and 30% of carbon fibers.

The systems have been produced by a DSM Microcompounder 15, equipped with two co-rotating screws and a recirculation system. The applied thermal profile leads to a melt temperature of 184 °C and a mixing time of 60 seconds has been set.

Dog-bone samples (ISO 527 1BA specimen) have been produced by injection moulding, using a DSM Micro Injection Moulding Machine 10cc. Injection and mould temperature respectively of 210 °C and 55 °C have been set, as well as an injection/holding pressure of 12 bar and a holding time of 8 seconds.

Material characterization

Thermal stability has been measured via dynamic TGA scan test (20 °C/min) from room temperature to 600 °C in a nitrogen atmosphere. The composites morphology has been analysed by SEM-FEG. Electrical properties have been studied by mean of conductivity test.

Mechanical properties have been analysed by mean of an electronic dynamometer with no external strain gage. On this regards, strain controlled (5 mm/min) tensile test have been carried out following the guidelines of ISO 527 standard.

RESULTS AND DISCUSSION

The neat rHDPE based systems processing ability has been revealed very critical. The problem has been solved by mean of the addition of few weight fractions of Erucamide, also in the case of highly reinforced systems containing also the coupling agent. On the other hands, the addition of this product leads to a slight decrease in the system thermal stability and mechanical strenght and stiffness, while the strain at break increases.

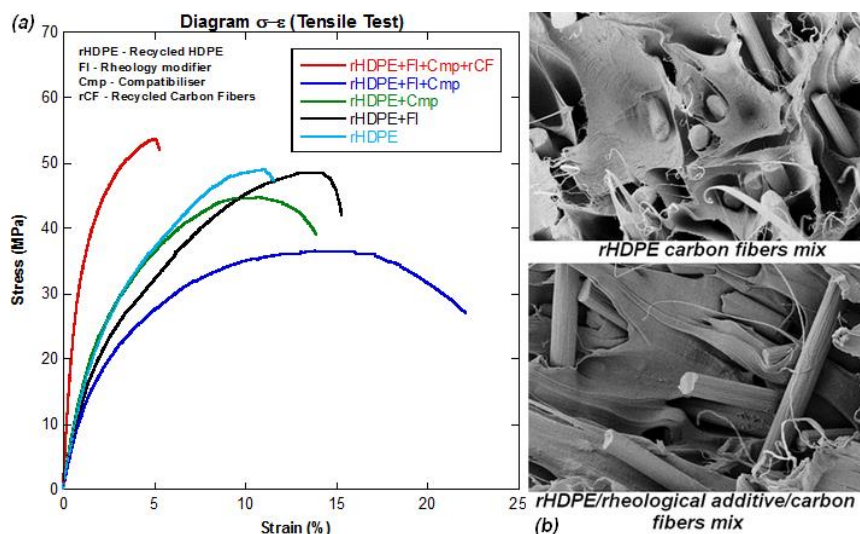


Fig. 1 rHDPE based composites Stress-strain diagram (part a) and morphology (part b).

The addition of short carbon fibers leads to a slight decrease in the investigated system strain at break, to a moderate increase in the tensile strenght and thermal stability, but also to a dramatic increase in the related stiffness. On the other hands, the reinforced systems behave as electrical insulating materials, as, despite the used fibers are characterised by a high electrical conductivity, they lie perfectly aligned in a single direction (the melt flow one related to the injection moulding stage) and without forming any conduction pathway.

Acknowledgment

This work has been financially supported by European Union - NextGenerationEU under the Italian Ministry of University and Research (MUR) National Innovation Ecosystem grant ECS00000041 - VITALITY.

References

- 1) A. Borkar, A. Hendlmeier, Z. Simon, J.D. Randall, F. Stojcevski, L.C. Henderson, “A comparison of mechanical properties of recycled high-density polyethylene/waste carbon fiber via injection molding and 3D printing”. *Polymer Composites*. 2022;43:2408–2418.
- 2) S. Karuppanan Gopalraj, T. Kärki, “A review on the recycling of waste carbon fibre/glass fibre-reinforced composites: fibre recovery, properties and life-cycle analysis”. *SN Applied Sciences* (2020) 2:433;

ROLE OF NANOLIGNIN AND METAL OXIDE NANOPARTICLES ON PLLA UV PHOTODEGRADATION

Debora Puglia¹, Erlantz Lizundia^{2,3}, Ilaria Armentano⁴, Francesca Luzi⁵, Alessandro Di Michele⁶, Roccoaldo Sardella⁷, Andrea Carotti⁷, Antonio Macchiarulo⁷, Luigi Torre¹

¹Department of Civil and Environmental Engineering, University of Perugia, UdR INSTM, Italy

²Life Cycle Thinking Group, Department of Graphic Design and Engineering Projects, Faculty of Engineering in Bilbao, University of the Basque Country (UPV/EHU), Bilbao

³Spain BCMaterials, Basque Center for Materials, Applications and Nanostructures, UPV/EHU Science Park, Leioa, Spain

⁴Department of Economics, Engineering, Society and Business Organization (DEIM), University of Tuscia, Viterbo, Italy

⁵Department of Science and Engineering of Matter, Environment and Urban Planning (SIMAU), Università Politecnica Delle Marche, UdR INSTM, Ancona, Italy

⁶Department of Physics and Geology, University of Perugia, Perugia, Italy

⁷Department of Pharmaceutical Sciences, University of Perugia, Italy

debora.puglia@unipg.it

INTRODUCTION

When considering the UV degradation of Poly(L-lactide) (PLLA)/lignin nanocomposites with the addition of metal oxides, several factors come into play: metal oxides can act as UV filters, shielding the PLLA/lignin matrix from harmful UV rays or some of them exhibit photocatalytic activity, which can lead to the degradation of organic compounds under UV irradiation. This property may affect the stability of the PLLA/lignin matrix, potentially accelerating degradation processes. Size and dispersion of metal oxide nanoparticles within the composite also play a crucial role in their UV protection effectiveness. Smaller nanoparticles with better dispersion tend to provide more efficient UV protection, due to increased surface area and uniform coverage. Besides UV radiation, other environmental factors such as temperature, humidity, and oxygen exposure can also influence the degradation behavior of PLLA/lignin nanocomposites containing metal oxides.

In this work, we addressed the fast UV-light induced degradation of polylactide through nanocomposite approach. The effect of the introduction of both inorganic and organic nanoparticles within the PLLA matrix on the physical integrity, appearance, thermal transitions, and physico-chemical conformation of PLLA has been thoroughly studied. Overall, the visual appearance and physical integrity of the materials is better kept upon the introduction of metal oxide nanoparticles and lignin nanoparticles, indicating that the UV-induced degradation of PLLA is markedly reduced because of the UV blocking effect of such nanoparticles.

EXPERIMENTAL

Binary and ternary nanocomposites were prepared by the solution cast method in chloroform. For the realization of PLLA binary films, a specific amount of LNPs (1 wt %) or metal oxide (ZnFe₂O₄, Fe₂O₃, WO₃, TiO₂, Ag₂O) nanoparticles (0.5 wt %) was dispersed in CHCl₃ using a tip sonication in an ice bath for 2 min at 30% amplitude (nanoparticle/CHCl₃ ratio was selected at 1 wt %/v). Polymeric solution and NP suspensions (except for Fe₂O₃) were mixed at RT under a magnetic stirrer for 1 h and then cast. In the case of Fe₂O₃-based films, polymer and metal oxide dispersions were mixed using tip sonication for 2 min at 30% amplitude. For the preparation of PLLA ternary nanocomposites, LNPs and metal oxide NP suspensions

were previously mixed using tip sonication (2 min at 30% amplitude) and added to the PLLA solution; the combination of LNPs and metal oxide NPs was performed following the same procedure reported for the PLLA binary-based films.

Accelerated photodegradation studies have been carried out by using a UVACUBE 2000 UV curing chamber at a power of 2000 W. Samples were placed at an arc length of 200 mm to irradiate the samples at a power output of 100 W/cm. 1 h of irradiation under these experimental conditions correspond approximately to 17.000 hours of irradiation.

In order to deeper investigate the synergic stabilizing effect on the photodegradation of the PLLA observed by adding lignin nanoparticles to the nanocomposites, four in silico molecular dynamic simulations (MDs) have been performed for selected reference systems, namely PLLA, PLLA/1LNP, PLLA/0.5TiO₂, PLLA/1LNP/0.5TiO₂.

RESULTS AND DISCUSSION

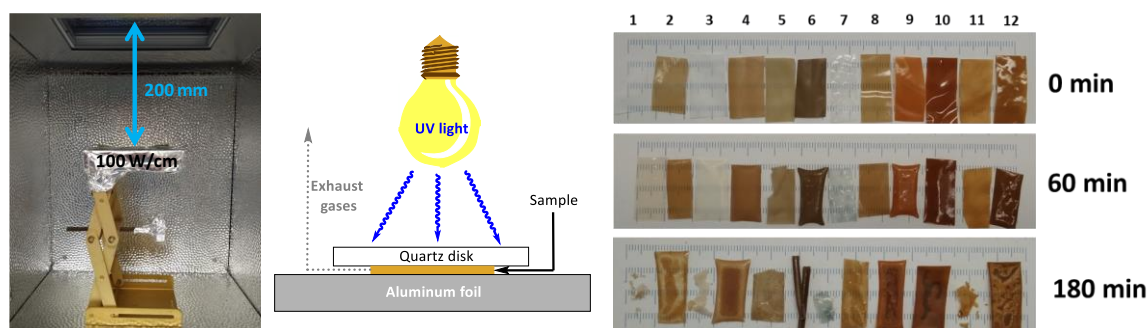


Figure 1. Experimental set up and visual observation of poly(lactide)-based nanocomposites during accelerated UV aging. From left to right: Visual images (1, PLLA; 2, PLLA/1LNP; 3, PLLA/0.5TiO₂; 4, PLLA/1LNP/0.5TiO₂; 5, PLLA/0.5Ag₂O; 6, PLLA/1LNP/0.5Ag₂O; 7, PLLA/0.5WO₃; 8, PLLA/1LNP/0.5WO₃; 9, PLLA/0.5Fe₂O₃; 10, PLLA/1LNP/0.5Fe₂O₃; 11, PLLA/0.5ZnFe₂O₄; 12, PLLA/1LNP/0.5ZnFe₂O₄)

UV induced photooxidation of PLLA is driven by the formation of a radical via the abstraction of tertiary H from the main chain with the concomitant formation of a tertiary radical (P•). In this framework, photochemical degradation of polymers could be delayed upon the introduction of stabilizers, which are classified as UV screening, UV absorption, excited state deactivation and free radical scavenging. Some materials can absorb UV light and dissipate this energy in the form of harmless long wavelength radiation, where the energy of the excited state is usually transferred to a quencher molecule which may dissipate the energy to a harmless form. Transition metal chelates can be used as quenchers. Additionally, radical scavengers inhibit the propagation step in the photooxidation process. Therefore, in this work we combined UV screening materials (metal oxide nanoparticles), with a radical scavenger of natural origin, lignin. The results of the investigation reveal a concomitant effect of metal oxide nanoparticles and lignin nanoparticles on the protection of PLLA against discoloration and photodegradation during UV irradiation as a function of chemical structure and dimension of the MOs nanoparticles.

References

- 1) Lizundia E, Armentano I, Luzi F, Bertoglio F, Restivo E, Visai L, Torre L, Puglia D. ACS Appl Bio Mater. 2020 Aug 17;3(8):5263-5274. doi: 10.1021/acsbm.0c006372
- 2) Russo S., Muscetta M., Amato P., Venezia V., Verrillo M., Rega R., Lettieri S., Cocca M., Marotta R., Vitiello G., Chemosphere, 346, 2024, 140605, doi: 10.1016/j.chemosphere.2023.140605.

UNDERSTANDING AND COUNTERATING THERMO-OXIDATIVE DEGRADATION DURING MECHANICAL RECYCLING OF PA 6,6

A. Rech^{1,2*}, K. Almdal¹, A.E. Daugaard²

¹Department of Chemistry, Technical University of Denmark, Kemitorvet, Kgs. Lyngby, Denmark

²Danish Polymer Centre, Department of Chemical Engineering, Technical University of Denmark, Søltofts Plads, Kgs. Lyngby, Denmark

*arirec@kt.dtu.dk

INTRODUCTION

In recent decades, despite the extensive advantages offered by plastic materials, there has been a growing environmental apprehension surrounding their use. The durability of plastic, coupled with its widespread production, poses significant challenges in managing disposed plastic. (1) Additionally, since plastic is produced mainly from oil, its production contributes to the depletion of raw materials, which has been increasing at twice the rate of population growth over the last decades. (2) Currently, only 9% of globally produced plastic is recycled (3); to minimize the environmental impact and raw material depletion caused by plastic materials, it is crucial to maximize recycling opportunities.

The study explored the mechanical recyclability of post-industrial waste (PIW) polyamide 6,6 (PA 6,6). The detrimental impacts of mechanical recycling on these materials were investigated through rheology and strategies to mitigate these effects were proposed. The ultimate aim was to enable the thermoprocessing of plastic products meeting industrial quality standards, utilizing mechanically recycled PA 6,6.

EXPERIMENTAL

Materials

The Lego group provided pellets of PA 6,6 in natural and red colors, virgin, processed 1 and 10 cycles. Among the additives, the antioxidants (AO), Pentaerythritol tetrakis(3,5-di-tert-butyl-4-hydroxyhydrocinnamate) and Tris(2,4-di-tert-butylphenyl) phosphite, were purchased from Merck while the chain extender (CE), 2,2'-Bis(2-oxazoline) was purchased from TCI Europe.

Preparation

The effect of mechanical recycling of PA6,6 was investigated on virgin PA6,6 in its natural color, on PA6,6 processed 1 cycle in its natural color and red, and on PA 6,6 processed 10 cycles in its natural color and red. The investigations were conducted on injected discs with a diameter of 25 mm and a thickness of 1.5 mm.

The counteracting of thermo-oxidative degradation during mechanical recycling of PA 6,6 was investigated by reprocessing PA6,6 red alone, with 1 pph of a mixture 1:1 of two antioxidants (AO), and with the combination of 1 pph of the mix of antioxidants together with 2 pph of chain extender (AO+CE). The processing was executed with the use of a twin-screw extruder operated at 100 rpm and the following temperature profile: 250-270-290-290-290-290-290°C. The materials were collected after 1 or 5 extrusion cycles, and the additives were either added only on the first cycle (1) or repeatedly during the 5 cycles (5). The investigations were conducted on discs injected as described previously.

Characterization

Changes in molecular weight, chain scission, and crosslinking were observed through rheology by executing a time test of 1 h, at 2% strain, a low angular frequency of 0.1 rad/s and a temperature of 290°C, using a 25 mm parallel plate geometry.

RESULTS AND DISCUSSION

The study initially focused on assessing the effects of thermo-oxidation during mechanical recycling. A time test at low frequencies was found to be the most descriptive of the differences between the virgin and reprocessed samples. As illustrated in Figure 1a, in PA6,6 natural crosslinking was minor but predominant in the first extrusion, as evidenced by higher values of the storage modulus (G'). Conversely, chain scission was predominant over ten extrusions, as indicated by lower G' values compared to virgin PA6,6. Notably, the presence of the red dye significantly accelerated PA6,6 chain scission, as shown from the lower initial G' values, and the crosslinking process, as shown from the increased slope in the G' curve.

In a subsequent step, efforts were made to reduce the detrimental effects of mechanical recycling on the red PA 6,6, which was found to be the most prone to thermo-oxidative degradation. Antioxidants or a combination of antioxidants and a chain extender were introduced during the reprocessing cycles, and the impact of increased initial stabilization versus recurrent stabilization at each reprocessing cycle was examined. As shown by the comparison of Figures 1b and 1c, the combination of AO+CE was the most effective, with G' values falling between those of the virgin reference and the reference processed 1 cycle. Finally, the repetitive addition of additives at each reprocessing cycle proved most effective in mitigating crosslinking phenomena. The use of AO+CE demonstrated a reduction in molecular changes during mechanical recycling, though further optimization is needed to maintain material quality at a constant level throughout mechanical recycling.

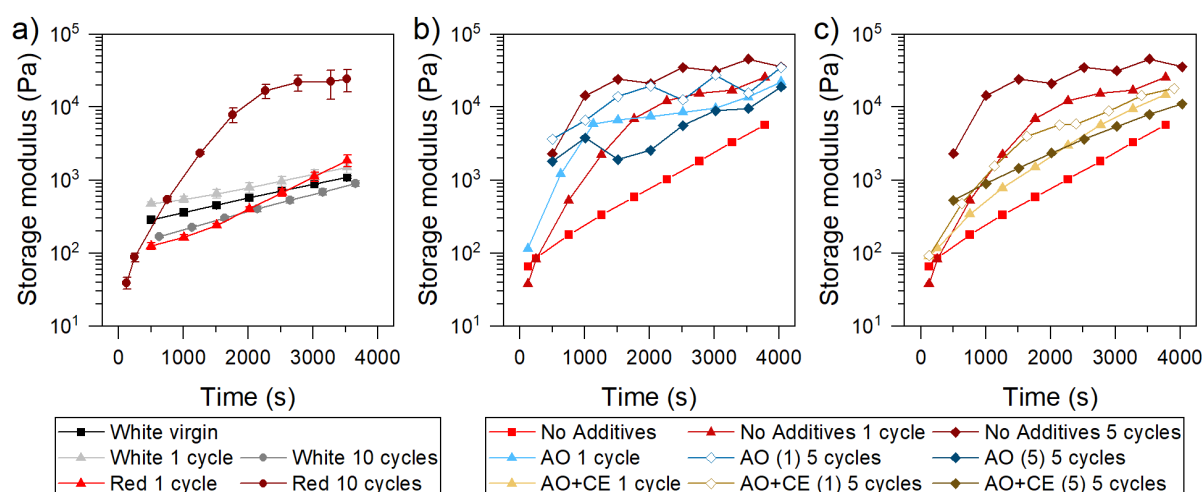


Fig. 1 Rheological analysis comparing (a) reprocessed PA 6,6 nature and red, (b) red PA6,6 reprocessed alone or with antioxidants, and (c) red PA6,6 reprocessed alone or with a combination of antioxidants and chain extender.

Acknowledgment

This work has been financially supported by Innovation Fund Denmark and TRACE through grant number 1153-00001B.

References

- 1) M. Rujnić-Sokele, A. L. Pilipović, Waste Management and Research, **35**, 132-140 (2017)
- 2) OECD Publishing, OECD Global Material Resources Outlook to 2060: Economic Drivers and Environmental Consequences (2019)
- 3) OECD Publishing, OECD Global Plastic Outlook: Policy Scenarios to 2060 (2022)

INCORPORATING RECYCLED MASKS INTO BITUMEN: A SUSTAINABLE SOLUTION

Maria Chiara Riccelli¹, Paola Scarfato¹, Alessia Romano², Marinella Levi², Giulia Infurna³, Nadka Tz. Dintcheva³, Loredana Incarnato¹

¹Department of Industrial Engineering, University of Salerno, Via Giovanni Paolo II, Fisciano, SA, Italy

²Department of Chemistry, Materials, and Chemical Engineering “Giulio Natta”, Politecnico di Milano, Piazza Leonardo da Vinci, Milano, Italy

³Department of Engineering, University of Palermo, Viale delle Scienze, Palermo, Italy

INTRODUCTION

The COVID-19 emergency has increased the use of personal protective equipment such as face masks, which are made of polypropylene (PP). Although essential for health, the short lifespan of masks creates disposal problems. Moreover, governments around the world have inherited huge quantities of unused surgical masks.

A sustainable solution to this problem can be achieved by incorporating masks into bitumen for road construction. This process not only reduces waste but also improves the properties of the asphalt, making it more durable and resistant.

In this work PP masks have been used as a modifier of bitumen at different concentrations (0.5, 1, 3, and 5 wt%) for the production of Polymer Modified Bitumen (PMB). For improving the compatibility between PP and bitumen, a compatibilizer made of PP grafted with 0.5 wt% of maleic anhydride was used. The study involved a thorough material characterization of the masks, the preparation of PMB mixtures, and their characterization.

EXPERIMENTAL

Materials

The surgical masks used in this study are unused masks from five different brands on the market, ensuring adequate representativeness. Only the three layers of non-woven polypropylene fabric were selected as modifiers for the bitumen. Virgin polypropylene with a density of 0.90 g/cm³, supplied by LyondellBasell, was used for comparison.

A compatibilizer, called Intune, a polypropylene-based olefin block copolymer, was supplied by Dow in the form of granules ($T_g = -58.0$ °C; $T_m = 67.8$ °C).

One paving grade bitumen with penetration degree of 75/100 was supplied by ENI and used as comparison.

Preparation

The bitumen, previously warmed up to 180°C until complete fluidization, was modified by incorporating into it different amounts (0.5wt%, 1wt%, 3wt%, and 5wt%) of mask shreds, with and without the addition of the Intune compatibilizer at 5wt%. The mixtures were then kept under stirring at this temperature at 1000 rpm for 10 min until complete homogenization.

Characterization of bituminous mixtures

Penetration tests developed specifically for bituminous mixtures were conducted. By using a CMT4000 SANS dynamometer and a 100 N load cell, the penetration force and the penetration energy of the samples were evaluated up to 10 mm of depth at room temperature.

Finally, using the HAAKE Viscotester C rotational viscometer from Thermo Scientific (Germany), the viscosity at 135°C of the bituminous mixtures was measured (ISO 2555).

RESULTS AND DISCUSSION

Fig. 1 provides information on the consistency of bitumen at a given (room) temperature. As can be seen by the graph, the modification of the bitumen with the mask shreds increased the value of the penetration force of bituminous mixtures in all cases. The extent of the improvement significantly increases with the mask shreds loadings and with the addition of Intune compatibilizer. In particular, the most performing mixture, added with 5wt% of compatibilized masks, shows a penetration force almost double than the neat bitumen.

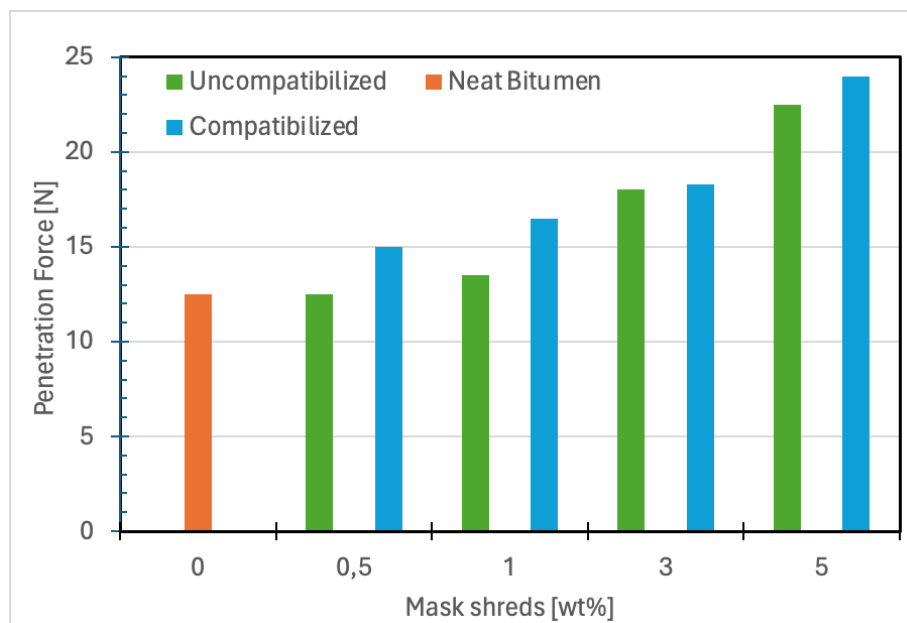


Fig. 1 Penetration force [N] for neat bitumen and for compatibilized and non-compatibilized bituminous mixtures

Similar behavior was also found in the viscosity of the bituminous mixtures, measured at 135°C. Also, in this case, with respect to the neat bitumen that has viscosity value of 200 MPa/s, the most viscous systems are the mixtures at 5wt% of masks, which shows a viscosity value of 495 MPa/s and 450 MPa/s for the compatibilized and un-compatibilized systems, respectively.

However, since bitumen is a temperature-sensitive material, the effect of the temperature above and below the ambient temperature on stiffness and viscosity of the bitumen mixtures will be investigated to evaluate their performance in different environmental conditions.

Acknowledgment

This work has been financially supported by the MIUR Project "FUTUREVAL-PPE" (FUNCTIONAL Technology Unlocking and VALORIZATION of Personal Protective Equipment production scrap and waste).

References

- 1) L. Lyu, M. Bagchi, N. Markoglou, C. An, H. Peng, H. Bi, X. Yang, H. Sun, *Journal of Hazardous Materials*, **461**, 132566 (2024)
- 2) M. Porto, P. Caputo, V. Loise, S. Eskandarsefat, B. Teltayev, C. Rossi, *Applied Sciences*, **9** (2019)

CHARACTERIZATION, PHOTO-OXIDATION AND DEGRADATION IN COMPOST OF WOOD FLOUR AND HAZELNUT SHELLS POLYLACTIDE-BASED BIOCOMPOSITES

M. Baiamonte^{1,2}, M. Rapisarda³, M.C. Mistretta^{1,2}, G. Impallomeni³, F.P. La Mantia^{1,2*}
and P. Rizzarelli^{3**}

¹ Dipartimento di Ingegneria, Università di Palermo, Palermo, Italy

² INSTM, Consorzio Interuniversitario Nazionale per la Scienza e Tecnologia dei Materiali, Firenze, Italy

³ Istituto per i Polimeri, Compositi e Biomateriali (IPCB) – SS di Catania, Consiglio Nazionale delle Ricerche (CNR), Catania, Italy

*francescopaolo.lamantia@unipa.it, **paola.rizzarelli@cnr.it

INTRODUCTION

In order to reduce the environmental impact of plastics, biocomposites are an important tool produced by loading a biodegradable matrix with organic fillers, which modify some properties of the polymer matrix. Biocomposites are, then, biodegradable and, depending on the matrix, compostable.

In this work, polylactide (PLA) was loaded with wood flour (WF) or hazelnut shells (HS) (10 and 20% of fillers). The matrix and biocomposites were thoroughly examined for their mechanical and rheological properties to evaluate their processability and performance. Compost burial degradation test, with and without prior photo-oxidation, was carried out to check their biodegradability after outdoor exposure.

EXPERIMENTAL

Materials

PLA was supplied by NatureWorks (USA), WF, primarily from beech trees, and HS powders were provided by La.So.Le. (Percoto, Italy) and Agrindustria Tecco (Cuneo, Italy), respectively. The compost was furnished by Biofactory S.p.A. (Calcinatè, BG, Italy)

Preparation

Biocomposites were prepared using a twin-screw extruder (OMC, Saronno, Italy) (screw diameter = 19 mm, length-to-diameter ratio = 25). The temperature profile was set from 150 °C to 180 °C with a screw speed of 160 rpm. Specimens for testing were prepared by compression molding (Carver laboratory press, USA) at 180 °C for 3 min. at 300 psi. PLA and biocomposites underwent accelerated weathering in a QUV chamber with eight UVB-313 lamps (Q-Labs Corp., USA). The exposure cycle involved 8h of UV irradiation at 60 °C followed by 4h of condensation at 40 °C. To assess humidity's impact during weathering, comparative tests were carried out with the same irradiation cycle but only under UV exposure. Samples were monitored at different intervals: 12, 24 and 36h.

Rheological and physico-chemical characterization

Mechanical characterization was conducted using an Instron 3365 universal testing machine, following ASTM D638 standards. At least seven specimens per sample were tested, with data validated by one-way ANOVA. Rheological characterization was performed at 180 °C. ATR-FTIR spectra were recorded using 8 scans at 4 cm⁻¹ resolution, normalized at 2995 cm⁻¹ for CH₃ group stretching. SEM images were taken after samples were cracked in liquid nitrogen, analyzed using ImageJ software. Nuclear magnetic resonance (¹H NMR) experiments were performed at 500 MHz at 27 °C in CDCl₃ with 0.03% TMS and the spectra were processed with Mestre-Nova software. Surface wettability was measured using a contact angle goniometer at room temperature after samples have been equilibrated at 40 °C for 30 min, with at least five values recorded. Compost burial test was performed up to 30 days at 58.0 ± 0.1 °C and degradation monitored through weight loss (WL).

RESULTS AND DISCUSSION

In polymer composites, inert fillers usually increase viscosity (1), which can worsen processability. However, in this study, the biocomposite samples exhibited lower viscosity than the virgin PLA matrix, particularly the biocomposite with WF. This unusual behavior is attributed to strong incompatibility and poor adhesion between the PLA matrix and fillers, leading to slippage between the phases and possibly more severe thermomechanical degradation, which reduces molecular weight. This poor adhesion also caused decreased tensile strength and elongation at break, although the PLA matrix itself is brittle. Mechanical properties showed a slight increase in modulus, especially in the WF biocomposite. UV irradiation and humidity effects were also studied. The biocomposites with bio-wastes showed increased UV resistance and slower compost degradation, attributed to lignin in the fillers, which acts as a stabilizer against photo-oxidation. Both fillers increased resistance to compost degradation, though photo-oxidation accelerated it. Overall, the biocomposites demonstrated improved mechanical properties, enhanced UV resistance, and reduced compost degradation susceptibility. WL after 30 days was about 25% for PLA and 10-15% for the biocomposites (2). Photo-oxidation increased WL in both types of biocomposites with extended weathering time and condensation cycles, in agreement with previous studies (3). This study represents an example of circular economy, from the cradle to the grave (Fig 1).

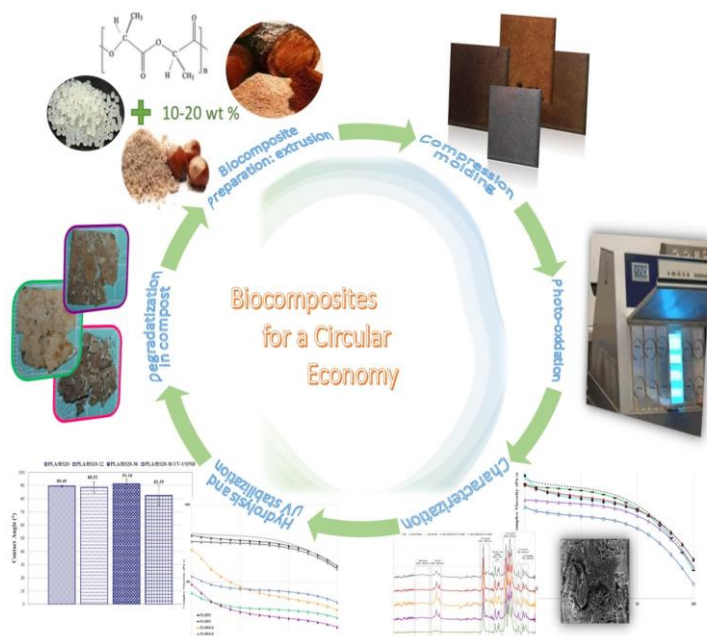


Fig. 1 Studying PLA-based biocomposites from the cradle to the grave.

Acknowledgment

This research was partially financially supported by Sicilian Region PO FESR 2014–2020. Action 1.1.5, project “New therapeutic strategies in ophthalmology: bacterial, viral and microbial infections – NUSTEO”, CUP:G68I18000700007 – application code 08CT2120090065. Biofactory S.p.A (Calcinatè, BG, Italy) is gratefully acknowledged for supplying the compost for degradation tests.

References

- 1) M. Gardette, S. Therias, J.L. Gardette, M. Murariu, F. Dubois, *Polym. Degrad. Stab.*, **96**, 616-623 (2011).
- 2) M. Baiamonte, M. Rapisarda, M.C. Mistretta, G. Impallomeni, F.P. La Mantia, P. Rizzarelli, *Polym. Compos.*, 1-17 (2024).
- 3) P. Rizzarelli, M. Rapisarda, L. Ascione, F. Degli Innocenti, F.P. La Mantia, *Polym. Degrad. Stab.*, **188**, 109578 (2021).

CHEMICAL AND PHOTOCHEMICAL DEGRADATION OF PLA-BASED GREEN COMPOSITES

A. Maio, E.F. Gulino, M. Gammino, M.C. Citarrella, **R. Scaffaro***

Department of Engineering, University of Palermo, Viale delle Scienze, Palermo, Italy

andrea.maio@unipa.it, emmanuelfortunato.gulino@unipa.it, mariaclara.citarrella@unipa.it, michele.gammino@unipa.it, roberto.scaffaro@unipa.it (corresponding author)

INTRODUCTION

Degradability of bioplastic-based green composites in different scenarios is crucial for properly assessing their environmental performance. Biodegradable polyesters, such as poly(lactic acid) (PLA), are susceptible to various degradation mechanisms during processing, usage, and disposal. The presence of green filler coming from waste biomass can either accelerate or delay these processes, depending on several factors. While degradation during processing and service life should be minimized, rapid degradation during disposal is desirable. Therefore, understanding the degradability of PLA-based green composites under different conditions is strategic to optimize their overall performance, from both an economic and environmental point of view.

EXPERIMENTAL

Materials

Poly(lactic acid) 2003 D (PLA) was chosen as the polymer matrix. The lignocellulosic fillers selected were flours obtained from waste *Posidonia oceanica* leaves (POL), *Ailanthus altissima* (AA) and *Chamaerops humilis* (dwarf palm) leaves (CHL). Chloroform, and buffer solutions at pH 7.4 and pH 10 were purchased from Sigma Aldrich.

Preparation and characterizations

Green composites containing 10 wt.% or 20 wt.% of POL, AA, and CHL were prepared by twin-screw extrusion and compression molding. The samples were subjected to various types of degradation.

- (i) Photochemical aging: performed in a Q-UV Solar Eye weatherometer equipped with UB-B lamps (313 nm), with cycles comprising 4 h of irradiation at T=55 °C followed by 2 h of dark/condensation at T=35 °C.
- (ii) Chemical aging: conducted in neutral (pH 7.4) and alkaline (pH 10) environments to monitor the disintegrability of materials.

At predetermined time intervals, aged samples were withdrawn, and the evolution of key properties was monitored. Water uptake and mass loss degree were evaluated by gravimetric measurements, mechanical behavior was investigated by tensile testing, surface wettability was assessed by water contact angle (WCA), morphology was analyzed by scanning electron microscopy (SEM), structural changes in the polymer were evaluated by FTIR/ATR spectroscopy and intrinsic viscosity.

RESULTS AND DISCUSSION

Depending on the type and amount of natural fibers, the durability of PLA-based green composites can be modulated during either photochemical or chemical aging. In particular, the lignin domains in the fillers generally protect the polymer from photochemical reactions, likely exerting shielding effect. Conversely, the hydrophilicity and porous nature of the fillers can increase the water transfer throughout the samples, occasionally accelerating hydrolytic degradation in some specific scenarios. In this latter context, the intraphase – that is, the capability of macromolecules to enter the lumens of fillers and thereby increase the matrix-

filler contact area – can play multiple roles and different functions. This may either accelerate or delay the degradation, depending on several factors. For instance, PLA-POL biocomposites proved to degrade much faster than PLA in aqueous conditions, with the POL fillers offering preferential gateways for water penetration through filler-matrix interphase by capillarity and swelling-aided polymer cracking (Fig. 1). More generally, by monitoring the morphological and chemical characteristics of composites it is possible to tune their durability and degradability. This allows for the fabrication of green composites that combine adequate performance during their service life with relatively fast disintegration after disposal.

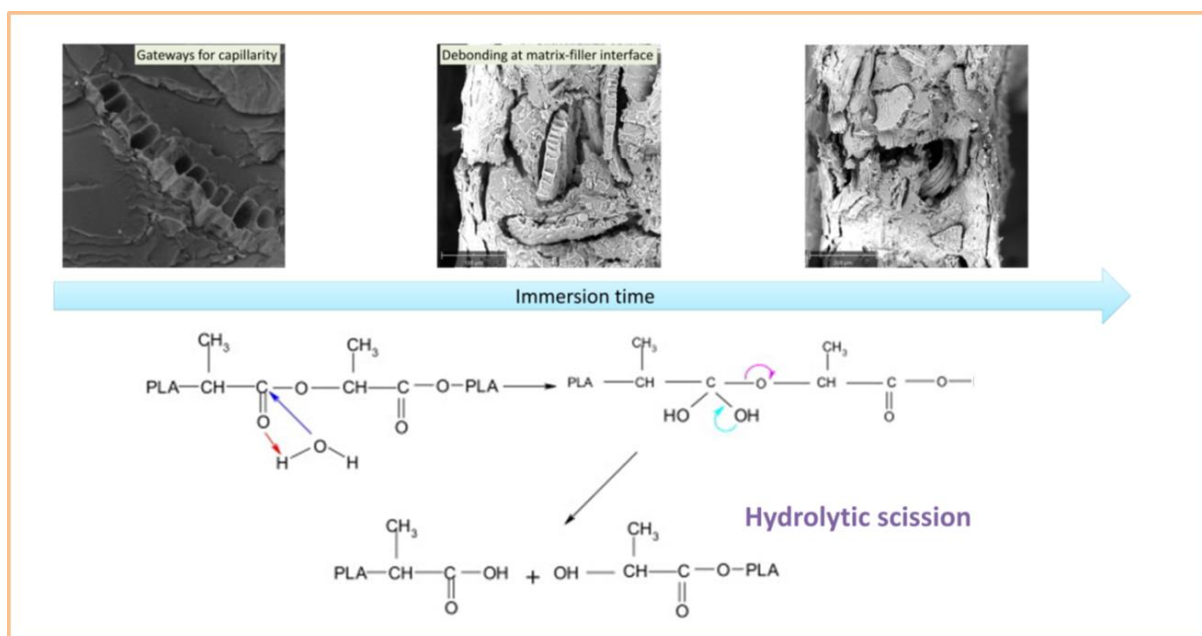


Fig. 1 Time-evolution of hydrolytic degradation pathways for a PLA-POL green composite. Prior to degradation, POL provide gateways for water penetration via capillarity. Debonding at matrix-filler interface and polymer cracking are caused by POL swelling and PLA embrittlement upon degradation, which is further enhanced by solvent propagation, thus resulting in erosive events.

Acknowledgment

This study was carried out within the MICS (Made in Italy - circular and Sustainable) Extended Partnership and received funding from the European Union Next-GenerationEU (PIANO NAZIONALE DI RIPRESA E RESILIENZA (PNRR) - MISSIONE 4 COMPONENTE 2, INVESTIMENTO 1.3 - D.D. 1551.11-10-2022, PE00000004). This manuscript reflects only the authors' views and opinions, neither the European Union nor the European Commission can be considered responsible for them.

This study was carried out within the SAMOTHRACE (Sicilian micro and nano technology research and innovation center) Extended Partnership and received funding from the European Union Next-GenerationEU (PIANO NAZIONALE DI RIPRESA E RESILIENZA (PNRR) – MISSIONE 4 COMPONENTE 2, INVESTIMENTO 1.5). This manuscript reflects only the authors' views and opinions, neither the European Union nor the European Commission can be considered responsible for them.

PRIN: Green composites based on biodegradable polymers and vegetal biomasses of Mediterranean area: processing, characterization and degradability - Bando 2022 - Prot. 20228WNZ2Z.

DEVELOPMENT, PERFORMANCE, AND DEGRADATION BEHAVIOR OF BIOCOMPOSITES BASED ON PBS AND GLOCHIDS FROM OPUNTIA FICUS-INDICA

F. Marchetta¹, L. D'Arienzo¹, L. Di Maio¹, L. Botta², M.C. Mistretta², P. Rizzarelli³, M. Leanza³, P. Scarfato^{1,*}

¹Department of Industrial Engineering, University of Salerno, Via Giovanni Paolo II 132, Fisciano (SA), Italy

²Department of Engineering, University of Palermo, Viale delle Scienze, Ed. 6, Palermo, Italy

³Institute for Polymers, Composites and Biomaterials (IPCB), Via P. Gaifami 18, Catania, Italy

*pscarfato@unisa.it

INTRODUCTION

The design and development of biocomposites entirely made from materials derived from renewable resources offer significant advantages in terms of eco-sustainability as they promote the development of circular economies, encouraging the use of natural, even waste materials, and can be responsibly disposed of, reducing the risk of environmental pollution and damage to ecosystems while ensuring the same technological functionality as traditional composites.

In this work, for the compositional design of biocomposites with enhanced performance, in terms of mechanical properties, functional characteristics and sustainability, the polymer matrix based on PBS (polybutylene succinate) was added with fibers derived from waste in the local agri-food supply chain. Specifically, the glochids of *Opuntia ficus-indica* were chosen because they have a surface with numerous hooks that can potentially ensure high interfacial adhesion with the polymer matrix (1).

The experimental activity involved the production of biocomposites, varying the polymer/reinforcement ratio, and their morphological and chemical-mechanical characterization.

EXPERIMENTAL

Materials and Biocomposites Preparation

The polymer matrix was a polybutylene succinate sourced from renewable sources, commercially named Bio PBS FZ91 (density=1.26 g/cm³, T_m=115°C), produced by Mitsubishi Chemical Corporation (Tokyo, Japan). Different percentages by weight of glochids the small and thin hairs, much like spines, from prickly pear fruits, were added as reinforcing elements.

Composites were prepared at different spines concentrations (0, 14, 20, and 30 wt%) using the melt compounding technique in a twin-screw extruder (Dr. Collin GmbH - ZK 25-48D) with co-rotating intermeshing screws (D_{screw}=25 mm, L/D = 42).

Morphological and thermo-mechanical characterization

Morphological investigations were carried out using a FESEM LEO 1525 (Carl Zeiss SMT AG, Oberkochen, Germany) on the sample sections cryo-fractured perpendicularly to the extrusion direction.

Thermal characterization was performed by using the differential scanning calorimetry (Chip-DSC 100, Linseis, Germany), to evaluate the melting temperature and the degree of crystallinity of biocomposites during the first heating.

Mechanical tests were carried out, following ASTM standard D882, by a CMT6000 Series dynamometer (SANS, Shenzhen, China), equipped with a load cell of 1 kN, at a crosshead speed of 5 mm/min.

RESULTS AND DISCUSSION

The morphology of the produced biocomposites was analyzed by SEM analysis. Fig. 1 shows SEM micrographs obtained on cross-sections of the PBS sample with 20wt% glochids added.

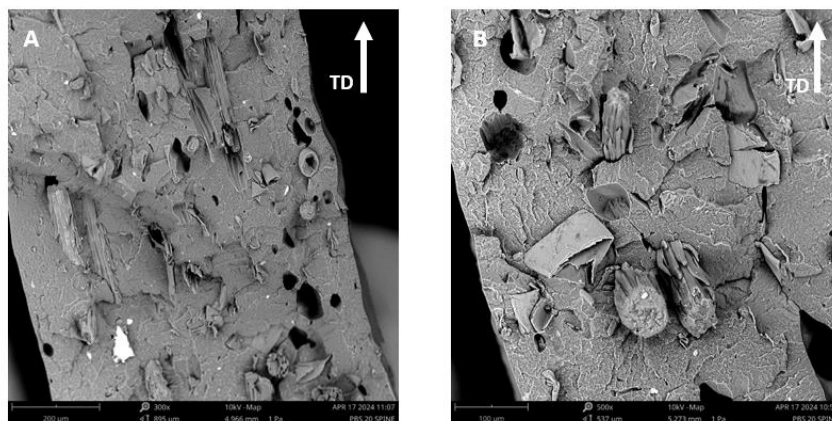


Fig. 1 SEM micrographs of PBS composites loaded with 20wt% of glochids at different magnifications in transverse direction (TD): A. 300x; B. 500x.

The glochids are dispersed and rather homogeneously distributed in the PBS matrix, with a preferential orientation in the extrusion direction. They exhibit a microfibrillar structure with a rough surface, and their scales appear closed towards the fiber axis. The adhesion between the two phases appears good, given the absence of interfacial voids, indicative of the good wettability of the fiber by the polymer, while the circular cavities observable in the matrix are the result of the debonding and pull-out of the fibers that occurred following cryo-fracture of the specimen.

The degree of crystallinity of the biocomposites is higher than that of unloaded PBS and progressively increases with the glochids content, passing from ca. 56% to 69% for the sample at 30wt% loading.

The presence of the tiny spines within the PBS matrix results in a significant increase in the values of Young's modulus and thus in the stiffness of the samples, which progressively rise with the increasing filler content (up to 73% for the sample at 30wt% loading). The mechanical performance enhancement can be attributed to the combined effect of the increased crystallinity of the biocomposites and the ability of the glochids to act as a reinforcing agent due to their good adhesion with the polymeric matrix, as shown by SEM.

The designed and produced systems prioritize the principles of the Circular Economy by efficiently using materials and resources and valorizing agri-food waste. They not only provide the opportunity to obtain high-performance biocomposite systems capable of fully integrating into the natural cycle but also contribute to reducing the amount of waste generated.

Acknowledgment

This work has been financially supported by the project "Sustainable routes to high Performance and Recycling of Biodegradable plastics for a circular economy - SuperBio" (PRIN PNRR 2022, project no. P2022M3FTM, CUP: D53D23018670001), funded by the Next Generation EU instrument, Italian National Recovery and Resilience Plan (NRRP), M4C2 – Investment 1.1.

References

- 1) A. Ulloa-Leitón, M.E. Álvarez-Sánchez, C. García-Osorio, F. Gavi-Reyes, R. Maldonado-Torres, *Rev. fitotec. Mex.*, **44**, 201–209 (2021).

Polylactic acid electrospun membrane as a proof of concept for intestinal barrier reconstruction

M. Testa^{1,2}, C. Di Marco², G. Serio³, C. Gentile³, V. La Carrubba², F. Lopresti²

1 Department of Biomedicina, Neuroscienze e Diagnostica avanzata, University of Palermo, Palermo, Italy

2 Department of Engineering, University of Palermo, Palermo, Italy

3 Department of Biological, Chemical and Pharmaceutical Sciences and Technologies, University of Palermo, Palermo, Italy

INTRODUCTION

Biomolecules transport across the intestinal epithelium is a key process of interest in biomedical and nutritional fields [1]. Recent developments in cellular biology and biomaterials science and technology have allowed the development of powerful tools to develop advanced *in vitro* models.

Deviating from commercial polycarbonate membranes, commonly used to reproduce barrier tissues *in-vitro*, this study explores the potential of electrospun scaffold (ES) as substrate for Caco-2 cells culture. Electrospinning allows to produce scaffolds composed of nano- or micro-fibers, offering a favorable microenvironment for cells and tissue growth [2]. Due to its similarity with the topography of the native extracellular matrix, electrospun microfibers can act as an ideal substrate for biofabricating *in-vitro* intestinal epithelium models addressing the challenge of maintaining the normal physiological status of primary intestinal epithelium. Among the different materials processable via electrospinning, polylactic acid (PLA) is one of the most interesting due to its chemical physical properties and biocompatibility [3]. PLA has been approved by the US Food and Drug Administration (FDA) for biomedical applications [4] however, as the hydrophobicity of the material may lead to poor cell adhesion, air-cold plasma treatment was adopted to improve Caco-2 proliferation and intestinal epithelium maintenance in a long-term culture.

EXPERIMENTAL

Materials

PLA (Ingeo 2002D) was supplied by NatureWorks (NatureWorks LLC, Minnetonka, MN, USA) while, Ethanol (Et-OH), Acetone (Ac) and Chloroforms (TCM), isopropyl alcohol, Caco-2 cell line, Dulbecco's Modified Eagle Medium (DMEM) and antibiotic-antimycotic solution were purchased from Sigma Aldrich (Merck KGaA, Darmstadt, Germany). Commercial polymethyl methacrylate (PMMA) was purchased from Clarex, Nitto Jushi Kogyo Co. Ltd., Tokyo, Japan and processed by means of a CO₂ laser cutter (Maitech, 40 W)

Methods

The PLA electrospun scaffolds were produced according to our previous works [5,6]. After fabrication the membrane was subjected to air cold-plasma, in order to improve its hydrophilicity and biocompatibility, according to [5]. After functionalization the scaffold were cut in 12 mm diameter circles and fitted into two PMMA rings obtained via laser cutter to act as an Transwell-like device. The surface of the membrane exposed to the cell is equal to 0.33 cm², according to a 96-well plate. Before cells seeding, the scaffolds were sterilized by immersing them in a 70:30 v:v ethanol aqueous solution for 30 minutes, followed by 3 washing with PBS in order to remove any residual of ethanol.

The scaffolds were then positioned in a 24-well plate and seeded with 30000 Caco-2 cells by dropping 50 μL of DMEM (600 cells/ μl) on the top of the ES surface and 500 μL of DMEM were filled in the well.

Scanning electron microscope (SEM, Phenom ProX, Phenom-World) analysis was performed on the scaffolds before and after cell culture at 7, 14 and 21 days. Cellularized samples were washed with PBS and fixed with 4% (v/v) glutaraldehyde at 4 $^{\circ}\text{C}$ for 2 h. Then, they were rinsed with water and dehydrated with ethanol series (25%, 50%, 75% v/v and pure ethanol) and dried under fume hood. Before the analysis, all the samples were gold sputtered.

RESULTS AND DISCUSSION

The Transwell-like device, integrated with an electrospun membrane (shown in Fig. 1a), after assembly appears intact and functional avoiding the shrinking phenomena and ensuring an efficient seeding. Scanning electron microscopy micrographs of ES after air-cold plasma shows randomly oriented micrometric fibers with homogeneous diameter size distribution (Fig. 1b). After 21 days of culture (Fig. 1c), Caco-2 cells formed intact confluent cell monolayers on scaffold surfaces with different villi-like architectures. At higher magnification (Fig. 1d), it is possible to observe that the cells tightly adhere each other in the villi. In fact, adjacent cells show a morphology that suggests the formation of tight junctions, essential for the barrier function of the tissue model. Furthermore, the same image highlights the presence of irregular particles at the edge of the villi-like structures that can be ascribed to the ability of cells to produce microvillus-derived vesicles, an important intercellular messenger for maintaining intestinal homeostasis.

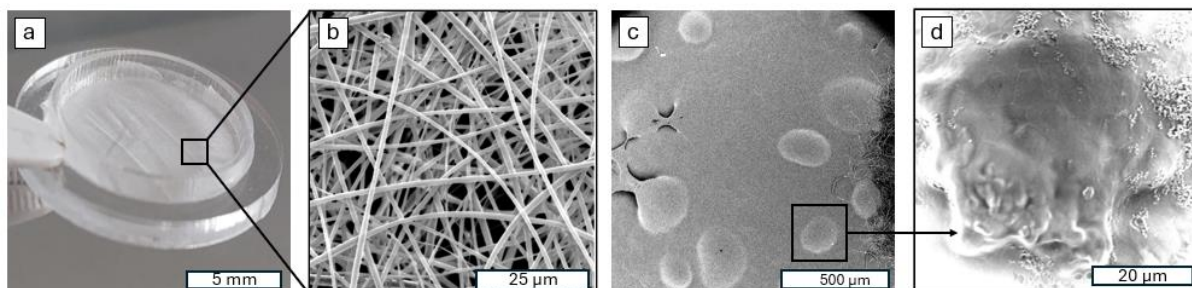


Figure 1. a) Picture of the Transwell-like device including the electrospun membrane; b) SEM image of the ES after plasma treatment; c) and d) SEM image of the Caco-2 cells cultured for 21 days on the ES

Concluding, in this study a Transwell-like device containing an electrospun membrane was successfully fabricated and applied for the biofabrication of an *in vitro* intestinal model.

References

- [1] Y. Xu, N. Shrestha, V. Pr eat, A. Beloqui, *Adv Drug Deliv Rev*, **175**, 113795 (2021).
- [2] D.I. Braghirolli, D. Steffens, P. Pranke, *Drug Discov Today*, **19**, 743–753 (2014).
- [3] O. Bjorgvinsdottir, S.J. Ferguson, B.S. Snorradottir, T. Gudjonsson, K. Wuertz-Kozak, *Mater Today Bio*, 101060, (2024).
- [4] E. Capuana, F. Lopresti, M. Ceraulo, V. La Carrubba, *Polymers (Basel)*, **14**, (2022).
- [5] F. Lopresti, S. Campora, G. Tirri, et al., *Materials Science and Engineering: C*, **127**, 112248 (2021).
- [6] F. Lopresti, S. Campora, S. Rigogliuso, et al., *Int J Mol Sci*, **25**, 2507 (2024).

Physical and Antibacterial Properties of Biodegradable PLA/PBAT Blends Containing Carvacrol

V. Titone^a, L. Botta^a, M.C. Mistretta^a, S. Russello^a, G. Garofalo^b and R. Gaglio^b

^aDepartment of Engineering, RU INSTM, University of Palermo, Viale delle Scienze, 90128 Palermo, Italy

^bDepartment of Agricultural, Food and Forest Sciences, University of Palermo, Viale delle Scienze, Bldg. 5, 90128 Palermo, Italy
vincenzo.titone@unipa.it

INTRODUCTION

Over the years, polymer blends have found wide applications because of the ability to combine different properties to make materials that meet specific needs. Recently, however, the focus has increasingly shifted to the use of biodegradable products, and the packaging industry is also considering the use of these materials. However, what is emerging of particular note is the development of materials with antimicrobial properties capable of maintaining the organoleptic properties of food.

The aim of this work was to addition of an essential oil in poly(lactide) (PLA) and poly(butylene adipate-co-terephthalate) (PBAT) blends and to study the effect of the blend composition on the properties of the obtained material paying particular attention on the evaluation of oil release kinetics and on the antibacterial properties of these systems.

EXPERIMENTAL

Materials

The raw materials used in this work were:

- Poly(lactic acid) (PLA), trade name PLA Ingeo 4032D, purchased from NatureWorks. Density: 1.24 g/cm³; melt flow index (MFI): 7g/10 min (210 °C, 2.16 kg), melting temperature: 155–179 °C;
- Poly(butylene adipate-co-terephthalate) (PBAT), trade name Ecoflex F C1200, purchased from BASF. Density: 1.25–1.27 g/cm³; melt flow index (MFI): 2.7–4.9 g/10 min (190 °C, 2.16 kg), melting temperature: 130–140 °C;
- Carvacrol (CRV), antimicrobial agent, was purchased from Sigma-Aldrich (Sigma-Aldrich, USA).

Preparation

The materials were prepared with a Brabender mixer mod. PLE330 (Brabender, Duisburg, Germany) operating at 180 °C at 60 rpm for 5 min.

CRV loading was added after four minutes during the process to minimize evaporation. Before blending, to prevent hydrolysis phenomena, (24) PLA and PBAT were dried in a vacuum oven overnight at 60°C

All compositions are shown in Table 1.

Sample code	PLA, %wt	PBAT, %wt	CRV, phr
PLA	100	-	-
PBAT	-	100	-
PLA/CRV	100	-	20
PBAT/CRV	-	100	20
75/25	75	25	-
25/75	25	75	-
75/25/CRV	75	25	20
25/75/CRV	25	75	20

Table 1 – Formulation of all composition investigated.

Characterization

Rheological measurements were performed on ARES G2 rotational rheometer at temperatures of 180 °C with a gap of about 1.5 mm between the plates.

Tensile tests were performed using an Instron universal testing machine

Water contact angle (WCA) measurement was carried out using a First Ten Angstrom FTA1000C system, with demineralized water.

Release tests were performed in a Specord 252 UV-vis spectrophotometer.

The antibacterial properties of the polymers were evaluated in vitro on solid and liquid media through the disc diffusion and the plate count method.

RESULTS AND DISCUSSION

As shown in Figure 1, both PLA and PBAT show a Newtonian plateau at low frequencies and non-Newtonian behavior at higher frequencies, with PLA having a higher overall viscosity than PBAT. The blends show slight shear-thinning behavior without a Newtonian plateau, with viscosity higher than that of the individual components. The addition of PBAT increases the elasticity and melt strength of PLA, while carvacrol reduces viscosity with slightly less pronounced non-Newtonian behavior due to its plasticizing effect.

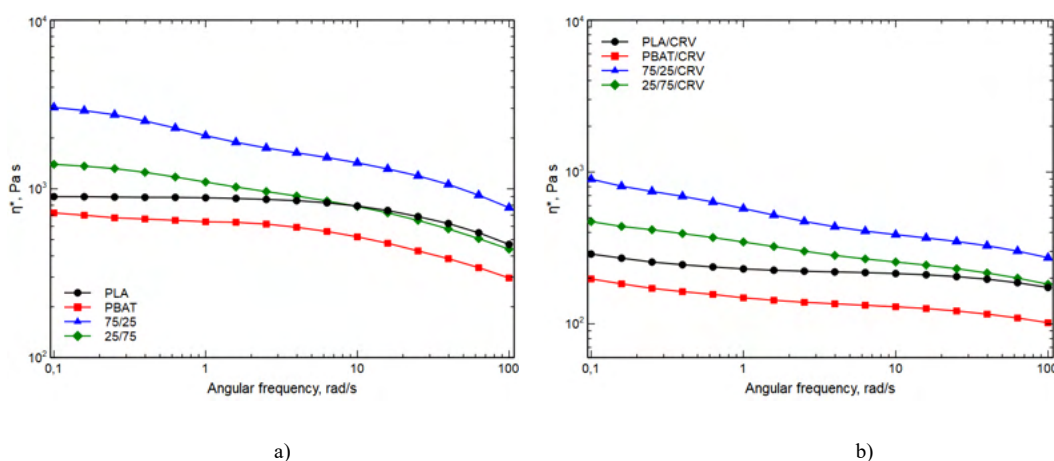


Figure 2 – Complex viscosity curves as a function angular frequency: a) without oil; b) with added oil.

The mechanical properties show that adding PBAT to PLA increases flexibility, while adding PLA to PBAT increases stiffness, with the plasticization effects of carvacrol being stronger in the PLA phase. Furthermore, both pure polymers and blends with carvacrol showed a decrease in contact angle values, due to a smoother surface that resulted in less roughness and consequently higher wettability.

Finally, data on their microbiological investigation in liquid media showed the ability of all CRV-containing materials to exert antibacterial activity against *L. monocytogenes* and *S. Enteritidis*. More specifically, PLA and the PLA blend showed a bacteriostatic effect, while PBAT and the PBAT blend showed a bactericidal effect.

References

1. Y. Deng; C. Yu; P. Wongwiwattana; N. L. Thomas J. Polym. Environ. 2018, 26, 3802.
2. R. Gaglio, L. Botta, G. Garofalo, A. Miceli, L. Settanni, F. Lopresti Food Packag. Shelf Life 2021, 28, 100633.
3. F. Lopresti, L. Botta, V. La Carrubba, L. Di Pasquale, L. Settanni, R. Gaglio Int. J. Biol. Macromol. 2021, 193, 117

Flame Retardants on Textiles: A novel steady-state experimental approach for mechanistic investigations

N. Tomasik^{1,3}, R. Otto^{2,3}, T. Mayer-Gall^{2,3}, and B. Atakan^{1,3}

¹Thermodynamics (EMPI), University of Duisburg-Essen, Duisburg, Germany

²Deutsches Textilforschungszentrum Nord-West gGmbH, Krefeld, Germany

³Center for Nanointegration Duisburg-Essen (CENIDE), Duisburg, Germany

niklas.tomasik@uni-due.de

INTRODUCTION

Currently generic experiments are lacking, which separate the effects of flow, heat and mass transfer, solid-state reactions, gas-phase-reactions, and flame propagation for heterogeneous flame retardant (FR) substrate systems. Many standard flammability tests lead to complicated time and space dependent pyrolysis and combustion situations, which defeat investigating the details of the (sub-)mechanism of flame retardancy. Some studies approach a separation by focusing on pure gas flames doped with FRs and analyzing gas flames properties like laminar flame speed variations (1); this is important, but not sufficient to learn more about heterogeneous systems. Even with advanced gas phase diagnostics the interpretation of the results of polymer flame retardant blends is difficult (2).

In combustion science, the separation of different effects and sub-mechanisms has led to much progress in the last decades. For such an approach simplifying generic experiments are needed, which is addressed here. The idea is to use the possibility to perfuse moving – later FR coated – permeable textiles with gases of different composition and temperatures. The textile velocity is controlled, to obtain a situation where the textile decomposition or combustion takes place at the same speed, such that a steady-state is obtained. In such an experiment, the surface composition and the gas-phase composition can be investigated for longer periods of times at well-defined non-fluctuating conditions, while variables can be changed one at a time. With such a set-up the solid phase can be analyzed as well as the gas phase, e.g. by mass spectrometry. The actual contribution addresses the experimental setup, especially the control of steady-state conditions using optically determined pyrolysis rates. Validation is carried out by surface analysis using uncoated cotton as an often-studied textile to verify the concept with inert gas/oxygen mixtures of different compositions and temperatures.

EXPERIMENTAL

The experimental setup is shown in Figure 1. Gas mixtures of argon or nitrogen and oxygen of variable composition (x_{O_2} : 0 – 20 %) and velocity (0,1 – 10 m/s) are heated to the desired temperature (300 – 1000 K) with a tube furnace. The gas flows orthogonally on the moving textile. The textile is moved between two coils using a motor with speed control. The flowing hot gas mixture on the textile surface causes chemical reactions, the burnt or pyrolyzed area on the textile becomes darker, as monitored by a camera, which is used for control, together with thermocouple temperature measurements.

The resulting *images* are evaluated with a computer regarding the intensity at the burnt area. A PID controller realized in LabVIEW uses the measured intensity, compares it with an adjustable set intensity and uses this to specify a

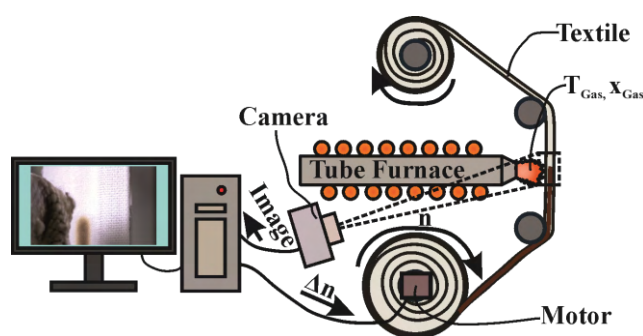


Figure 1: Sketch of the experimental setup.

speed change Δn for the motor. Utilizing the PID controller ensures the steady-state conditions of the burnt area. The intensity dependent composition of the product gas, released by the textile, will be analyzed with mass spectrometry in future work. Space dependent surface infrared (IR) spectra were used after the experiments, to validate steady-state conditions

RESULTS AND DISCUSSION

Starting with time and temperature dependent pyrolysis rate determinations for different mixtures with and without oxygen, the correct motor velocity range was selected, to obtain steady state conditions. The in-situ control was first investigated for different positions and conditions, also using the different color channels of the camera. The setup works best, when no hole is formed in the textile; the asymmetry due to gravity can be well controlled. The deviation of the surface composition along the textile movement direction is analyzed by IR spectroscopy and is shown for ten positions in Figure 2.

The qualitative infrared spectra agree very well for all positions and show that the chemical composition of the controlled moving textile is nearly identical at different positions. The coefficient of variation was calculated indicating the local composition fluctuation. The value is 0.1 for a large part of the spectrum; at points with high intensity, it even falls below 0.01. At points with low intensity, it is just above 1.

The temperature as well as the oxygen content dependency on the burnt area on the textile was investigated, both showing a similar behavior. With rising temperature or oxygen content the intensity measured by the camera decreases faster without textile movement. This indicates an increase in the reaction rate with temperature and oxygen content as expected, because both promote reactions in combustion or pyrolysis experiments. Therefore, for maintaining a constant intensity level with rising temperature or oxygen content the velocity of the textile must be adjusted. This is successfully achieved by the control for various gas composition as well as temperature of up to 600 K. At higher temperatures, a hole prevails in the textile, which can also be held at steady state when needed. In summary, it is shown, that steady-state conditions during the partial combustion or pyrolysis of cotton textiles are achievable with this experimental setup and can be used for detailed investigations of flame retardants on textiles in the future.

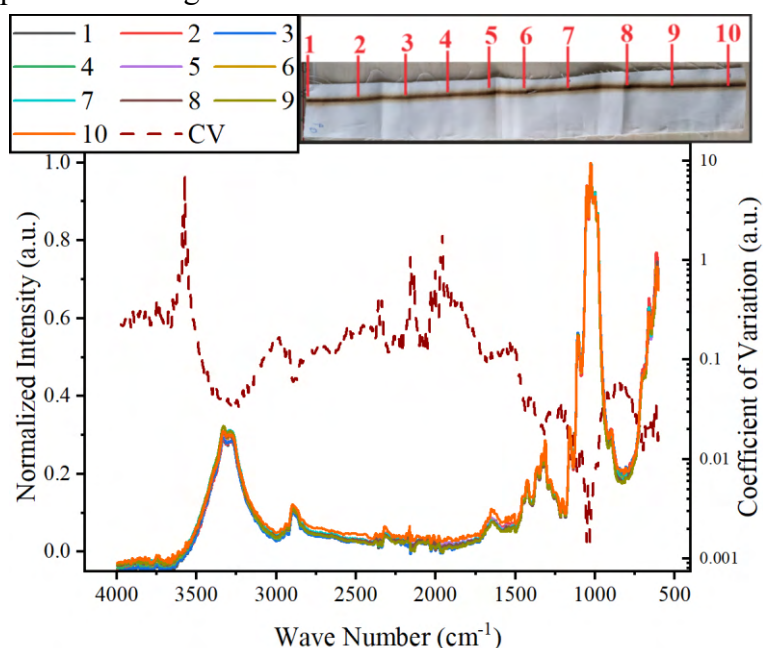


Figure 2: IR Spectra at different locations on a controlled textile strip which was moving from position 1 to 10 with defined orthogonal flow of air at 400°C.

At higher temperatures, a hole prevails in the textile, which can also be held at steady state when needed. In summary, it is shown, that steady-state conditions during the partial combustion or pyrolysis of cotton textiles are achievable with this experimental setup and can be used for detailed investigations of flame retardants on textiles in the future.

Acknowledgment

Financial supported by the Deutsche Forschungsgemeinschaft (DFG, Project number 517869745) is gratefully acknowledged.

References

- 1) Sikes, Travis, et al. 2019. 10.1016/j.proci.2018.05.042.
- 2) Trubachev, S. A., et al. 2020. 10.1063/5.0033887.

PHOTO-DEGRADATION EFFECTS OF BIO-POLYBUTYLENE-SUCCINATE EXPOSED TO UVC RAYS

Cristina Scolaro^a, Annamaria Visco^{a,b}, Salim Brahim^a

^a Department of Engineering, University of Messina, C.da Di Dio, 98166 Messina, Italy

^b Institute for Polymers, Composites and Biomaterials - CNR IPCB, Via Paolo Gaifami 18, 9-95126-Catania, Italy avisco@unime.it, cscolaro@unime.it, salim.brahimi@studenti.unime.it

INTRODUCTION

Bioderived and biodegradable Poly Butylene Succinate (PBS) represents an alternative to fossil-based plastics, since it possesses physical-mechanical characteristics like polyethylene [1]. Its applications range from textiles, to packaging for food/cosmetics, to biomedical fields (scaffolds for tissue engineering, micro and nanoparticles for drug delivery, wound dressing, 3 D or 4D printing, electrospinning processing) [2].

The sterilizability of plastics with UVC-rays is of particular interest following the recently concluded pandemic. UVC can affect microorganisms, but it is also re-sponsible for the decomposition and degradation of many organic compounds (such as polymers). Nevertheless, in many cases (as for example biomedical, medical, food, drinks, pharma, cosmetics applications) manufactures are subjected to sterilization processes before use, therefore the influence of UVC on polymers is of crucial importance.

In this study, the resistance of PBS to UVC exposure at room temperature has been evaluated and compared to PBS pure and PBS with an UV adsorber, the carbon black (CB).

EXPERIMENTAL

Materials

The blend of PBS, pure and with 2 wt.% of CB, has been mixed in a Brabender Plasticorder PL2100 chamber at 140°C, speed 40 rpm, for ten minutes. The resulting blends were thermoformed in a uniaxial hot press PM 20-200, at 140°C for 15 minutes, p=100 bar. Dog-bone samples, 1 mm thick, have been obtained by a Ray-Ran cutter machine according to ASTM D638 M-3.

UVC exposure

Samples have been exposed in a black chamber to UVC rays (UVP lamp mod. UVG-54 handheld, 254 nm, 230V/6W, 2200 μ W at 7.62 cm, LLC, Upland, CA), for 2-4-8-16-24h at distance from the lamp of 15 cm, T=25°C, RH=21%. The UVC average intensity at the dog-bone surface was 860 μ W \cdot cm⁻² \pm 10 μ W \cdot cm⁻² (Blak-Ray model J-225 Ultraviolet Meter). The treatment doses ranged from \sim 6.2 to 74.3 J/cm⁻² (intensity per time).

Physico-chemical characterization

Surface (roughness, water contact angle, shore D hardness, morphology) calorimetric (DSC), mechanical (static tensile) tests were carried out on all the blends, before and during the UVC rays' exposure.

RESULTS AND DISCUSSION

The experimental results indicated UVC induced progressively severe damages in pure PBS. This effect is strongly reduced by the presence of CB, which absorbs UV rays and preserves the degradation of the bioplastic. Experimental results showed a modification effect

on both the surface and the bulk of samples tested. UVC rays degrade PBS due to photooxidation reactions. PBS loses its ductility and hardness and becomes brittle after only two hours of exposure (see fig.1-mechanical tensile and hardness Shore-D test graphs). The probable chain scission reactions in the amorphous part make PBS rougher and more hydrophilic (see fig.1-wettability test graphs). Due to the intrinsic affinity of carbon black with blood, a greater blood-philicity was observed in PBS-CB compared to PBS. This phenomenon increases with increasing irradiation time. UVC rays are used for the sterilization process, which is necessary in some applications such as biomedical, cosmetic, pharmaceutical, food, and other products. Since UVA-UVB rays are less powerful than UVC rays, a material well resistant to UVC rays, can easily resist UVA-UVB rays.

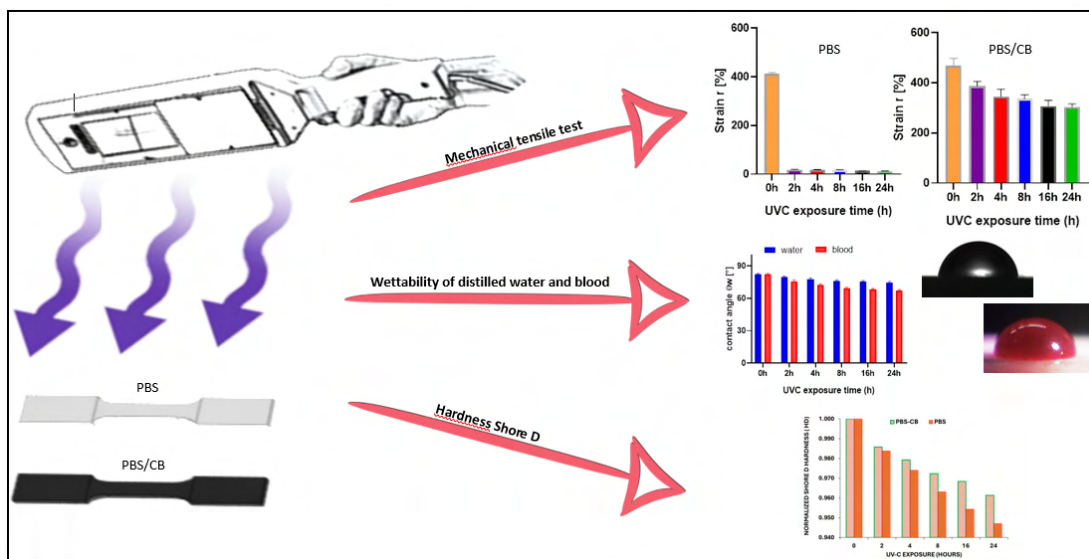


Fig. 1. Mechanical tensile test, wettability in water and blood, normalized shore D hardness of samples during the UVC exposure.

CONCLUSIONS

PBS, tested under accelerated aging conditions, was extremely sensitive to UVC photodegradation. However, CB highly reduces this effect. Further studies will be dedicated to optimizing exposure/dose times to kill different pathogens, defining the optimal amount by weight of CB in PBS and comparing the effect of carbon black with the effect of a white filler with less aesthetic impact (such as titanium dioxide) or others. These studies should be combined with a biological investigation of irradiated PBS and PBS-CB, to confirm the theoretical estimate of pathogen reduction.

Acknowledgment

Authors thanks LIFE project for the Environment and Climate Action” Project LIFE2021-SAP-ENV-101074314 LIFE-Reuse of bEer SpenT grAin foR bioplasTics – RESTART, co funded by European Community.

References

- 1) Scolaro, C.; Brahimi, S.; Falcone, A.; Beghetto, V.; Visco, A.. *Polymers*, 16,2024
- 2) Rafiqah, S.A.; Khalina, A.; Harmaen, A.S.; Tawakkal, I.A.; Zaman, K.; Asim, M.; Nurrazi, M.N.; Lee, C.H. *Polymers*, 13, 2021.

FILMS BASED ON HYALURONIC ACID/ELLAGIC ACID– BIOLOGICAL STUDIES

L. Zasada¹, B. Kaczmarek-Szczepańska¹, K. Kleszczyński², D. Chmielniak¹, M.B. Hollerung², K. Steinbrink², and S. Grabska-Zielińska³

¹ Department of Biomaterials and Cosmetics Chemistry, Faculty of Chemistry, Nicolaus Copernicus University in Torun, Poland;

² Department of Dermatology, University of Münster, Germany;

³ Faculty of Chemical Technology and Engineering, Bydgoszcz University of Science and Technology, Poland;

503555@doktorant.umk.pl (L.Z.); beata.kaczmarek@umk.pl (B.K-S.)

INTRODUCTION

Hyaluronic acid (HA), a naturally occurring glycosaminoglycan, is known for its excellent biocompatibility, biodegradability, and ability to promote hydration and tissue repair (1). Ellagic acid (EA), a polyphenolic compound found in various fruits and nuts, possesses potent antioxidant, anti-inflammatory, and anticancer properties (2). This study explores the synergistic effects of HA and EA composites for potential use in enhancing wound healing, protecting against oxidative stress, and supporting tissue regeneration.

EXPERIMENTAL

Materials

Hyaluronic acid sodium salt (HA, $M = 1.8 \times 10^6$ g/mol) and ellagic acid (EA, $M = 302.20$ g/mol, anhydrous) were purchased from Pol-Aura company (Poznań, Poland). Minimum Essential Medium Eagle (MEM) (1000 mg/L), 1% penicillin streptomycin solution, 0.05% trypsin/0.53 mM EDTA solution, 3-(4,5-dimethylthiazol-2-yl)-2,5-diphenyltetrazolium bromide (MTT), ethanol (EtOH), HCl, L-glutamine (200 mM), and isopropanol were purchased from Sigma (St. Louis, MO, USA). Fetal bovine serum was supplied by Thermo Fisher Scientific (Waltham, MA, USA). Plate count agar (PCA) for bacterial culture was from Biocorp (Warsaw, Poland).

Preparation

Hyaluronic acid (HA) was dissolved in deionized water at a concentration of 1% (w/v), while ellagic acid (EA) was dissolved at 4% (w/v) in either 0.0015 M NaOH or 0.1 M AcOH. The solutions of HA and EA were then combined in three different weight ratios: 80HA/20EA, 50HA/50EA, and 20HA/80EA. Each 40 mL mixture was stirred with a magnetic stirrer for 1 hour at room temperature (maintaining 400 r.p.m.) and then placed on a plastic holder measuring 10×10 cm.

Biological studies

Normal human epidermal keratinocytes (NHEKs) and dermal fibroblasts (NHDFs) were sourced from PromoCell and ATCC, respectively. NHEKs were cultured in Keratinocyte Growth Medium 2, while NHDFs and human melanoma cell lines A375 and G-361 were cultured in MEM medium with supplements. Cells were seeded at 0.5×10^5 cells/well, allowed to attach for 24 hours, and then cultured for 96 hours with media changes every 48 hours. Cell viability was assessed using the MTT assay, and antioxidant activity using the DPPH assay.

RESULTS AND DISCUSSION

The results showed a significant decrease in cell proliferation for both healthy and tumor cells, with viability drops ranging from 72% to 80% for acetic acid and 63% to 81% for sodium hydroxide (Fig. 1). This indicated that films with 20% or more ellagic acid were cytotoxic. All HA/EA films demonstrated positive radical scavenging activity, with no significant differences based on composition or solvent (Tab. 1).

Table 1. Radical scavenging activity (RSA) of HA/EA films (n = 3; * significant difference compared to the control sample (100HA) (p < 0.05)).

Specimen	RSA [%]
100HA	-21.50 ± 0.02
80HA/20EA/AcOH	85.40 ± 0.01*
50HA/50EA/AcOH	84.80 ± 0.01*
20HA/80EA/AcOH	85.11 ± 0.01*
80HA/20EA/NaOH	86.23 ± 0.06*
50HA/50EA/ NaOH	83.21 ± 0.07*
20HA/80EA/ NaOH	85.15 ± 0.04*

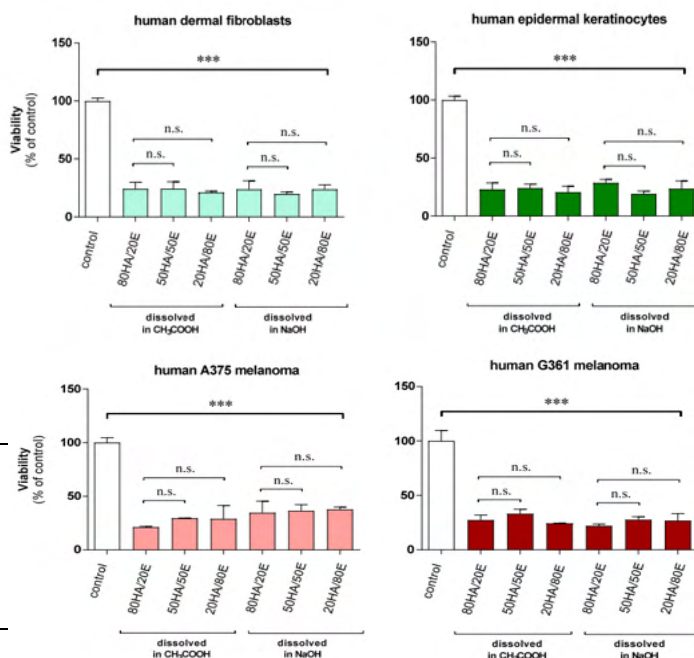


Figure 2. Human epidermal keratinocytes (NHEK) and dermal fibroblasts (NHDF), as well as human amelanotic melanoma cells (A375 and G-361), were seeded on respective hyaluronic acid (HA)/ellagic acid (EA)-loaded scaffolds and cultured for 96 h, and the viability was assessed using the MTT viability assay.

Ellagic acid (EA) adds antioxidant activity to hyaluronic acid (HA) films, confirmed by DPPH testing. No significant differences in antioxidant activity were found based on sample composition or EA solvent. HA is non-toxic and aids wound healing, but phenolic acids like EA can be toxic depending on concentration. Our studies showed that high concentrations of EA in hydrogels can be cytotoxic, suggesting the need to reduce EA content.

Acknowledgment

This work has been supported in some part by the Nicolaus Copernicus University in Torun (Torun, Poland) to maintain research potential, by the Excellence Initiative Research University competition for scientific groups-BIOdegradable PACKaging materials research group (4101.00000085), and by the grants of the German Research Foundation (Deutsche Forschungsgemeinschaft [DFG]): TR156/C05-246807620 (K.S.), SFB1009/B11-194468054 (K.S.), SFB1066/B06-213555243 (K.S.), SFB1450/C06-431460824 (K.S.), and KL2900/3-1(K.K.).

References

- 1) T.G. Sahana, P.D. Rekha, Mol Bio Rep., **45**,(6):2857-2867 (2018)
- 2) F. Shahidi, P. Ambigaipalan, J. of Functional Food, **18**, Part B, 820-897 (2015)

ENHANCING STABILITY: THE PROTECTIVE ROLE OF NANODIAMONDS AGAINST DEGRADATION AND BIODEGRADATION IN CELLULOSE ETHER DISPERSIONS

Elena Palmieri^{1,2}, Annamaria Alabiso³, Luciana Migliore³, Emanuela Tamburri¹, Silvia Orlanducci¹

¹ Dip.to di Scienze e Tecnologie Chimiche, Università degli Studi di Roma “Tor Vergata”, Via della Ricerca Scientifica, Rome, Italy

² Istituto per la Microelettronica e i Microsistemi, Consiglio Nazionale delle Ricerche, Via del Fosso del Cavaliere 100, Rome 00133, Italy

³ Dip.to di Biologia, Università degli Studi di Roma “Tor Vergata”, Via della Ricerca Scientifica, Rome, Italy

elena.palmieri@artov.imm.cnr.it; emanuela.tamburri@uniroma2.it

INTRODUCTION

Cellulosic polymers like hydroxyethyl cellulose (HEC) and hydroxypropyl cellulose (HPC) are widely used across industries due to their gel thickening, emulsifying, water-retaining, and stabilizing properties. These non-conducting polymers are valuable in cosmetics, electronics, pharmaceuticals, and medical fields. However, HEC and HPC can degrade under strong heat, radiation, oxidative conditions, strong acids, bases, and cellulase enzymes, which hydrolyze cellulose bonds and reduce viscosity. To enhance their stability, industrial products often include buffers and preservatives. This study examines the stability of HEC and HPC solutions and their composites with detonation nanodiamonds (DND), monitoring rheological behavior, viscosity, conductivity, and pH. It is found that DND significantly stabilize the polymeric dispersions and slow biodegradation, offering substantial benefits for various applications utilizing cellulose ethers.

EXPERIMENTAL

Materials

Hydroxyethyl cellulose (HEC) with MW~720 kDa and a quoted molar substitution (MS) of hydroxyethyl groups of 2.5. Hydroxypropyl cellulose (HPC), MW 370 kDa. Detonation Nano Diamond (DND) powders with primary sizes in the range of 5-10 nm were obtained from International Technology Center (ITC, USA).

Preparation

All HEC solutions were prepared by adding varying amounts of the polymer (as received) to a known volume of distilled water, followed by approximately 4 hours of magnetic stirring at 40°C to ensure complete dissolution. All HPC solutions were prepared by adding the proper amount of polymer (as received) to a known amount of distilled water, while mixing the solution, thus avoiding the formation of polymer aggregates. The obtained viscous solution was left for 24 hours to rest. The polymer concentrations are expressed as % ^{w/w}, based on the weight of the dry polymer per weight of the solvent (water).

The polymer-DND dispersions were prepared by adding nanodiamonds to deionized water, followed by an ultrasonic bath to prevent the formation of larger DND clusters. Once the DND dispersion was ready, the appropriate amount of polymer was added.

Rheological and physico-chemical characterization

Rheological characterization was performed using an AR 2000 rheometer by TA Instruments with a cone and plate measurement geometry. A 60 mm diameter 2° acrylic cone was used for all the solutions (correction for non-uniform shear field is automated in software).

The conductivity of the dispersions was estimated using a Pancellet LLC GELB WEISS conductivity meter.

The pH measurements were performed using a Pancellet LLC GELB WEISS pH meter.

RESULTS AND DISCUSSION

The stability of HEC and HPC polymer solutions at various weight concentrations, along with their composites, was assessed by monitoring rheological behavior. Rheological characterization was performed the day after preparation and continued weekly for up to three months at room temperature. Additionally, pH and conductivity changes were recorded. Microbial infection was evaluated by observing petri dishes filled with the dispersions, stored at room temperature, with daily monitoring of microorganism colony formation using an optical microscope.

No significant biodegradation was observed in HPC-based dispersions, while HEC-based dispersions exhibited severe biodegradation, especially those without DND (Figure 1a). The microorganism responsible for the degradation of HEC was identified as belonging to the *Actinomyces* sp. [1] [2]. After 7 days from preparation, HEC and HEC-DND dispersions were inoculated in agar-agar plates (Figure 1b) to amplify bacterial growth, confirming that HEC-DND dispersions showed reduced bacterial growth compared to HEC dispersions.

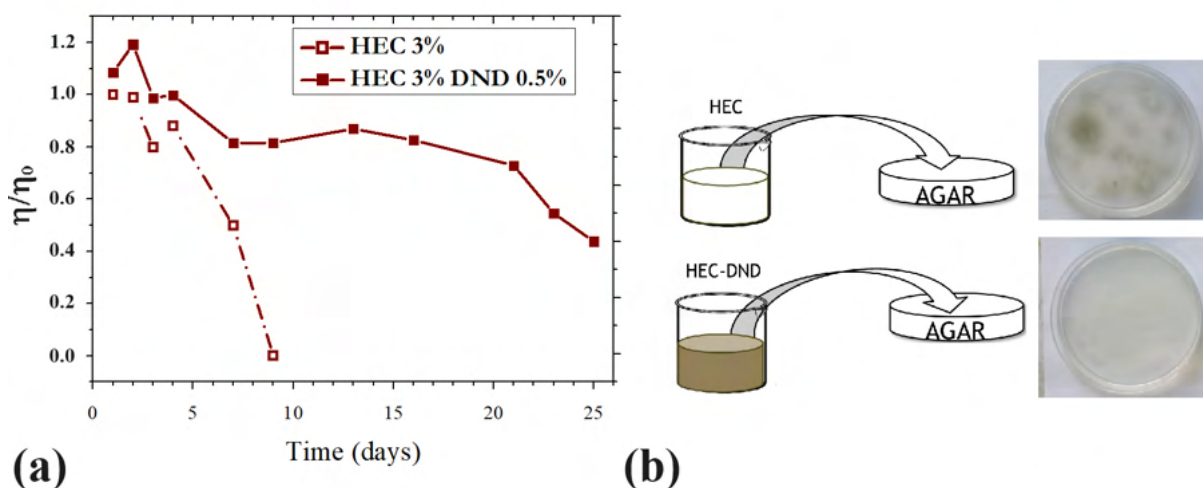


Fig. 1 (a) Normalized variation in zero-rate viscosity of HEC 3%, compared with DND-HEC composite, in a 25 days' period. (b) Agar-agar petri dishes inoculated with HEC 3% and HEC 3% DND after 7 days from preparation. In the agar-agar dish inoculated with the dispersion without DND it is possible to observe higher biological growth.

From the collected data, it can be concluded that HPC dispersions remained free from microbial degradation in the period examined, while HEC dispersions experienced biological degradation within days. The inclusion of DND in HEC composites enhanced their resistance to biodegradation, making them more stable compared to pure HEC dispersions.

References

- 1) Y. Diao et al. (2017) *Carb. Pol.* <http://dx.doi.org/10.1016/j.carbpol.2017.02.089>
- 2) Fergus, C. L. (1969). The Cellulolytic Activity of Thermophilic Fungi and Actinomycetes. *Mycologia*, 61(1), 120–129. doi:10.1080/00275514.1969.12018706

IMPACT OF CALCIUM HYDROXIDE TREATMENT ON SISAL FIBER PROPERTIES AND THEIR GEOPOLYMER COMPOSITES

C. Sanfilippo¹, V. Fiore¹, L. Calabrese², B. Megna¹, A. Valenza¹

¹Department of Engineering, University of Palermo, Viale delle Scienze, 90128, Palermo, Italy

²Department of Engineering, University of Messina, Contrada Di Dio (Sant'Agata), 98166 Messina, Italy

INTRODUCTION

Geopolymers are now recognized as environmentally friendly building materials, [1][2] offering good mechanical properties and resistance to hostile environments and high temperatures. However, their primary weakness is the brittle nature of the matrix, which limits their use in various industries. To overcome this issue, incorporating synthetic or natural fibers represents a potential solution [3]. In particular, natural fibers can be used to reinforce cement and geopolymer matrices due to their low density, relatively high specific mechanical properties, biodegradability, and wide availability [4].

EXPERIMENTAL

Materials

The main aim of this paper is to investigate how an innovative and eco-friendly fiber treatment can enhance the mechanical performance of sisal fiber-reinforced geopolymers by improving the fiber-matrix adhesion. Specifically, sisal fibers were soaked in a 2 wt% aqueous solution of calcium hydroxide for 24, 48, and 72 hours at 25°C. All geopolymeric samples were made using metakaolin as the precursor, activated with a 7M KOH solution and potassium silicate powder. River sand (2 mm nominal diameter) was used as the aggregate. Metakaolin was initially mixed with potassium silicate powder and river sand in a ratio of 1:0.5:2. Afterwards, the KOH solution was added to the mix to initiate geopolymerization. Fiber-reinforced geopolymer composites were manufactured by replacing 2 wt% of the aggregate with raw and treated sisal fibers.

Results

Chemical and morphological analyses were conducted on sisal fibers to evaluate the effectiveness of the proposed treatment. Specifically, changes in the functional groups on the fiber surface were assessed using Fourier transform infrared analysis (FTIR). Thermogravimetric analysis (TGA) and scanning electron microscope (SEM) observations were performed to investigate the thermal and morphological behavior of sisal fibers. Overall, these tests demonstrated that the proposed treatment is a useful alternative to traditional alkaline treatments (such as mercerization). Additionally, the mechanical performance of unreinforced and reinforced geopolymer materials was evaluated through compression, flexural, and indirect tensile tests (i.e., Brazilian). The experimental results indicated that the mechanical performance of geopolymer composites is influenced by the soaking time of the fiber treatment.

DISCUSSION

Overall, the proposed treatment has proven to be an effective technique for removing non-cellulosic components from sisal fibers, although it slightly reduced their mechanical properties. Additionally, it was found that the improved homogeneity and surface roughness of the natural fibers, along with the removal of surface impurities, enhance the adhesion with the geopolymer matrix. Mechanical characterization through compression, Brazilian, and

flexural tests demonstrated that fiber-reinforced geopolymer composites, when treated, enhance their mechanical performance with increasing fiber content.

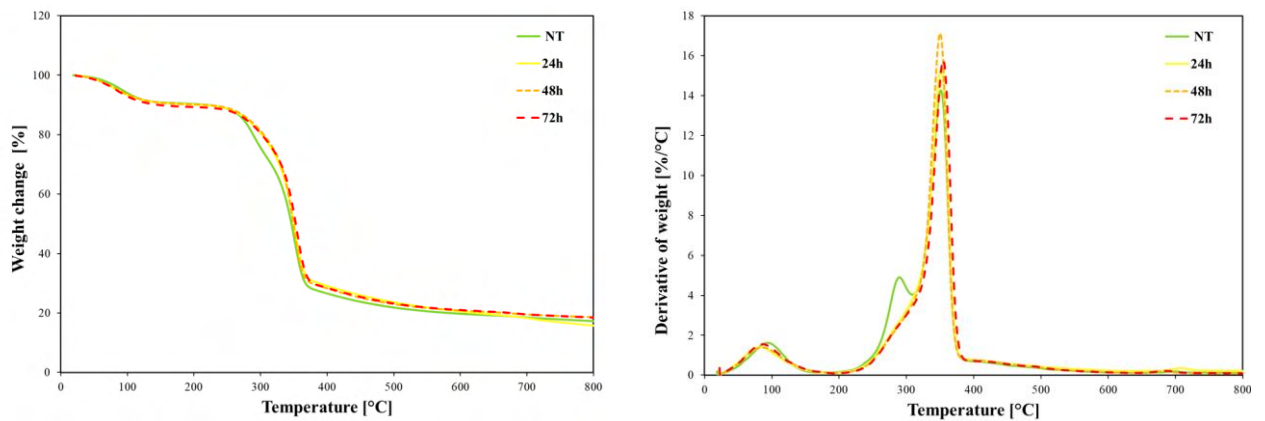


Fig 1: TG and DTG curves of untreated and treated sisal fibers

References

- 1) J. Davidovits, Geopolymers, *Journal of Thermal Analysis* **37** (1991) 1633–1656.
- 2) N.A. Al-Ghazali, F.N.A.A. Aziz, K. Abdan, N.A.M. Nasir, Mechanical Properties of Natural Fibre Reinforced Geopolymer Composites: A Review, *Pertanika J Sci Technol* **30** (2022) 2053–2069.
- 3) C. Lv, J. Liu, G. Guo, Y. Zhang, The Mechanical Properties of Plant Fiber-Reinforced Geopolymers: A Review, *Polymers (Basel)* **14** (2022).
- 4) P. Cong, Y. Cheng, Advances in geopolymer materials: A comprehensive review, *Journal of Traffic and Transportation Engineering (English Edition)* **8** (2021) 283–314.

Participant List

SURNAME	NAME	AFFILIATION	COUNTRY
Abe	Hideki	Bioplastic Research Team, RIKEN CSRS	Japan
Adoumaz	Ismail	Universite de Pau et des Pays de l'Adour	Morocco
Affato	Lorena	Institute of Polymers, Composites and Biomaterials - CNR	Italy
Aleeva	Yana	University of Palermo	Italy
Al-Malaika	Sahar	Aston University	UK
Ambrosio	Luigi	Institute of Polymers, Composites and Biomaterials - CNR	Italy
Antonucci	Vincenza	Institute of Polymers, Composites and Biomaterials - CNR	Italy
Arrigo	Rossella	Polytechnic of Turin	Italy
Avella	Angelica	Chalmers University of Technology	Sweden
Badia Valiente	Jose David	Universitat de València	Spain
Baiamonte	Marilena	University of Palermo	Italy
Bajer	Dagmara	Nicolaus Copernicus University	Poland
Balsamo	Marta	University of Palermo	Italy
Baron	Roxane	4D Pioneers	France
Becker	Richard	German Environment Agency (UBA)	Germany
Benito Hernandez	Elena Maria	University of Sevilla	Spain
Benzemma	Anais	IMP - Ingénierie des Matériaux Polymères	France
Bernagozzi	Giulia	Polytechnic of Turin	Italy

Berner	Valeria	Fraunhofer Institute for Chemical Technology ICT	Germany
Bondioli	Federica	Polytechnic of Turin	Italy
Botta	Luigi	University of Palermo	Italy
Bounor-Legare	Véronique	Université Claude Bernard Lyon 1	France
Bruzaud	Stephane	Université Bretagne Sud	France
Buccella	Giacomo	RSE S.p.A.	Italy
Bussiere	Pierre Olivier	Institut de Chimie de Clermont-Ferrand	France
Cabedo Mas	Luis	Universitat Jaume I	Spain
Calabrese	Luigi	University of Messina	Italy
Calandra	Pietro	Institute for the Study of Nanostructured Materials - CNR	Italy
Carbone	Camilla	University of Palermo	Italy
Carfagna	Cosimo	Institute of Polymers, Composites and Biomaterials - CNR	Italy
Cavodeau	Florian	Universty of Upper Alsace	France
Celauro	Clara	University of Palermo	Italy
Celina	Mathew	Editor in chief PDST	USA
Ceraulo	Manuela	University of Palermo	Italy
Chervanyov	Alexander	University of Münster	Germany
Ciaramitaro	Veronica Concetta	University of Palermo	Italy
Cicala	Gianluca	University of Catania	Italy
Citarrella	Maria Clara	University of Palermo	Italy
Coltelli	Maria Beatrice	University of Pisa	Italy

Colucci	Giovanna	Polytechnic of Turin	Italy
Combeau	Marie	IMT Mines Ales	France
Covas	José	University of Minho	Portugal
Cruz	Sandra	Federal University of São Carlos	Brasil
Deguines	Charles-Henry	Universty of Upper Alsace	France
Delarue	Laetizia	IMT Mines Alès	France
De-Paz	Maria Violante	University of Sevilla	Spain
Di Liberto	Erika Alessia	University of Palermo	Italy
Di Maio	Luciano	University of Salerno	Italy
Di Marco	Chiara	University of Palermo	Italy
Diaz-Carrasco	Fatima	University of Sevilla	Spain
Dintcheva	Nadka	University of Palermo	Italy
Doriat	Aurelien	Institut Pprime	France
Dorigato	Andrea	University of Trento	Italy
Duchamp	Alexy	Université Clermont Auvergne	France
Fabritius	Helge-Otto	Hamm-Lippstadt University of Applied Sciences	Germany
Filippone	Giovanni	University of Naples Federico II	Italy
Fiore	Vincenzo	University of Palermo	Italy
Fiorica	Calogero	University of Palermo	Italy
Fiorini	Maurizio	University of Bologna	Italy
Fiorio	Rudinei	Maastricht University	The Netherlands

Frache	Alberto	Polytechnic of Turin	Italy
Fredi	Giulia	University of Trento	Italy
Friscione	Lorenzo	Zwick Roell Srl	Italy
Fuchs	Sabine	Hamm-Lippstadt University of Applied Sciences	Germany
Fukata	Yuya	The University of Tokyo	Japan
Galbis Fuster	Elsa	University of Sevilla	Spain
Gamez-Pérez	José	University Jaume I	Spain
Gammino	Michele	University of Palermo	Italy
Garcia-Martin	Maria Gracia	University of Sevilla	Spain
Gardette	Jean-Luc	Université Clermont Auvergne	France
Garofalo	Emilia	University of Salerno	Italy
Gerard	Jean-Francois	<i>Université de Lyon - INSA</i>	France
Gijsman	Pieter	Gijsman Durability Advisory	The Netherlands
Gkaliou	Kyriaki	Grundfos Holding A/S	Denmark
Glerean	Paolo	Aliplast s.p.a.	Italy
Gnoffo	Chiara	Polytechnic of Turin	Italy
Gomez-Sanchez	Elena	Deutsches Bergbau-Museum Bochum	Germany
Goncalves Marques	Gabriela	Universite Claude Bernard Lyon 1	France
Gorecki	Karol	Jagiellonian University	Poland
Gratier	Léa	University of Lorraine	France
Grömmer	Roxana	Fraunhofer Institute for Chemical Technology	Germany

Gulino	Emmanuel Fortunato	University of Palermo	Italy
Gutierrez Silva	Karen Dayana	University of Valencia	Spain
Hiejima	Yusuke	Kanazawa University	Japan
Höhne	Karl-Cristoph	Fraunhofer Institute for Chemical Technology	Germany
Incarnato	Loredana	University of Salerno	Italy
Infurna	Giulia	University of Palermo	Italy
Inguanta	Rosalinda	University of Palermo	Italy
Ishida	Takato	Nagoya University	Japan
Ivanova	Tatjana	Riga Technical University	Latvia
Iwata	Tadahisa	University of Tokyo	Japan
Jakubowicz	Ignacy	RISE Research Institutes of Sweden	Sweden
Jankowski	Piotr	Łukasiewicz Research Network - Industrial Chemistry Institute	Poland
Jost	Chloé	Université Claude Bernard Lyon 1	France
Kabe	Taizo	The University of Tokyo	Japan
Killinger	Lukas	Fraunhofer Institute of Chemical Technology	Germany
Koike	Takanari	Kyoto University	Japan
Kowalonek	Jolanta	Nicolaus Copernicus University in Toruń	Poland
Kozłowska	Justyna	Nicolaus Copernicus University in Toruń	Poland
Kozłowski	Ryszard	Former Director of the Institute of Natural Fibres	Poland
Krukzala	Krzysztof	Jagiellonian University in Krakow	Poland
La Mantia	Francesco Paolo	University of Palermo	Italy

Lamattina	Giulia	University of Palermo	Italy
Latteri	Alberta	University of Catania	Italy
Lazeregue	Hiba	Arts et Métiers Institute of Technology	France
Leanza	Melania	Institute of Polymers, Composites and Biomaterials - CNR	Italy
Leem	Yoobin	Hokkaido University	Japan
Lo Bianco	Alessandro	University of Palermo	Italy
Lo Re	Giada	Chalmers University of Technology	Sweden
Luciano	Marco	University of Palermo	Italy
Maffezzoli	Alfonso	University of Salento	Italy
Maggiani	Mario	AMAPLAST	Italy
Maio	Andrea	University of Palermo	Italy
Masek	Anna	Lodz University of Technology	Poland
Mathieu	Camille	Arts et Métiers Institute of Technology	France
Mauro	Nicolò	University of Palermo	Italy
Mayer-Gall	Thomas	Deutsches Textilforschungszentrum Nord-West gGmbH	Germany
Mazzara	Francesca	University of Palermo	Italy
Megna	Bartolomeo	University of Palermo	Italy
Meng	Xiangze	Tsinghua University	China
Merijs-Meri	Remo	Riga Technical University	Latvia
Messori	Massimo	Polytechnic of Turin	Italy

Metzsch-Zilligen	Elke	Fraunhofer Institute for Structural Durability and System Reliability	Germany
Milazzo	Mario	University of Pisa	Italy
Mincheva	Rosica	University of Mons	Belgium
Miranda	Riccardo	University of Palermo	Italy
Mistretta	Maria Chiara	University of Palermo	Italy
Moretti	Federica	University of Trieste	Italy
Morreale	Marco	Kore University of Enna	Italy
Müller	Alejandro J.	University of the Basque Country	Spain
Muranaka	Yosuke	Kyoto University	Japan
Nag	Aniruddha	University of York	UK
Nakashima	Erika	Chubu University	Japan
Niccolai	Francesca	University of Pisa	Italy
Noè	Camilla	Polytechnic of Turin	Italy
Ørsnæs	Morten V.	GRUNDFOS Holding A/S	Denmark
Otto	Raphael	Deutsches Textilforschungszentrum Nord-West gGmbH	Germany
Paiva	Maria da Conceição	University of Minho	Portugal
Palmieri	Francesco	University of Salerno	Italy
Panagiotopoulos	Christos	National Technical University of Athens	Greece
Pantani	Roberto	University of Salerno	Italy
Papaspnyrides	Constantine D.	National Technical University of Athens	Greece

Patrick	Klein	Covestro Deutschland AG, Leverkusen	Germany
Paul	Adir Chandra	Tomas Bata University in Zlin	Czech Republic
Pegoretti	Alessandro	University of Trento	Italy
Penati	Mario Roberto	MP Strumenti	Italy
Pesenti	Theo	Université Paris-Saclay	France
Petrucci	Roberto	University of Perugia	Italy
Porfyrus	Athanasios	National Technical University of Athens	Greece
Puglia	Debora	University of Perugia	Italy
Pyrzyński	Kajetan	DELTA - Innovative Company	Poland
Quentin	Jean	University of Lyon, UJM-Saint- Etienne	France
Rech	Arianna	Technical University of Denmark	Germany
Regnier	Julie	GEMTEX - Génie et Matériaux Textiles	France
Riccelli	Maria Chiara	University of Salerno	Italy
Ricciardi	Maria Rosaria	Institute of Polymers, Composites and Biomaterials - CNR	Italy
Richaud	Emmanuel	Arts et Metiers Institute of Technology - CNRS	France
Rijavec	Tjasa	University of Ljubljana	Slovenia
Rizzarelli	Paola	Institute of Polymers, Composites and Biomaterials - CNR	Italy
Rizzo	Giuliana	University of Catania	Italy
Rodi	Erica	Irritec SpA	Italy
Saha	Petr	Tomas Bata University in Zlin	Czech Republic
Sanfilippo	Carmelo	University of Palermo	Italy

Scaffaro	Roberto	University of Palermo	Italy
Scarfato	Paola	University of Salerno	Italy
Schartel	Bernard	Bundesanstalt für Materialforschung und -prüfung	Germany
Schiera	Veronica	University of Palermo	Italy
Schwind	Bertram	Hamm-Lippstadt University of Applied Sciences	Germany
Scolaro	Cristina	University of Messina	Italy
Serrano	Stephane	University of Toulon	France
Skyronka	Victor	Université Jean Monnet, Saint- Etienne	France
Stam	Rachel	Maastricht University	The Neterlands
Stanzione	Mariaamelia	Institute of Polymers, Composites and Biomaterials - CNR	Italy
Szostak	Marek	Poznan University of Technology	Poland
Tamburri	Emanuela	Tor Vergata University of Rome	Italy
Tang	Guoshuo	Tsinghua University	China
Testa	Maria	University of Palermo	Italy
Therias	Sandrine	Université Clermont Auvergne	France
Titone	Vincenzo	University of Palermo	Italy
Tomasik	Niklas	University of Duisburg-Essen	Germany
Tomasik	Niklas	University of Duisburg-Essen	Germany
Torre	Luigi	University of Perugia	Italy
Torresi	Stefano	University of the Basque Country	Spain
Valenza	Antonino	University of Palermo	Italy

Vaytet	Théo	Universite Claude Bernard Lyon 1	France
Visco	Annamaria	University of Messina	Italy
Visinoni	Andrea	FKV SRL	Italy
Voulgaris	Dimistris	ELKEME SA	Greece
Vouyiouka	Stamatina	National Technical University of Athens	Greece
Watt	Fabien Allan	Hamm-Lippstadt University of Applied Sciences	Germany
Yang	Rui	Tsinghua University	China
Yarahmadi	Nazdaneh	RISE Research Institutes of Sweden	Sweden
Ye	Yan	Tsinghua University	China
Zasada	Lidia	Nicolaus Copernicus University in Torun	Poland

